

**A STUDY ON CLUSTER AND HEAVY PARTICLE
RADIOACTIVITY OF SUPERHEAVY NUCLEI**



*Thesis submitted to Bharathidasan University
in partial fulfillment of the requirements for the degree of*

Doctor of Philosophy in Physics

Submitted by

NAGARAJA A M

(Ref. No. 06977/Ph. D-K3/Physics/PT/April 2019)

Part time Research Scholar in Physics

St. Joseph's College (Autonomous)

Tiruchirappalli

Under the guidance of

Supervisor

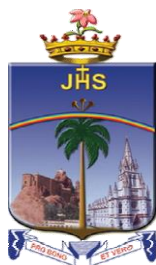
Dr. S. ALFRED CECIL RAJ

Associate Professor of Physics
St. Joseph's College (Autonomous)
Tiruchirappalli – 620 002
Tamilnadu

Co-Supervisor

Dr. H.C. MANJUNATHA

Associate Professor of Physics
Government College for Women
Kolar – 563 101
Karnataka



Department of Physics
St. Joseph's College (Autonomous)
(Affiliated to Bharathidasan University)
Tiruchirappalli-620 002

MAY 2022

Dr. S. Alfred Cecil Raj, M Sc., M.Phil., Ph.D.

Associate Professor

Department of Physics

St. Joseph's College (Autonomous)

Tiruchirappalli- 620 002



CERTIFICATE

This is to certify that the thesis entitled “**A STUDY ON CLUSTER AND HEAVY PARTICLE RADIOACTIVITY OF SUPERHEAVY NUCLEI**” submitted to the Bharathidasan University, Tiruchirappalli in partial fulfillment of the requirements for the award of the degree of Doctor of Philosophy in Physics, is a bonafide record of the work done by **Nagaraja A M** (Ref. No. 06977/Ph.D.-K3/Physics/PT/April 2019) from May 2019 to May 2022 under my supervision and guidance. This is an independent work on the part of the candidate under my guidance.

(Dr. S. Alfred Cecil Raj)
Supervisor

Place : Tiruchirappalli

Date :

Dr. H.C. Manjunatha, M Sc.,M.Phil.,Ph.D.

Associate Professor

Department of Physics

Govt. College for Women

Kolar - 563 101



CERTIFICATE

This is to certify that the thesis entitled **“A STUDY ON CLUSTER AND HEAVY PARTICLE RADIOACTIVITY OF SUPERHEAVY NUCLEI”** submitted to the Bharathidasan University, Tiruchirappalli in partial fulfillment of the requirements for the award of the degree of Doctor of Philosophy in Physics, is a bonafide record of the work done by **NAGARAJA A M** (Ref.No.06977/Ph.D-K3/Physics/PT/April 2019) from May 2019 to May 2022 under my supervision and guidance. This is an independent work on the part of the candidate under my guidance.

(Dr. H.C. Manjunatha)
Co-Supervisor

Place : Kolar

Date :

DECLARATION

I hereby declare that the thesis entitled **“A STUDY ON CLUSTER AND HEAVY PARTICLE RADIOACTIVITY OF SUPERHEAVY NUCLEI”** embodies the results of my research work carried out under the guidance and supervision of **Dr. S. Alfred Cecil Raj, M.Sc., M.Phil., Ph.D.** Supervisor, Associate Professor, Department of Physics, St. Joseph’s College (Autonomous), Tiruchirappalli & **Dr. H.C. Manjunatha, M.Sc., M.Phil., Ph.D.** Co-Supervisor, Associate Professor, Department of Physics, Govt. College for Women, Kolar, and that I have not submitted the above thesis to any University for any Degree, Diploma, Fellowship or any other similar titles previously.

(NAGARAJA A. M.)

Place : Tiruchirappalli

Date :

Department of Physics
St. Joseph's College (Autonomous)

(Affiliated to Bharathidasan University)
Tiruchirappalli – 620 002



CERTIFICATE OF PLAGIARISM CHECK

1.	Name of the Research Scholar	NAGARAJA A. M. (Ref. No. 06977/Ph. D-K3/Physics/PT/April 2019)
2.	Course of study	Ph.D. Physics
3.	Title of the Thesis	A STUDY ON CLUSTER AND HEAVY PARTICLE RADIOACTIVITY OF SUPER HEAVY NUCLEI
4.	Name of the Supervisor	Dr. S. Alfred Cecil Raj, M.Sc., M.Phil., Ph.D.
5.	Name of the Co-Supervisor	Dr. H.C. Manjunatha, M.Sc., M.Phil., Ph.D.
6.	Department/Institution/ Research Centre	Department of Physics St. Joseph's College (Autonomous) Tiruchirappalli -620 002
7.	Acceptable Maximum Limit	10%
8.	Percentage of similarity of content identified	0%
9.	Software Used	Ouriginal
10.	Date of Verification	23.05.2022

Report on plagiarism check, item with % of similarity is attached.

Signature of the Co-Supervisor

Signature of the Supervisor

Signature of the Candidate

Document Information

Analyzed document	NAGARAJA A M.pdf (D137587480)
Submitted	2022-05-23T07:00:00.0000000
Submitted by	Dorairajan
Submitter email	manavaidorai@gmail.com
Similarity	0%
Analysis address	manavaidorai.stjct@analysis.ouriginal.com

Sources included in the report

ACKNOWLEDGEMENT

I would like to express my sincere gratitude to my Supervisor **Dr. S. Alfred Cecil Raj**, Associate Professor, Department of Physics, St. Joseph's College (Autonomous), Tiruchirappalli for his continuous support of my Ph.D. work. As my research Supervisor, the valuable guidance given during the course of this investigation helped me to complete my Ph.D. work successfully. I thank my Supervisor for the extended support and encouragement over these years.

With immense pleasure and a deep sense of gratitude, I wish to express my sincere thanks to my Co-Supervisor **Dr. H.C. Manjunatha**, Associate Professor, Department of Physics, Government College for Women, Kolar, without his motivation, continuous encouragement, and suggestions, this research would not have been successfully completed.

I would like to extend my special thanks to Doctoral Committee Members **Dr. R. Radhakrishnan**, Associate Professor, Department of Physics, Jamal Mohamed College (Autonomous), Tiruchirappalli, and **Dr. M.M. Armstrong Arasu**, Assistant Professor, St. Joseph's College (Autonomous), Tiruchirappalli for their valuable and inspiring guidance which enabled me to bring out this research successfully.

I am grateful to **Rev. Dr. M. Arockiasamy Xavier S.J.**, Principal, St. Joseph's College (Autonomous), Tiruchirappalli for providing me with the facilities and many other resources needed for my research. I am extremely grateful to **Dr. N. Ravi**, HOD, and all the faculty members of the Department of Physics, St. Joseph's College (Autonomous), Tiruchirappalli for their consent, encouragement, and support in my research.

My sincere thanks to research colleagues **Dr. L. Seenappa**, **Dr. K.N. Sridhar**, **Dr. N. Sowmya** **Prof. K.V. Sathish**, **Prof. G.R. Sridhara**, **Prof. N. Nagaraja**, and **Prof. M.G. Srinivas** **Dr. Y.S. Vidya** and **Prof. B. Chinnappa Reddy**, fellow researchers **Mr. P.S. Damodara Gupta**, **Mr. N. Manjunath**, **Mr. R.Munirathnam**, and **Mr. B. Mahesh** and **Miss. S. Deepthi** for their cooperation, support, and encouragement during the research work.

My sincere thanks to the Principal, H.O.D, and faculties of the Physics department, Government First Grade College, Kolar. I wish to extend my profound sense of gratitude to my family members and friends for all the sacrifices they made during my research and also for providing me with moral support and encouragement whenever required.

NAGARAJA A M

CONTENTS

LIST OF FIGURES	iii
LIST OF TABLES	viii
ABSTRACT	x
1 Introduction	1
1.1 Superheavy elements	1
1.2 Decay of superheavy elements	4
1.2.1 Alpha decay	4
1.2.2 Spontaneous fission	5
1.2.3 Cluster radioactivity	6
1.2.4 Heavy paricle radioactivity	10
1.3 Objectives	13
2 Semi empirical formula for decay energy and half-lives of cluster radioactivity	14
2.1 Introduction	14
2.2 Theory	17
2.2.1 Semi-empirical formula for decay energies of cluster radioactivity	17
2.2.2 Semi-empirical formula for cluster decay half lives	22
2.3 Results	30
3 Cluster radioactivity	41
3.1 Introduction	41
3.2 Theory	44
3.2.1 Modified generalized liquid drop model(MGLDM)	44
3.2.2 Modified Proximity Potential 1977 (MP-77)	46
3.2.3 Proximity 1977 (Prox-77)	47
3.2.4 Modified proximity potential 1981 (MP-81)	47
3.2.5 Proximity 2013 (Prox-13)	47

3.2.6	Prox Ngo 1980 (Ng-80)	48
3.2.7	Denisov 2002 (DP-00)	48
3.3	Coulomb and Proximity potential (CPPM)	49
3.4	Results	50
4	Heavy particle radioactivity of superheavy elements	80
4.1	Theory	82
4.2	Results	82
4.2.1	Comparision of HPR with alpha decay and SF	90
5	Investigations on decay modes of superheavy nuclei	94
5.1	Introduction	94
5.2	Theory	97
5.2.1	Alpha and cluster decay	97
5.2.2	Beta decay	100
5.2.3	Spontaneous fission	104
5.3	Results	105
6	Summary and conclusion	120
6.1	Comparision of present work with microscopic theory	120
6.1.1	Selection of decay energy and suitable mass excess for the study of CR and HPR	120
6.1.2	Suitable microscopic and macroscopic model to study of CR and HPR .	122
6.2	Semiempirical formula for decay energies and half lives of CR	126
6.3	Cluster radioactivity in the SHN	127
6.3.1	Even nuclei	127
6.3.2	Odd nuclei	127
6.3.3	Theoretical evidence for neutron magic number 184 from cluster radioactivity studies	127
6.4	Heavy particle radioactivity	128
6.5	Investigations on decay modes of SHN	128
6.6	Scope of the Research work	130
	REFERENCES	130
	LIST OF PUBLICATIONS	177

List of Figures

2.1	The variation of Q-values with the mass number of daughter nuclei and atomic number of cluster nuclei.	18
2.2	The variation of Q-values as a function of during different cluster emissions such as ${}^4\text{He}$ to ${}^{46}\text{Ca}$ for the neutron number = 148 and 150.	21
2.3	The variation of logarithmic half-lives as a function of product of atomic number of daughter and inverse square root of energy released during the decay process for parent nuclei with $Z=110$	27
2.4	Variation of fitting constants A and B with product of atomic number and mass of cluster for $Z=110$	28
2.5	Variation of A_2 , A_1 , A_0 , B_2 , B_1 and B_0 with atomic number of parent nuclei . . .	29
2.6	A comparison of present formula with that of other theoretical method such as HFB [236, 237]	31
2.7	Percentage of deviation of present formula with that of the experiments [261, 262]	32
2.8	Percentage of deviation of present formula with that of the experiment [76, 263] .	33
2.9	A comparison of variation of available experimental values with present work . .	36
2.10	A prediction of α decay half-lives in the SH region $Z=118-126$	36
2.11	The comparison of average deviation of α decay half-lives with atomic number for different semi empirical relations	38
3.1	A plot of $Q(\text{MeV})$ of even nuclei within the atomic number range $104 \leq Z \leq 126$ as a function of Z^2/A	50
3.2	A plot of experimental $\log T_{1/2}(s)$ as a function of Z/\sqrt{Q}	51
3.3	A plot of Q value of even nuclei in the atomic number range $104 \leq Z \leq 126$ as a function of Sussmann central radii C_i	52
3.4	A plot of penetration probability of even nuclei in the atomic number range $104 \leq Z \leq 126$ evaluated using MGLDM model with mass number of parent nuclei. . .	53

3.5	A plot of $\log T_{1/2}(s)$ of even nuclei in the atomic number range $104 \leq Z \leq 126$ as a function of atomic number of daughter nuclei.	54
3.6	Comparison of $\log T_{1/2}(s)$ of even nuclei as a function of neutron number of cluster nuclei (N_C)	55
3.7	A plot of $\log T_{1/2}(s)$ of even nuclei within the atomic number range $104 \leq Z \leq 126$ as a function of $(N - Z)^2/A$ for different cluster emissions such as ^{12}C , ^{28}Si , ^{36}Ar and ^{40}Ca in case of (a) $Z=104$, (b) $Z=114$, (c) $Z=120$ and (d) $Z=126$	55
3.8	A plot of $\log T_{1/2}(s)$ of even nuclei within the atomic number range $104 \leq Z \leq 126$ as a function of $Z^2/A^{1/3}$ for different cluster emissions such as ^{12}C , ^{28}Si , ^{36}Ar and ^{40}Ca in case of (a) $Z=104$, (b) $Z=114$, (c) $Z=120$ and (d) $Z=126$	56
3.9	A plot of $\log T_{1/2}(s)$ of even nuclei within the atomic number range $104 \leq Z \leq 126$ as a function of pairing effect ($1/\sqrt{A}$).	57
3.10	A plot of logarithmic half-lives as function of shell corrections for (a) $Z=104$ and (b) 114.	58
3.11	A variation of total potential using different proximity potential functions such as MP-77, Prox-77, MP-81, Prox-13, Ng-80 and DP-00 with the separation distance between the two nuclei in case of ^{262}Db parent nuclei during the cluster emission of ^{14}C	59
3.12	Percentage of deviation of decay energies using mass excess models such as WS3+RBF, WS4, WS4+RBF, WS3, KTUY, FRLDM and WS with that of available experimental data as a function of Z^2/A	61
3.13	A plot of Q values of odd nuclei in the atomic number range $105 \leq Z \leq 125$ as a function of Sussmann central radii C_i	62
3.14	Comparison of $\log T_{1/2}(s)$ values obtained using different proximity functions both in case of CPPM and MGLDM as a function of Z/\sqrt{Q} with that of available experimental CD half-lives.	62
3.15	A plot of penetration probability of odd nuclei in the atomic number range $105 \leq Z \leq 125$ evaluated using MGLDM model with mass number of parent nuclei.	63
3.16	A plot of $\log T_{1/2}(s)$ of odd nuclei in the atomic number range $105 \leq Z \leq 125$ as a function of atomic number of daughter nuclei.	64
3.17	A plot of $\log T_{1/2}(s)$ of odd nuclei as a function of atomic number of cluster nuclei	65

3.18	Comparison of $\log T_{1/2}(s)$ of odd nuclei as a function of neutron number of cluster nuclei	66
3.19	A plot of $\log T_{1/2}(s)$ of odd nuclei within the atomic number range $105 \leq Z \leq 125$ as a function of Z^2/A	66
3.20	A plot of $\log T_{1/2}(s)$ of odd nuclei within the atomic number range $105 \leq Z \leq 125$ as a function of $(N - Z)/(N + Z)$	67
3.21	Plot of evaluated $\log T_{1/2}$ values vs mass number of parent nuclei for the emission of cluster (${}^4\text{He}$ to ${}^{48}\text{Ca}$) and spontaneous fission from SH region $104 \leq Z \leq 115$	69
3.22	Plot of evaluated $\log T_{1/2}$ values vs mass number of parent nuclei for the emission of cluster (${}^4\text{He}$ to ${}^{48}\text{Ca}$) and spontaneous fission from SH region $116 \leq Z \leq 126$	70
3.23	Map of nuclei reflecting the logarithmic half-lives corresponding to shortest cluster-decay half-lives for the mass number and atomic number of parent nuclei in the SHE in the region $104 \leq Z \leq 126$	74
3.24	Map of nuclei reflecting Q-values corresponding to shortest cluster-decay half-lives for the mass and atomic number of parent nuclei in SHE in the region $104 \leq Z \leq 126$	75
3.25	Map of nuclei reflecting the logarithmic half-lives corresponding to shortest cluster-decay half-lives for the neutron number and atomic number of parent nuclei in the SHE in the region $104 \leq Z \leq 126$	77
3.26	(a) Variation of logarithmic half-lives ($\log T_{1/2}$) of ${}^9\text{Be}$ cluster-decay as a function of neutron number of the daughter nuclei in the region 104-109, similarly,(b) 110-115, (c)116-121 and (d) 122-126.	78
4.1	A plot of Q value (MeV) as a function of Sussmann central radii (C_i) in the atomic number range $104 \leq Z \leq 126$ for the HPR of ${}^{86}\text{Kr}$	84
4.2	A plot of $\log T$ (s) as a function of (a) neutron number of cluster (N_c), (b)neutron number of parent nuclei (N_p), (c) atomic number of cluster nuclei (Z_c) and (d)atomic number of daughter nuclei (Z_d).	86
4.3	A plot of $\log T_{1/2}(s)$ as a function of relative neutron excess $(N - Z)/(N + Z)$ of parent nuclei.	87
4.4	A plot of $\log T_{1/2}(s)$ as a function of asymmetry effect $((N - Z)^2/A)$ for different HPR such as ${}^{86}\text{Kr}$, ${}^{91}\text{Y}$, ${}^{94}\text{Zr}$ and ${}^{96}\text{Mo}$ in case of (a) $Z=120$, (b) $Z=122$, (c) $Z=124$ and (d) $Z=126$	87

4.5	A plot of $\log T_{1/2}(s)$ as a function of pairing effect ($1/\sqrt{A}$) for different HPR such as ^{86}Kr , ^{91}Y , ^{94}Zr and ^{96}Mo in case of (a) $Z=120$, (b) $Z=122$, (c) $Z=124$ and (d) $Z=126$	88
4.6	A plot of $\log T_{1/2}(s)$ as a function of Coulomb effect ($Z^2/A^{1/3}$) for different HPR such as ^{86}Kr , ^{91}Y , ^{94}Zr and ^{96}Mo in case of (a) $Z=120$, (b) $Z=122$, (c) $Z=124$ and (d) $Z=126$	89
4.7	Comparison of $\log T_{1/2}(s)$ of HPR (HPR), α decay and SF (SF) as a function of mass number of the parent nuclei (A_P) for different SH elements.	91
5.1	Schematic presentation of molecular phase of the di-nuclear system. The daughter nucleus and the emitted (smaller) fragments. The distance between their geometrical centers and distance between the center of the heavier fragment and the circular sharp neck of radius a are denoted by ζ and ξ , respectively.	99
5.2	Map of nuclei reflecting the logarithmic α -decay half-lives for the isotopes of elements from $Z=104$ to 126 . The Q -values estimated using AME16 and FRDM95. The vertical line on the right side of the figure shows increase in $\log T_{1/2}$ values from navy blue region to brown region.	109
5.3	Predicted CD logarithmic half-lives in the atomic number range $Z=104-126$ using AME16 and FRDM95 mass excess values. The hallow bin with different colour in each panel shows the cluster emission for which half-lives are minimum.	110
5.4	Map of nuclei reflecting the logarithmic cluster-decay half-lives for the neutron number of parent and cluster isotopes of elements from $Z=104$ to 126	111
5.5	Heat map showing the variations of lowest logarithmic half lives of clusters of $104 < Z < 126$	112
5.6	Heat map showing the variations of logarithmic half lives of SF of $104 < Z < 126$	113
5.7	Chart of SF(purple), alpha-decay(brown), β^+ -decay(cyan) and cluster emitters(yellow) with atomic numbers $Z = 104-126$. The Q values are calculated using the FRDM95 mass tables	114
5.8	Heat map showing the variations of atomic number, mass number of parent and logarithmic half lives of different decay modes (<i>lifetimes</i>) of $104 < Z < 126$	116
6.1	A comparison of $Q_{exp} - Q_{th}$ values obtained using different mass excess values such as WS3+RBF, WS4, WS4+RBF, WS3, KTUY, FRLDM and WS with that of Z^2/A	121

6.2	Variation of $\log T_{1/2}(s)$ as a function of Z_d/\sqrt{Q} for (a) microscopic HFB [72], M3Y [81], RMFM [402], QMPP-WKB [70] and (b) macroscopic models MGLDM, CPPM, GLDM1, GLDM2 [407, 408].	123
6.3	Comparison of standard deviation obtained using microscopic and macroscopic models.	124
6.4	Variation of $\log T_{exp}/\log T_{semi}$ as a function of $Z_d Q^{-1/2}$ using different semi-empirical relations such as UNIV [409], NRDX [217], UDL [76], KPS [410], AZF [411], Horoi [214] and Poenaru et al., [71, 71].	125

List of Tables

2.1	Fitting parameters for present formula defined in equation 2.4 for even parent neutron number.	23
2.2	Co-efficient sets of A' and B'.	30
2.3	The range of isotopes and total number of isotopes considered for each atomic number (Z) in the present empirical formula.	30
2.4	Root mean square error in the present formula, FRDM95 [252] and HFB14 [252].	32
2.5	A comparison of experimental Q-values with the FRDM95, HFB14 and present formula having same A/Z during an α decay in the SH region $106 \geq Z \geq 118$. . .	34
2.6	Comparison of half-lives (s) of this work with UDL [224], Horoi et al., [214] Univ [227], Royer [212] and VSS [228] and experimental values.	37
2.7	Comparison of half-lives (s) of this work with Refers.[272–276]	38
2.8	A comparison of logarithmic half-lives(s) of present work with logarithmic half-lives(s) UNIV [227], NRDX [217], UDL [224], and Horoi [214]	39
3.1	The standard deviation obtained using different mass excess values with that of experimental Q-values.	52
3.2	The standard deviation obtained using different mass excess values with that of experimental Q-values.	60
3.3	Comparison of cluster-decay half-lives evaluated using present work (PW) with the available experiments.	68
3.4	Isotopes of heavy and SH nuclei having longer life time in the atomic number region $104 \leq Z \leq 118$	71
3.5	Logarithmic half- lives for different decay modes and their dominant decay mode	72
3.6	Logarithmic half- lives of different decay modes and their dominant decay mode .	73
3.7	Tabulation of parent (A_P), daughter (A_D) and cluster nuclei (A_C) along with the Q-values and $\log T_{1/2}$ values corresponding to magic number of neutrons of parent/daughter nuclei.	76

4.1	Tabulation of Q-values obtained using different mass excess values such as WS3+RBF, WS4, WS4+RBF, WS3, KTUY, FRLDM, WS with experimental Q-values . . .	82
4.2	The standard deviation obtained using different mass excess values with that of experimental Q-values.	83
4.3	A comparison of cluster decay half-lives [305] obtained using CPPM and MGLDM with that of available experiments.	85
4.4	Decay chain of predicted heavy particle emitters in the SHN region $118 \leq Z \leq 126$. Tabulation of Q-values, half-lives of HPR (HPR), α , β^\pm -decay and SF along with dominant decay mode.	92
5.1	Tabulation of cluster-decay half-lives evaluated using present work (PW) and available experiments.	106
5.2	Comparison of logarithm half-lives (years) of SF in the SH region $104 \leq Z \leq 114$ from present work with the available experiments.	107
5.3	Comparison of present work(PW) with the available experimental(Exp)values . .	108
5.4	Identified cluster emitters in the SHN	113
5.5	Identified alpha emitters in the SHN region	115
5.6	Identified β^+ emitters in the SHN region	117
5.7	SHN with double decay mode and its branching ratios	118
6.1	The standard deviation obtained using different mass excess values with that of experimental Q-values.	122
6.2	The standard deviation obtained using different semi empirical relations with that of experimental $\log T_{1/2}$ -values.	124

ABSTRACT

A detailed investigation is carried out on the cluster and heavy particle radioactivity of superheavy nuclei. A semi-empirical formula is formulated for decay energies, alpha decay, and cluster decay half-life in the superheavy region $104 \leq Z \leq 126$ for the emission of clusters (${}^4\text{He}$, ${}^9\text{Be}$, ${}^{10,11}\text{B}$, ${}^{12}\text{C}$, ${}^{14}\text{N}$, ${}^{16}\text{O}$, ${}^{19}\text{F}$, ${}^{20-22}\text{Ne}$, ${}^{23}\text{Na}$, ${}^{24-26}\text{Mg}$, ${}^{27}\text{Al}$, ${}^{28-30}\text{Si}$, ${}^{31}\text{P}$, ${}^{32-34}\text{S}$, ${}^{35}\text{Cl}$, ${}^{36,38,40}\text{Ar}$, ${}^{39,41}\text{K}$ and ${}^{40,42-44,46}\text{Ca}$), with simple inputs of the mass number of daughter nuclei (Z_d), atomic number of cluster emission (Z_c), and neutron number of parent nuclei (N_p). To check the predictive power of constructed formula, the values produced by the formula are compared with that of the experiments. The process of cluster and heavy particle radioactivity of superheavy nuclei is studied using the Coulomb and Proximity potential Model (CPPM) and modified generalized liquid drop model (MGLDM). The role of the Coulomb effect, asymmetry effect, pairing effect, entrance channel parameters, and shell effect on cluster radioactivity are studied. Six different proximity functions and various mass excess values were used in the evaluation of cluster decay half-lives.

A detailed investigation of different decay modes such as alpha-decay, beta-decay, and cluster-decay including the heavy particle emission ($Z_c > 28$) and spontaneous fission leads to identifying the new cluster and beta-plus emitters in the superheavy region $104 \leq Z \leq 126$. For the first time around 21 beta-plus and seven heavy particle emitters are identified in the superheavy nuclei. The reported regions of beta-plus and heavy particle radioactivity for the superheavy nuclei are stronger than alpha-decay. The studied macroscopic models such as the modified generalized liquid drop model (MGLDM), Coulomb and proximity potential model (CPPM), and generalized liquid drop model (GLDM) were compared with the microscopic models. The detailed investigations show that among macroscopic models, MGLDM predicts cluster decay half-lives close to experiments. Whereas, among the microscopic models, the Relativistic Mean Field model (RMFM) predicts cluster decay half-lives close to the experiments. Similarly, among available semi-empirical formulae, AZF(A Zoospermia Factor) produces less deviation.

During the study of cluster radioactivity of superheavy nuclei, surprisingly it is observed that the shortest half-lives of cluster decay in all superheavy elements are observed for daughter neutron number 184 and nearly equal to that. This is clear evidence of the existence of the neutron magic number $N=184$. This study is useful in the understanding of superheavy element nuclei structure.

CHAPTER 1

Introduction

1.1 Superheavy elements

Superheavy elements (SHE) are chemical elements with an atomic number larger than 103, in the periodic table. They are beyond the actinides, and can be synthesised in a laboratory. They are named for physicists and chemists, as well as the locations where the elements are synthesised. In 1940, Flerov et al., [1] observed that, the SF of ^{238}U heavy nuclei might break into two halves. Bohr and Wheeler [2], presented liquid-drop model, depicted that a nucleus is a drop of charged liquid. A potential barrier prevents the drop from splitting when the surface tension is greater than coulomb repulsive force on protons. However, The supply of energy to the nucleus can overcome this. The liquid-drop model predicted that Plutonium, Curium, and Californium would have similar lifetimes. Many isotopes of transuranium elements were identified by researchers [3] at the JINR in Dubna.

One of the most unresolved question till date is the synthesis of superheavy nuclei $Z > 118$. More than thirty superheavy nuclei have been synthesized by cold and hot fusion reactions [4–8]. In addition to above experimental evidence, Many attempts have been repeatedly conducted in order to synthesize the superheavy element $Z > 118$ using the projectiles such as Sc, Ti, V, Cr, Mn, Fe and Co [9, 10]. Using relativistic mean field theory and self-consistent calculations [11–13] the proton magicities have been predicted for $Z=114, 120, 124$ and 126 . Consequently, many the-

oretical studies proposes suitable projectile target combinations to extend the periodic table up to $Z=126$ [14–21]. Among which, the atomic number $Z=120$, 124 and 126 are paid more attention in order to disclose the existence of magic nuclei.

The identification of the new synthesized superheavy nuclei is carried out when excited compound nuclei attains ground state through the decay modes. The transition from excited state to ground state occurs mainly by an alpha decay [22, 23]. In addition spontaneous fission [24, 25] is also observed in the superheavy region. Hence, main decay modes are identified as alpha and spontaneous fission in the superheavy region. In addition, cluster and heavy particle radioactivity [26–29] is also observed in the heavy and superheavy nuclei.

On the experimental side, the emission of heavier clusters (^{14}C , ^{20}O , ^{24}Ne , ^{28}Mg and ^{32}Si) leading to doubly magic nuclei ^{208}Pb [27, 30, 31]. The experimental confirmation of ^{24}Ne cluster from the heavy nuclei ^{232}U was attained during the year 1985 [32]. Neon cluster emissions were also successfully observed from the isotopes of uranium i.e $^{232,234,235}U$ [33]. Cluster emission of ^{23}F and ^{24}Ne from the ^{231}Pa was experimentally observed [34]. Bonetti et al., [35] experimentally studied the $^{22,24}Ne$ cluster emission from ^{230}U . The cluster radioactivity $^{28,30}Mg$, $^{32,34}Si$ was experimentally observed in the heavy nuclei ^{238}Pu and ^{242}Cm [36].

Gong et al., [37] found that Mc, Rg, Mt, Ds, Lv, Og and Ts, were classified as metals, whereas Fl and Nh are classified as metalloids. In the last few decades, spectacular advances in relativistic quantum theory and computational algorithms [38] enabled precise computations of properties of SHEs and their compounds. The majority of the works, especially those relating to experimental studies, and the importance of relativistic effects for the strongest elements is explained, in the range $108 \leq Z \leq 120$ and $166 \leq Z \leq 182$. Bürvenich et al., [39] explore the systematics of fission barriers(SFB) in SHE. The life times of recently created isotopes of SHE with $Z=112$, 114, 116, and 118, as well as certain decay products, are theoretically computed [40] using microscopic

nuclear interaction potentials within the WKB approximation.

The inability of complete fusion reactions to synthesis of SHE is understood [41] in terms of the superheavy precursors generated in these reactions having poor survival probabilities or the failure to achieve complete fusion. In light of these findings, more attempts to synthesis these elements utilising full fusion, deep inelastic transfer processes. The brief overviews of theoretical [42] and experimental measurements of fundamental features such as SF $T_{1/2}$, fission barriers(FB) and total kinetic energy released during fission were given special attention.

For SHE evaporation residue cross sections have been investigated [43] and found to be maximum at a given initial temperature. Using Multiconfiguration Dirac-Fock (MDF) approach, Indelicato et al., [44] examined the effects of incorporating Breit interaction into the self-consistent field process on all orders are demonstrated. Brodziński and Skalski [45] use the macroscopic-microscopic, Woods-Saxon and Skyrme SLy6 Hartree-Fock plus and BCS models to investigate energy landscapes for chosen SH even-even system with $Z=128$ to 148 . The current state of research on the synthesis and characteristics of SHE were [46] examined. Theoretical examination of relativistic impacts on the characteristics of these components receives special emphasis. The excitation energy, ionisation potentials and polarizabilities of the SHE rutherfordium, lawrencium and nobelium are calculated [47] using all order single double and coupled cluster technique. The production cross sections [48] in hot fusion reactions of SHN are thoroughly examined. The SHE $Z=110$, $Z=111$, and $Z= 112$ their EDT (electric dipole transition) rates and isotopic shifts are determined. All the three elements and their subsequent ionisation potentials are computed and compared to lighter comparable elements. The currently studied elements are reviewed [49] through many theoretical investigations.

To comprehend the static and dynamic features of the atomic nucleus, various models and hypotheses have been developed. The nucleus is thought to have energy that comes from sur-

face tension and coulomb repulsion of the protons. Cluster radioactivity shown by superheavy nuclei leads to the production of a doubly magic ^{208}Pb daughter nucleus. CR is an intermediate between α -decay and SF. Hence, it becomes an important to establish a relation for decay energies in heavy and superheavy region. Prediction of $T_{1/2}$ and its decay energies will identify the existence of SHN. Detail investigations also enables us to examine the possible isotopes and its shell structure in the superheavy region $104 \leq Z \leq 126$. There are many theoretical microscopic and macroscopic models whose predictive power to predict cluster radioactivity $T_{1/2}$ is also important.

1.2 Decay of superheavy elements

The most common types of radiation are alpha, beta, and gamma radiations, but there are several other modes in which a radioactive nucleus can decay. Other modes of decay that a nucleus may undergo proton emission, neutron emission, cluster decay, spontaneous fission, positron emission, electron capture, double beta decay, isomeric transitions, internal conversion, and so on. The most common decay modes of heavy and SHN, α decay, cluster decay, and SF, have been discussed in detail in the sections below.

1.2.1 Alpha decay

Rutherford's discovery of alpha decay in the 1920s [50], was addressed by quantum mechanics. Becquerel [51] observed α decay for the first time in 1896 as an unknown radiation from the radioactive uranium nucleus. α decay is thought to be an asymmetric fission process with varying charge densities. A simple empirical relation for predicting the alpha half lives [52] has been successfully derived. The formula for describing [53] $T_{1/2}$ values for heavy and SHN is proposed. α -decay of even nuclei is reviewed and evaluated [54] across the periodic table. In even-even

nucleids, an empirical relation for predicting the half-life of the favoured transition [52] has been successfully obtained. Poenaru et al., [55] proposed a semi-empirical formula for α decay.

Akrawy, et al., [56] calculated the α decay $T_{1/2}$ in the SH region $106 \leq Z \leq 118$ using UDL, MGD and CPPM. Santhosh and Priyanka [57] calculated half-lives for deformed nuclei using the recently proposed CPPMDN model. Based on several observed transitions [58], a level scheme for ^{210}At is proposed.

1.2.2 Spontaneous fission

A semi-empirical WKB framework, the SF process for even nuclei of $Z \geq 92$ is investigated. The role of quadrupole and hexadecapole distortion parameters were included to evaluate alpha decay half-lives [59] for SHN of Z close to 114 and N towards 184. Estimation of SF $T_{1/2}$ shows a relative stability near closed-shell nucleon numbers. Xu and Ren [60] proposed SF half-lives for heavy elements with $Z \geq 90$.

The super fluid model of nuclei is used [61] to analyse spontaneous fission $T_{1/2}$. The effect of pair correlation on parameters determining potential barrier penetrability for fission is investigated. The difference in the spontaneous fission period for even and odd-mass nuclei is explained. The empirical Swiatecki formula is supported for even nuclei, Previous correlations of spontaneous fission $T_{1/2}$ vs Z^2/A predict that even-even isotopes $T_{1/2}$ increase with A . A deviation from the above correlation is discussed, and it is demonstrated [62] that the spontaneous fission $T_{1/2}$ of even-even isotopes reach a maximum as A increases.

The shorter spontaneous fission $T_{1/2}$ beyond the maximum may be due to the greater deformations of the larger- A nuclides. Some observations are made about fission thresholds, because of the dramatic changes in properties observed in the region of the heavy fermium isotopes and for still heavier elements, the spontaneous fission (SF) of the heaviest actinides and transactinides

is of particular interest. Existing experimental data on SF properties, such as half-life systematics, fragment kinetic energy and mass yield distributions, prompt neutron emission, and gamma emission, will be reviewed. The potential for extending studies of SF properties to other regions is discussed, the potential for obtaining additional information about low-energy fission properties. Swiatecki's work on the correlation of spontaneous fission $T_{1/2}$ has been modified [63] and expanded to include elements with Z greater than 100. On these bases, the values of spontaneous fission $T_{1/2}$ predicted are unexpectedly high. The partial half-life of $Z=106$, $A=271$ is predicted to be around 13 years.

1.2.3 Cluster radioactivity

cluster radioactivity(CD) is an asymmetric fission process which is an intermediate between spontaneous fission and α -decay. Before 1980's the radioactive disintegration was experimentally observed either by α -decay or spontaneous fission. Later the concept of cluster radioactivity phenomenon in the heavy and superheavy nuclei was first suggested by Sandulescu et al., [64]. Rose and Jones [30] experimentally observed cluster radioactivity in 1984 and later Aleksandrov et al.,[65] found ^{14}C cluster emission from ^{223}Ra . Later on, cluster emission such as ^{20}O , ^{23}F , $^{22,24,26}\text{Ne}$, $^{28,30}\text{Mg}$ and $^{32,34}\text{Si}$ were experimentally observed [66, 67]. The cluster ^{34}Si emission was experimentally observed [68, 69] in heavy nuclei ^{242}Cm and ^{238}U .

Several theoretical models such as preformed cluster model (PCM) by Gupta et al., [70], superasymmetric fission model by Poenaru et al., [71] explains the cluster radioactivity. There are also several theoretical models [72–76] were successfully predicts the cluster radioactivity in the heavy and superheavy nuclei. Microscopic measurements for the formation of cluster probability and barrier penetrability [75, 76] have been made by using R matrix description of the process.

Within the microscopic model Warda et al., [77] investigated cluster radioactivity in the super-heavy element $Z=116$. In all these different models a collection of various proximity potentials is a benchmark to evaluate the half-lives.

Zhang et al., [78] studied large cluster radioactivity in even-even nuclei by using fourteen proximity potential functions. The results indicate that with experimental data, the effects of proximity potential such as Bass 77 and Denisov potentials are more appropriate. Raj Kumar [79] investigated cluster radioactivity by using different proximity potential functions. Santhosh et al., [80] analysed cluster radioactivity half-lives in the superheavy nuclei $^{280-314}116$ by studying Coulomb and proximity potentials. By using the folding density dependent M3Y effective interaction method, Routray et al., [81] investigated cluster radioactivity in heavy nuclei. Within the density-dependent cluster model, Ismail et al., [82, 83] studied cluster radioactivity half-lives in the superheavy element $Z=121$ and 122 . The shorter half-lives were theoretically observed during cluster emissions of ^{14}C , ^{20}O , ^{20}Ne , and ^{24}Ne cluster emissions from heavy and superheavy nuclei. The role of deformation parameter and the orientation of different nuclei during the cluster radioactivity leading to doubly magic nuclei ^{208}Pb were studied by Arun and Gupta [84]. Kuklin et al., [85] examined cluster radioactivity by using dinuclear system concept in the actinide region. Iriondo et al., [86] studied cluster radioactivity by using Gamow potential model for formation and then penetration probability of the particle through the Coulomb barrier. The earlier researcher's [87, 87–94, 94–98] were extensively studied cluster radioactivity in heavy and superheavy region.

Using super asymmetric fission model Poenaru et al., [99] predicted the cluster emission (^{12}C , ^{16}O , $^{30,32}\text{Si}$, $^{48,50}\text{Ca}$, and ^{68}Ni) half-lives of $T > 10^{40}\text{s}$. The two-step process such as cluster formation and quantum-mechanical fragmentation was successfully explained in the heavy region [100]. Many theoretical models such as Yukawa plus exponential model (CYEM) [101], preformed cluster model (PCM) [102], mean-field HartreeFock-Bogoliubov theory [103], Coulomb

and proximity potential model (CPPM) [104, 105], double-folded model with the renormalized M3Y interaction (RM3Y) [106], microscopic density dependent cluster model (DDCM) [107], Generalised liquid drop model [108] and effective liquid drop model [109]. All the above models predict the cluster decay half-lives, microscopic understanding of cluster decay and nuclear structure information. Among the different decay models the generalized liquid drop model which describes the process of fusion barrier [110], fission [111], cluster decay [112], investigation of charge asymmetry, deformation and proximity effects and nuclear structure parameters such as nuclear radius and mass [113, 114].

Earlier, researchers have effectively used different models such as CPPM, MGLDM, ELDM and semi-empirical relations to evaluate decay modes in the heavy and superheavy nuclei [87, 88, 92, 94, 94, 96, 115–117, 117–119]. The goal of this contribution is to study the range of isotopes in the superheavy nuclei $Z=126$ using different proximity potentials within the modified generalised liquid drop model (MGLDM). These different versions of the proximity potentials involves different parameters and the proximity function $\phi(S_0)$. Hence, the systematic behaviors of different proximity potentials in the heavy particle radioactivity were important in order to explore the nuclear structure. By using the method of extrapolation towards the superheavy nuclei $Z=126$ and comparison of proximity potential function with that of available experiments increases the predictive power of the model during heavy particle radioactivity half-lives.

The existence of greater stability in the realm of unknown SHE is anticipated by [120] nuclear theory. The values of the pre-formation factors were obtained [121] from experimental cluster decay $T_{1/2}$ using the preformed cluster model technique, assuming that the heavy ion emission decay constant is the function of the assault frequency, pre-formation factor and penetrability. In some SHN, cluster radioactivity, which is well known in light actinides, could become the dominating decay route. Warda et al., [77] observed a distinct fission fragment mass distribution, with the

heaviest fragment around ^{208}Pb . The unified description formula (UD), universal curve (UNIV), Horoi formula, and universal decay law (UDL) were used [122] to investigate the cluster radioactivity of $^{294}118$, $^{296}120$, and $^{298}122$. The competition between α -decay and CR for $Z=104-124$ is investigated. Poenaru et al., [74] altered the idea of CR to emitted particles with $Ze > 28$ from $Z > 110$ parent nuclei. To calculate Q values, a table of measured masses and theoretical values are used. In the superheavy region, [123] the probability of decay and heavy-cluster decay are studied. A new formula is used to calculate the pre-formation probability for the cluster emissions, which are based on the decay of Q values. CR and α -decay of several SHN in the atomic number range $Z = 119 - 126$, they may be synthesised in future, were also examined [124]. The half lives against CR are calculated by two models such as ASAFM (Analytical Super Asymmetric Fission model) and UNIV. The decay $T_{1/2}$ are calculated using four different models such as ASAF, UNIV, semi-empirical formula based on Fission Theory (semFIS), and AKRA. The Q-values are determined by the WS4 atomic masses. Xiao Jun Bao et al., [125] Starting with the alpha-like R-matrix theory, a recently proposed UDL for α -decay and CR $T_{1/2}$ was introduced. The mass and charge numbers of the charged particle, as well as the Q value.

The stability of the nucleus is well defined by its magicity of protons or neutrons. Shell closure effects were studied using cluster decay in ^{218}U [126]. Gupta et al., [127] have shown stability of atom is either due to magicity of neutrons or protons.

From the literature it is observed that all these investigations gives incomplete information of cluster radioactivity in the superheavy nuclei region $Z=104-126$. Hence in the present work we have analysed cluster radioactivity in the superheavy region of wide range from $Z=104-126$ using modified generalised liquid drop model (MGLDM). The half-lives of different cluster emissions such as ^4He , ^6Li , ^9Be , ^{20}Ne , ^{23}Na , ^{24}Mg , ^{27}Al , ^{28}Si , ^{31}P , ^{32}S , ^{35}Cl , ^{36}Ar , ^{39}K and ^{40}Ca were evaluated in the superheavy region $Z=104-126$ using Ng80 [128] which produces the less deviation when

compared to other proximity functions as mentioned in the earlier work [87].

1.2.4 Heavy particle radioactivity

The process of emitted particles with $Z_e > 28$ from parents with $Z > 110$ and daughter around ^{208}Pb is termed as heavy-particle radioactivity (HPR). This phenomenon was experimentally confirmed [30, 68] in heavy parent nuclei with $Z = 87 - 96$ by measuring half-lives during the emission of ^{14}C , ^{20}O , ^{23}F , $^{22,24-26}\text{Ne}$, $^{28,30}\text{Mg}$, $^{32,34}\text{S}$. The concept of HPR was changed [129] by studying the cluster emission of atomic number $Z_e \geq 28$. The Heavy particle radioactivity with cluster emission of atomic number $Z_e^{max} = Z - 28$ allowing to get daughter of doubly magic nuclei ^{208}Pb from parent nuclei with $Z > 110$.

It is also predicted [130] that superheavy element $Z=122$ with $A=292$ might belong to a new class of long-lived high spin super- and hyperdeformed isomeric states. The relativistic mean-field (RMF) and nonrelativistic Skyrme Hartree-Fock (SHF) formalisms [131] predicts that the superheavy element $Z = 122$ with $A = 290$ is highly oblate to a large prolate shape, which may be considered as the superdeformed and hyperdeformed structure. The Coulomb and proximity potential model (CPPM) [132] predicts that SHN with $Z = 122$ with $A = 295 - 307$ having measurable alpha decay half-lives. In addition to this many theories predicts the possible isotopes for $Z = 122$ [82, 91, 92, 133–135]. Previous researchers predicted the projectile-target combinations using various models such as statistical model [91, 136, 137], dynamical cluster-decay model (DCM) [138, 138–140], dinuclear system model (DNS) [141–143, 143]. Some phenomenological models such as density-dependent cluster model [60, 82], coulomb and proximity potential model [144] modified generalized liquid drop model (MGLDM) [145] analytical superasymmetric fission model [146] are used in the study of cluster radioactivity of superheavy nuclei.

The original Generalized Liquid Drop Model (GLDM) was proposed by Royer et al., [108, 147]. Later, it is modified by including the different proximity potentials, pre-formation factor with iso-spin parameter, size of cluster and daughter nucleus and the modified pre-formation factor which is termed as modified liquid drop model (MGLDM) [97, 145, 148]. The theory which is based on the super asymmetric fission model used to study the α -decay, proton emission, cluster radioactivity and cold fission is referred as the effective liquid drop model (ELDM) and it was proposed by Goncalves and Duarte[149]. This model is also experimentally validated by many experiments [149–155]. The effective liquid drop model (ELDM) was proposed by Goncalves and Duarte[149] which is super asymmetric fission model to study α -decay, proton emission, cluster radioactivity and cold fission in a unified framework. This model is validated by many experiments[149–155]. In the Coulomb and proximity potential model (CPPM), for separated fragments, from touching configuration on-wards total potential is taken as the sum of the coulomb potential and canonical proximity potential [104, 156, 157]. Studies on the decay properties from previous researchers [90, 117, 145, 158–166]. Using preformed cluster model (PCM) [29, 167, 168] researchers have theoretically studied heavy particle radioactivity, spontaneous fission, binary and ternary fission in heavy and superheavy nuclei. Several theoretical investigations [169, 170] anticipated the island of stability around the atomic numbers $Z=114, 120, 122$ and 126 with neutron number of $N=184$. Since, in near future the experimental synthesis and decay of compound nuclei of superheavy elements from $Z=119$ to 126 is expected. The analysis of radioactivity in the transactinide elements with $Z \geq 104$ allows for a better provides an opportunity in understanding of a matter's structure and properties. The cold fusion reactions with lead and bismuth as a target and hot fusion reactions with a ^{48}Ca projectile on an actinide target are used to synthesize the superheavy element. [9, 171–180]. By the cold and hot fusion reactions, the formed compound nuclei achieve a stable state by many decay methods such as α -decay, cluster-decay,

β -decay and spontaneous fission. However, in the superheavy region the formed nuclei decay mainly through an α -decay followed by the spontaneous fission and in few cases mainly by the spontaneous fission. The possibility of the heavy particle radioactivity (HPR) was also predicted in the superheavy nuclei [129, 181].

Many theoretical models such as cluster model [182], multi-channel cluster model[183], the density dependent M3Y (DDM3Y) effective interaction[184, 185],generalized liquid drop model (GLDM) [186], coulomb and proximity potential model (CPPM) [187], generalized density depended cluster model[188], unified model for α -decay and α -capture (UMADAC) [189] were involved in order to evaluate the α decay half-lives. The method of QRPA (quasiparticle random phase approximation) were used to evaluate the β -decay half-lives [190]. The beta decay half-lives are evaluated using the widely accepted models [191–193]

The spontaneous fission half-lives were first predicted by Bohr and Wheeler [194] and later on experimentally confirmed by the Flerov and Petrzak [1]. During the year 1955 Swiatecki [195] evaluated the spontaneous fission half-lives using the fissility parameter Z^2/A in a liquid drop model. Previous researchers [196–198] studied spontaneous fission half-lives using shell correction in a modified liquid drop model. Furthermore, cluster-decay is an intermediate between an alpha decay and spontaneous fission [64] and experimentally confirmed during the year 1984 [30]. Cluster-decay such as ^{14}C , $^{16,18}\text{O}$, $^{22,24,26}\text{Ne}$, ^{23}F , $^{28,30}\text{Mg}$, ^{34}Si and so on were experimentally observed from the parent nuclei ^{221}Fr to ^{242}Cm [199]. The cluster decay half-lives are evaluated using the various models such as Super-asymmetric fission model (SAFM) [71, 200] unified fission model [201, 202] preformation cluster model (PCM) [70, 203]. The cluster decay half-lives are also evaluated using semi-microscopic methods [204–206]. Earlier researchers were studied different decay modes using the different models and semi-empirical relations to evaluate the half-lives [87–98, 145, 207].

The different models such as CPPM, MGLDM, ELDM, and different proximity potentials and semi-empirical relations are used to evaluate different decay modes in the heavy and superheavy nuclei [87, 88, 92, 94, 94, 96, 115–117, 117–119] of various Z . In literature there is no systematic study with respect to the atomic number range from $104 \leq Z \leq 126$ for cluster and heavy particle emission in the SH region. The present work is an attempt to test the possibility of cluster emission and heavy particle emission in the SHN region $104 \leq Z \leq 126$.

1.3 Objectives

By studying detail literature survey, to study the CR and HPR, the following objectives are framed

- To Construct semi-empirical formula for decay energies and $T_{1/2}$ in case of heavy and super heavy nuclei.
- Application of well-established theoretical models such as CPPM and MGLDM to study the cluster radioactivity in the heavy and super heavy nuclei.
- Study of heavy particle radioactivity using theoretical models such as CPPM and MGLDM in the heavy and super heavy nuclei.
- To study competition between different decay modes such as spontaneous fission, cluster radioactivity, α -decay, and heavy particle radioactivity.
- Study of shell structure (Search for magic number) using cluster radioactivity.
- Study of the predictive power of microscopic and macroscopic models in cluster radioactivity.

CHAPTER 2

Semi empirical formula for decay energy and half-lives of cluster radioactivity

2.1 Introduction

There are many models for the study of α decay and CR, such as nuclear interaction potentials and semi empirical models(SEM), and these are considered effective methods for studying α decay and cluster decay(CD) half-lives. The cluster and α decay [30, 208] were discovered at the end of the twentieth century. Poenaru et al., [74, 129] investigated the competition between cluster and α decay. Geiger and Nuttal [209] proposed an empirical relationship and systematically observed variation in α decay half-lives. Gamow [210] used the quantum tunnelling effect to explain α decay half-lives. Viola and Seaborg [211] developed a semi empirical relationship for α decay half-lives. Royer [212] developed an empirical formula for α decay half-lives based on a liquid drop model that takes proximity into account. Brown [213] developed an empirical formula based on the experimental variation of logarithmic half-lives. Horoi et al., [214] proposed a scaling law for the decay time of an α particle, which is generalised for CD. Poenaru et al., [215] proposed the SemFIS formula for SHN α decay half-lives, taking into account magic numbers of nucleons, the analytical super asymmetric fission model, and universal curves. Sobiczewski and Parkhomenko [198] proposed a formula for heavy and SHN for α decay half lives. Poenaru et al., [216] presented a single universal curve for α decay as well as CR. Wang et al., [154] used

recent NUBASE2012 data to evaluate α decay half-lives while taking ground state spin and parity of parent and daughter into account, using the WKB barrier penetration probability Ni et al., [217] developed a semi-empirical formula for α decay half-lives and CD half-lives. Previous studies [154, 218] looked into the α decay energies and half-lives of SHE. Mirea et al., [219] investigated the half-lives of various decay modes in ^{222}Ra . Brown [213] proposed an empirical relationship for α decay half-lives in SHN. Sobiczewski et al., [220] investigated α decay and SF. Akrawy et al., [221] studied α decay half-lives in the SH region using various relationships. Previous workers [154, 215, 222–225] presented an empirical formula for α decay half lives in heavy nuclei.

Sobiczewski and Pomorski [198] investigated the properties of SHN. Dong et al., [226] investigated the α decay half lives of heavy nuclei. Previous studies [227] used a multichannel cluster model to calculate the α decay half-lives of deformed nuclei. Gurvitz and Kalbermann [228] investigated decay width and energy shift in a metastable state. Sun et al., [229] investigated the α decay half-lives in heavy and SHN. Greiner et al., [200] investigated CD in ^{223}Ra . Poenaru et al., [230] investigated shell effects and α decay half-lives in SHN. Previous researchers [88, 91, 92, 116] investigated and compared the half lives of SF, ternary fission, and CD of this predicted nuclei for $Z=122, 124, \text{ and } 126$. By studying the fusion barrier characteristics of 14054 projectile target combinations. An empirical formula developed for fusion barrier heights, positions, and curvature of the inverted parabola of SHN with atomic numbers $104 \leq Z \leq 136$. Experiments [231] are used to compare the values produced by the current formula with the simple inputs of mass number (A) and atomic number (Z). Previous researchers [224] developed a semi-empirical formula for the α decay half lives of heavy and SHN and parameterized the fusion-fission cross section [232] for heavy and SHN.

The nuclear masses are the very important quantities in the nuclear physics. A large number of precise experimental data on the mass excess values have been collected by means of mass

spectroscopy and the reaction Q-values. The knowledge about the Q-values have been further extended by the complete information on the binding energies. There were many remarkable successful formula such as Weizsacker-Bethe [233, 234] mass formula. These mass formulas are not only useful for practical purpose but also give link between empirical and pure theories. Previous workers [191, 235] studied the ground state properties within the Finite Liquid Droplet Model (FRDM). Audi et al., [236] and Goriely et al., [237] were studied the ground state properties of the nuclei within the Hartree Fock Bogoliubov (HFB) method. The experimental mass excess values were also included along with the FRDM and HFB-14. Audi et al., [238] presented the nuclear decay properties in the ground and isomeric states from the NUBASE evaluation. Manjunatha et al., [158, 239] proposed semi-empirical formula for mass excess of nuclei in the atomic number range $57 \leq Z \leq 126$. The studied mass excess values using the semi-empirical formula were compared with the theoretical models such as FRDM and HFB. The proposed semi empirical formula successfully reproduces the mass excess values in agreement with the available values.

Previous researchers [239] also proposed a semi empirical formula for an α and CR, which exactly reproduce the experimental values. The experimental α decay half-lives of heavy nuclei were compared with the generalized liquid drop model(GLDM) and Viola-Seaborg-Sobiczewski formula by Royer and Zhang [240, 241] using the amount of energy released during α decay. Negra et al., [242] studied the β decay characteristics in case of neutron deficient isotopes such as Sr, Y and Zr and also deduced the mass excess values using Q_β measurements. Borrel et al., [243] studied the β decayed two proton and mass excess values in the nuclei ^{31}Ar and ^{27}S . Mayer et al., [244] investigated the mass excess values and the excited states of neutron-rich nuclei $^{33-35}\text{Si}$, $^{35-36}\text{P}$ and $^{37-38}\text{S}$ from the study of ^{14}C and ^{18}O induced reactions on ^{36}S . David [217] studied the mass excess values near the neutron rich isotopes of iron. Scheerer et al., [245] measured Q value of the reaction of $^{144}\text{Sm} (^3\text{He}, d)^{145}\text{Eu}$ and also evaluated the mass excess of ^{145}Eu . Pre-

vious researchers [246, 247] experimentally measured the Q-values for the $^{40,42,51}\text{Ca}$ and hence determined the mass excess values. Earlier researchers [88, 90–92, 94, 137, 248, 249] were extensively used the mass excess values and studied the Q-values of the reaction in heavy and SHN region. Manjunatha et al., [231, 232, 250] parameterized the fusion and fission cross sections, fusion barrier and barrier positions in case of heavy and SHN. From the detail study it has been observed that there are many semi-empirical formulas for α and CD half-lives, α decay energy, mass excess values fusion and fission cross sections and fusion barriers. But there is no simple empirical formula to obtain the Q-values in case of cluster and an α decay. Hence, in the present work is an attempt to parameterize decay energies during an α and CD in the atomic number range $103 \leq Z \leq 126$.

2.2 Theory

2.2.1 Semi-empirical formula for decay energies of cluster radioactivity

To derive the empirical formula for decay energy (Q) during the cluster emissions (^4He , ^6Li , ^9Be , $^{20,22}\text{Ne}$, ^{23}Na , $^{24-26}\text{Mg}$, ^{27}Al , $^{28-30}\text{Si}$, $^{32-34}\text{S}$, ^{35}Cl , $^{36,38,40}\text{Ar}$, $^{39,41}\text{K}$ and $^{40,42-44,46}\text{Ca}$), it is assumed that decay energy is directly proportional to the mass number of daughter nuclei (A_d) and inversely proportional to atomic number of cluster (Z_c). The figure 2.1 shows the variation of Q-values with the mass number of daughter nuclei (A_d) and atomic number of cluster nuclei (Z_c). The Geiger and Nuttall law (GNL) [209] and universal decay law (UDL) [76] relates the Q-values during cluster emission depends on the daughter nucleus and emitted cluster nucleus. The microscopic and macroscopic approach [191, 196, 251–253] were extensively used in the calculation of decay energy of α particle in the heavy and SH region. Furthermore, some of the formulae [226, 254–257] are based on the ideology of liquid drop model and shell-models assumed that decay energy is a function of atomic mass and neutron number.

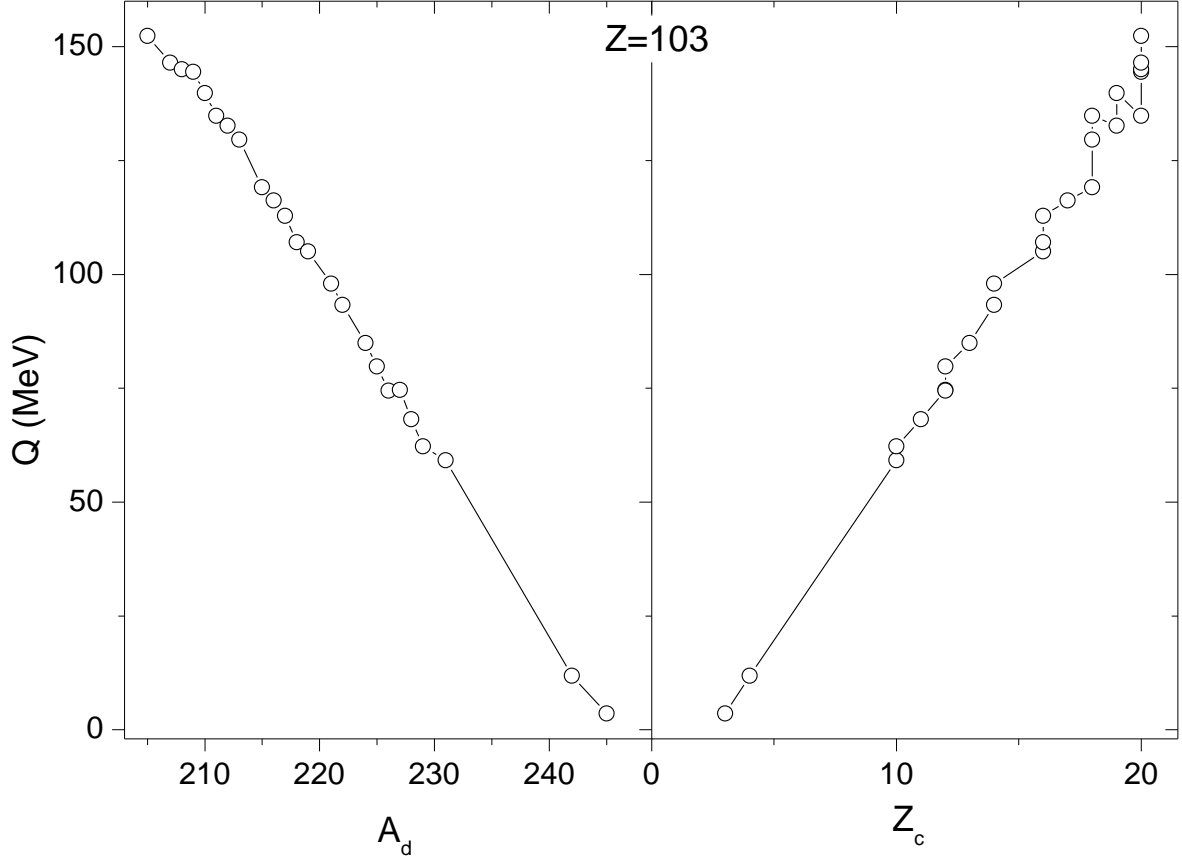


Fig. 2.1 The variation of Q-values with the mass number of daughter nuclei and atomic number of cluster nuclei.

$$Q_{\alpha} = f(A, N, Z) \quad (2.1)$$

For an instance, Perlmann and Rasmussen [254] proposed the Q-value formula in the SH region for the α decay in terms of standard recoil energy and electron shielding corrections and it is as follows;

$$Q_{\alpha} = \frac{A}{A-4} E_{\alpha} [6.53(Z-2)^{7/5} - 8.0(Z-2)^{2/5}] \times 10^{-5} \text{ MeV} \quad (2.2)$$

Where A and Z are the mass number and atomic number of the parent nucleus. Babu and Kumar [255] removed the discrepancy between the Q_{α} and the experimental Q_{α} by including the $\ln 2$

function in the equation 2.2 and it is as follows;

$$Q_\alpha = \frac{A}{A-4} E_\alpha [6.53(Z-2)^{7/5} - 8.0(Z-2)^{2/5}] \times 10^{-5} - \ln 2 \text{ MeV} \quad (2.3)$$

The above defined relations are applicable in the SH region with atomic number range. $110 \leq Z \leq 128$. Later on, Dong et al., [226] proposed an α decay energy in the heavy and SH region ($Z \geq 98$ and $N \geq 140$) and it is given as follows;

$$Q_\alpha = B_\alpha + [a_v(A-4)^2 - a_v A] + [a_s A^{2/3} - a_s^{2/3(A-4)}] + [-a_c(Z-2)^2(A-4)^{-1/3} + a_c Z^2 A^{-1/3}] \quad (2.4)$$

$$\begin{aligned} &+ \left[-a_a \left(\frac{N-Z}{2} \right)^2 (A-4)^{-1} + a_a \left(\frac{N-Z}{2} \right) A^{-1} \right] + [a_p \delta (A-4)^{-1/2} - a_p \delta A^{-1/2}] \\ &+ \left[a_6 \frac{|A-256|}{A-4} - a_6 \frac{|A-252|}{A} \right] + \left[a_7 \frac{|N-254|}{N-2} + a_7 \frac{|N-252|}{N} \right] \\ &+ \left[a_8 \frac{|N-Z-50|}{A-4} - a_8 \frac{|N-Z-50|}{A} \right] \end{aligned}$$

Here $a_s, a_c, a_a, a_p, a_6, a_7$ and a_8 are the fitting parameters [256]. Eventually, Dong et al., [226] simplified and proposed five-parameter Q-value formula by considering liquid drop model.

$$\begin{aligned} Q_\alpha^{Th}(\text{MeV})_\alpha = & \alpha Z A^{-4/3} (3A - Z) + \beta \left(\frac{N-A}{A} \right)^2 + \gamma \left[\frac{|N-252|}{N} + a_7 - \frac{|N-254|}{N-2} \right] \quad (2.5) \\ & + \delta \left[\frac{|Z-110|}{Z} - \frac{|Z-112|}{Z-2} \right] + \epsilon \end{aligned}$$

Further simplified formula was also given by Dong et al., [257] for the SHEs $Z \geq 110$ using liquid drop model by neglecting the effect of shell energy.

$$Q_\alpha(\text{MeV}) = \alpha Z A^{-4/3} (3A - Z) + b \left(\frac{N-Z}{A} \right)^2 + e \quad (2.6)$$

Where a, b and e are fitting parameters [257]. The first two terms include the Coulomb energy and symmetry energy respectively. The above set of equations (2.2-2.6) were defined by the previous researchers to predict the decay energies of an α by using atomic number (Z), mass number (A) and neutron number (N) of parent nucleus, atomic number of daughter nuclei ($Z_d = Z - 2$). The survey reveals that there is no empirical formula available for the prediction of the decay energies during the cluster emission. Hence, in the present work constructed empirical formula for decay energies of cluster emission by assuming the fact that decay energy is a function of mass number of the daughter nucleus, atomic number of the cluster nucleus and neutron number of the parent nucleus.

$$Q_\alpha = f(A_d, N_c, Z_p) \quad (2.7)$$

In the above function, the parent nuclei information is obtained from the neutron number (N_p), the cluster emission information is availed from the (Z_c) and daughter nuclei information is considered from (A_d).

$$Q_\alpha = f(A_d/Z_c) \quad (2.8)$$

The function $f(A_d/Z_c)$ is evaluated by studying the variation of Q-values with A_d/Z_c , and is presented in figure 2.2. This figure shows the variation of Q-values as a function of A_d/Z_c during different cluster emissions from ${}^4\text{He}$ to ${}^{46}\text{Ca}$ for the parent neutron number $Z = 148$ and 150 . This type of variation is observed for all types of studied clusters. From the figure it is observed that there is systematic variation of Q-values with the A_d/Z_c . Based on this variation, constructed the

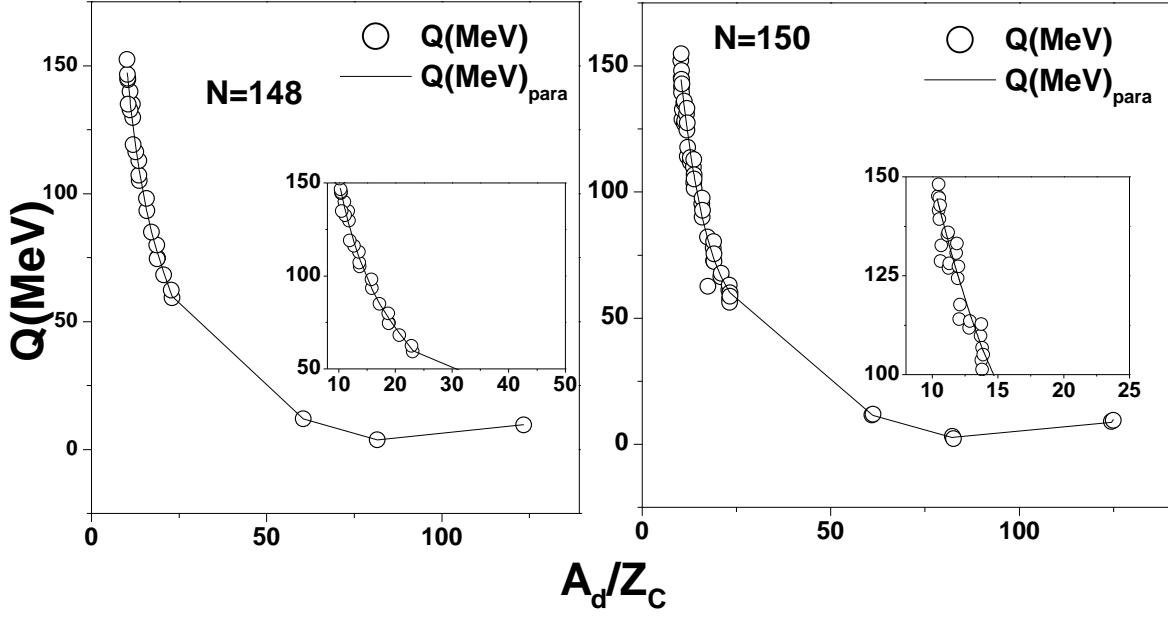


Fig. 2.2 The variation of Q-values as a function of during different cluster emissions such as ${}^4\text{He}$ to ${}^{46}\text{Ca}$ for the neutron number = 148 and 150.

function for Q-values in terms of A_d/Z_c and it is given as follows;

$$Q = \sum_{i=1}^6 a_i(N) (A_d/Z_c)^i \quad (2.9)$$

Here $a_6(N)$ to $a_0(Z)$ were the fitting constants and these constants were evaluated by studying the variation of $a_i(N)$ with neutron number (N). In the present formulae the sixth power of the polynomial function such that it has small co-efficient of determination and residual sum of powers nearly equal to unity, which produces the Q-values more accurately. In the above equation $a_i(N)$ is considered as function of neutron number. By this the complete information for the decay process is considered while proposing the semi-empirical formulae for the Q-values. The detail studies of fitting parameters $a_i(N)$ with neutron number enable us to construct the following function;

$$a_i = \sum_{j=0}^2 a_{ij} N^j \quad (2.10)$$

Final expression for decay energy (Q) is obtained by substituting the equation (2.10) in equation (2.8);

$$Q = \left\{ \sum_{i=0}^6 \sum_{j=0}^2 a_{ij} N^j \left(\frac{A_d}{Z_C} \right)^i \right\} \quad (2.11)$$

The above equation produces the decay energies of SHN during the emission of different clusters such as ^4He , ^6Li , ^9Be , $^{20,22}\text{Ne}$, ^{23}Na , $^{24-26}\text{Mg}$, ^{27}Al , $^{28-30}\text{Si}$, $^{32-34}\text{S}$, ^{35}Cl , $^{36,38,40}\text{Ar}$, $^{39,41}\text{K}$ and $^{40,42-44,46}\text{Ca}$. The values of fitting parameters for even parent neutron number are given in the table 2.1. Although the proposed semi-empirical formulae is in the sixth order, but the simple input of A_d , Z_C and neutron number of parent nuclei produces the Q-values more accurately and precisely without the knowledge of mass excess values.

2.2.2 Semi-empirical formula for cluster decay half lives

The cluster decay half lives are evaluated using formalism explained below.

The potential $V(R)$ is considered as the sum of the Coulomb, the nuclear and the centrifugal potentials

$$V(R) = V_c(R) + V_N(R) + V_{cf}(R) \quad (2.12)$$

Coulomb potential is written as

$$V_c(R) = Z_1 Z_2 e^2 \begin{cases} \frac{1}{R} & \text{for } (R > R_c) \\ \frac{1}{2R_c} \left[3 - \left(\frac{R}{R_c} \right) \right] & \text{for } (R < R_c) \end{cases} \quad (2.13)$$

In above equation, Z_1 and Z_2 are the atomic numbers of the daughter and emitted alpha/ cluster respectively. The radial distance is obtained using the equation $R_c = 1.24(R_e + R_d)$.

Table 2.1 Fitting parameters for present formula defined in equation 2.4 for even parent neutron number.

N_p	a_{62}	a_{61}	a_{60}	a_{52}	a_{51}	a_{50}
148-152	5.847718707E-09	-1.766676560E-06	1.334346597E-04	-1.812370062E-06	5.475851439E-04	-4.136238721E-02
154-158	5.912525308E-11	-1.878646742E-08	1.495389196E-06	-2.401845174E-08	7.635230728E-06	-6.082073466E-04
160-164	9.418879041E-11	-3.064941013E-08	2.495873156E-06	-4.177148343E-08	1.359261030E-05	-1.106944522E-03
166-170	-1.112380457E-10	3.766826569E-08	-3.184435911E-06	4.900664364E-08	-1.662274279E-05	1.407444919E-03
172-176	7.653701093E-12	-3.047609801E-09	3.013214213E-07	-2.433934491E-09	1.030792088E-06	-1.070339171E-04
178-182	-3.623620934E-12	1.388448821E-09	-1.311978445E-07	2.666310035E-09	-1.003426922E-06	9.354381984E-05
184-188	-4.341816698E-11	1.610594947E-08	-1.492032491E-06	2.230833397E-08	-8.277984019E-06	7.670884789E-04
190-194	8.310606371E-11	-3.206394882E-08	3.093538238E-06	-5.302429919E-08	2.042396389E-05	-1.967180004E-03
196-200	4.019136011E-05	-1.593646000E-02	1.579554871E+00	-5.351532684E-03	2.121960843E+00	-2.103198462E+02
202-206	4.814175881E-06	-1.985825316E-03	2.046392943E-01	-6.603989113E-04	2.723525779E-01	-2.806010781E+01
208-212	3.428784319E-05	-1.437743115E-02	1.507158973E+00	-4.510174598E-03	1.891006832E+00	-1.982122279E+02
N_p	a_{42}	a_{41}	a_{40}	a_{32}	a_{31}	a_{30}
148-152	2.038492841E-04	-6.159855413E-02	4.653669178E+00	-1.034146920E-02	3.125672492E+00	-2.362090773E+02
154-158	3.756420434E-06	-1.194719035E-03	9.524964220E-02	-2.830616883E-04	9.007926952E-02	-7.189479330E+00
160-164	7.141266164E-06	-2.323746809E-03	1.892501379E-01	-5.893256505E-04	1.917557365E-01	-1.561816483E+01
166-170	-8.258304740E-06	2.806295788E-03	-2.380047961E-01	6.659664818E-04	-2.267593094E-01	1.926586349E+01
172-176	2.423035785E-07	-1.179932007E-04	1.345861991E-02	-2.085247871E-06	3.657718757E-03	-5.984906945E-01
178-182	-6.696151123E-07	2.496198150E-04	-2.309539200E-02	7.657912641E-05	-2.836344125E-02	2.609651811E+00
184-188	-4.421236379E-06	1.641032553E-03	-1.521007462E-01	4.230461589E-04	-1.570473753E-01	1.455703254E+01
190-194	1.252045729E-05	-4.817291665E-03	4.634633781E-01	-1.380111984E-03	5.305928820E-01	-5.100772486E+01
196-200	2.924207238E-01	-1.159492676E+02	1.149242204E+04	-8.384395965E+00	3.324551256E+03	-3.295171040E+05
202-206	3.733995244E-02	-1.539496117E+01	1.585701627E+03	-1.112244703E+00	4.584192739E+02	-4.720305333E+04
208-212	2.421927344E-01	-1.015341678E+02	1.064148258E+04	-6.787841379E+00	2.845281259E+03	-2.981666740E+05
N_p	a_{22}	a_{21}	a_{20}	a_{12}	a_{11}	a_{10}
148-152	2.410849840E-01	-7.289909917E+01	5.512240687E+03	-2.486481140E+00	7.524616662E+02	-5.696272086E+04
154-158	1.045598746E-02	-3.330628158E+00	2.663182017E+02	-1.676149576E-01	5.352502151E+01	-4.299818364E+03
160-164	2.400977868E-02	-7.811971547E+00	6.363932302E+02	-4.413342062E-01	1.436098838E+02	-1.170698612E+04
166-170	-2.625096649E-02	8.958157859E+00	-7.625148228E+02	4.624089838E-01	-1.582117071E+02	1.349279688E+04
172-176	-1.353345735E-03	3.498704829E-01	-1.865174037E+01	1.116563197E-01	-3.688772375E+01	3.005812904E+03
178-182	-4.264610445E-03	1.570896961E+00	-1.437670947E+02	1.104809197E-01	-4.048972825E+01	3.683388730E+03
184-188	-1.993375660E-02	7.399772958E+00	-6.857375675E+02	4.178312608E-01	-1.550569426E+02	1.435654616E+04
190-194	7.280682920E-02	-2.797578725E+01	2.688004656E+03	-1.660868203E+00	6.379396561E+02	-6.127831798E+04
196-200	1.329121601E+02	-5.270212142E+04	5.223663017E+06	-1.103624062E+03	4.376100930E+05	-4.337478030E+07
202-206	1.837625467E+01	-7.571137037E+03	7.793234113E+05	-1.593728046E+02	6.563730153E+04	-6.753811161E+06
208-212	1.046304833E+02	-4.385138981E+04	4.594633672E+06	-8.408028043E+02	3.523208143E+05	-3.690859840E+07
N_p	a_{02}	a_{01}	a_{00}			
148-152	9.299020413E+00	-2.817320729E+03	2.137703873E+05			
154-158	7.014099006E-01	-2.268605096E+02	1.865986458E+04			
160-164	3.150336986E+00	-1.025881256E+03	8.382030958E+04			
166-170	-3.252437223E+00	1.116598599E+03	-9.540410103E+04			
172-176	-3.032970202E+00	1.049934540E+03	-9.045768767E+04			
178-182	-1.103723007E+00	4.038214548E+02	-3.654291406E+04			
184-188	-3.170460158E+00	1.176944722E+03	-1.088101887E+05			
190-194	1.270224229E+01	-4.877486620E+03	4.685758406E+05			
196-200	3.748536102E+03	-1.486384417E+06	1.473279656E+08			
202-206	5.658595515E+02	-2.329574253E+05	2.396181655E+07			
208-212	2.752281816E+03	-1.153033566E+06	1.207647837E+08			

where R_e and R_d are respectively the radii of the emitted alpha/cluster and daughter nuclei. The nuclear potential $V_N(R)$ is calculated from the proximity potential.

$$V_N(Z) = 4\pi\gamma \left(\frac{C_1 C_2}{C_1 + C_2} \right) \phi(\xi) MeV \quad (2.14)$$

Using the droplet model [258], the radius C_i was calculated as

$$C_i = R_i + \frac{N_i}{A_i} t_i \quad (2.15)$$

$$R_i(\alpha_i) = R_{0i} \left[1 + \sum_{\lambda} (\beta_{\lambda} Y_{\lambda}^0(\alpha_i)) \right] \quad (2.16)$$

In this case, α_i is the angle formed by the radius vector and the i^{th} nuclei symmetry axis. R_{0i} denotes the half-density radii of the charge distribution and t_i is the neutron skin of the nucleus.

The nuclear charge, is given by the relation

$$R_{ooi} = 1.244 A_i^{1/3} \left[1 + \frac{1 + 1.646}{A_i} - 0.191 \frac{A_i - 2Z_i}{A_i} \right] fm \text{ (for } i=1,2) \quad (2.17)$$

The half-density radius c_i

$$R_{oi} = R_{ooi} \left[1 - \frac{7}{2} \frac{b^2}{R_{ooi}^2} - \frac{49}{8} \frac{b^4}{R_{ooi}^4} + \dots \right] (i = 1, 2) \quad (2.18)$$

Using the droplet model, neutron skin t_i reads as (i=1,2)

$$t_i = \frac{3}{2} r_0 \left[\frac{J I_i - \frac{1}{12} c_1 Z_i A_i^{-1/3}}{Q + \frac{9}{4} J A_i^{-1/3}} \right] \quad (2.19)$$

Here, $r_0 = 1.14$ fm, the nuclear symmetric energy coefficient $J = 32.65$ MeV, $I_i = \frac{N_i}{A_i}$, and $c_1 = 3e^2/5r_0 = 0.757895$ MeV. The neutron skin stiffness coefficient Q was set at 35.4 MeV. In terms of neutron skin, the nuclear surface energy coefficient was given as

$$\nu = \frac{1}{4\pi r_0^2} \left[18.63(\text{MeV}) - Q \frac{t_1^2 + t_2^2}{2r_0^2} \right] \quad (2.20)$$

where t_1 and t_2 were calculated using above equation. The universal function for this is given by

$$\phi(\xi) = -0.1353 + \sum_{n=0}^5 \frac{c_n}{n+1} (2.5 - \xi)^{n+1}, \text{ for } 0 \leq \xi \leq 2.5 \quad (2.21)$$

$$\phi(\xi) = -\exp \left[\frac{2.75 - \xi}{0.7176} \right], \text{ for } \xi \geq 2.5 \quad (2.22)$$

where $\zeta = R - C_1 - C_2$, The values of different constants c_n were $c_0 = -0.1886$, $c_1 = -0.2628$, $c_2 = -0.15216$, $c_3 = -0.04562$, $c_4 = 0.069136$, and $c_5 = -0.011454$. The Langer modified centrifugal barrier is adopted [259] in the present calculation.

$$V_{cf} = \frac{\hbar^2 [l + \frac{1}{2}]^2}{4\pi\mu R^2} \quad (2.23)$$

According to WKB approximation (Wentzel-Kramers-Brillouin) the penetration probability P through the potential barrier studied by the following equation;

$$P = \exp \left[-\frac{2}{\hbar} \int_{R_a}^{R_b} \sqrt{2\mu[V_T(r) - Q]} dr \right] \quad (2.24)$$

where μ is the reduced mass α decay or CD system, R_a/R_c and R_b are the inner and outer turning points and these turning points are calculated by

$$V_T(R_a/R_c) = Q = V_T(R_b) \quad (2.25)$$

The decay half-life of parent nuclei with the emission of α particle or cluster particle is studied by

$$T_{1/2} = \frac{\ln 2}{\lambda} = \frac{\ln 2}{\nu p} \quad (2.26)$$

Where λ is the decay constant and ν is the assault frequency and is expressed as

$$\nu = \frac{\omega}{2\pi} = \frac{2E_\nu}{h} \quad (2.27)$$

where E_ν is the empirical vibrational energy. The evaluated cluster and α decay half lives are used in the construction of formula. The relationship between logarithmic half-lives and the product of atomic number of daughter and square root of reciprocal of energy released ($Z_d Q^{-1/2}$) is found to be linear. Figure 2.3 depicts the variation of logarithmic half-lives with $Z_d Q^{-1/2}$, such as parent nuclei $Z=110$. The linear equation is sufficient to fit logarithmic half-lives in terms of $Z_d Q^{-1/2}$. The following is the fitted equation for logarithmic half-lives in terms of $Z_d Q^{-1/2}$:

$$\log T_{1/2} = A(Z_d Q^{-1/2}) + B \quad (2.28)$$

$$A = A(Z_c A_c) \quad \text{and} \quad B = B(Z_c A_c) \quad (2.29)$$

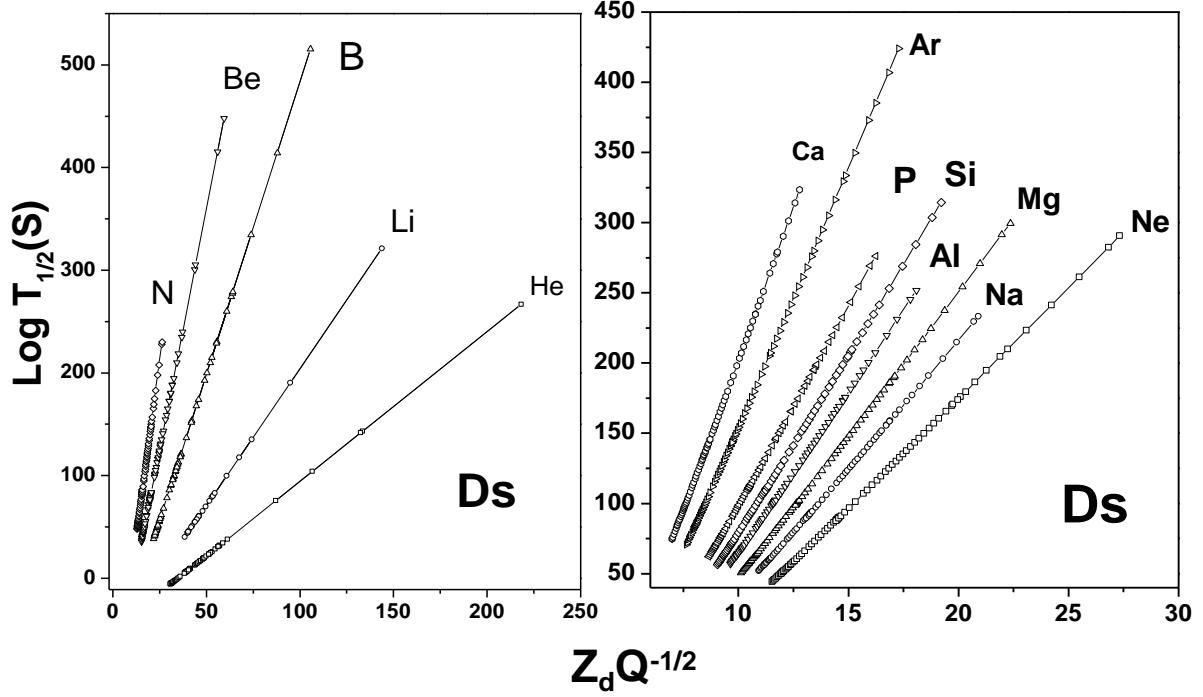


Fig. 2.3 The variation of logarithmic half-lives as a function of product of atomic number of daughter and inverse square root of energy released during the decay process for parent nuclei with $Z=110$

Where A and B in the above equation are the fitting parameters, depends on the type of cluster emitted and the parent nuclei. The variation of A and B which is used to evaluate the fitting parameters A and B . Where Z_c is the cluster atomic number and A_c is the cluster mass number. Figure 2.4 depicts the variation of fitting constants A and B with the product of atomic number and cluster mass $Z_c A_c^{-1/3}$, for example, $Z = 110$, all SHN in the atomic number range $104 \leq Z \leq 130$ show similar variation.

$$A = A_2(Z_c A_c^{-1/3})^2 + A_1(Z_c A_c^{-1/3}) + A_0 \quad (2.30)$$

$$B = B_2(Z_c A_c^{-1/3})^2 + B_1(Z_c A_c^{-1/3}) + B_0 \quad (2.31)$$

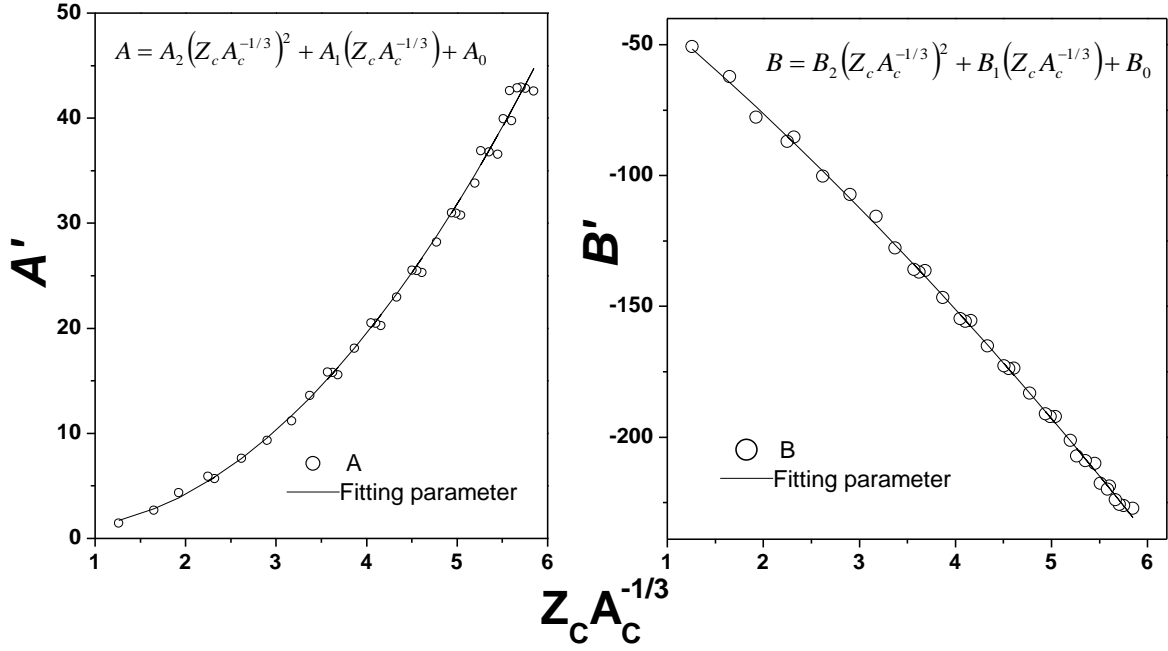


Fig. 2.4 Variation of fitting constants A and B with product of atomic number and mass of cluster for Z=110

The fitting parameters A_2 , A_1 , A_0 , and B_2 , B_1 , B_0 are determined by the atomic number of the parent nuclei. As a result, the above fitting parameters can be expressed as $A_2 = A_2(Z)$, $A_1 = A_1(Z)$, $A_0 = A_0(Z)$, $B_2 = B_2(Z)$, $B_1 = B_1(Z)$, and $B_0 = B_0(Z)$. The variation of A_2 , A_1 , A_0 , B_2 , B_1 and B_0 with the atomic number of parent nuclei is used to evaluate these fitting parameters. Figure 2.5 depicts the relationship between A_2 , A_1 , A_0 , B_2 , B_1 and B_0 and the atomic number of parent nuclei. According to this graph, there is a systematic variation in fitting parameters with the atomic number of parent nuclei, in terms of atomic number, a second order polynomial to these fitting parameters.

$$A_2 = \sum_{i=0}^2 A_{2i} Z^i, A_1 = \sum_{i=0}^2 A_{1i} Z^i, A_0 = \sum_{i=0}^2 A_{0i} Z^i \quad (2.32)$$

$$B_2 = \sum_{i=0}^2 0.53 \times B_{2i} Z^i, B_1 = \sum_{i=0}^2 0.53 \times B_{1i} Z^i, B_0 = \sum_{i=0}^2 B_{0i} Z^i \quad (2.33)$$

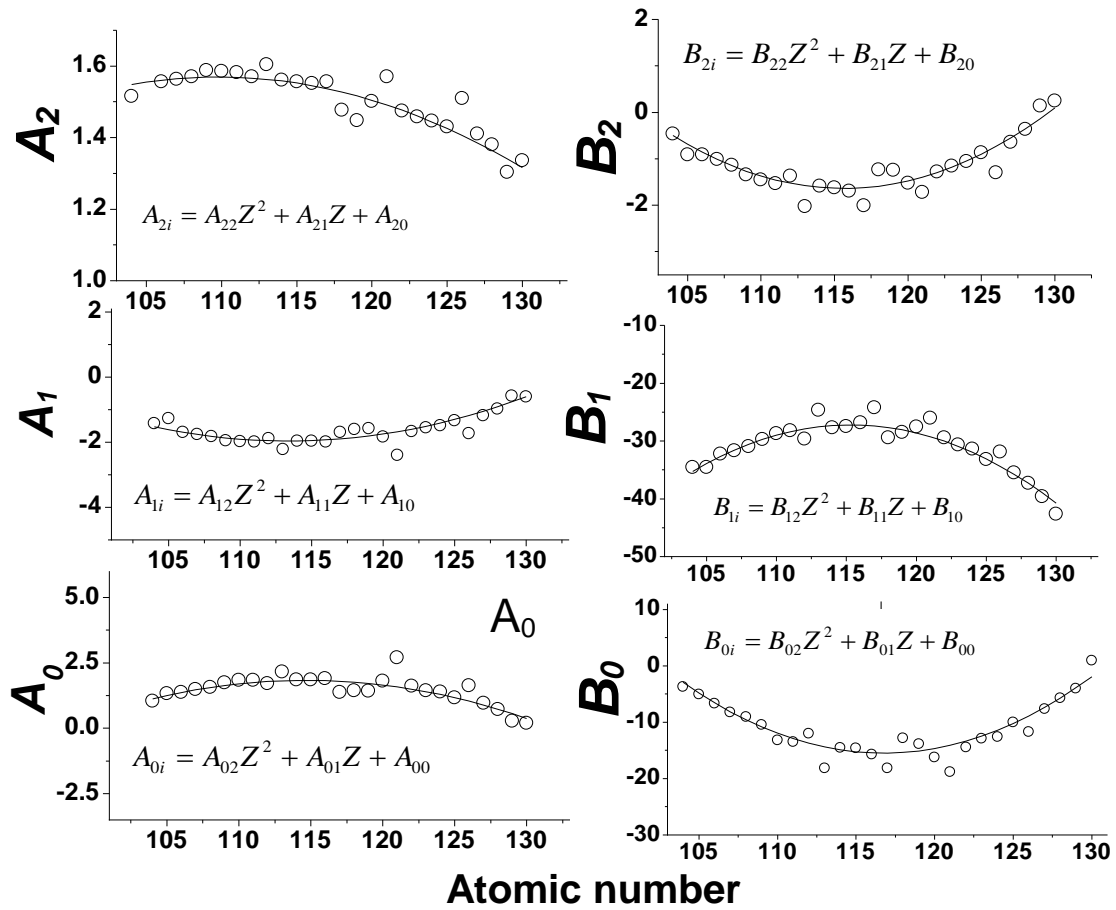


Fig. 2.5 Variation of A_2 , A_1 , A_0 , B_2 , B_1 and B_0 with atomic number of parent nuclei

Table 2.2 Co-efficient sets of A' and B'.

i	A_{2i}	A_{1i}	A_{0i}	B_{2i}	B_{1i}	B_{0i}
2	-6.19E-04	4.93E-03	-6.17E-03	8.41E-03	-6.28E-02	7.73E-02
1	0.135994	-1.11765	1.414481	-1.94459	14.48453	-18.0448
0	-5.8946	61.40271	-79.2567	110.7946	-862.417	1037.946

Table 2.3 The range of isotopes and total number of isotopes considered for each atomic number (Z) in the present empirical formula.

Z	Range of isotopes	Total isotopes	Z	Range of isotopes	Total isotopes	Z	Range of isotopes	Total isotopes
104	$253 \geq A \geq 270$	17	112	$277 \geq A \geq 286$	9	120	$295 \geq A \geq 310$	15
105	$258 \geq A \geq 272$	14	113	$278 \geq A \geq 290$	12	121	$295 \geq A \geq 310$	15
106	$258 \geq A \geq 271$	13	114	$284 \geq A \geq 290$	6	122	$299 \geq A \geq 310$	11
107	$260 \geq A \geq 278$	18	115	$287 \geq A \geq 290$	3	123	$297 \geq A \geq 339$	42
108	$263 \geq A \geq 277$	14	116	$288 \geq A \geq 294$	6	124	$309 \geq A \geq 320$	11
109	$266 \geq A \geq 282$	16	117	$290 \geq A \geq 310$	20	125	$303 \geq A \geq 339$	36
110	$267 \geq A \geq 281$	14	118	$290 \geq A \geq 300$	10	126	$306 \geq A \geq 339$	36

The fitting parameters in the above equations are A_{2i} , A_{1i} , A_{0i} , B_{2i} , B_{1i} , and B_{0i} , as shown in table 2.2. The final expression for logarithmic half-lives of α decay and CD is obtained by substituting equations (2.30) and (2.31) in equation (2.28).

$$\log T_{1/2} = \left[(Z_c A_c^{-1/3})^2 \sum_{i=0}^2 Z^i A_{2i} + (Z_c A_c^{-1/3}) \sum_{i=0}^2 Z^i A_{1i} + \sum_{i=0}^2 Z^i A_{0i} \right] \frac{Z_d Q^{-1/2}}{2} \quad (2.34)$$

$$+ \left[(Z_c A_c^{-1/3})^2 \sum_{i=0}^2 Z^i B_{2i} + (Z_c A_c^{-1/3}) \sum_{i=0}^2 0.53 Z^i B_{1i} + \sum_{i=0}^2 Z^i B_{0i} \right]$$

This formula yields logarithmic half-lives for α and CD from parent SHN in the atomic number range $104 \leq Z \leq 130$.

2.3 Results

The constructed empirical formula for decay energies of SHN during the emission of different clusters produces the decay energies (Q-value) of SHN of atomic number range $104 \leq Z_p \leq 126$ (corresponding mass numbers of isotopes are listed in the table 2.3) during the cluster emission of atomic number range $2 \leq Z_c \leq 20$ with mass number range $4 \leq A_c \leq 46$. To evaluate the fitting

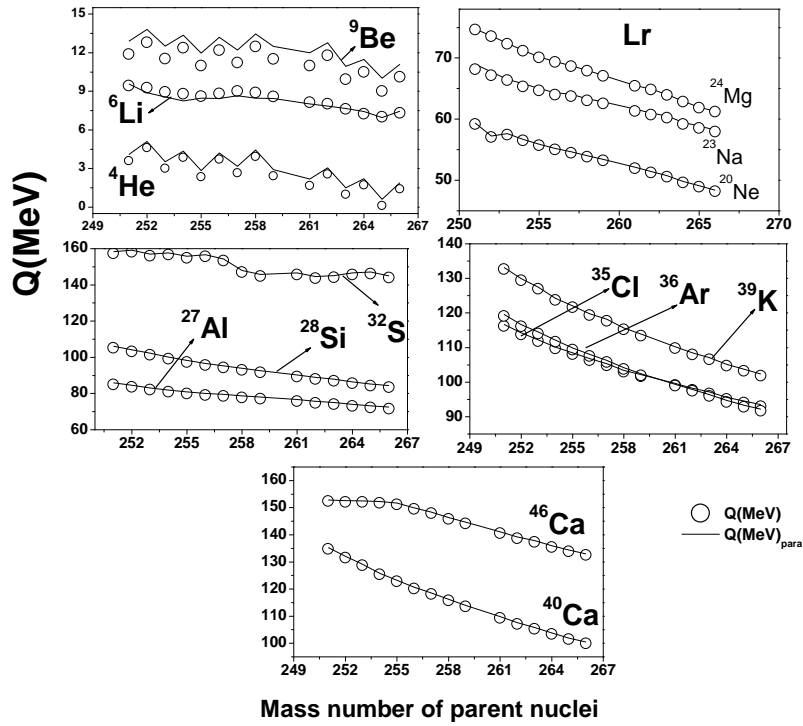


Fig. 2.6 A comparison of present formula with that of other theoretical method such as HFB [236, 237]

parameters the mass excess values available in the literature are used [260]. This formula also predicts the different Q-values correspond to different cluster emissions of same A_d/Z_c ratio. The figure 2.2 shows the variation of Q-values with the function of ratio of mass number of daughter nuclei to the atomic number of emitted cluster. The present work is compared with that of the other theoretical models. Figure 2.6 shows the comparison of present formula with that of other theoretical method such as HFB [236, 237] for SHE $Z=104$. From the figure it is clearly observed that there is close agreement of the present formula with that of HFB. Similarly, present formula produces Q-values close to the other theoretical models. In order to check the predictive power of present constructed formula, the values produced by the present formula is compared with that of the available experiments [261, 262]. Figure 2.7 shows the comparison of present formula with that of the experiments for different values. From the figure it is clearly observed that the values produced by the present formula is close to the experiments. Hence the constructed semi

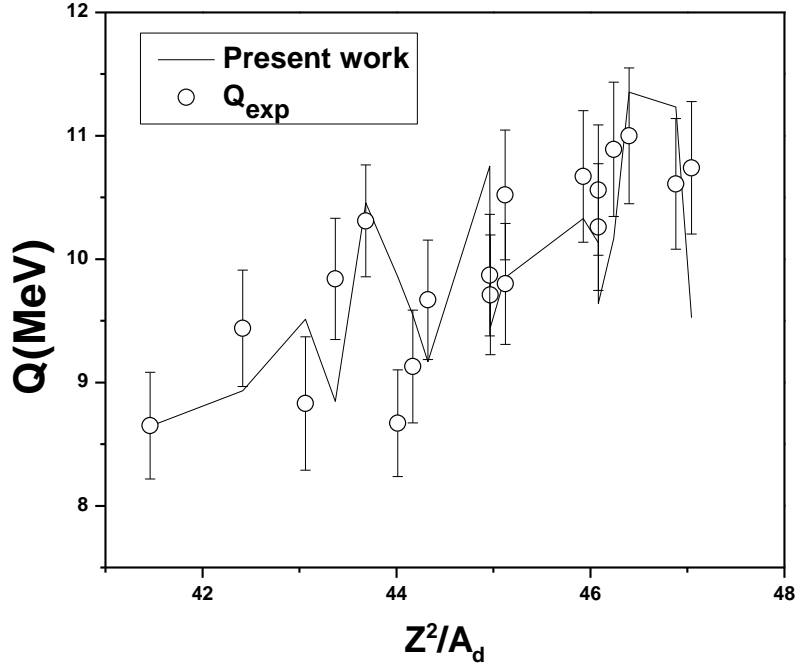


Fig. 2.7 Percentage of deviation of present formula with that of the experiments [261, 262]

empirical formula can produce the Q-values by simple inputs of mass number of daughter nuclei, atomic number of cluster emission and neutron number of parent nuclei. To evaluate predictive power of the present formula, the percentage of deviation and root mean square error (RMSE) of present formula is calculated using following equations;

$$Deviation(\%) = \left(\frac{Q_{exp} - Q_{PF}}{Q_{exp}} \right) \times 100 \quad (2.35)$$

$$RMSE = \sqrt{\frac{\sum_{i=1}^N (Q_{cal} - Q_{exp})^2}{N}} \quad (2.36)$$

The evaluated percentage of deviation of present formula is shown in the figure 2.8. From this

Table 2.4 Root mean square error in the present formula, FRDM95 [252] and HFB14 [252].

Method	Present formula	FRDM95	HFB14
Root mean square error	0.919477465	1.137312	1.137324

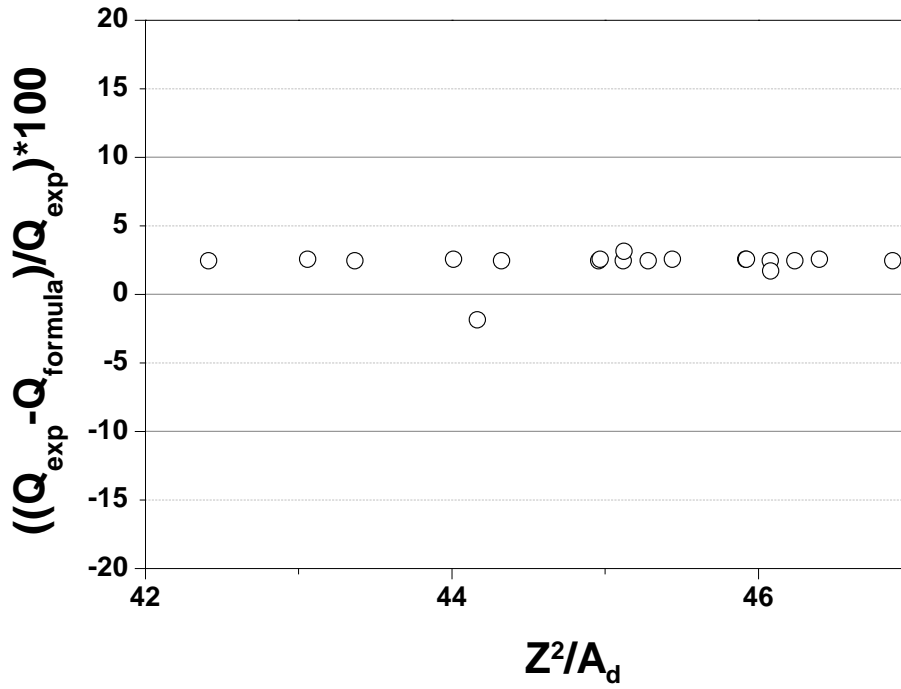


Fig. 2.8 Percentage of deviation of present formula with that of the experiment [76, 263]

figure it is observed that percentage of deviation is less than the ± 5 percent. The evaluated RMSE for present formula and also other theoretical methods given in the table 2.4. Even though the ratio between A/Z correspond to the same values, but due to different cluster emission, formation of daughter nuclei, isotope of the parent nuclei and the Q -value released during the decay process changes, hence different Q -values for the same A/Z ratio. The experimental results having same A/Z ratio during an α decay and corresponding Q -values are given in table 2.5. The available formulae [226, 254–257] in the literature uses up to eight terms to predict decay energies correspond to only α emission. Eventually, seven terms with sixth order to produce decay energies of (${}^4\text{He}$, ${}^6\text{Li}$, ${}^9\text{Be}$, ${}^{20,22}\text{Ne}$, ${}^{23}\text{Na}$, ${}^{24-26}\text{Mg}$, ${}^{27}\text{Al}$, ${}^{28-30}\text{Si}$, ${}^{32-34}\text{S}$, ${}^{35}\text{Cl}$, ${}^{36,38,40}\text{Ar}$, ${}^{39,41}\text{K}$ and ${}^{40,42-44,46}\text{Ca}$). 27 clusters including α in the SH region. All the proposed semi empirical formulae produces the energy during an α -decay only. The formula proposed to produce decay energies of cluster emission is first of its kind. Hence, the constructed new formula will produce the decay energies of SHN without the knowledge of the mass excess.

The amount of energy released $Q(\text{MeV})$ during CD [${}^4\text{He}$, ${}^9\text{Be}$, ${}^{10,11}\text{B}$, ${}^{12}\text{C}$, ${}^{14}\text{N}$, ${}^{16}\text{O}$, ${}^{19}\text{F}$,

Table 2.5 A comparison of experimental Q-values with the FRDM95, HFB14 and present formula having same A/Z during an α decay in the SH region $106 \geq Z \geq 118$.

Parent	Daughter	A/Z	Q-values			
			FRDM95	HFB14	EXP	PF
${}^{269}\text{Sg}$	${}^{265}\text{Rf}$	41.77	8.8	8.8	7.46 ± 0.06	8.64
${}^{271}\text{Sg}$	${}^{267}\text{Rf}$	41.461	8.7	8.7	8.65 ± 0.4325	8.64
${}^{275}\text{Hs}$	${}^{271}\text{Sg}$	42.415	9.199	9.199	9.44 ± 0.472	8.93
${}^{277}\text{Ds}$	${}^{273}\text{Hs}$	43.682	10.3	10.3	10.31 ± 0.453	10.46
${}^{279}\text{Ds}$	${}^{275}\text{Hs}$	43.369	9.6	9.6	9.84 ± 0.492	8.85
${}^{281}\text{Ds}$	${}^{277}\text{Hs}$	43.06	8.958	8.958	8.83 ± 0.5415	9.51
${}^{283}\text{Cn}$	${}^{279}\text{Ds}$	44.325	9.62	9.62	9.67 ± 0.4835	9.17
${}^{284}\text{Cn}$	${}^{280}\text{Ds}$	44.169	9.301	9.301	9.13 ± 0.4565	9.55
${}^{285}\text{Cn}$	${}^{281}\text{Ds}$	44.014	8.793	8.793	8.67 ± 0.4335	9.86
${}^{283}\text{Nh}$	${}^{279}\text{Rg}$	45.12	10.6	10.6	10.52 ± 0.526	9.86
${}^{284}\text{Nh}$	${}^{280}\text{Rg}$	44.961	10.25	10.25	9.87 ± 0.4935	10.75
${}^{286}\text{Fl}$	${}^{282}\text{Cn}$	45.441	10.7	10.7	10.35 ± 0.5175	8.63
${}^{287}\text{Fl}$	${}^{283}\text{Cn}$	45.282	10.436	10.436	10.29 ± 0.5145	9.56
${}^{288}\text{Fl}$	${}^{284}\text{Cn}$	45.125	9.969	9.969	9.8 ± 0.49	9.85
${}^{289}\text{Fl}$	${}^{285}\text{Cn}$	44.969	9.847	9.847	9.71 ± 0.4855	9.45
${}^{287}\text{Mc}$	${}^{283}\text{Nh}$	46.08	11.3	11.3	10.26 ± 0.513	10.13
${}^{288}\text{Mc}$	${}^{284}\text{Nh}$	45.92	10.999	10.999	10.15 ± 0.5075	8.46
${}^{290}\text{Lv}$	${}^{286}\text{Fl}$	46.4	11.3	11.3	11 ± 0.55	11.35
${}^{291}\text{Lv}$	${}^{287}\text{Fl}$	46.241	11	11	10.89 ± 0.5445	10.17
${}^{292}\text{Lv}$	${}^{288}\text{Fl}$	46.082	10.707	10.707	10.56 ± 0.528	9.64
${}^{293}\text{Lv}$	${}^{289}\text{Fl}$	45.925	8.886	8.886	10.67 ± 0.5335	10.33
${}^{291}\text{Ts}$	${}^{287}\text{Mc}$	47.041	11.9	11.9	10.74 ± 0.537	9.53
${}^{292}\text{Ts}$	${}^{288}\text{Mc}$	46.88	11.6	11.6	10.61 ± 0.5305	11.23
${}^{294}\text{Og}$	${}^{290}\text{Lv}$	47.361	8.47	8.47	11.81 ± 0.06	9.98

${}^{20-22}\text{Ne}$, ${}^{23}\text{Na}$, ${}^{24-26}\text{Mg}$, ${}^{27}\text{Al}$, ${}^{28-30}\text{Si}$, ${}^{31}\text{P}$, ${}^{32-34}\text{S}$, ${}^{35}\text{Cl}$, ${}^{36,38,40}\text{Ar}$, ${}^{39,41}\text{K}$ and ${}^{40,42-44,46}\text{Ca}$] including α decay from parent SHN in the atomic number range $104 \leq Z \leq 126$ is calculated from the following equation;

$$Q = \delta M_p - (\Delta M_i + \delta M_j) + k(Z_p^e - Z_d^e) \quad (2.37)$$

where M_p , M_i , and M_j denote the mass excess of parent and fission fragments, respectively. The atomic electron effect is represented by the last term in the above equation. The total binding energy of Z electrons in the atom, where $k = 8.7 \text{ eV}$ for $Z \geq 60$. The experimental mass excess

values [264] were used in the current study, where experimental mass excess values are unavailable, theoretical mass excess values are considered [238, 239, 265, 266]. CD half-lives (^4He , ^9Be , $^{10,11}\text{B}$, ^{12}C , ^{14}N , ^{16}O , ^{19}F , $^{20-22}\text{Ne}$, ^{23}Na , $^{24-26}\text{Mg}$, ^{27}Al , $^{28-30}\text{Si}$, ^{31}P , $^{32-34}\text{S}$, ^{35}Cl , $^{36,38,40}\text{Ar}$, $^{39,41}\text{K}$ and $^{40,42-44,46}\text{Ca}$) including α decay are calculated for SHN in the atomic number range $104 \leq Z \leq 130$. The constructed universal semi empirical formula for α decay and CD for SHN with atomic number range $104 \leq Z \leq 130$, using simple inputs such as cluster mass number (A_c), daughter nuclei mass number (A_d), energy released during decay (Q), and parent nuclei atomic number (Z). To validate the current work, the logarithmic half lives produced by the present formula are compared to those produced by experiments and other formulae such as Universal Decay Law (UDL) [76] and Horoi et al., [214], Univ [216], Royer [212], and VSS [211]. Table 2.6 shows a comparison of calculated α half-lives with UDL, Horoi et al., Univ, Royer, and VSS values, as well as experimental values.

According to the detailed literature review, there are no experiments on the CD of SHN, but experimental values for α decay in the SHN region are available. As a result, in this study, the values produced by the current formula for α decay half lives are compared with those obtained from experiments. Figure 2.9 depicts a comparison of experimental half lives [178, 252, 268–271] for α decay with the values produced by the current formula. Table 2.7 comparison of present work with calculated half-lives from the literature [272–276] and experimental half-lives of $Z=114, 116$, and 118 with that of the current work. Due to the lack of experimental CD half-lives in the SH region, CD logarithmic half-lives predicted in the present work are compared with theoretical models such as Univ, NRDX [217], UDL [224], and Horoi et al., [214] which are tabulated in table 2.8. Because the predicted half-lives of SHN are close to the experimental values in the SH region $Z=118-126$, which is shown in figure 2.10. To assess the predictive power of the current formula, the percentage of deviation between calculated and experimental α decay half-lives were

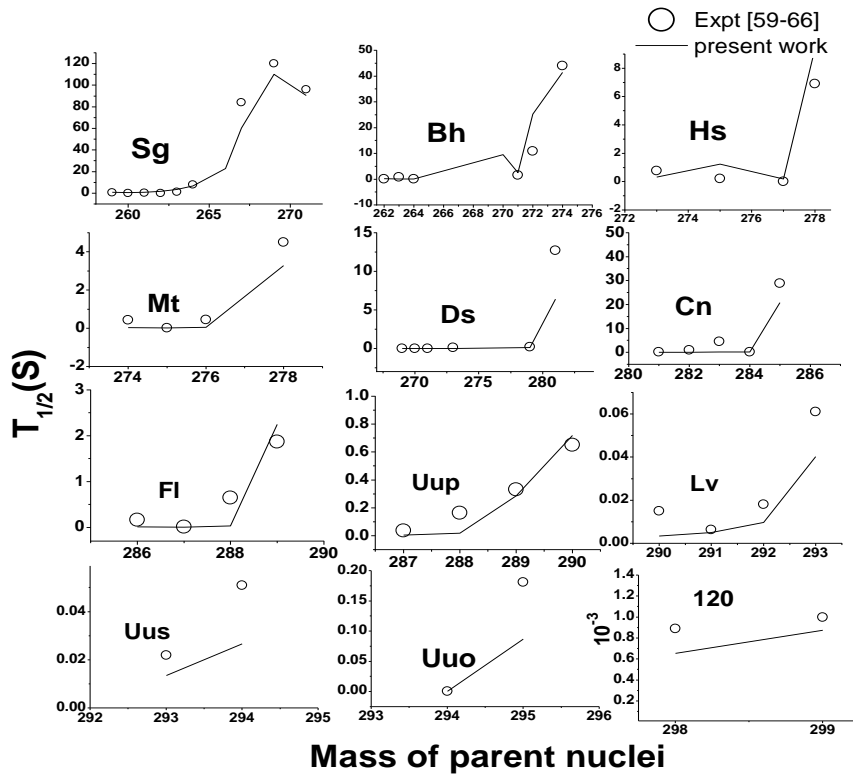


Fig. 2.9 A comparison of variation of available experimental values with present work

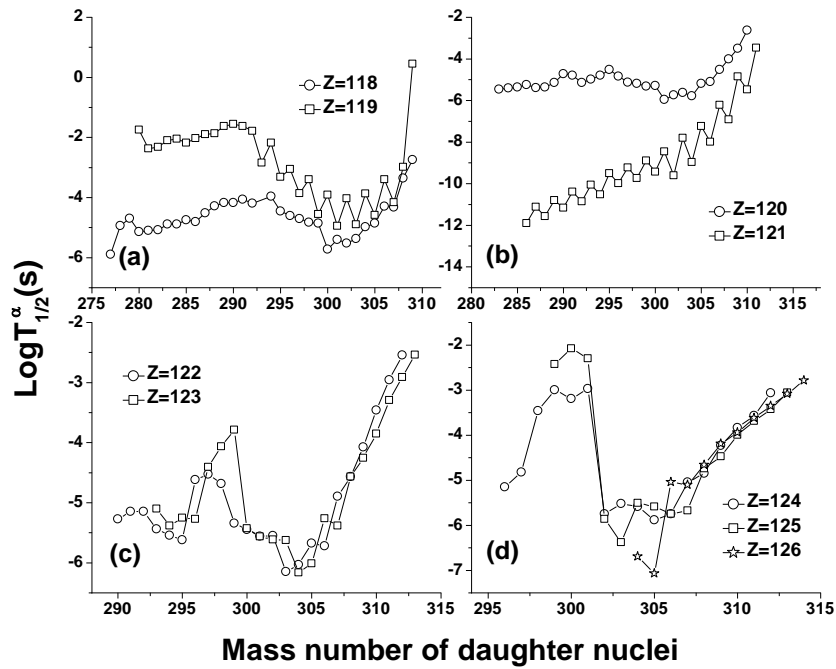


Fig. 2.10 A prediction of α decay half-lives in the SH region $Z=118-126$

Table 2.6 Comparison of half-lives (s) of this work with UDL [224], Horoi et al., [214] Univ [227], Royer [212] and VSS [228] and experimental values.

Isotopes	Experimental α -decay half-lives (s)	Q_α (MeV)	Present Work (s)	UDL (s)	Horoi et al., (s)	Univ (s)	Royer (s)	VSS (s)
²⁷⁵ 106	144 ^{+4.3} ₋₁ [225]	8.65±0.08	57.6	57.6	18.42	28.86	11.4	21.6
²⁷¹ 106	114 ^{+2.4} _{-0.6} [215]	8.54±0.08	90.6	90.6	45	62.4	30.6	59.4
²⁷⁴ 107	53 ⁺²⁵⁰ ₋₂₄ [223]	8.93±0.08	9.51	6.88	8.51	3.56	6.86	12.58
²⁷⁵ 108	0.19 ^{+0.22} _{-0.07} [215]	9.3±0.06	1.28	1.44	1.51	0.59	1.13	2.01
²⁷⁵ 108	0.15 ^{+0.27} _{-0.06} [225]	9.44±0.07	0.76	0.6	0.62	0.23	0.43	0.77
²⁷⁵ 109	0.097 ⁺⁴⁶ _{-4.4} [267]	10.48±	0.012	0.0036	0.029	0.0086	0.0013	0.0023
²⁷⁸ 109	7.7 ⁺³⁷ _{-3.5} [223]	9.69±0.19	0.19	0.27	0.26	0.09	0.17	0.31
²⁷⁹ 110	0.18 ^{+0.05} _{-0.03} [225]	9.84±0.06	0.078	0.25	0.21	0.07	0.14	0.25
²⁷⁹ 111	0.17 ⁺⁸¹⁰ ₋₈₀ [267]	10.52±	0.0057	0.012	0.0085	0.0026	0.00045	0.0079
²⁸² 111	0.51 ^{+2.5} _{-0.23} [223]	9.13±0.1	0.998	43.07	36.43	17.62	39.15	73.54
²⁸⁵ 112	3.4 ⁺¹⁷ ₋₉ [225]	9.29±0.06	0.492	31.79	25.17	11.45	25.86	50.8
²⁸³ 112	4 ^{+1.3} _{-0.7} [225]	9.67±0.06	0.11	3.06	2.24	0.91	1.96	3.54
²⁸³ 112	0.038 ^{+1.2} _{-0.27} [215]	9.54±0.06	0.18	6.86	5.03	2.18	4.79	8.66
²⁸⁵ 112	34 ⁺¹⁷ ₋₉ [224]	9.16±0.06	0.84	74.89	59.5	29.08	66.8	131.18
²⁸⁵ 113	5.5 ⁺⁵ _{-1.8} [223]	9.88±0.08	0.051	1.93	1.21	0.47	1.02	1.84
²⁸⁶ 113	0.02 ⁺⁹⁴ ₋₉ [223]	9.76±0.1	0.029	0.191	0.131	0.046	0.095	0.15
²⁸³ 113	0.1 ⁺⁴⁹⁰ ₋₄₅ [267]	10.26±	0.169	5.893	3.176	1.275	2.9141	5.473
²⁸⁸ 114	0.018 ^{+2.1} _{-0.6} [218]	9.83±0.05	0.082	1.596	1.014	0.386	0.859	1.545
²⁸⁷ 114	0.00048 ^{+3.2} _{-0.09} [215]	10.02±0.06	0.035142	1.6	1.01	0.385	0.858	1.54
²⁸⁹ 114	0.053 ^{+1.4} _{-0.19} [224]	9.82±0.06	0.176	5.49	3.38	1.31	2.99	5.86
²⁸⁸ 114	0.63 ^{+0.27} _{-0.14} [224]	9.95±0.08	0.11	2.35	1.541	0.583	1.31	2.451
²⁸⁶ 114	0.29 ^{+0.54} _{-0.11} [224]	10.03±0.31	0.079	1.51	0.954	0.376	0.84	1.45
²⁸⁸ 114	0.63 ^{+0.27} _{-0.14} [224]	9.95±0.08	0.11	2.58	1.54	0.58	1.31	2.45
²⁸⁶ 114	0.29 ^{+0.54} _{-0.11} [224]	10.03±0.31	0.079273	1.46	0.96	0.38	0.84	1.45
²⁸⁹ 114	2.7 ^{+1.4} _{-0.7} [225]	9.96±0.06	0.12	2.283	1.454	0.526	1.171	2.29
²⁸⁸ 114	0.8 ^{+0.32} _{-0.18} [225]	10.09±0.07	0.064	1.092	0.67	0.238	0.52	0.98
²⁸⁷ 114	0.51 ^{+0.18} _{-0.1} [225]	10.16±0.06	0.049	0.75	0.45	0.16	0.35	0.63
²⁸⁶ 114	0.16 ^{+0.07} _{-0.03} [225]	10.35±0.06	0.025	0.23	0.151	0.05	0.11	0.19
²⁸⁹ 114	2.7 ^{+1.4} _{-0.7} [225]	9.96±0.06	0.1	2.28	1.45	0.53	1.17	2.29
²⁸⁸ 114	0.8 ^{+0.32} _{-0.18} [225]	10.09±0.07	0.06	1.09	0.67	0.24	0.52	0.98
²⁸⁹ 115	0.22 ⁺²⁶⁰ ₋₈₀ [223]	10.45±0.09	0.022	0.315	0.164	0.053	0.12	0.21
²⁸⁷ 115	0.032 ⁺¹⁵⁵ ₋₁₄ [267]	10.74±	0.0081	0.057	0.033	0.01	0.021	0.035
²⁹⁰ 115	0.016 ⁺⁷⁵ ₋₈ [223]	10.09±0.4	0.083	2.36	1.29	0.48	1.1	2.1
²⁹⁰ 116	0.015 ⁺²⁶ ₋₆ [221]	11±0.08	0.00428	0.031	0.015	0.004	0.0089	0.015
²⁹¹ 116	0.063 ^{+11.6} _{-2.5} [221]	10.89±0.07	0.0069	0.059	0.028	0.0078	0.016	0.028
²⁹² 116	0.018 ⁺¹⁶ ₋₆ [222]	10.8±0.07	0.0096	0.087	0.045	0.012	0.026	0.049
²⁹³ 116	0.053 ⁺⁶² ₋₁₉ [221]	10.67±0.06	0.014	0.177	0.091	0.026	0.055	0.18
²⁸⁶ 116	0.13 ^{+0.04} _{-0.02} [215]	10.19±0.06	0.086	2.63	1.35	0.64	1.55	2.22
²⁹⁴ 117	0.178 ⁺³⁷⁰ ₋₃₆ [223]	10.96±0.1	0.0091	0.074	0.036	0.0097	0.02	0.038
²⁹³ 117	0.014 ⁺¹¹ ₋₄ [223]	11.18±0.08	0.0045	0.022	0.011	0.0029	0.0061	0.01
²⁹⁴ 118	0.0006 ^{+1.07} _{-0.31} [215]	11.65±0.06	0.0018	0.0056	2.054	0.0047	0.00912	0.00105

determined, using the expression.

$$Deviation = \frac{\log(T_{1/2,i}^{expt}) - \log(T_{1/2,i}^{cal})}{\log(T_{1/2,i}^{expt})} \quad (2.38)$$

Table 2.7 Comparison of half-lives (s) of this work with Refers.[272–276]

Isotopes	Q (MeV)	$T_{1/2}^{Prev.Work}$ (s)	$T_{1/2}^{exp.}$ (s)	$T_{1/2}^{Presentwork}$ (s)
^{286}Fl	10.35	8.48×10^{-3} [272, 273]	2×10^{-1}	1.05×10^{-2}
^{286}Fl	10.07	4.7×10^{-2} [272, 273]	6.6×10^{-1}	2.91×10^{-2}
^{288}Fl	9.94	6.14×10^{-2} [275]	3.5×10^{-1}	4.76×10^{-2}
^{290}Lv	11	7.36×10^{-4} [272, 273]	8.3×10^{-3}	2.06×10^{-3}
^{292}Lv	10.78	2.51×10^{-3} [272, 273]	1.3×10^{-2}	4.36×10^{-3}
^{290}Lv	10.88	5.52×10^{-3} [275]	8×10^{-3}	3.09×10^{-3}
^{292}Lv	10.92	1.93×10^{-2} [275]	2.4×10^{-2}	2.7×10^{-3}
^{293}Og	12.241	0.354×10^{-3} [274]	-	1.24×10^{-4}
^{293}Og	11.92	2.96×10^{-4} [276]	1×10^{-3}	3.21×10^{-4}
^{294}Og	11.82	3.27×10^{-5} [272, 273]	6.9×10^{-4}	4.35×10^{-4}
^{294}Og	11.97	2.24×10^{-4} [275]	1.15×10^{-3}	2.76×10^{-4}
^{295}Og	11.9	1.336×10^{-3} [274]	-	3.4×10^{-4}
^{295}Og	11.7	5.49×10^{-4} [276]	1×10^{-2}	6.29×10^{-4}
^{296}Og	11.65	7.3×10^{-5} [272, 273]	8.25×10^{-4}	7.24×10^{-4}
^{296}Og	11.75	0.869×10^{-3} [274]	-	5.37×10^{-4}
^{297}Og	12.1	0.361×10^{-3} [274]	-	1.85×10^{-4}
^{297}Og	12	1.04×10^{-4} [276]	-	2.52×10^{-4}

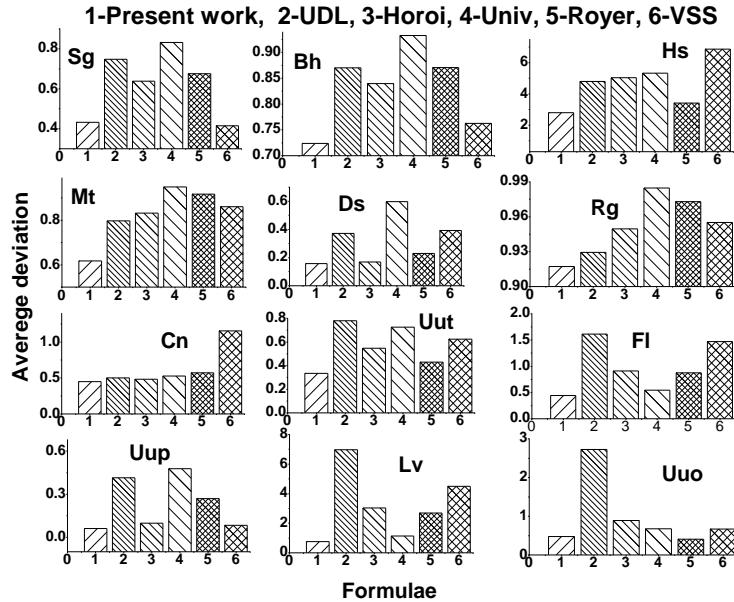


Fig. 2.11 The comparison of average deviation of α decay half-lives with atomic number for different semi empirical relations

Table 2.8 A comparison of logarithmic half-lives(s) of present work with logarithmic half-lives(s) UNIV [227], NRDX [217], UDL [224], and Horoi [214]

Isotopes	log $T_{1/2}$									
	^{24}Mg					^{34}S				
	Present Work	Univ	NRDX	UDL	Horoi	Present Work	Univ	NRDX	UDL	Horoi
^{263}Rf	36.189	44.406	45.8	50.01	46.58	36.165	41.94	45.5	44.84	46.48
^{270}Db	38.49	49.77	50.02	56.034	52.02	37.546	45.592	48.12	49.356	50.69
^{259}Sg	28.01	32.57	33.4	36.82	35.14	28.84	32.05	33.58	32.8	36.59
^{267}Bh	30.182	37.05	42.04	42.086	40.034	31.35	36.48	39.9	38.49	41.82
^{265}Hs	30.18	37.054	41.34	42.085	40.034	31.31	36.479	39.82	38.49	41.82
^{278}Mt	32.7	43.033	45.22	49.056	46.42	32.21	39.06	43.252	41.94	45.52
^{277}Ds	27.85	34.94	39.4	39.98	38.84	28.65	33.49	38.32	35.084	40.12
^{282}Rg	39.42	57.45	61.52	64.983	59.52	37.13	49.45	55.05	54.59	55.65
^{281}Cn	26.12	32.78	38.215	37.67	37.15	26.87	31.16	39.37	32.29	38.37
^{283}Nh	25.43	31.84	35.4	36.62	36.44	26.16	30.154	38.65	31.072	37.552
^{289}Fl	28.56	37.56	43.72	43.37	42.22	29.75	36.37	45.35	39.11	44.35
^{289}Mc	25.87	32.82	36.35	37.99	37.85	26.98	31.55	38.77	33.06	39.77
^{292}Lv	28.73	38.01	41.36	44.05	42.86	28.93	34.89	42.36	37.41	43.36
^{294}Ts	27.99	36.43	40.086	42.34	41.59	49.02	74.17	77.25	83.4	78.25
^{295}Og	26.7	33.8	37.75	39.37	39.25	27.31	31.52	39.55	33.27	40.55

Isotopes	^{30}Si					^{40}Ca				
	Present Work	Univ	NRDX	UDL	Horoi	Present Work	Univ	NRDX	UDL	Horoi
^{263}Rf	30.22	37.06	41.5	40.171	40.95	59.84	64.762	68.672	70.34	68.67
^{270}Db	31.016	39.51	43.67	43.21	43.977	63.85	73.569	75.086	80.639	77.09
^{259}Sg	24.45	29.41	31.153	31.03	33.13	45.28	43.8	44.73	45.41	49.473
^{267}Bh	25.45	31.69	33.2	33.97	36.19	51.89	54.55	59.9	58.76	60.29
^{265}Hs	25.75	32.194	35.67	34.59	36.69	51.89	54.55	59.29	58.76	60.29
^{278}Mt	26.17	34.05	38.261	37.09	39.6	55.63	61.998	67.2	67.97	68.2
^{277}Ds	23.04	29.12	33.75	31.089	34.72	49.93	53.01	59.15	57.35	60.25
^{282}Rg	31.64	45.83	50.813	51.19	51.128	60.85	72.6	78.171	80.53	77.71
^{281}Cn	21.51	27.22	34.3	28.86	33.2	47.05	48.91	58.19	52.6	57.19
^{283}Nh	20.99	26.55	33.88	28.097	32.88	46.001	47.37	57.1	50.81	56.098
^{289}Fl	24.07	32.09	38.42	35.14	38.93	51.14	55.92	63.92	61.46	64.42
^{289}Mc	21.79	28.06	34.54	30.17	35.036	46.69	48.41	55.36	52.36	57.86
^{292}Lv	23.66	31.37	38.11	34.41	38.61	48.9	51.96	60.92	56.88	61.42
^{294}Ts	23.07	30.08	37.07	32.88	37.57	48.42	50.87	60.24	55.65	60.74
^{295}Og	22.17	28.18	35.37	30.56	35.87	46.29	46.91	56.92	50.83	57.42

Figure 2.11 depicts the average deviation factor of α decay half-lives for different atomic numbers in the SH region $104 \leq Z \leq 130$. In comparison to UDL [224], Horoi et al., [214] Univ [227], Royer [212], and VSS [228], the average deviation factor of the current formula is small. As a result, our universal semi empirical formula produces α decay half-lives with less variation than other formulae such as UDL, Horoi et al., Univ, Royer, and VSS. The developed formula for logarithmic half lives of α decay and CD is limited to SHN with atomic numbers $104 \leq Z \leq 130$.

CHAPTER 3

Cluster radioactivity

3.1 Introduction

Cluster radioactivity (CR) in the region of SHN has become an interesting topic in the recent era. CR is a type of highly asymmetric decay which exists between process of an α -decay and spontaneous fission. During CR, atom emits cluster of protons and neutrons whose number lies between an α -particle and binary fission fragment. CR is similar to that of an α -decay which can occur only if the cluster passes through the potential barrier. Sandulescu et al., [277] discovered the first theoretically based prediction of CR. Experimental based CR phenomenon was first found by Rose et al., [30] during decay of ^{223}Ra . Furthermore, systematics of CR and related decay constants calculation using microscopic approach is performed by Blendowske et al., [73].

Lovas et al., [278] investigated CR using different microscopic approach. Poenaru and Griener [279] evaluated CR using macroscopic and microscopic approach. Furthermore, Santhosh et al., [280] proposed semi empirical formula for radioactive nuclei's exhibiting CR. In addition to the above empirical relations many microscopic models such as DDCM with usage of M3Y nucleon-nucleon interaction [281, 282], DFT [283], Optical potential calculations based on RMF theory [284], exotic cluster decay in heavy nuclei using Folding Density Dependent M3Y (FDDM3Y) [81], super fluid phenomena and resonance effects using Continuum Hopping Model (CHM) [285], GDDCM [286], Realistic α pre-formation factors of odd-A and odd-odd nuclei within the DFT

[287], PCM [69], ASAF [288] and Skyrme-SLy4 effective nucleon–nucleon interaction (SLy4) [289] were extensively used to study CR.

Furthermore CD explained by macroscopic models viz., half lives of CR as a asymmetric spontaneous fission is studied by generalized liquid drop model(GLDM) [112]. CR of neutron-deficient nuclei in trans-tin region was studied using ELDM [290], CD half-lives and preformation probabilities by CPPM [291]. Earlier researchers [87, 292–296] have studied CR in the SH region. Super asymmetric fission theory is extended from CD to nanophysics by LDM [288].

Zhang et al., [121] deduced preformation factors using experimental CD half-lives within preformed cluster model approach. CR is investigated using RMF theory [297]. Experimental investigation of the CR of atomic nuclei by Tretyakova and Mikheev [298]. Ahmed et al., [299] studied the α and cluster preformation factors in the formation of even even SHN in the atomic numbers range $82 \leq Z \leq 114$. Ghodsi et al., studied α - decay properties of even even SHN by including preformation factor with in the cluster formation model [300]. Various studies on CR using different proximity potentials within CPP [88, 90, 92, 96, 115, 117] are available in literature. With the detail analysis of literature, a comprehensive investigation is carried out using MGLDM and CPPM theoretical models to find effect of CR in the formation even-even SHN with in the atomic range $104 \leq Z \leq 126$.

The discovery of natural radioactivity at the beginning of 20th century opens a new era in Nuclear Physics. If the atomic nuclei emits a cluster of neutrons or protons, then the nuclear decay is called CD. Sandulescu et al., first predicted CR on the basis of QMFT. Experimentally, Rose and Jones [30] first observed CD in the radioactive decay of Radium-223 by the emission of carbon particle. From literature survey [68, 301], heavy CR such as Oxygen, Neon, Magnesium and Silicon were observed. Poenaru et al., [129] explored the heavy-particle radioactivity of SH nuclei. Some theoretical models such as superasymmetric fission model [71], the unified fission

model (UFM) [219] and the PCDM [302] have been used to explain CR. The experiments were conducted to measure the CD of ^{230}U and ^{225}Ac and the most probable clusters are ^{22}Ne and ^{14}C respectively [68].

The microscopic point of view enters particularly into the evaluation of the preformation probability by use of many-body wave functions. It seems to be difficult to extend the procedure to clusters heavier than Oxygen due to the large number of nucleons involved in these calculations [73]. By considering the quantum tunnelling of a preformed cluster at the nuclear surface, the decay modes such as microscopic theories of α -decay and CR can be explained [303]. The double magic structure of the heavy fragment clearly shows the strong influence of shell effects on CR. Assuming the preformed cluster tunnels through a potential barrier the cluster radioactivity is explained in terms of the Gamow model of α decay [77]. GNL gave a semi-empirical relationship of the α -decay half-life with the range of α -particles and it is explained by Gamow using the tunnelling [304].

Half-lives of CR are studied within the WKB barrier-penetration probability by constructing the potential barrier using a GLDM [112]. Half-lives of clusters emitted from radioactive nuclei whose mass numbers vary from 221 to 242, emitting C, O, F, Ne, Mg and Si clusters are calculated using modified generalized liquid drop model. For the existing generalized liquid drop model with proximity 77 potential, a new pre-formation factor is added in the modified generalized liquid drop model [305]. Nagaraja et al., [87, 292–296] have studied CR in the SH region. The two-proton radioactivity half-lives of the ground state of nuclei are studied using generalized liquid drop model (GLDM). Previous researchers used many theoretical approaches which include the direct decay model, the simultaneous versus sequential decay model and the diproton model to estimate the half-lives of 2p radioactivity [306]. Zhang et al., [122] investigated CR of SH nuclei $^{294}_{118}$, $^{296}_{120}$ and $^{298}_{122}$ were studied using different models. Poenaru et al., [307] observed that

CR is one of the important decay modes for SH nuclei with branching ratio larger than that of α decay for $Z \geq 121$ nuclei by the analytical supersymmetric fission (ASAF) model.

Several experimental techniques are developed to investigate the extremely rare decay mode of heavy nuclei. CR is an intermediate position between alpha-particle radioactivity and spontaneous fission. An experiment was conducted to measure the CD of ^{242}Cm and the most probable clusters are ^{34}Si and ^{208}Pb respectively.

Using R matrix description of the process, microscopic estimation of cluster formation probability and barrier penetrability were investigated [75, 308]. Various studies on CR using different proximity potentials [88, 90, 92, 96, 115, 117] were available in heavy and SH nuclei. The use of different universal functions are the fundamental advantage of the proximity potential model. In the present analysis, different versions of the proximity functions such as MP-77, Prox-77, MP-81, Prox-13, Ng-80, Dp-00 are used in Coulomb and Proximity potential model (CPPM) and modified generalised liquid drop model (MGLDM). Using these different proximity potentials, the CR of odd SH nuclei within the atomic number range $105 \leq Z \leq 125$, were studied.

3.2 Theory

3.2.1 Modified generalized liquid drop model(MGLDM)

In MGLDM [108, 147], total energy during CR is the sum of volume E_V , surface E_S , Coulomb E_C , proximity E_P and centrifugal E_l energies and it is expressed as;

$$E = E_V + E_s + E_c + E_P + E_l \quad (3.1)$$

When the nuclei are far apart, then

$$E_V = -15.494(1 - 1.8I^2)A \text{ MeV} \quad (3.2)$$

$$E_s = 17.9439(1 - 2.6I^2)A^{2/3} \frac{S}{4\pi R_0^2} \text{ MeV} \quad (3.3)$$

$$E_c = 0.6e^2(Z^2/R_0) \times 0.5 \quad (3.4)$$

$$\int (V(\theta)/V_0)(R(\theta)/R_0)^3 \sin(\theta) d\theta \text{ MeV}$$

where S and I are the surface area of the deformed nucleus and relative neutron excess respectively. V_0 and $V(\theta)$ are the surface potential of the sphere and electrostatic potential at the surface respectively. For post-scission region the equation 3.1 to 3.4 are rewritten as explained in the literature [148]. The term E_ℓ is expressed as;

$$E_\ell(r) = \frac{\hbar^2}{2\mu} \frac{\ell(\ell + 1)}{r^2} \quad (3.5)$$

where μ is the reduced mass, r is the distance between the mass centers and ℓ is the angular momentum. The nuclear proximity potential [78] is given by;

$$V_N(R) = 4\pi\gamma\bar{R}\Phi(s) \quad (3.6)$$

here \bar{R} is the mean curvature radius and it is given by $\bar{R} = \frac{C_1 C_2}{C_1 + C_2}$ and C_i is the Sussmann central radii and is evaluated as follows;

$$C_i = R_i - \left(\frac{b^2}{R_i} \right) \quad (3.7)$$

Sharp radii R_i is expressed as;

$$R_i = 1.28A_i^{1/3} - 0.76 + 0.8A_i^{-1/3} \quad (3.8)$$

In the equation (3.6), γ is defined as;

$$\gamma = \gamma_0 \left[1 - I_s \left(\frac{N - Z}{A} \right)^2 \right] \text{MeV}/\text{fm}^2 \quad (3.9)$$

where $\gamma_0 = 1.460734 \text{ MeV}/\text{fm}^2$ and $I_s = 4.0$ and various universal proximity function in equation 3.6.

3.2.2 Modified Proximity Potential 1977 (MP-77)

The proximity potential function of the Blocki and Swiatecki [156] improved by Dutt [309] is expressed as;

$$\Phi(S) = \begin{cases} -1.7817 + 0.927S + 0.143S^2 - 0.090S^3 & S < 0 \\ -1.7817 + 0.927S + 0.01696S^2 - 0.05148S^3 & 0 < S < 1.9475 \\ -4.41 \exp(-S/0.7176) & S > 1.9475 \end{cases} \quad (3.10)$$

here $S = (r - C_1 - C_2)/b$ and the surface width, $b = (\pi/\sqrt{3})a$ with $a = 0.55 \text{ fm}$.

3.2.3 Proximity 1977 (Prox-77)

Based on generalized theorem the universal function [310] is as follows;

$$\phi(S) = \begin{cases} \left(-\frac{1}{2}\right) (S_0 - 2.54)^2 - 0.0852(S_0 - 2.54)^3 & \text{for } S_0 < 1.2511 \\ -3.437 \exp\left(-\frac{S_0}{0.75}\right)^3 & \text{for } S_0 \geq 1.2511 \end{cases} \quad (3.11)$$

3.2.4 Modified proximity potential 1981 (MP-81)

Based on gently curved surfaces, Blocki et al., [310] proposed proximity potential. Later, during 1981 Blocki and Swiatecki [156] improved the proximity potential and it is given by;

$$\Phi(S) = \begin{cases} -1.7817 + 0.927S + 0.01696S^2 - 0.05148S^3 & 0 < S < 1.9475 \\ -4.41 \exp(-S/0.7176) & S > 1.9475 \end{cases} \quad (3.12)$$

3.2.5 Proximity 2013 (Prox-13)

Using double-folding model (DFM) with the density-dependent nucleon-nucleon interaction Zhang et al., [311] studied the universal function and it is expressed as;

$$\phi(S_0) = \frac{P_1}{1 + \exp\left(\frac{S_0 + P_2}{P_3}\right)} \quad (3.13)$$

with $S_0 = \frac{R-R_1-R_2}{b}$ and P_1 , P_2 and P_3 are the constants whose values are -7.65, 1.02 and 0.89 respectively [311].

3.2.6 Prox Ngo 1980 (Ng-80)

In 1980 Ngo [128] proposed a proximity potential between two gently curved surfaces and it is as follows;

$$\Phi(S) = \begin{cases} -33 + 5.4(S - S_0)^2 & S < S_0 \\ -33\exp[-1/5](S - S_0)^2 & S \geq S_0 \end{cases} \quad (3.14)$$

where $S_0 = -1.6fm$ [128].

3.2.7 Denisov 2002 (DP-00)

Using semi-microscopic potential approach Denisov [312] proposed proximity potential $\phi(S = r - R_1 - R_2 - 2.65)$ and is given by;

$$\Phi(S) = \begin{cases} 1 - S/0.7881663 + 1.229218S^2 - 0.2234277S^3 - 0.1038769S^4 \\ -\frac{R_1R_2}{R_1+R_2}(0.1844935S^2 + 0.07570101S^3) & \text{for } -5.65 \leq S \leq 0 \\ +(I_1 + I_2)(0.04470645S^2 + 0.0334687S^3) \\ 1 - S^2 \left[0.05410106 \frac{R_1R_2}{R_1+R_2} \exp\left(-\frac{S}{0.7881663}\right) \right] - 0.5395420(I_1 + I_2) \\ \exp\left(-\frac{S}{2.424408}\right) \times \exp\left(-\frac{S}{0.7881663}\right) & \text{for } S \geq 0 \end{cases}$$

The penetration probability using WKB integral is given by;

$$P = \exp \left[-\frac{2}{\hbar} \int_{R_{in}}^{R_{out}} \sqrt{2B(r)E(r) - E(sphere)} \right] \quad (3.15)$$

here R_{in} and R_{out} are the classical turning points with the conditions $V(r = R_{in}) = V(r = R_{out}) = Q$. μ is the reduced mass of the cluster and daughter nuclei. The half-lives of cluster

emission from the odd SH nuclei in the atomic number range $105 \leq Z \leq 125$ were evaluated using the following equation;

$$T_{1/2} = \left(\frac{\ln 2}{\lambda} \right) = \left(\frac{\ln 2}{P_0 \nu P} \right) \quad (3.16)$$

here decay constant λ is a function of assault frequency $\nu = \left(\frac{\omega}{2\pi} \right) = \left(\frac{2E_\nu}{h} \right)$. Here E_ν is the empirical zero point vibrational energy and it is expressed as;

$$E_\nu = Q \left[0.056 + 0.039 \exp \left(\frac{4 - A_e}{2.5} \right) \right] \text{ MeV} \quad (3.17)$$

Here A_e is the mass number of the emitted cluster particle. The term P in equation (3.16) is the penetration probability of the CD.

3.3 Coulomb and Proximity potential (CPPM)

The total potential is the sum of Coulomb ($V_c(R)$) and proximity ($V_N(R)$) potentials and it is evaluated as;

$$V(R) = V_N(R) + V_c(R) \quad (3.18)$$

The Coulomb potential is evaluated as follows;

$$V_c(R) = Z_1 Z_2 e^2 \begin{cases} \frac{1}{R} & \text{for } (R > R_c) \\ \frac{1}{2R_c} \left[3 - \left(\frac{R}{R_c} \right) \right] & \text{for } (R < R_c) \end{cases} \quad (3.19)$$

where Z_1 and Z_2 are the atomic numbers of daughter and cluster nuclei respectively. The radial distance is given by $R_c = 1.24(R_e + R_d)$. The different proximity functions such as MP-77,

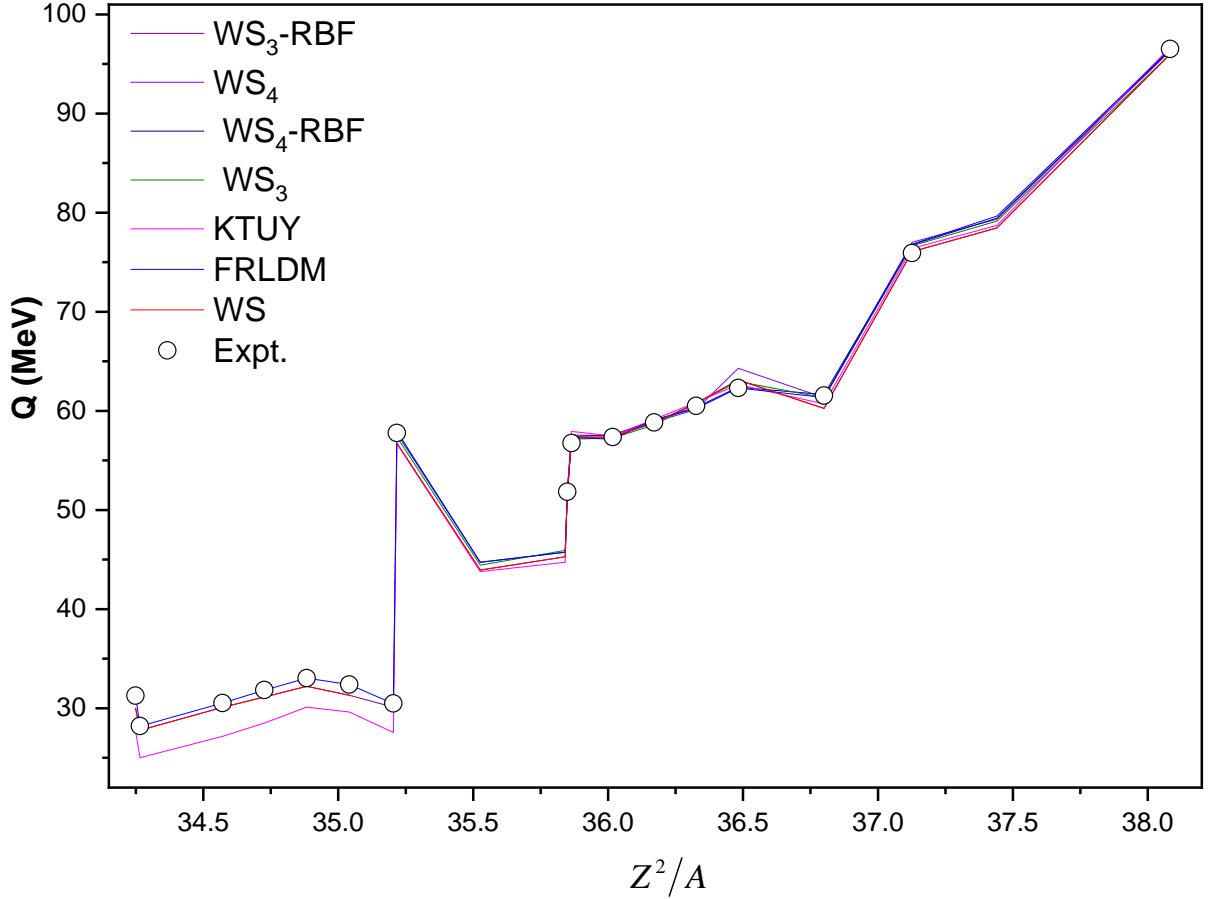


Fig. 3.1 A plot of $Q(\text{MeV})$ of even nuclei within the atomic number range $104 \leq Z \leq 126$ as a function of Z^2/A .

Prox-77, MP-81, Prox-13, Ng-80 and Dp-00 which were used in the evaluation of MGLDM are used to evaluate total potential. The penetration probability and half-lives are evaluated using the theory given in detail in Section 3.2.1.

3.4 Results

The sensitivity of Q-values in the evaluation of CD half-lives using different mass excess values such as Finite-Range Liquid-Drop Model (FRLDM) [313], Kourra-Tachibaba-Uno-Yamada (KTUY) [265, 314], Weizsacker-Skyrme (WS4) model [315], WS3+RBF [316], WS3 [317], WS [318] and Weizsacker-Skyrme (WS)+radial basis function (RBF) i.e WS4+RBF [315] were studied for the available experimental Q-values of cluster-radioactivity. The figure 3.1 shows plot of

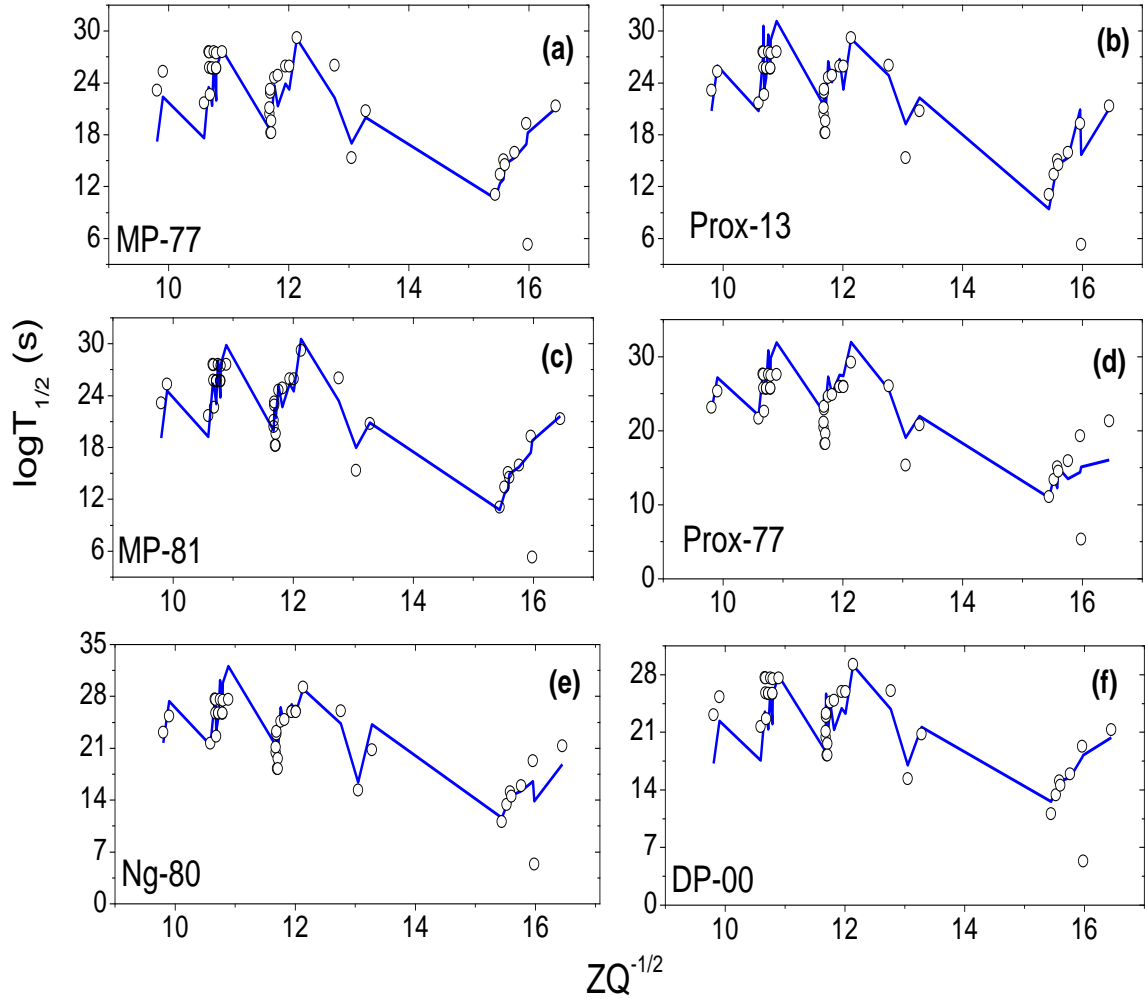


Fig. 3.2 A plot of experimental $\log T_{1/2}(s)$ as a function of Z/\sqrt{Q} .

Q-values using different mass excess values as a function of Z^2/A . The Q-values increases with increase in the function. The overall behaviour of Q-values are in good agreement with that of experimental Q-values. In order to identify the closure reproduction of experimental Q-values, the standard deviation is evaluated as follows;

$$\sigma = \left(\frac{1}{(n-1)} \sum_{i=1}^n (Q^{cal} - Q^{exp})^2 \right)^{1/2} \quad (3.20)$$

here n is the number of nuclei considered during CR. The deviation obtained using each mass excess values is tabulated in table 3.1. From the table it is inferred that the deviation obtained

Table 3.1 The standard deviation obtained using different mass excess values with that of experimental Q-values.

WS3-RBF	WS4	WS4-RBF	WS3	KTUY	FRLDM	WS
7.08	8.13	8.55	8.33	7.15	6.98	7.18

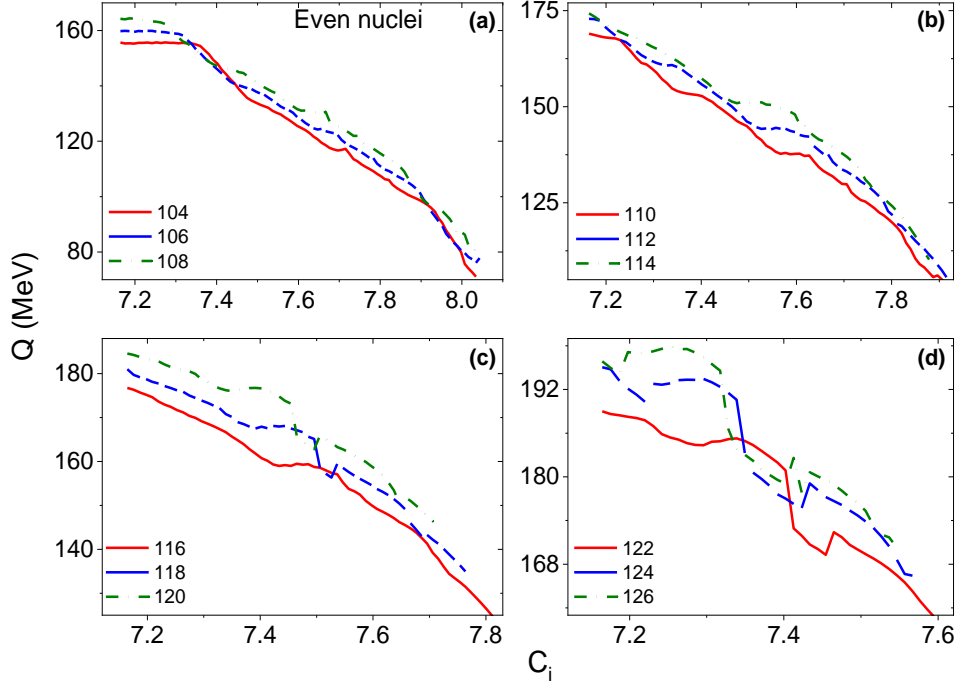


Fig. 3.3 A plot of Q value of even nuclei in the atomic number range $104 \leq Z \leq 126$ as a function of Sussmann central radii C_i .

using FRLDM is found to be smaller when compared to other models studied. Hence, in further investigation of CD half-lives, FRLDM mass excess values are used.

Furthermore, the suitable proximity potential is selected by plotting experimental $\log T_{1/2}(s)$ using different proximity functions as a function of Z/\sqrt{Q} and it is shown in figure 3.2. The standard deviation obtained for Prox-2013 is about $\sigma = 1.62$ with that of available experiments. Hence, in further analysis, Prox-2013 proximity function is considered for the evaluation of cluster-decay half-lives. Evaluation of cluster emitters within the range He to Ca viz; ${}^4\text{He}$, ${}^6\text{Li}$, ${}^9\text{Be}$, ${}^{20-22}\text{Ne}$, ${}^{23}\text{Na}$, ${}^{24-26}\text{Mg}$, ${}^{27}\text{Al}$, ${}^{28-30}\text{Si}$, ${}^{31}\text{P}$, ${}^{32-34}\text{S}$, ${}^{35}\text{Cl}$, ${}^{36,38,40}\text{Ar}$, ${}^{39}\text{K}$ and ${}^{40,42-44,46}\text{Ca}$ is evaluated for the even SH nuclei within the atomic number range $104 \leq Z \leq 126$.

In the figure 3.3, variation of Q-value with the Sussmann central radii C_i is represented for

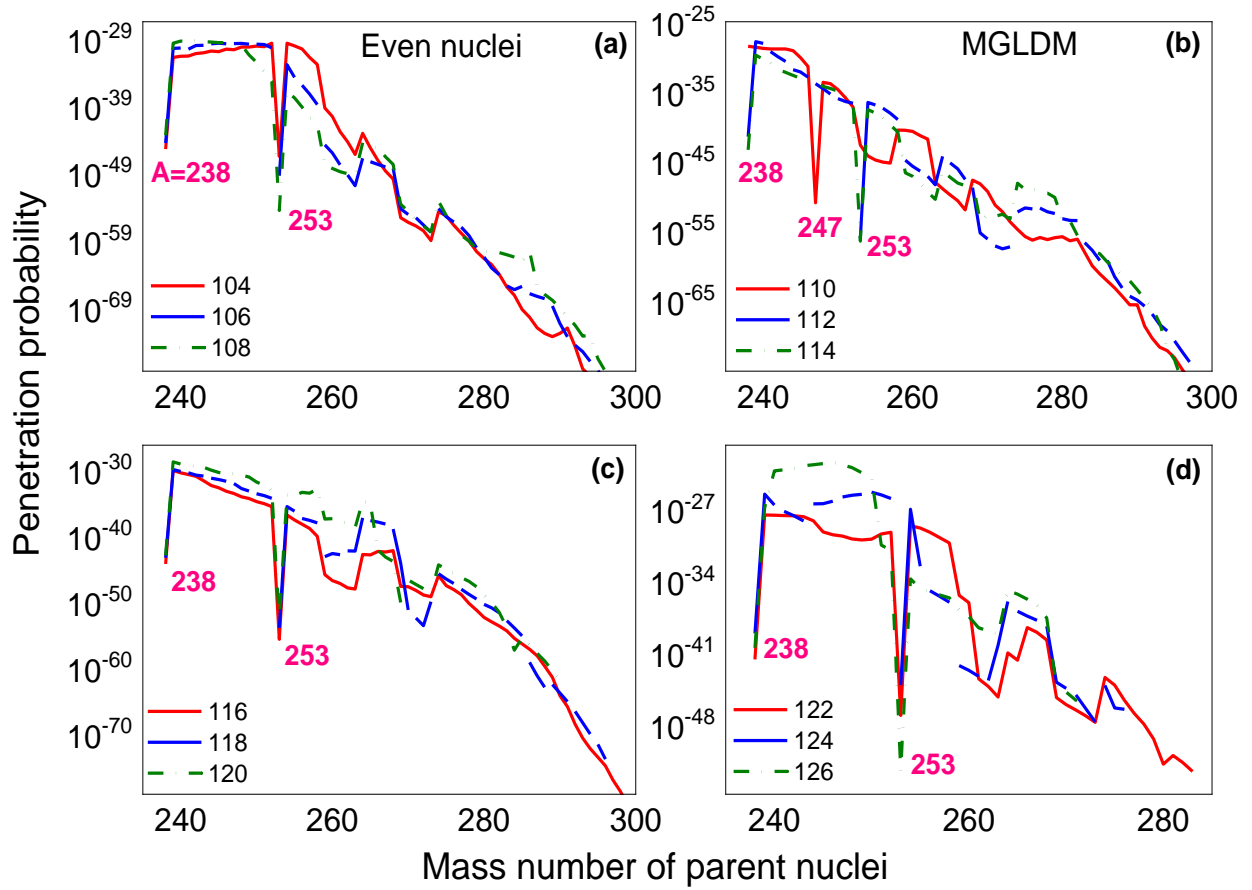


Fig. 3.4 A plot of penetration probability of even nuclei in the atomic number range $104 \leq Z \leq 126$ evaluated using MGLDM model with mass number of parent nuclei.

even nuclei's with in the atomic number range $104 \leq Z \leq 126$. From the graph it is clear that Q-value is varying inversely proportional to the Sussmann central radii. The penetration probability evaluated within the atomic number range $104 \leq Z \leq 126$ and it is represented in figure 3.4. As the mass number of parent nuclei increases the penetration probability gradually decreases. There is a sudden decrease in the penetration probability when $A=238$ and $A=253$ within the atomic number range $104 \leq Z \leq 126$. The penetration probability is inversely proportional to half-lives. hence the smaller penetration probability leads to larger the half-lives when mass of the parent nuclei is equal to 238 and 253.

Once, the penetration probability is evaluated using the WKB integral with the boundary conditions, half-lives of even nuclei within the atomic number range $104 \leq Z \leq 126$ is studied.

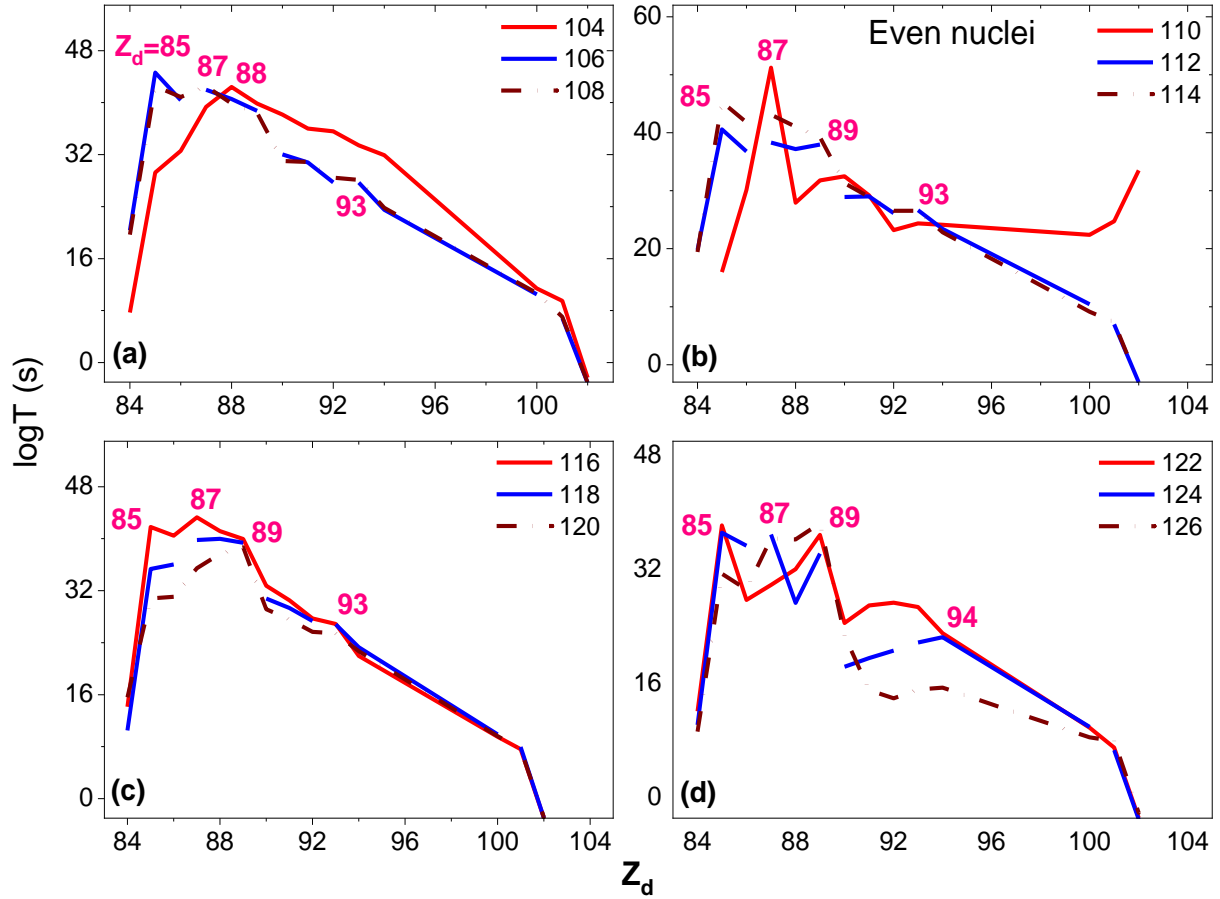


Fig. 3.5 A plot of $\log T_{1/2}(s)$ of even nuclei in the atomic number range $104 \leq Z \leq 126$ as a function of atomic number of daughter nuclei.

The figure 3.5 shows plot of $\log T_{1/2}(s)$ as a function of Z_d . In all the even SH nuclei, the larger $\log T_{1/2}$ is observed when Z_d is with in atomic range 85 to 89, i.e when atomic number is near the magic number.

In addition to plot of $\log T_{1/2}$ as a function of Z_d and also plotted $\log T_{1/2}$ as function of N_C . The figure 3.6 shows an increase in logarithmic half-lives with increase in cluster neutron number. It reaches maximum when N_C is equal to 20 and again it gradually decreases. The figure 3.6(a) and (b) shows larger stability when N_C is equal to 20 and 23 when compared to their neighbouring nuclei. Similarly, the figure 3.6(c) shows peaks when N_C is equal to 16, 20 and 23. Furthermore, the logarithmic half-lives are larger in case of even SH nuclei with $Z=122$ and 124 at $N_C=11, 16, 20$ and 23 . Hence, the even SH nuclei with $104 \leq Z \leq 126$ shows stability against these cluster

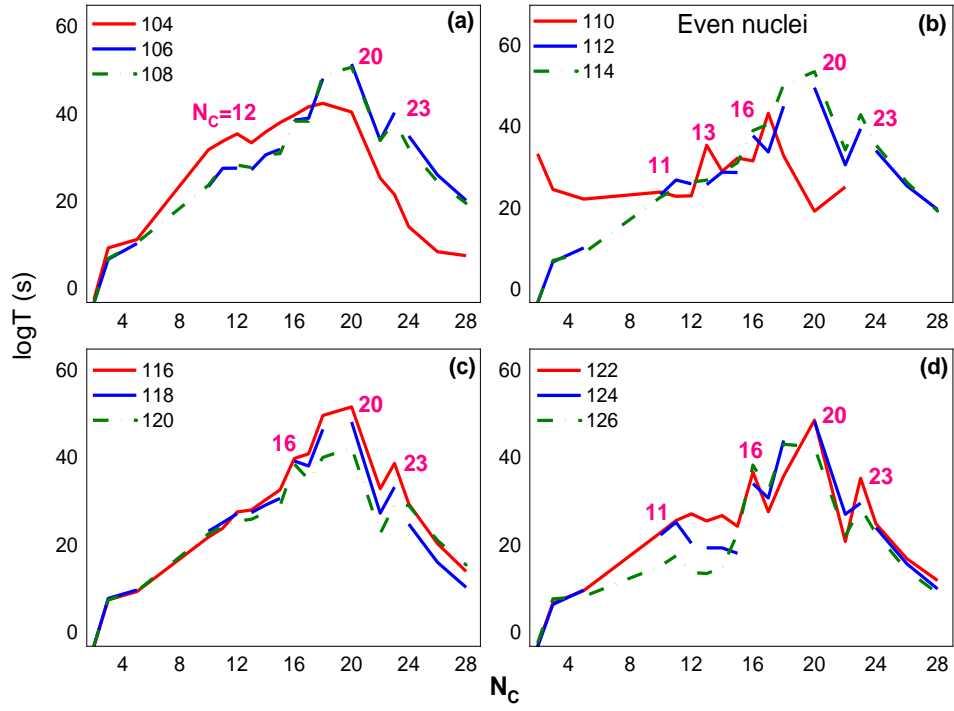


Fig. 3.6 Comparison of $\log T_{1/2}(s)$ of even nuclei as a function of neutron number of cluster nuclei (N_c)

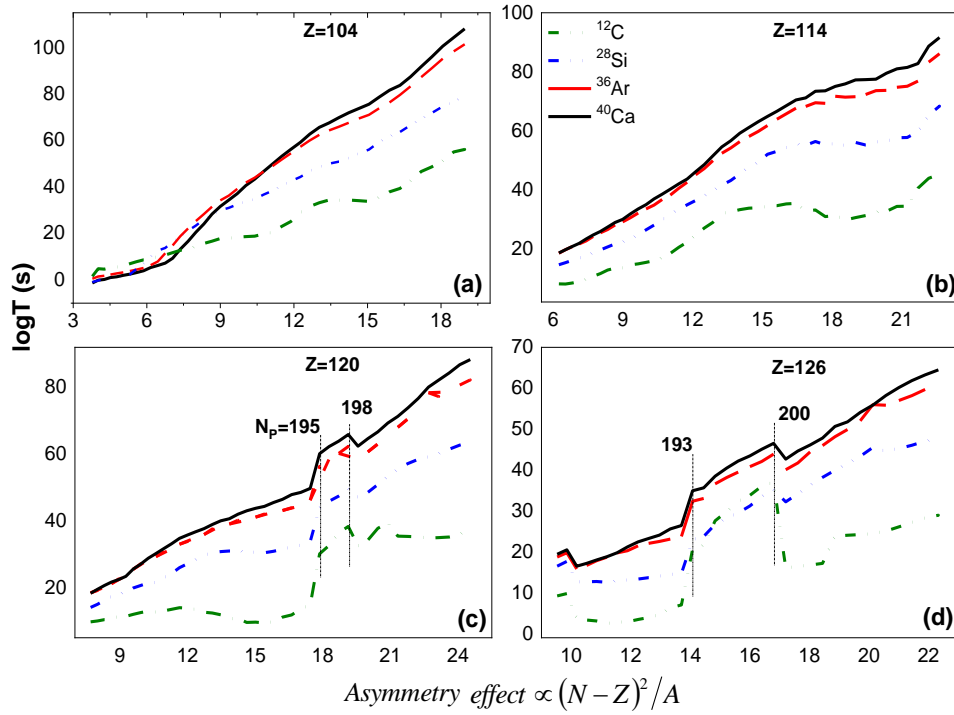


Fig. 3.7 A plot of $\log T_{1/2}(s)$ of even nuclei within the atomic number range $104 \leq Z \leq 126$ as a function of $(N - Z)^2/A$ for different cluster emissions such as ^{12}C , ^{28}Si , ^{36}Ar and ^{40}Ca in case of (a) $Z=104$, (b) $Z=114$, (c) $Z=120$ and (d) $Z=126$.

emissions with neutron number is between 11 to 23.

The number of neutrons and protons significantly contributes the logarithmic half-lives. A plot of logarithmic half-lives as a function of $(N - Z)^2/A$ is shown in figure 3.7. The $\log T_{1/2}$ values increases with increase in $(N - Z)^2/A$ value. The disparity between emitted protons and neutrons causes a sudden increase in $\log T_{1/2}$ values when $(N - Z)^2/A$ is nearly equal to 12 and above in case of $Z=104$ during ^{12}C emission. Similarly, in case of $Z=114$, the $\log T_{1/2}$ value decreases when $(N - Z)^2/A$ is greater than 12. In case of $Z=120$ and 126 the $(N - Z)^2/A$ is 18 and 14 respectively at which the $\log T_{1/2}$ value shows an unexpected increase.

The function $Z^2/A^{1/3}$ is involved in the Coulomb effect in the evaluation of binding en-

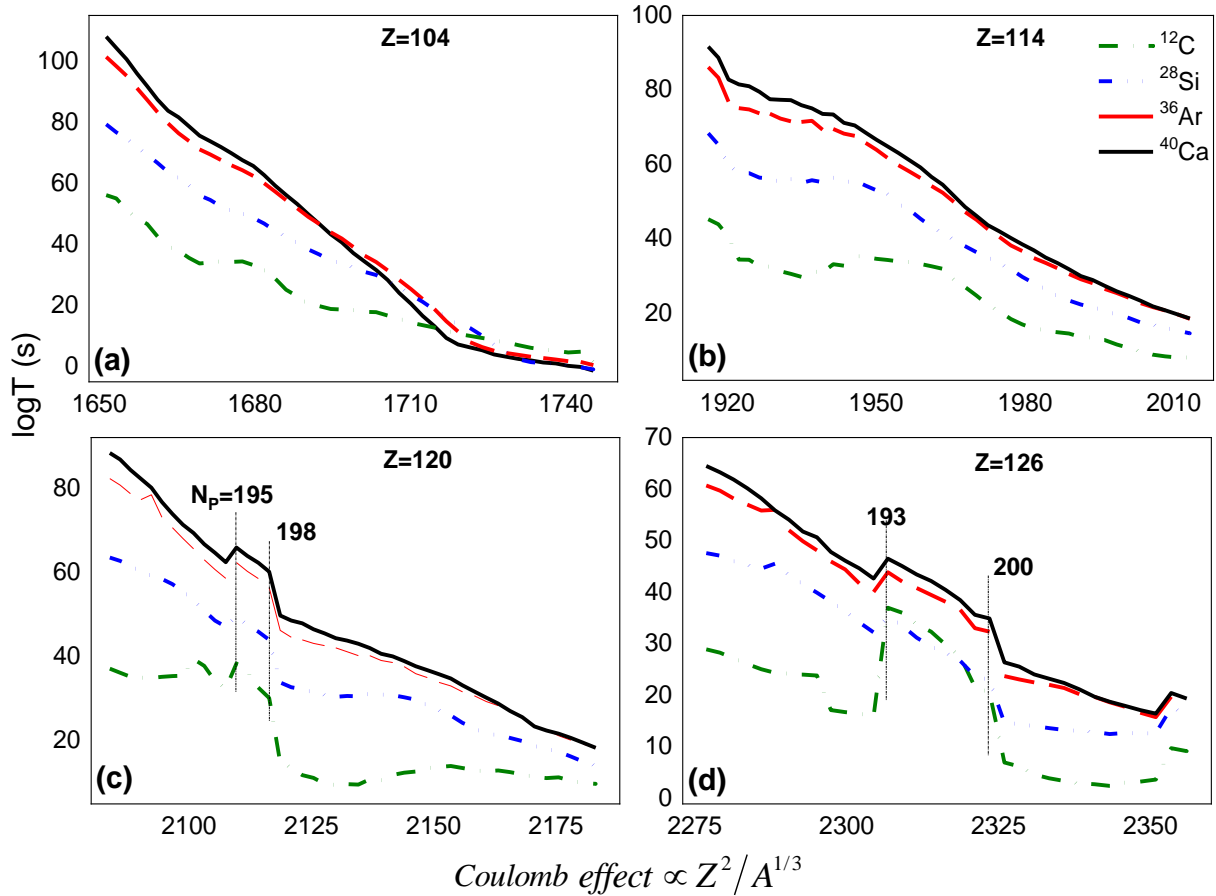


Fig. 3.8 A plot of $\log T_{1/2}(s)$ of even nuclei within the atomic number range $104 \leq Z \leq 126$ as a function of $Z^2/A^{1/3}$ for different cluster emissions such as ^{12}C , ^{28}Si , ^{36}Ar and ^{40}Ca in case of (a) $Z=104$, (b) $Z=114$, (c) $Z=120$ and (d) $Z=126$.

ergy. The repulsive force between two nuclei reduces the binding energy. It is also evident that as

$Z^2/A^{1/3}$ increases the logarithmic half-lives gradually decreases i.e when there is an increase in Coulomb repulsive force then the life-time of the compound nuclei gradually decreases. A plot of $\log T_{1/2}$ as a function of $Z^2/A^{1/3}$ is shown in figure 3.8(a-d) for atomic number $Z=104, 114, 120$ and 126 .

Another important term is pairing effect, it is an attractive interaction between two nucleons.

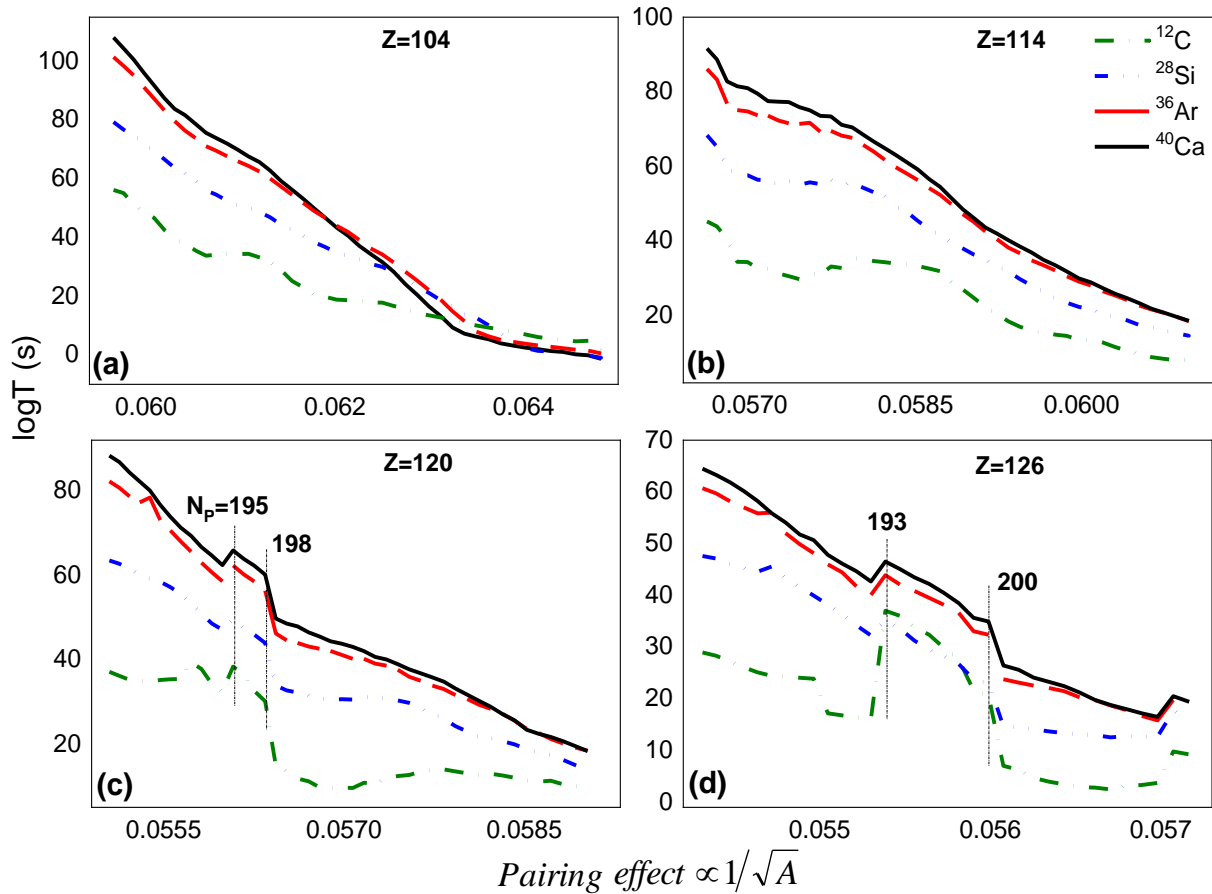


Fig. 3.9 A plot of $\log T_{1/2}(s)$ of even nuclei within the atomic number range $104 \leq Z \leq 126$ as a function of pairing effect ($1/\sqrt{A}$).

Earlier studies [319, 320] were pointed out that the pairing energy of protons are greater than that of neutrons with $N=50$ and $N=82$. The figure 3.9(a-d) shows a plot of $\log T_{1/2}$ as function of pairing effect i.e $1/\sqrt{A}$. As the effect of pairing effect increases between two nuclei the corresponding half-lives decreases. The attractive interaction between two nucleons decreases when the two nuclei are far apart. Hence, the half-lives of parent nuclei also decreases. From the figure 3.9(c) the

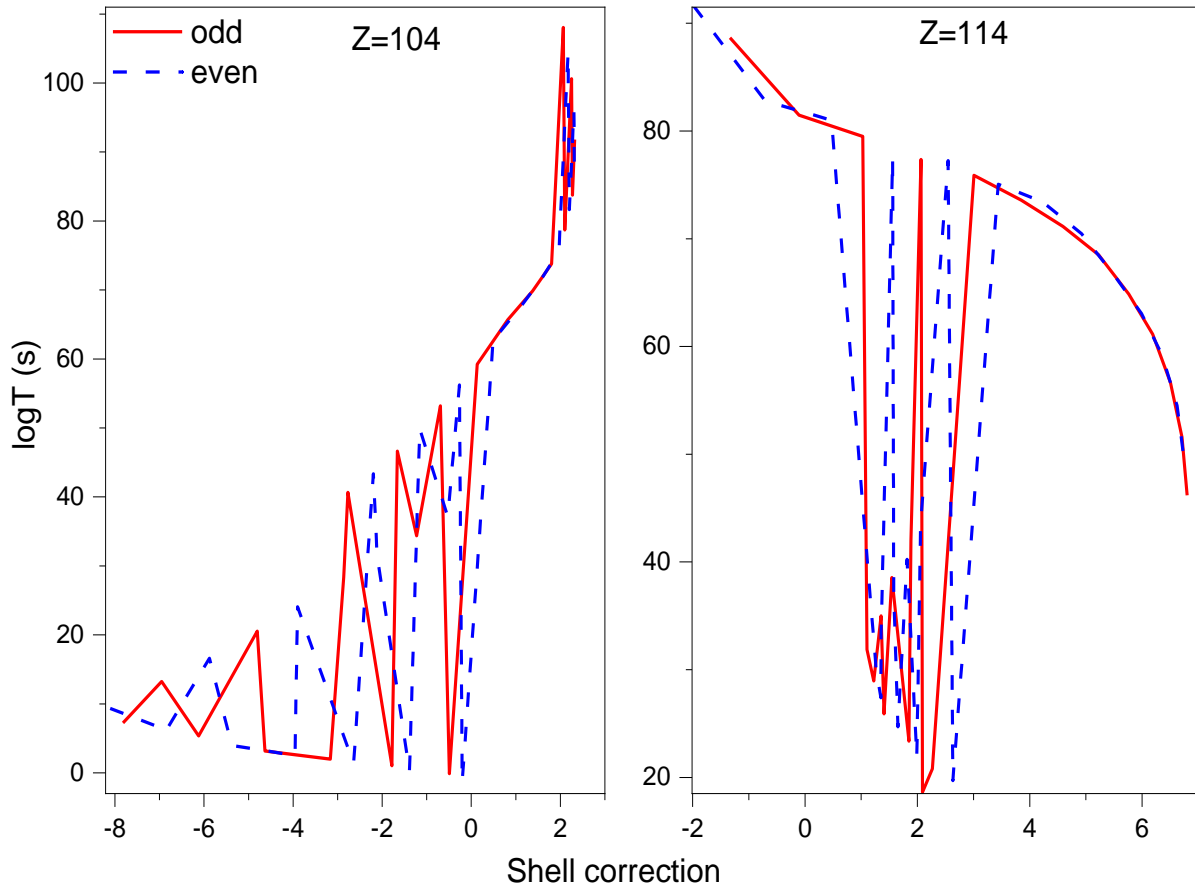


Fig. 3.10 A plot of logarithmic half-lives as function of shell corrections for (a) $Z=104$ and (b) 114 .

stability of half-lives when pairing effect value is above 0.560, that is when the neutron number is from 195 to 198 which is near the second generation magic number $N=196$. Hence, due to shell effects the unexpected increase in the $\log T_{1/2}$ values were observed from the parent nuclei $Z=120$. Similarly, in case of $Z=126$ unexpected increase in the $\log T_{1/2}$ values were observed when $N=193$ and $N=200$ and is as shown in figure 3.9(d) for the parent nuclei $Z=126$.

Seeger[321] effectively introduced the shell correction term which is a function of neutron and proton number. The shell correction term allows for the explanation of magical nuclei by anticipating different factors such as proton separation energies, neutron separation energies, and so on. It also play an important role in shell structure. The figure 3.10 illustrate the role of shell effects on the logarithmic half-lives in case of $Z=104$ and 114 . Both odd and even mass of daugh-

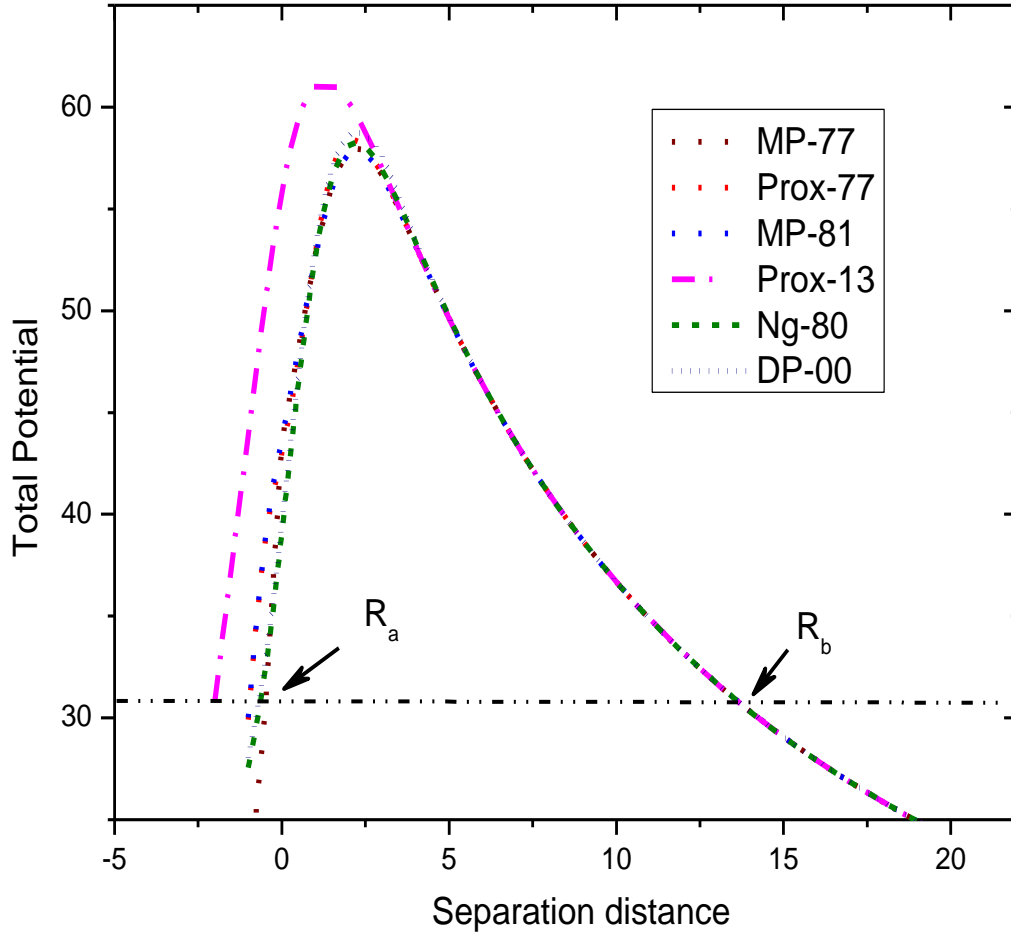


Fig. 3.11 A variation of total potential using different proximity potential functions such as MP-77, Prox-77, MP-81, Prox-13, Ng-80 and DP-00 with the separation distance between the two nuclei in case of ^{262}Db parent nuclei during the cluster emission of ^{14}C .

ter nuclei is considered during an evaluation of half-lives. In both the cases, the continuous line specifies the data corresponding to odd mass number of daughter nuclei and dotted lines for the even nuclei. However, no systematic variation of logarithmic half-lives is observed with respect to shell corrections. From the detail analysis of logarithmic half-lives as function of Coulomb term, asymmetry term, pairing term and shell corrections on CR half-lives in the even SH nuclei within the atomic number range $104 \leq Z \leq 126$ will guide for further investigations. Both MGLDM and CPPM is used to evaluate cluster emitters such as ^4He , ^6Li , ^9Be , $^{20-22}\text{Ne}$, ^{23}Na , $^{24-26}\text{Mg}$, ^{27}Al , $^{28-30}\text{Si}$, ^{31}P , $^{32-34}\text{S}$, ^{35}Cl , $^{36,38,40}\text{Ar}$, ^{39}K and $^{40,42-44,46}\text{Ca}$ using various versions of proximity functions such as MP-77, Prox-77, MP-81, Prox-13, Ng-80 and Dp-00 for the odd SH nuclei within

Table 3.2 The standard deviation obtained using different mass excess values with that of experimental Q-values.

WS3-RBF	WS4	WS4-RBF	WS3	KTUY	FRLDM	WS
7.08	8.13	8.55	8.33	7.15	6.98	7.18

the atomic number range $105 \leq Z \leq 125$.

The figure 3.11 presents the variation of total scattering potential as a function of separation distance between two nuclei. The SHN ^{262}Db as an example, the comparable potential distributions have been also observed in the case of other studied nuclei. It is also well known fact that the area under the curve gives penetration probability. Again penetration probability is inversely proportional to half-lives. Smaller penetration probability results in longer half-lives and vice-versa. The figure clearly shows larger area for proximity function Prox-13 when compared to other proximity functions studied. It is also evident that the values obtained from the proximity functions such as MP-77, Prox-77, MP-81, Ng-80 and Dp-00 produces total potential almost of same nature. The penetration probability is evaluated using the boundary conditions as shown in figure 3.11.

The sensitivity of Q-values in the evaluation of CD half-lives using different mass excess values such as Finite-Range Liquid-Drop Model (FRLDM) [313], Kourra-Tachibaba-Uno-Yamada (KTUY) [265, 314], Weizsacker-Skyrme (WS4) model [315], WS3+RBF [316], WS3 [317], WS [318] and Weizsacker-Skyrme (WS)+radial basis function (RBF) i.e WS4+RBF [315] were studied.

The percentage of deviation obtained using various mass excess values with that of experiments is shown in figure 3.12. The experimental Q-values are extracted from the literature [280]. From the figure it is noticed that the values obtained from FRLDM is found to be in good agreement with that of experimental Q-values. The standard deviation produced by each mass excess

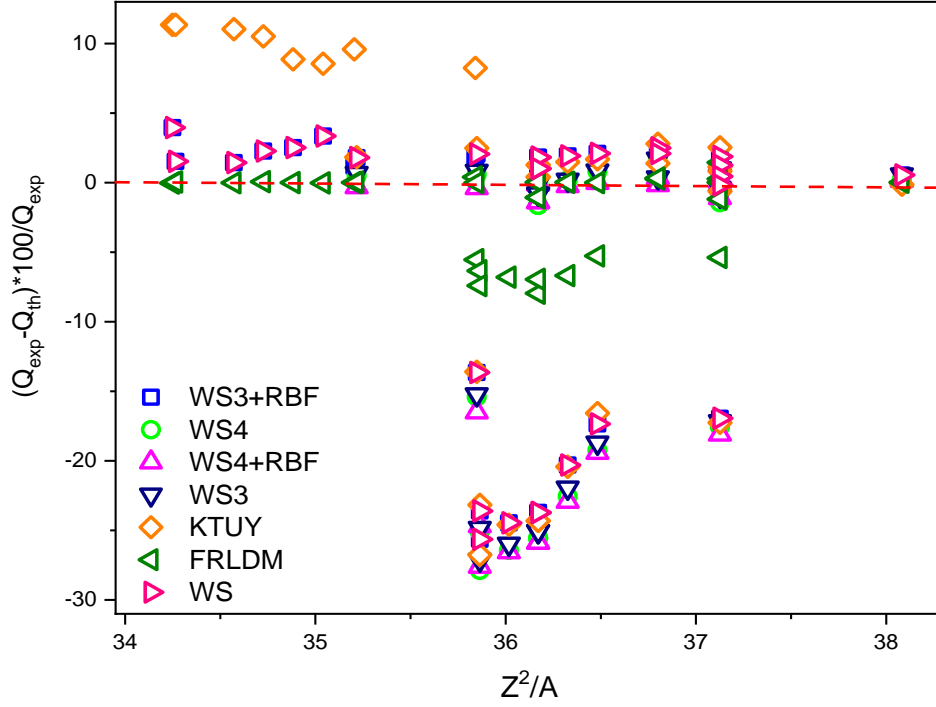


Fig. 3.12 Percentage of deviation of decay energies using mass excess models such as WS3+RBF, WS4, WS4+RBF, WS3, KTUY, FRLDM and WS with that of available experimental data as a function of Z^2/A .

values are evaluated as follows;

$$\sigma = \left(\frac{1}{(n-1)} \sum_{i=1}^n (Q^{cal} - Q^{exp})^2 \right)^{1/2} \quad (3.21)$$

here n is the number of nuclei considered during CR. The deviation obtained using each mass excess values is tabulated in table 3.2. From the table it is inferred that the deviation obtained using FRLDM is found to be smaller when compared to other models studied. Hence, in further investigation of CD half-lives FRLDM mass excess values are used.

Further, confirmation of Q -values with close reproduction of experimental values, the variation of Q -values as a function of Sussmann central radii C_i in the atomic number range $105 \leq Z \leq 125$ is studied. A plot of Q -values as a function of C_i is plotted in figure 3.13. The Q -values decreases with increase in Sussman central radii.

The different proximity functions such as MP-77, Prox-77, MP-81, Prox-13, Ng-80 and

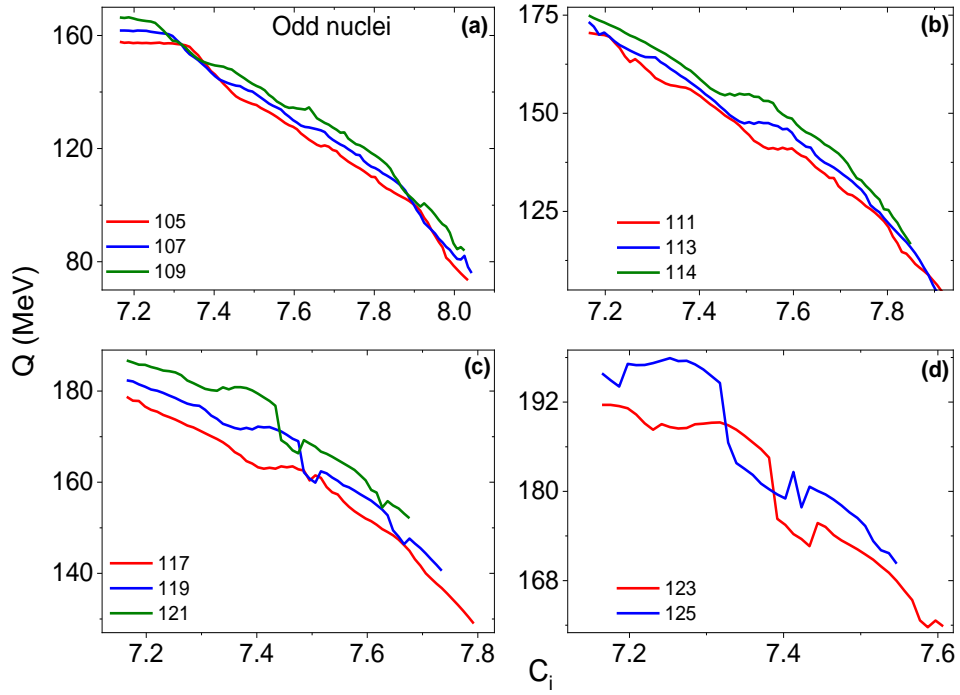


Fig. 3.13 A plot of Q values of odd nuclei in the atomic number range $105 \leq Z \leq 125$ as a function of Sussmann central radii C_i .

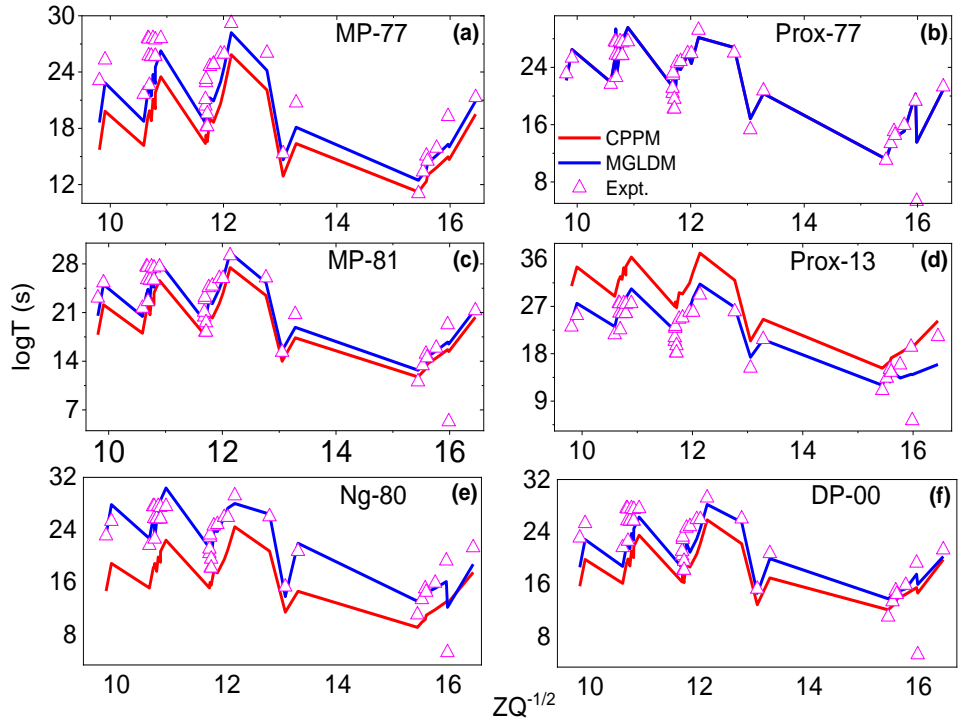


Fig. 3.14 Comparison of $\log T_{1/2}(s)$ values obtained using different proximity functions both in case of CPPM and MGLDM as a function of Z/\sqrt{Q} with that of available experimental CD half-lives.

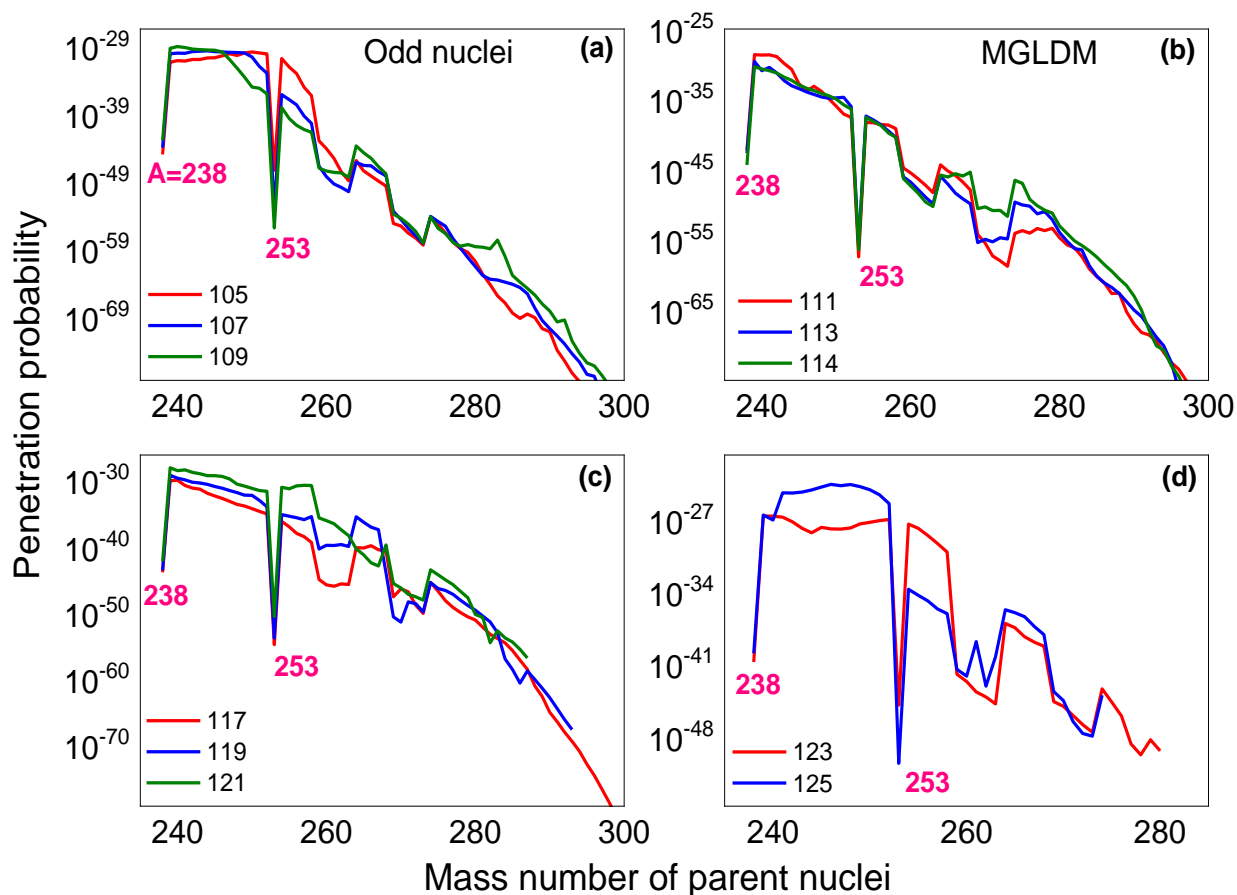


Fig. 3.15 A plot of penetration probability of odd nuclei in the atomic number range $105 \leq Z \leq 125$ evaluated using MGLDM model with mass number of parent nuclei.

DP-00 were used to evaluate half-lives using CPPM and MGLDM. The values obtained using different proximity potentials were compared with that of available experimental data [280]. The figure 3.14 shows the plot of logarithmic half-lives of CR with that of Z/\sqrt{Q} . The closure look of the figure shows the logarithmic half-lives obtained using Prox-13 proximity potential produces less deviation when compared to other studied proximity functions both in case of CPPM and MGLDM.

The penetration probability evaluated using MGLDM model using Proximity function Prox-13 within the atomic number range $105 \leq Z \leq 125$ and it is represented in figure 3.15. As the mass number of parent nuclei increases the penetration probability gradually decreases. Similar trend is also observed in the CPPM. There is a sudden decrease in the penetration probability

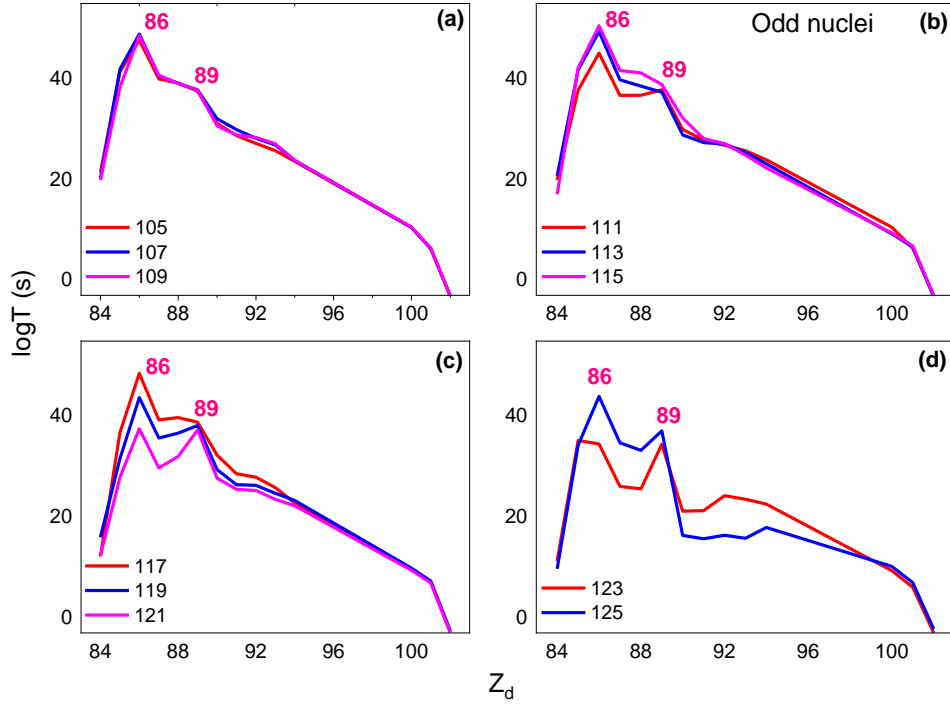


Fig. 3.16 A plot of $\log T_{1/2}(s)$ of odd nuclei in the atomic number range $105 \leq Z \leq 125$ as a function of atomic number of daughter nuclei.

when $A=238$ and $A=253$ within the atomic number range $105 \leq Z \leq 125$, since the penetration probability is inversely proportional to half-lives. Hence, the smaller penetration probability leads to larger half-lives when mass of the parent nuclei is equal to 238 and 253. Once, the penetration probability is evaluated using the WKB integral with the boundary conditions, half-lives of odd nuclei within the atomic number range $105 \leq Z \leq 125$ is studied. The standard deviation produced by CPPM is found to be $\sigma = 1.73$ and in case of MGLDM the deviation is about $\sigma = 1.62$. Hence, in our further analysis CD half-lives produced by MGLDM with less deviation with respect to experimental data is considered. The figure 3.16 shows plot of $\log T_{1/2}(s)$ as a function of Z_d . In all the odd SH nuclei, the larger $\log T_{1/2}$ is observed when Z_d is equal to 86 and 89. The larger value of $\log T_{1/2}$ is observed when atomic number is near the magic number.

The atomic number of different cluster emissions from Helium to Calcium were considered. The corresponding logarithmic half-lives were plotted as a function of Z_C and it is as shown in figure 3.17. From the figure 3.17(a), larger half-lives are observed when Z_C is nearly equal to 16

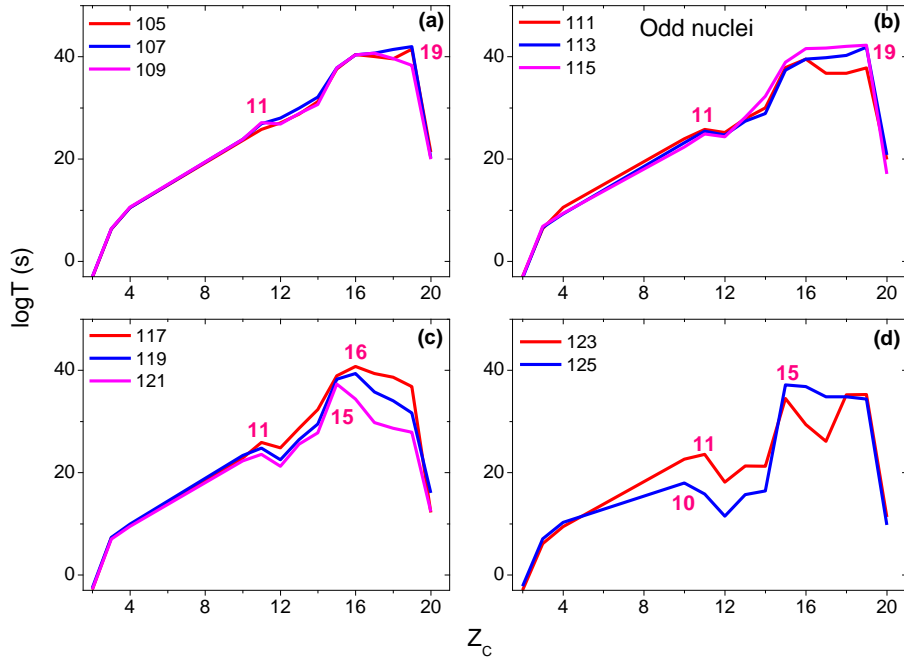


Fig. 3.17 A plot of $\log T_{1/2}(s)$ of odd nuclei as a function of atomic number of cluster nuclei and 19 in case of $Z=105, 107$ and 109 . Similarly, larger half-lives were also observed in case of odd SH nuclei from $Z=111$ to 125 as shown in figure 3.17(b-c) when Z_C is nearly equal to 16 and 19. In case of figure 3.17(d), the larger half-lives are observed when Z_C is equal to 15 and 19. The larger half-lives are due to magic number of cluster atomic number i.e these odd SH nuclei are more stable when Z_C is from Sulphur to Potassium.

In addition to plot of $\log T_{1/2}$ as a function of Z_d and Z_c , $\log T_{1/2}$ as function of N_C is also plotted. The figure 3.18 shows an increase in logarithmic half-lives with increase in cluster neutron number. It reaches maximum when N_C is equal to 20 and again it gradually decreases. The figure 3.18(a) and (b) shows larger stability when N_C is equal to 11 and 20. Similarly, the figure 3.18(c) shows peaks when N_C is equal to 12, 16 and 20. Furthermore, the logarithmic half-lives are larger in case of odd SH nuclei with $Z=123$ and 125 at $N_C=11, 16$ and 20 . Hence, the odd SH nuclei with $105 \leq Z \leq 125$ shows stability against these cluster emissions with neutron number between 11 to 20.

In addition to evaluation of half-lives, the role of entrance channel parameters such as Z^2/A

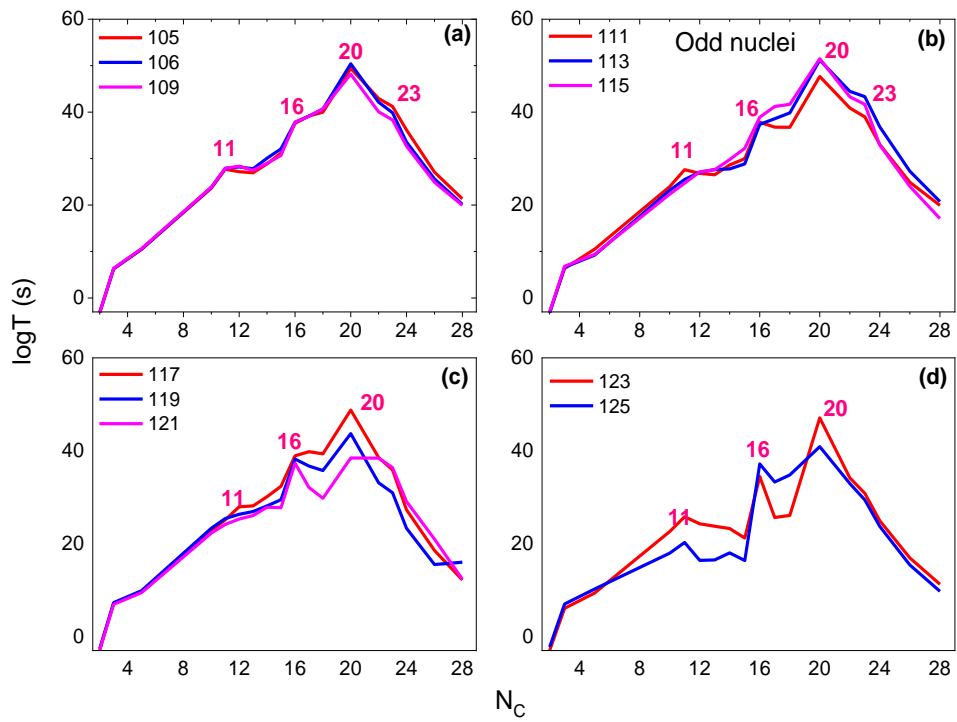


Fig. 3.18 Comparison of $\log T_{1/2}(s)$ of odd nuclei as a function of neutron number of cluster nuclei

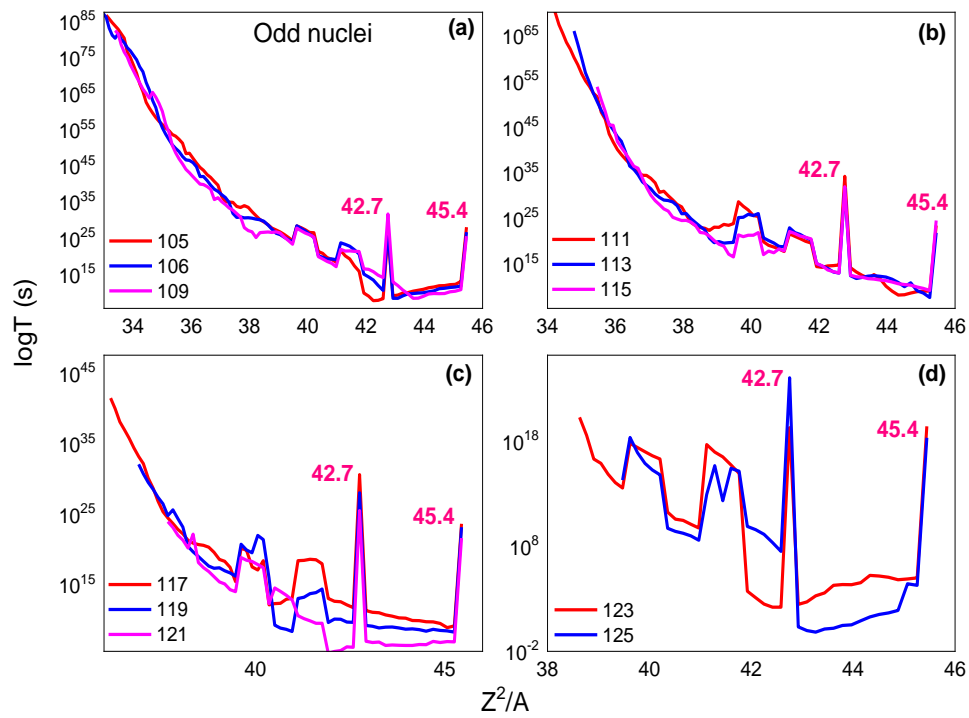


Fig. 3.19 A plot of $\log T_{1/2}(s)$ of odd nuclei within the atomic number range $105 \leq Z \leq 125$ as a function of Z^2/A .

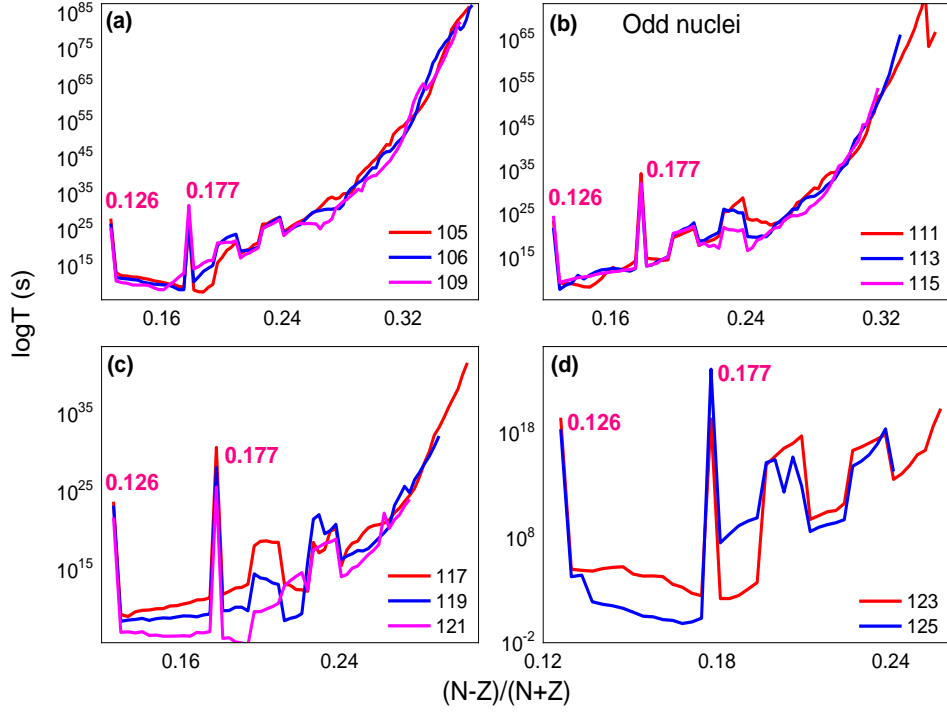


Fig. 3.20 A plot of $\log T_{1/2}(s)$ of odd nuclei within the atomic number range $105 \leq Z \leq 125$ as a function of $(N - Z)/(N + Z)$.

and $(N - Z)/(N + Z)$ are also studied. A plot of $\log T_{1/2}$ as a function of Z^2/A is shown in figure 3.19. The linear dependence of logarithmic half-lives were observed as a function of Z^2/A . From the figure 3.19(a) larger $\log T_{1/2}$ is observed when Z^2/A nearly equal to 42.7 and 45.4 for the atomic number $Z=105, 107$ and 109 . Similar variation is also observed in case of odd SH nuclei in the atomic number range $111 \leq Z \leq 125$. Hence, these nuclei also shows extra stability when Z^2/A is at 42.7 and 45.4. Similarly, the variation of $\log T_{1/2}$ as a function of entrance channel parameter $(N - Z)/(N + Z)$ is studied. Figure 3.20 shows plot of $\log T_{1/2}$ as function of $(N - Z)/(N + Z)$. As the value of $(N - Z)/(N + Z)$ increases the $\log T_{1/2}$ value gradually decreases. The larger value of $\log T_{1/2}$ is observed when the value of $(N - Z)/(N + Z)$ is equal to 0.126 and 0.177. Hence, the overall stability of odd SH nuclei within the atomic number range $105 \leq Z \leq 125$ were observed to be more stable against different cluster emissions when atomic and neutron number is nearly equal to magic number. The CR half-lives of experimentally available cluster emitters were evaluated using MGLDM as explained in the theory section 3.2.

Here, the experimental Q-values for the evaluation of cluster-decay half-lives for the experimentally available cluster emitters are used. The table 3.3 shows evaluated cluster-decay half-lives

Table 3.3 Comparison of cluster-decay half-lives evaluated using present work (PW) with the available experiments.

Decay	Q_{Exp} (MeV)	$\log T_{1/2}^{exp}$	$\log T_{1/2}^{PW}$
$^{221}\text{Fr} \rightarrow ^{14}\text{C} + ^{207}\text{Tl}$	31.317	14.51[322]	15.59
$^{221}\text{Ra} \rightarrow ^{14}\text{C} + ^{207}\text{Pb}$	32.396	13.37[322]	14.56
$^{222}\text{Ra} \rightarrow ^{14}\text{C} + ^{208}\text{Pb}$	33.05	11.05[323]	13.70
$^{223}\text{Ra} \rightarrow ^{14}\text{C} + ^{209}\text{Pb}$	31.829	15.05[323]	14.94
$^{224}\text{Ra} \rightarrow ^{14}\text{C} + ^{210}\text{Pb}$	30.54	15.9[324]	16.52
$^{226}\text{Ra} \rightarrow ^{14}\text{C} + ^{212}\text{Pb}$	28.2	21.29[325]	22.74
$^{225}\text{Ac} \rightarrow ^{14}\text{C} + ^{211}\text{Bi}$	30.477	17.16[326]	17.86
$^{228}\text{Th} \rightarrow ^{20}\text{O} + ^{208}\text{Pb}$	44.72	20.73[327]	21.94
$^{230}\text{U} \rightarrow ^{22}\text{Ne} + ^{208}\text{Pb}$	61.4	19.56[328]	19.21
$^{230}\text{Th} \rightarrow ^{24}\text{Ne} + ^{206}\text{Hg}$	57.571	24.61[280]	23.87
$^{231}\text{Pa} \rightarrow ^{24}\text{Ne} + ^{207}\text{Tl}$	60.417	22.89[280]	22.07
$^{232}\text{U} \rightarrow ^{24}\text{Ne} + ^{208}\text{Pb}$	62.31	20.39[329]	21.25
$^{233}\text{U} \rightarrow ^{24}\text{Ne} + ^{209}\text{Pb}$	60.486	24.84[280]	23.75
$^{234}\text{U} \rightarrow ^{26}\text{Ne} + ^{208}\text{Pb}$	59.466	25.93[330, 331]	24.46
$^{234}\text{U} \rightarrow ^{28}\text{Mg} + ^{206}\text{Hg}$	74.11	25.74[332]	26.04
$^{236}\text{Pu} \rightarrow ^{28}\text{Mg} + ^{208}\text{Pb}$	79.67	21.65[280]	22.67
$^{238}\text{Pu} \rightarrow ^{28}\text{Mg} + ^{210}\text{Pb}$	75.912	25.66[333]	26.93
$^{238}\text{Pu} \rightarrow ^{30}\text{Mg} + ^{208}\text{Pb}$	77	25.66[333]	25.26
$^{238}\text{Pu} \rightarrow ^{32}\text{Si} + ^{206}\text{Hg}$	91.19	25.3[334]	27.85
$^{242}\text{Cm} \rightarrow ^{34}\text{Si} + ^{208}\text{Pb}$	96.509	23.11[335]	23.24

using MGLDM with the available experiments. The average deviation and standard deviation is evaluated using the following expressions;

$$\delta = \frac{1}{n} \sum_{i=1}^n |\log T_{1/2}^{PW} - \log_{1/2}^{exp}| \quad (3.22)$$

and

$$\sqrt{\delta^2} = \sqrt{\frac{1}{n} \sum_{i=1}^n [\log T_{1/2}^{PW} - \log_{1/2}^{exp}]^2} \quad (3.23)$$

The average deviation (δ) and standard deviation ($\sqrt{\delta^2}$) are evaluated for 20 experimental val-

ues available in the literature. The value of δ and $\sqrt{\delta^2}$ are found to be 1.01 and 1.202, respectively.

The amount of energy released during the CR is evaluated using the mass excess values avail-

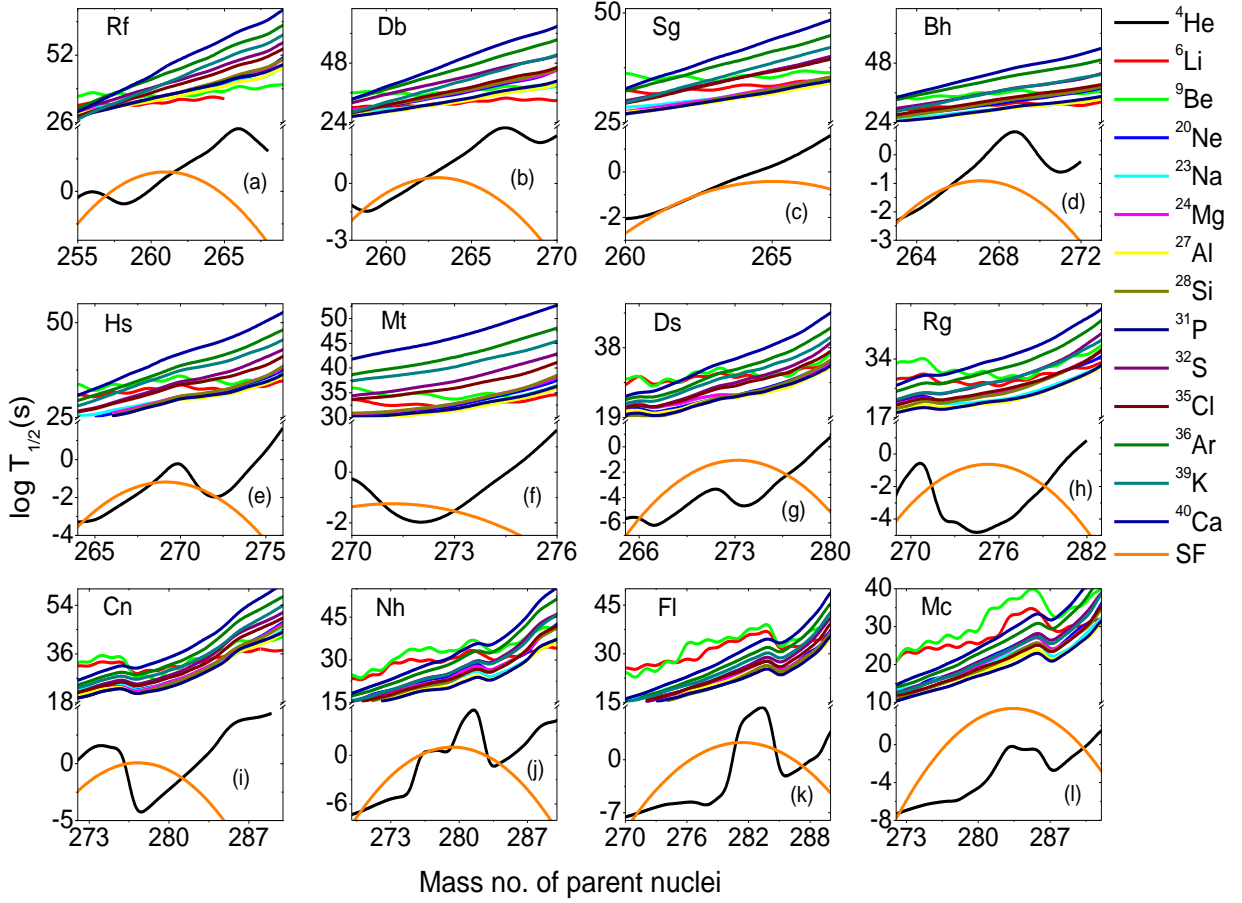


Fig. 3.21 Plot of evaluated $\log T_{1/2}$ values vs mass number of parent nuclei for the emission of cluster (${}^4\text{He}$ to ${}^{48}\text{Ca}$) and spontaneous fission from SH region $104 \leq Z \leq 115$.

able in the literature [336]. In figure 3.21 and 3.22, the half-lives of possible cluster emissions from ${}^4\text{He}$ to ${}^{40}\text{Ca}$ and spontaneous fission in the SH region $104 \leq Z \leq 115$ and $116 \leq Z \leq 126$ respectively are studied. The spontaneous fission half-lives of SH nuclei in the region $104 \leq Z \leq 126$ are evaluated using semi-empirical formula proposed by Xu et al., [337] is as follows;

$$T_{1/2} = \exp[2\pi (C_0 + C_1A + C_2A^2 + C_3Z^4 + C_4(N - Z)^2) - (0.13323Z^2/A^{1/3} - 11.64)] \quad (3.24)$$

where, C_0, C_1, C_2, C_3 and C_4 are -195.09227, 3.10156, -0.04386, 1.40301×10^{-6} and -0.03199

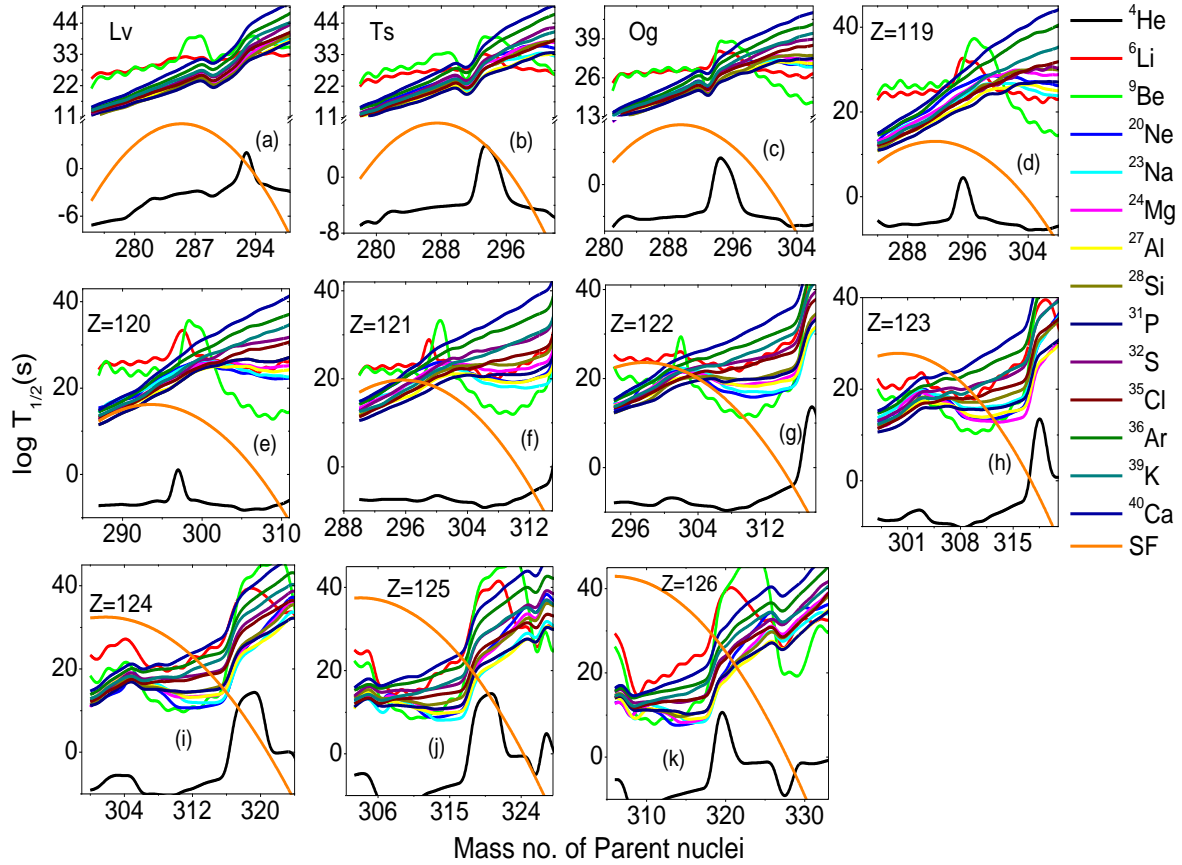


Fig. 3.22 Plot of evaluated $\log T_{1/2}$ values vs mass number of parent nuclei for the emission of cluster (${}^4\text{He}$ to ${}^{48}\text{Ca}$) and spontaneous fission from SH region $116 \leq Z \leq 126$.

respectively. From these plots it is clear that the ${}^4\text{He}$ emission and spontaneous fission half-lives shows smaller logarithmic half-life values when compared to other cluster emissions studied. Figure 3.21(a) shows smaller half-lives in the isotopes of SH nuclei ${}^{257-262}\text{Rf}$ when compared to other cluster emissions studied. The neutron number corresponding to isotopes of SH nuclei ${}^{257-261}\text{Rf}$ varies between $N=153-157$ which are near the magic numbers of 184. Similarly, the figure 3.21(b-l) depicts shorter α -decay half-lives when compared to other different decay modes in the isotopes of SH nuclei ${}^{259-262}\text{Db}$, ${}^{261-262}\text{Sg}$, ${}^{263-265}\text{Bh}$, ${}^{265-268}\text{Hs}$, ${}^{271-273}\text{Mt}$, ${}^{267-275}\text{Ds}$, ${}^{271-278}\text{Rg}$, ${}^{276-281}\text{Cn}$, ${}^{271-283}\text{Nh}$, ${}^{272-287}\text{Fl}$, ${}^{273-290}\text{Mc}$, ${}^{275-292}\text{Lv}$, ${}^{278-293,295-298}\text{Ts}$, ${}^{281-301}\text{Og}$, ${}^{284-304}\text{119}$, ${}^{287-308}\text{120}$, ${}^{290-305,308-311}\text{121}$, ${}^{294-314}\text{122}$, ${}^{297-317}\text{123}$, ${}^{300-305,308-317}\text{124}$, ${}^{303-323}\text{125}$ and ${}^{306-325}\text{126}$.

Table 3.4 Isotopes of heavy and SH nuclei having longer life time in the atomic number region $104 \leq Z \leq 118$.

Element	N	logT	Element	N	logT
²⁶⁷ ₁₀₄ Rf	163	3.67	²⁸⁶ ₁₁₂ Cn	174	2.82
²⁶⁸ ₁₀₅ Db	163	5.00	²⁸⁶ ₁₁₃ Nh	173	0.98
²⁶⁹ ₁₀₆ Sg	163	2.27	²⁹⁰ ₁₁₄ Fl	176	1.28
²⁷⁸ ₁₀₇ Bh	171	3.06	²⁹⁰ ₁₁₅ Mc	175	-0.19
²⁷⁸ ₁₀₈ Hs	170	3.06	²⁹³ ₁₁₆ Lv	177	-1.28
²⁸² ₁₀₉ Mt	173	1.82	²⁹⁴ ₁₁₇ Ts	177	-1.29
²⁸² ₁₁₀ Ds	172	1.82	²⁹⁴ ₁₁₈ Og	176	-3.24
²⁸⁶ ₁₁₁ Rg	175	2.82			

In order to explore new isotopes of SH nuclei with magic nuclei, first shell closures of the atoms are analysed in heavy and SH nuclei in the region $104 \leq Z \leq 118$. The table 3.4 presents the tabulation of nuclei having specific neutron number and larger half-lives. It has been observed that these tabulated nuclei with atomic number (Z) or neutron number (N) are much more stable than their neighbouring nuclei. The tabulated atomic nuclei is having comparatively higher binding energy per nucleon. Thus, these nuclei possess longer half-lives and hence more stable against different nuclear decay. From the table it is inferred that the neutron number with N=163-177 shows complete shell closures within the atomic nuclei. So the neutron numbers with shell closures are having larger half-lives which are near magic nuclei or magic nuclei. Hence, with this background work, is extended to predict magic or semi-magic neutron numbers in atomic number region $104 \leq Z \leq 126$.

Table 3.5 and 3.6 shows tabulated logarithmic half-lives of different decay modes such as α , β^+ , spontaneous fission half-lives and shortest logarithmic half-life corresponding to CD. The dominant decay mode among different decay modes studied is also shown in the 6th, 12th and 18th column of the table 3.5 and 3.6. From these tables it is observed that the SH nuclei ²⁶²Rf is having neutron number N=158 with logarithmic half-life of 1.13s which undergoes spontaneous fission. The nuclei ²⁶²Rf is more stable when compared to their neighbouring nuclei. Similarly, the SH nuclei ²⁶²Db with N=157 and α -decay logarithmic half-life of -0.44s, ²⁶²Sg(N=156) and $\log T_{1/2}$

Table 3.5 Logarithmic half- lives for different decay modes and their dominant decay mode

Parent Nuclei	log $T_{1/2}$				Decay mode	Parent Nuclei	log $T_{1/2}$				Decay mode	Parent Nuclei	log $T_{1/2}$				Decay mode
	α	β^+	Sf	Cluster			α	β^+	Sf	Cluster			α	β^+	Sf	Cluster	
²⁵⁷ Rf ₁₅₃	-2.11	0.23	-0.19	30.93(³¹ P)	α	²⁷⁰ Nh ₁₅₇	-6.05	-3.77	-6.73	13.54(³¹ P)	Sf	²⁸⁹ Lv ₁₇₃	-3.21	-2.19	4.53	20.32(³¹ P)	α
²⁵⁸ Rf ₁₅₄	-1.86	0.46	0.43	32.43(²⁷ Al)	α	²⁷¹ Nh ₁₅₈	-5.57	-3.55	-5.15	14.41(³¹ P)	α	²⁹⁰ Lv ₁₇₄	-2.98	-1.97	3.80	22.75(³¹ P)	α
²⁵⁹ Rf ₁₅₅	-1.22	5.17	0.88	31.77(⁶ Li)	α	²⁷² Nh ₁₅₉	-5.23	-3.33	-3.75	15.43(³¹ P)	α	²⁹¹ Lv ₁₇₅	-2.78	-1.76	2.90	24.25(³¹ P)	α
²⁶⁰ Rf ₁₅₆	-0.29	1.42	1.14	34.1(²⁷ Al)	α	²⁷³ Nh ₁₆₀	-5.00	-3.11	-2.53	16.08(³¹ P)	α	²⁹² Lv ₁₇₆	-2.61	-1.54	1.82	26.76(²⁷ Al)	α
²⁶¹ Rf ₁₅₇	0.39	1.82	1.23	32.77(⁶ Li)	α	²⁷⁴ Nh ₁₆₁	-4.84	-2.89	-1.49	16.94(³¹ P)	α	²⁷⁸ Ts ₁₆₁	-7.26	-5.41	-0.24	10.27(³¹ P)	α
²⁶² Rf ₁₅₈	1.17	2.06	1.13	35.71(⁶ Li)	Sf	²⁷⁵ Nh ₁₆₂	-4.74	-2.67	-0.63	18.08(³¹ P)	α	²⁷⁹ Ts ₁₆₂	-7.18	-5.19	1.37	11.49(³¹ P)	α
²⁵⁹ Db ₁₅₄	-2.69	0.49	-1.12	27.14(³¹ P)	α	²⁷⁶ Nh ₁₆₃	-4.69	-2.45	0.06	19.03(³¹ P)	α	²⁸⁰ Ts ₁₆₃	-7.15	-4.98	2.80	11.96(³¹ P)	α
²⁶⁰ Db ₁₅₅	-1.89	0.73	-0.49	28.3(²⁷ Al)	α	²⁷⁹ Nh ₁₆₆	-3.49	-1.79	1.04	19.98(³¹ P)	α	²⁸¹ Ts ₁₆₄	-7.14	-4.76	4.04	13.2(³¹ P)	α
²⁶¹ Db ₁₅₆	-1.26	0.96	-0.04	28.85(²⁷ Al)	α	²⁸³ Nh ₁₇₀	-1.55	-0.90	-0.15	22.2(³¹ P)	α	²⁸² Ts ₁₆₅	-6.76	-4.55	5.11	14.07(³¹ P)	α
²⁶² Db ₁₅₇	-0.44	1.20	0.23	29.82(⁶ Li)	α	²⁷¹ Fl ₁₅₇	-6.71	-4.40	-7.32	12.8(²⁸ Si)	Sf	²⁸³ Ts ₁₆₆	-6.41	-4.34	6.00	14.59(³¹ P)	α
²⁶¹ Sg ₁₅₅	-2.69	0.11	-1.86	27.73(²⁸ Si)	α	²⁷² Fl ₁₅₈	-6.41	-4.18	-5.55	13.72(²⁸ Si)	α	²⁸⁴ Ts ₁₆₇	-6.04	-4.12	6.72	15.71(³¹ P)	α
²⁶² Sg ₁₅₆	-1.88	0.34	-1.22	28.74(²⁸ Si)	α	²⁷³ Fl ₁₅₉	-5.99	-3.96	-3.97	14.44(²⁸ Si)	α	²⁸⁵ Ts ₁₆₈	-5.47	-3.91	7.25	16.28(³¹ P)	α
²⁶³ Bh ₁₅₆	-2.74	-0.28	-2.39	24.33(³¹ P)	α	²⁷⁴ Fl ₁₆₀	-5.68	-3.74	-2.56	15.52(²⁸ Si)	α	²⁸⁶ Ts ₁₆₉	-5.09	-3.69	7.60	17.32(³¹ P)	α
²⁶⁴ Bh ₁₅₇	-1.92	-0.05	-1.75	25.17(³¹ P)	α	²⁷⁵ Fl ₁₆₁	-5.49	-3.52	-1.34	16.35(²⁸ Si)	α	²⁸⁷ Ts ₁₇₀	-4.78	-3.48	7.78	18.43(³¹ P)	α
²⁶⁵ Bh ₁₅₈	-1.39	0.19	-1.28	25.83(³¹ P)	α	²⁷⁶ Fl ₁₆₂	-5.38	-3.30	-0.29	17.41(²⁸ Si)	α	²⁸⁸ Ts ₁₇₁	-4.51	-3.27	7.78	19.75(³¹ P)	α
²⁶⁶ Bh ₁₅₉	-0.98	0.42	-1.00	26.89(²⁷ Al)	Sf	²⁷⁷ Fl ₁₆₃	-5.33	-3.08	0.58	18.17(²⁸ Si)	α	²⁸⁹ Ts ₁₇₂	-4.29	-3.05	7.59	20.62(³¹ P)	α
²⁶⁴ Hs ₁₅₆	-3.32	-0.90	-3.53	23.74(²⁸ Si)	Sf	²⁷⁸ Fl ₁₆₄	-5.30	-2.86	1.27	18.92(²⁸ Si)	α	²⁹⁰ Ts ₁₇₃	-4.10	-2.84	7.24	22(³¹ P)	α
²⁶⁵ Hs ₁₅₇	-2.83	-0.67	-2.70	24.31(³¹ P)	α	²⁷⁹ Fl ₁₆₅	-4.84	-2.64	1.79	19.98(³¹ P)	α	²⁹¹ Ts ₁₇₄	-3.79	-2.63	6.70	18.22(³¹ P)	α
²⁶⁶ Hs ₁₅₈	-2.17	-0.44	-2.05	25.41(³¹ P)	α	²⁸⁰ Fl ₁₆₆	-4.43	-2.42	2.12	20.95(²⁸ Si)	α	²⁹² Ts ₁₇₅	-3.52	-2.41	5.98	20.2(³¹ P)	α
²⁶⁷ Hs ₁₅₉	-1.69	-0.21	-1.58	26.11(³¹ P)	α	²⁸¹ Fl ₁₆₇	-3.86	-2.20	2.28	21.86(³¹ P)	α	²⁹³ Ts ₁₇₆	-3.30	-2.20	5.09	25.07(³¹ P)	α
²⁶⁸ Hs ₁₆₀	-1.36	0.02	-1.29	27.6(²⁷ Al)	α	²⁸⁶ Fl ₁₇₂	-1.80	-1.11	0.37	24.79(³¹ P)	α	²⁹⁵ Ts ₁₇₈	-2.92	-1.77	2.76	27.21(³¹ P)	α
²⁷¹ Hs ₁₆₃	-0.88	0.71	-1.48	29.73(²⁷ Al)	Sf	²⁸⁷ Fl ₁₇₃	-1.46	-0.89	-0.54	26.38(³¹ P)	α	²⁹⁶ Ts ₁₇₉	-2.74	-1.56	1.33	27.57(⁶ Li)	α
²⁷² Hs ₁₆₄	-0.82	0.94	-1.90	30.77(²⁷ Al)	Sf	²⁷² Mc ₁₅₇	-7.22	-5.02	-7.81	10.4(³¹ P)	Sf	²⁹⁷ Ts ₁₈₀	-2.55	-1.34	-0.28	29.14(³¹ P)	α
²⁷¹ Mt ₁₆₂	-1.91	-0.15	-1.23	29.73(²⁷ Al)	α	²⁷³ Mc ₁₅₈	-6.90	-4.80	-5.86	11.17(³¹ P)	α	²⁹⁸ Ts ₁₈₁	-2.35	-1.13	-2.06	27.1(⁶ Li)	α
²⁷² Mt ₁₆₃	-1.80	0.08	-1.29	30.77(²⁷ Al)	α	²⁷⁴ Mc ₁₅₉	-6.65	-4.58	-4.09	12(³¹ P)	α	²⁹⁹ Ts ₁₈₂	-2.15	-0.91	-4.03	28.69(⁶ Li)	Sf
²⁷³ Mt ₁₆₄	-1.73	0.31	-1.52	30.89(⁶ Li)	α	²⁷⁵ Mc ₁₆₀	-6.47	-4.37	-2.49	12.74(³¹ P)	α	²⁸¹ Og ₁₆₃	-7.63	-5.61	3.78	10.74(²⁴ Mg)	α
²⁶⁶ Ds ₁₅₆	-5.16	-2.14	-5.69	19.85(²⁸ Si)	Sf	²⁷⁶ Mc ₁₆₁	-6.35	-4.15	-1.08	13.52(³¹ P)	α	²⁸² Og ₁₆₄	-7.63	-5.40	5.21	12.47(²⁸ Si)	α
²⁶⁷ Ds ₁₅₇	-4.73	-1.91	-4.49	18.87(²⁸ Si)	α	²⁷⁷ Mc ₁₆₂	-6.28	-3.93	0.15	14.11(³¹ P)	α	²⁸³ Og ₁₆₅	-7.20	-5.19	6.47	13.24(²⁸ Si)	α
²⁶⁸ Ds ₁₅₈	-4.21	-1.68	-3.47	19.83(²⁸ Si)	α	²⁷⁸ Mc ₁₆₃	-6.24	-3.71	1.21	15.14(³¹ P)	α	²⁸⁴ Og ₁₆₆	-6.82	-4.97	7.54	14.01(²⁸ Si)	α
²⁶⁹ Ds ₁₅₉	-3.74	-1.46	-2.63	20.49(²⁸ Si)	α	²⁷⁹ Mc ₁₆₄	-6.23	-3.50	2.09	16.21(³¹ P)	α	²⁸⁵ Og ₁₆₇	-6.49	-4.76	8.44	14.9(²⁸ Si)	α
²⁷⁰ Ds ₁₆₀	-3.43	-1.23	-1.96	22.09(³¹ P)	α	²⁸⁰ Mc ₁₆₅	-5.52	-3.28	2.78	17.07(³¹ P)	α	²⁸⁶ Og ₁₆₈	-6.19	-4.55	9.16	15.93(³¹ P)	α
²⁷¹ Ds ₁₆₁	-3.23	-1.00	-1.48	22.87(³¹ P)	α	²⁸¹ Mc ₁₆₆	-5.06	-3.06	3.30	17.77(³¹ P)	α	²⁸⁷ Og ₁₆₉	-5.73	-4.34	9.70	16.85(³¹ P)	α
²⁷² Ds ₁₆₂	-3.09	-0.78	-1.17	24.3(³¹ P)	α	²⁸² Mc ₁₆₇	-4.65	-2.84	3.64	18.81(³¹ P)	α	²⁸⁸ Og ₁₇₀	-5.34	-4.13	10.06	17.86(³¹ P)	α
²⁷³ Ds ₁₆₃	-3.01	-0.55	-1.04	24.03(²⁷ Al)	α	²⁸³ Mc ₁₆₈	-4.30	-2.63	3.81	19.57(³¹ P)	α	²⁸⁹ Og ₁₇₁	-5.05	-3.91	10.24	19.07(³¹ P)	α
²⁷⁴ Ds ₁₆₄	-2.97	-0.33	-1.10	25.31(²⁷ Al)	α	²⁸⁴ Mc ₁₆₉	-3.77	-2.41	3.79	20.75(³¹ P)	α	²⁹⁰ Og ₁₇₂	-4.81	-3.70	10.25	20(³¹ P)	α
²⁷⁵ Ds ₁₆₅	-2.39	-0.10	-1.32	25.33(²⁷ Al)	α	²⁸⁵ Mc ₁₇₀	-3.34	-2.19	3.59	22.3(³¹ P)	α	²⁹¹ Og ₁₇₃	-4.60	-3.49	10.07	21.06(³¹ P)	α
²⁷⁶ Ds ₁₆₆	-1.65	0.13	-1.73	26.42(²⁷ Al)	Sf	²⁸⁶ Mc ₁₇₁	-3.00	-1.97	3.22	23.69(³¹ P)	α	²⁹² Og ₁₇₄	-4.43	-3.28	9.72	22.41(³¹ P)	α
²⁷⁷ Ds ₁₆₇	-1.10	0.35	-2.32	27.17(²⁷ Al)	Sf	²⁸⁷ Mc ₁₇₂	-2.73	-1.76	2.67	20.05(³¹ P)	α	²⁹³ Og ₁₇₅	-4.28	-3.07	9.19	14.23(⁹ Be)	α
²⁷⁸ Ds ₁₆₈	-0.62	0.58	-3.08	29.2(²⁷ Al)	Sf	²⁸⁸ Mc ₁₇₃	-2.49	-1.54	1.94	22.14(³¹ P)	α	²⁹⁴ Og ₁₇₆	-4.14	-2.85	8.48	24.33(³¹ P)	α
²⁷⁹ Ds ₁₆₉	0.12	0.81	-4.03	30.68(²⁷ Al)	Sf	²⁸⁹ Mc ₁₇₄	-2.29	-1.32	1.03	23.72(³¹ P)	α	²⁹⁵ Og ₁₇₇	-4.00	-2.64	7.59	24.92(³¹ P)	α
²⁷¹ Rg ₁₆₀	-3.82	-1.86	-2.22	20.14(³¹ P)	α	²⁹⁰ Mc ₁₇₅	-2.03	-1.10	-0.06	25.92(²⁷ Al)	α	²⁹⁶ Og ₁₇₈	-3.69	-2.43	6.52	26.34(³¹ P)	α
²⁷² Rg ₁₆₁	-3.59	-1.63	-1.55	19.02(³¹ P)	α	²⁷⁵ Lv ₁₅₉	-7.12	-5.21	-4.09	10.92(²⁸ Si)	α	²⁹⁷ Og ₁₇₉	-3.45	-2.22	5.28	27.59(³¹ P)	α
²⁷³ Rg ₁₆₂	-3.45	-1.41	-1.06	19.9(³¹ P)	α	²⁷⁶ Lv ₁₆₀	-6.93	-4.99	-2.32	11.87(²⁸ Si)	α	²⁹⁸ Og ₁₈₀	-3.22	-2.00	3.86	27.49(³¹ P)	α
²⁷⁴ Rg ₁₆₃	-3.37	-1.18	-0.75	20.33(²⁷ Al)	α	²⁷⁷ Lv ₁₆₁	-6.80	-4.78	-0.72	12.94(²⁸ Si)	α	²⁹⁹ Og ₁₈₁	-3.00	-1.79	2.26	24.57(⁹ Be)	α
²⁷⁵ Rg ₁₆₄	-3.33	-0.96	-0.61	20.99(²⁷ Al)	α	²⁷⁸ Lv ₁₆₂	-6.73	-4.56	0.70	13.76(²⁸ Si)	α	³⁰⁰ Og ₁₈₂	-2.78	-1.58	0.48	27.78(⁹ Be)	α
²⁷⁶ Rg ₁₆₅	-2.81	-0.73	-0.66	21.21(²⁷ Al)	α	²⁷⁹ Lv ₁₆₃	-6.70	-4.35	1.94	14.44(²⁸ Si)	α	³⁰¹ Og ₁₈₃	-2.56	-1.37	-1.48	22.12(⁹ Be)	α
²⁷⁷ Rg ₁₆₆	-2.20	-0.51	-0.88	21.84(²⁷ Al)	α	²⁸⁰ Lv ₁₆₄	-6.69	-4.13	3.00	15.85(²⁸ Si)	α	³⁰² Og ₁₈₄	-2.33	-1.16	-3.62	24.98(⁹ Be)	Sf
²⁷⁸ Rg ₁₆₇	-1.54	-0.29	-1.28	23.03(²⁷ Al)	α	²⁸¹ Lv ₁₆₅	-6.33	-3.91	3.89	16.78(²⁸ Si)	α	³⁰³ Og ₁₈₅	-2.10	-0.94	-5.93	18.26(⁹ Be)	Sf
²⁷⁹ Rg ₁₆₈	-1.03	-0.06	-1.86	24.16(²⁷ Al)	Sf	²⁸² Lv ₁₆₆	-5.74	-3.70	4.59	17.59(²⁸ Si)	α	²⁸⁴ 119 ₁₆₅	-7.69	-5.82	7.96	10.61(²⁷ Al)	α
²⁷⁶ Cn ₁₆₄	-3.90	-1.59	-0.06	23.5(³¹ P)	α	²⁸³ Lv ₁₆₇	-5.26	-3.48	5.12	18.51(³¹ P)	α	²⁸⁵ 119 ₁₆₆	-7.26	-5.61	9.23	11.21(³¹ P)	α
²⁷⁷ Cn ₁₆₅	-3.30	-1.37	0.08	20.71(³¹ P)	α	²⁸⁴ Lv ₁₆₈	-4.87	-3.27	5.47	19.55(³¹ P)	α	²⁸⁶ 11					

Table 3.6 Logarithmic half- lives of different decay modes and their dominant decay mode

Parent Nuclei	log $T_{1/2}$				Decay mode	Parent Nuclei	log $T_{1/2}$				Decay mode	Parent Nuclei	log $T_{1/2}$				Decay mode
	α	β^+	Sf	Cluster			α	β^+	Sf	Cluster			α	β^+	Sf	Cluster	
²⁹¹ 119 ₁₇₂	-5.37	-4.35	13.04	16.59(³¹ P)	α	³⁰⁴ 121 ₁₈₃	-4.55	-3.37	13.48	16.54(⁹ Be)	α	³⁰⁵ 124 ₁₈₁	-6.54	-5.78	31.54	17.06(²³ Na)	α
²⁹² 119 ₁₇₃	-5.14	-4.14	13.05	17.49(³¹ P)	α	³⁰⁵ 121 ₁₈₄	-4.35	-3.17	11.90	17.57(⁹ Be)	α	³⁰⁸ 124 ₁₈₄	-6.10	-5.18	29.00	13.05(⁹ Be)	α
²⁹³ 119 ₁₇₄	-4.95	-3.93	12.89	18.6(³¹ P)	α	³⁰⁸ 121 ₁₈₇	-3.66	-2.55	6.09	11.15(⁹ Be)	α	³⁰⁹ 124 ₁₈₅	-5.94	-4.97	27.80	9(⁹ Be)	α
²⁹⁴ 119 ₁₇₅	-4.78	-3.72	12.54	19.78(³¹ P)	α	³⁰⁹ 121 ₁₈₈	-3.26	-2.34	3.79	13.36(⁹ Be)	α	³¹⁰ 124 ₁₈₆	-5.78	-4.77	26.41	10.69(²⁰ Ne)	α
²⁹⁵ 119 ₁₇₆	-4.63	-3.51	12.02	20.49(³¹ P)	α	³¹⁰ 121 ₁₈₉	-2.95	-2.13	1.32	10.86(⁹ Be)	α	³¹¹ 124 ₁₈₇	-5.40	-4.57	24.85	8.76(⁹ Be)	α
²⁹⁶ 119 ₁₇₇	-4.49	-3.30	11.31	21.04(³¹ P)	α	³¹¹ 121 ₁₉₀	-2.67	-1.93	-1.33	14.83(⁹ Be)	α	³¹² 124 ₁₈₈	-5.11	-4.37	23.11	10.61(²⁰ Ne)	α
²⁹⁷ 119 ₁₇₈	-4.35	-3.09	10.43	21.81(³¹ P)	α	³¹² 121 ₁₉₁	-2.39	-1.72	-4.16	12.65(⁹ Be)	Sf	³¹³ 124 ₁₈₉	-4.85	-4.17	21.19	9.56(⁹ Be)	α
²⁹⁸ 119 ₁₇₉	-4.21	-2.88	9.37	23.62(³¹ P)	α	²⁹⁴ 122 ₁₇₂	-6.87	-6.29	22.39	12.23(²⁸ Si)	α	³¹⁴ 124 ₁₉₀	-4.61	-3.97	19.10	11.12(²⁰ Ne)	α
²⁹⁹ 119 ₁₈₀	-4.06	-2.67	8.13	24.44(³¹ P)	α	²⁹⁵ 122 ₁₇₃	-6.70	-6.09	22.96	12.89(²⁸ Si)	α	³¹⁵ 124 ₁₉₁	-4.37	-3.77	16.82	11.51(²⁰ Ne)	α
³⁰⁰ 119 ₁₈₁	-3.91	-2.46	6.72	24.14(³¹ P)	α	²⁹⁶ 122 ₁₇₄	-6.56	-5.88	23.34	13.69(³¹ P)	α	³¹⁶ 124 ₁₉₂	-4.14	-3.56	14.37	12.44(²⁰ Ne)	α
³⁰¹ 119 ₁₈₂	-3.51	-2.25	5.12	24.64(³¹ P)	α	²⁹⁷ 122 ₁₇₅	-6.44	-5.68	23.55	14.04(³¹ P)	α	³¹⁷ 124 ₁₉₃	-3.92	-3.36	11.74	20.12(²³ Na)	α
³⁰² 119 ₁₈₃	-3.23	-2.04	3.35	20.22(⁹ Be)	α	²⁹⁸ 122 ₁₇₆	-6.33	-5.48	23.59	14.71(³¹ P)	α	³⁰³ 125 ₁₇₈	-7.42	-7.04	37.47	10.84(²⁷ Al)	α
³⁰³ 119 ₁₈₄	-2.97	-1.83	1.40	21.62(⁹ Be)	α	²⁹⁹ 122 ₁₇₇	-6.22	-5.27	23.44	15.12(³¹ P)	α	³⁰⁴ 125 ₁₇₉	-7.27	-6.84	37.52	12.84(³¹ P)	α
³⁰⁴ 119 ₁₈₅	-2.71	-1.62	-0.73	16.24(⁹ Be)	α	³⁰⁰ 122 ₁₇₈	-6.11	-5.07	23.11	16.71(³¹ P)	α	³⁰⁵ 125 ₁₈₀	-7.13	-6.64	37.40	13.57(²³ Na)	α
³⁰⁵ 119 ₁₈₆	-2.46	-1.41	-3.04	18.72(⁹ Be)	Sf	³⁰¹ 122 ₁₇₉	-6.00	-4.86	22.61	17.83(³¹ P)	α	³⁰⁶ 125 ₁₈₁	-6.98	-6.44	37.09	10.12(²³ Na)	α
³⁰⁶ 119 ₁₈₇	-2.21	-1.20	-5.53	14.1(⁹ Be)	Sf	³⁰² 122 ₁₈₀	-5.88	-4.66	21.93	18.65(³¹ P)	α	³⁰⁷ 125 ₁₈₂	-6.83	-6.24	36.61	9.51(²³ Na)	α
³⁰⁷ 119 ₁₈₈	-1.96	-0.98	-8.19	16.53(⁹ Be)	Sf	³⁰³ 122 ₁₈₁	-5.58	-4.45	21.06	16.8(⁹ Be)	α	³⁰⁸ 125 ₁₈₃	-6.67	-6.04	35.94	10.16(⁹ Be)	α
²⁸⁷ 120 ₁₆₇	-7.34	-6.04	12.33	11.47(³¹ P)	α	³⁰⁴ 122 ₁₈₂	-5.33	-4.25	20.02	19.28(⁹ Be)	α	³⁰⁹ 125 ₁₈₄	-6.51	-5.85	35.10	10.77(⁹ Be)	α
²⁸⁸ 120 ₁₆₈	-7.00	-5.83	13.42	12.22(³¹ P)	α	³⁰⁵ 122 ₁₈₃	-5.11	-4.04	18.81	14.64(⁹ Be)	α	³¹⁰ 125 ₁₈₅	-6.34	-5.65	34.08	7.74(⁹ Be)	α
²⁸⁹ 120 ₁₆₉	-6.71	-5.62	14.33	13.29(³¹ P)	α	³⁰⁶ 122 ₁₈₄	-4.89	-3.84	17.41	16.37(⁹ Be)	α	³¹¹ 125 ₁₈₆	-6.17	-5.45	32.89	9.31(⁹ Be)	α
²⁹⁰ 120 ₁₇₀	-6.46	-5.42	15.06	14.25(³¹ P)	α	³⁰⁷ 122 ₁₈₅	-4.67	-3.63	15.84	11.4(⁹ Be)	α	³¹² 125 ₁₈₇	-6.00	-5.25	31.51	8.07(⁹ Be)	α
²⁹¹ 120 ₁₇₁	-6.26	-5.21	15.62	14.96(³¹ P)	α	³⁰⁸ 122 ₁₈₆	-4.46	-3.43	14.08	13.9(⁹ Be)	α	³¹³ 125 ₁₈₈	-5.83	-5.05	29.96	7.97(²³ Na)	α
²⁹² 120 ₁₇₂	-6.08	-5.00	15.99	15.71(³¹ P)	α	³⁰⁹ 122 ₁₈₇	-4.24	-3.22	12.15	10.13(⁹ Be)	α	³¹⁴ 125 ₁₈₉	-5.56	-4.85	28.22	8.2(²³ Na)	α
²⁹³ 120 ₁₇₃	-5.93	-4.79	16.19	17.07(³¹ P)	α	³¹⁰ 122 ₁₈₈	-4.03	-3.02	10.04	12.89(⁹ Be)	α	³¹⁵ 125 ₁₉₀	-5.20	-4.65	26.31	8.11(²³ Na)	α
²⁹⁴ 120 ₁₇₄	-5.56	-4.58	16.20	18.17(³¹ P)	α	³¹¹ 122 ₁₈₉	-3.82	-2.81	7.75	10.22(⁹ Be)	α	³¹⁶ 125 ₁₉₁	-4.92	-4.45	24.22	8.4(²³ Na)	α
²⁹⁵ 120 ₁₇₅	-5.36	-4.37	16.04	18.92(³¹ P)	α	³¹² 122 ₁₉₀	-3.41	-2.61	5.29	15.45(⁹ Be)	α	³¹⁷ 125 ₁₉₂	-4.67	-4.25	21.95	8.76(²³ Na)	α
²⁹⁶ 120 ₁₇₆	-5.18	-4.16	15.70	19.77(³¹ P)	α	³¹³ 122 ₁₉₁	-3.06	-2.40	2.65	12.2(⁹ Be)	α	³¹⁸ 125 ₁₉₃	-4.43	-4.05	19.51	16.88(²³ Na)	α
²⁹⁷ 120 ₁₇₇	-5.02	-3.96	15.19	21.18(³¹ P)	α	³¹⁴ 122 ₁₉₂	-2.76	-2.20	-0.18	17.22(²⁰ Ne)	α	³¹⁹ 125 ₁₉₄	-4.20	-3.85	16.89	19.46(²³ Na)	α
²⁹⁸ 120 ₁₇₈	-4.87	-3.75	14.49	22.38(³¹ P)	α	³¹⁵ 122 ₁₉₃	-2.47	-1.99	-3.18	15.91(⁹ Be)	Sf	³²⁰ 125 ₁₉₅	-3.97	-3.65	14.08	20.73(²³ Na)	α
²⁹⁹ 120 ₁₇₉	-4.72	-3.54	13.62	23.69(²⁷ Al)	α	²⁹⁷ 123 ₁₇₄	-6.98	-6.54	27.19	10.6(³¹ P)	α	³²² 125 ₁₉₇	-3.50	-3.25	7.94	23.26(²⁷ Al)	α
³⁰⁰ 120 ₁₈₀	-4.56	-3.33	12.56	24.4(²⁷ Al)	α	²⁹⁸ 123 ₁₇₅	-6.85	-6.33	27.58	10.96(³¹ P)	α	³²³ 125 ₁₉₈	-3.06	-3.05	4.61	24.59(²⁷ Al)	α
³⁰¹ 120 ₁₈₁	-4.40	-3.12	11.33	24.76(²⁷ Al)	α	²⁹⁹ 123 ₁₇₆	-6.73	-6.13	27.80	11.4(³¹ P)	α	³⁰⁶ 126 ₁₈₀	-7.72	-7.31	42.98	12.78(²⁴ Mg)	α
³⁰² 120 ₁₈₂	-4.22	-2.91	9.92	22.84(⁹ Be)	α	³⁰⁰ 123 ₁₇₇	-6.62	-5.93	27.84	12.14(³¹ P)	α	³⁰⁷ 126 ₁₈₁	-7.49	-7.11	42.86	13.39(²⁴ Mg)	α
³⁰³ 120 ₁₈₃	-4.05	-2.70	8.33	17.56(⁹ Be)	α	³⁰¹ 123 ₁₇₈	-6.51	-5.72	27.70	13.29(³¹ P)	α	³⁰⁸ 126 ₁₈₂	-7.31	-6.91	42.56	8.14(²⁰ Ne)	α
³⁰⁴ 120 ₁₈₄	-3.86	-2.50	6.57	19.84(⁹ Be)	α	³⁰² 123 ₁₇₉	-6.39	-5.52	27.38	14.76(³¹ P)	α	³⁰⁹ 126 ₁₈₃	-7.12	-6.71	42.08	8.13(⁹ Be)	α
³⁰⁵ 120 ₁₈₅	-3.43	-2.29	4.62	14.32(⁹ Be)	α	³⁰³ 123 ₁₈₀	-6.27	-5.32	26.88	16.16(³¹ P)	α	³¹⁰ 126 ₁₈₄	-6.94	-6.52	41.43	10(⁹ Be)	α
³⁰⁶ 120 ₁₈₆	-3.13	-2.08	2.50	17.29(⁹ Be)	α	³⁰⁴ 123 ₁₈₁	-6.14	-5.11	26.20	15.12(⁹ Be)	α	³¹¹ 126 ₁₈₅	-6.76	-6.32	40.59	6.69(⁹ Be)	α
³⁰⁷ 120 ₁₈₇	-2.84	-1.87	0.20	12.21(⁹ Be)	α	³⁰⁵ 123 ₁₈₂	-6.01	-4.91	25.35	15.86(³¹ P)	α	³¹² 126 ₁₈₆	-6.58	-6.12	39.58	10.24(⁹ Be)	α
³⁰⁸ 120 ₁₈₈	-2.57	-1.66	-2.28	14.97(⁹ Be)	α	³⁰⁶ 123 ₁₈₃	-5.86	-4.71	24.32	13.31(⁹ Be)	α	³¹³ 126 ₁₈₇	-6.40	-5.92	38.39	7.63(²⁰ Ne)	α
³⁰⁹ 120 ₁₈₉	-2.31	-1.45	-4.94	11.41(⁹ Be)	Sf	³⁰⁷ 123 ₁₈₄	-5.55	-4.51	23.11	14.27(⁹ Be)	α	³¹⁴ 126 ₁₈₈	-6.22	-5.72	37.02	7.56(²⁰ Ne)	α
³¹⁰ 120 ₁₉₀	-2.05	-1.25	-7.77	16.04(⁹ Be)	Sf	³⁰⁸ 123 ₁₈₅	-5.26	-4.30	21.72	9.96(⁹ Be)	α	³¹⁵ 126 ₁₈₉	-6.04	-5.53	35.47	7.75(²⁰ Ne)	α
²⁹⁰ 121 ₁₆₉	-7.14	-6.27	16.89	10.45(³¹ P)	α	³⁰⁹ 123 ₁₈₆	-5.01	-4.10	20.15	11.95(⁹ Be)	α	³¹⁶ 126 ₁₉₀	-5.86	-5.33	33.75	8.21(²⁰ Ne)	α
²⁹¹ 121 ₁₇₀	-6.87	-6.06	17.80	10.97(³¹ P)	α	³¹⁰ 123 ₁₈₇	-4.77	-3.90	18.40	9.48(⁹ Be)	α	³¹⁷ 126 ₁₉₁	-5.69	-5.13	31.84	8.24(²³ Na)	α
²⁹² 121 ₁₇₁	-6.65	-5.85	18.54	11.92(³¹ P)	α	³¹¹ 123 ₁₈₈	-4.54	-3.69	16.48	11.77(⁹ Be)	α	³¹⁸ 126 ₁₉₂	-5.30	-4.93	29.76	8.83(²³ Na)	α
²⁹³ 121 ₁₇₂	-6.46	-5.65	19.10	12.59(³¹ P)	α	³¹² 123 ₁₈₉	-4.31	-3.49	14.38	10(⁹ Be)	α	³¹⁹ 126 ₁₉₃	-5.00	-4.74	27.50	17.18(²⁷ Al)	α
²⁹⁴ 121 ₁₇₃	-6.31	-5.44	19.48	13.49(³¹ P)	α	³¹³ 123 ₁₉₀	-4.09	-3.29	12.09	12.7(²⁴ Mg)	α	³²⁰ 126 ₁₉₄	-4.73	-4.54	25.06	17.93(²⁷ Al)	α
²⁹⁵ 121 ₁₇₄	-6.17	-5.23	19.69	14.06(³¹ P)	α	³¹⁴ 123 ₁₉₁	-3.87	-3.08	9.64	12.2(⁹ Be)	α	³²¹ 126 ₁₉₅	-4.49	-4.34	22.44	20.48(²⁷ Al)	α
²⁹⁶ 121 ₁₇₅	-6.05	-5.03	19.71	14.84(³¹ P)	α	³¹⁵ 123 ₁₉₂	-3.61	-2.88	7.00	13.28(²⁴ Mg)	α	³²² 126 ₁₉₆	-4.25	-4.14	19.65	22.14(²⁷ Al)	α
²⁹⁷ 121 ₁₇₆	-5.94	-4.82	19.56	15.61(³¹ P)	α	³¹⁶ 123 ₁₉₃	-3.17	-2.68	4.18	13.61(²⁴ Mg)	α	³²³ 126 ₁₉₇	-4.02	-3.94	16.67	23.05(²⁷ Al)	α
²⁹⁸ 121 ₁₇₇	-5.70	-4.61	19.22	16.47(³¹ P)	α												

of -1.88ms in case of α -decay, ^{266}Bh [N=159, -1.0s(sf)], ^{272}Hs [N=164, -1.9s(sf)], ^{273}Mt [164,-1.73s(α)], ^{276}Ds [166,-1.73s(sf)], ^{279}Rg [168,-1.86s(sf)], ^{281}Cn [169,-1.16s(α)], ^{283}Nh [170,-1.55s(α)], ^{287}Fl [173,-1.46(α)], ^{289}Mc [175,-2.03s(α)], ^{292}Lv [176,-2.61s(α)], ^{299}Ts [182,-4.03s(sf)], ^{302}Og [184,-3.62s(sf)], $^{305}\text{119}$ [186,-3.04s(sf)], $^{309}\text{120}$ [189,-4.94s(sf)], $^{312}\text{121}$ [191,-4.16s(sf)], $^{315}\text{122}$ [193,-3.18s(α)], $^{317}\text{123}$ [194,-2.85s(α)], $^{317}\text{124}$ [193,-3.92s(α)], $^{323}\text{125}$ [198,-3.06s(α)] and $^{329}\text{126}$ [203,-4.91s(sf)] shows comparably larger life times than their neighbouring nuclei. This signifies that there may be semi magic nuclei exist between neutron numbers N=157-203. More detail experimental/theoretical study is necessary to draw the definite conclusion in this aspect.

Even-though, an α and spontaneous fission are dominant in the studied table, but in further

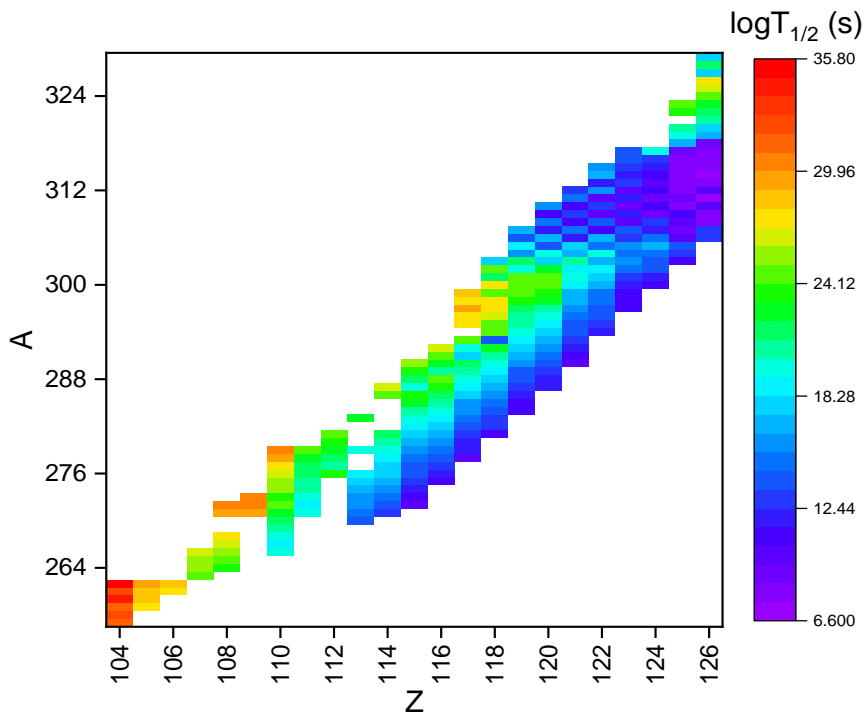


Fig. 3.23 Map of nuclei reflecting the logarithmic half-lives corresponding to shortest cluster-decay half-lives for the mass number and atomic number of parent nuclei in the SHE in the region $104 \leq Z \leq 126$.

analysis CR of shorter half-lives are considered . A map of nuclei reflects the shortest logarithmic half-lives of cluster emissions studied in the SH region $104 \leq Z \leq 126$ is shown in figure 3.23.

This figure enable to predict shortest half-lives among the studied cluster emissions and it is shown

on right side of the figure with the vertical bar. The shorter half-lives are shown with the colour indigo which ranges from 6.6s to 10.97s in the SH region $121 \leq Z \leq 126$ which includes the cluster emissions such as ${}^9\text{Be}$, ${}^{20}\text{Ne}$, ${}^{23}\text{Na}$, ${}^{24}\text{Mg}$, ${}^{27}\text{Al}$ and ${}^{31}\text{P}$. These shorter half-lives are due to magic number of neutrons in the SH region which ranges between 170 to 192. Among these half-lives the SH nuclei ${}^{309}125$ and ${}^{310}126$ has neutron number of 184 with $\log T_{1/2}=10.77\text{s}$ and 10s respectively, for the cluster emission of ${}^9\text{Be}$. Similarly, the $\log T_{1/2}$ corresponding to ${}^{311}126$ shows shortest value of 6.6 in which $Z=126$ is a magic nuclei. Further, dark blue colour to light

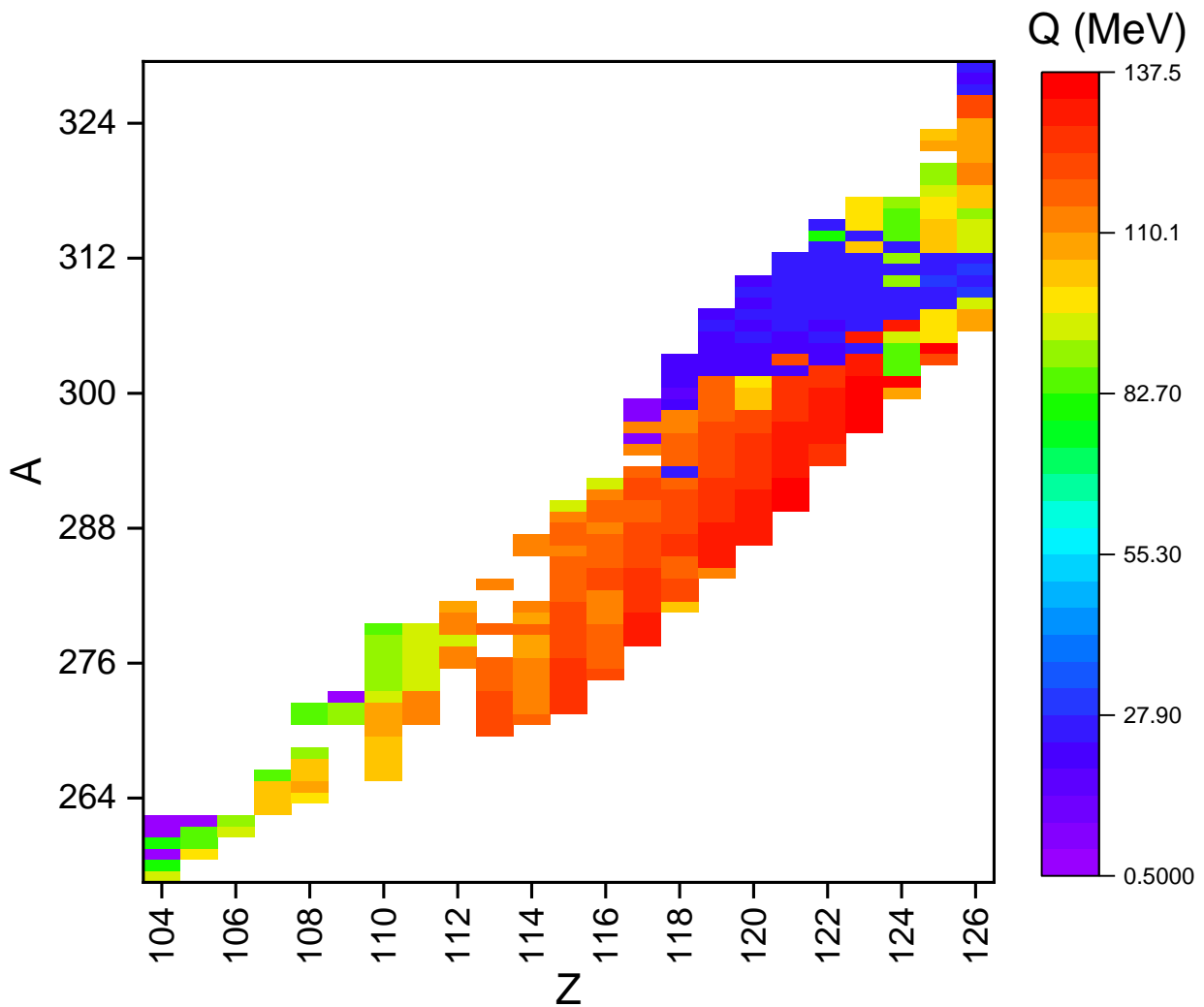


Fig. 3.24 Map of nuclei reflecting Q-values corresponding to shortest cluster-decay half-lives for the mass and atomic number of parent nuclei in SHE in the region $104 \leq Z \leq 126$.

blue shows the $\log T_{1/2}$ values of 11.12s to 18.98s within the SH region of $119 \leq Z \leq 126$ with

the cluster emissions such as ${}^9\text{Be}$, ${}^{20}\text{Ne}$, ${}^{23}\text{Na}$, ${}^{24}\text{Mg}$, ${}^{27}\text{Al}$ and ${}^{31}\text{P}$. Among these, the nuclei ${}^{322}_{126}$ is having magic neutron number with $N=196$, nuclei, ${}^{304}_{120}$, ${}^{305}_{121}$, ${}^{306}_{122}$ and ${}^{308}_{124}$ which carry magic neutron number with $N=184$. Logarithmic half-lives from cyan to red colour varies from 18s to 35.80s in the SH region $104 \leq Z \leq 122$ and $124 \leq Z \leq 126$.

The Q-values play a major role in the evaluation of cluster decay half-lives. The figure 3.24 shows Q-values corresponding to shortest CD half-lives for the mass and atomic number of SHE region $104 \leq Z \leq 126$. The Q-value of CD varies from 0.5MeV to 27.90MeV from indigo to blue colour for which logarithmic half-lives are smaller. Further, the Q-values above 27.90MeV to 137.5MeV corresponding to light blue to red colour for which logarithmic half-lives were found to be larger.

Similarly, the figure 3.25 shows the shortest cluster-decay half-lives for the neutron number

Table 3.7 Tabulation of parent (A_P), daughter (A_D) and cluster nuclei (A_C) along with the Q-values and $\log T_{1/2}$ values corresponding to magic number of neutrons of parent/daughter nuclei.

A_P	A_D	A_C	Q(MeV)	$\log T_{1/2}$
${}^{309}_{120}_{189}$	${}^{300}\text{Lv}_{184}$	${}^9\text{Be}_5$	24.84	11.41
${}^{310}_{121}_{189}$	${}^{301}\text{Ts}_{184}$	${}^9\text{Be}_5$	25.35	10.86
${}^{311}_{122}_{189}$	${}^{302}\text{Og}_{184}$	${}^9\text{Be}_5$	25.93	10.22
${}^{312}_{123}_{189}$	${}^{303}_{119}_{184}$	${}^9\text{Be}_5$	26.31	10
${}^{313}_{124}_{189}$	${}^{304}_{120}_{184}$	${}^9\text{Be}_5$	26.81	9.56
${}^{323}_{125}_{198}$	${}^{296}\text{Cn}_{184}$	${}^{27}\text{Al}_{14}$	105.15	24.59
${}^{324}_{126}_{198}$	${}^{297}\text{Nh}_{184}$	${}^{27}\text{Al}_{14}$	106.15	24.66
${}^{326}_{126}_{200}$	${}^{295}\text{Rg}_{184}$	${}^{31}\text{P}_{16}$	121.61	27.89
${}^{302}_{118}_{184}$	${}^{293}\text{Fl}_{179}$	${}^9\text{Be}_5$	19.35	24.98
${}^{303}_{119}_{184}$	${}^{294}\text{Mc}_{179}$	${}^9\text{Be}_5$	20.66	21.62
${}^{304}_{120}_{184}$	${}^{295}\text{Lv}_{179}$	${}^9\text{Be}_5$	21.52	19.84
${}^{305}_{121}_{184}$	${}^{296}\text{Ts}_{179}$	${}^9\text{Be}_5$	22.62	17.57
${}^{306}_{122}_{184}$	${}^{297}\text{Og}_{179}$	${}^9\text{Be}_5$	23.33	16.37
${}^{307}_{123}_{184}$	${}^{298}_{119}_{179}$	${}^9\text{Be}_5$	24.46	14.27
${}^{308}_{124}_{184}$	${}^{299}_{120}_{179}$	${}^9\text{Be}_5$	25.27	13.05
${}^{309}_{125}_{184}$	${}^{300}_{121}_{179}$	${}^9\text{Be}_5$	26.59	10.77
${}^{310}_{126}_{184}$	${}^{301}_{122}_{179}$	${}^9\text{Be}_5$	27.25	10
${}^{311}_{126}_{185}$	${}^{302}_{122}_{180}$	${}^9\text{Be}_5$	28.95	6.69
${}^{322}_{126}_{196}$	${}^{295}\text{Nh}_{182}$	${}^{27}\text{Al}_{14}$	108.47	22.14

and atomic number of parent nuclei in the SHE in the region $104 \leq Z \leq 126$. Indigo to blue

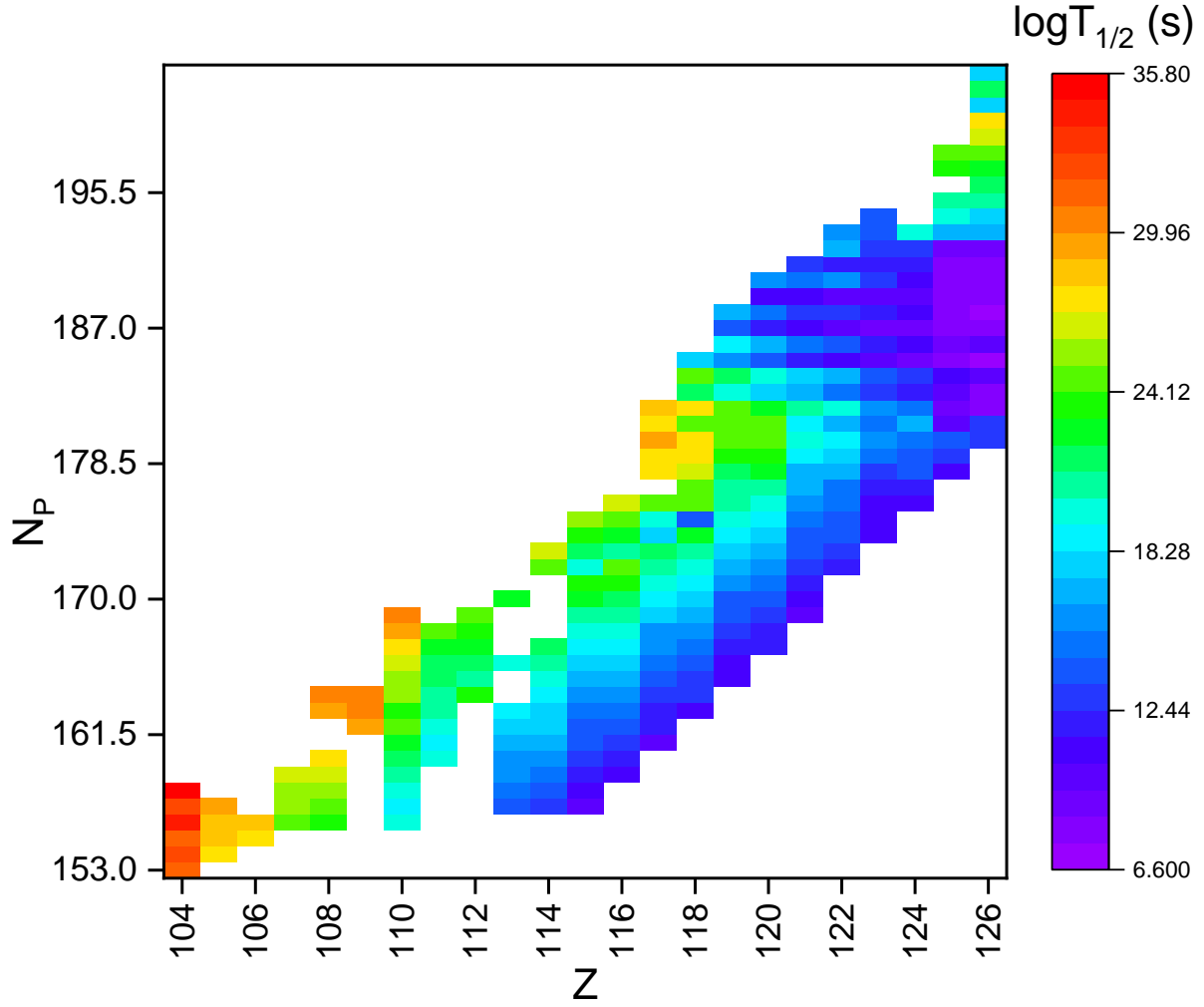


Fig. 3.25 Map of nuclei reflecting the logarithmic half-lives corresponding to shortest cluster-decay half-lives for the neutron number and atomic number of parent nuclei in the SHE in the region $104 \leq Z \leq 126$.

colour shows neutron number for which $\log T_{1/2}$ values presents shorter half-lives and cyan to red colour are related to larger half-lives.

The table 3.7 shows the tabulation of parent (A_P), daughter(A_D) and cluster nuclei (A_C) along with the Q-values and $\log T_{1/2}$ values corresponding to magic number of neutrons of parent/daughter nuclei. In case of parent nuclei $^{309}_{120}_{189}$ $\log T_{1/2}$ value of 11.41 is observed with the Q-value of 24.84MeV during the cluster emission of 9Be_5 , resulting in the daughter nuclei $^{300}_{184}_{184}$ in which neutron number of daughter nuclei is N=184. Similarly, the identified neutron number with magic number either in case of parent nuclei or daughter nuclei. From the detail study

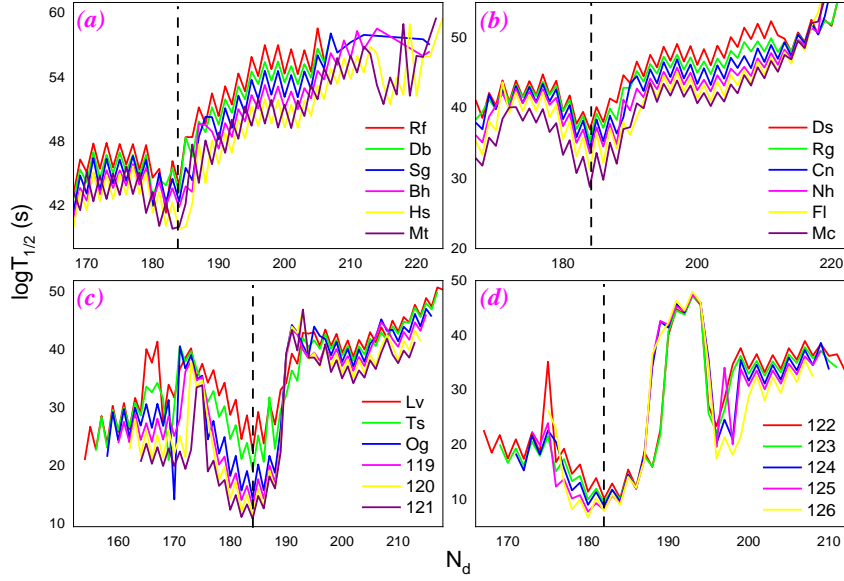


Fig. 3.26 (a) Variation of logarithmic half-lives ($\log T_{1/2}$) of ${}^9\text{Be}$ cluster-decay as a function of neutron number of the daughter nuclei in the region 104-109, similarly, (b) 110-115, (c) 116-121 and (d) 122-126.

of different decay modes and identification of shell closures in the SH region $104 \leq Z \leq 126$, there may exist daughter nuclei with magic number $N=184$ or near magic number if the nuclei undergoes CR. After detail investigation on CR in SHEs reveals that the shortest half-lives are observed for decay of SHEs through ${}^9\text{Be}$. The shortest half-lives corresponds to CD is referred as T_c . The figure 3.26 exhibits the connection between the $\log T_c$ and neutron number of daughter nuclei (N_d). Surprisingly it is observed that the shortest half-lives of CD in all SHEs is observed for neutron number $N_d = 184$ and near to that. However, many theoretical predictions also [11, 338, 339] have shown stability of nuclei when neutron number is equal or nearly equal to 184. The shorter CD half-lives are observed when $N_d = 184$ exhibits stronger shell effects due to their magicity when compared to their neighbouring ones. This is the clear evidence for the existence of the magic number corresponds to neutron number $N=184$.

Further, there is no experimental evidence on CR studies in the SH region. But, experimental CR in the actinide region is reported in table 3.3. The model used in the present work is validated by producing CR half-lives of experiments. The cluster-decay half-lives tabulated in table 3.7

evaluated using present model shows that the half-lives corresponds to the daughter neutron number ≈ 184 are having smaller value. Eventually, there is a tendency to form daughter nucleus with neutron number $N=184$. Hence, this may be the clue for the existence of neutron magic nuclei with $N=184$.

CHAPTER 4

Heavy particle radioactivity of superheavy elements

Synthesis of heavy elements is achieved by both cold fusion [340] and hot fusion [8] with different projectile target combinations up to atomic numbers $Z=118$, and heavy elements $Z=120$ synthesis is under attempt. A new kind of radioactivity with element ^{223}Ra named as heavy nuclei radioactivity was first identified by Rose et al., [30]. In 1980 Poenaru et al., [181] described calculations indicating a new type of decay known as heavy element decay which is in between α -decay and SF.

Furthermore, complex cluster radioactivity is studied in the region of heavy nuclei using density dependent cluster model (DCCM) with the use of M3Y nucleon-nucleon interaction [301]. The concept of HPR in the super heavy element with atomic number 126 using modified generalized liquid drop model (MGLDM) [292] is studied. Also studied ground state to ground state α decay in heavy nuclei region by Buck et al., [341] using Square-well potential model (SWPM). The potential energy surface for binary decay modes of ^{228}Th versus the distance between the fragment centers and the mass asymmetry is calculated by using Numerical super asymmetric fission (NuSAF) model and the analytical super asymmetric fission (ASAF) model [129, 181]. The binding energies, α -decay energies, and α -decay half-lives for heavy and SHN region is studied using the generalized density-dependent cluster model (GDCCM) [188]. Charity made a systematic description of evaporation spectra for light and heavy compound nuclei using macroscopic models

of the nucleus such as the rotating liquid-drop model (RLDM) [342]. Further more a theoretical investigation of the feasibility of α decay and cluster radioactivity from proton rich heavy isotope viz., Osmium (Os) isotopes with mass number ranging from 162–190 is studied by Nithu Ashok et al., [343] using Effective Liquid Drop Model (ELDM) and the α -decay half-lives of nuclei in the ground states and isomeric states have been calculated within the WKB approximation and Royer's formulae by a generalized liquid drop model (GLDM) [226].

Apart from the above theoretical approach many have studied the significance of certain terms viz; surface term, volume term, Coulomb term, shell term and asymmetric term in HPR. In the phenomenon of HPR, to establish a link between microscopic and macroscopic models by the method of self consistent semi classical description was studied by Brack et al.,[344]. The study of isobaric yield ratios and symmetry energy in heavy-ion reactions near the Fermi energy based on the Coulomb term was studied by Huang et al., [345]. Analysis of various competing binary and ternary decay processes of the ^{253}Es nucleus was studied by Sharma et al., [346] and conclude that closed shell effects play a significant role in the symmetric and asymmetric fission of binary and ternary fission. Further calculation of fission barriers for heavy and super heavy nuclei where formulations with the treatment of the surface-asymmetry term studied by Nix [347].

Earlier researchers have studied different decay modes such as binary fission, ternary fission, α -decay, β -decay, SF, cluster radioactivity and HPR [87, 88, 90–92, 94, 96, 117, 118, 160, 248, 348] in heavy and SHN.

The concept of HPR was introduced by previous researcher [129] by studying the cluster emission of atomic number $Z_e \geq 28$. The HPR with cluster emission of atomic number $Z_e^{max} = Z - 82$ allowing to get daughter of doubly magic nuclei ^{208}Pb from parent nuclei with $Z > 110$. The study of HPE in the SH region is important for nuclear structure analysis. Hence in the present work, systematically studied HPE in the SH region using CPPM and MGLDM models. It is also

identified the heavy particle emitters and its decay chain.

4.1 Theory

Among the various models, the MGLDM and CPPM are the successful models which describe the fusion, fission, α -decay, light particle emission, cluster emission, HPR and nuclear structure parameters such as nuclear radius and mass, investigation of charge asymmetry, deformation and proximity effects, for deformed nuclei. These theoretical models used in the chapter-3 of section 3.2, are extended for the study of HPR in SHN.

4.2 Results

Table 4.1 Tabulation of Q-values obtained using different mass excess values such as WS3+RBF, WS4, WS4+RBF, WS3, KTUY, FRLDM, WS with experimental Q-values

Parent	Daughter	Expt	WS3+RBF	WS4	WS4+RBF	WS3	KTUY	RIPL	WS
²³⁰ Th	²⁰⁶ Hg	57.57	56.74	57.49	57.95	57.39	56.72	57.76	56.74
²³¹ Pa	²⁰⁸ Pb	60.42	50.78	51.54	52.03	51.41	50.55	51.84	50.78
²³¹ Pa	²⁰⁷ Tl	60.42	58.92	59.83	60.39	59.74	58.89	60.41	58.92
²³⁰ U	²⁰⁸ Pb	61.4	60.02	60.39	61.33	60.50	59.83	61.39	60.02
²³² U	²⁰⁸ Pb	62.31	61.00	61.81	62.31	61.78	61.26	62.31	61.00
²³³ U	²⁰⁹ Pb	60.49	59.34	60.39	60.64	60.39	59.60	60.49	59.34
²³⁴ U	²⁰⁶ Hg	74.11	72.80	73.88	74.06	73.59	73.15	74.11	72.80
²³⁴ U	²¹⁰ Pb	58.83	57.77	58.85	58.90	58.85	58.09	58.83	57.77
²³⁴ U	²⁰⁸ Pb	59.47	58.25	59.80	59.66	59.31	58.60	59.47	58.25
²³⁶ Pu	²⁰⁸ Pb	79.67	78.47	79.34	79.45	79.14	78.72	79.67	78.47
²³⁸ Pu	²⁰⁶ Hg	91.19	90.08	90.57	90.97	90.25	90.32	91.19	90.08
²³⁸ Pu	²¹⁰ Pb	75.91	75.59	76.38	75.86	76.25	75.07	75.91	75.59
²³⁸ Pu	²⁰⁸ Pb	77.00	76.06	77.02	76.76	76.66	76.40	76.82	76.06
²⁴² Cm	²⁰⁸ Pb	96.51	96.00	96.31	96.39	95.98	96.67	96.51	96.00

The Q-values obtained using different mass excess values were tabulated in table 4.1. The standard deviation obtained from each Q-values using different mass excess values are evaluated

Table 4.2 The standard deviation obtained using different mass excess values with that of experimental Q-values.

WS3+RBF	WS4	WS4+RBF	WS3	KTUY	FRLDM	WS
2.90	2.50	2.33	2.55	2.91	2.38	2.90

as follows;

$$\sigma = \left(\frac{1}{(n-1)} \sum_{i=1}^n (Q^{cal} - Q^{exp})^2 \right)^{1/2} \quad (4.1)$$

The evaluated standard deviation of Q-values produced by various mass excess values are tabulated in table 6.1. From the table it is clear that the values obtained using WS4+RBF with respect to available experimental Q-values produces less deviation when compared to other studied models. Whereas, KTUY mass excess values produces larger deviation with respect to experimental Q-values. Hence, in our further analysis, WS4+RBF mass excess values are used to evaluate HPR. The experimental logarithmic half-lives of cluster radioactivity from ^{221}Fr to ^{238}Pu are evaluated using both CPPM and MGLDM. Both models are successively reproducing experimental cluster decay half-lives. Since both models were good enough to reproduce experimental values, the standard deviation obtained by these CPPM and MGLDM is found to be $\sigma=2.902$ and $\sigma=1.342$ respectively. From the standard deviation it is found that the MGLDM model produces less deviation when compared to CPPM. Hence, in our further analysis MGLDM is used to investigate HPR half-lives in the atomic number range $104 \leq Z \leq 126$.

Figure 4.1(a)-(d) shows the variation of amount of energy released during ^{86}Kr HPR from the even SH element $Z=104, 112, 120$ and 126 . Similarly, 4.1(e)-(h) shows variation of Q-values as function of Sussmann central radii for odd SH element $Z=107, 113, 117$ and 123 . As the Sussmann central radius increases, the Q-value gradually decreases. From the figure 4.1(a) it is noticed that the Q-value will be large for the nuclei with even number of neutrons compared to their immediate neighbours which is due to pairing of electrons. In the neighbourhood of the Sussmann central

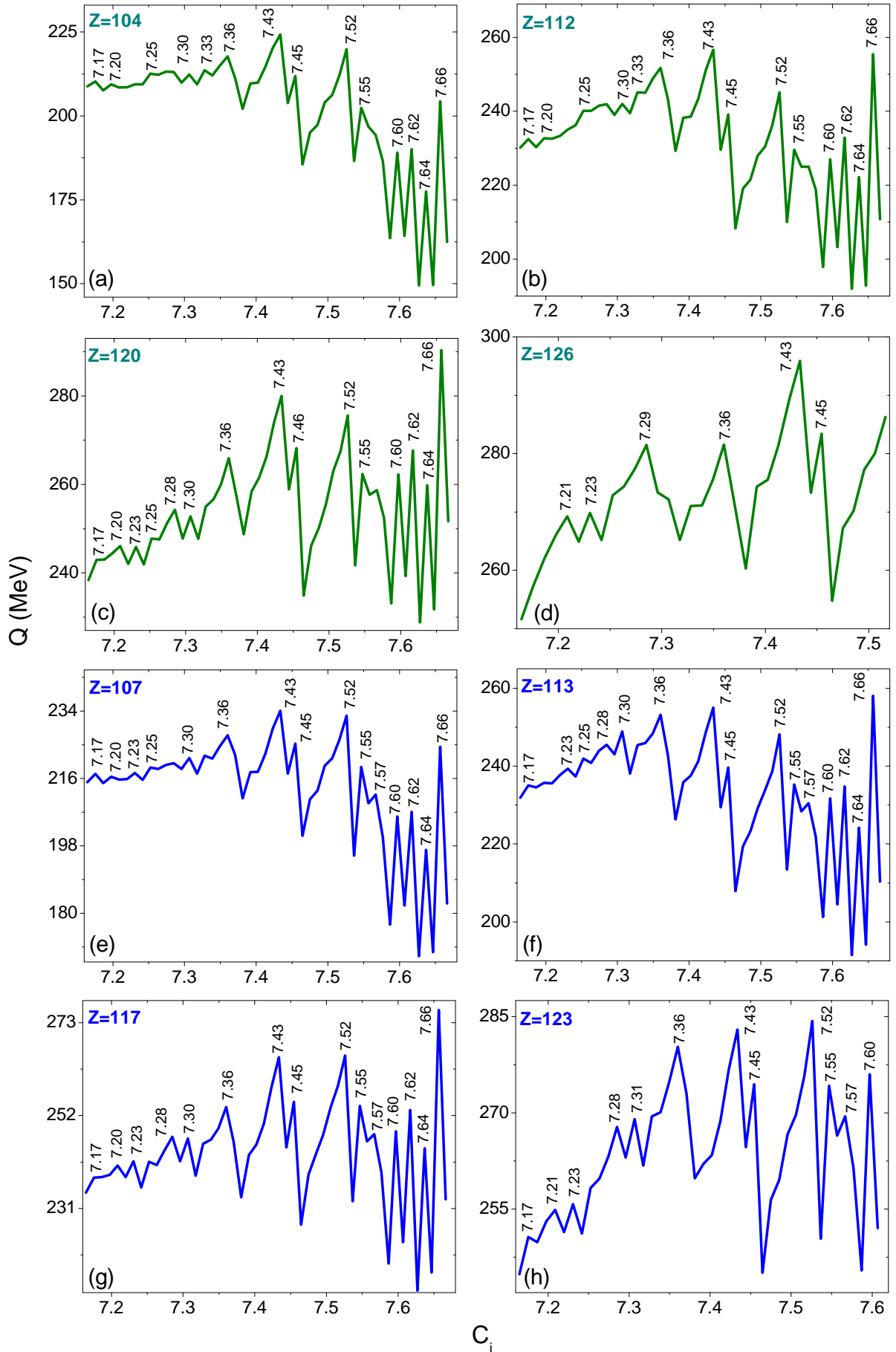


Fig. 4.1 A plot of Q value (MeV) as a function of Sussmann central radii (C_i) in the atomic number range $104 \leq Z \leq 126$ for the HPR of ^{86}Kr .

Table 4.3 A comparison of cluster decay half-lives [305] obtained using CPPM and MGLDM with that of available experiments.

Parent	Daughter	CPPM	MGLDM	Expt.	Parent	Daughter	CPPM	MGLDM	Expt.
²²¹ Fr	²⁰⁷ Tl	12.99	14.43	14.51	²³⁸ Pu	²⁰⁸ Pb	23.68	25.26	25.66
²²¹ Ra	²⁰⁷ Pb	11.93	13.86	13.37	²³⁸ Pu	²⁰⁶ Hg	22.87	27.85	25.3
²²² Ra	²⁰⁸ Pb	9.14	13.13	11.05	²⁴² Cm	²⁰⁸ Pb	21.66	23.24	23.11
²²³ Ra	²⁰⁹ Pb	13.33	14.03	15.05	²³¹ Pa	²⁰⁷ Tl	25.98	22.07	23.23
²²⁴ Ra	²¹⁰ Pb	13.84	15.08	15.9	²³³ Th	²⁰⁷ Hg	24.46	28	29.2
²²⁶ Ra	²¹² Pb	19.52	18.76	21.29	²²⁶ Th	²¹² Po	12.8	12.18	15.3
²²⁵ Ac	²¹¹ Bi	13.03	16.11	19.28	²²⁶ Th	²⁰⁸ Pb	12.47	13.83	15.3
²²⁸ Th	²⁰⁸ Pb	24.62	21.94	20.73	²³⁰ U	²⁰⁸ Pb	17.57	19.21	18.2
²³¹ Pa	²⁰⁸ Pb	24.75	26.39	26.02	²³⁰ U	²⁰⁶ Pb	17.68	19.12	18.2
²³⁰ U	²⁰⁸ Pb	17.57	18.63	19.56	²³² U	²⁰⁸ Pb	23.75	21.25	21.08
²³⁰ Th	²⁰⁶ Hg	27.71	23.87	24.61	²³² U	²⁰⁴ Hg	20.87	22.78	22.6
²³¹ Pa	²⁰⁷ Tl	25.98	22.07	22.89	²³³ U	²⁰⁹ Pb	27.45	23.75	24.83
²³² U	²⁰⁸ Pb	18.14	21.25	20.39	²³³ U	²⁰⁵ Hg	28.24	25.9	27.59
²³³ U	²⁰⁹ Pb	22.45	23.75	24.84	²³⁴ U	²¹⁰ Pb	19.46	25.9	25.92
²³⁴ U	²¹⁰ Pb	23.46	25.9	25.93	²³⁴ U	²⁰⁸ Pb	22.97	27.32	25.92
²³⁴ U	²⁰⁸ Pb	22.97	27.32	25.93	²³⁴ U	²⁰⁶ Hg	18.4	26.04	27.54
²³⁴ U	²⁰⁶ Hg	21.4	26.04	25.74	²³⁶ U	²⁰⁸ Hg	22.43	30.39	27.58
²³⁵ U	²⁰⁷ Hg	25.71	28.54	27.44	²³⁶ U	²⁰⁶ Hg	19.87	27.43	27.58
²³⁶ Pu	²⁰⁸ Pb	20.13	22.67	21.65	²³⁸ Pu	²¹⁰ Pb	19.07	26.93	25.7
²³⁸ Pu	²¹⁰ Pb	22.07	26.93	25.66	²³⁸ Pu	²⁰⁸ Pb	17.68	25.26	25.7

radii 7.61 and 7.63, Q-value is almost minimum. Similarly, the minimum Q-value due to pairing effect is also observed for both odd and even SHN.

In HPR, different emissions such as ⁵⁸Ni, ⁵⁹Cu, ⁶⁰Zn, ⁶¹Ga, ⁶²Ge, ⁶³As, ⁶⁴Se, ⁶⁵Br, ⁶⁶Kr, ⁶⁷Rb, ⁶⁸Sr, ⁶⁹Y, ⁷⁰Zr, ⁷¹Nb, ⁷²Mo, ⁷³Tc, ⁷⁴Ru, ⁷⁵Rh, ⁷⁶Pd, ⁷⁷Ag, ⁷⁸Cd, ⁷⁹In, ⁸⁰Sn, ⁸¹Sb, ⁸²Te, ⁸³I, ⁸⁴Xe, ⁸⁵Cs, ⁸⁶Ba, ⁸⁷La, ⁸⁸Ce, ⁸⁹Pr, ⁹⁰Nd, ⁹¹Pm and ⁹²Sm were studied using the conditions such that $Z_e^{min} = 28$ and maximum HPR is $Z_e^{max} = Z - 82$ [26]. Further, a plot of logarithmic half life as a function of (a) neutron number of cluster (N_c), (b) neutron number of parent nuclei (N_p), (c) atomic number of cluster nuclei (Z_c) and (d) atomic number of daughter nuclei (Z_d) is shown in figure 4.2 for the SH region $120 \leq Z \leq 126$. This figure depicts that logarithmic half life increases with the neutron number of both cluster and parent nuclei. It is clearly observed from the figure 4.2(a) that the logarithmic half-lives have larger values for which neutron number of cluster emission $N_C = 37, 45, 56$ and 68 . That is the parent nuclei is more stable for these neutron

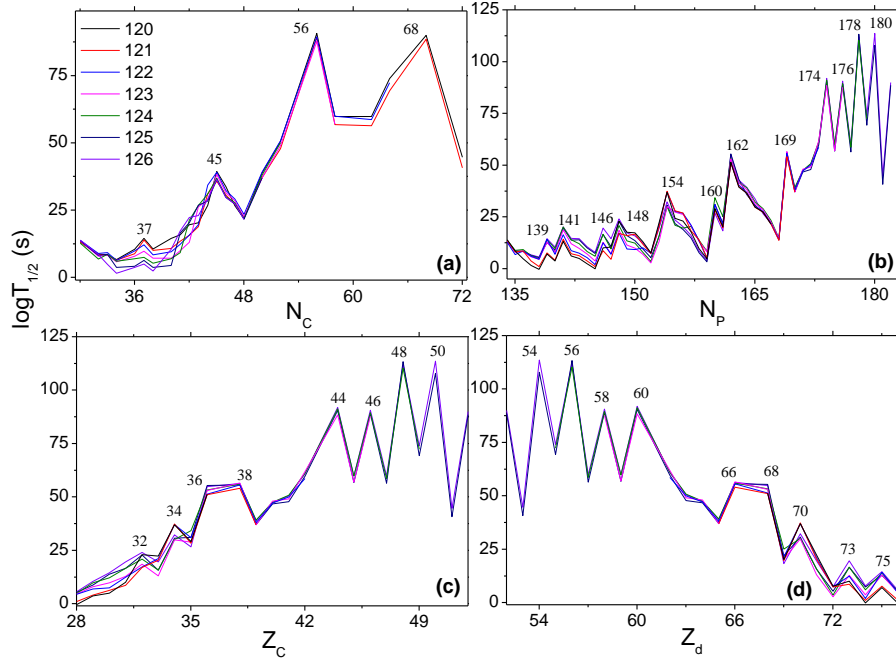


Fig. 4.2 A plot of $\log T_{1/2}$ (s) as a function of (a) neutron number of cluster (N_C), (b) neutron number of parent nuclei (N_P), (c) atomic number of cluster nuclei (Z_C) and (d) atomic number of daughter nuclei (Z_d).

cluster emissions. The parent nuclei is more stable when neutron number is equal to $N_P=139-180$ in which larger half-lives are observed when most of the neutron number is even due to pairing effects. Similarly, the $\log T_{1/2}$ values increases with increase in Z_C and parent nuclei becomes more stable when Z_C are found to be even numbers and vice versa in case of Z_d . Hence, the HPE from the parent nuclei and its half-lives fairly depends on the neutron and atomic number of cluster, daughter and parent nuclei.

Further, the relative neutron excess also plays an important role in the stability of nuclei. Hence, half-lives of parent nuclei is studied as a function of relative neutron excess and it is presented in figure 4.3. The $\log T_{1/2}$ values increases with increase in relative neutron excess value. The half-lives of parent nuclei shows more stability when the relative neutron excess values are between 0.133 to 0.267 in the atomic number range $120 \leq Z \leq 126$. The quantity of neutrons and protons has a substantial impact on logarithmic half-lives. A plot of $\log T_{1/2}$ as function of asymmetry effect $((N - Z)^2/A)$ for different HPR of ^{86}Kr , ^{91}Y , ^{94}Zr and ^{96}Mo in case of $Z=120$,

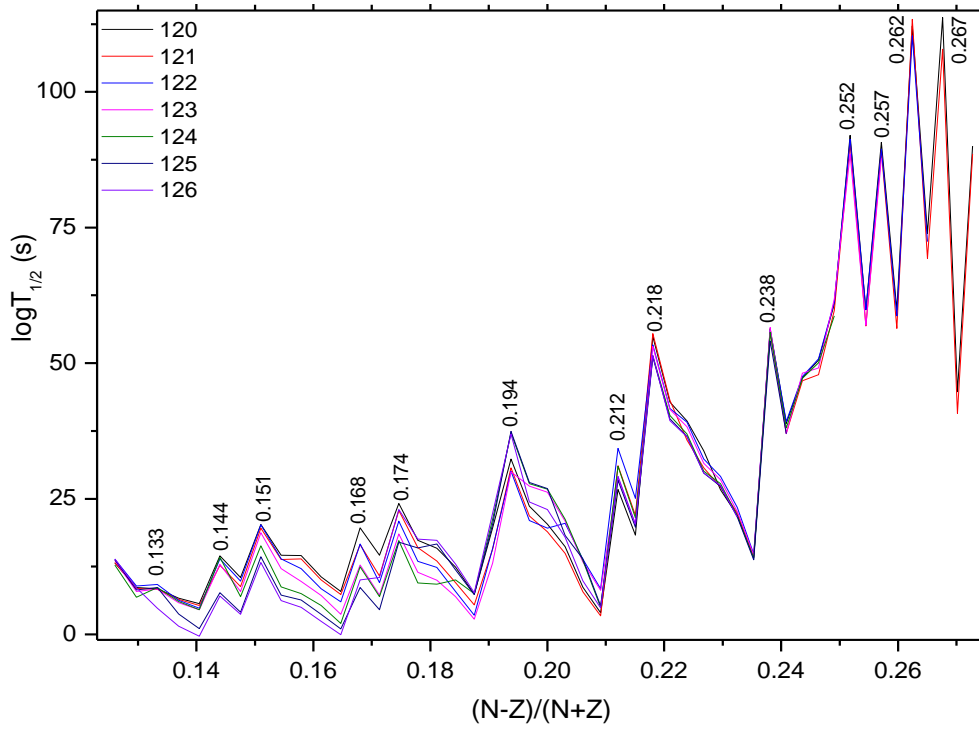


Fig. 4.3 A plot of $\log T_{1/2}(s)$ as a function of relative neutron excess $(N - Z)/(N + Z)$ of parent nuclei.

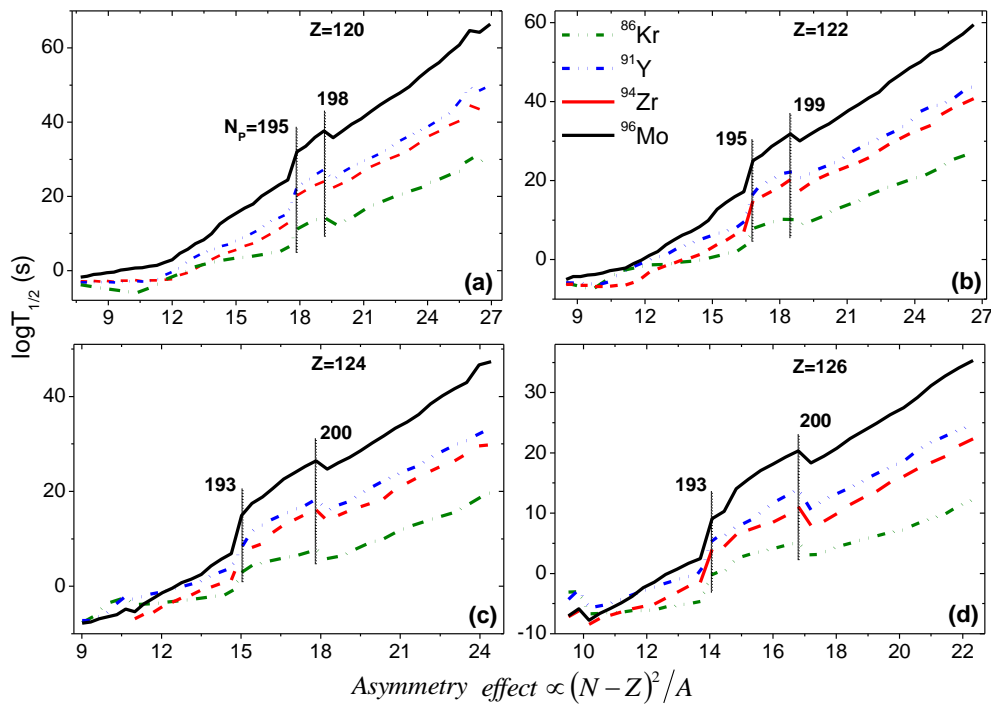


Fig. 4.4 A plot of $\log T_{1/2}(s)$ as a function of asymmetry effect $((N - Z)^2/A)$ for different HPR such as ^{86}Kr , ^{91}Y , ^{94}Zr and ^{96}Mo in case of (a) $Z=120$, (b) $Z=122$, (c) $Z=124$ and (d) $Z=126$.

122, 124 and 126 is presented in figure 4.4. As the value of asymmetry effect $((N - Z)^2/A)$ increases the corresponding half-lives gradually increases. However, larger stability is observed when $(N - Z)^2/A=195$ to 198 in case of $Z=120$ and 122. Similarly, higher stability is observed when asymmetry effect is equal to 193 to 200 in case of $Z=124$ and 126. Another key phrase

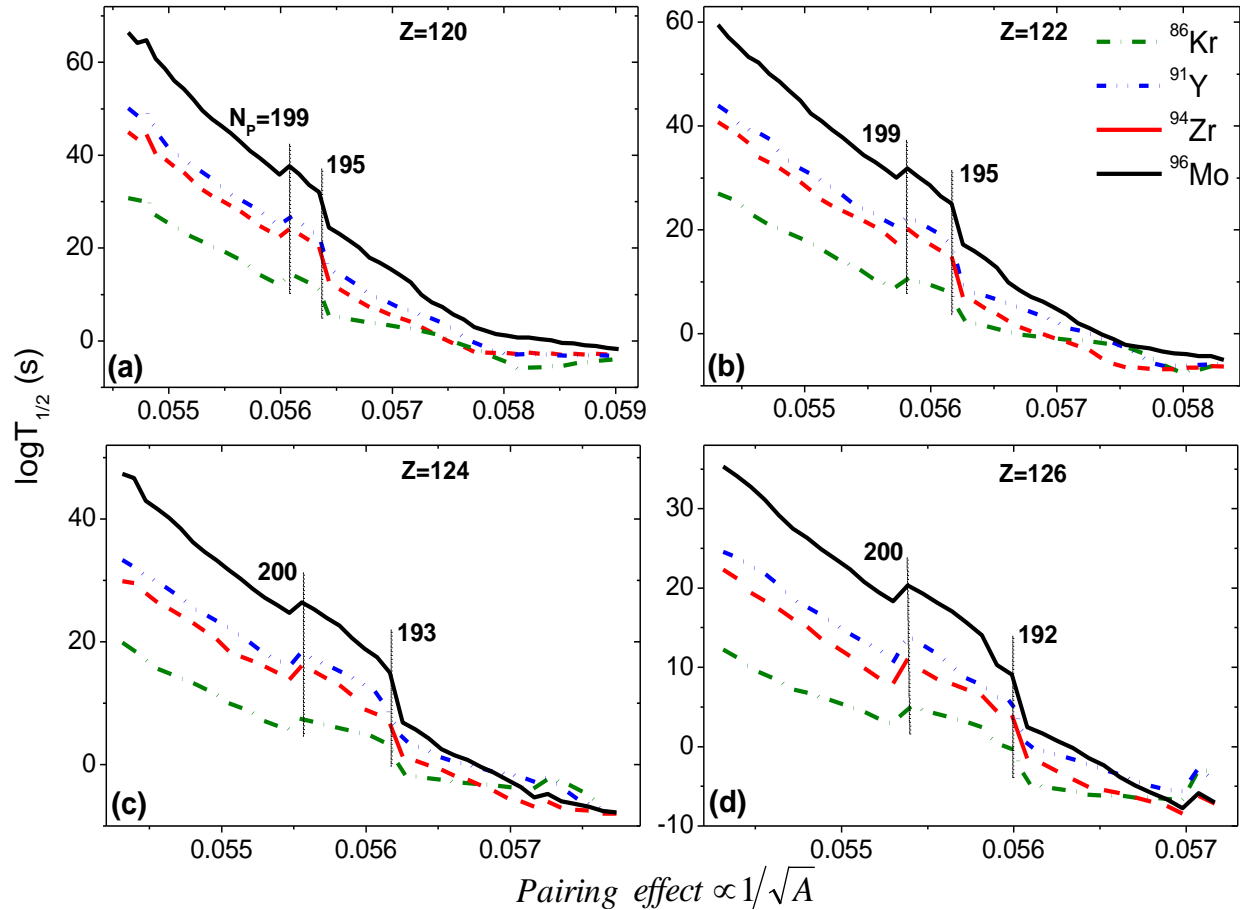


Fig. 4.5 A plot of $\log T_{1/2}(s)$ as a function of pairing effect ($1/\sqrt{A}$) for different HPR such as ^{86}Kr , ^{91}Y , ^{94}Zr and ^{96}Mo in case of (a) $Z=120$, (b) $Z=122$, (c) $Z=124$ and (d) $Z=126$.

is pairing effect, which refers to the attractive interaction of two nucleons. Previous researches [319, 320] has shown that the pairing energy of protons is larger than that of neutrons for $N=50$ and $N=82$. The figure 4.5(a-d) represents the plot of $\log T_{1/2}$ as function of pairing effect for different HPR such as ^{86}Kr , ^{91}Y , ^{94}Zr and ^{96}Mo in case of (a) $Z=120$, (b) $Z=122$, (c) $Z=124$ and (d) $Z=126$. The gradual increase in the effect of pairing effect results in the decrease of $\log T_{1/2}$ values. When two nuclei are far away, the attractive interaction between them reduces and hence life-time of

parent nuclei also decreases. From the figure 4.5(a-d) shows stability of half-lives when pairing effect nearly equal to 0.0555 to 0.056 for which broad valley of neutron number with N=192 to 200 is observed. These results are on far with the prediction of band of neutron numbers which lies between N=172-184 [349].

The Coulomb effect of is also involved in the HPR. The Coulomb term $Z^2/A^{1/3}$ i.e repulsive

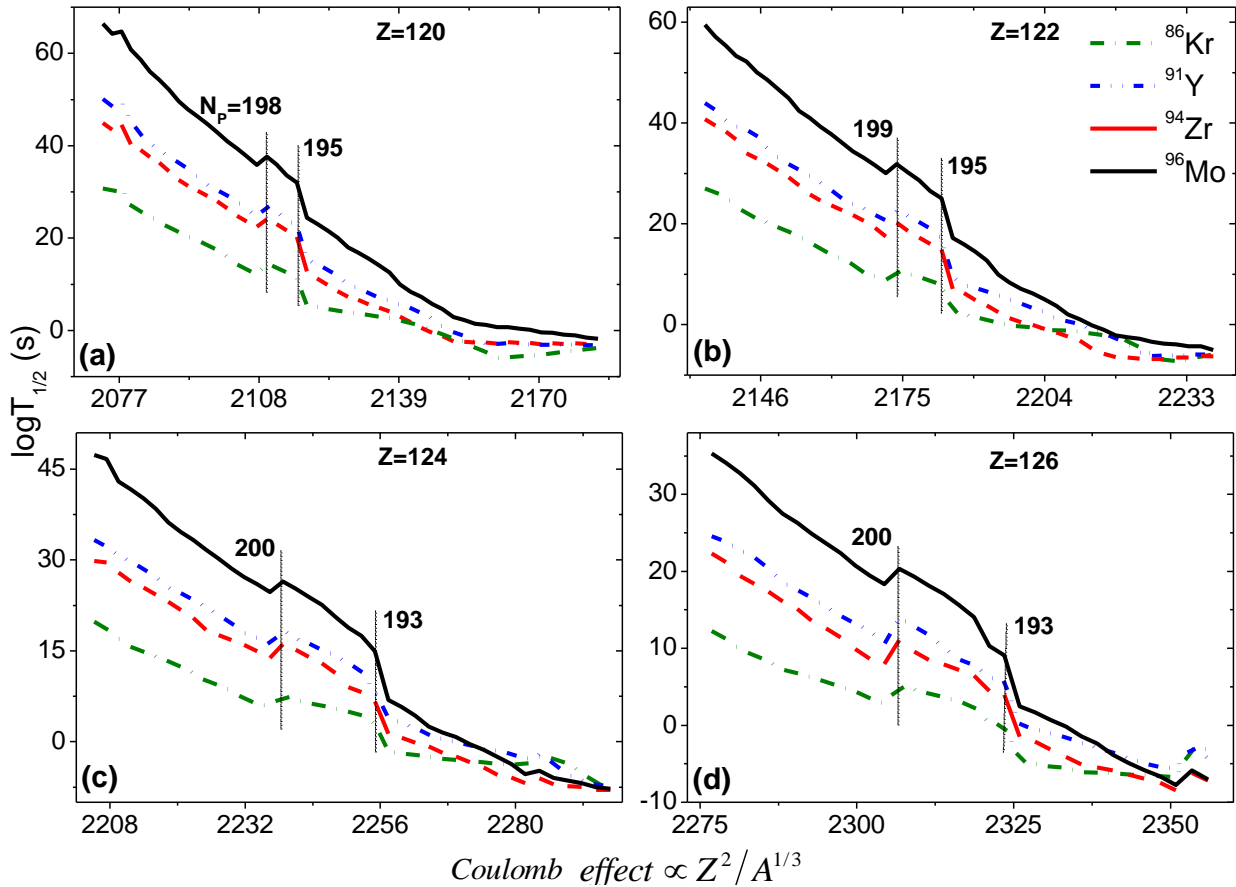


Fig. 4.6 A plot of $\log T_{1/2}(s)$ as a function of Coulomb effect ($Z^2/A^{1/3}$) for different HPR such as ^{86}Kr , ^{91}Y , ^{94}Zr and ^{96}Mo in case of (a) $Z=120$, (b) $Z=122$, (c) $Z=124$ and (d) $Z=126$.

force between the two nuclei is studied. A plot of $\log T_{1/2}(s)$ as a function of Coulomb effect ($Z^2/A^{1/3}$) for different HPE such as ^{86}Kr , ^{91}Y , ^{94}Zr and ^{96}Mo in case of $Z=120$, $Z=122$, $Z=124$ and $Z=126$ are presented in figure 4.6. As the Coulomb effect increases, the logarithmic half-lives decreases. That is when the Coulomb effect becomes dominant, the force of attraction between the two nuclei decreases and hence there is a decrease in the half-lives. As similar to asymmetry effect

and pairing effect, a band of neutron number from 193-200 is observed for which the logarithmic half-lives is found to be larger when compared to their neighbouring nuclei.

4.2.1 Comparison of HPR with alpha decay and SF

After detail analysis of HPR on asymmetry effect, relative neutron excess, pairing effect and Coulomb effect an effort was made to investigate dominant decay modes such as SF and α -decay. The SF half-lives [350] are evaluated as follows;

$$T_{1/2} = \exp \left(2\pi \left[c_0 + c_1 A + c_2 Z^2 + c_3 Z^4 + c_4 (N - Z)^2 - \left(0.13323 \frac{Z^2}{A^{1/3}} - 11.64 \right) \right] \right) \quad (4.2)$$

here A is the mass number of parent nuclei, N and Z are the neutron and atomic number of parent nuclei, respectively.

Semi-empirical formula including angular momentum by Dong, et al., [226] is as follows;

$$\log T_{1/2}^{Dong} = aZQ^{-1/2} + bA^{1/6}Z^{1/2} + c + \frac{\ell(\ell + 1)}{\sqrt{(A - 4)(Z - 2)A^{-2/3}}} \quad (4.3)$$

Where a, b and c are fitting parameters.

From the earlier studies [351] it is noticed that ^{86}Kr is dominant in SH element Z=118 when compared to all other studied HPR. Similarly, for SH element Z=122 the dominant HPR is found to be ^{94}Zr , for Z=123 it is ^{91}Y and for Z=124 and Z=126 the HPR is found to be ^{96}Mo . Hence, in the present comparison, HPR half-lives of ^{86}Kr , ^{94}Zr , ^{91}Y and ^{96}Mo were compared with that of SF and α -decay. The figure shows the plot of $\log T_{1/2}$ as a function of mass number of parent nuclei. The figure 4.7(a) shows the comparison of different decay modes of ^{86}Kr HPR, SF and α -decay half-lives of SH element Z=118 as a function of mass number of parent nuclei. Here, α decay is dominant in the mass number $^{281-291}\text{Og}$, in case of $^{292-295}\text{Og}$ HPR is dominant, again

α -decay is dominant in the SHN $^{296-302}\text{Og}$. The SF is dominant in $^{303-304}\text{Og}$ and beyond ^{305}Og , α -decay is dominant. Similarly, examined the possible dominant decay mode in the SH element $Z=122$ to 124 and 126 , it is also presented in figure 4.7(b-e).

Later, also studied decay chains for the identified HPR. The identified HPR and its decay

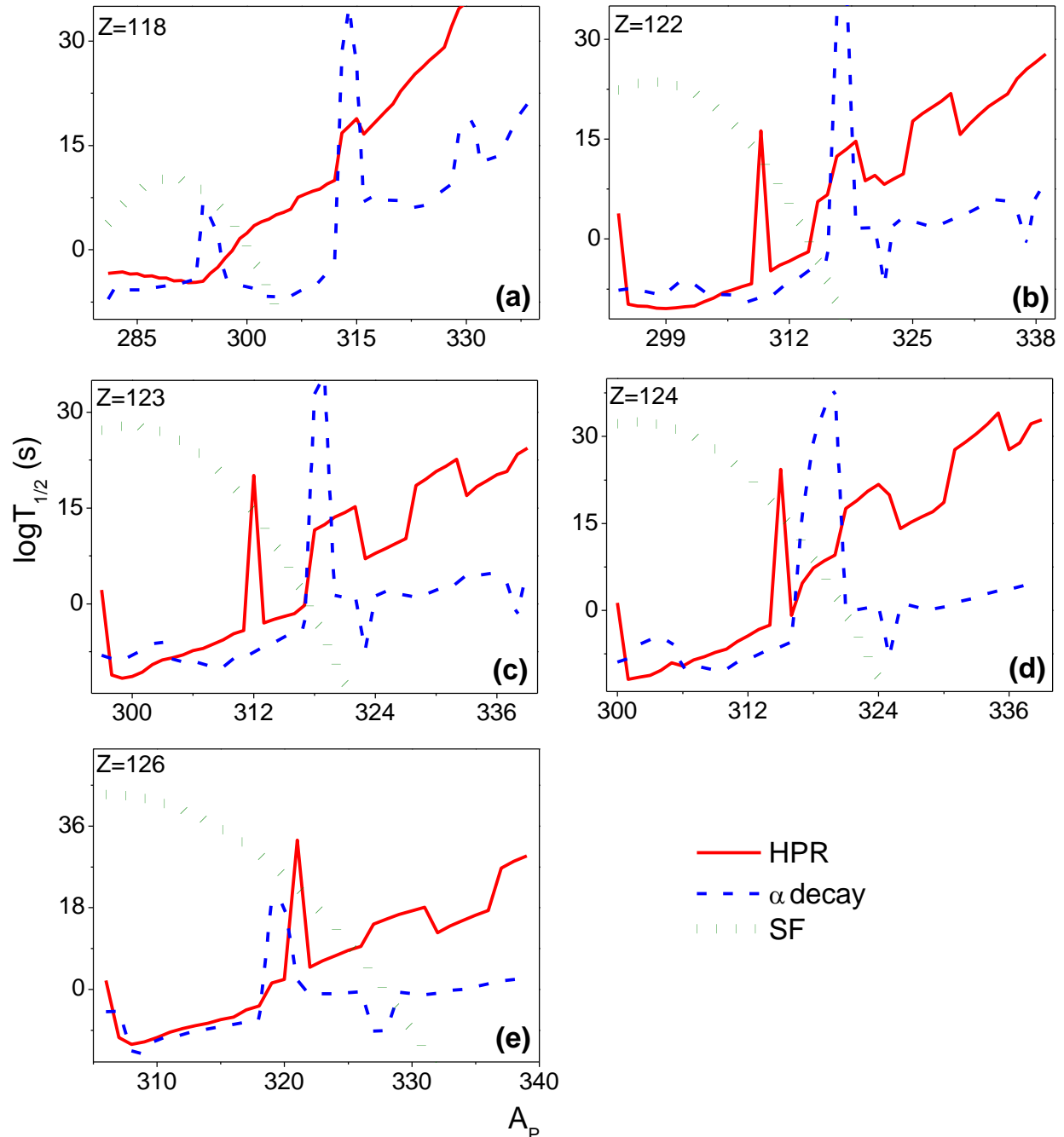


Fig. 4.7 Comparison of $\log T_{1/2}(s)$ of HPR (HPR), α decay and SF (SF) as a function of mass number of the parent nuclei (A_P) for different SH elements.

chains in the SH region $118 \leq Z \leq 126$ are tabulated in table 4.4. In addition to α -decay and SF

Table 4.4 Decay chain of predicted heavy particle emitters in the SHN region $118 \leq Z \leq 126$. Tabulation of Q-values, half-lives of HPR (HPR), α , β^\pm -decay and SF along with dominant decay mode.

Nuclei	Q (MeV)	HPR	α	β^+	β^-	SF	Decay mode
^{292}Og ^{206}Pb	300.79	1.90E-05	7.22E-05	3.23E-04	8.52E+08	5.26E+09	HPR(^{86}Kr) Stable
^{293}Og ^{207}Pb	300.45	2.19E-05	9.60E-05	1.95E-04	5.18E+08	1.55E+09	HPR(^{86}Kr) Stable
^{294}Og ^{208}Pb	300.03	2.86E-05	3.67E+05	8.59E-04	3.15E+08	3.02E+08	HPR(^{86}Kr) Stable
^{295}Og ^{209}Pb	297.96	3.86E-04	5.17E+03	5.19E-04	1.92E+08	3.90E+07	HPR(^{86}Kr) Beta-
^{209}Bi ^{205}Tl	3.138	3.94E+42	6.34E+26	8.13E+26	7.20+26	9.87E+41	α Stable
$^{300}\text{122}$ ^{206}Pb	336.31	2.03E-07	9.80E-07	5.27E-06	8.27E+09	1.29E+23	HPR(^{94}Zr) Stable
$^{301}\text{122}$ ^{207}Pb	335.73	2.90E-07	1.37E-06	3.13E-06	5.04E+09	4.05E+22	HPR(^{94}Zr) Stable
$^{302}\text{122}$ ^{208}Pb	335.28	3.56E-07	7.88E-07	1.35E-05	3.08E+09	8.41E+21	HPR(^{94}Zr) Stable
$^{297}\text{123}$ ^{206}Po	338.25	4.27E-08	5.06E-08	6.59E-08	1.73E+11	1.54E+27	HPR(^{91}Y) Beta+
^{206}Bi ^{206}Pb	2.735	6.10E+50	1.47E+19	5.39E+05	8.51E+05	2.01E+36	Beta+ Stable
$^{299}\text{123}$ ^{208}Po	338.29	2.07E-08	2.98E-08	1.68E-07	6.44E+10	6.30E+27	HPR(^{91}Y) α
^{204}Pb ^{200}Hg	1.969	7.89E+58	4.42E+21	3.99E+24	1.53E+23	2.15E+39	α Stable
$^{301}\text{123}$ ^{210}Po	336.67	7.48E-08	5.94E-07	4.28E-07	2.40E+10	4.98E+27	HPR(^{91}Y) α
^{206}Pb	5.407	2.11E+55	1.20E+07	3.76E+07	1.45E+07	1.84E+37	Stable
$^{301}\text{124}$ ^{205}Pb	355.63	3.02E-08	3.21E-08	5.90E-08	1.14E+11	2.73E+32	HPR(^{96}Mo) SF
$^{302}\text{126}$ ^{206}Pb	354.06	1.46E-07	4.04E-06	2.53E-07	6.97E+10	3.02E+32	HPR(^{96}Mo) Stable

of evaluated β^+ and β^- -decay as explained in literature [160]. For SHN ^{292}Og , HPR, α -decay, SF and β^\pm -decay half-lives are evaluated as seen in table 4.4. From the comparison of all these different decay modes, it is clearly seen that the HPR half-life is smaller when compared to other studied decay modes. Hence, HPR of ^{86}Kr is dominant in the SHN ^{292}Og and parent nuclei becomes ^{206}Pb and then it becomes stable. Similarly, ^{293}Og and ^{294}Og both undergoes ^{86}Kr radioactivity and then

the parent nuclei becomes stable by lead (Pb) residual nuclei. However, the nuclei ^{295}Og follows ^{86}Kr radioactivity then β -decay followed by an α -decay, then the nuclei ^{205}Tl becomes stable. In case of $^{300-302}122$ shows smaller half-lives for HPR of ^{94}Zr and in all these cases the Pb is the stable nuclei. Further, the nuclei $^{297,299,301}123$ undergoes ^{91}Y HPR it reaches stable nuclei. Similarly, the SHN $^{301}124$ experiences ^{96}Mo HPR and stable nuclei is reached with the lead (Pb) nuclei. Similar case is also observed for the SHN $^{302}126$.

After detail investigation on decay chain of predicted heavy particle emitters, 11 heavy particle emitters are identified in the SH region such as ^{292}Og , ^{293}Og , ^{294}Og , ^{295}Og , $^{300}122$, $^{301}122$, $^{302}122$, $^{297}123$, $^{299}123$, $^{301}124$, $^{302}124$ and $^{302}126$. Almost all these heavy particle emitters end their decay chain by forming stable lead. It is found that SH elements may be formed in supernova explosion through nuclear process such as r process [352] and multi-nucleon transfer reactions [353]. The formed SH nucleus is having very short lifetimes and it undergoes decay to form stable nucleus such as lead. It is also observed that the abundance of elements in supernova and galaxy spectrum shows larger quantities of Pb [354, 355]. Hence, present work may find useful in nuclear astrophysics aspect.

CHAPTER 5

Investigations on decay modes of superheavy nuclei

5.1 Introduction

The unanswered questions in the field of Nuclear Physics are; what is the heaviest SHN that can exist? Do very long-lived SHN exist in the nature?. Over the past ten years have been marked by remarkable progress in the science of SH elements and nuclei. The existence of the SHN above $Z=103$ can be studied by its limitations such as whether it is naturally occurring or synthesised in the laboratory. There is no conclusive remarks on the existence of SHN naturally. Instead, these SHN is synthesised using the cold and hot fusion reactions with half-lives ranging between days to μs . The cold fusion reactions include either lead or bismuth as targets [9] and hot fusion reactions includes ^{48}Ca beams on various actinide targets [178]. Many theoretical predictions such as microscopic-macroscopic [356] (single-particle potential) and self-consistent approaches includes nucleus-nucleus potential [357, 358], relativistic field model [359, 360] and Multinucleon transfer reactions [361] provides an information such as structure of the nuclei, location of shell closure and decay modes in the heavy and SHN.

The discovery of SH elements [175, 340] are assumed to be near the island of stability. Boilley et al., [362] predicted evaporation residue cross sections in the SH elements and also influence of shell effects [363]. The entrance channel dynamics using ^{48}Ca projectile and ^{208}Pb as target [364]. During the year 1966, two groups of researchers- Mayers and Swiatecki, Viola and Seaborg [365]

separately predicted the presence of heavy nuclei which is near the island of stability. Later on, Sobiczewski et al., [366] predicted that the nucleus $Z=114$ will be the center of island of stability and neutron number $N=184$. In the year 1955 Nilsson [367] proposed shell model which includes deformation property of the nuclei. Bender et al., [368] uses skyrme energy density functional model and studied the deformation properties of closed proton and neutron shells. The nuclear mass, radius and spectroscopy far away from the valley of stability and were experimentally analysed by earlier researchers [369]. Investigation of the isomers for SHN ^{254}No is the stepping stone towards the island of stability [370]. Previous researchers [371] have analysed the nuclear shell structure and have found that there is an extra stability near the magic nuclei. The present scenario is almost near to the center of presumed island of stability, but the final landing is yet to be completed and intriguing question is how these SHN is still accessible.

On the other hand, the identification of SHN is based on the observations of decay chains. The SHN, $Z=114-118$ were observed by its consistent decay chains which end in the isotopes of Rutherfordium(Rf) and Dubnium(Db). The SF and α -decay are the main dominant decay modes in the SHN and also limits the stability of SHN. Furthermore, the newly synthesised SH elements are mainly identified by its decay chains from unknown nuclei to the known daughter nuclei with the help of the parent and daughter correlation.

Previous researchers [87, 87–93, 95–98, 207] were extensively studied the competition between different decay modes such as ternary fission, SF, CD, proton decay, β -decay and α -decay in the heavy and SH region using various theoretical models such as CPPM, MGLDM, ELDM and temperature dependent proximity potential model(TDPPM). The possible decay modes in the SHN $Z=119$ and 120 were predicted [372]. From the literature [373] it is clearly observed that the isotopes of SHN $Z=104-112$ is having α -decay and SF as dominant decay modes. Whereas, only α -decay is dominant in the isotopes of SHN $Z=113, 115-118$. While the isotopes of SHN, $Z=114$

is having SF as dominant in the nuclei ^{284}Fl and α -decay is dominant in the nuclei $^{286-289}\text{Fl}$ and β^+ is dominant in the nuclei ^{290}Fl . On the other hand, the concept of heavy particle radioactivity [129] in the SH region also finds an important application during the synthesis of SHN. In spite of significant development in the experimental and theoretical progressions, but there exists many unanswered questions related to decay modes of the SHN. Until now only α -decay and SF were successfully observed in the experiments.

Experimental results suggesting a considerable increase in the lifetime of nuclei as they approach the closed proton and neutron shells [374]. The lifetimes of most known SHN are governed by the competition between α -decay and SF. The existence of island of stability has been confirmed experimentally during previous decade [8]. Some theoretical studies reveals that the SH element with 114 and 164 protons are stable against the fission, alpha and beta decays [375]. Various phenomenological and microscopic models such as fission model(FM) [71], cluster model (CM) [376], GLDM [241], UMADAC [187] are available in the literature to study the different decay modes of SHN. In addition to the above study many literature's are available in relation to an α - decay and SF of SHN[377–379]. Simple empirical formulae is also available in determining decay half-lives [216]. The possible isotopes for new SH elements are identified by studying the competition between different probable decay modes such as α , β , cluster-decay and SF. This work focus on the different decay modes of SHN in the atomic number range $104 \leq Z \leq 126$. After detail investigation on the competition between different decay modes, the possible isotopes and their decay modes with branching ratios are identified in the SHN region. Hence, the current work is significant in predicting the most possible decay mode in SHN and identifying possible emitters in this SH region. The theoretical formalism is explained in section 5.2.

5.2 Theory

5.2.1 Alpha and cluster decay

In an effective liquid-drop model (ELDM), the α decay half-life is computed using the relation

$$T_{1/2}(s) = \frac{\ln 2}{\nu_0 P P_\alpha} \quad (5.1)$$

Where ν_0 is the assault frequency on the barrier and $\nu_0 = 1.8 \times 10^{22} s^{-1}$ [380]. P_α is the pre-formation factor is closely related with the shell structure [381]. The empirical formula for P_α is expressed as;

$$\log P_\alpha = p_1 + p_2(Z - Z_1)(Z_2 - Z) + p_3(N - N_1)(N_2 - N) + p_4 A \quad (5.2)$$

where N, Z and A are the neutron, charge and mass number of the parent nucleus respectively, Z_1 and Z_2 are the proton magic numbers around Z ($Z_1 \leq Z \leq Z_2$) and N_1 and N_2 the neutron magic numbers around N ($N_1 \leq N \leq N_2$). p_1, p_2 and p_3 corresponds to parameters in the region even(Z)-even(N), even(Z)-odd(N), odd(Z)-even(N) and odd(Z)-odd(N) are tabulated in table I of reference [382]. P is Gamow penetrability factor given by the expression

$$P = \exp \left[-\frac{2}{\hbar} \int_{\zeta_0}^{\zeta_c} \sqrt{2\mu[V(\zeta) - Q]} d\zeta \right] \quad (5.3)$$

where μ is the inertial coefficient resulted due to the approximation of Werner- Wheeler[383]. The limits of integration ζ_0 and ζ_c are the inner and outer turning points, expressed as $\zeta_0 = R_p - \bar{R}_1$ and $\zeta_c = \frac{Z_1 Z_2 e^2}{Q}$. R_p is the radius of the parent nucleus and \bar{R}_1 is the final radius of the emitted cluster.

In the effective liquid drop model, the studies have shown the total potential as sum of Coulomb,

proximity and centrifugal potential [384, 385]. Hence, one may use effective one-dimensional total potential energy as follows;

$$V = V_c + V_s + V_\ell \quad (5.4)$$

In order to evaluate the Coulomb contribution in terms of deformation parameter, V_c is used as defined in reference [386]

$$V_C(R) = \frac{e^2 Z_1 Z_2}{R} + 3Z_1 Z_2 e^2 \sum_{\lambda, i=1,2} \times \frac{R_i^\lambda(\alpha_i, T)}{(2\lambda + 1)} Y_\lambda^{(0)}(\theta_i) \left[\beta_{\lambda i} + \frac{4}{7} \beta_{\lambda i}^2 Y_\lambda^{(0)}(\theta_i) \right] \quad (5.5)$$

with

$$R_i(\alpha_i) = R_{oi} \left[1 + \sum_{\lambda} \beta_{\lambda i} Y_\lambda^{(0)}(\alpha_i) \right] \quad (5.6)$$

where $\beta_{\lambda i}$ is the deformation parameter and $Y_{\lambda(0)}$ is the spherical harmonics and $R_{oi} = 1.28A_i^{1/3} - 0.76 + 0.8A_i^{-1/3}$ The effective surface potential can be calculated by

$$V_s = \sigma_{eff}(S_1 + S_2) \quad (5.7)$$

where S_1 and S_2 are the surface areas of the spherical fragments. σ_{eff} is the effective surface tension which is defined as

$$\sigma_{eff} = \frac{1}{4(R^2 - R_1^2 - R_2^2)} \left(Q - \frac{3}{20\pi\epsilon_0} e^2 \left[\frac{Z^2}{R} - \frac{Z_1^2}{R_1} - \frac{Z_2^2}{R_2} \right] \right) \quad (5.8)$$

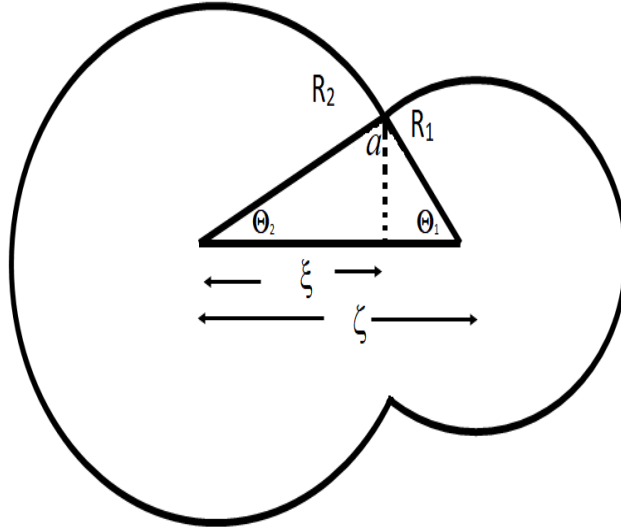


Fig. 5.1 Schematic presentation of molecular phase of the di-nuclear system. The daughter nucleus and the emitted (smaller) fragments. The distance between their geometrical centers and distance between the center of the heavier fragment and the circular sharp neck of radius a are denoted by ζ and ξ , respectively.

where R_2 is the final radius of the daughter fragment. The centrifugal potential energy is determined by

$$V_\ell = \frac{\hbar^2 \ell(\ell + 1)}{2\mu\zeta^2} \quad (5.9)$$

where ℓ is the angular momentum of emitted alpha/cluster and it is calculated using the selection rules. In case of an alpha/CD [148, 387], the selection rules follows the condition that;

$$|J_p - J_d| \leq \ell_\alpha \leq |J_p + J_d| \quad \text{and} \quad \frac{\pi_p}{\pi_d} = (-1)^{\ell_\alpha} \quad (5.10)$$

where J_p, π_p and J_d, π_d spin and parity of the parent and daughter nuclei, respectively. $\mu = \frac{M_1 M_2}{M_1 + M_2}$ is the reduced mass of the fragments. M_1 and M_2 represent their atomic masses. In ELDM, system having two intersecting spherical nuclei with different radii is considered [384]. The schematic diagram for the representation of four independent coordinates such as R_1, R_2, ζ and ξ are shown in figure 5.1. Three constraints are used to reduce 4-dimensional spherical problem to an equivalent

1-dimensional problem. A geometric constraint given below is introduced such that the spherical segments remain in contact.

$$R_1^2 - (\zeta - \xi)^2 = R^2 - \xi^2 \quad (5.11)$$

The variable ζ and ξ are the distance between the geometrical centers and distance between the center of the heavier fragment and the circular sharp neck of radius [149, 385]. Assuming nuclear matter as in-compressible, constraints for the conservation of systems total volume is

$$2(R_1^3 + R_2^3) + 3[R_1^2(\zeta - \xi) + R_2^2\xi] - [(\zeta - \xi)^2 + \xi^3] = 4R^3 \quad (5.12)$$

Where $R = r_0A^{1/3}$ is the radius of the parent nucleus, $r_0=1.34$ fm - is the adjustable parameter and A is the mass number of the parent. Radius of the α particle R_1 is assumed to be constant in varying mass asymmetry shape (VMAS) description

$$R_1 - \bar{R}_1 = 0 \quad (5.13)$$

Where $\bar{R}_1 = \left(\frac{Z_i}{Z}\right)^{1/3} R$ $i=1,2$ \bar{R}_1 gives the final radius of the α particle. Where Z_1, Z_2, Z are the atomic numbers of the α particle, daughter nucleus and parent nucleus respectively.

5.2.2 Beta decay

For all types of β processes, the expression for the half life T_β is given by [388]

$$\frac{1}{T_\beta} = \frac{1}{T_{\beta^+}} + \frac{1}{T_{\beta^-}} + \frac{1}{EC} \quad (5.14)$$

Here EC is the electron capture. For a particular type β decay, the expression for the half life is given by

$$f_0^b T_b = \ln 2 \left[\frac{g^2 m_e^5 c^4}{2\pi^3 \hbar^7} |M_{if}|^2 \right]^{-1} \quad (5.15)$$

Here, f_0^b is the fermi function, $b=\beta^\pm$ or EC, m_e is mass of the electron and M_{if} is the transition matrix element between initial and final states. The R.H.S of above may be approximated by a constant for each kind of β -decay [389]. For allowed and forbidden case of beta decay, this constant is different. For allowed β -decays, previous work has given this constant value as 5.7 ± 1.1 [390]. The equation (5.15) reduces to;

$$\log_{10}[f_0^b T_b(\text{sec})] = 5.7 \pm 1.1 \quad (5.16)$$

$$\log_{10}[f_0^b T_b] = 4.7 \quad (5.17)$$

5.2.2.1 β^\pm decays

Fermi function for β decay is given by the expression,

$$f_0^\beta \pm = \int_1^{E_0} F(E, Z) P(E) (E_0 - E)^2 dE \quad (5.18)$$

Here, $P(E)$ is the momentum of the particle, $F(E,Z)$ can be computed at the nuclear surface using the magnitude of radial electron/positron wave function. The first approximation of $F(E,Z)$ is

$$F_0(E, Z) = \frac{2(\gamma + 1)(2pR)^{2(\gamma-1)} \exp\left[\frac{\pi\xi}{p}\right] |\Gamma(\gamma + i\frac{\xi}{p})|^2}{\Gamma^2(2\gamma + 1)} \quad (5.19)$$

Here, $\gamma = \sqrt{1 - \alpha^2 Z^2}$, $\xi = \pm \alpha ZE$ (+ for β^- decay and - for β^+ decay), $\alpha=1/137$ is the fine structure constant, R is the radius of the nucleus and Γ is the gamma function.

At the surface of the nucleus (for β^+ decay) orbital electrons screening effect has a big impact on the β electron/positron wave function. Thus $F(E,Z)$ becomes,

$$F(E, Z) = F_0(E \pm V_0, Z) \alpha^{\pm} (E \pm V_0, Z) \frac{p(E \pm V_0)(E \pm V_0)}{p(E)E} \quad (5.20)$$

Here, $V_0 = 1.81\alpha^2 Z^{4/3}$, α is the finite wavelength of β particle, $p(E) = \sqrt{E^2 - 1}$ is the momentum of the β particle, $E_0 = 1 + Q_{\beta^{\pm}}/m_e c^2$ is the total limit energy of the β decay and $E = 1 + \varepsilon/m_e c^2$; ε is the kinetic energy of the β particle

The expression for the energy released in β^+ decay is

$$Q_{\beta^+} = M(A, Z) - M(A, Z - 1) - 2m_e c^2 \quad (5.21)$$

Similarly for β^- decay,

$$Q_{\beta^-} = M(A, Z) - M(A, Z - 1) \quad (5.22)$$

5.2.2.2 Electron Capture

The value of Q for the electron capture is given by the relation,

$$Q_{EC} = M(A, Z) - M(A, Z - 1) - B_e = Q_{\beta^+} + 2m_e c^2 - B_e \quad (5.23)$$

Here, B_e is the electron binding energy. Hence, even for the forbidden β^+ decay, electron capture is allowed. The capture of electrons of K-shell in lower Z and L-shell in higher Z is the major

contributors to the electron capture. Contributions of electrons of higher shells is negligible. Thus, Fermi function becomes,

$$f_0^{EC} = f_0^K + f_0^{L_I} + f_0^{L_{II}} \quad (5.24)$$

In general, for any shell,

$$f_0^X = \frac{\pi}{2} [E(Q_{EC}) + E_X]^2 [g_X^2(Z_X) + f_X^2(Z_X)] \quad X = K, L_I, L_{II} \quad (5.25)$$

E_X is the total energy of the electron, given by

$$E_K = \gamma, E_L = \left(\frac{1 + \gamma}{2}\right)^{1/2} \quad (5.26)$$

Where Z_X is the effective charge, which considers the screening of Coulomb field of the nucleus by other electrons[391]

$$Z_K = Z - 0.35 \quad \text{and} \quad Z_L = Z - 4.15 \quad (5.27)$$

The non zero components of radial parts (g_X and f_X) of wave function of relativistic electron of orbit X are

$$g_K^2(Z) = \frac{4(1 + \gamma)(2\alpha Z R)^{2(\gamma-1)}(\alpha Z)^3}{\Gamma(2\gamma + 1)} \quad (5.28)$$

$$g_{L_I}^2(Z) = \frac{[(2\gamma + 2)^{1/2} + 2](2\gamma + 1)(2\alpha Z R)^{2(\gamma-1)}(\alpha Z)^3}{\Gamma(2\gamma + 1)[(2\gamma + 2)^{1/2} + 1](2\gamma + 2)^\gamma} \quad (5.29)$$

$$g_{L_{II}}^2(Z) = \frac{3}{16}(\alpha Z)^2 g_{L_I}^2(Z) \quad (5.30)$$

5.2.3 Spontaneous fission

The SF decay is studied by employing the effect of quantum tunneling through the potential barrier.

The decay constant of SF is expressed as;

$$\lambda = \frac{\ln 2}{T_{sf}} = \nu S P_s \quad (5.31)$$

where ν , S and P_s are the model dependent quantities such as assault frequency, preformation probability and barrier penetrability respectively. In the above equation $P = S P_s$ and the SF half-lives are calculated as;

$$T = \frac{\ln 2}{\nu P} = \frac{h \ln 2}{2} \frac{1}{E_\nu P} \quad (5.32)$$

where h is the Planck constant and $E_\nu = h\nu/2$ is the zero point vibration energy. The penetration probability is evaluated using the action integral, K ;

$$P = \exp(-K) \quad (5.33)$$

and hence the decimal logarithm of T(s) is given by

$$\log_{10} T = 0.43429 K - 20.8436 - \log_{10} E_\nu \quad (5.34)$$

if $E_\nu=0.5\text{MeV}$ then the above equation becomes $\log_{10}T = -\log_{10}P - 20.5426$. The action integral K is evaluated as follows;

$$K = \frac{2\sqrt{2m}}{\hbar} \int_{R_a}^{R_b} (B(r)[E(R) - Q])^{1/2} dR \quad (5.35)$$

The term $E(R)$ is the macroscopic energy in terms of surface, volume, coulomb, proximity energy(CPE), shell correction and pairing energy term [392] and m is the rest mass of neutron. Few of the superheavies are spherical, the rest are deformed, mainly prolate or oblate. To include this effect, deformations are also involved in the calculation of $E(r)$ which is adopted from the previous work [392]. In the above equation R is the separation distance between center of the fission fragments, R_a and R_b are the turning points, is evaluated using the boundary conditions $E(R_a)$ and $E(R_b)=Q$. However, the term $B(r)$ is the inertia with respect to r and it is evaluated using the semi-empirical model for the inertia [393].

$$B(r) = \mu(1 + \text{ke}xp[-\frac{128}{51}(r - R_{sph}/R_0)]) \quad (5.36)$$

where μ and k are the reduced mass of the fission fragments semi-empirical constant ($k=14.8$) respectively. R_{sph} is the distance between the center of masses between the fission fragments, where as $R_{sph}/R_0=0.75$ in the symmetric case. The decay constant (λ) and total fission decay constant is evaluated as described in the reference [392]

5.3 Results

The mass excess values play a major role in the prediction of decay mode and its corresponding half-lives. The predicted half-lives are sensitive to the Q-values and small change in the Q-values results in the notable change in the half-lives with the magnitude of order 10^1 to 10^2 [129]. Mass

excess tables such as WS4 [315], EBW [394], HFB28 and HFB29 [395], DZ10 [396], KTUY [265], finite range droplet model (FRDM) [264] and AME16 [397] are available in the literature. In the present work, the updated AME16 [397] mass excess values up to $Z=118$ and above $Z>118$ the mass excess values are taken from the finite range droplet model (FRDM) [264]. The dominant decay mode is identified by studying the competition between different decay modes such as α -decay, β -decay, CD and SF in the SHN region $104 \leq Z \leq 126$.

Table 5.1 Tabulation of cluster-decay half-lives evaluated using present work (PW) and available experiments.

Decay	$Q_{Exp}(\text{MeV})$	$\log T_{1/2}^{exp}$ [280]	$\log T_{1/2}^{PW}$
$^{221}\text{Fr} \rightarrow ^{14}\text{C} + ^{207}\text{Tl}$	31.317	14.51	14.91
$^{221}\text{Ra} \rightarrow ^{14}\text{C} + ^{207}\text{Pb}$	32.396	13.37	13.56
$^{222}\text{Ra} \rightarrow ^{14}\text{C} + ^{208}\text{Pb}$	33.05	11.05	12.70
$^{223}\text{Ra} \rightarrow ^{14}\text{C} + ^{209}\text{Pb}$	31.829	15.05	13.94
$^{224}\text{Ra} \rightarrow ^{14}\text{C} + ^{210}\text{Pb}$	30.54	15.9	15.52
$^{226}\text{Ra} \rightarrow ^{14}\text{C} + ^{212}\text{Pb}$	28.2	21.29	22.74
$^{225}\text{Ac} \rightarrow ^{14}\text{C} + ^{211}\text{Bi}$	30.477	17.16	17.06
$^{228}\text{Th} \rightarrow ^{20}\text{O} + ^{208}\text{Pb}$	44.72	20.73	22.04
$^{230}\text{U} \rightarrow ^{22}\text{Ne} + ^{208}\text{Pb}$	61.4	19.56	20.21
$^{230}\text{Th} \rightarrow ^{24}\text{Ne} + ^{206}\text{Hg}$	57.571	24.61	25.07
$^{231}\text{Pa} \rightarrow ^{24}\text{Ne} + ^{207}\text{Tl}$	60.417	22.89	23.07
$^{232}\text{U} \rightarrow ^{24}\text{Ne} + ^{208}\text{Pb}$	62.31	20.39	22.25
$^{233}\text{U} \rightarrow ^{24}\text{Ne} + ^{209}\text{Pb}$	60.486	24.84	25.05
$^{234}\text{U} \rightarrow ^{26}\text{Ne} + ^{208}\text{Pb}$	59.466	25.93	25.62
$^{234}\text{U} \rightarrow ^{28}\text{Mg} + ^{206}\text{Hg}$	74.11	25.74	26.04
$^{236}\text{Pu} \rightarrow ^{28}\text{Mg} + ^{208}\text{Pb}$	79.67	21.65	22.07
$^{238}\text{Pu} \rightarrow ^{28}\text{Mg} + ^{210}\text{Pb}$	75.912	25.66	25.98
$^{238}\text{Pu} \rightarrow ^{30}\text{Mg} + ^{208}\text{Pb}$	77	25.66	26.25
$^{238}\text{Pu} \rightarrow ^{32}\text{Si} + ^{206}\text{Hg}$	91.19	25.3	26.05
$^{242}\text{Cm} \rightarrow ^{34}\text{Si} + ^{208}\text{Pb}$	96.509	23.11	24.24

In the detail study of literature survey, there is no experimental evidence for cluster radioactivity in the SH region. Furthermore, experimental studies on CD in the actinide region are available. To validate the present work, the CD half-lives produced by the present work in the actinide region are compared with the experiments. The values produced by present work agrees well with the experiments. With this confidence, the CD is studied in the SH region and it is

Table 5.2 Comparison of logarithm half-lives (years) of SF in the SH region $104 \leq Z \leq 114$ from present work with the available experiments.

Parent nuclei	$\log T_{SF}^{Expt}$ yr [337]	$\log T_{SF}^{Th}$ yr
^{254}Rf	-12.1	-10.91
^{256}Rf	-9.71	-8.48
^{258}Rf	-9.35	-7.06
^{260}Rf	-9.2	-6.35
^{262}Rf	-7.18	-6.36
^{258}Sg	-10	-11.33
^{260}Sg	-9.65	-10.17
^{262}Sg	-9.32	-8.722
^{264}Sg	-8.93	-7.98
^{266}Sg	-7.86	-7.96
^{264}Hs	-10.2	-11.02
^{270}Ds	-8.6	-9.46
^{282}Cn	-10.6	-9.39
^{284}Cn	-8.5	-7.98
^{286}Fl	-8.08	-7.58

tabulated in table 5.1. Similarly, table 5.2 shows studied logarithmic half-lives (in years) of SF from present work with the available experiments. The CD and SF half-lives produced by the present work are close to the experiments. As a part of this investigation, α -decay properties of SHN are studied using the formalism explained in the theory section. The predicted alpha decay half-lives are validated by comparing with the available experiments in the SH region. The comparison of predicted α -decay half-lives with that of the experiments are given in the table 5.3. From the comparison it is observed that the predicted half-lives are in good agreement with that of experiments. With this confidence, the alpha decay half lives of SHN are predicted in the region $104 \leq Z \leq 126$. Figure 5.2 shows wide range of α -decay half-lives. For a given SHN, alpha decay half-lives increases with increase in the neutron number of its isotopes. For instance, α -decay half-lives are in the order of nanosecond at $N/Z = 1.307692$ for Rutherfordium, whereas for the same SH element α -decay half-lives are in the order of $10^2 s$ at $N/Z = 1.504762$. Similarly, all the neutron rich SHN are having comparably longer α -decay half-lives and this is in concurrence with the report available in the literature [398]. The evaluated α -decay half-lives of all possible

Table 5.3 Comparison of present work(PW) with the available experimental(Exp)values

Parent nuclei	Q_α (MeV)	$\log T_{1/2}(\text{exp})$	$\log T_{1/2}(\text{PW})$	Parent nuclei	Q_α (MeV)	$\log T_{1/2}(\text{exp})$	$\log T_{1/2}(\text{PW})$
²⁶¹ Bh	8.649	1.515	1.86	²⁸⁴ Cn	9.301	1.013	1.78
²⁶⁰ Db	9.379	-0.295	0.11	²⁷⁷ Cn	11.622	-2.551	-2.65
²⁶⁹ Sg	8.8	2.27	2.12	²⁸⁶ Nh	9.68	0.978	1.22
²⁶⁵ Sg	9.078	0.869	1.15	²⁸⁵ Nh	10.02	0.623	0.76
²⁶³ Sg	9.391	-0.932	0.12	²⁸⁴ Nh	10.25	-0.013	0.08
²⁶¹ Sg	9.803	-1.469	-1.21	²⁸³ Nh	10.6	-1.125	-0.98
²⁷² Bh	9.3	1.025	0.78	²⁸⁹ Fl	9.847	0.279	0.96
²⁷¹ Bh	9.5	0.176	0.18	²⁸⁸ Fl	9.969	-0.18	-0.16
²⁷⁰ Bh	9.3	1.785	1.02	²⁸⁷ Fl	10.436	-0.319	-0.28
²⁷⁷ Hs	8.4	-2.523	-1.02	²⁸⁶ Fl	10.7	-0.921	-0.87
²⁷³ Hs	9.9	-0.119	-0.32	²⁸⁵ Fl	11	-0.824	-1.89
²⁶⁹ Hs	9.629	0.851	0.65	²⁹⁰ Mc	10.3	-0.187	0.18
²⁷⁴ Hs	9.5	0.079	0.21	²⁸⁹ Mc	10.6	-0.481	-0.35
²⁷⁸ Mt	9.1	0.653	1.65	²⁹³ Lv	8.886	-1.244	0.12
²⁷⁶ Mt	9.8	-0.284	0.05	²⁹² Lv	10.707	-1.886	-0.96
²⁷⁴ Mt	10.5	-0.357	-0.98	²⁹¹ Lv	11	-1.721	-1.45
²⁸¹ Ds	8.958	1.104	1.45	²⁸⁹ Lv	11.7	-2.848	-2.97
²⁸² Rg	9.38	2	1.85	²⁹⁴ Ts	8.963	-1.292	0.06
²⁸⁰ Rg	9.98	0.623	0.55	²⁹⁴ Og	8.47	-3.161	-2.45
²⁷⁹ Rg	10.45	-1.046	-1.04	²⁹⁵ Og	9.056	-1.745	0.58
²⁸⁵ Cn	8.793	1.447	2.85	²⁹⁸ 120	13.355	-3.051	-4.68
²⁸³ Cn	9.62	0.623	0.89	²⁹⁹ 120	13.105	-3.15	-1.58
²⁸¹ Cn	10.28	-0.886	-0.68				

SHN are represented in the heat map 5.2. The right vertical bar of the figure shows the magnitude of $\log T_{1/2}$ values. The variation of colours from navy blue to wine colour shows the values in the range $10^{-10}s$ to 10^2s . The contrast of the blue region lies between $10^{-10}s$ to $10^{-7}s$, green region lies within $10^{-6}s$ to $10^{-4}s$, $10^{-4}s$ to $10^{-3}s$ information is presented in yellow region. Finally the red to wine region shows the higher half-lives of the order of $10^{-2}s$ to 10^2s . The inset of the figure 5.2 on the left top side gives an information on the magnified portion α -decay half-lives in the SH region $Z=104-114$. whereas, the bottom right inset gives an information on the magnified portion of the SH region $Z=115-126$. After the detail investigation on the α - decay, a search was made to identify the cluster emitters in the SH region. The cluster radioactivity is energetically favour if the Q-values are positive. The possibility of CD with $3 \leq Z_c \leq 45$ in the SH region

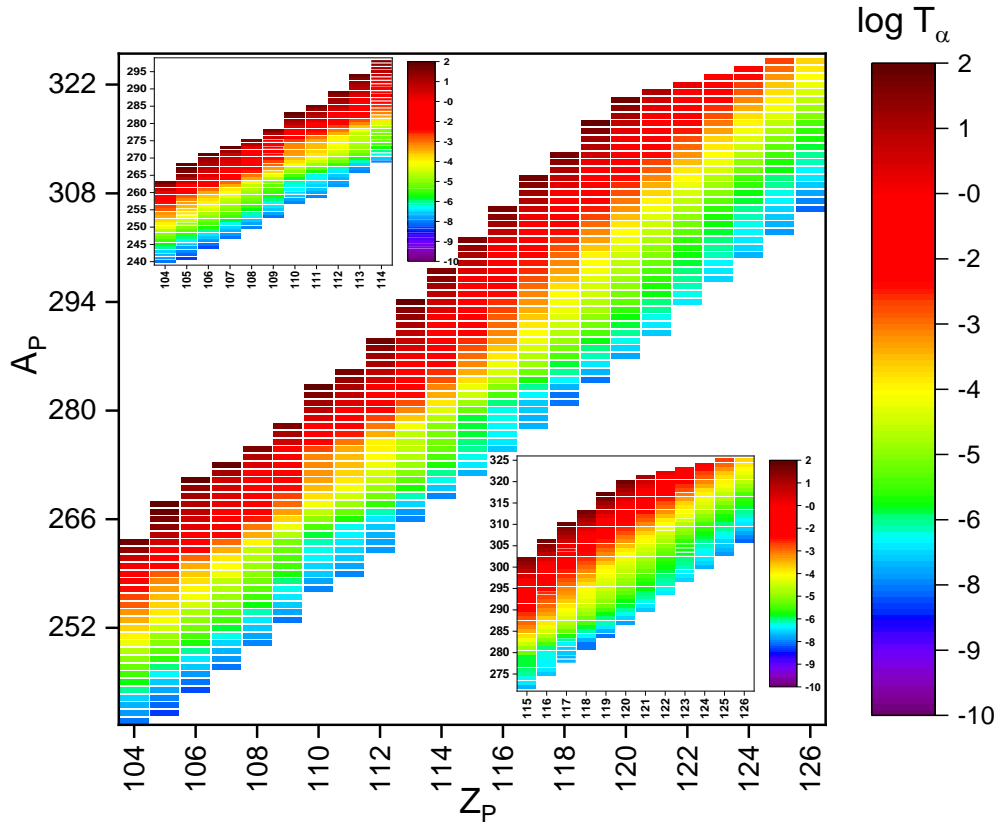


Fig. 5.2 Map of nuclei reflecting the logarithmic α -decay half-lives for the isotopes of elements from $Z=104$ to 126 . The Q -values estimated using AME16 and FRDM95. The vertical line on the right side of the figure shows increase in $\log T_{1/2}$ values from navy blue region to brown region.

$104 \leq Z \leq 126$ is studied. For a given parent nuclei, the half-lives corresponds to various cluster emission are evaluated and identified the cluster corresponds to shorter half-lives. Furthermore, the cluster emitters corresponds to shorter half-lives for different isotopes of given SH element are also identified. Eventually, cluster emissions corresponds to the shortest half-lives T_c are identified and this is referred as CD half-lives (T_c). The predicted CD half-lives in the atomic number region $104 \leq Z \leq 126$ corresponds to all the studied cluster emissions are shown in figure 5.3. This figure enable us to identify the cluster emission corresponds to the shorter half-lives of given SH element. The half-lives of SHN with $Z=115-120$ against cluster radioactivities are shorter for ^{86}Kr than that of the other studied clusters. The SHN with $Z=104, 106, 108, 110, 112, 114, 124$ and 126 have the shorter half-lives against ^{96}Mo cluster emission than that of the other studied clusters. The decay half-lives are shorter for ^{91}Y emission from the SHN with $Z=109, 111, 113,$

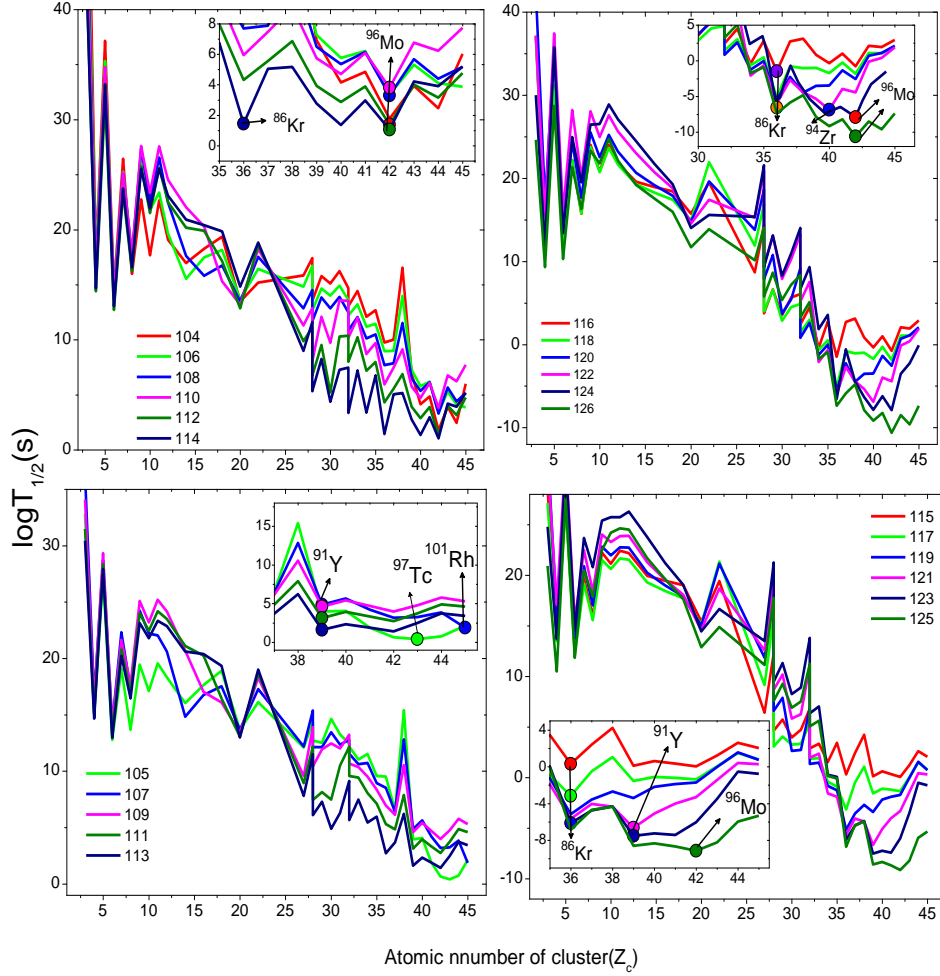


Fig. 5.3 Predicted CD logarithmic half-lives in the atomic number range $Z=104-126$ using AME16 and FRDM95 mass excess values. The hallow bin with different colour in each panel shows the cluster emission for which half-lives are minimum.

121 and 123. Similarly, The half-lives of SHN with $Z=105$ and 107 against cluster radioactivities are shorter for ^{97}Tc and ^{101}Rh than that of the other studied clusters.

The cluster radioactivities in the SHN region are having shorter half-lives for cluster neutron numbers such as 44-48 from the parent nuclei with neutron numbers 130-200 and the same is depicted in the figure 5.4. The range of CD half-lives for the SH elements with $104 \leq Z \leq 126$ are shown in the figure 5.5. The shorter half-lives are observed for the $N/Z > 1.37068$ and larger values of half-lives are observed for the $N/Z < 1.37068$. From the figure, it is clear that up to SHN $104 \leq Z \leq 115$ the larger CD half-lives were observed, whereas, shorter CD half-lives in the SH region $116 \leq Z \leq 126$. The inset of the figure 5.5 on the top left side gives the magnified

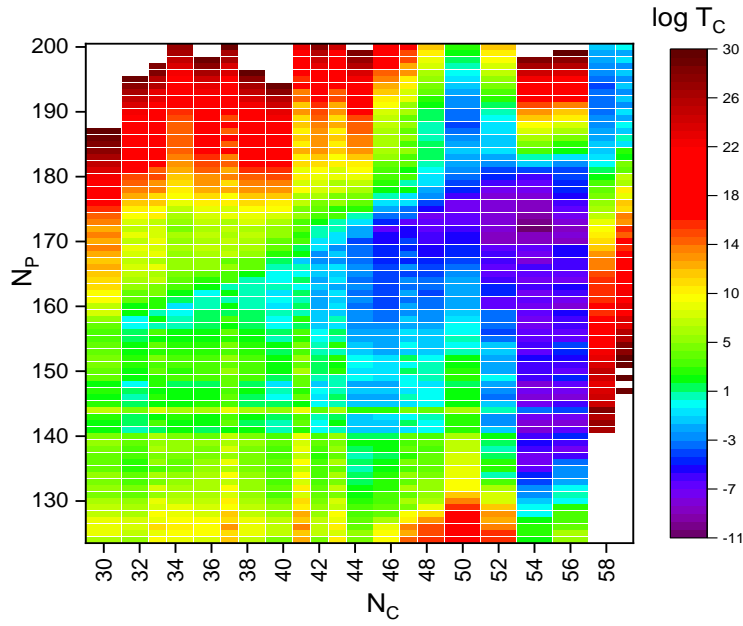


Fig. 5.4 Map of nuclei reflecting the logarithmic cluster-decay half-lives for the neutron number of parent and cluster isotopes of elements from $Z=104$ to 126.

portion of logarithmic half-lives (T_c) in the SH region $104 \leq Z \leq 114$. Whereas, the inset placed in right bottom gives magnified portion of shorter logarithmic half-lives (T_c) in the SH region $115 \leq Z \leq 126$. This figure also depicts that some of the SHN having the life times in terms of ns to μs and decays through the CD modes also.

The other prominent decay mode studied is the SF and it is also energetically feasible in the heavy and SHN. It may occur in the heavy and SHN due to an increase in the Coulomb interactions. From the available literature's [8, 175, 177, 179, 268, 269, 340] the consistent α -decay chains were observed from the SHN followed by the SF. The SF half-lives are studied using the theory explained in the section 5.2.3. A figure of nuclides includes over a wide range of studied SF half-lives in the SH region $Z=104-126$ is presented in figure 5.6. The $\log T_{SF}$ values varies between -50 (dark blue region) to 50 (dark red region). For an instance, the atomic number with $Z=104$ shows the $\log T_{1/2}(SF)$ of isotopes from 245 to 275, whose corresponding $\log T_{1/2}(SF)$ ranges from -50 to 5 and the half-lives with smaller values were depicted by the range of blue colour from navy blue to blue colour. The half-lives ranging from nanoseconds (ns) to 10^5 s were

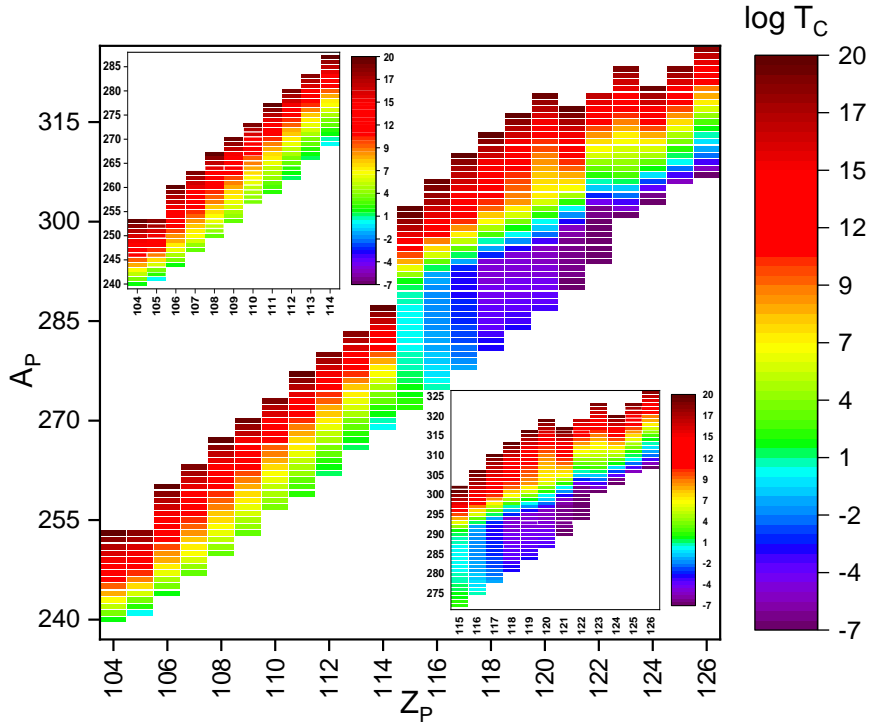


Fig. 5.5 Heat map showing the variations of lowest logarithmic half lives of clusters of $104 < Z < 126$

shown from the colour yellow to light orange. Similarly, in the atomic number range $Z=119$ and above the larger values of SF logarithmic half-lives were shown by the range of red colours. Thus, on either side of the figure 5.6 the isotopes of the atomic number range $Z=104-126$, have found to be smaller half-lives and in the middle region of the figure larger values of the $\log T_{1/2}$ is observed up to $Z=116$. Whereas, the smaller half-lives were observed on top of the higher isotopes of $Z > 116$ and larger $\log T_{1/2}$ for the lower isotopes of $Z > 116$. The similar trend is also observed by the previous researchers [399] in which they have compared half-lives of nuclei $Z=92-104$ with that of the experimentally available values.

A detail investigation on Q-values corresponds to the β -decay in the SH region reveals that β^+ -decay is energetically possible with $Z=105, 107, 113, 114, 115, 117, 119, 121, 123, 125$ and 126 whereas, the β^- -decay is energetically not possible. Furthermore, β -decay half-lives are studied using the formalism explained in the section 5.2.2.1.

The competition between different possible decay modes such as α -decay, cluster-decay, β -

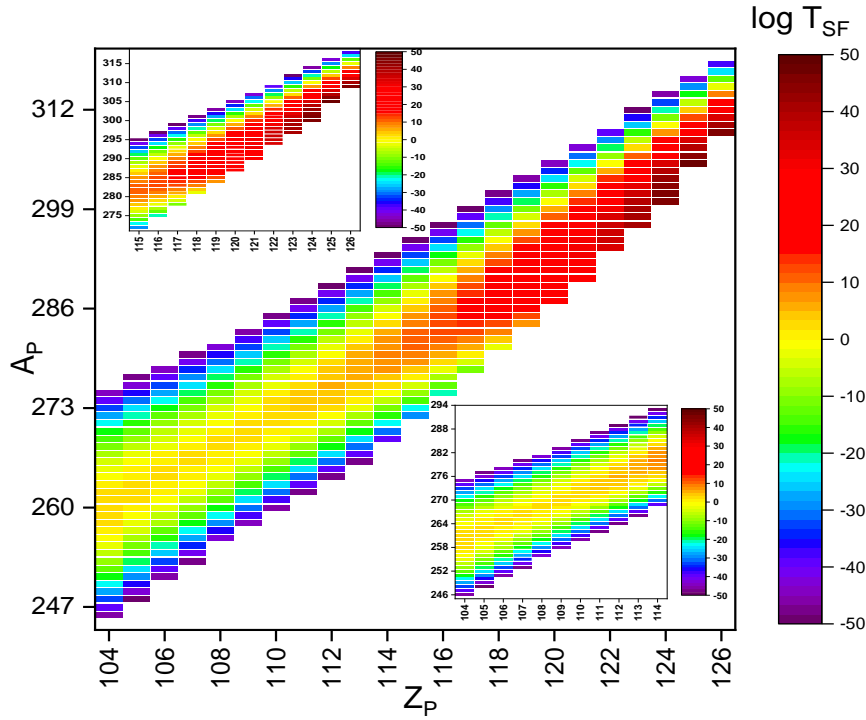


Fig. 5.6 Heat map showing the variations of logarithmic half lives of SF of $104 < Z < 126$

decay and SF enable us to identify the dominant decay mode for the SH elements in the atomic number region $104 \leq Z \leq 126$ of all possible isotopes. Figure 5.7 depicts the decay modes of the SHN. In the studied SH region around 21 β^+ emitters are identified and these β^+ emitters are tabulated in the table 5.6. Furthermore, 07 cluster emitters are identified in the SH region and the same were tabulated in the table 5.4. Among the studied possible decay modes in the SHN,

Table 5.4 Identified cluster emitters in the SHN

Parent nuclei	Q (MeV)	$\log(T_{1/2})$	cluster
^{292}Og	304.08	-5.08	^{86}Kr
^{293}Og	303.63	-4.63	^{86}Kr
$^{298}\text{122}$	338.25	-6.02	^{94}Zr
$^{300}\text{122}$	337.45	-6.21	^{94}Zr
$^{299}\text{123}$	338.66	-7.18	^{91}Y
$^{300}\text{124}$	356.06	-7.35	^{96}Mo
$^{306}\text{126}$	364.27	-8.78	^{96}Mo

the majority of the nuclei undergoes α -decay and SF. The α emitting SHN are tabulated in the table 5.5. [94] The identified alpha emitters having half-lives around μs to 100s in the SH region

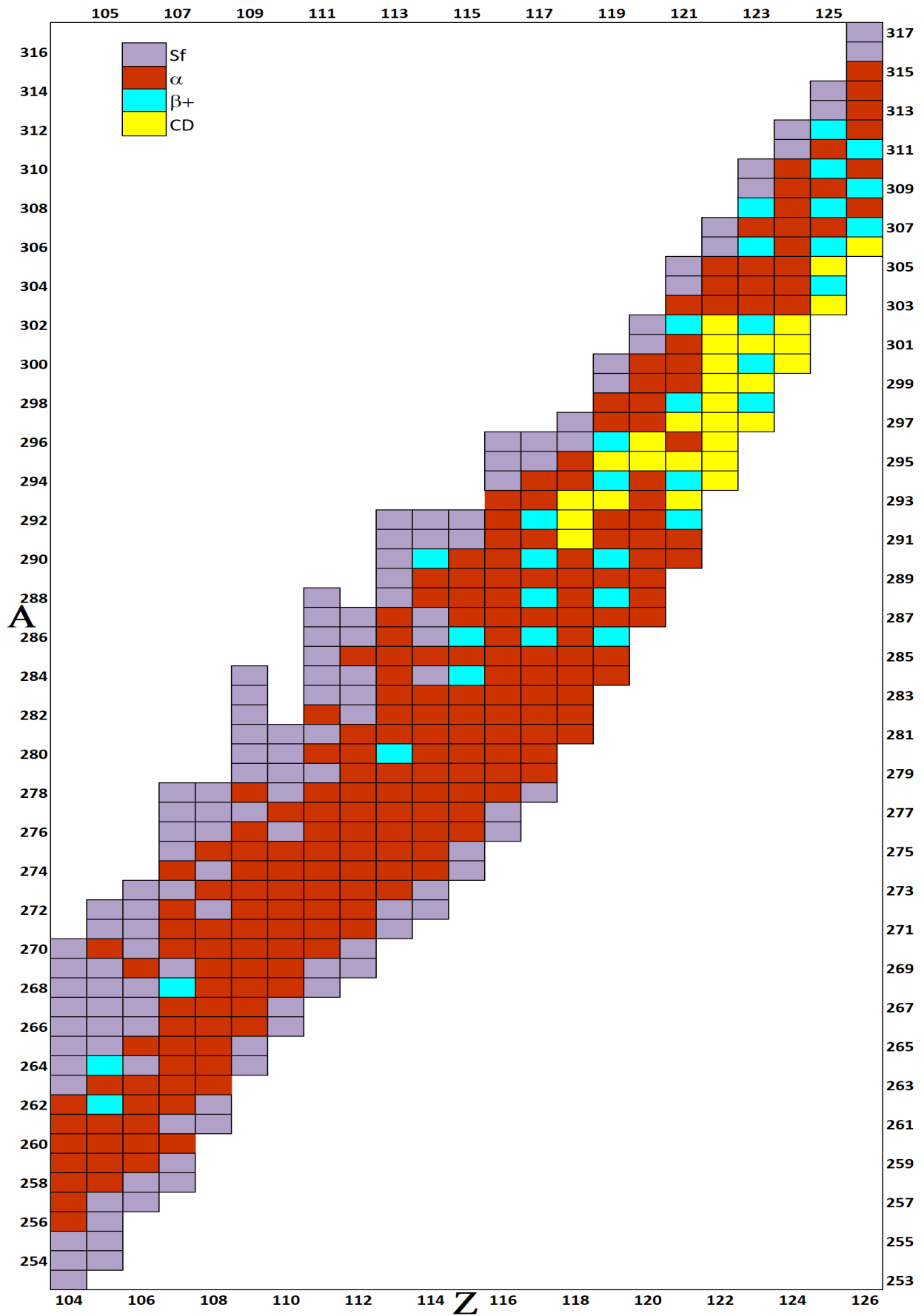


Fig. 5.7 Chart of SF(purple), alpha-decay(brown), β^+ -decay(cyan) and cluster emitters(yellow) with atomic numbers $Z = 104$ -126. The Q values are calculated using the FRDM95 mass tables

Table 5.5 Identified alpha emitters in the SHN region

Parent Nuclei	Q (MeV)	$\log(T_{1/2})$	Parent Nuclei	Q (MeV)	$\log(T_{1/2})$	Parent Nuclei	Q (MeV)	$\log(T_{1/2})$
²⁵⁶ Rf	10.15	0.92	²⁷⁷ Ds	10.34	-2.51	²⁸⁰ Lv	13.59	-6.78
²⁵⁷ Rf	10.05	0.78	²⁷¹ Rg	11.61	-3.72	²⁸¹ Lv	13.35	-6.98
²⁵⁸ Rf	9.94	-0.16	²⁷³ Rg	11.44	-3.56	²⁸² Lv	13.13	-5.14
²⁵⁹ Rf	9.67	0.35	²⁷⁵ Rg	11.37	-3.42	²⁸³ Lv	12.91	-5.78
²⁶⁰ Rf	9.4	-1.12	²⁷⁷ Rg	10.88	-2.21	²⁸⁴ Lv	12.7	-3.89
²⁶¹ Rf	9.14	1.56	²⁷⁹ Rg	10.44	-1.23	²⁸⁵ Lv	12.51	-3.99
²⁶² Rf	8.92	0.52	²⁸⁰ Rg	10.24	0.62	²⁸⁶ Lv	12.34	-4.25
²⁵⁸ Db	10.45	0.55	²⁸² Rg	9.89	2.15	²⁸⁷ Lv	12.19	-3.98
²⁵⁹ Db	10.36	-0.35	²⁷¹ Cn	12.1	-4.89	²⁸⁸ Lv	12.06	-3.56
²⁶⁰ Db	10.08	0.26	²⁷² Cn	11.96	-4.65	²⁹⁰ Lv	11.83	-1.75
²⁶¹ Db	9.81	0.65	²⁷³ Cn	11.87	-4.33	²⁹¹ Lv	11.73	-2.36
²⁶³ Db	9.34	1.52	²⁷⁴ Cn	11.8	-4.16	²⁹² Lv	11.64	-1.88
²⁷⁰ Db	8.45	3.25	²⁷⁵ Cn	11.76	-3.98	²⁹³ Lv	11.55	-1.23
²⁵⁹ Sg	10.84	-0.15	²⁷⁶ Cn	11.74	-2.98	²⁷⁹ Ts	14.06	-7.36
²⁶⁰ Sg	10.74	-2.16	²⁷⁷ Cn	11.49	-3.15	²⁸¹ Ts	14.02	-8.25
²⁶¹ Sg	10.47	-0.48	²⁷⁸ Cn	11.25	-2.47	²⁸³ Ts	13.56	-5.36
²⁶² Sg	10.2	-1.86	²⁷⁹ Cn	11.03	-2.36	²⁸⁵ Ts	13.14	-5.12
²⁶³ Sg	9.95	0.25	²⁸⁰ Cn	10.81	-1.78	²⁸⁷ Ts	12.78	-4.88
²⁶⁹ Sg	9.16	2.56	²⁸¹ Cn	10.62	-0.99	²⁸⁹ Ts	12.5	-4.65
²⁶⁰ Bh	11.21	-1.42	²⁸⁵ Cn	10	1.56	²⁹¹ Ts	12.28	-2.98
²⁶³ Bh	10.59	-1.76	²⁷³ Nh	12.4	-5.65	²⁹⁴ Ts	12	-1.45
²⁶⁵ Bh	10.12	0.12	²⁷⁵ Nh	12.24	-4.79	²⁸¹ Og	14.44	-7.65
²⁶⁶ Bh	9.94	0.22	²⁷⁶ Nh	12.2	-4.78	²⁸² Og	14.43	-7.63
²⁷⁰ Bh	9.56	1.89	²⁷⁷ Nh	12.18	-4.52	²⁸³ Og	14.19	-7.45
²⁷¹ Bh	9.53	0.18	²⁷⁹ Nh	11.7	-2.89	²⁸⁴ Og	13.97	-6.25
²⁷² Bh	9.27	1.12	²⁸¹ Nh	11.26	-2.12	²⁸⁵ Og	13.76	-6.41
²⁷⁴ Bh	8.78	1.23	²⁸² Nh	11.07	-1.69	²⁸⁶ Og	13.56	-6.24
²⁶³ Hs	11.27	-2.56	²⁸⁴ Nh	10.73	-0.16	²⁸⁷ Og	13.37	-5.25
²⁶⁵ Hs	10.77	-4.56	²⁸⁵ Nh	10.59	0.78	²⁸⁸ Og	13.21	-5.98
²⁶⁶ Hs	10.55	-1.85	²⁸⁶ Nh	10.47	0.88	²⁹⁴ Og	12.53	-3.88
²⁶⁷ Hs	10.37	-1.42	²⁸⁷ Nh	10.35	0.76	²⁹⁵ Og	12.44	-1.25
²⁶⁸ Hs	10.23	0.69	²⁷⁵ Fl	12.78	-4.69	²⁸⁵ 119	14.37	-5.69
²⁶⁹ Hs	10.13	1.42	²⁷⁶ Fl	12.72	-5.12	²⁸⁷ 119	13.96	-4.25
²⁷⁰ Hs	10.05	1.78	²⁷⁷ Fl	12.68	-5.36	²⁸⁹ 119	13.62	-5.97
²⁷¹ Hs	10	0.45	²⁷⁸ Fl	12.66	-5.46	²⁹² 119	13.23	-5.28
²⁷³ Hs	9.71	-0.56	²⁷⁹ Fl	12.42	-4.12	²⁹⁷ 119	12.78	-3.97
²⁷⁵ Hs	9.23	-0.15	²⁸⁰ Fl	12.19	-4.36	²⁸⁷ 120	14.56	-6.58
²⁶⁶ Mt	11.27	-1.93	²⁸¹ Fl	11.96	-3.78	²⁸⁸ 120	14.37	-6.25
²⁶⁷ Mt	11.06	-2.52	²⁸² Fl	11.76	-3.15	²⁹⁰ 120	14.03	-6.46
²⁶⁹ Mt	10.74	-2.32	²⁸³ Fl	11.56	-2.99	²⁹² 120	13.76	-5.85
²⁷¹ Mt	10.57	-1.85	²⁸⁸ Fl	10.86	-0.25	²⁹⁸ 120	13.2	-3.87
²⁷³ Mt	10.49	-1.23	²⁸⁹ Fl	10.75	0.62	²⁹⁹ 120	13.11	-4.12
²⁷⁴ Mt	10.23	-0.12	²⁷⁷ Mc	13.19	-6.85	³⁰⁰ 120	13.02	-4.36
²⁷⁵ Mt	9.99	-1.25	²⁷⁸ Mc	13.16	-6.48	²⁹⁰ 121	14.59	-6.28
²⁷⁶ Mt	9.75	-0.36	²⁷⁹ Mc	13.14	-5.96	²⁹⁶ 121	13.87	-5.48
²⁷⁸ Mt	9.33	1.36	²⁸⁰ Mc	12.9	-5.12	³⁰⁰ 121	13.53	-5.22
²⁶⁸ Ds	11.62	-3.56	²⁸¹ Mc	12.67	-5.36	³⁰³ 122	13.77	-4.98
²⁶⁹ Ds	11.45	-3.24	²⁸³ Mc	12.24	-4.25	³⁰⁴ 122	13.67	-4.99
²⁷⁰ Ds	11.31	-3.68	²⁸⁵ Mc	11.88	-3.12	³⁰⁴ 123	14.18	-5.12
²⁷¹ Ds	11.21	-0.58	²⁸⁸ Mc	11.47	-0.89	³⁰⁶ 124	14.49	-5.66
²⁷² Ds	11.14	-3.09	²⁸⁹ Mc	11.36	-0.52	³⁰⁸ 124	14.28	-5.98
²⁷³ Ds	11.1	-2.96	²⁹⁰ Mc	11.26	-0.25	³¹⁰ 124	14.05	-5.87
²⁷⁴ Ds	11.07	-2.45	²⁷⁸ Lv	13.64	-6.75			
²⁷⁵ Ds	10.81	-2.12	²⁷⁹ Lv	13.61	-6.12			

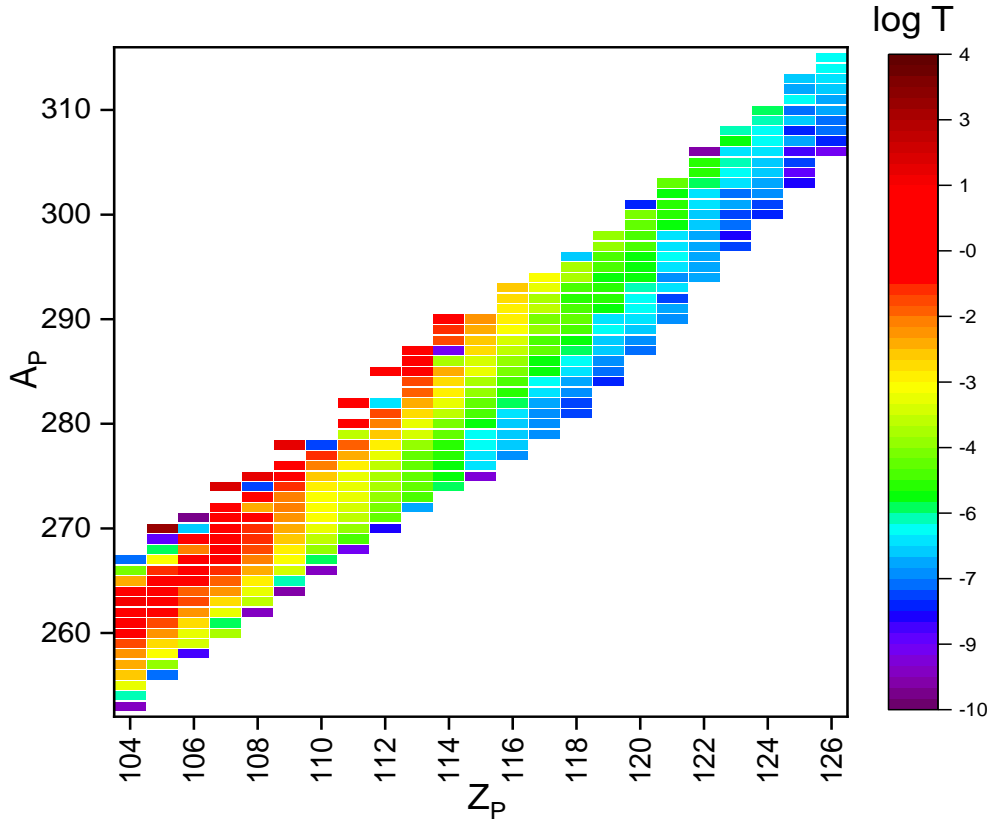


Fig. 5.8 Heat map showing the variations of atomic number, mass number of parent and logarithmic half lives of different decay modes (*lifetimes*) of $104 < Z < 126$

$104 \leq Z \leq 126$. The table 5.4 shows the identified cluster emissions with the corresponding half-lives. The amount of energy released during cluster emission, cluster emitted and $\log T_{1/2}$ values are tabulated in the table. The minimum CD half-lives corresponds to ^{86}Kr , ^{94}Zr , ^{91}Y and ^{96}Mo for the nuclei $^{292-293}\text{Og}$, $^{298,300}\text{122}$, $^{299}\text{123}$, $^{300}\text{124}$ and $^{306}\text{126}$ respectively. From the available literature it is also evident that the heavy particle radioactivity of ^{86}Kr is observed in the SHN $Z=118$ [129, 400]. In addition the cluster emission such as Rb, Sr, Y, Zr, Nb, and Mo [401] were observed for the SH region $Z= 119-124$ respectively. In concurrence to the previous work, present work also shows shorter half-lives in the SH region $Z=118, 122-124$ and 126 with the cluster emissions such as ^{86}Kr , ^{94}Zr , ^{91}Y and ^{96}Mo respectively. Similarly, around 20 possible β^+ emitters were identified in the SH region $105 \leq Z \leq 125$ and the same were tabulated in the table 5.6.

Table 5.6 Identified β^+ emitters in the SHN region

Parent nuclei	Q (MeV)	$\log(T_{1/2})$
^{264}Db	2.24	-0.04
^{268}Bh	2.93	-0.83
^{290}Fl	0.79	1.28
^{286}Mc	4.53	-3.68
^{292}Ts	4.96	-4.12
$^{290}119$	7.20	-6.27
$^{296}119$	5.75	-5.01
$^{292}121$	8.29	-7.56
$^{294}121$	8.06	-7.15
$^{298}121$	6.83	-6.32
$^{302}121$	5.12	-5.49
$^{298}123$	8.42	-8.04
$^{300}123$	8.27	-7.64
$^{302}123$	6.72	-7.23
$^{306}123$	5.73	-6.42
$^{304}125$	7.81	-8.55
$^{306}125$	7.61	-8.15
$^{308}125$	6.99	-7.75
$^{310}125$	6.47	-7.35
$^{312}125$	5.79	-6.96

The table 5.7 gives an information of half-lives and branching ratios, which has ambiguity in deciding the single decay mode. The branching ratios relative to minimum half-lives among the studied decay modes is evaluated and second column of the table shows the $\log T_{1/2}$ values corresponding to SF, α , β^+ and CD half-lives. For instance, the SHN ^{263}Rf shows shorter $\log T_{1/2}$ values for SF and β^+ -decay when compared to other decay modes. The branching ratio among the SF and β^+ -decay is evaluated and it is found that the branching ratio corresponding to SF and β^+ is found to be 55% and 45% respectively. Similarly, the branching ratios for the SH region $104 \leq Z \leq 126$ were identified and tabulated in the table 5.7. Finally, investigated life times of the SH elements after studying the competition between different decay modes are pictorially represented in the figure 5.8. This figure shows that the life-times of the SH element varies from ns to minutes. It has been observed that life-times of the SH element decreases with increase in atomic number. For instance, the average life-time of SH element with $Z=104$ is around 10min

Table 5.7 SHN with double decay mode and its branching ratios

Parent nuclei	log($T_{1/2}$)				Decay mode		Parent nuclei	log($T_{1/2}$)				Decay mode	
	Sf	α	β^+	CD	Sf	α		β^+	CD	Sf	α	β^+	CD
²⁶³ Rf	1.25	1.98	1.65	36.6	Sf = 57%	β^+ = 43%	²⁹⁶ 120	19.58	-4.87	-4.38	-5.45	CD = 53%	α = 47%
²⁶² Db	2.31	-0.48	-0.51	34.76	β^+ = 52%	α = 48%	²⁹¹ 120	25.45	-6.21	-5.85	-4.69	α = 51%	β^+ = 49%
²⁶⁴ Bh	0.71	-1.65	-1.75	20.58	β^+ = 51%	α = 49%	²⁹⁷ 120	15.36	-4.25	-4.6	-3.62	β^+ = 52%	α = 48%
²⁶² Bh	-3.25	-3.25	-2.22	17.73	Sf = 50%	Sf = 50%	²⁸⁹ 120	21.36	-6.31	-6.27	-4.3	α = 50%	β^+ = 50%
²⁶⁶ Bh	1.62	-1.89	-1.29	23.6	α = 59%	β^+ = 41%	²⁹³ 120	25.32	-5.18	-5.43	-5.06	β^+ = 51%	α = 49%
²⁶⁴ Hs	-2.98	-3.15	-1.11	15.37	α = 51%	Sf = 49%	²⁹³ 121	29.32	-6.98	-6.29	-6.47	α = 52%	CD = 48%
²⁷⁰ Mt	2.11	-2.45	-2.08	19.43	α = 54%	β^+ = 46%	²⁹⁹ 121	18.56	-4.75	-5.05	-5.43	CD = 52%	β^+ = 48%
²⁷² Mt	1.35	-1.65	-1.63	22.66	α = 50%	β^+ = 50%	³⁰³ 121	-4.36	-3.52	-4.22	2.35	Sf = 51%	β^+ = 49%
²⁶⁸ Mt	0.99	-2.78	-2.54	16.53	α = 52%	β^+ = 48%	²⁹¹ 121	25.87	-5.94	-6.7	-6.65	β^+ = 50%	CD = 50%
²⁷⁶ Ds	-1.72	-1.65	-0.09	23.61	Sf = 51%	α = 49%	²⁹⁵ 121	30.36	-5.78	-5.88	-6.34	CD = 52%	β^+ = 48%
²⁷² Rg	2.22	-3.15	-3.34	12.55	β^+ = 51%	α = 49%	²⁹⁷ 121	26.9	-4.77	-5.46	-6.33	CD = 54%	β^+ = 46%
²⁷⁶ Rg	2.42	-2.16	-2.44	18.44	β^+ = 53%	α = 47%	³⁰¹ 121	8.25	-5.36	-4.64	-1.47	α = 54%	β^+ = 46%
²⁶⁹ Rg	-3.98	-3.86	-2.95	9.04	Sf = 51%	α = 49%	²⁹⁴ 122	30.65	-5.98	-6.51	-6.89	CD = 51%	β^+ = 49%
²⁷⁰ Rg	-1.56	-3.87	-3.79	10.12	α = 51%	β^+ = 49%	²⁹⁵ 122	34.25	-5.99	-6.73	-6.78	CD = 50%	β^+ = 50%
²⁷⁸ Rg	-1.32	-1.54	-1.99	21.54	β^+ = 56%	α = 44%	²⁹⁶ 122	36.89	-6.24	-6.1	-6.83	CD = 52%	α = 48%
²⁷⁴ Rg	3.56	-3.22	-2.89	15.4	α = 53%	β^+ = 47%	²⁹⁷ 122	34.22	-6.96	-6.32	-6.77	α = 51%	CD = 49%
²⁸³ Nh	-1.55	-1.89	-1.55	18.55	α = 55%	Sf = 45%	³⁰⁵ 122	-0.58	-4.98	-4.68	-0.68	α = 52%	β^+ = 48%
²⁷⁴ Nh	0.65	-4.01	-4.6	6.88	β^+ = 53%	α = 47%	³⁰² 122	18.21	-5.27	-4.87	-6.31	CD = 54%	α = 46%
²⁸⁰ Nh	4.98	-2.78	-3.27	14.3	β^+ = 54%	α = 46%	³⁰¹ 122	23.56	-5.96	-5.5	-6.46	CD = 52%	α = 48%
²⁷⁸ Nh	5.88	-3.87	-3.72	11.51	α = 51%	β^+ = 49%	²⁹⁹ 122	30.89	-6.14	-5.91	-6.7	CD = 52%	α = 48%
²⁷⁴ Fl	-5.12	-4.89	-3.95	3.62	Sf = 51%	α = 49%	³⁰³ 122	13.77	-5.11	-5.09	-4.33	α = 50%	β^+ = 50%
²⁸⁵ Fl	-0.45	-2.11	-1.97	16.71	α = 52%	β^+ = 48%	³⁰³ 123	27.89	-6.36	-5.96	-3.66	α = 52%	β^+ = 48%
²⁸² Mc	11.02	-3.78	-4.55	0.52	β^+ = 55%	α = 45%	²⁹⁷ 123	38.48	-6.17	-7.18	-7.51	CD = 51%	β^+ = 49%
²⁸⁷ Mc	1.32	-2.98	-2.4	0.5	α = 55%	β^+ = 45%	³⁰¹ 123	35.02	-6.18	-6.37	-6.86	CD = 52%	β^+ = 48%
²⁸⁴ Mc	8.98	-3.58	-4.12	0.37	β^+ = 54%	α = 46%	³⁰⁷ 123	2.18	-4.98	-5.15	2.81	β^+ = 51%	α = 49%
²⁷⁶ Mc	-3.12	-5.89	-5.86	1.45	α = 50%	β^+ = 50%	³⁰⁵ 123	15.58	-5.48	-5.56	-0.65	β^+ = 50%	α = 50%
²⁷⁷ Lv	-6.85	-5.78	-5.42	0.18	Sf = 54%	α = 46%	³⁰⁸ 123	-4.89	-5.26	-6.01	3.61	β^+ = 53%	α = 47%
²⁸⁹ Lv	3.15	-3.05	-2.83	-1.32	α = 52%	β^+ = 48%	³⁰³ 124	40.25	-6.25	-6.83	-6.77	β^+ = 50%	CD = 50%
²⁹³ Ts	-2.98	-3.58	-2.84	-2.88	α = 55%	Sf = 45%	³⁰⁵ 124	33.21	-5.12	-6.42	-4.29	β^+ = 56%	α = 44%
²⁸⁴ Ts	13.25	-5.25	-5.83	-2.5	β^+ = 53%	α = 47%	³⁰² 124	40.25	-5.96	-6.6	-7.13	CD = 52%	β^+ = 48%
²⁸⁶ Ts	14.55	-5.16	-5.4	-2.6	β^+ = 51%	α = 49%	³⁰⁴ 124	35.85	-6.01	-6.19	-6.45	CD = 51%	β^+ = 49%
²⁹⁰ Ts	9.18	-4.36	-4.55	-3.09	β^+ = 51%	α = 49%	³⁰⁷ 124	22.14	-5.97	-6.02	-0.09	β^+ = 50%	α = 50%
²⁸⁸ Ts	13.78	-4.87	-4.98	-2.91	β^+ = 51%	α = 49%	³⁰¹ 124	44.14	-6.04	-7.23	-7.53	CD = 51%	β^+ = 49%
²⁸⁰ Ts	0.68	-6.25	-6.69	-2.01	β^+ = 52%	α = 48%	³⁰⁹ 124	6.87	-5.11	-5.62	3.17	β^+ = 52%	α = 48%
²⁸² Ts	8.58	-5.85	-6.26	-2.19	β^+ = 52%	α = 48%	³⁰⁹ 125	26.25	-6.51	-6.49	0.26	α = 50%	β^+ = 50%
²⁹⁰ Og	16.98	-3.78	-3.91	-4.72	CD = 55%	β^+ = 45%	³⁰⁷ 125	38.21	-6.21	-6.89	-3.75	β^+ = 53%	α = 47%
²⁹¹ Og	14.89	-3.78	-4.13	-4.9	CD = 54%	β^+ = 46%	³¹¹ 125	11.58	-5.75	-6.09	2.43	β^+ = 51%	α = 49%
²⁸⁹ Og	18.74	-5.25	-4.56	-4.46	α = 54%	β^+ = 46%	³⁰⁵ 125	45.35	-6.87	-7.29	-7.5	CD = 51%	β^+ = 49%
²⁸⁴ 119	5.95	-6.68	-7.53	-3.17	β^+ = 53%	α = 47%	³⁰³ 125	45.25	-6.96	-7.69	-8.07	CD = 51%	β^+ = 49%
²⁹³ 119	18.29	-3.98	-4.57	-5.15	CD = 53%	β^+ = 47%	³¹⁵ 126	-1.58	-5.75	-6.17	2.82	β^+ = 52%	α = 48%
²⁸⁶ 119	14.98	-7.25	-7.11	-3.79	α = 50%	β^+ = 50%	³¹³ 126	15.25	-6.24	-6.57	0.85	β^+ = 51%	α = 49%
²⁹⁴ 119	15.98	-3.89	-5.43	-5.15	β^+ = 51%	CD = 49%	³⁰⁸ 126	48.21	-6.87	-7.12	-5.37	β^+ = 51%	α = 49%
²⁸⁸ 119	19.35	-5.85	-6.69	-4.15	β^+ = 53%	α = 47%	³¹¹ 126	32.21	-5.12	-6.96	-0.97	β^+ = 58%	α = 42%
²⁹⁸ 119	-4.85	-3.22	-4.59	0.23	Sf = 51%	β^+ = 49%	³¹⁰ 126	39.21	-6.32	-6.73	-1.99	β^+ = 52%	α = 48%
²⁹¹ 119	21.25	-4.58	-4.99	-4.74	β^+ = 51%	CD = 49%	³⁰⁹ 126	44.58	-6.58	-7.36	-3.69	β^+ = 53%	α = 47%
²⁹⁵ 119	11.35	-4.23	-4.15	-5.03	CD = 54%	α = 46%	³¹² 126	26.12	-5.74	-6.33	0.01	β^+ = 52%	α = 48%
²⁹⁵ 120	22.15	-4.78	-5.02	-5.46	CD = 52%	β^+ = 48%	³⁰⁷ 126	51.32	-7.11	-7.75	-6.99	β^+ = 52%	α = 48%
²⁹⁴ 120	23.58	-4.22	-4.79	-5.36	CD = 53%	β^+ = 47%	³¹⁴ 126	7.56	-6.21	-5.94	1.7	α = 51%	β^+ = 49%

whereas, average life-time of hypothetical SH element with $Z=126$ is of the order *m.s.*

CHAPTER 6

Summary and conclusion

6.1 Comparison of present work with microscopic theory

Even though, many microscopic, macroscopic and semi-empirical relations are available in literature, a consolidated outcome of all these models are essential in order to predict CD half-lives for heavy and SHN. A detail investigation is carried out to identify the model which produces the experimental half-lives with less deviation, and also to test the predictive power of theoretical models used in the study of cluster and HPR. In the present work, the macroscopic models such as modified generalised liquid drop model (MGLDM) and Coulomb and proximity potential model (CPPM) were used. To test the predictive powers these macroscopic models they are compared with microscopic models such as Hartree-Fock-Bogoliubov (HFB) [72], M3Y effective interaction [81], Relativistic Mean Field model (RMFM) [402], quantum-mechanical fragmentation process and WKB penetrability (QMPP-WKB) [70]. In the modified generalized liquid drop model (MGLDM) [108, 147].

6.1.1 Selection of decay energy and suitable mass excess for the study of CR and HPR

The role of Q-values plays major role in the evaluation of alpha-decay half-lives as well as CD half-lives [403]. The evaluation of half-lives are directly sensitive to Q-values and these Q-values depends on exact selection of mass excess values. A slight change in Q-values of 0.1MeV causes

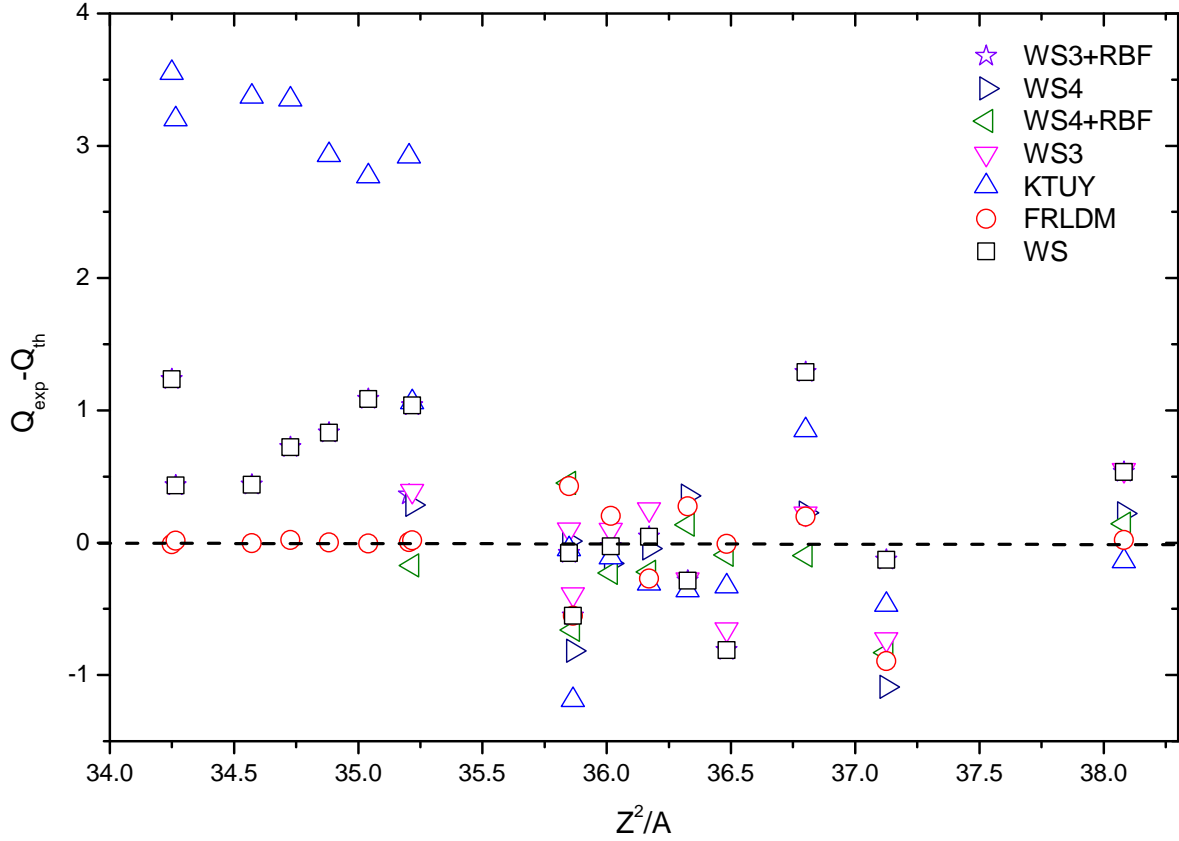


Fig. 6.1 A comparison of $Q_{exp} - Q_{th}$ values obtained using different mass excess values such as WS3+RBF, WS4, WS4+RBF, WS3, KTUY, FRLDM and WS with that of Z^2/A .

a significant variance in half-lives of the order of $10^{-1}s$ to $10^{-2}s$. As a result, the importance of Q-values in predicting accurate half-lives improves. The role of mass excess values in predicting exact experimental Q-value i.e $Q_{exp} - Q_{th}$ is plotted as seen in figure 6.1. The various mass excess values such as WS3+RBF [316], Weizsacker-Skyrme (WS4) model [315], WS4+RBF [315], WS3 [317], Kourra-Tachibaba-Uno-Yamada (KTUY) [265], finite-range liquid-drop model (FRLDM) [313] and WS [404] is used to notice the deviation obtained from theoretical and experimental Q-values from each mass excess value. The comprehensive of the figure shows all these different mass excess values in evaluation of Q-values are fairly reproduces the experimental Q-values. However, the deviation produced by KTUY is larger when compared to other Q-values evaluated using different mass excess values. Hence, the standard deviation is calculated for each Q-value

obtained using different mass excess values. The evaluated standard deviation is as follows;

$$\sigma = \left(\frac{1}{(n-1)} \sum_{i=1}^n (Q^{cal} - Q^{exp})^2 \right)^{1/2} \quad (6.1)$$

The standard deviation is evaluated for n=23 clusters which are available in literature [280, 322, 324, 405, 406]. The σ obtained for each Q-values using different mass excess values are tabulated in table 6.1. From the table it is clearly seen that the value of σ is less in case of FRLDM i.e the mass excess values used in the evaluation of Q-values produces less deviation when compared to other mass models.

Table 6.1 The standard deviation obtained using different mass excess values with that of experimental Q-values.

WS3+RBF	WS4	WS4+RBF	WS3	KTUY	FRLDM	WS
0.73	0.83	0.41	0.44	2.15	0.31	0.75

6.1.2 Suitable microscopic and macroscopic model to study of CR and HPR

Further, the half-lives are evaluated using different microscopic and macroscopic models. The cluster-decay half-lives using macroscopic models such as MGLDM, CPPM [407] from the present work and data available from GLDM1 and GLDM2 [112] were studied in the mass and atomic number range $221 \leq A \leq 242$, $87 \leq Z \leq 96$ respectively. Similarly, the CR half-lives using microscopic models such as Hartree-Fock-Bogoliubov (HFB) [72], M3Y effective interaction [81], Relativistic Mean Field model (RMFM) [402], quantum-mechanical fragmentation process and WKB penetrability (QMPP-WKB) [70]. The experimental $\log T_{1/2}$ values are extracted from the literature [280]. The figure 6.2(a) shows plot of $\log T_{exp}/\log T_{th}$ as a function of $Z_d Q^{-1/2}$ in which $\log T_{th}$ specifies the values corresponding to microscopic cluster-decay half-lives. Similarly, the ratio of experimental to macroscopic CD half-lives are presented in figure 6.2(b). In case of microscopic CD half-lives, the value of $\log T_{exp}/\log T_{th}$ ranges between -0.8 to +1.3. Like-

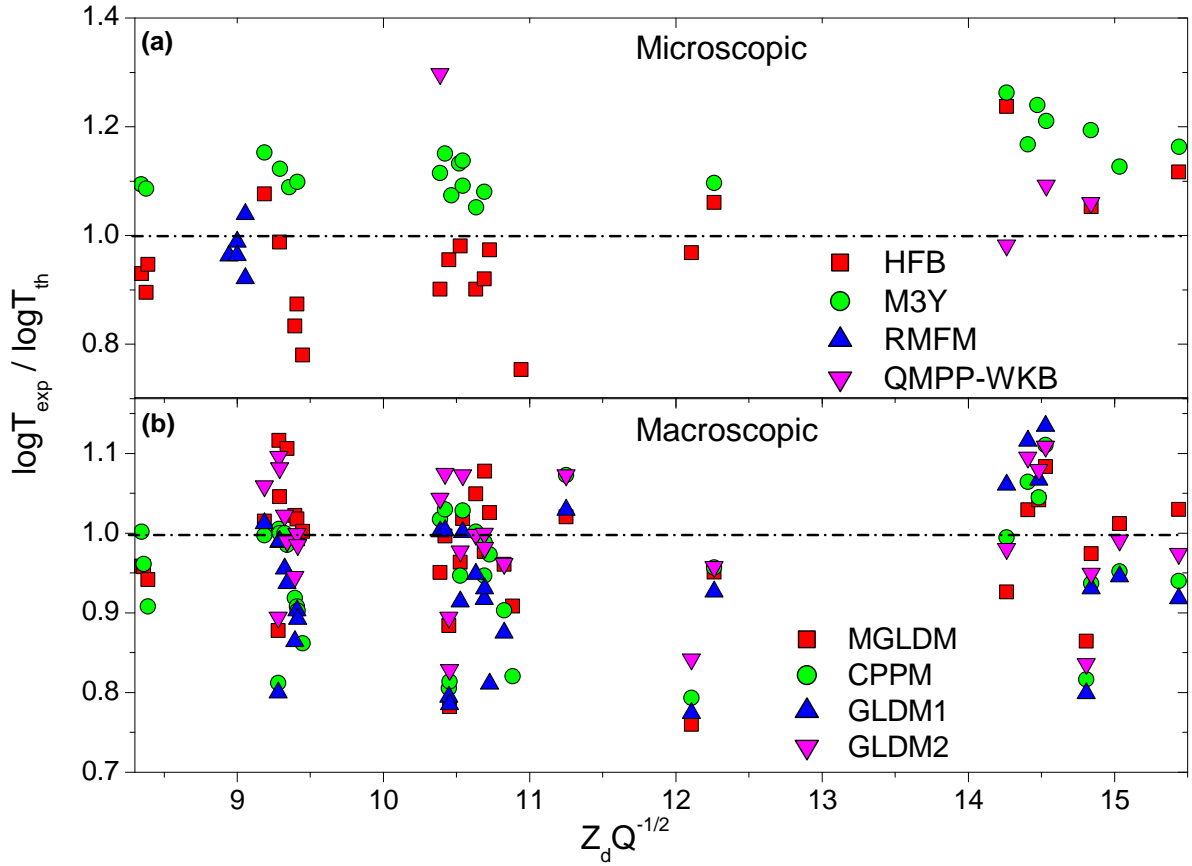


Fig. 6.2 Variation of $\log T_{1/2}(s)$ as a function of Z_d/\sqrt{Q} for (a) microscopic HFB [72], M3Y [81], RMFM [402], QMPP-WKB [70] and (b) macroscopic models MGLDM, CPPM, GLDM1, GLDM2 [407, 408].

wise, in case of macroscopic models the ratio of $\log T_{exp}$ to $\log T_{th}$ values ranges between -0.8 to +1.2. Since definite conclusions could not be able to draw from the figure, standard deviation is evaluated. The figure 6.3 shows comparison of CD half-lives evaluated using microscopic and macroscopic models with respect to experiments. From this comparison it is observed that the model such as Relativistic Mean Field model (RMFM) produces less deviation when compared to other studied models. Equivalently, the Hartree-Fock-Bogoliubov (HFB) produces more deviation when compared to all other models studied. In addition, the MGLDM model produces less deviation in case of macroscopic models.

Thereafter, the investigated semi-empirical relations such as One single line of universal (Univ) [409], NRDX [217], Universal decay law (UDL) [76], KPS [410], AZF [411], Horoi [214]

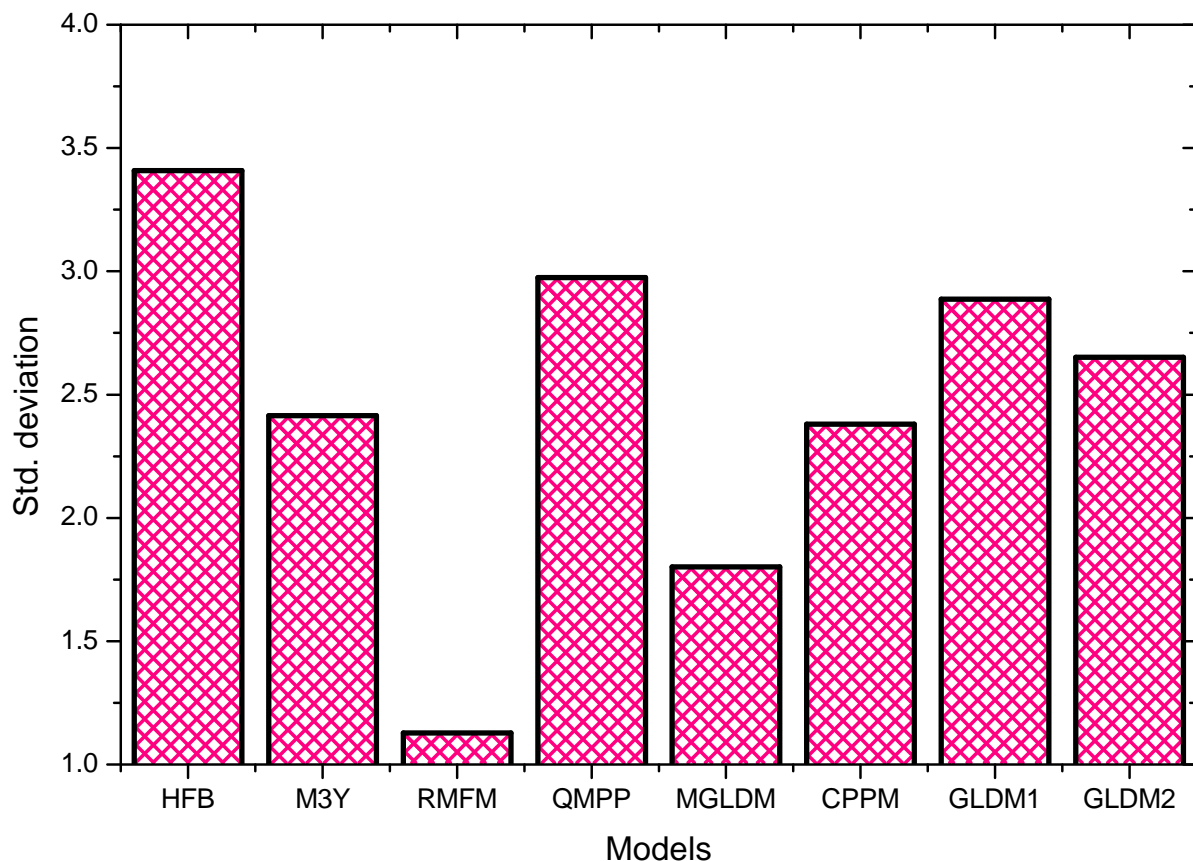


Fig. 6.3 Comparison of standard deviation obtained using microscopic and macroscopic models.

Table 6.2 The standard deviation obtained using different semi empirical relations with that of experimental $\log T_{1/2}$ -values.

Models	σ
UNIV [409]	2.67
NRDX [217]	2.94
UDL [76]	2.84
KPS [410]	3.03
AZF [411]	1.03
Horoi [214]	1.11
Poenaru [71, 71]	1.18

and Poenaru et al., [71, 71] which are available for CR. A plot of $\log T_{exp}/\log T_{semi}$ is plotted as a function of $Z_d Q^{-1/2}$ for experimental cluster-decay half-lives to different CD half-lives using semi-empirical relations is shown in figure 6.4. From the figure, it is noticed that the ratio of $\log T_{exp}/\log T_{semi}$ varies between 0.8 to 1.4. The close examination of figure shows that majority of AZF [411], Horoi [214] and Poenaru et al., [71, 71] lies close to unity i.e the value produced

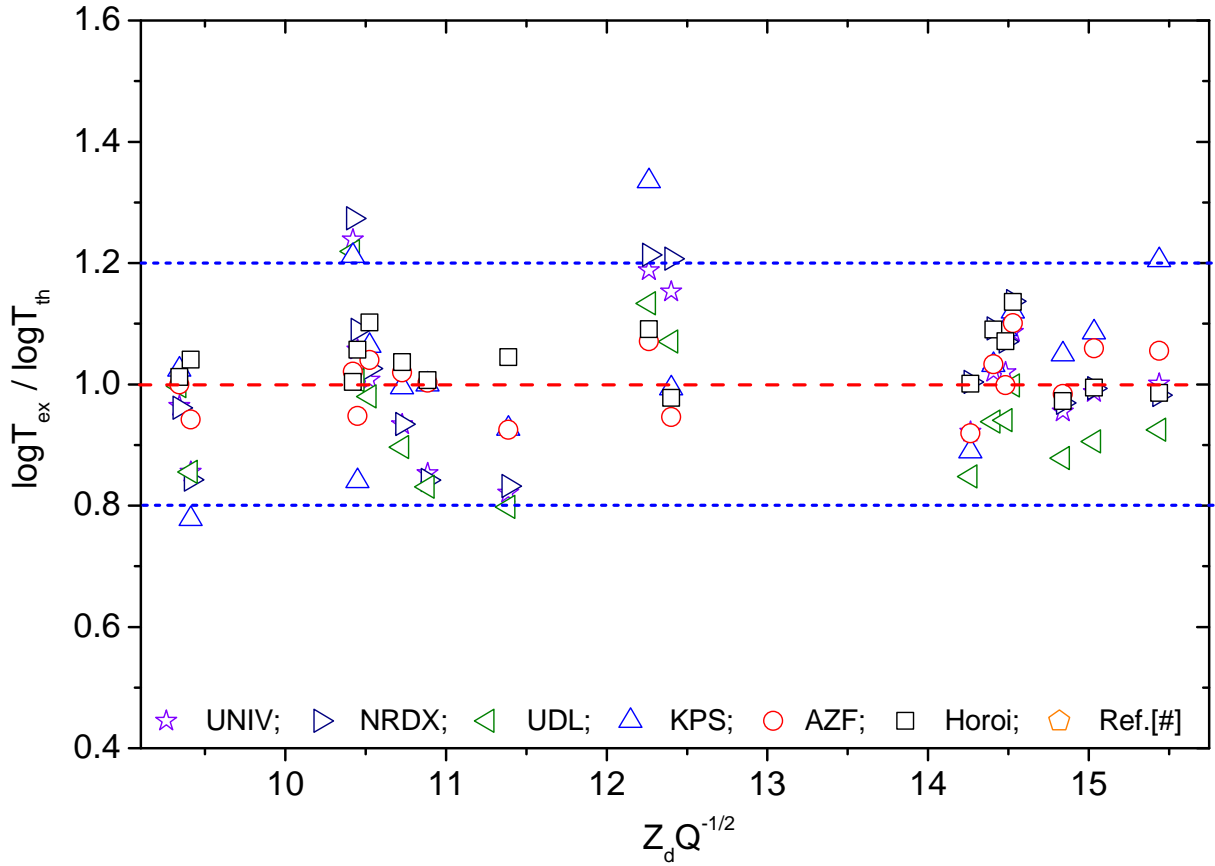


Fig. 6.4 Variation of $\log T_{exp}/\log T_{semi}$ as a function of $Z_d Q^{-1/2}$ using different semi-empirical relations such as UNIV [409], NRDX [217], UDL [76], KPS [410], AZF [411], Horoi [214] and Poenaru et al., [71, 71].

by these semi-empirical relations is almost equal to experimental CD half-lives. Since, no clear conclusions can be taken from the figure, the evaluated standard deviation produced by each semi-empirical relation. The table 6.2 shows standard deviation obtained using each semi-empirical relation with that of experiments. The standard deviation accompanied by AZF [411], Horoi [214] and Poenaru et al., [71] are nearly equal to unity. However, among these semi-empirical relations AZF produces the deviation which is equal to 1.02. Hence, the capability of reproducing experimental CD in macroscopic, microscopic and semi-empirical formulae gives an insight into prediction in the heavy and SH region for unknown nuclei. The cluster-decay half-lives are evaluated using macroscopic models such as MGLDM and CPPM. In addition to this the cluster-decay half-lives using GLDM were studied. Further, the cluster-decay half-lives obtained using

microscopic models such as HFB, M3Y, RMFM and QMPP-WKB were analysed. The half-lives obtained using macroscopic and microscopic models were compared with that of available experiments. The standard deviation is less in case of MGLDM macroscopic model. Furthermore, RMFM microscopic models produces less deviation when compared to other microscopic models. Similarly, the less deviation is observed in AZF semi-empirical formulae. Hence, these results gives an insight into prediction of CD half-lives in heavy and SH region for unknown nuclei. The accurate prediction of CD process enables us to study the shell structure of the heavy nucleus.

6.2 Semiempirical formula for decay energies and half lives of CR

A semi empirical formula for alpha decay half-lives and cluster decay half-lives is formulated for superheavy nuclei of atomic number range $104 \leq Z \leq 130$. The logarithmic half lives produced by the present formula with that of experiments and other formulae such as Universal Decay Law (UDL) [224] and Horoi et al., [214], Univ [227], Royer [212] and VSS [228]. The constructed formula produces logarithmic half lives for alpha and cluster decay (${}^4\text{He}$, ${}^6\text{Li}$, ${}^9\text{Be}$, ${}^{20,22}\text{Ne}$, ${}^{23}\text{Na}$, ${}^{24-26}\text{Mg}$, ${}^{27}\text{Al}$, ${}^{28-30}\text{Si}$, ${}^{32-34}\text{S}$, ${}^{35}\text{Cl}$, ${}^{36,38,40}\text{Ar}$, ${}^{39,41}\text{K}$ and ${}^{40,42-44,46}\text{Ca}$), in superheavy nuclei of atomic number range $104 \leq Z \leq 130$. The proposed a new empirical formula for alpha decay and cluster decay half-lives agree with the experiments and other formulae available in literature. Further an attempt is made to parameterize decay energies (Q) during the same cluster emissions from the SHN region $103 \leq Z \leq 126$. To check the predictive power of constructed formula and compared the decay energies produced by the present formula with that the experiments. The constructed empirical formula can reproduce the Q-values during the cluster emissions using simple input of mass number of daughter nuclei, atomic number of cluster emission, and neutron number of parent nuclei. The constructed the semiempirical formula successfully produces Q-values for superheavy elements during the cluster decay.

6.3 Cluster radioactivity in the SHN

6.3.1 Even nuclei

The radioactive decay with different cluster emissions in the isotopes of Helium to Calcium nuclei is studied. The nuclear proximity potential is studied using Prox-13 proximity function. The CR half-lives have been evaluated within WKB integral method. The estimated CD half-lives from the present work is precisely reproduce the experimental data. Predictions are made in the even SHN in the atomic number range $104 \leq Z \leq 126$. The role of Coulomb effect ($Z^2/A^{2/3}$), asymmetry effect ($(N - Z)^2/A$), pairing effect (\sqrt{A}) and shell effect on half-lives gives an insight in to future experiments on CR.

6.3.2 Odd nuclei

The radioactive decay with the different mass excess values were considered during an evaluation of CD half-lives. The mass excess values produced by FRLDM are in good agreement between available experimental data. The different proximity functions such as MP-77, Prox-77, MP-81, Prox-13, Ng-80 and DP-00 were used in both CPPM and MGLDM models. The CR half-lives have been evaluated within WKB integral method using different proximity potential functions. The estimated CD half-lives using Prox-13 proximity function precisely reproduce the experimental data. Predictions are made in the odd SHN in the atomic number range $105 \leq Z \leq 125$. The role of entrance channel parameters such as Z^2/A and $(N - Z)/(N + Z)$ on logarithmic half-lives gives an insight in to future experiments on CR.

6.3.3 Theoretical evidence for neutron magic number 184 from cluster radioactivity studies

The neutron number corresponding to studied SHN with $N = 179-184$ are having shorter CD half-lives. The shortest CD half-lives corresponds to SHN $^{311}_{126}185$ with ^9Be cluster emission.

The existence of neutron magic number 184 is also demonstrated through the CD studies. In addition to this, shorter half-lives are also observed for the magic or near magic neutron number of daughter nuclei. Hence, we have predicted possibility of magic neutron number or near magic neutron number in the SH element $104 \leq Z \leq 126$.

6.4 Heavy particle radioactivity

The HPR in the SH region $104 \leq Z \leq 126$ is studied using CPPM and MGLDM. The standard deviation of Q-values using different mass excess values are evaluated and among all the different mass excess values the WS4+RBF produces less deviation. Similarly, we have also evaluated CD half-lives and compared with that of available experimental values. The standard deviation produced by MGLDM is less when compared to CPPM. Furthermore, the HPR of ^{58}Ni to ^{92}Sm were studied. The role of asymmetry effect, relative neutron excess, pairing effect and Coulomb effect on half-lives were studied. The HPR of ^{86}Kr , ^{94}Zr , ^{91}Y and ^{96}Mo is observed in the SH element $Z=118$, 122-124 and 126. The HPR of ^{86}Kr , ^{94}Zr , ^{91}Y and ^{96}Mo is compared with the spontaneous fission, α -decay and β^\pm -decay. The decay chains of these SHElement is also predicted. These SHElements with shorter half-lives undergoes decay and stable lead nuclei is formed. The larger quantities of Pb is observed in supernova and galaxy spectrum. As a result, the current research might be valuable in the field of nuclear astrophysics.

6.5 Investigations on decay modes of SHN

systematically investigated all possible decay modes such as α , β , cluster-decay and spontaneous fission in the SH region $104 \leq Z \leq 126$. The present work is validated by comparing with experiments. It has been found around 20 β^+ and seven heavy particle-emitters in the SH region. Furthermore, the nuclei which shows almost same half-lives for two decay modes are

also reported with the corresponding branching ratios. However, through experimental study is necessary to draw the definite conclusions in this aspect.

6.6 Scope of the Research work

The accurate prediction of the CD process enables us to study the shell structure of the heavy nucleus and it gives an insight into a prediction of CD half-lives in the heavy and super heavy regions. This work will be the reference for identifying possible decay modes in the super heavy region. The existence of neutron magic number 184 is predicted through CD studies, in the super heavy nuclei region $104 \leq Z \leq 126$. The dominant decay mode is identified by studying the competition between different decay modes such as α -decay, β -decay, cluster-decay, and spontaneous fission in the super heavy nuclei region $104 \leq Z \leq 126$, for unknown nuclei. The study of cluster and HPR enable to predict the new magic number and shell structure of the heavy nucleus. During the study of cluster radioactivity of superheavy nuclei, surprisingly it is observed that the shortest half-lives of cluster decay in all superheavy elements are observed for daughter neutron number 184 and nearly equal to that. This is a clear evidence for the existence of the neutron magic number $N=184$. This study is useful in the understanding of superheavy element nuclei structure

References

- [1] G. N. Flerov and K. A. Petrzhak. Spontaneous fission of uranium. *Phys. Rev*, 58(89):275–279, 1940.
- [2] N. Bohr and J. A. Wheeler. The mechanism of nuclear fission. *Physical Review*, 56(5):426, 1939.
- [3] Glenn T. Seaborg. The transuranium elements. *Nuclear Science and Engineering*, 9(4):475–487, 1961.
- [4] Y. T. Oganessian, V. K. Utyonkov, Y. V. Lobanov, F. S. Abdullin, A. N. Polyakov, I. V. Shirokovsky, Y. S. Tsyganov, G. G. Gulbekian, S. L. Bogomolov, B. N. Gikal, A. N. Mezentsev, S. Iliev, V. G. Subbotin, A. M. Sukhov, A. A. Voinov, G. V. Buklanov, K. Subotic, V. I. Zagrebaev, M. G. Itkis, J. B. Patin, K. J. Moody, J. F. Wild, M. A. Stoyer, N. J. Stoyer, D. A. Shaughnessy, J. M. Kenneally, P. A. Wilk, R. W. Loughheed, R. I. Il'kaev, and S. P. Vesnovskii. Measurements of cross sections and decay properties of the isotopes of elements 112, 114, and 116 produced in the fusion reactions $^{233,238}\text{U}$, ^{242}Pu , and $^{248}\text{Cm}+^{48}\text{Ca}$. *Phys. Rev. C*, 70:064609, Dec 2004.
- [5] Yu. Ts. Oganessian, V. K. Utyonkov, Y. V. Lobanov, F. Sh. Abdullin, A. N. Polyakov, R. N. Sagaidak, I. V. Shirokovsky, Y. S. Tsyganov, A. A. Voinov, G. G. Gulbekian, S. L. Bogomolov, B. N. Gikal, A. N. Mezentsev, S. Iliev, V. G. Subbotin, A. M. Sukhov, K. Subotic, V. I. Zagrebaev, G. K. Vostokin, M. G. Itkis, K. J. Moody, J. B. Patin, D. A. Shaughnessy,

- M. A. Stoyer, N. J. Stoyer, P. A. Wilk, J. M. Kenneally, J. H. Landrum, J. F. Wild, and R. W. Lougheed. Synthesis of the isotopes of elements 118 and 116 in the ^{249}Cf and $^{245}\text{Cm} + ^{48}\text{Ca}$ fusion reactions. *Phys. Rev. C*, 74:044602, Oct 2006.
- [6] Y. T. Oganessian, F. S. Abdullin, C. Alexander, J. Binder, R. A. Boll, S. N. Dmitriev, J. Ezold, K. Felker, J. M. Gostic, R. K. Grzywacz, J. H. Hamilton, R. A. Henderson, M. G. Itkis, K. Miernik, D. Miller, K. J. Moody, A. N. Polyakov, A. V. Ramayya, J. B. Roberto, M. A. Ryabinkin, K. P. Rykaczewski, R. N. Sagaidak, D. A. Shaughnessy, I. V. Shirokovsky, M. V. Shumeiko, M. A. Stoyer, N. J. Stoyer, V. G. Subbotin, A. M. Sukhov, Yu. S. Tsyganov, V. K. Utyonkov, A. A. Voinov, and G. K. Vostokin. Experimental studies of the $^{249}\text{Bk} + ^{48}\text{Ca}$ reaction including decay properties and excitation function for isotopes of element 117, and discovery of the new isotope ^{277}Mt . *Phys. Rev. C*, 87:054621, May 2013.
- [7] G. Munzenberg, S. Grevy, N. Alamanos, N. Amar, J. C. Angelique, R. Anne, G. Auger, F. Becker, R. Dayras, A. Drouart, et al. Experiment on the synthesis of element 113 in the reaction $^{209}\text{Bi}(^{70}\text{Zn}, n)^{278}113$. *Rev. Mod. Phys*, 72:733, 2000.
- [8] Y. Oganessian. Heaviest nuclei from 48ca-induced reactions. *Journal of Physics G: Nuclear and Particle Physics*, 34(4):R165, 2007.
- [9] F. P. Heßberger, S. Hofmann, D. Ackermann, V. Ninov, M. Leino, G. Münzenberg, S. Saro, A. Lavrentev, A. G. Popeko, A. V. Yeremin, et al. Decay properties of neutron-deficient isotopes 256, 257 db, 255 rf, 252, 253 lr. *The European Physical Journal A-Hadrons and Nuclei*, 12(1):57–67, 2001.
- [10] J. H. Hamilton, S. Hofmann, and Y. T. Oganessian. Search for superheavy nuclei. *Annual Review of Nuclear and Particle Science*, 63:383–405, 2013.

- [11] S. Ćwiok, J. Dobaczewski, P. H. Heenen, P. Magierski, and W. Nazarewicz. Shell structure of the superheavy elements. *Nuclear Physics A*, 611(2-3):211–246, 1996.
- [12] K. Rutz, Michaël Bender, T. Bürvenich, T. Schilling, P. G. Reinhard, J. A. Maruhn, and W. Greiner. Superheavy nuclei in self-consistent nuclear calculations. *Physical Review C*, 56(1):238, 1997.
- [13] Michaël Bender, K. Rutz, P. G. Reinhard, J. A. Maruhn, and W. Greiner. Shell structure of superheavy nuclei in self-consistent mean-field models. *Physical Review C*, 60(3):034304, 1999.
- [14] G. G. Adamian, N. V. Antonenko, W. Scheid, and V. V. Volkov. Fusion cross sections for superheavy nuclei in the dinuclear system concept. *Nuclear Physics A*, 633(3):409–420, 1998.
- [15] Y. Aritomo, T. Wada, M. Ohta, and Y. Abe. Fluctuation-dissipation model for synthesis of superheavy elements. *Phys. Rev. C*, 59:796–809, Feb 1999.
- [16] V. I. Zagrebaev. Synthesis of superheavy nuclei: Nucleon collectivization as a mechanism for compound nucleus formation. *Phys. Rev. C*, 64:034606, Aug 2001.
- [17] L. Zu-Hua and B. Jing-Dong. Effects of isospin equilibrium on cold fusion of superheavy nuclei. *Chinese Physics Letters*, 22(12):3044, 2005.
- [18] H. C. Manjunatha and K. N. Sridhar. Survival and compound nucleus probability of super heavy element $z=117$. *The European Physical Journal A*, 53(5):1–11, 2017.
- [19] M. G. Itkis, E. Vardaci, I. M. Itkis, G. N. Knyazheva, and E. M. Kozulin. Fusion and fission of heavy and superheavy nuclei (experiment). *Nuclear Physics A*, 944:204–237, 2015.

- [20] H. C. Manjunatha and K. N. Sridhar. Projectile target combination to synthesis superheavy nuclei $z=126$. *Nuclear Physics A*, 962:7–23, 2017.
- [21] T. Nhan Hao, N. N. Duy, K. Y. Chae, N. Quang Hung, and N. Nhu Le. Investigation of the synthesis of the unknown superheavy nuclei $309, 312, 126$. *International Journal of Modern Physics E*, 28(07):1950056, 2019.
- [22] Y. T. Oganessian, V. K. Utyonkov, Yu. V. Lobanov, F. Sh. Abdullin, A. N. Polyakov, I. V. Shirokovsky, Yu. S. Tsyganov, G. G. Gulbekian, S. L. Bogomolov, B. N. Gikal, A. N. Mezentsev, S. Iliev, V. G. Subbotin, A. M. Sukhov, O. V. Ivanov, G. V. Buklanov, K. Subotic, M. G. Itkis, K. J. Moody, J. F. Wild, N. J. Stoyer, M. A. Stoyer, and R. W. Loughheed. Synthesis of superheavy nuclei in the $^{48}\text{Ca}+^{244}\text{Pu}$ reaction: $^{288}114$. *Phys. Rev. C*, 62:041604, Sep 2000.
- [23] Y. T. Oganessian and V. K. Utyonkov. Superheavy nuclei from 48ca-induced reactions. *Nuclear Physics A*, 944:62–98, 2015.
- [24] Michael Thoennessen. Spontaneous fission. In *The Discovery of Isotopes*, pages 245–250. Springer, 2016.
- [25] D. N. Poenaru and R. A. Gherghescu. Spontaneous fission of the superheavy nucleus ^{286}Fl . *Phys. Rev. C*, 94:014309, Jul 2016.
- [26] D. N. Poenaru, R. A. Gherghescu, and W. Greiner. Heavy-particle radioactivity of superheavy nuclei. *Phys. Rev. Lett.*, 107:062503, Aug 2011.
- [27] P. B. Price. Heavy-particle radioactivity (α & α'). *Annual Review of Nuclear and Particle Science*, 39(1):19–42, 1989.

- [28] K. P. Santhosh and B. Priyanka. Heavy particle radioactivity from superheavy nuclei leading to 298114 daughter nuclei. *Nuclear Physics A*, 929:20–37, 2014.
- [29] G. Sawhney, K. Sandhu, M. K. Sharma, and R. K. Gupta. Role of nuclear deformations and proximity interactions in heavy particle radioactivity. *The European Physical Journal A*, 50(11):1–11, 2014.
- [30] H. J. Rose and G. A. Jones. A new kind of natural radioactivity. *Nature*, 307(5948):245–247, 1984.
- [31] E. Hourani, M. Hussonnois, and D. N. Poenaru. Radioactivities by light fragment (c, ne, mg) emission. In *Annales de Physique*, volume 14, pages 311–396, 1989.
- [32] S. W. Barwick, P. B. Price, and J. D. Stevenson. Radioactive decay of ^{232}U by ^{24}Ne emission. *Phys. Rev. C*, 31:1984–1986, May 1985.
- [33] R. Bonetti, C. Chiesa, A. Guglielmetti, C. Migliorino, A. Cesana, M. Terrani, and P. B. Price. Neon radioactivity of uranium isotopes. *Phys. Rev. C*, 44:888–890, Aug 1991.
- [34] P. B. Price, R. Bonetti, A. Guglielmetti, C. Chiesa, R. Matheoud, C. Migliorino, and K. J. Moody. Emission of ^{23}F and ^{24}Ne in cluster radioactivity of ^{231}Pa . *Phys. Rev. C*, 46:1939–1945, Nov 1992.
- [35] R. Bonetti, C. Carbonini, A. Guglielmetti, M. Hussonnois, D. Trubert, and C. Le Naour. Cluster decay of ^{230}U via ne emission. *Nuclear Physics A*, 686(1-4):64–70, 2001.
- [36] K. P. Santhosh, B. Priyanka, and M. S. Unnikrishnan. Cluster decay half-lives of trans-lead nuclei within the coulomb and proximity potential model. *Nuclear Physics A*, 889:29–50, 2012.

- [37] S. Gong, W. Wu, F. Q. Wang, J. Liu, Y. Zhao, Y. Shen, S. Wang, Q. Sun, and Q. Wang. Classifying superheavy elements by machine learning. *Physical Review A*, 99(2):022110, 2019.
- [38] V. Pershina. Electronic structure and properties of superheavy elements. *Nuclear Physics A*, 944:578–613, 2015.
- [39] Thomas Bürvenich, Michaël Bender, Joachim Alexander Maruhn, and P-G Reinhard. Systematics of fission barriers in superheavy elements. *Physical Review C*, 69(1):014307, 2004.
- [40] P. R. Chowdhury, C. Samanta, and D. N. Basu. α decay half-lives of new superheavy elements. *Physical Review C*, 73(1):014612, 2006.
- [41] G. T. Seaborg, W. Loveland, and D. J. Morrissey. Superheavy elements: a crossroads. *Science*, 203(4382):711–717, 1979.
- [42] F. P. Heßberger. Spontaneous fission properties of superheavy elements. *The European Physical Journal A*, 53(4):1–32, 2017.
- [43] R. K. Gupta, M. Balasubramaniam, R. Kumar, N. Singh, M. Manhas, and W. Greiner. Optimum orientations of deformed nuclei for cold synthesis of superheavy elements and the role of higher multipole deformations. *Journal of Physics G: Nuclear and Particle Physics*, 31(7):631, 2005.
- [44] P. Indelicato, José Paulo Santos, Stephan Boucard, and J. P. Desclaux. Qed and relativistic corrections in superheavy elements. *The European Physical Journal D*, 45(1):155–170, 2007.

- [45] W. Brodziński and J. Skalski. Predictions for superheavy elements beyond $z=126$. *Physical Review C*, 88(4):044307, 2013.
- [46] Y. T. Oganessian and Sergey N. D. Synthesis and study of properties of superheavy atoms. factory of superheavy elements. *Russian Chemical Reviews*, 85(9):901, 2016.
- [47] V. A. Dzuba, M. S. Safronova, and U. I. Safronova. Atomic properties of superheavy elements no, lr, and rf. *Physical Review A*, 90(1):012504, 2014.
- [48] L. Zhu, W. J. Xie, and F. S. Zhang. Production cross sections of superheavy elements $z=119$ and 120 in hot fusion reactions. *Physical Review C*, 89(2):024615, 2014.
- [49] B. G. C. Lackenby, V. A. Dzuba, and V. V. Flambaum. Calculation of atomic properties of superheavy elements $z=110$ – 112 and their ions. *Physical Review A*, 101(1):012514, 2020.
- [50] E. Rutherford. E. rutherford, proc. roy. soc., a97, 374 1920.
- [51] Jean Becquerel and JA Crowther. Discovery of radioactivity. *Nature*, 161(4094):609, 1948.
- [52] Y. Hatsukawa, H. Nakahara, and D. C. Hoffman. Systematics of alpha decay half-lives. *Physical Review C*, 42(2):674, 1990.
- [53] A. Parkhomenko and A. Sobiczewski. Phenomenological formula for alpha-decay half-lives of heaviest nuclei. *Acta physica polonica B*, 36(10):3095, 2005.
- [54] Y. A. Akovali. Review of alpha–decay data from doubly–even nuclei. *Nuclear Data Sheets*, 84(1):1–114, 1998.
- [55] D. N. Poenaru, M. Ivascu, and D. Mazilu. A new semiempirical formula for the alpha decay half-lives. *Journal de Physique Lettres*, 41(24):589–590, 1980.

- [56] D. T. Akrawy, H. Hassanabadi, S. S. Hosseini, and K. P. Santhosh. Systematic study of alpha decay half-lives using new universal decay law. *International Journal of Modern Physics E*, 28(09):1950075, 2019.
- [57] K. P. Santhosh and B. Priyanka. Alpha-decay studies on 130-153 eu nuclei. *International Journal of Modern Physics E*, 22(11):1350081, 2013.
- [58] D. F. Torgerson, R. A. Gough, and R. D. Macfarlane. Alpha decay of the isomers of fr 214. *Physical Review*, 174(4):1494, 1968.
- [59] Sven Gösta Nilsson, J. R. Nix, A. Sobiczewski, Z. Szymański, S. Wycech, C. Gustafson, and P. Möller. On the spontaneous fission of nuclei with z near 114 and n near 184. *Nuclear Physics A*, 115(3):545–562, 1968.
- [60] C. Xu and Z. Ren. Systematical law of spontaneous fission half-lives of heavy nuclei. *Physical Review C*, 71(1):014309, 2005.
- [61] M. G. Urin and D. F. Zaretsky. On the spontaneous fission of nuclei. *Nuclear Physics*, 75(1):101–108, 1966.
- [62] J. R. Huizenga. Spontaneous fission systematics. *Physical Review*, 94(1):158, 1954.
- [63] D. W. Dorn. Predictions of spontaneous fission half-lives for heavy nuclei. *Physical Review*, 121(6):1740, 1961.
- [64] A. Sandulescu, D. N. Poenaru, and W. Greiner. New type of decay of heavy nuclei intermediate between fission and. cap alpha. decay. *Sov. J. Particles Nucl.(Engl. Transl.);(United States)*, 11(6), 1980.
- [65] D. V. Aleksandrov, A. F. Belyatskij, Y. A. Glukhov, E. Y. Nkol'skij, B. G. Novatskij, A. A.

- Ogloblin, and D.N. Stepanov. Observation of spontaneous emission of ^{14}C nuclei from ^{223}Ra . *Pis'ma v Zhurnal Eksperimental'noj i Teoreticheskoy Fiziki*, 40(4):152–154, 1984.
- [66] R. K. Gupta and W. Greiner. Cluster radioactivity. *International Journal of Modern Physics E*, 3(supp01):335–433, 1994.
- [67] Y. S. Zamyatnin, V. L. Mikheev, and S. P. Tret'yakova. V. I. Furman, S. G. Kadenskii and Yu. M. Chulvil'skii, *Sov. J. Part. Nucl.*, 21:231, 1990.
- [68] R. Bonetti and A. Guglielmetti. Cluster radioactivity: an overview after twenty years. *Romanian reports in Physics*, 59(2):301, 2007.
- [69] S. K. Arun, R. K. Gupta, S. Kanwar, B. Singh, and M. K. Sharma. Cluster radioactivity with effects of deformations and orientations of nuclei included. *Physical Review C*, 80(3):034317, 2009.
- [70] S. S. Malik and R. K. Gupta. Theory of cluster radioactive decay and of cluster formation in nuclei. *Physical Review C*, 39(5):1992, 1989.
- [71] D. N. Poenaru, M. Ivaşcu, A. Sandulescu, and W. Greiner. Atomic nuclei decay modes by spontaneous emission of heavy ions. *Physical Review C*, 32(2):572, 1985.
- [72] M. Warda and L. M. Robledo. Microscopic description of cluster radioactivity in actinide nuclei. *Physical Review C*, 84(4):044608, 2011.
- [73] R. Blendowske and H. Walliser. Systematics of cluster-radioactivity-decay constants as suggested by microscopic calculations. *Physical review letters*, 61(17):1930, 1988.
- [74] D. N. Poenaru, R.A. Gherghescu, and W. Greiner. Cluster decay of superheavy nuclei. *Physical Review C*, 85(3):034615, 2012.

- [75] Rezső G. Lovas, R. J. Liotta, A. Insolia, K. Varga, and D. S. Delion. Microscopic theory of cluster radioactivity. *Physics reports*, 294(5):265–362, 1998.
- [76] C. Qi, F. Xu, R. J. Liotta, and R. Wyss. Universal decay law in charged-particle emission and exotic cluster radioactivity. *Physical review letters*, 103(7):072501, 2009.
- [77] M. Warda, A. Zdeb, and Luis M. Robledo. Cluster radioactivity in superheavy nuclei. *Physical Review C*, 98(4):041602, 2018.
- [78] G. L. Zhang, Y. J. Yao, M. F. Guo, M. Pan, G. X. Zhang, and X. X. Liu. Comparative studies for different proximity potentials applied to large cluster radioactivity of nuclei. *Nuclear Physics A*, 951:86–96, 2016.
- [79] R. Kumar. Cluster radioactivity using various versions of nuclear proximity potentials. *Physical Review C*, 86(4):044612, 2012.
- [80] K. P. Santhosh and R. K. Biju. Neutron and proton shell closure in the superheavy region via cluster radioactivity in 280–314 116 isotopes. *Pramana*, 72(4):689–707, 2009.
- [81] T. R. Routray, J. Nayak, and D. N. Basu. Cluster radioactivity in very heavy nuclei: a new perspective. *Nuclear Physics A*, 826(3-4):223–229, 2009.
- [82] M. Ismail and A. Adel. Prediction of α -decay chains and cluster radioactivity of $^{300-304}_{121}$ and $^{302-306}_{122}$ isotopes using the double-folding potential. *Physical Review C*, 101(2):024607, 2020.
- [83] M. Ismail, W. M. Seif, and A. Abdurrahman. Relative stability and magic numbers of nuclei deduced from behavior of cluster emission half-lives. *Physical Review C*, 94(2):024316, 2016.

- [84] S. K. Arun, R. K. Gupta, B. Singh, S. Kanwar, and M. K. Sharma. ^{208}Pb -daughter cluster radioactivity and the deformations and orientations of nuclei. *Physical Review C*, 79(6):064616, 2009.
- [85] S. N. Kuklin, G. G. Adamian, and N. V. Antonenko. Spectroscopic factors and barrier penetrabilities in cluster radioactivity. *Physics of Atomic Nuclei*, 68(9):1443–1452, 2005.
- [86] M. Iriondo, D. Jerrestam, and R. J. Liotta. Cluster radioactivity and clustering formation in nuclei. *Nuclear Physics A*, 454(2):252–266, 1986.
- [87] A. M. Nagaraja, H. C. Manjunatha, N. Sowmya, N. Manjunath, and S. A. C. Raj. Cluster radioactivity of superheavy nuclei $^{290-310}120$ using different proximity functions. *The European Physical Journal Plus*, 135(10):1–16, 2020.
- [88] H. C. Manjunatha and N. Sowmya. Competition between spontaneous fission ternary fission cluster decay and alpha decay in the super heavy nuclei of $z=126$. *Nuclear Physics A*, 969:68–82, 2018.
- [89] N. Sowmya, H. C. Manjunatha, N. Dhananjaya, and A. M. Nagaraja. Competition between binary fission, ternary fission, cluster radioactivity and alpha decay of 281 ds. *Journal of Radioanalytical and Nuclear Chemistry*, 323(3):1347–1351, 2020.
- [90] G. R. Sridhar, H. C. Manjunatha, N. Sowmya, P. S. Gupta, and H. B. Ramalingam. Atlas of cluster radioactivity in actinide nuclei. *The European Physical Journal Plus*, 135(3):1–28, 2020.
- [91] H. C. Manjunatha, K. N. Sridhar, and N. Sowmya. Investigations of the synthesis of the superheavy element $z=122$. *Physical Review C*, 98(2):024308, 2018.

- [92] H. C. Manjunatha and N. Sowmya. Decay modes of superheavy nuclei $z=124$. *International Journal of Modern Physics E*, 27(05):1850041, 2018.
- [93] N. Sowmya and H. C. Manjunatha. Investigations on different decay modes of darmstadtium. *Physics of Particles and Nuclei Letters*, 17(3):370–378, 2020.
- [94] N. Sowmya and H. C. Manjunatha. Competition between different decay modes of superheavy element $z=116$ and synthesis of possible isotopes. *Brazilian Journal of Physics*, 49(6):874–886, 2019.
- [95] N. Sowmya, H. C. Manjunatha, and P. S. Damodara Gupta. Competition between decay modes of superheavy nuclei 281-310og. *International Journal of Modern Physics E*, 2020.
- [96] N. Sowmya and H. C. Manjunatha. Investigations on different decay modes of darmstadtium. *Physics of Particles and Nuclei Letters*, 17(3):370–378, 2020.
- [97] N. Sowmya, H. C. Manjunatha, P. S. Damodara Gupta, and N. Dhananjaya. Competition between cluster and alpha decay in odd z superheavy nuclei $111 \leq z \leq 125$. *Brazilian Journal of Physics*, pages 1–37, 2020.
- [98] K. N. Sridhar, H. C. Manjunatha, and H. B. Ramalingam. Search for possible fusion reactions to synthesize the superheavy element $z=121$. *Physical Review C*, 98(6):064605, 2018.
- [99] D. N. Poenaru, W. Greiner, M. Ivascu, and A. Sandulescu. Heavy cluster decay of trans-zirconium “stable” nuclides. *Phys. Rev. C*, 32:2198–2200, Dec 1985.
- [100] S. S. Malik, S. Singh, R. K. Puri, S. Kumar, and R. K. Gupta. Clustering phenomena in radioactive and stable nuclei and in heavy-ion collisions. *Pramana*, 32(4):419–433, 1989.

- [101] G. Shanmugam and B. Kamalaharan. Application of a cubic barrier in exotic decay studies. *Phys. Rev. C*, 38:1377–1381, Sep 1988.
- [102] S. S. Malik and Raj K. Gupta. Theory of cluster radioactive decay and of cluster formation in nuclei. *Phys. Rev. C*, 39:1992–2000, May 1989.
- [103] M. Warda and L. M. Robledo. Microscopic description of cluster radioactivity in actinide nuclei. *Phys. Rev. C*, 84:044608, Oct 2011.
- [104] Y. J. Shi and W. J. Swiatecki. Estimates of radioactive decay by the emission of nuclei heavier than α -particles. *Nuclear Physics A*, 438(2):450–460, 1985.
- [105] K. P. Santhosh and A. Joseph. Exotic decay in cerium isotopes. *Pramana*, 58(4):611–621, 2002.
- [106] A. M. Kobos, B. A. Brown, P. E. Hodgson, G. R. Satchler, and A. Budzanowski. Folding model analysis of α -particle elastic scattering with a semirealistic density-dependent effective interaction. *Nuclear Physics A*, 384(1-2):65–87, 1982.
- [107] C. Xu and Z. Ren. Global calculation of α -decay half-lives with a deformed density-dependent cluster model. *Phys. Rev. C*, 74:014304, Jul 2006.
- [108] G. Royer and R. Moustabchir. Light nucleus emission within a generalized liquid-drop model and quasimolecular shapes. *Nuclear Physics A*, 683(1-4):182–206, 2001.
- [109] M. Goncalves and S. B. Duarte. Effective liquid drop description for the exotic decay of nuclei. *Phys. Rev. C*, 48:2409–2414, Nov 1993.
- [110] G. Royer and B. Remaud. Static and dynamic fusion barriers in heavy-ion reactions. *Nuclear Physics A*, 444(3):477–497, 1985.

- [111] G. Royer and R. A. Gherghescu. On the formation and alpha decay of superheavy elements. *Nuclear Physics A*, 699(3-4):479–492, 2002.
- [112] X. J. Bao, H. F. Zhang, B. S. Hu, G. Royer, and J. Q. Li. Half-lives of cluster radioactivity with a generalized liquid-drop model. *Journal of Physics G: Nuclear and Particle Physics*, 39(9):095103, 2012.
- [113] J. M. Wang, H. F. Zhang, and J. Q. Li. α decay half-lives for $z= 108, 114, 120, 126$ isotopes and $n= 162, 184$ isotones. *Journal of Physics G: Nuclear and Particle Physics*, 40(4):045103, 2013.
- [114] H. Zhang, W. Zuo, J. Li, and G. Royer. α decay half-lives of new superheavy nuclei within a generalized liquid drop model. *Phys. Rev. C*, 74:017304, Jul 2006.
- [115] H. C. Manjunatha, K. N. Sridhar, and N. Sowmya. Investigations of the synthesis of the superheavy element $z = 122$. *Phys. Rev. C*, 98:024308, Aug 2018.
- [116] H. C. Manjunatha. Alpha decay properties of superheavy nuclei $z= 126$. *Nuclear Physics A*, 945:42–57, 2016.
- [117] N. Sowmya, H. C. Manjunatha, N. Dhananjaya, and A. M. Nagaraja. Competition between binary fission, ternary fission, cluster radioactivity and alpha decay of 281ds. *Journal of Radioanalytical and Nuclear Chemistry*, 323(3):1347–1351, 2020.
- [118] N. Sowmya, H. C. Manjunatha, P. S. Damodara Gupta, and N. Dhananjaya. Competition between cluster and alpha decay in odd z superheavy nuclei $111 \leq z \leq 125$. *Brazilian Journal of Physics*, 51(1):99–135, 2021.
- [119] N. Sowmya, H. C. Manjunatha, et al. Decay properties of superheavy nuclei 269–290 fl. *Physics of Particles and Nuclei Letters*, 18(2):177–184, 2021.

- [120] Y. T. Oganessian. Superheavy elements. *Pure and applied chemistry*, 76(9):1715–1734, 2004.
- [121] H. F. Zhang, J. M. Dong, G. Royer, W. Zuo, and J. Q. Li. Preformation of clusters in heavy nuclei and cluster radioactivity. *Physical Review C*, 80(3):037307, 2009.
- [122] Y. L. Zhang, Y. Z. Wang, et al. Systematic study of cluster radioactivity of superheavy nuclei. *Physical Review C*, 97(1):014318, 2018.
- [123] K. P. Santhosh and C. Nithya. Systematic studies of α and heavy-cluster emissions from superheavy nuclei. *Physical Review C*, 97(6):064616, 2018.
- [124] D. N. Poenaru, H. Stöcker, and R. A. Gherghescu. Cluster and alpha decay of superheavy nuclei. *European Physical Journal A—Hadrons and Nuclei*, 54(2), 2018.
- [125] X. J. Bao, H. F. Zhang, J. M. Dong, J. Q. Li, and H. F. Zhang. Competition between α decay and cluster radioactivity for superheavy nuclei with a universal decay-law formula. *Physical Review C*, 89(6):067301, 2014.
- [126] S. Kumar, R. Rani, and R. Kumar. Shell closure effects studied via cluster decay in heavy nuclei. *Journal of Physics G: Nuclear and Particle Physics*, 36(1):015110, 2008.
- [127] R. K. Gupta, S. Kumar, R. Kumar, M. Balasubramaniam, and W. Scheid. Structure effects in the region of superheavy elements via the α -decay chain of 293118. *Journal of Physics G: Nuclear and Particle Physics*, 28(11):2875, 2002.
- [128] H. Ngo and C. Ngô. Calculation of the real part of the interaction potential between two heavy ions in the sudden approximation. *Nuclear Physics A*, 348(1):140–156, 1980.
- [129] D. N. Poenaru, R. A. Gherghescu, and W. Greiner. Heavy-particle radioactivity of superheavy nuclei. *Physical review letters*, 107(6):062503, 2011.

- [130] A. Marinov, I. Rodushkin, D. Kolb, A. Pape, Y. Kashiv, R. Brandt, R. V. Gentry, and H. W. Miller. Evidence for the possible existence of a long-lived superheavy nucleus with atomic mass number $a = 292$ and atomic number $z \cong 122$ in natural th. *International journal of modern physics E*, 19(01):131–140, 2010.
- [131] S. K. Patra, M. Bhuyan, M. S. Mehta, and R. K. Gupta. Superdeformed and hyperdeformed states in $z = 122$ isotopes. *Physical Review C*, 80(3):034312, 2009.
- [132] O. Nagib. α -decay half-lives of superheavy nuclei with $z = 122$ – 125 . *Physical Review C*, 101(1):014610, 2020.
- [133] T. A. Siddiqui, A. Quddus, S. Ahmad, and S. K. Patra. A search for neutron magicity in the isotopic series of $z = 122, 128$ superheavy nuclei. *Journal of Physics G: Nuclear and Particle Physics*, 47(11):115103, 2020.
- [134] G. Naveya, S. Santhosh Kumar, S. I. A. Philominraj, and A. Stephen. Alpha-decay chains of $z = 122$ superheavy nuclei using cubic plus proximity potential with improved transfer matrix method. *Indian Journal of Pure and Applied Physics*, 58:397–403, 2020.
- [135] T. A. Siddiqui, S. Ahmad, and K. Afaque. Structural properties of superheavy isotopes $z = 122$ with cdf approach. In *Proceedings of the DAE-BRNS symposium on nuclear physics*. V. 62, 2017.
- [136] N. Ghahramany and A. Ansari. Synthesis and decay process of superheavy nuclei with $z = 119$ – 122 via hot-fusion reactions. *The European Physical Journal A*, 52(9):1–12, 2016.
- [137] H. C. Manjunatha, K. N. Sridhar, and N. Sowmya. Investigations on $ni64 + zana \rightarrow z = 104$ – 123 (shn) $a = 250$ – 310 reactions. *Nuclear Physics A*, 987:382–395, 2019.

- [138] S. Chopra, R. K. Gupta, et al. Synthesis of the $z=122$ superheavy nucleus via fe 58- and ni 64-induced reactions using the dynamical cluster-decay model. *Physical Review C*, 95(4):044603, 2017.
- [139] A. Deep, R. Kharab, R. Singh, S. Chopra, et al. Examining the entrance channel effects on the synthesis of the double deformed nucleus hs 270: A theoretical study using the dynamical cluster-decay model including skyrme forces. *Physical Review C*, 102(3):034607, 2020.
- [140] M. Panigrahi, R. N. Panda, M. Bhuyan, and S. K. Patra. Exploring the α -decay chain of 302122 within relativistic mean-field formalism. *Canadian Journal of Physics*, 99(999):1–8, 2021.
- [141] A. S. Zubov, G. G. Adamian, and N. V. Antonenko. Application of statistical methods for analysis of heavy-ion reactions in the framework of a dinuclear system model. *Physics of Particles and Nuclei*, 40(6):847–889, 2009.
- [142] G. Giardina, G. Fazio, G. Mandaglio, M. Manganaro, A. K. Nasirov, M. V. Romaniuk, and C. Sacca. Expectations and limits to synthesize nuclei with $z \geq 120$. *International Journal of Modern Physics E*, 19(05n06):882–893, 2010.
- [143] L. Zhu, J. Su, C. Y. Huang, and F. S. Zhang. Effects of entrance channel on fusion probability in hot fusion reactions. *Chinese Physics C*, 40(12):124105, 2016.
- [144] H. C. Manjunatha, N. Sowmya, N. Manjunath, and L. Seenappa. Investigations on the superheavy nuclei with magic number of neutrons and protons. *International Journal of Modern Physics E*, 29(5):2050028–673, 2020.
- [145] A. M. Nagaraja, H. C. Manjunatha, N. Sowmya, N. Manjunath, and S. A. Raj. Cluster

- radioactivity of superheavy nuclei 290–310 120 using different proximity functions. *The European Physical Journal Plus*, 135(10):1–16, 2020.
- [146] D. N. Poenaru, R. A. Gherghescu, and W. Greiner. Nuclear inertia and the decay modes of superheavy nuclei. *Journal of Physics G: Nuclear and Particle Physics*, 40(10):105105, 2013.
- [147] G. Royer and B. Remaud. Fission processes through compact and creviced shapes. *Journal of Physics G: Nuclear Physics*, 10(8):1057, 1984.
- [148] H. C. Manjunatha, G. R. Sridhar, N. Sowmya, P. S. Gupta, and H. B. Ramalingam. A systematic study of alpha decay in actinide nuclei using modified generalized liquid drop model. *International Journal of Modern Physics E*, 30(2):2150013–201, 2021.
- [149] M. Goncalves and S. B. Duarte. Effective liquid drop description for the exotic decay of nuclei. *Physical Review C*, 48(5):2409, 1993.
- [150] M. Gonçalves, S. B. Duarte, F. Garcia, and O. Rodriguez. Prescold: Calculation of the half-life for alpha decay, cluster radioactivity and cold fission processes. *Computer physics communications*, 107(1-3):246–252, 1997.
- [151] O. A. P. Tavares, S. B. Duarte, O. Rodríguez, F. Guzmán, M. Gonçalves, and F. García. Effective liquid drop description for alpha decay of atomic nuclei. *Journal of Physics G: Nuclear and Particle Physics*, 24(9):1757, 1998.
- [152] J. P. Cui, Y. L. Zhang, S. Zhang, Y. Z. Wang, et al. α -decay half-lives of superheavy nuclei. *Physical Review C*, 97(1):014316, 2018.
- [153] S. B. Duarte, O. A. P. Tavares, F. Guzman, A. Dimarco, F. Garcia, O. Rodriguez, and M. Goncalves. Half-lives for proton emission, alpha decay, cluster radioactivity, and cold

- fission processes calculated in a unified theoretical framework. Technical report, Centro Brasileiro de Pesquisas Fisicas (CBPF), 2002.
- [154] Z. Y. Wang, Z. M. Niu, Q. Liu, and J. Y. Guo. Systematic calculations of α -decay half-lives with an improved empirical formula. *Journal of Physics G: Nuclear and Particle Physics*, 42(5):055112, 2015.
- [155] S. Zong-Qiang, S. Liang-Ping, F. Guang-Wei, M. Ying, and Q. Jian-Fa. Investigation of proton radioactivity with the effective liquid drop model. *Chinese Physics C*, 39(2):024102, 2015.
- [156] J. Blocki and W. J. Swiatecki. A generalization of the proximity force theorem. *Annals of Physics*, 132(1):53–65, 1981.
- [157] Y. J. Shi and W. J. Swiatecki. Estimates of the influence of nuclear deformations and shell effects on the lifetimes of exotic radioactivities. *Nuclear Physics A*, 464(2):205–222, 1987.
- [158] H. C. Manjunatha and N. Sowmya. Pocket formula for mass excess of nuclei in the range $57 \leq Z \leq 103$. *Modern Physics Letters A*, 34(15):1950112, 2019.
- [159] G. R. Sridhara, H. C. Manjunatha, K. N. Sridhar, and H. B. Ramalingam. Systematic study of the α decay properties of actinides. *Pramana*, 93(5):1–14, 2019.
- [160] M. G. Srinivas, H. C. Manjunatha, K. N. Sridhar, N. Sowmya, and A. C. Raj. Proton decay of actinide nuclei. *Nuclear Physics A*, 995:121689, 2020.
- [161] N. Sowmya, H. C. Manjunatha, N. Dhananjaya, and A. M. Nagaraja. Competition between binary fission, ternary fission, cluster radioactivity and alpha decay of ^{281}ds . *Journal of Radioanalytical and Nuclear Chemistry*, 323(3):1347–1351, 2020.

- [162] H. C. Manjunatha, G. R. Sridhar, P. S. Damodara Gupta, H. B. Ramalingam, and V. H. Doddamani. Pocket formula for alpha decay energies and half-lives of actinide nuclei. *Zeitschrift für Naturforschung A*, 75(6), 2020.
- [163] M. G. Srinivas, H. C. Manjunatha, N. Sowmya, P. S. Damodara Gupta, and A. C. Raj. Systematics of proton decay of actinides. *Indian journal of Pure and Applied Physics*, 58, 2020.
- [164] H. C. Manjunatha, G. R. Sridhar, P. S. Gupta, K. N. Sridhar, M. G. Srinivas, and H. B. Ramalingam. Decay modes of uranium in the range $203 < a < 299$. *Indian journal of Pure and Applied Physics*, 58, 2020.
- [165] H. C. Manjunatha and K. N. Sridhar. Radioactive decay of rutherfordium. *Iranian Journal of Science and Technology, Transactions A: Science*, 44(4), 2020.
- [166] H. C. Manjunatha, M. G. Srinivas, N. Sowmya, P. S. Damodara Gupta, and A. C. Raj. Proton radioactivity of heavy nuclei of atomic number range $72 < z < 88$. *Physics of Particles and Nuclei Letters*, 17(7):909–915, 2020.
- [167] K. Sharma, G. Sawhney, and M. K. Sharma. Spontaneous fission and competing ground state decay modes of actinide and transactinide nuclei. *Phys. Rev. C*, 96:054307, Nov 2017.
- [168] N. Sharma, A. Kaur, and M. K. Sharma. Analysis of various competing binary and ternary decay processes of the ^{253}Es nucleus. *Phys. Rev. C*, 102:064603, Dec 2020.
- [169] Y. T. Oganessian and V. K. Utyonkov. Super-heavy element research. *Reports on Progress in Physics*, 78(3):036301, 2015.
- [170] N. Ghahramany and E. Yazdankish. Determination of deuteron dipole moment in nuclear quark-like model. *Communications in Theoretical Physics*, 59(5):579, 2013.

- [171] Y. T. Oganessian, A. G. Demin, A. S. Iljinov, S. P. Tretyakova, A. A. Pleve, Y. E. Penionzhkevich, M. P. Ivanov, and Y. P. Tretyakov. Experiments on the synthesis of neutron-deficient kurchatovium isotopes in reactions induced by ^{50}Ti ions. *Nuclear Physics A*, 239(1):157–171, 1975.
- [172] G. Münzenberg, S. Hofmann, H. Folger, F. P. Hessberger, J. Keller, K. Poppensieker, B. Quint, W. Reisdorf, K. H. Schmidt, H. J. Schött, et al. The isotopes $^{259}106$, $^{260}106$, and $^{261}106$. *Zeitschrift für Physik A Atoms and Nuclei*, 322(2):227–235, 1985.
- [173] C. M. Folden III, S. L. Nelson, C. E. Düllmann, J. M. Schwantes, R. Sudowe, P. M. Zielinski, K. E. Gregorich, H. Nitsche, and D. C. Hoffman. Excitation function for the production of $^{262}107$ ($z=107$) in the odd- z -projectile reaction $^{208}\text{Pb}(^{55}\text{Mn}, n)$. *Physical Review C*, 73(1):014611, 2006.
- [174] S. Hofmann, F. P. Heßberger, V. Ninov, et al. Excitation function for the production of $^{265}108$ and $^{266}109$. *Zeitschrift für Physik A Hadrons and Nuclei*, 358(4):377–378, 1997.
- [175] S. Hofmann, V. Ninov, F. P. Heßberger, P. Armbruster, H. Folger, G. Münzenberg, H. J. Schött, A. G. Popeko, A. V. Yeremin, A. N. Andreyev, et al. Production and decay of $^{269}110$. *Zeitschrift für Physik A Hadrons and Nuclei*, 350(4):277–280, 1995.
- [176] S. Hofmann, F. P. Heßberger, D. Ackermann, et al. New results on elements 111 and 112. *The European Physical Journal A-Hadrons and Nuclei*, 14(2):147–157, 2002.
- [177] K. Morita, K. Morimoto, D. Kaji, T. Akiyama, S. Goto, H. Haba, E. Ideguchi, R. Kanungo, K. Katori, H. Koura, et al. Experiment on the synthesis of element 113 in the reaction $^{209}\text{Bi}(^{70}\text{Zn}, n)$ $^{278}113$. *Journal of the physical Society of Japan*, 73(10):2593–2596, 2004.
- [178] Y. T. Oganessian, V. K. Utyonkov, Y. V. Lobanov, F. S. Abdullin, A. N. Polyakov, I. V. Shi-

- rokovsky, Y. S. Tsyganov, G. G. Gulbekian, S. L. Bogomolov, B. N. Gikal, et al. Publisher's note: Measurements of cross sections and decay properties of the isotopes of elements 112, 114, and 116 produced in the fusion reactions u 233, 238, pu 242, and cm 248+ ca 48 [phys. rev. c 70, 064609 (2004)]. *Physical Review C*, 71(2):029902, 2005.
- [179] Y. T. Oganessian, V. K. Utyonkov, Y. V. Lobanov, et al. Synthesis of superheavy nuclei in the $^{48}\text{Ca}+^{244}\text{Pu}$ reaction: $^{288}114$. *Phys. Rev. C*, 62:041604, Sep 2000.
- [180] Y. T. Oganessian, V. K. Utyonkoy, Y. V. Lobanov, et al. Experiments on the synthesis of element 115 in the reaction $^{243}\text{Am}(^{48}\text{Ca}, xn)^{291-x}115$. *Phys. Rev. C*, 69:021601, Feb 2004.
- [181] D. N. Poenaru, R. A. Gherghescu, and W. Greiner. Heavy-particle radioactivity. In *Journal of Physics: Conference Series*, volume 436, page 012056. IOP Publishing, 2013.
- [182] B. Buck, A. C. Merchant, and S. M. Perez. Recent developments in the theory of alpha decay. *Modern Physics Letters A*, 6(27):2453–2461, 1991.
- [183] D. Ni and Z. Ren. New approach for α -decay calculations of deformed nuclei. *Physical Review C*, 81(6):064318, 2010.
- [184] P. R. Chowdhury, C. Samanta, and D. N. Basu. Search for long lived heaviest nuclei beyond the valley of stability. *Physical Review C*, 77(4):044603, 2008.
- [185] C. Samanta, P. R. Chowdhury, and D. N. Basu. Predictions of alpha decay half lives of heavy and superheavy elements. *Nuclear Physics A*, 789(1-4):142–154, 2007.
- [186] Y. Z. Wang, J. M. Dong, B. B. Peng, and H. F. Zhang. Fine structure of α decay to rotational states of heavy nuclei. *Physical Review C*, 81(6):067301, 2010.
- [187] V. Y. Denisov and H. Ikezoe. α -nucleus potential for α -decay and sub-barrier fusion. *Phys. Rev. C*, 72:064613, Dec 2005.

- [188] D. Ni and Z. Ren. Binding energies, α -decay energies, and α -decay half-lives for heavy and superheavy nuclei. *Nuclear Physics A*, 893:13–26, 2012.
- [189] V. Y. Denisov and A. A. Khudenko. α -decay half-lives: Empirical relations. *Phys. Rev. C*, 79:054614, May 2009.
- [190] J. Engel, M. Bender, J. Dobaczewski, W. Nazarewicz, and R. Surman. β decay rates of r-process waiting-point nuclei in a self-consistent approach. *Physical Review C*, 60(1):014302, 1999.
- [191] P. Möller, J. R. Nix, W. D. Wyers, and W. J. Swiatecki. At. data and nucl. data tables 59, 185 (1995); p. möller, jr nix, and k. L. Kratz, *At. Data and Nucl. Data Tables*, 66:131, 1997.
- [192] P. Möller, B. Pfeiffer, and K. L. Kratz. New calculations of gross β -decay properties for astrophysical applications: Speeding-up the classical r process. *Physical Review C*, 67(5):055802, 2003.
- [193] I N Borzov, Stéphane Goriely, and J M Pearson. Microscopic calculations of β -decay characteristics near the $a=130$ r-process peak. *Nuclear Physics A*, 621(1-2):307–310, 1997.
- [194] J. A. Wheeler N. Bohr. *Phys. Rev.*, 56:426, 1936.
- [195] W. J. Swiatecki. Systematics of spontaneous fission half-lives. *Physical Review*, 100(3):937, 1955.
- [196] V. M. Strutinsky. Shell effects in nuclear masses and deformation energies. *Nuclear Physics A*, 95(2):420–442, 1967.
- [197] P. Möller, D. G. Madland, A. J. Sierk, and A. Iwamoto. Nuclear fission modes and fragment mass asymmetries in a five-dimensional deformation space. *Nature*, 409(6822):785–790, 2001.

- [198] A. Sobiczewski and K. Pomorski. Description of structure and properties of superheavy nuclei. *Progress in Particle and Nuclear Physics*, 58(1):292–349, 2007.
- [199] K. P. Santhosh and T. A. Jose. Alpha and cluster decay using modified generalized liquid drop model with iso-spin dependent pre-formation factor. *Nuclear Physics A*, 992:121626, 2019.
- [200] W. Greiner, M. Ivascu, D. N. Poenaru, and A. Sandulescu. On exotic nuclear decay of ^{223}Ra by emission of ^{14}C nuclei. *Zeitschrift für Physik A Atoms and Nuclei*, 320(2):347–348, 1985.
- [201] Y. J. Shi and W. J. Swiatecki. Theoretical estimates of the rates of radioactive decay of radium isotopes by ^{14}C emission. *Physical review letters*, 54(4):300, 1985.
- [202] B. Buck and A. C. Merchant. A consistent cluster model treatment of exotic decays and alpha decays from heavy nuclei. *Journal of Physics G: Nuclear and Particle Physics*, 15(5):615, 1989.
- [203] S. Kumar and R. K. Gupta. Neck formation and deformation effects in a preformed cluster model of exotic cluster decays. *Physical Review C*, 55(1):218, 1997.
- [204] D. N. Poenaru, Y. Nagame, R. A. Gherghescu, and W. Greiner. Erratum: Systematics of cluster decay modes [phys. rev. c 65, 054308 (2002)]. *Physical Review C*, 66(4):049902, 2002.
- [205] D. N. Poenaru, Y. Nagame, R. A. Gherghescu, and W. Greiner. Systematics of cluster decay modes. *Physical Review C*, 65(5):054308, 2002.
- [206] M. A. Hooshyar, I. Reichstein, and F. B. Malik. *Nuclear Fission and Cluster Radioactivity: An Energy-Density Functional Approach*. Springer Science and Business Media, 2005.

- [207] N. Sowmya and H. C. Manjunatha. Competition between different decay modes of super-heavy element $Z = 116$ and synthesis of possible isotopes. *Brazilian Journal of Physics*, 49(6):874–886, 2019.
- [208] J. K. Pansaers. Iii. table des comptes-rendus. *Revue Philosophique de Louvain*, 20(80):24–67, 1913.
- [209] H. Geiger and J. M. Nuttall. Lvii. the ranges of the α particles from various radioactive substances and a relation between range and period of transformation. *The London, Edinburgh, and Dublin Philosophical Magazine and Journal of Science*, 22(130):613–621, 1911.
- [210] G. Gamow. Zur quantentheorie des atomkernes. *Zeitschrift für Physik*, 51(3):204–212, 1928.
- [211] V. E. Viola Jr and G. T. Seaborg. Nuclear systematics of the heavy elements—ii lifetimes for alpha, beta and spontaneous fission decay. *Journal of Inorganic and Nuclear Chemistry*, 28(3):741–761, 1966.
- [212] G. Royer. Alpha emission and spontaneous fission through quasi-molecular shapes. *Journal of Physics G: Nuclear and Particle Physics*, 26(8):1149, 2000.
- [213] B. A. Brown. Simple relation for alpha decay half-lives. *Physical Review C*, 46(2):811, 1992.
- [214] Mihai Horoi. Scaling behaviour in cluster decay. *Journal of Physics G: Nuclear and Particle Physics*, 30(7):945, 2004.
- [215] D. N. Poenaru, I. H. Plonski, and W. Greiner. α -decay half-lives of superheavy nuclei. *Physical Review C*, 74(1):014312, 2006.

- [216] D. N. Poenaru, R. A. Gherghescu, and W Greiner. Single universal curve for cluster radioactivities and α decay. *Physical Review C*, 83(1):014601, 2011.
- [217] D. Ni, Z. Ren, T. Dong, and C. Xu. Unified formula of half-lives for α decay and cluster radioactivity. *Physical Review C*, 78(4):044310, 2008.
- [218] A. I. Budaca, R. Budaca, and I. Silisteanu. Extended systematics of alpha decay half lives for exotic superheavy nuclei. *Nuclear Physics A*, 951:60–74, 2016.
- [219] M. Mirea, R. Budaca, and A. Sandulescu. Spontaneous fission, cluster emission and alpha decay of ^{222}Ra in a unified description. *Annals of Physics*, 380:154–167, 2017.
- [220] A. Sobiczewski, Z. Patyk, and S. Ćwiok. Deformed superheavy nuclei. *Physics letters B*, 224(1-2):1–4, 1989.
- [221] D. T. Akrawy, H. Hassanabadi, S. S. Hosseini, and K. P. Santhosh. Systematic study of α -decay half-lives using royer and related formula. *Nuclear Physics A*, 971:130–137, 2018.
- [222] G. Royer. Analytic expressions for alpha-decay half-lives and potential barriers. *Nuclear Physics A*, 848(3-4):279–291, 2010.
- [223] B. Sahu, R. Paira, and B. Rath. General decay law for emission of charged particles and exotic cluster radioactivity. *Nuclear Physics A*, 908:40–50, 2013.
- [224] H. C. Manjunatha and K. N. Sridhar. New semi-empirical formula for α -decay half-lives of the heavy and superheavy nuclei. *The European Physical Journal A*, 53(7):1–9, 2017.
- [225] D. T. Akrawy and D. N. Poenaru. Alpha decay calculations with a new formula. *Journal of Physics G: Nuclear and Particle Physics*, 44(10):105105, 2017.

- [226] J. Dong, H. Zhang, Y. Wang, W. Zuo, and J. Li. Alpha-decay for heavy nuclei in the ground and isomeric states. *Nuclear Physics A*, 832(3-4):198–208, 2010.
- [227] C. Xu and Z. Ren. Global calculation of α -decay half-lives with a deformed density-dependent cluster model. *Physical Review C*, 74(1):014304, 2006.
- [228] S. A. Gurvitz and G. Kalbermann. Decay width and the shift of a quasistationary state. *Physical review letters*, 59(3):262, 1987.
- [229] X. D. Sun, P. Guo, and X. H. Li. Systematic study of α decay half-lives for even-even nuclei within a two-potential approach. *Physical Review C*, 93(3):034316, 2016.
- [230] D. N. Poenaru, I. H. Plonski, R. A. Gherghescu, and W. Greiner. Valleys due to pb and sn on the potential energy surface of superheavy and lighter α -emitting nuclei. *Journal of Physics G: Nuclear and Particle Physics*, 32(9):1223, 2006.
- [231] H. C. Manjunatha, K. N. Sridhar, N. Nagaraja, and N. Sowmya. Pocket formula for fusion barriers of superheavy nuclei. *The European Physical Journal Plus*, 133(6):1–9, 2018.
- [232] H. C. Manjunatha and N. Sowmya. Parametrisation of the experimental fusion–fission cross-sections. *Pramana*, 90(5):1–16, 2018.
- [233] C. F. von Weizsäcker. Zur theorie der kernmassen. *Zeitschrift für Physik*, 96(7):431–458, 1935.
- [234] H. A. Bethe and R. F. Bacher. Nuclear physics a. stationary states of nuclei. *Reviews of Modern Physics*, 8(2):82, 1936.
- [235] P. Möller and J. R. Nix. Atomic masses and nuclear ground-state deformations calculated with a new macroscopic-microscopic model. *Atomic Data and Nuclear Data Tables*, 26(2):165–196, 1981.

- [236] G. Audi, A. H. Wapstra, and C. Thibault. The ame2003 atomic mass evaluation:(ii). tables, graphs and references. *Nuclear physics A*, 729(1):337–676, 2003.
- [237] Stéphane Goriely, M. Samyn, and J. M. Pearson. Further explorations of skyrme-hartree-fock-bogoliubov mass formulas. vii. simultaneous fits to masses and fission barriers. *Physical Review C*, 75(6):064312, 2007.
- [238] H. C. Manjunatha, B. M. Chandrika, and L. Seenappa. Empirical formula for mass excess of heavy and superheavy nuclei. *Modern Physics Letters A*, 31(28):1650162, 2016.
- [239] H. C. Manjunatha, N. Sowmya, and A. M. Nagaraja. Semi-empirical formula for alpha and cluster decay half-lives of superheavy nuclei. *Modern Physics Letters A*, 35(06):2050016, 2020.
- [240] G. Royer and H. F. Zhang. Recent α decay half-lives and analytic expression predictions including superheavy nuclei. *Physical Review C*, 77(3):037602, 2008.
- [241] H. F. Zhang and G. Royer. Theoretical and experimental α decay half-lives of the heaviest odd-z elements and general predictions. *Physical Review C*, 76(4):047304, 2007.
- [242] S. Della Negra, H. Gauvin, D. Jacquet, and Y. Le Beyec. Q_β measurements and mass excess values for neutron deficient isotopes near $z = 40$. *Zeitschrift für Physik A Atoms and Nuclei*, 307(4):305–321, 1982.
- [243] V. Borrel, J. C. Jacmart, F. Pougheon, R. Anne, C. Detraz, D. Guillemaud-Mueller, A. C. Mueller, D. Bazin, R. Del Moral, J. P. Dufour, et al. 31ar and 27s: Beta-delayed two-proton emission and mass excess. *Nuclear Physics A*, 531(2):353–369, 1991.
- [244] W. A. Mayer, W. Henning, R. Holzwarth, H. J. Körner, G. Korschinek, G. Rosner, and H. J.

- Scheerer. Mass excess and excited states of neutron-rich silicon, phosphorus and sulphur isotopes. *Zeitschrift für Physik A Atoms and Nuclei*, 319(3):287–293, 1984.
- [245] H. J. Scheerer, D. Pereira, A. Chalupka, R. Gyufko, and C. A. Wiedner. Mass excess of ^{145}Eu . *Zeitschrift für Physik A Atoms and Nuclei*, 308(2):183–184, 1982.
- [246] M. Brauner, D. Rychel, R. Gyufko, C. A. Wiedner, and S. T. Thornton. Mass excess of ^{51}Ca . *Phys. Lett., B;(Netherlands)*, 150, 1985.
- [247] C. Miehé, P. Dessagne, P. Baumann, A. Huck, G. Klotz, A. Knipper, G. Walter, and G. Marguier. Experimental mass excess of ^{40}Cl and ^{42}Cl . *Physical Review C*, 39(3):992, 1989.
- [248] H. C. Manjunatha, N. Sowmya, K. N. Sridhar, and L. Seenappa. A study of probable alpha-ternary fission fragments of ^{257}Fm . *Journal of Radioanalytical and Nuclear Chemistry*, 314(2):991–999, 2017.
- [249] N. Sowmya and H. C. Manjunatha. A study of binary fission and ternary fission. *Bulg. J. Phys*, 46:16–27, 2019.
- [250] H. C. Manjunatha, N. Sowmya, N. Manjunatha, P. S. Damodara Gupta, L. Seenappa, K. N. Sridhar, T. Ganesh, and T. Nandi. Entrance channel dependent hot fusion reactions for superheavy element synthesis. *Physical Review C*, 102(6):064605, 2020.
- [251] P. Moller and J. R. Nix. Stability of heavy and superheavy elements. *Journal of Physics G: Nuclear and Particle Physics*, 20(11):1681, 1994.
- [252] Y. T. Oganessian, V. K. Utyonkov, Y. V. Lobanov, F. S. Abdullin, A. N. Polyakov, R. N. Sagaidak, I. V. Shirokovsky, Y. S. Tsyganov, A. A. Voinov, G. G. Gulbekian, et al. Synthesis of the isotopes of elements 118 and 116 in the ^{249}Cf and $^{245}\text{Cm} + ^{48}\text{Ca}$ fusion reactions. *Physical Review C*, 74(4):044602, 2006.

- [253] M. Brack, J. Damgaard, A. S. Jensen, H. C. Pauli, V. M. Strutinsky, and C. Y. Wong. Funny hills: The shell-correction approach to nuclear shell effects and its applications to the fission process. *Reviews of Modern Physics*, 44(2):320, 1972.
- [254] I. Perlman and J. O. Rasmussen. Handbuch der physik. *Springer-Verlag*, 42:145, 1957.
- [255] R. Rengaiyan, A. V. Babu, and S. S. Kumar. Level density and structural changes in the neutron deficient doubly magic nucleus 100 sn. In *Proceedings of the DAE Symp. on Nucl. Phys*, volume 58, page 362, 2013.
- [256] T. Dong, Z. Ren, et al. Improved version of a binding energy formula for heavy and super-heavy nuclei with $z \geq 90$ and $n \geq 140$. *Physical Review C*, 77(6):064310, 2008.
- [257] J. Dong, W. Zuo, and W. Scheid. Correlation between α -decay energies of superheavy nuclei involving the effects of symmetry energy. *Physical Review Letters*, 107(1):012501, 2011.
- [258] W. D. Myers and WJ Świątecki. Nucleus-nucleus proximity potential and superheavy nuclei. *Physical Review C*, 62(4):044610, 2000.
- [259] M. Ismail, A. Y. Ellithi, M. M. Botros, and A. Adel. Systematics of α -decay half-lives around shell closures. *Physical Review C*, 81(2):024602, 2010.
- [260] P. Möller, A. J. Sierk, T. Ichikawa, and H. Sagawa. Nuclear ground-state masses and deformations: Frdm (2012). *Atomic Data and Nuclear Data Tables*, 109:1–204, 2016.
- [261] H. Zhang, W. Zuo, J. Li, and G. Royer. α decay half-lives of new superheavy nuclei within a generalized liquid drop model. *Physical Review C*, 74(1):017304, 2006.
- [262] S. B. Duarte, O. A. P. Tavares, M. Gonçalves, O. Rodríguez, F. Guzmán, T. N. Barbosa,

- F. García, and A. Dimarco. Half-life predictions for decay modes of superheavy nuclei. *Journal of Physics G: Nuclear and Particle Physics*, 30(10):1487, 2004.
- [263] P. Moller and J. R. Nix. Stability of heavy and superheavy elements. *Journal of Physics G: Nuclear and Particle Physics*, 20(11):1681–1747, nov 1994.
- [264] Reference input parameter library (ripl-3). <https://www-nds.iaea.org/RIPL-3.html>.
- [265] H. Koura, T. Tachibana, M. Uno, and M. Yamada. Nuclidic mass formula on a spherical basis with an improved even-odd term. *Progress of theoretical physics*, 113(2):305–325, 2005.
- [266] M. Kowal, P. Jachimowicz, and J. Skalski. Ground state and saddle point: masses and deformations for even-even superheavy nuclei with $98 \leq Z \leq 126$ and $134 \leq N \leq 192$. *arXiv preprint arXiv:1203.5013*, 2012.
- [267] R. Taageper and M. Nurmia. On the relations between half-life and energy release in alpha decay. *Ann. Acad. Sci. Fennicae, Ser. A*, 6, 1961.
- [268] Y. T. Oganessian, V. K. Utyonkov, Y. V. Lobanov, F. S. Abdullin, A. N. Polyakov, I. V. Shirokovsky, Y. S. Tsyganov, G. G. Gulbekian, S. L. Bogomolov, B. N. Gikal, et al. Measurements of cross sections for the fusion-evaporation reactions $^{244}\text{Pu}(\text{ca } 48, x n) 292\text{-}x 114$ and $^{245}\text{Cm}(\text{ca } 48, x n) 293\text{-}x 116$. *Physical Review C*, 69(5):054607, 2004.
- [269] Y. T. Oganessian, V. K. Utyonkov, Y. V. Lobanov, F. S. Abdullin, A. N. Polyakov, I. V. Shirokovsky, Y. S. Tsyganov, G. G. Gulbekian, S. L. Bogomolov, B. N. Gikal, et al. Observation of the decay of $^{292}116$. *Physical Review C*, 63(1):011301, 2000.

- [270] Y. T. Oganessian, F. S. Abdullin, P. D. Bailey, D. E. Benker, M. E. Bennett, S. N. Dmitriev, J. G. Ezold, J. H. Hamilton, R. A. Henderson, M. G. Itkis, et al. Eleven new heaviest isotopes of elements $z=105$ to $z=117$ identified among the products of $bk\ 249+ca\ 48$ reactions. *Physical Review C*, 83(5):054315, 2011.
- [271] H. Zhang, J. Li, W. Zuo, Z. Ma, B. Chen, and S. Im. Properties of the superheavy element $287\ 115$ and its α -decay time. *Physical Review C*, 71(5):054312, 2005.
- [272] P. Mohr. α -decay properties of $118\ 296$ from double-folding potentials. *Physical Review C*, 95(1):011302, 2017.
- [273] A. Sobiczewski. Theoretical predictions for the nucleus $118\ 296$. *Physical Review C*, 94(5):051302, 2016.
- [274] X. J. Bao, S. Q. Guo, H. F. Zhang, J. Q. Li, et al. Theoretical predictions for the decay chain of the nuclei $og\ 293, 295-297$. *Physical Review C*, 95(3):034323, 2017.
- [275] J. G. Deng, J. C. Zhao, J. L. Chen, X. J. Wu, and X. H. Li. α decay properties of $296og$ within the two-potential approach. *Chinese Physics C*, 42(4):044102, 2018.
- [276] J. G. Deng, J. H. Cheng, B. Zheng, and X. H. Li. α decay properties of $297og$ within the two-potential approach. *Chinese Physics C*, 41(12):124109, 2017.
- [277] A. Sandulescu, D. N. Poenaru, and W. Greiner. New type of decay of heavy nuclei intermediate between fission and α decay. *Sov. J. Particles Nucl. (Engl. Transl.); (United States)*, 11(6), 11 1980.
- [278] R.G. Lovas, R.J. Liotta, A. Insolia, K. Varga, and D.S. Delion. Microscopic theory of cluster radioactivity. *Physics Reports*, 294(5):265–362, 1998.

- [279] D. N. Poenaru and W. Greiner. Cluster radioactivity. In *Clusters in Nuclei*, pages 1–56. Springer, 2010.
- [280] K. P. Santhosh, R. K. Biju, and A. Joseph. A semi-empirical model for alpha and cluster radioactivity. *Journal of Physics G: Nuclear and Particle Physics*, 35(8):085102, 2008.
- [281] Z. Ren, C. Xu, and Z. Wang. New perspective on complex cluster radioactivity of heavy nuclei. *Phys. Rev. C*, 70:034304, Sep 2004.
- [282] R. Zhong-Zhou and X. Chang. Density-dependent cluster model study of α -decay and cluster radioactivity of nuclei. *Nuclear Physics Review*, 22(4):344–350, 2005.
- [283] Z. Matheson, S. A. Giuliani, W. Nazarewicz, J. Sadhukhan, and N. Schunck. Cluster radioactivity of ^{294}og . *arXiv preprint arXiv:1812.06490*, 2018.
- [284] B. Singh, M. Bhuyan, S. K. Patra, and R. K. Gupta. Optical potential obtained from relativistic-mean-field theory-based microscopic nucleon–nucleon interaction: applied to cluster radioactive decays. *Journal of Physics G: Nuclear and Particle Physics*, 39(2):025101, 2012.
- [285] I. Silisteanu and W. Scheid. Half-lives of cluster radioactivity within a model including superfluid phenomena and resonance effects. *Physical Review C*, 51(4):2023, 1995.
- [286] D. Ni and Z. Ren. Half-lives and cluster preformation factors for various cluster emissions in trans-lead nuclei. *Physical Review C*, 82(2):024311, 2010.
- [287] D. Deng, Z. Ren, D. Ni, and Y. Qian. Realistic α preformation factors of odd-a and odd-odd nuclei within the cluster-formation model. *Journal of Physics G: Nuclear and Particle Physics*, 42(7):075106, 2015.

- [288] D. N. Poenaru and W. Greiner. Extension of superasymmetric fission theory from cluster decay to nanophysics. *Nuclear Physics A*, 834(1-4):163c–166c, 2010.
- [289] W. M. Seif, A. R. Abdulghany, and Z. N. Hussein. Change in neutron skin thickness after cluster-decay. *Journal of Physics G: Nuclear and Particle Physics*, 48(2):025111, 2021.
- [290] Y. Gao, J. Cui, Y. Wang, and J. Gu. Cluster radioactivity of neutron-deficient nuclei in trans-tin region. *Scientific Reports*, 10(1):1–15, 2020.
- [291] M. Ismail, A. Y. Ellithi, M. M. Selim, N. Abou-Samra, and O. A. Mohamedien. Cluster decay half-lives and preformation probabilities. *Physica Scripta*, 95(7):075303, 2020.
- [292] A. M. Nagaraja, H. C. Manjunatha, N. Sowmya, L. Seenappa, P. S. Damodara Gupta, N. Manjunatha, and S. A. C. Raj. Heavy particle radioactivity of superheavy element $z=126$. *Nuclear Physics A*, 1015:122306, 2021.
- [293] A. M. Nagaraja, H. C. Manjunatha, N. Sowmya, N. Manjunath, and S. A. C. Raj. Cluster radioactivity of superheavy nuclei 290–310 120 using different proximity functions. *The European Physical Journal Plus*, 135(10):1–16, 2020.
- [294] A. M. Nagaraja, H. C. Manjunatha, N. Sowmya, P. S. Gupta, and S. Raj. Decay of dinuclear systems formed from dubnium. *Pramana*, 95(4):1–8, 2021.
- [295] H. C. Manjunatha, S. A. C. Raj, A. M. Nagaraja, and N. Sowmya. Cluster radioactivity in superheavy nuclei 299-306122. *Journal of Nuclear Physics, Material Sciences, Radiation and Applications*, 8(1):55–63, 2020.
- [296] H. C. Manjunatha and A. M. Nagaraja. Cluster radioactivity in superheavy nuclei $z=124$. In *Proceedings of the DAE Symp. on Nucl. Phys*, volume 64, page 170, 2019.

- [297] O. A. P. Tavares and E. L. Medeiros. A simple description of cluster radioactivity. *Physica Scripta*, 86(1):015201, 2012.
- [298] S. P. Tretyakova and V. L. Mikheev. Experimental investigation of the cluster radioactivity of atomic nuclei. *Il Nuovo Cimento A (1971-1996)*, 110(9-10):1043–1048, 1997.
- [299] S. M. S. Ahmed, R. Yahaya, S. Radiman, and M. S. Yasir. Alpha-cluster preformation factors in alpha decay for even–even heavy nuclei using the cluster-formation model. *Journal of Physics G: Nuclear and Particle Physics*, 40(6):065105, 2013.
- [300] O. N. Ghodsi and M. Hassanzad. α -decay properties of even-even superheavy nuclei. *Physical Review C*, 101(3):034606, 2020.
- [301] Z. Ren, C. Xu, and Z. Wang. New perspective on complex cluster radioactivity of heavy nuclei. *Physical Review C*, 70(3):034304, 2004.
- [302] R. K. Gupta, R. Kumar, N. K. Dhiman, M. Balasubramaniam, W. Scheid, and C. Beck. Cluster decay of hot $^{56}\text{Ni}^*$ formed in the $^{32}\text{S}+^{24}\text{Mg}$ reaction. *Phys. Rev. C*, 68:014610, Jul 2003.
- [303] D. N. Poenaru and R. A. Gherghescu. Cluster preformation at the nuclear surface in cold fission. *EPL (Europhysics Letters)*, 118(2):22001, 2017.
- [304] D. N. Poenaru and W. Greiner. Cluster radioactivities—past, present and future. *International Journal of Modern Physics E*, 17(10):2255–2263, 2008.
- [305] K. P. Santhosh and T. A. Jose. Half-lives of cluster radioactivity using the modified generalized liquid drop model with a new preformation factor. *Physical Review C*, 99(6):064604, 2019.

- [306] J. P. Cui, Y. H. Gao, Y. Z. Wang, J. Z. Gu, et al. Two-proton radioactivity within a generalized liquid drop model. *Physical Review C*, 101(1):014301, 2020.
- [307] D. N. Poenaru, R. A. Gherghescu, and W. Greiner. Cluster decay of superheavy nuclei. *Phys. Rev. C*, 85:034615, Mar 2012.
- [308] C. Qi, F. R. Xu, R. J. Liotta, and R. Wyss. Universal decay law in charged-particle emission and exotic cluster radioactivity. *Phys. Rev. Lett.*, 103:072501, Aug 2009.
- [309] Ishwar Dutt. The role of various parameters used in proximity potential in heavy-ion fusion reactions: New extension. *Pramana*, 76(6):921–931, 2011.
- [310] J. Blocki, J. Randrup, W. J. Świątecki, and C. F. Tsang. Proximity forces. *Annals of Physics*, 105(2):427–462, 1977.
- [311] G. L. Zhang, H. B. Zheng, and W. W. Qu. Study of the universal function of nuclear proximity potential between α and nuclei from density-dependent nucleon-nucleon interaction. *The European Physical Journal A*, 49(1):1–6, 2013.
- [312] V.Yu. Denisov. Interaction potential between heavy ions. *Physics Letters B*, 526(3):315–321, 2002.
- [313] P. Möller and J. R. Nix. Wd myers and wj swiatecki. *Atom. Data and Nucl. Data Tables*, 59:185, 1995.
- [314] H. KOURA et al. Calculated atomic masses and nuclear deformations (ktuy05). https://wwwndc.jaea.go.jp/nuclldata/mass/KTUY05_m246S12np.pdf.
- [315] N. Wang, M. Liu, X. Wu, and J. Meng. Surface diffuseness correction in global mass formula. *Physics Letters B*, 734:215–219, 2014.

- [316] N. Wang and M. Liu. Nuclear mass predictions with a radial basis function approach. *Physical Review C*, 84(5):051303, 2011.
- [317] M. Liu, N. Wang, Y. Deng, and X. Wu. Further improvements on a global nuclear mass model. *Physical Review C*, 84(1):014333, 2011.
- [318] N. Wang, Z. Liang, M. Liu, and X. Wu. Mirror nuclei constraint in nuclear mass formula. *Physical Review C*, 82(4):044304, 2010.
- [319] H. E. Suess. Magic numbers and the missing elements technetium and promethium. *Physical Review*, 81(6):1071, 1951.
- [320] L. Kowarski. Magic numbers and elements with no stable isotopes. *Physical Review*, 78(4):477, 1950.
- [321] P. A. Seeger. Semiempirical atomic mass law. *Nuclear Physics*, 25:1–IN1, 1961.
- [322] R. Bonetti, C. Chiesa, A. Guglielmetti, C. Migliorino, P. Monti, A. L. Pasinetti, and H. L. Ravn. Carbon radioactivity of ^{221}Fr and ^{221}Ra and the hindered decay of exotic odd-a emitters. *Nuclear Physics A*, 576(1):21–28, 1994.
- [323] P. B. Price, J. D. Stevenson, S. W. Barwick, and H. L. Ravn. Discovery of radioactive decay of ^{222}Ra and ^{224}Ra by ^{14}C emission. *Phys. Rev. Lett.*, 54:297–299, Jan 1985.
- [324] E. Hourani, L. Rosier, G. Berrier-Ronsin, A. Elayi, A. C. Mueller, G. Rappenecker, G. Rotbard, G. Renou, A. Liebe, L. Stab, et al. Fine structure in α emission from ^{223}Ra and ^{224}Ra . *Physical Review C*, 44(4):1424, 1991.
- [325] E. Hourani, M. Hussonnois, L. Stab, L. Brillard, S. Gales, and J. P. Schapira. Evidence for the radioactive decay of ^{226}Ra by α emission. *Physics Letters B*, 160(6):375–379, 1985.

- [326] R. Bonetti, C. Chiesa, A. Guglielmetti, R. Matheoud, C. Migliorino, A. L. Pasinetti, and H. L. Ravn. Nuclear structure effects in the exotic decay of ^{225}Ac via ^{14}C emission. *Nuclear Physics A*, 562(1):32–40, 1993.
- [327] R. Bonetti, C. Chiesa, A. Guglielmetti, C. Migliorino, A. Cesana, and M. Terrani. Discovery of oxygen radioactivity of atomic nuclei. *Nuclear Physics A*, 556(1):115–122, 1993.
- [328] M. Hussonnois, J.F Le Du, L. Brillard, J. Dalmasso, and G. Ardisson. Search for a fine structure in the ^{14}C decay of ^{222}Ra . *Physical Review C*, 43(6):2599, 1991.
- [329] S. W. Barwick, P. B. Price, and J. D. Stevenson. Radioactive decay of ^{232}U by ^{24}Ne emission. *Physical Review C*, 31(5):1984, 1985.
- [330] R. Bonetti, C. Chiesa, A. Guglielmetti, C. Migliorino, A. Cesana, M. Terrani, and P. B. Price. Neon radioactivity of uranium isotopes. *Physical review C*, 44(2):888, 1991.
- [331] K. J. Moody, E. K. Hulet, S. Wang, and P. B. Price. Heavy-fragment radioactivity of ^{234}U . *Physical Review C*, 39(6):2445, 1989.
- [332] SP Tretyakova, Yu S Zamyatnin, V. N. Kovantsev, Y. S. Korotkin, V. L. Mikheev, and G. A. Timofeev. Observation of nucleon clusters in the spontaneous decay of ^{234}U . *Zeitschrift für Physik A Atomic Nuclei*, 333(4):349–353, 1989.
- [333] S. Wang, D. Snowden-Ifft, P. B. Price, K. J. Moody, and E. K. Hulet. Heavy fragment radioactivity of ^{238}Pu : Si and mg emission. *Physical Review C*, 39(4):1647, 1989.
- [334] J. M. Dong, H. F. Zhang, J. Q. Li, and W. Scheid. Cluster preformation in heavy nuclei and radioactivity half-lives. *The European Physical Journal A*, 41(2):197–204, 2009.
- [335] A. Sandulescu and W. Greiner. Cluster decays. *Reports on Progress in Physics*, 55(9):1423, 1992.

- [336] M. Wang, W. J. Huang, F. G. Kondev, G. Audi, and S. Naimi. The ame 2020 atomic mass evaluation (ii). tables, graphs and references. *Chinese Physics C*, 45(3):030003, 2021.
- [337] C. Xu, Z. Ren, and Y. Guo. Competition between α decay and spontaneous fission for heavy and superheavy nuclei. *Phys. Rev. C*, 78:044329, Oct 2008.
- [338] A. T. Kruppa, M. Bender, W. Nazarewicz, P. G. Reinhard, T. Vertse, and S. wiok. Shell corrections of superheavy nuclei in self-consistent calculations. *Phys. Rev. C*, 61:034313, Feb 2000.
- [339] J. P. Cui, Y. L. Zhang, S. Zhang, and Y. Z. Wang. α -decay half-lives of superheavy nuclei. *Phys. Rev. C*, 97:014316, Jan 2018.
- [340] S. Hofmann and G. Munzenberg. The discovery of the heaviest elements. *Reviews of Modern Physics*, 72(3):733, 2000.
- [341] B. Buck, A. C. Merchant, and S. M. Perez. Ground state to ground state alpha decays of heavy even-even nuclei. *Journal of Physics G: Nuclear and Particle Physics*, 17(8):1223, 1991.
- [342] R. J. Charity. Systematic description of evaporation spectra for light and heavy compound nuclei. *Physical Review C*, 82(1):014610, 2010.
- [343] N. Ashok, D. M. Joseph, and A. Joseph. Cluster decay in osmium isotopes using hartree–fock–bogoliubov theory. *Modern Physics Letters A*, 31(07):1650045, 2016.
- [344] M. Brack, C. Guet, and H. B. Hakansson. Selfconsistent semiclassical description of average nuclear properties—a link between microscopic and macroscopic models. *Physics Reports*, 123(5):275–364, 1985.

- [345] M. Huang, Z. Chen, S. Kowalski, Y. G. Ma, R. Wada, T. Keutgen, K. Hagel, M. Barbui, A. Bonasera, C. Bottosso, et al. Isobaric yield ratios and the symmetry energy in heavy-ion reactions near the fermi energy. *Physical Review C*, 81(4):044620, 2010.
- [346] N. Sharma, A. Kaur, and M. K. Sharma. Analysis of various competing binary and ternary decay processes of the es 253 nucleus. *Physical Review C*, 102(6):064603, 2020.
- [347] J. R. Nix. Calculation of fission barriers for heavy and superheavy nuclei. *Annual Review of Nuclear Science*, 22(1):65–120, 1972.
- [348] H. C. Manjunatha, N. Sowmya, and P. S. Gupta. Competition between different decay modes in the isotopes of actinide nuclei. *Iranian Journal of Science and Technology, Transactions A: Science*, 45(6):2201–2217, 2021.
- [349] M. Bender, W. Nazarewicz, and P. G. Reinhard. Shell stabilization of super-and hyperheavy nuclei without magic gaps. *Physics Letters B*, 515(1-2):42–48, 2001.
- [350] C. Xu, Z. Ren, and Y. Guo. Competition between α decay and spontaneous fission for heavy and superheavy nuclei. *Physical Review C*, 78(4):044329, 2008.
- [351] H. C. Manjunatha, N. Sowmya, P. S. Damodara Gupta, K. N. Sridhar, A. M. Nagaraja, L. Seenappa, and S. Alfred Cecil Raj. Investigation of decay modes of superheavy nuclei. *Nuclear Science and Techniques*, 32(11):1–17, 2021.
- [352] I. V. Panov. Formation of superheavy elements in nature. *Physics of Atomic Nuclei*, 81(1):68–75, 2018.
- [353] V. I. Zagrebaev, A. V. Karpov, I. N. Mishustin, and W. Greiner. Formation of super-heavy elements in astrophysical nucleosynthesis. In *AIP Conference Proceedings*, volume 1491, pages 269–272. American Institute of Physics, 2012.

- [354] C. Sneden and J. J. Cowan. Genesis of the heaviest elements in the milky way galaxy. *Science*, 299(5603):70–75, 2003.
- [355] J. J. Cowan and F. K. Thielemann. R-process nucleosynthesis in supernovae. *Physics Today*, 57(10):47–54, 2004.
- [356] G. G. Adamian, N. V. Antonenko, and W. Scheid. High-spin isomers in some of the heaviest nuclei: Spectra, decays, and population. *Phys. Rev. C*, 81:024320, Feb 2010.
- [357] A. T. Kruppa, M. Bender, W. Nazarewicz, et al. Shell corrections of superheavy nuclei in self-consistent calculations. *Phys. Rev. C*, 61:034313, Feb 2000.
- [358] Y Shi, D. E. Ward, B. G. Carlsson, et al. Structure of superheavy nuclei along decay chains of element 115. *Phys. Rev. C*, 90:014308, Jul 2014.
- [359] X. Meng, B. Lu, and S. Zhou. Ground state properties and potential energy surfaces of ^{270}Hs from multidimensionally-constrained relativistic mean field model. *SCIENCE CHINA Physics, Mechanics and Astronomy*, 63(1):1–11, 2020.
- [360] R. R. Swain and B. B. Sahu. Structure and reaction dynamics of she $z= 130$. *Chinese Physics C*, 43(10):104103, 2019.
- [361] F. Niu, P. H. Chen, H. G. Cheng, and Z. Q. Feng. Multinucleon transfer dynamics in nearly symmetric nuclear reactions. *Nuclear Science and Techniques*, 31:1–8, 2020.
- [362] D. Boilley, B. Cauchois, H. Lü, A. Marchix, Y. Abe, and C. Shen. How accurately can we predict synthesis cross sections of superheavy elements? *Nuclear Science and Techniques*, 29(12):1–6, 2018.
- [363] D. Naderi and S. A. Alavi. Influence of the shell effects on evaporation residue cross section of superheavy nuclei. *Nuclear Science and Techniques*, 29(11):1–9, 2018.

- [364] X. Li, Z. Wu, and L. Guo. Entrance-channel dynamics in the reaction $^{40}\text{Ca} + ^{208}\text{Pb}$. *SCIENCE CHINA-PHYSICS MECHANICS and ASTRONOMY*, 62(12), 2019.
- [365] Y. T. Oganessian and K. P. Rykaczewski. A beachhead on the island of stability. *Physics Today*, 68(8), 2015.
- [366] A. Sobiczewski, F. A. Gareev, and B. N. Kalinkin. Closed shells for $Z > 82$ and $N > 126$ in a diffuse potential well. *Physics Letters*, 22(4):500–502, 1966.
- [367] S. Nilsson. Binding states of individual nucleons in strongly deformed nuclei. *Dan. Mat. Fys. Medd.*, 29(CERN-55-30):1–69, 1955.
- [368] M. Bender, K. Bennaceur, T. Duguet, et al. Tensor part of the skyrme energy density functional. ii. deformation properties of magic and semi-magic nuclei. *Phys. Rev. C*, 80:064302, Dec 2009.
- [369] B. A. Brown. The nuclear shell model towards the drip lines. *Progress in Particle and Nuclear Physics*, 47(2):517–599, 2001.
- [370] R. D. Herzberg, P. T. Greenlees, P. A. Butler, et al. Nuclear isomers in superheavy elements as stepping stones towards the island of stability. *Nature*, 442(7105):896–899, 2006.
- [371] D. Tománek and M. A. Schlüter. Calculation of magic numbers and the stability of small si clusters. *Phys. Rev. Lett.*, 56:1055–1058, Mar 1986.
- [372] A. Soylu. Search for decay modes of heavy and superheavy nuclei. *Chinese Physics C*, 43(7):074102, 2019.
- [373] Nuclear live chart. <https://www-nds.iaea.org/relnsd/vcharthtml/VChartHTML.html>.

- [374] Y. T. Oganessian. Route to islands of stability of superheavy elements. *Physics of Atomic Nuclei*, 63(8):1315–1336, 2000.
- [375] J. Grumann, U. Mosel, B. Fink, et al. Investigation of the stability of superheavy nuclei around $Z=114$ and $Z=164$. *Zeitschrift für Physik*, 228(5):371–386, 1969.
- [376] B. Buck, A. C. Merchant, and S. M. Perez. α decay calculations with a realistic potential. *Phys. Rev. C*, 45:2247–2253, May 1992.
- [377] P. Möller, G. A. Leander, and J. R. Nix. On the stability of the transeinsteinium elements. *Zeitschrift für Physik A Atomic Nuclei*, 323(1):41–45, 1986.
- [378] F. R. Xu, E. G. Zhao, R. Wyss, and P. M. Walker. Enhanced stability of superheavy nuclei due to high-spin isomerism. *Phys. Rev. Lett.*, 92:252501, Jun 2004.
- [379] C.Y. Wong. Additional evidence of stability of the superheavy element 310126 according to the shell model. *Physics Letters*, 21(6):688–690, 1966.
- [380] S. B. Duarte, F. G. OAP T, and A. Dimarco. Half-lives for proton emission, alpha decay, cluster radioactivity, and cold fission processes calculated in a unified theoretical framework. *Atomic Data and Nuclear Data Tables*, 80(2):235, 2002.
- [381] H. F. Zhang, G. Royer, Y. J. Wang, J. M. Dong, W. Zuo, and J. Q. Li. Analytic expressions for α particle preformation in heavy nuclei. *Phys. Rev. C*, 80:057301, Nov 2009.
- [382] Z. Shan, Z. Yanli, C. Jianpo, et al. Improved semi-empirical relationship for α -decay half-lives. *Phys. Rev. C*, 95:014311, Jan 2017.
- [383] D. N. Poenaru, J. A. Maruhn, W. Greiner, et al. Inertia and fission paths in a wide range of mass asymmetry. *Zeitschrift für Physik A Atomic Nuclei*, 333:291, 1989.

- [384] M. Gonçalves and S. B. Duarte. Effective liquid drop description for the exotic decay of nuclei. *Phys. Rev. C*, 48:2409–2414, Nov 1993.
- [385] M. Gonçalves, N. Teruya, O. A. P. Tavares, and S. B. Duarte. Two-proton emission half-lives in the effective liquid drop model. *Physics Letters B*, 774:14–19, 2017.
- [386] K.P. Santhosh and R.K. Biju. Stability of $^{248-254}\text{Cf}$ isotopes against alpha and cluster radioactivity. *Annals of Physics*, 334:280–287, 2013.
- [387] N. Maroufi, V. Dehghani, and S. A. Alavi. Alpha and cluster decay of some deformed heavy and superheavy nuclei. *Nuclear Physics A*, 983:77–89, 2019.
- [388] B. S. Dzhelepov, L. N. Zyryanova, and Y. P. Suslov. Beta processes functions for the analysis of beta spectra and electron capture. page 373, 1972.
- [389] A. V. Karpov, V. I. Zagrebaev, Y. Martinez Palenzuela, et al. Decay properties and stability of heaviest elements. *International Journal of Modern Physics E*, 21(02):1250013, 2012.
- [390] C. S. Wu and S. A. Moszkowski. Beta decay. page 183, 1966.
- [391] M. A. Preston. Addison-Wesley Publishing Company, Inc.,, 1962.
- [392] X. Bao, H. Zhang, G. Royer, et al. Spontaneous fission half-lives of heavy and superheavy nuclei within a generalized liquid drop model. *Nuclear Physics A*, 906:1–13, 2013.
- [393] J. Randrup, S. E. Larsson, P. Möller, Sven Gösta Nilsson, K. Pomorski, and A. Sobiczewski. Spontaneous-fission half-lives for even nuclei with $z \geq 92$. *Physical Review C*, 13(1):229, 1976.
- [394] M. W. Kirson. Mutual influence of terms in a semi-empirical mass formula. *Nuclear Physics A*, 798(1-2):29–60, 2008.

- [395] S. Goriely. Further explorations of skyrme–hartree–fock–bogoliubov mass formulas. xv: The spin–orbit coupling. *Nuclear Physics A*, 933:68–81, 2015.
- [396] J. Duflo and A.P. Zuker. Microscopic mass formulas. *Phys. Rev. C*, 52:R23–R27, Jul 1995.
- [397] M. Wang, G. Audi, F. G. Kondev, et al. The ame2016 atomic mass evaluation (ii). tables, graphs and references. *Chinese Physics C*, 41(3):030003, 2017.
- [398] J. P. Wieleczko, E. Bonnet, J. Gomez del Campo, et al. Influence of the n/z ratio on disintegration modes of compound nuclei. In *AIP Conference Proceedings*, volume 1098, pages 64–69. American Institute of Physics, 2009.
- [399] A. Baran, K. Pomorski, A. Lukasiak, et al. A dynamic analysis of spontaneous-fission half-lives. *Nuclear Physics A*, 361(1):83–101, 1981.
- [400] Z. Matheson, S. A. Giuliani, W. Nazarewicz, et al. Cluster radioactivity of $^{294}_{118}\text{Og}_{176}$. *Phys. Rev. C*, 99:041304, Apr 2019.
- [401] D. N. Poenaru, R. A. Gherghescu, and W. Greiner. Heavy-particle radioactivity. *Journal of Physics: Conference Series*, 436:012056, apr 2013.
- [402] M. Bhattacharya and G. Gangopadhyay. Cluster decay in very heavy nuclei in a relativistic mean field model. *Physical Review C*, 77(2):027603, 2008.
- [403] H. C. Manjunatha, L. Seenappa, and K. N. Sridhar. Uncertainties in the empirical formulae for alpha decay half-lives of heavy and superheavy nuclei. *The European Physical Journal Plus*, 134(9):477, 2019.
- [404] N. Wang, M. Liu, and X. Wu. Modification of nuclear mass formula by considering isospin effects. *Physical Review C*, 81(4):044322, 2010.

- [405] P. B. Price, J. D. Stevenson, S. W. Barwick, and H. L. Ravn. Discovery of radioactive decay of ^{222}Ra and ^{224}Ra by ^{14}C emission. *Physical review letters*, 54(4):297, 1985.
- [406] P. B. Price, R. Bonetti, A. Guglielmetti, C. Chiesa, R. Matheoud, C. Migliorino, and K. J. Moody. Emission of ^{23}F and ^{24}Ne in cluster radioactivity of ^{231}Pa . *Physical Review C*, 46(5):1939, 1992.
- [407] K. P. Santhosh and T. A. Jose. Half-lives of cluster radioactivity using the modified generalized liquid drop model with a new preformation factor. *Phys. Rev. C*, 99:064604, Jun 2019.
- [408] X. J. Bao, H. F. Zhang, B. S. Hu, G. Royer, and J. Q. Li. Half-lives of cluster radioactivity with a generalized liquid-drop model. *Journal of Physics G: Nuclear and Particle Physics*, 39(9):095103, jul 2012.
- [409] D. N. Poenaru, R. A. Gherghescu, and W. Greiner. Single universal curve for cluster radioactivities and α decay. *Phys. Rev. C*, 83:014601, Jan 2011.
- [410] K. P. Santhosh, R. K. Biju, and Antony J. A semi-empirical model for alpha and cluster radioactivity. *Journal of Physics G: Nuclear and Particle Physics*, 35(8):085102, jul 2008.
- [411] M. Balasubramaniam, S. Kumarasamy, N. Arunachalam, and R. K. Gupta. New semiempirical formula for exotic cluster decay. *Physical Review C*, 70(1):017301, 2004.

LIST OF PUBLICATIONS

Journal publications

1. A. M. Nagaraja, H. C. Manjunatha, N. Sowmya, N. Manjunath and S. Alfred Cecil Raj. Cluster radioactivity of super heavy nuclei 290–310120 using different proximity functions. *Eur. Phys. J. Plus* 135 (2020) 814. ISSN:2190-5444.
2. A.M..Nagaraja, H.C.Manjunatha, N.Sowmya, L.Seenappa, P.S.Damodara Gupta, N.Manjunatha and S. Alfred Cecil Raj. Heavy particle radioactivity of super heavy element $Z = 126$. *Nuclear Physics A* 1015 (2021) 122306. ISSN: 1873-1554.
3. H. C. Manjunatha, N. Sowmya and A. M. Nagaraja. The semi-empirical formula for alpha and cluster decay half-lives of super heavy nuclei. *Modern Physics Letters A*. 35, (2020) 2050016. ISSN: 1793-6632.
4. H. C. Manjunatha, A. M Nagaraja, N. Sowmya and K. N. Sridhar. An attempt to parameterize decay energies of super heavy nuclei $103 < Z < 126$ during alpha and cluster decay. *Indian Journal of Physics* 96 (2022) 1237–1246. ISSN: 0974-9845
5. A. M. Nagaraja, H. C. Manjunatha, K.N. Sridhar and S. Alfred Cecil Raj. Systematics of ^{12}C Emission from Super heavy Nuclei. *Bulg. J. Phys.* 46, (2019) 202–213. ISSN: 1314-2666
6. A.M. Nagaraja, K.N. Sridhar, L. Seenappa, R. Munirathnam, N. Sowmya, H.C. Manjunatha, S. Alfred Cecil Raj, Surface, Asymmetric, Coulomb, Pairing and Shell Effects on Cluster

Radioactivity of Superheavy Nuclei with $104 \leq Z \leq 126$. *Brazilian Journal of Physics*, 52 (2022) 97. ISSN: 1678-4448

7. H.C. Manjunatha, S. Alfred Cecil Raj, A.M. Nagaraja, and N. Sowmya. Cluster radioactivity in super-heavy nuclei 299-306122. *J. Nucl. Phys. Mat. Sci. Rad. A.* 8 (2020) 55–63. ISSN:2321-9289
8. Nagaraja. A.M, N.Sowmya, H.C.Manjunatha, and S. Alfred Cecil Raj. Cluster radioactivity in super heavy nuclei ^{299–302}120. *Indian Journal of Pure and Applied Physics* 58, (2020) 207-212. ISSN: 0975-1041
9. A. M. Nagaraja, H. C. Manjunatha, N. Sowmya, P. S. Damodara gupta and S. Alfred Cecil Raj. Decay of dinuclear systems formed from dubnium. *Pramana J. Phys.* 95(2021)194. ISSN: 0304-4289.
10. A. M. Nagaraja, H. C. Manjunatha, N. Sowmya, K. N. Sridhar, Theoretical evidence for neutron magic number 184 from cluster radioactivity studies P. S. Damodara Gupta and S. Alfred Cecil Raj. *International Journal of Modern Physics E* 31, 1 (2022) 2250004. ISSN: 0218-3013.
11. N. Sowmya, H. C. Manjunatha, N. Dhananjaya, A. M. Nagaraja. Competition between binary fission, ternary fission, cluster radioactivity and alpha decay of ²⁸¹Ds. *J Radioanal Nucl Chem* 323, (2020) 1347–1351 ISSN: 0236-5731
12. A. M. Nagaraja, R. Munirathnam, H.C.Manjunatha, N.Sowmya K.N.Sridhar, L.Seenappa, S.Alfred Cecil Raj. Heavy particle radioactivity of superheavy nuclei. (communicated to Journal)
13. A. M. Nagaraja, K.N.Sridhar, L.Seenappa, R.Munirathnam,N.Sowmya, H.C.Manjunatha,

S.Alfred Cecil Raj. Prediction of cluster decay using CPPM and MGLDM models for superheavy nuclei with $105 \leq Z \leq 125$. (Communicated to journal)

14. A. M. Nagaraja, R. Munirathnam, H.C.Manjunatha1, N.Sowmya K.N.Sridhar, L.Seenappa, S.Alfred Cecil Raj. Predictive power of theoretical models in Cluster radioactivity. (communicated to Journal)

Full papers in conference proceedings

1. H. C. Manjunatha, Nagaraja A. M, N. Sowmya. Cluster radioactivity in super heavy nuclei $Z=124$. Proceedings of the DAE Symposium.on Nuclear Physics (ISBN: 818372083-8). Volume 64 (2019)
2. A. M. Nagaraja, N. Sowmya, H. C. Manjunatha, P. S. Damodara Gupta and S. Alfred Cecil Raj. Study of heavy particle radioactivity of $^{294}118$. Proceedings of the DAE Symposium.on Nuclear Physics (ISBN: 818372084-6). Volume 65 (2021).
3. A.M. Nagaraja, N. Sowmya, H.C. Manjunatha, Damodara Gupta, L. Seenappa K.N.Sridhar, S. Alfred Cecil Raj Cluster radioactivity in ^{287}Mc using modified generalized liquid drop model. *J Adv Sci Res*, 2021; ICITNAS: 230-234. ISSN: 0976-9595.
4. A. M. Nagaraja, H. C. Manjunatha, K. N. Sridhar and S. Alfred Cecil Raj. Li Radioactivity from Super heavy nuclei. Proceedings (ISBN:978-93-88680-09-7) of the National Conference on Environmental Monitoring, Impact Assessment and Management (NCEMIAM-19), SSN College of Engineering, Chennai 16th March (2019) 23-25.

Papers presented

1. N. Sowmya, H. C. Manjunatha, N. Dhananjaya and A. M. Nagaraja. Competition between binary fission, ternary fission, Cluster radioactivity and alpha decay of ^{281}Ds . paper presented at National symposium (NUCAR 2019) held from 15th to 19th Jan 2019 at Bhabha Atomic Research Centre (BARC)-MUMBAI.
2. A. M. Nagaraja, H. C. Manjunatha, K. N. Sridhar and S. Alfred Cecil Raj. “Li Radioactivity from Super heavy nuclei” paper presented in National Conference on Environmental Monitoring Impact Assessment and Management (NCEMIAM-2019) (ISBN:978-93-88680-09-7) held on 16th March 2019 at SSN College of Engineering, CHENNAI.
3. A. M. Nagaraja, N. Sowmya, H. C. Manjunatha and S. Alfred Cecil Raj “Cluster radioactivity in nuclei $^{299-302}\text{120}$ ” paper presented in International conference(ICNFNP-2019) held from 14th to 17th October 2019 at Banaras Hindu University, VARANASI.
4. A. M. Nagaraja, H. C. Manjunatha, N. Sowmya and S Alfred Cecil Raj. “Cluster radioactivity in super-heavy nuclei $^{299-306}\text{122}$ ” paper presented at National symposium (NSRP-22) held from 8th to 10th November 2019 at Jawaharlal Nehru University, New Delhi.
5. A. M. Nagaraja, N. Sowmya, H. C. Manjunatha, P. S. Damodara Gupta and S. Alfred Cecil Raj. “Study of heavy particle radioactivity of $^{294}\text{118}$.” 65th DAE-BRNS Symposium on Nuclear Physics, December 1-5, 2021, DAE Convention Centre, Anushaktinagar, Mumbai, Maharashtra, 400094
6. A. M. Nagaraja, N. Sowmya, H. C. Manjunatha, and P. S. Damodara Gupta. “Alpha accompanied cold ternary fission of Fermium of $^{242}\text{100}$; $^{260}\text{100}$.” paper presented in the 19th Annual/5th international Science Fiction Online Conference 2020(IFSC-2020) During 7-9

December 2020. Bangalore University, Bangalore.

7. Nagaraja A. M. Sowmya, N, Manjunatha H. C, Damodara Gupta P. S. Seenappa, L. Sridhar, K. N. and Alfred Cecil Raj S. “Cluster Radioactivity in ^{287}Mc using Modified Generalized Liquid Drop Model.” Paper presented in International Conference on Innovative Trends in Natural and Applied Sciences (ICITANS-2021) 17-18 August 2021, Mahathma Gandhi College of Science, Gadchandur, Chandrapur- 442908(M.S), India.



Cluster radioactivity of superheavy nuclei $^{290-310}120$ using different proximity functions

A. M. Nagaraja^{1,2}, H. C. Manjunatha^{1,a}, N. Sowmya¹, N. Manjunath¹,
S. Alfred Cecil Raj²

¹ Department of Physics, Government College for Women, Kolar 563101, India

² Department of Physics, St. Joseph's College, Affiliated to Bharathidasan University, Tiruchirapalli 62002, India

Received: 27 May 2020 / Accepted: 5 October 2020

© Società Italiana di Fisica and Springer-Verlag GmbH Germany, part of Springer Nature 2020

Abstract The present work used eight different proximity functions in the modified liquid drop model [MGLDM] to study the cluster and alpha decay half-lives in the superheavy nuclei $Z = 120$. The values produced by the present work are compared with experiments. We have explored the proximity function is suitable in MGLDM for the cluster and alpha radioactivity of superheavy nuclei. The present work is useful in the study of decay modes of superheavy nuclei $Z = 120$.

1 Introduction

Cluster radioactivity is an intermediate process between spontaneous fission and alpha decay. During 1980, Sandulescu et al. [1] predicted that the cluster radioactivity is an intermediate process and later Rose and Jones [2] experimentally confirmed the same. Over a last four decades, cluster radioactivity of C, O, N, Mg and Si was observed from the parent nuclei ^{221}Fr – ^{242}Cm leading to doubly magic nuclei ^{208}Pb or its nearby nuclei. The concept of heavy particle radioactivity was further explored by Poenaru et al. [3, 4]. Various theoretical models were developed to describe cluster radioactivity. The super-asymmetric fission model (SAFM) [5, 6] has made a major contribution to the knowledge of nuclear hadronic decays. The unified fission model [5, 7–13] in which the cluster formation probability is studied using the internal barrier penetration and preformation cluster model (PCM) [14–17] is evaluated by solving the Schrodinger equation in case of dynamic flow of charges and masses. Cluster radioactivity is a process of quantum tunneling in which the cluster must penetrate the potential barrier to emerge from the parent nucleus. In case of UFM (unified fission model) and PCM, the cluster can penetrate the potential barrier with the existing Q-values, which plays vital role in the measurement of the emitted cluster half-lives [18].

The concept of proximity potential was extensively used in the nuclear physics. Shi and Swaiateki [19] were the first to empirically explore the proximity potential, and later Gupta et al. [15, 20] were extensively used the same method in preformation cluster model. Various proximity potentials have recently been used to analyze the cross sections above and below the Coulomb barrier for nuclear decay and nuclear fusion reaction. In addition, several changes

^a e-mail: manjunathhc@rediffmail.com (corresponding author)

have been made to the proximity potential. Dutta and Puri [21, 22] have used various versions of proximity potentials to test the fusion cross sections of different target–projectile combinations. Earlier researchers [23, 24] were studied the role of deformations and orientations of the radioactive nuclei, mainly for the doubly magic nuclei ^{208}Pb . The earlier researchers [25–42] studied the different decay modes using the different proximity functions.

The proximity potential function essentially consists of two parts. One depends on the shape and geometry of daughter nuclei and cluster nuclei, and the other is the universal function related to separation distance between the two nuclei. At present, there were different forms of proximity potentials. The differences in the proximity functions are based on the $\phi(S)$ and the different parameters which were used in the evaluation of $\phi(S)$. Until now the systematic study of alpha decay, fission and cluster half-lives was evaluated using the different theoretical models such as unified fission model, generalized liquid drop model, Coulomb and proximity models and so on in case of $Z = 120$. All these models were efficiently predicted the alpha decay half-lives and corresponding decay chains of the same. Hence, in the present work we have used eight different proximity functions in the modified liquid drop model [MGLDM] to evaluate cluster and alpha decay half-lives in the superheavy nuclei $Z = 120$. Then in accordance with the available experimental results, we explored which proximity function is suitable for the cluster and alpha radioactivity and also explained the reason for same. This paper is structured as follows: The theoretical study of cluster and alpha decay is presented in Sect. 2. The evaluation of half-lives is given in Sect. 3. The results and discussions are displayed in Sect. 4. The conclusions are given in Sect. 5.

2 Theoretical framework

The macroscopic modified generalized liquid drop energy between the two nuclei is taken as a sum of volume, surface, Coulomb, proximity and centrifugal energies and is expressed as:

$$E = E_V + E_S + E_C + E_{\text{Prox}} + E_I \quad (1)$$

The expressions for the volume, surface and Coulomb energies are given by:

$$E_V = -15.494(1 - 1.8I^2)A \text{ MeV} \quad (2)$$

$$E_S = 17.9439(1 - 2.6I^2)A^{2/3}(S/4\pi R_0^2) \text{ MeV} \quad (3)$$

$$E_C = 0.6e^2(Z^2/R_0) \times 0.5 \int (V(\theta)/V_0)(R(\theta)/R_0)^3 \sin \theta \, d\theta \text{ MeV} \quad (4)$$

where I is the relative neutron excess, S is the surface area of the deformed nucleus, $V(\theta)$ is the electrostatic potential at the surface and V_0 is the surface potential of the sphere, respectively. When the nuclei are far apart, then the equations are written as:

$$E_V = -15.494[(1 - 1.8I_1^2)A_1 + (1 - 1.8I_2^2)A_2] \text{ MeV} \quad (5)$$

$$E_S = 17.9439[(1 - 2.6I_1^2)A_1^{2/3} + (1 - 2.6I_2^2)A_2^{2/3}] \text{ MeV} \quad (6)$$

$$E_C = 0.6e^2Z_1^2/R_1 + 0.6e^2Z_2^2/R_2 + e^2Z_1Z_2/r \quad (7)$$

Here, A_i is the mass number, Z_i is the atomic number, R_i is the radii of the two nuclei, and I_i is the relative neutron excess of the two nuclei. The relative neutron excess $I_2 = 0$ to ensure negative E_V and positive E_S . The radius R_i of the daughter nuclei is given by:

$$R_i = (1.28A_i^{1/3} - 0.76 + 0.8A_i^{-1/3}) \text{ fm}, \quad i = 1, 2 \tag{8}$$

The centrifugal energy E_l of the emitted cluster is given by:

$$E_l(r) = \frac{\hbar^2 l(l+1)}{2\mu r^2} \tag{9}$$

where μ , l and r are the reduced mass, the angular momentum and the distance between the mass centers, respectively. The proximity function E_{Prox} is defined as:

$$E_{Prox}(Z) = 4\pi\gamma\bar{R}\Phi\left(\frac{z}{b}\right) \tag{10}$$

where Φ is the universal proximity potential function and z is distance between the near surfaces of the fragments, respectively. $b \approx 0.99$ is the nuclear surface thickness. In Eq. (10), \bar{R} is the mean curvature radius and C_i is the Sussmann central radii, expressed as:

$$\bar{R} = \frac{C_1 C_2}{C_1 + C_2} \tag{11}$$

$$C_i = R_i - \left(\frac{b^2}{R_i}\right) \tag{12}$$

R_i is evaluated using Eq. (8). γ in Eq. (10) is expressed as:

$$\gamma = \gamma_0 \left[1 - K_S \left(\frac{N - Z}{A} \right)^2 \right] \text{ MeV/fm}^2 \tag{13}$$

where $\gamma_0 = 1.460734 \text{ MeV/fm}^2$ and $K_S = 4.0$.

We have evaluated the half-lives of cluster and alpha radioactivity by using eight different universal proximity potentials and were expressed as follows:

2.1 Modified Prox 1977 (MP 77)

The modified form due to Blocki and Swiatecki [43] is expressed as [44]:

$$\phi(S) = \begin{cases} -1.7817 + 0.927S + 0.143S^2 - 0.09S^3 & S < 0 \\ -1.7817 + 0.927S + 0.01696S^2 - 0.05148S^3 & 0 < S < 1.9475 \\ -4.41 \exp(-S/0.7176) & S > 1.9475 \end{cases} \tag{14}$$

where $S = (r - C_1 - C_2)/b$ and b is the surface width, $b = (\pi/\sqrt{3})a$ with $a = 0.55 \text{ fm}$ and it is nearly equal to unity.

2.2 Prox 1977 (Prox 77)

Blocki et al. [43] suggested a generalized proximity theorem according to which the force between the two gently curved objects is proportional to the potential per unit area between two flat surfaces made of the same material and the proportionality constant is a function of the mean curvature of the two objects. The whole theorem leads to the formula for the interaction potential between the two nuclei leading a function of simple geometrical factor and universal separation function. The universal function is expressed as:

$$\phi(S) = \begin{cases} -0.5(S - 2.54)^2 - 0.0852(S - 2.54)^3 & S < 1.2511 \\ -3.437 \exp(-S/0.75) & S > 1.2511 \end{cases} \tag{15}$$

with $S = (r - C_1 - C_2)/b$ and $b \approx 1$.

2.3 Modified proximity potential 1981 (MP 81)

Blocki et al. [43] first proposed the Proximity 1977 which is valid for gently curved surfaces; again Blocki and Swiatecki [45] improved the proximity potential function and included the surfaces which have large curvature which are still characterized by small angles between the significant portions of the interacting surfaces. They proposed general proof for the proximity force for the gap configuration which goes over into a crevice after contact and the improved formula for the proximity potential function were expressed as:

$$\phi(S) = \begin{cases} -1.7817 + 0.927S + 0.0169S^2 - 0.0514S^3 & 0 < S < 1.9475 \\ -4.41 \exp(-S/0.7176) & S > 1.9475 \end{cases} \quad (16)$$

2.4 Bass 1977 (Bass 77)

The actual potential in the external region consists of an influence of Coulomb, centrifugal and nuclear potential. On the basis of the liquid drop model, the later can be interpreted as the change in surface energy of the two fragments due to their mutual interaction. Assuming that the specific surface energy is exponentially depended on local fragment separation, simple geometrical arguments resulted in terms of explicit expression for masses of the fragment nuclei. The effective potential is expressed as:

$$E^{\text{Prox}} = -\frac{d}{R_{12}} a_s A_1^{1/3} A_2^{1/3} \exp\left(-\frac{r - R_{12}}{d}\right) \quad (17)$$

where $R_{12} = r_0(A_1^{1/3} + A_2^{1/3})$, $d = 1.35$ fm and $a_s = 17.0$ MeV. The nuclear part of total interaction potential is expressed as follows:

$$E^{\text{Prox}} = -a_s A_1^{1/3} A_2^{1/3} \frac{d}{R_{12}} \exp\left(-\frac{r - R_{12}}{d}\right) \quad (18)$$

By using liquid drop model and geometric interpretations, Bass [46] presented the nuclear aspect of the interaction potential from the knowledge based on the experimental evidence of the fusion cross sections.

$$E^{\text{Prox}} = -\frac{R_1 R_2}{R_1 + R_2} \Phi(r - R_1 - R_2) \quad (19)$$

Universal function $\Phi(r - R_1 - R_2)$ has the following form

$$\phi(S) = \left[0.033 \exp\left(\frac{S}{d_1}\right) + 0.007 \exp\left(\frac{S}{d_2}\right) \right]^{-1} \quad (20)$$

2.5 Prox 2013 (Prox 13)

Zhang et al. [47] studied the universal function using double-folding model (DFM) with the density-dependent nucleon–nucleon interaction. When the overlap between the two nuclei increases, the proximity potential model becomes complex due to nuclear potential which overlaps in the smaller distances of the nuclear surfaces. Hence, the DFM with the density-

dependent nucleon–nucleon interaction was used to calculate nuclear potential and then proposed universal function, and it is expressed as:

$$\Phi(\varepsilon) = \frac{p_1}{1 + \exp\left(\frac{s_0 + p_2}{p_3}\right)} \tag{21}$$

$$\text{With } s_0 = \frac{R - R_1 - R_2}{b} \tag{22}$$

Here, p_1 , p_2 and p_3 are -7.65 , 1.02 and 0.89 , respectively [44].

2.6 Prox Ngo 1980 (Ng80)

In 1980, Ngo [48] proposed a proximity function between two gently curved surfaces that is a function of the separation degree of freedom. The evaluated nuclear potential is expressed as:

$$\phi(S) = \begin{cases} -33 + 5.4(S - S_o)^2 & \text{for } S < S_o \\ -33 \exp\left[-\frac{1}{5}\right](S - S_o)^2 & \text{for } S \geq S_o \end{cases} \tag{23}$$

where $S_o = -1.6$ fm.

2.7 Denisov 2002 (DP00)

In 2002, Denisov [49] proposed the proximity potential function by using semi-microscopic potential between heavy ions evaluated for different colliding ions in the approach of frozen densities in the extended framework of Thomas–Fermi approximation with \hbar^2 correction term and the universal function $\Phi(S = r - R_1 - R_2 - 2.65)$ is given by:

$$\Phi(S) = \begin{cases} 1 - s/0.7881663 + 1.229218S^2 - 0.2234277S^3 - 0.1038769S^4 \\ - \frac{R_1 R_2}{R_1 + R_2} (0.1844935S^2 + 0.07570101S^3) + (I_1 + I_2)(0.04470645S^2 + 0.0334687S^3) & \text{for } -5.65 \leq S \leq 0 \\ 1 - S^2 \left[0.05410106 \frac{R_1 R_2}{R_1 + R_2} \exp\left(-\frac{S}{1.760580}\right) \right] \\ - 0.5395420(I_1 + I_2) \exp\left(-\frac{S}{2.424408}\right) \times \exp\left(-\frac{S}{0.7881663}\right) & \text{for } S \geq 0 \end{cases} \tag{24}$$

2.8 Prox 2000 (Prox 00)

In the year 2000, Myers and Swiatecki proposed the proximity function [50] especially for the superheavy region and it is expressed as:

$$\Phi(S) = \begin{cases} -0.1353 + \sum_{n=0}^5 [C_n/(n - 1)](2.5 - S)^{n+1} & (0 < S \leq 2.5) \\ -0.0955 \exp\left(\frac{2.75 - S}{0.7176}\right) & (S \geq 2.5) \end{cases} \tag{25}$$

The different values of constant C_n were $C_0 = -0.1886$, $C_1 = 0.2628$, $C_2 = -0.15216$, $C_3 = -0.04562$, $C_4 = 0.069136$, and $C_5 = -0.011454$.

3 Evaluation of half-live

According to WKB (Wentzel–Kramers–Brillouin) approximation, the penetration probability P through the potential barrier was studied for the cluster and alpha decay by the following equation:

$$P = \exp \left\{ -\frac{2}{\hbar} \int_{R_a}^{R_b} \sqrt{2\mu(E - Q)} dr \right\} \quad (26)$$

where the total energy is evaluated using Eq. (1) by using different proximity functions and in case of Bass 77 we have used Eq. (19). μ is the reduced mass alpha decay or cluster decay system, R_a and R_b are the inner and outer turning points, and these turning points were evaluated using the following conditions:

$$V_T(R_a) = Q = V_T(R_b) \quad (27)$$

The cluster and alpha decay half-life of parent nuclei is studied by:

$$T_{1/2} = \frac{\ln 2}{\lambda} = \frac{\ln 2}{\nu P} \quad (28)$$

where λ is the decay constant and ν is the assault frequency and is expressed as

$$\nu = \frac{\omega}{2\pi} = \frac{2E_v}{h} \quad (29)$$

The E_v , the empirical vibration energy, is given as:

$$E_v = Q \left\{ 0.056 + 0.039 \exp \left[\frac{4 - A_2}{2.5} \right] \right\} \quad \text{for } A_2 \geq 4 \quad (30)$$

4 Results and discussion

We have studied different cluster emissions such as ${}^4\text{He}$, ${}^6\text{Li}$, ${}^9\text{Be}$, ${}^{20-22}\text{Ne}$, ${}^{23}\text{Na}$, ${}^{24-26}\text{Mg}$, ${}^{27}\text{Al}$, ${}^{28-30}\text{Si}$, ${}^{31}\text{P}$, ${}^{32-34}\text{S}$, ${}^{35}\text{Cl}$, ${}^{36,38,40}\text{Ar}$, ${}^{39}\text{K}$ and ${}^{40,42-44,46}\text{Ca}$ by using the different proximity functions such as Mp 77, Prox 77, MP 81, Bass 77, Prox 13, Ng80, DP00 and Prox 00. We know that the cluster and alpha decay half-lives were depended on the penetration probability which is associated with the total energy and the amount of energy released during cluster and alpha decay. In the above calculations, the value of the Coulomb potential remains the same but the value of proximity potentials differs in each case. Figure 1 shows the variation of total potential/energy with the increase in separation distance between the two nuclei. Here, we have selected the superheavy nuclei ${}^{302}120$ as an example, and we have also observed similar distributions of potential in case of other nuclei. In different potential wells, we have observed that the value of the V changes up to 4 fm and then above 4 fm and more than the Q_α ; there are no much differences between the total potential. However, the Bass 77 produces the lower barrier height when compared to other potentials. The distribution of potential in case of Prox 00 was observed to be slightly higher when compared to Bass 77. From the figure, it is also clearly observed that the distribution of the $V(\text{MeV})$ values was almost similar in case of MP 77, Prox 77, MP 81, Prox 13 and Ng80. It is also observed that the DP00 was in between the distribution of all other proximity potential function values. The studied different proximity potential energies for the superheavy region ${}^{290-310}120$ are presented in Fig. 2. Figure 2 depicts the variation of total potential/energy using different

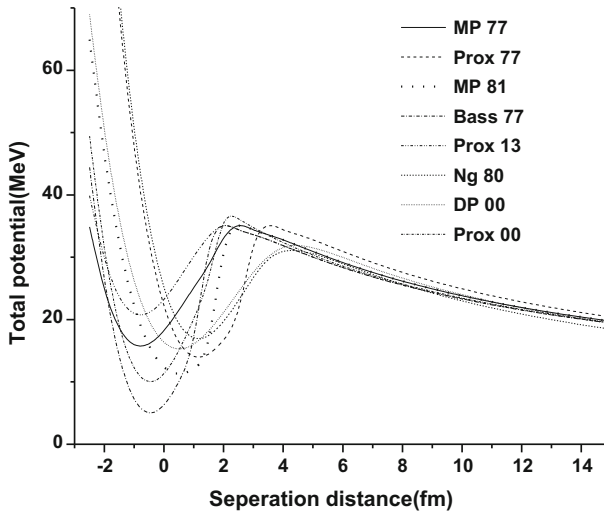


Fig. 1 A variation of total potential/energy using different proximity potential functions with the separation distance between the two nuclei

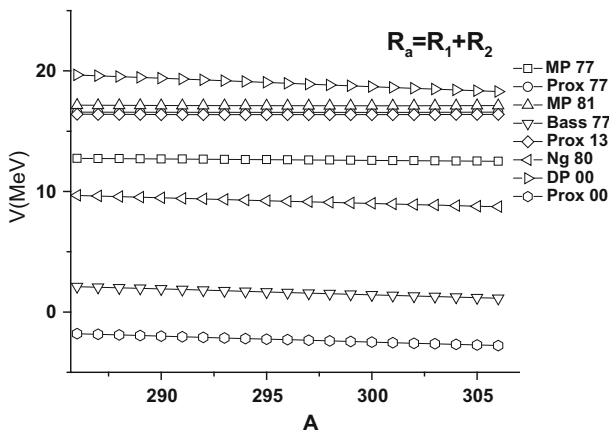


Fig. 2 A variation of total potential/energy using different proximity potential functions with the mass number of parent nuclei during an alpha decay at a separation distance of $R_a = R_1 + R_2$

proximity potential functions with the mass number of parent nuclei during an alpha decay at a separation distance of $R_a = R_1 + R_2$ in the superheavy region $^{290-310}120$. Since we have observed different potential wells in case of Fig. 1, here also we have observed the different $V(\text{MeV})$ by using different proximity functions.

The amount of energy released during different cluster and alpha emissions was studied using the mass excess values available in the literature [51–55]. The Q-values were taken as a difference between the mass excess of parent and fragment nuclei. The amount of energy released during different cluster emissions with mass number of parent nuclei for the $^{290-310}120$ is presented in Fig. 3. From the figure, it has been observed that as the mass number of cluster increases corresponding Q-values were also increased. Once the total potential/energy and amount of energy released during different cluster emissions were

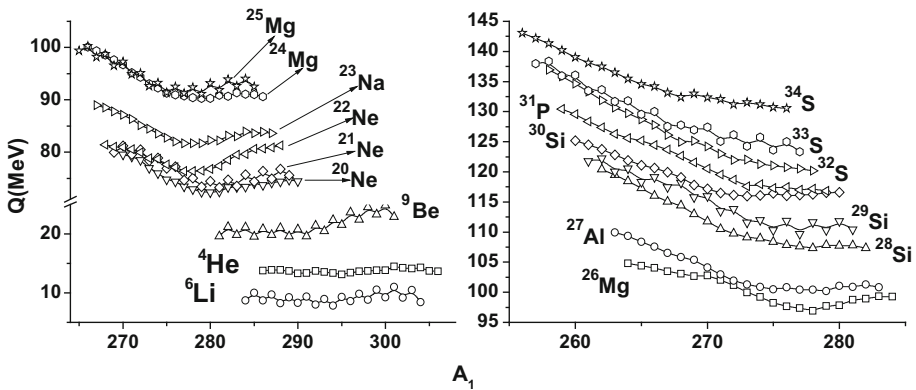


Fig. 3 Amount of energy released during different cluster emissions with mass number of parent nuclei

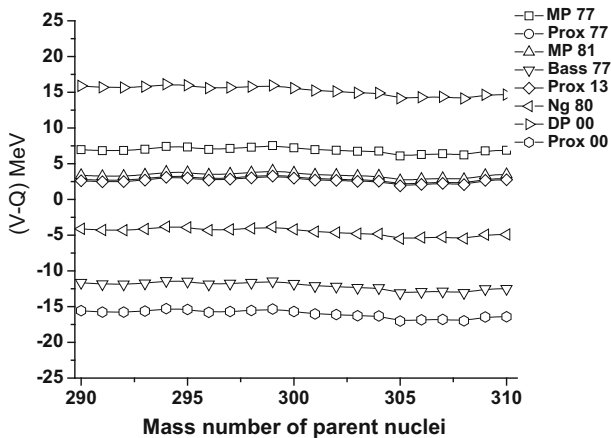


Fig. 4 The variation of driving potential using different proximity potential functions with the mass number of parent nuclei

studied, then the driving potentials for all the cluster and alpha emissions were studied using different proximity functions. Figure 4 represents the variation of driving potential using different proximity potential functions with the mass number of parent nuclei at a separation distance of $R_a = R_1 + R_2$ in the superheavy region $^{290-310}120$. From Fig. 4 it is observed that the driving potential of Prox 00 is lesser when compared to all other proximity functions. Although the scale of driving potentials is quite different for MP 77, Prox 77, MP 81, Bass 77, Prox 13, Ng80, DP00 and Prox 00, their potential energy surface area is similar and exhibits the similar alpha potential well with slight different values.

The difference between the V and Q plays an important role in the estimation of half-lives. The half-lives were inversely proportional to the barrier penetration probability and it is evaluated using the WKB integral. From Fig. 5 it is evident that the alpha decay logarithmic half-life of superheavy nuclei $^{290-310}120$ was decreased with an increase in neutron number. However, we have observed minimum logarithmic half-life values when compared to neighboring nuclei near the magic nuclei $N = 176$ and 185 . The tabulated values of logarithmic half-lives using MP 77, Prox 77, MP 81, Bass 77, Prox 13, Ng80, DP00 and Prox 00 for

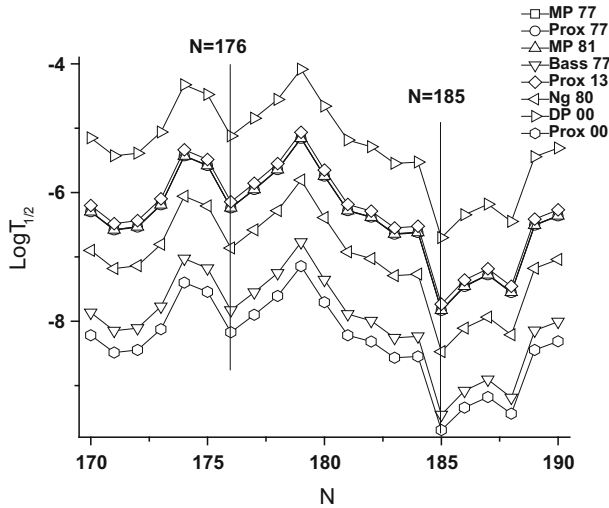


Fig. 5 A variation of logarithmic half-lives with the neutron number for the superheavy region $^{290-310}120$ by using different proximity functions

cluster emissions such as ^4He , ^6Li , ^9Be , $^{20-22}\text{Ne}$, ^{23}Na , $^{24-26}\text{Mg}$, ^{27}Al , $^{28-30}\text{Si}$, ^{31}P , $^{32-34}\text{S}$ and ^{46}Ca for superheavy nuclei $^{302}120$ are shown in Table 1. In order to study the effects of the proximity functions, MP 77, Prox 77, MP 81, Bass 77, Prox 13, Ng80, DP00 and Prox 00 used in the present study were also compared with the available experimental values [56] in the superheavy region $Z = 104-118$. The table gives the comparison between the logarithmic half-lives of different proximity functions with the available experimental values. From the comparison, it is clear that the magnitude of half-lives of different cluster emissions such as ^4He , ^6Li , ^9Be , $^{20-22}\text{Ne}$, ^{23}Na , $^{24-26}\text{Mg}$, ^{27}Al , $^{28-30}\text{Si}$, ^{31}P , $^{32-34}\text{S}$ and ^{46}Ca in case of MP 77, Prox 77, MP 81, Prox 13 and Ng80 was found to be similar, but the value of half-lives was found to be little different in in the Bass 77, DP00 and Prox 00. Depending on Fig. 1, we can inference that the variation of the half-lives in Table 1 was due to the distribution of total potential.

To be more accurate with the results obtained from the different proximity potentials, we have compared the logarithmic half-lives using the proximity functions such as MP 77, Prox 77, MP 81, Bass 77, Prox 13, Ng80, DP00 and Prox 00 with that of available experimental values [52] in the superheavy region $104 < Z < 118$ which are tabulated in Table 2. From the tabulated values, it is observed that there are similar magnitude values for the MP 77, Prox 77, MP 81, Prox 13 and Ng80 and slight variation in case of Bass 77, DP00 and Prox 00. The ratio of experimental and calculated half-lives using different proximity functions was studied, and it is expressed as:

$$\log(r) = \frac{\log_{\text{exp}}(T_{1/2})}{\log_{\text{cal}}(T_{1/2})} \tag{31}$$

Figure 6 shows a deviation between the logarithmic half-lives using different proximity functions such as MP 77, Prox 77, MP 81, Bass 77, Prox 13, Ng80, DP00 and Prox 00 and experimental logarithm half-lives during an alpha decay for the superheavy nuclei $104 < Z < 118$. From the figure, it is observed that the many of the points lies in between + 1 and -1 in case of MP 77, Prox 77, MP 81, Prox 13 and Ng80 and little deviations in case of

Table 1 Tabulation of logarithmic half-lives using Mp 77, Prox 77, MP 81, Bass 77, Prox 13, Ng80, DP00 and Prox 00 for cluster emissions such as ^4He , ^6Li , ^9Be , ^{20}Ne , ^{23}Na , ^{24}Mg , ^{27}Al , ^{28}Si , ^{31}P , ^{32}S and ^{46}Ca for superheavy nuclei ^{302}Z

Parent Nuclei	Daughter Nuclei	Emitted Cluster	Q(MeV)	LogT _{1/2}	MP 77	Prox 77	MP 81	Bass 77	Prox 13	Ng 80	DP 00	Prox 00
302 ₁₂₀	298 ₁₁₈	^4He	13.715	- 6.379	- 6.386	- 6.379	- 7.992	- 7.992	- 6.287	- 7.026	- 5.287	- 8.315
302 ₁₂₀	296 ₁₁₇	^6Li	8.603	27.198	27.206	27.198	41.108	41.108	27.540	26.906	28.348	40.589
302 ₁₂₀	293 ₁₁₆	^9Be	20.512	23.083	23.093	23.083	21.452	21.452	23.840	22.841	17.924	20.583
302 ₁₂₀	282 ₁₁₀	^{20}Ne	73.342	24.474	24.496	24.473	28.149	28.149	26.084	24.462	27.265	24.444
302 ₁₂₀	281 ₁₁₀	^{21}Ne	73.262	25.206	25.229	25.206	28.210	28.210	26.918	25.205	28.132	24.809
302 ₁₂₀	280 ₁₁₀	^{22}Ne	76.797	20.823	20.847	20.823	22.126	22.126	22.706	20.832	23.991	19.121
302 ₁₂₀	279 ₁₀₉	^{23}Na	81.657	26.235	26.260	26.235	30.581	30.581	28.069	26.259	29.304	26.378
302 ₁₂₀	278 ₁₀₈	^{24}Mg	90.414	26.107	24.447	24.419	30.846	30.846	26.536	24.490	27.838	24.918
302 ₁₂₀	277 ₁₀₈	^{25}Mg	91.237	25.369	25.395	25.369	30.853	30.853	27.343	25.417	28.610	25.736
302 ₁₂₀	276 ₁₀₈	^{26}Mg	97.655	17.969	17.997	17.968	20.058	20.058	20.174	18.031	21.540	16.211
302 ₁₂₀	275 ₁₀₇	^{27}Al	100.449	25.095	25.124	25.095	31.762	31.762	27.201	25.166	28.497	25.701
302 ₁₂₀	274 ₁₀₆	^{28}Si	108.923	25.034	25.063	25.033	34.274	34.274	27.167	25.116	28.459	26.180
302 ₁₂₀	273 ₁₀₆	^{29}Si	111.565	22.299	22.330	22.299	29.176	29.176	24.575	22.394	25.919	22.758
302 ₁₂₀	272 ₁₀₆	^{30}Si	116.155	17.706	17.738	17.705	21.652	21.652	20.180	17.817	21.602	16.777
302 ₁₂₀	271 ₁₀₅	^{31}P	119.531	23.381	23.414	23.381	32.239	32.239	25.763	23.497	27.124	24.211
302 ₁₂₀	270 ₁₀₄	^{32}S	124.186	27.324	27.357	27.324	40.850	40.850	29.660	27.445	30.986	29.178
302 ₁₂₀	269 ₁₀₄	^{33}S	126.946,	24.617	24.651	24.617	35.285	35.285	27.091	24.751	28.465	25.853
302 ₁₂₀	268 ₁₀₄	^{34}S	132.378	19.060	19.096	19.059	25.919	25.919	21.747	19.213	23.203	19.016
302 ₁₂₀	256 ₁₀₀	^{46}Ca	175.095	10.154	10.207	10.154	12.521	12.521	13.999	10.463	15.760	6.563

Table 2 A comparison of logarithmic half-life different proximity functions such as Mp 77, Prox 77, MP 81, Bass 77, Prox 13, Ng80, DP00 and Prox 00 for the available experimental values [52]

Parent nuclei	Daughter nuclei	Log $T_{1/2}$											(Log $T_{1/2}$)Exp
		MP 77	Prox 77	MP 81	Bass 77	Prox 13	Ng 80	DP 00	Prox 00				
^{256}Rf	^{252}No	0.856	0.741	0.744	-0.869	0.834	0.096	0.847	-1.098	0.32			
^{258}Rf	^{254}No	0.670	-0.109	-0.106	-1.715	-0.016	-0.754	1.001	-1.960	-0.98			
^{260}Rf	^{256}No	0.008	-0.004	0.043	-0.026	0.022	0.020	0.045	-0.058	0.02			
^{260}Sg	^{256}Rf	-0.733	-1.456	-1.451	-3.045	-1.360	-2.083	-0.325	-3.302	-1.91			
^{264}Hs	^{260}Sg	-1.948	-2.656	-2.650	-4.235	-2.559	-3.274	-1.514	-4.514	-2.97			
^{268}Hs	^{264}Sg	0.369	-0.103	-0.101	-0.230	-0.011	-0.276	-0.274	-0.206	0.15			
^{270}Hs	^{266}Sg	2.404	1.575	1.576	-0.079	0.864	0.894	2.619	-0.292	0.95			
^{270}Ds	^{266}Hs	-2.668	-3.401	-3.395	-4.982	-3.303	-4.021	-2.264	-5.285	-3.69			
^{286}Fl	^{282}Cn	0.474	-0.376	-0.374	-2.038	-0.286	-1.062	0.645	-2.256	-0.46			
^{288}Fl	^{284}Cn	0.239	0.194	0.195	-0.155	0.332	-0.257	0.244	-0.145	-0.12			
^{290}Lv	^{286}Fl	-0.641	-1.482	-1.480	-3.136	-1.391	-2.161	-0.455	-3.361	-2.1			
^{292}Lv	^{288}Fl	-0.057	-0.901	-0.900	-2.569	-0.811	-1.592	0.108	-2.788	-1.62			
^{294}Og	^{290}Lv	-2.094	-2.918	-2.915	-4.557	-2.825	-3.584	-1.875	-4.799	-2.94			

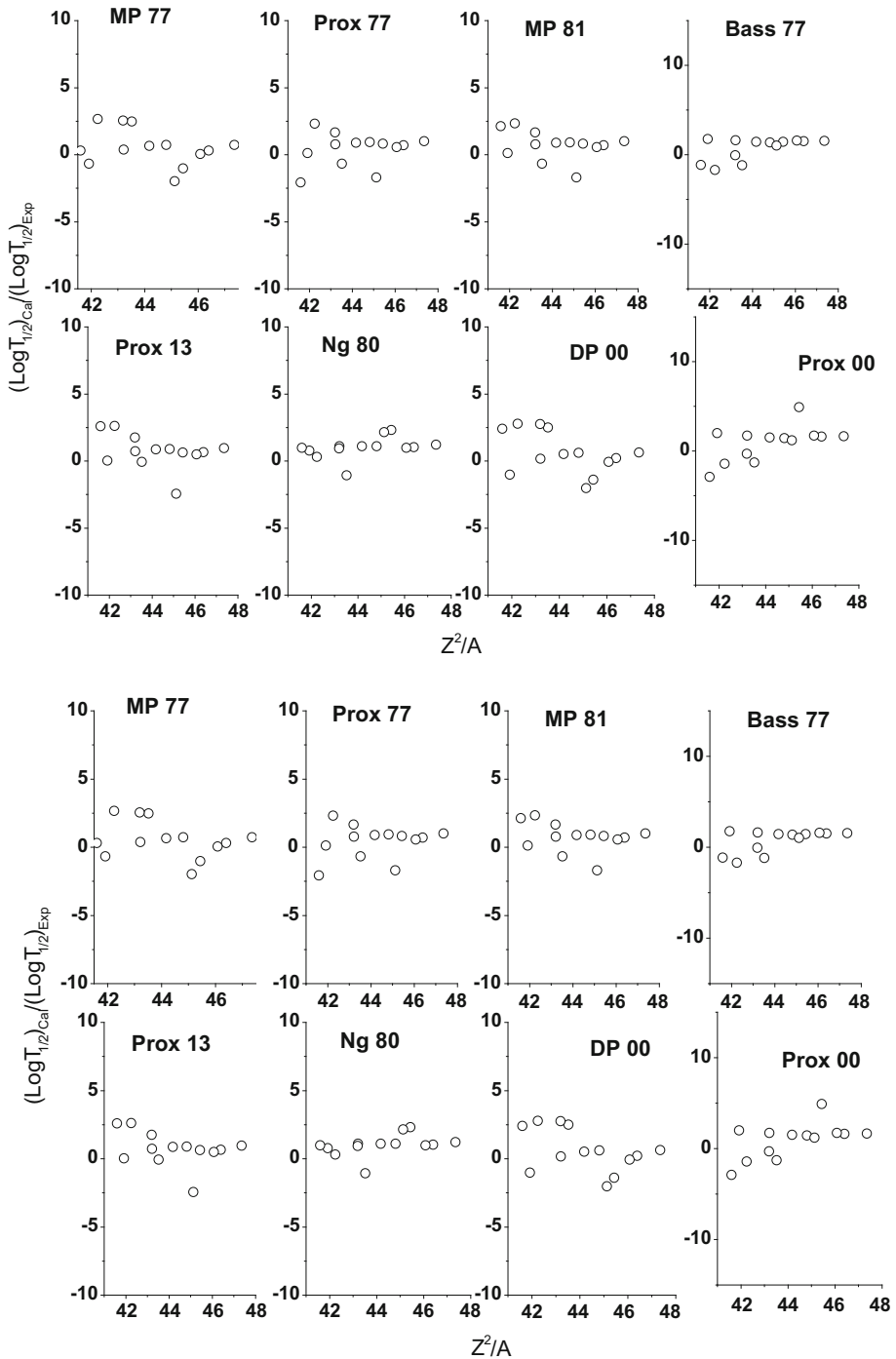


Fig. 6 A deviation between the logarithmic half-lives using different proximity functions such as Mp 77, Prox 77, MP 81, Bass 77, Prox 13, Ng80, DP00 and Prox 00 and experimental logarithm half-lives during an alpha decay for the superheavy nuclei $104 < Z < 118$

Table 3 Standard deviation values between the experimental and different proximity functions such as Mp 77, Prox 77, MP 81, Bass 77, Prox 13, Ng80, DP00 and Prox 00

$\sigma_{MP\ 77}$	$\sigma_{Prox\ 77}$	$\sigma_{MP\ 81}$	$\sigma_{Bass\ 77}$	$\sigma_{Prox\ 13}$	$\sigma_{Ng\ 80}$	$\sigma_{DP\ 00}$	$\sigma_{Prox\ 00}$
0.552	0.556	0.735	0.832	0.538	0.932	0.264	0.749

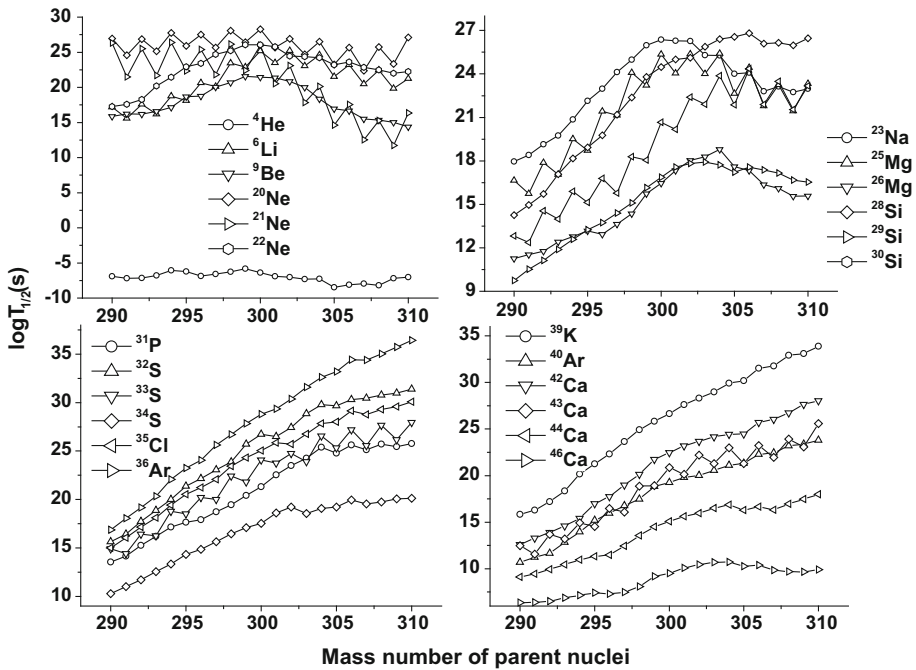


Fig. 7 A variation of logarithmic half-lives of superheavy nuclei $^{290-310}120$ during the cluster emission of as ^4He , ^6Li , ^9Be , $^{20-22}\text{Ne}$, ^{23}Na , $^{24-26}\text{Mg}$, ^{27}Al , $^{28-30}\text{Si}$, ^{31}P , $^{32-34}\text{S}$, ^{35}Cl , $^{36,38,40}\text{Ar}$, ^{39}K and $^{40,42-44,46}\text{Ca}$ by using proximity function Ng 80

Bass 77, DP00 and Prox 00. The Q-values were evaluated by using the mass excess values. We have used experimental mass excess values [51]. For those nuclei, where experimental mass excess was unavailable, we have used theoretical mass excess values [52–55].

The standard deviation of half-lives by using different proximity functions was evaluated with that of experimental values, and it is expressed as:

$$\sigma = \left(\frac{1}{(n - 1)} \sum_{i=1}^n \left(\log T_{1/2}^{\text{cal}} - \log T_{1/2}^{\text{exp}} \right)^2 \right)^{1/2} \tag{32}$$

The evaluated standard deviation is shown in Table 3. From the comparison, it is obtained that the standard deviation of half-lives for MP 77, Prox 77, Prox 13 was observed to be of the same order and the deviation produced by the MP 81 and Prox 00 is of the same order. The DP00 produces the large deviation, whereas Ng 80 values were nearly equal to unity. Henceforth, Fig. 7 shows the variation of logarithmic half-lives of superheavy nuclei $^{290-310}120$ during the different cluster emissions by using proximity function Ng 80 and the

Table 4 tabulation of logarithmic half-lives of superheavy nuclei $^{290-310}120$ during the cluster emission of as ^4He , ^6Li , ^9Be , $^{20-22}\text{Ne}$, ^{23}Na , $^{24-26}\text{Mg}$, ^{27}Al , $^{28-30}\text{Si}$, ^{31}P , $^{32-34}\text{S}$, ^{35}Cl , $^{36,38,40}\text{Ar}$, ^{39}K and $^{40,42-44,46}\text{Ca}$ by using proximity function Ng 80

Parent nuclei	Logarithmic half-lives											
	^4He	^6Li	^9Be	^{20}Ne	^{21}Ne	^{22}Ne	^{23}Na	^{25}Mg	^{26}Mg	^{28}Si	^{29}Si	^{30}Si
290	- 6.90	26.95	26.32	17.26	17.20	15.87	17.95	16.66	11.25	14.25	12.82	9.74
291	- 7.18	24.57	21.48	17.61	15.56	16.21	18.40	15.73	11.53	14.96	12.36	10.52
292	- 7.14	26.89	25.52	18.26	17.58	16.20	19.15	17.88	11.76	15.71	14.54	11.12
293	- 6.80	25.15	21.68	20.20	16.20	16.58	19.75	17.06	12.42	17.07	13.98	11.88
294	- 6.06	27.75	26.38	21.45	18.77	17.16	20.86	19.51	12.78	18.17	15.89	12.59
295	- 6.21	25.92	22.35	22.92	18.11	18.67	22.14	18.72	13.16	18.92	15.13	13.24
296	- 6.86	27.52	25.37	23.43	20.64	18.76	22.98	21.43	12.94	19.77	16.79	13.72
297	- 6.58	25.66	21.79	24.68	20.13	20.03	24.12	21.15	13.63	21.19	15.77	14.40
298	- 6.28	28.06	26.16	25.22	23.44	20.70	24.98	24.09	14.35	22.38	18.28	15.10
299	- 5.81	26.41	22.40	26.08	22.88	21.59	25.97	23.20	15.74	23.80	18.06	16.14
300	- 6.39	28.29	25.97	26.07	25.17	21.45	26.37	25.35	16.45	24.49	20.65	16.87
301	- 6.92	25.67	20.52	25.80	23.49	21.36	26.28	24.04	17.34	25.01	20.17	17.57
302	- 7.03	26.91	23.08	24.46	25.21	20.83	26.26	25.37	18.03	25.12	22.39	17.82
303	- 7.29	24.71	17.82	24.39	23.06	20.00	25.29	24.02	18.30	25.88	21.90	17.91
304	- 7.27	26.51	20.10	24.23	24.63	18.37	25.28	25.41	18.79	26.41	23.88	17.71
305	- 8.47	23.26	14.61	23.21	21.54	16.97	24.00	22.66	17.61	26.57	21.87	17.22
306	- 8.11	25.65	17.57	23.61	23.19	16.66	24.08	24.43	17.34	26.81	24.37	17.56
307	- 7.93	22.35	12.52	22.84	20.50	15.51	22.80	21.79	16.36	26.09	21.89	17.37
308	- 8.21	25.76	15.27	22.47	22.45	15.35	23.13	23.25	16.11	26.16	23.48	17.16
309	- 7.18	23.32	11.74	22.01	19.83	15.02	22.74	21.45	15.56	25.97	21.54	16.68
310	- 7.04	27.09	16.35	22.23	21.25	14.37	22.98	23.33	15.57	26.46	23.16	16.53
Parent nuclei	^{31}P	^{32}Si	^{33}S	^{34}S	^{35}Cl	^{36}Ar	^{39}K	^{40}Ar	^{42}Ca	^{43}Ca	^{44}Ca	^{46}Ca
290	13.55	15.64	14.90	10.30	14.99	16.87	15.84	10.69	12.60	12.49	9.11	6.35
291	14.16	16.43	14.40	11.01	16.04	18.05	16.30	11.24	13.29	11.56	9.44	6.38
292	15.26	17.73	16.42	11.71	17.14	19.17	17.20	11.66	13.90	13.68	9.92	6.52
293	16.21	18.86	16.25	12.55	18.10	20.32	18.35	12.84	14.60	13.19	10.46	6.88
294	17.17	20.01	18.78	13.33	19.42	22.08	20.15	13.96	15.42	14.94	10.95	7.16
295	17.66	21.37	18.52	14.34	20.54	23.24	21.27	15.21	17.00	14.54	11.31	7.42
296	17.91	22.16	20.21	14.86	21.23	24.04	22.32	15.95	17.75	16.49	11.48	7.31
297	18.72	23.05	20.01	15.65	22.09	25.63	23.63	16.78	19.00	16.09	12.46	7.49
298	19.46	23.88	22.41	16.46	23.45	26.70	24.91	17.47	20.14	18.87	13.57	8.09
299	20.40	25.71	21.81	17.08	24.31	27.85	25.83	18.85	21.73	18.93	14.49	9.18
300	21.33	26.74	24.09	17.53	25.05	28.79	26.65	19.26	22.48	20.85	15.07	9.52
301	22.53	26.50	23.76	18.61	25.87	29.36	27.60	19.79	23.20	20.15	15.62	10.09
302	23.50	27.45	24.75	19.21	25.72	30.38	28.30	20.00	23.68	22.19	15.96	10.46
303	24.26	28.85	23.90	18.55	26.76	31.58	28.97	20.55	24.15	21.28	16.49	10.69
304	25.38	29.80	26.56	19.08	27.83	32.62	29.93	21.10	24.44	22.97	16.86	10.73

corresponding half-lives are tabulated in Table 4. From the figure and table, we have observed that the alpha decay half-lives were smaller when compared to different cluster emissions.

5 Conclusions

The present work used eight different proximity functions in the modified liquid drop model [MGLDM] to study the cluster and alpha decay half-lives in the superheavy nuclei $Z = 120$. We have explored the proximity function suitable in MGLDM for the cluster and alpha radioactivity of superheavy nuclei. The present work is useful in the study of decay modes of superheavy nuclei $Z = 120$.

References

1. A. Sandulescu, D.N. Poenaru, W. Greiner, *Sov. J. Part. Nucl.* **11**, 528 (1980)
2. H.J. Rose, G.A. Jones, *Nature* **307**, 245 (1984)
3. D.N. Poenaru, R.A. Gherghescu, W. Greiner, *Phys. Rev. Lett.* **107**, 062503 (2011)
4. D.N. Poenaru, R.A. Gherghescu, W. Greiner, *Phys. Rev. C* **85**, 034615 (2012)
5. D.N. Poenaru, M. Ivascu, A. Sandulescu, W. Greiner, *Phys. Rev. C* **32**, 572 (1985)
6. W. Greiner, M. Ivascu, D.N. Poenaru, A. Sandulescu, *Z. Phys. A* **320**, 347 (1985)
7. D.N. Poenaru, W. Greiner, K. Depta, M. Ivascu, D. Mazilu, A. Sandulescu, *At. Data Nucl. Data Tables* **34**, 423 (1986)
8. Y.J. Shi, W.J. Swiatecki, *Phys. Rev. Lett.* **54**, 300 (1985)
9. G. A. Pik-Pichak, *Fiz. Elem. Chastits At. Yadra* **44**, 1421 (1986); *Sov. J. Part. Nucl.* **44**, 923 (1986)
10. G. Shanmugam, B.K. Kamalharan, *Phys. Rev. C* **38**, 1377 (1988)
11. B. Buck, A.C. Merchant, *J. Phys. G* **15**, 615 (1989)
12. A. Sandulescu, R.K. Gupta, W. Greiner, F. Carstoiu, M. Horoi, *Int. J. Mod. Phys. E* **1**, 379 (1992)
13. G. Royer, R.K. Gupta, V.Yu. Denisov, *Nucl. Phys. A* **632**, 275 (1988)
14. R. K. Gupta, in *Proceedings of the 5th International Conference on Nuclear Reaction Mechanisms*, edited by E. Gadioli (Ricerca Scientifica ed Educazione Permanente, Milan, 1988), p. 416
15. S.S. Malik, R.K. Gupta, *Phys. Rev. C* **39**, 1992 (1989)
16. S. Kumar, R.K. Gupta, *Phys. Rev. C* **55**, 218 (1997)
17. R. K. Gupta, in *Heavy Elements and Related New Phenomena*, Vol. II, edited by W. Greiner and R. K. Gupta (World Scientific, Singapore, 1999), Chap. 18, p. 731
18. S.K. Arun, R.K. Gupta, B.B. Singh, S. Kanwar, M.K. Sharma, *Phys. Rev. C* **79**, 064616 (2009)
19. Y.J. Shi, W.J. Swiatecki, *Nucl. Phys. A* **438**, 450 (1985)
20. S.S. Malik, S. Singh, R.K. Puri, S. Kumar, R.K. Gupta, *Pramana. J. Phys.* **32**, 419 (1989)
21. I. Dutt, R.K. Puri, *Phys. Rev. C* **81**, 064608 (2010)
22. I. Dutt, R.K. Puri, *Phys. Rev. C* **81**, 064609 (2010)
23. G. Sawhney, K. Sandhu, M.K. Sharma, R.K. Gupta, *Eur. Phys. J. A* **50**, 175 (2014)
24. N. Malhotra, R.K. Gupta, *Phys. Rev. C* **31**, 1179 (1985)
25. H.C. Manjunatha, *Int. J. Modern Phys. E* **25**, 1650074-85 (2016)
26. H.C. Manjunatha, *Nucl. Phys. A* **945**, 42–57 (2016)
27. H.C. Manjunatha, K.N. Sridhar, *Nucl. Phys. A* **962**, 7–23 (2017)
28. H.C. Manjunatha, N. Sowmya, *Nucl. Phys. A* **969**, 68–82 (2018)
29. H.C. Manjunatha, N. Sowmya, *Int. J. Mod Phys. E* **27**(5), 1850041:1-17, (2018)
30. N. Sowmya, H.C. Manjunatha, *Proc. DAE Symp. Nucl. Phys.* **63**, 200–201 (2018)
31. H.C. Manjunatha, K.N. Sridhar, N. Sowmya *Phy. Rev. C* **98**, 024308 (2018)
32. H.C. Manjunatha, K.N. Sridhar, N. Sowmya, *Nucl. Phys. A* **987**, 382–395 (2019)
33. K.N. Sridhar, H.C. Manjunatha, H.B. Ramalingam, *Phys. Rev. C* **98**(6), 064605 (2018)
34. H.C. Manjunatha, K.N. Sridhar, *Nucl. Phys. A* **975**, 136–153 (2018)
35. N. Sowmya, H.C. Manjunatha, *Braz. J. Phys.* **49**, 874 (2019)
36. N. Sowmya, H.C. Manjunatha, *Bulg. J. Phys.* **46**, 16–27 (2019)
37. G.R. Sridhar, H.C. Manjunatha, N. Sowmya, P.S.D. Gupta, H.B. Ramalingam, *Eur. Phys. J. Plus* **135**(3), 1–28 (2020)

38. M.G. Srinivas, H.C. Manjunatha, K.N. Sridhar, N. Sowmya, Alfred Cecil Raj Nucl. Phys. A **995**, 1216 (2020)
39. N. Sowmya, H.C. Manjunatha, N. Dhananjaya, A.M. Nagaraja, J. Radioanal. Nucl. Chem. **323**(3), 1347–1351 (2020)
40. A.M. Nagaraja, H.C. Manjunatha, K.N. Sridhara, S. Alfred Cecil Raj, Bulg. J. Phys. **46**, 202–213 (2019)
41. A.M. Nagaraja, H.C. Manjunatha, N. Sowmya, S. Alfred Cecil Raj, Indian J. Pure Appl. Phys. **58**, 207–212 (2020)
42. N. Sowmya, H.C. Manjunatha, A.M. Nagaraja, N. Dhananjaya, Indian J. Pure Appl. Phys. **58**, 267–270 (2020)
43. J. Błocki, J. Randrup, W.J. Świątecki, C.F. Tsang, Ann Phys (NY) **105**, 427 (1977)
44. I Dutt, Pramana, J. Phys. **76**, 6, 921-931, (2011)
45. J. Błocki, W.J. Świątecki, Ann. Phys. (NY) **132**, 53 (1981)
46. R. Bass, Phys. Rev. Lett. **39**, 265 (1977)
47. G.L. Zhang, H.B. Zheng, W.W. Qu, Eur. Phys. J. A **49**, 10 (2013)
48. H. NgO, C. Ngo, Nucl. Phys. A **348**, 140 (1980)
49. V.Y. Denisov, Phys. Lett. B **526**, 315 (2002)
50. W.D. Myers, W.J. Świątecki, Phys. Rev. C **62**, 044610 (2000)
51. <https://www-nds.iaea.org/RIPL-3/>
52. H. Koura, T. Tachibana, M. Uno, M. Yamada, Prog. Theor. Phys. **113**, 305 (2005)
53. M. Kowal, P. Jachimowicz, J. Skalski, [arXiv:1203.5013](https://arxiv.org/abs/1203.5013)
54. H.C. Manjunatha, B.M. Chandrika, L. Seenappa, Mod. Phys. Lett. A **31**(28), 1650162 (2016)
55. H.C. Manjunatha, N.Sowmya Mod. Phys. Lett. A (2019) 1650162
56. G. Audi, F. Kondev, M. Wang, W. Huang, S. Naimi, Chin. Phys. C **41**, 030001 (2017)



Heavy particle radioactivity of superheavy element $Z = 126$

A.M. Nagaraja^{a,b}, H.C. Manjunatha^{a,*}, N. Sowmya^{a,*}, L. Seenappa^a,
P.S. Damodara Gupta^a, N. Manjunatha^a, S. Alfred Cecil Raj^b

^a Department of Physics, Government College for Women, Kolar, 563101, Karnataka, India

^b Department of Physics, St. Joseph's College (Autonomous), Affiliated to Bharathidasan University, Tiruchirapalli, 62002, India

Received 2 August 2021; received in revised form 26 August 2021; accepted 27 August 2021

Available online 1 September 2021

Abstract

The concept of heavy particle radioactivity is studied using modified generalised liquid drop model (MGLDM) in the superheavy element $Z = 126$. The eight different proximity functions and different mass excess values were used to evaluate cluster/HPR. The logarithmic half-lives using different proximity functions and mass excess values are compared with that of experiments. The HPR of ^{60}Ni to ^{102}Ru have been studied in the superheavy region $^{306}126$ to $^{326}126$. The HPR half-lives has been compared with the different decay modes such as α -decay, β -decay and spontaneous fission. 9 HPR emitters, 4 α emitters, 1 β^+ emitter and 7 spontaneous fission nuclei were identified in the superheavy nuclei $^{306-314}126$, $^{315-318}126$, $^{319}126$ and $^{320-326}126$ respectively.

© 2021 Elsevier B.V. All rights reserved.

Keywords: Superheavy nuclei; Alpha-decay; Cluster-decay; Q-values

1. Introduction

One of the most unresolved question till date is the synthesis of superheavy nuclei $Z > 118$. More than thirty superheavy nuclei have been synthesized by cold and hot fusion reactions [1–5].

* Corresponding authors.

E-mail addresses: manjunthc@rediffmail.com (H.C. Manjunatha), sowmyaparakash8@gmail.com (N. Sowmya).

In addition to above experimental evidence, many attempts have been repeatedly conducted in order to synthesize the superheavy element $Z > 118$ using the projectiles such as Sc, Ti, V, Cr, Mn, Fe and Co [6,7]. Using relativistic mean field theory and self-consistent calculations [8–10] the proton magicities have been predicted for $Z = 114, 120, 124$ and 126 . Consequently, many theoretical studies propose suitable projectile target combinations to extend the periodic table up to $Z = 126$ [11–18]. Among which, the atomic number $Z = 120, 124$ and 126 are paid more attention in order to disclose the existence of magic nuclei.

The identification of the new synthesized superheavy nuclei is carried out when excited compound nuclei attains ground state through the decay modes. The transition from excited state to ground state occurs mainly by an alpha decay [19,20]. In addition spontaneous fission [21,22] is also observed in the superheavy region. Hence, main decay modes are identified as alpha and spontaneous fission in the superheavy region. In addition, cluster and heavy particle radioactivity [23–26] is also observed in the heavy and superheavy nuclei.

On the experimental side, the emission of heavier clusters (^{14}C , ^{20}O , ^{24}Ne , ^{28}Mg and ^{32}Si) leading to doubly magic nuclei ^{208}Pb [24,27,28]. The experimental confirmation of ^{24}Ne cluster from the heavy nuclei ^{232}U was attained during the year 1985 [29]. Neon cluster emissions were also successfully observed from the isotopes of uranium i.e. $^{232,234,235}\text{U}$ [30]. Cluster emission of ^{23}F and ^{24}Ne from the ^{231}Pa was experimentally observed [31]. Bonetti et al., [32] experimentally studied the $^{22,24}\text{Ne}$ cluster emission from ^{230}U . The cluster radioactivity $^{28,30}\text{Mg}$, $^{32,34}\text{Si}$ was experimentally observed in the heavy nuclei ^{238}Pu and ^{242}Cm [33].

Using super asymmetric fission model Poenaru et al., [34] predicted the cluster emission (^{12}C , ^{16}O , $^{30,32}\text{Si}$, $^{48,50}\text{Ca}$, and ^{68}Ni) half-lives of $T > 10^{40}$ s. The two-step process such as cluster formation and quantum-mechanical fragmentation was successfully explained in the heavy region [35]. Many theoretical models such as Yukawa plus exponential model (CYEM) [36], preformed cluster model (PCM) [37], mean-field HartreeFock-Bogoliubov theory [38], Coulomb and proximity potential model (CPPM) [39,40], double-folded model with the renormalized M3Y interaction (RM3Y) [41], microscopic density dependent cluster model (DDCM) [42], generalised liquid drop model [43] and effective liquid drop model [44]. All the above models predict the cluster decay half-lives, microscopic understanding of cluster decay and nuclear structure information. Among the different decay models the generalized liquid drop model which describes the process of fusion barrier [45], fission [46], cluster decay [47], investigation of charge asymmetry, deformation and proximity effects and nuclear structure parameters such as nuclear radius and mass [48,49].

Earlier, researchers have effectively used different models such as CPPM, MGLDM, ELDM and semi-empirical relations to evaluate decay modes in the heavy and superheavy nuclei [50–59]. The goal of this contribution is to study the range of isotopes in the superheavy nuclei $Z = 126$ using different proximity potentials within the modified generalised liquid drop model (MGLDM). These different versions of the proximity potentials involve different parameters and the proximity function $\phi(S_0)$. Hence, the systematic behaviours of different proximity potentials in the heavy particle radioactivity were important in order to explore the nuclear structure. By using the method of extrapolation towards the superheavy nuclei $Z = 126$ and comparison of proximity potential function with that of available experiments increases the predictive power of the model during heavy particle radioactivity half-lives. The theory used to evaluate the half-lives using different proximity potential functions is briefly described in section 2. The results using the present work are discussed in section 3. The conclusions out of the present work are given in section 4.

2. Theory

Among the various models, the MGLDM is one of the successful models which describes the fusion, fission, α and light particle emissions and nuclear structure parameters such as nuclear radius and mass, investigation of charge asymmetry, deformation and proximity effects. For a deformed nucleus, total energy is the sum of the volume (E_v), surface (E_s), coulomb (E_c) and proximity (E_{prox}) energies and the same were expressed as;

$$E = E_v + E_s + E_c + E_{prox} + E_l \quad (1)$$

For the deformed nuclei the volume (E_v), surface (E_s) and coulomb energies (E_c) are given by;

$$E_v = -15.494(1 - 1.8I^2)A \text{ MeV} \quad (2)$$

$$E_s = 17.9439(1 - 2.6I^2)A^{2/3} \frac{S}{4\pi R_0^2} \text{ MeV} \quad (3)$$

$$E_c = 0.6e^2(Z^2/R_0) \times 0.5 \int (V(\theta)/V_0)(R(\theta)/R_0)^3 \sin(\theta) d\theta \text{ MeV} \quad (4)$$

where I is the relative neutron excess, S is the surface area of the deformed nucleus, $V(\theta)$ is the electrostatic potential at the surface and V_0 is the surface potential of the sphere. When the nuclei are far apart then the equations are written as;

$$E_v = -15.494(1 - 1.8I_1^2)A_1 + (1 - 1.8I_2^2)A_2 \text{ MeV} \quad (5)$$

$$E_s = 17.9439(1 - 2.6I_1^2)A_1^{2/3} + (1 - 2.6I_2^2)A_2^{2/3} \text{ MeV} \quad (6)$$

$$E_c = 0.6e^2(Z_1^2/R_1) + 0.6e^2(Z_2^2/R_2) + e^2 Z_1 Z_2 / r \text{ MeV} \quad (7)$$

Here A_i , Z_i , R_i and I_i are with the usual notations such as mass number, atomic number, radii of the two nuclei and relative neutron excess of the two nuclei respectively. The $I_2 = 0$ such that E_v and E_s possesses negative and positive values. The radii R_i of the daughter nuclei are defined as;

$$R_i = (1.26A_i^{1/3} - 0.76 + 0.8A_i^{-1/3}) \text{ fm} \quad i = 1, 2, \dots \quad (8)$$

The centrifugal energy E_l of the emitted proton is expressed as;

$$E_l(r) = \frac{\hbar^2}{2\mu} \frac{\ell(\ell + 1)}{r^2} \quad (9)$$

where μ , ℓ and r are usual notations with reduced mass, angular momentum and the distance between the mass centers respectively. The proximity function is taken from the reference [60] and it is expressed as;

$$V_p(Z) = 4\pi\gamma\Phi\bar{R} \left(\frac{Z}{b} \right) \quad (10)$$

here ϕ is the universal proximity potential and z is the distance between the near surfaces of the fragments. $b \approx 0.99$ is the nuclear surface thickness. In the above equation (10), is the mean curvature radius and it is calculated using the following relation;

$$\bar{R} = \frac{C_1 C_2}{C_1 + C_2} \quad (11)$$

The Sussmann central radii C_i is given by;

$$C_i = R_i - \left(\frac{b^2}{R_i} \right) \tag{12}$$

sharp radii R_i is expressed as;

$$R_i = 1.28A_i^{1/3} - 0.76 + 0.8A_i^{-1/3} \tag{13}$$

In the equation (10), γ is given defined as;

$$\gamma = \gamma_0 \left[1 - I_s \left(\frac{N - Z}{A} \right)^2 \right] \text{ MeV/fm}^2 \tag{14}$$

where $\gamma_0 = 1.460734 \text{ MeV/fm}^2$ and $I_s = 4.0$ and the various universal proximity function in equation (10) is as follows.

2.1. Modified proximity potential 1977 (MP77)

Ishwar Dutt has modified the original proximity potential [60] using different data available for universal function and surface energy co-efficient. The radius formula has improved using the data available on charge distribution. The proposed proximity potential reproduced the potential barrier heights less than 5% on average and hence can be used to evaluate the fusion cross sections; The proposed proximity potential [61] function is expressed as;

$$\Phi(S) = \begin{cases} -1.7817 + 0.927S + 0.143S^2 \\ -0.09S^3 & S < 0 \\ -1.7817 + 0.927S + \\ 0.01696S^2 - 0.05148S^3 & 0 < S < 1.9475 \\ -4.41 \exp(-S/0.7176) & S > 1.9475 \end{cases} \tag{15}$$

With $S = (r - C_1 - C_2)/b$ and $b = (\pi/\sqrt{3})a$ with $a = 0.55 \text{ fm}$ [61].

2.2. Proximity 1977 (Prox77)

The generalized theorem is based on the force between two gently curved objects in close proximity is directly proportional to the interaction potential per unit area between two flat surfaces and the constant of proportionality is measure of the mean curvature of the two objects. The formula resulting in product of geometrical factor and a universal function is as follows;

$$\phi(S) = \begin{cases} \left(-\frac{1}{2} \right) (S_0 - 2.54)^2 \\ -0.0852(S_0 - 2.54)^3 & \text{for } S_0 < 1.2511 \\ -3.437 \exp\left(-\frac{S_0}{0.75} \right)^3 & \text{for } S_0 \geq 1.2511 \end{cases} \tag{16}$$

2.3. Modified proximity potential 1981 (Mp81)

The conventional proximity force theorem states that the proximity force between gently curved surfaces is directly proportional to interaction energy per unit area between two flat surfaces. The geometrical configurations will include the cases in which the shape is in the form of

single object or two or more fission fragments. The gap between two gently curved surfaces are separated or overlapped by distance S . The improved proximity potential function of the Blocki and Swiatecki [62] includes the surfaces which have large curvature which are still characterized by small angles between the significant portions of the interacting surfaces. The proposed proximity potential function is expressed as;

$$\Phi(S) = \begin{cases} -1.7817 + 0.927S + 0.143S^2 - \\ 0.090S^3 & 0 < S < 1.9475 \\ -4.41 \exp(-S/0.7176) & S > 1.9475 \end{cases} \quad (17)$$

2.4. Bass 1977 (Bass77)

Bass [63] investigated the interaction of two heavy nuclei using a simple, classical model that allows for quantitative predictions of interaction and fusion reactions, as well as angular momenta limits in surface and fusion reactions. Bass suggested an exponential factor for the proximity potential based on a model of liquid drop that consists of mutual separation of two fission fragments by change in surface energy and in multiplying geometrical argument that leads internally to nuclear part of its potential to interact. The effective potential is expressed as;

$$E^{Prox} = -\frac{d}{R_{12}} a_s A_1^{1/3} A_2^{1/3} \exp\left(-\frac{r - R_1}{d}\right) \quad (18)$$

where $R_{12} = r_0(A_1^{1/3} + A_2^{1/3})$, r is the separation distance, $d = 1.35$ fm and $a_s = 17.0$ MeV [60]. By using liquid drop model and geometric interpretations, the nuclear interaction is taken from proximity method and it is given by:

$$E^{Prox} = -\frac{R_1 R_2}{R_1 R_2} \Phi(r - R_1 - R_2) \quad (19)$$

Universal function $\phi(r - R_1 - R_2)$ has the following form;

$$\phi(S) = \left[A \exp\left(\frac{S}{d_1}\right) + B \exp\left(\frac{S}{d_2}\right) \right]^{-1} \quad (20)$$

with $A = 0.030$ fm/MeV, $B = 0.0061$ fm/MeV, $d_1 = 3.30$ fm and $d_2 = 0.65$ fm [64].

2.5. Proximity 2013 (Prox 13)

When the overlap of two nuclei increases, the proximity potential model becomes less accurate due to complication of nuclear potential at the small distance in the overlap region of nuclear surfaces. While, double-folding model (DFM) gives the average results of the effective nucleon-nucleon interaction at all nuclear densities. Surface effects from the nuclear surface region are immediately taken into consideration. Since the DFM has a great validity at the tail of the potential, Zhang et al., [65] studied the universal function using double-folding model (DFM) with the density-dependent nucleon-nucleon interaction. Then the proposed universal function and it is expressed as;

$$\phi(S_0) = \frac{P_1}{1 + \exp\left(\frac{S_0 + P_2}{P_3}\right)} \quad (21)$$

with $S_0 = \frac{R-R_1-R_2}{b}$ and P_1 , P_2 and P_3 are the constants whose values are -7.65 , 1.02 and 0.89 respectively [65].

2.6. Prox Ngo 1980 (Ng80)

In 1980 Ngo [66] proposed a proximity potential between two gently curved surfaces that is a function of the separation degree of freedom and it is proportional to the interaction potential per unit area and the proximity factor is 2ϕ times the reciprocal of the square root of the Gaussian curvature of the gap width function at the point of closest approach. The force between two gently curved surfaces depends on the interaction potential between two nuclei. Ngo calculated the interaction between two heavy ions using the energy density formalism and Fermi distributions. Thus Ng80 proximity potential was constructed based on the energy density formalism and Fermi distributions. This proximity potential was constructed by considering the experimental fusion barriers.

$$\Phi(S) = \begin{cases} -33 + 5.4(S - S_0)^2 & S < S_0 \\ -33 \exp[-1/5](S - S_0)^2 & S \geq S_0 \end{cases} \quad (22)$$

where $S_0 = -1.6$ fm [66].

2.7. Denisov 2002 (DP00)

In 2002 Denisov [67] suggested the possible proximity relation through the use of semi-microscopic potential between heavy ions for the specific colliding ions in the framework of Thomas–Fermi approximation with correction term. The proton and neutron densities of each ion are obtained in the Hartree–Fock–Bogoliubov approximation with SkM* parameter set of the Skyrme force. An expression for the ion–ion potential well fits the semi-microscopic potentials in the wide range of both colliding ions and distances between them and the universal function $\phi(S = r - R_1 - R_2 - 2.65)$ is given by;

$$\Phi(S) = \begin{cases} 1 - S/0.7881663 + 1.229218S^2 \\ -0.2234277S^3 - 0.1038769S^4 \\ -\frac{R_1R_2}{R_1+R_2}(0.1844935S^2 + 0.07570101S^3 \\ + (I_1 + I_2)) \\ (0.04470645S^2 + \\ 0.0334687S^3) & \text{for } -5.65 \leq S \leq 0 \\ 1 - S^2 \left[0.05410106 \frac{R_1R_2}{R_1+R_2} \exp\left(-\frac{S}{0.7881663}\right) \right] \\ -0.5395420(I_1 + I_2) \\ \exp\left(-\frac{S}{2.424408}\right) \times \exp\left(-\frac{S}{0.7881663}\right) & \text{for } S \geq 0 \end{cases}$$

2.8. Prox 2000 (Prox 00)

Myers and Swiatecki [68] considered the nuclear properties including the surface energy coefficient and nuclear radii using nuclear parameters. The proximity 1977 treatment of nucleus–nucleus interaction is confronted with 113 measured fusion barriers specially in the superheavy region and it is expressed as;

$$\phi(S) = \begin{cases} -0.1353 + \sum_{n=0}^5 \left[\frac{C_n}{(n-1)} \right] \times \\ (2.5 - S)^{(n+1)} & 0 < S \leq 2.5 \\ -0.0955 \exp\left(\frac{2.75-S}{0.7176}\right) & S \geq 2.5 \end{cases} \quad (23)$$

The values of constant C_n are $C_0 = -0.1886$, $C_2 = 0.2628$, $C_2 = -0.15216$, $C_3 = -0.04562$, $C_4 = 0.069136$ and $C_5 = -0.011454$ [68]. The proximity and coulomb function are enough to achieve the α -decay and cluster radioactivity and the probability of penetration is studied using the WKB integration;

$$P = \exp \left[-\frac{2}{\hbar} \int_{R_{in}}^{R_{out}} \sqrt{2B(r)E(r) - E(\text{sphere})} \right] \quad (24)$$

here R_{in} and R_{out} are the inside and outside classical turning points and which can be evaluated from the condition that the $V(r = R_{in}) = V(r = R_{out}) = Q$ and μ is the reduced mass of the cluster and daughter nuclei. The half-lives of cluster emission from the superheavy nuclei $Z = 104-126$ were evaluated using the following equation;

$$T_{1/2} = \left(\frac{\ln 2}{\lambda} \right) = \left(\frac{\ln 2}{P_0 \nu P} \right) \quad (25)$$

where λ is the decay constant and it is a function of assault frequency $\nu = \left(\frac{\omega}{2\pi} \right) = \left(\frac{2E_v}{h} \right)$. Here E_v is the empirical zero point vibrational energy and it is expressed as;

$$E_v = Q \left[0.056 + 0.039 \exp\left(\frac{4 - A_e}{2.5}\right) \right] \text{ MeV} \quad (26)$$

Here A_e is the mass number of the emitted alpha and cluster particle. The term P and P_0 in equation (25) are the penetration probability and preformation probability for cluster decay. The P_0 play a major role in heavy and superheavy nuclei [69,70]. The P_0 for heavy particle radioactivity is evaluated as follows [71];

$$P_0 = 10^{aQ+bQ^2+c} \quad (27)$$

where Q is decay energy released during heavy particle radioactivity. Here, a , b and c are the fitting parameters with -0.25736 , 6.37291×10^{-4} and 3.35106 , respectively.

3. Results and discussions

The present study is carried with the two step process. Firstly, logarithmic half-lives obtained from the eight proximity potentials are compared with the available experiments. The standard deviation of logarithmic half-lives produced by using different proximity potentials are evaluated. The proximity potential which produces logarithmic half-lives with least standard deviation is identified. In the second part, the role of Q -values in the prediction of logarithmic half-lives were studied using different mass excess values such as Kourra-Tachibaba-Uno-Yamada (KTUY) [72], finite-range liquid-drop model (FRLDM) [73], Weizsacker-Skyrme (WS4) model [74], Weizsacker-Skyrme (WS)+radial basis function (RBF) i.e. WS4+RBF [74], WS3+RBF [75], WS3 [76], WS* [77]. Finally predicted the HPR half-lives by using suitable proximity function and mass excess values in the superheavy element $Z = 126$.

Table 1

Comparison of logarithmic half-lives obtained using eight proximity potentials such as MP77, Prox77 MP81, Bass77, Prox13, Ng80, DP00 and Prox00 with that of experiments.

Decay	Q_{Exp} (MeV)	$LogT_{1/2}$ (s)								
		<i>Expt.</i>	<i>MP77</i>	<i>Prox77</i>	<i>MP81</i>	<i>Bass77</i>	<i>Prox13</i>	<i>Ng80</i>	<i>DP00</i>	<i>Prox00</i>
$^{221}Fr \rightarrow ^{14}C + ^{207}Tl$	31.317	14.51 [78]	14.28	14.25	13.60	18.99	13.96	15.59	13.79	13.83
$^{221}Ra \rightarrow ^{14}C + ^{207}Pb$	32.396	13.37 [78]	13.14	13.11	12.44	19.46	12.88	14.56	12.74	12.89
$^{222}Ra \rightarrow ^{14}C + ^{208}Pb$	33.05	11.05 [79]	11.22	12.42	11.74	16.86	12.25	13.70	12.13	11.97
$^{223}Ra \rightarrow ^{14}C + ^{209}Pb$	31.829	15.05 [79]	15.29	15.27	15.28	14.66	14.54	14.94	13.16	12.83
$^{224}Ra \rightarrow ^{14}C + ^{210}Pb$	30.54	15.9 [80]	15.12	15.09	14.47	12.75	14.71	16.52	14.51	14.02
$^{226}Ra \rightarrow ^{14}C + ^{212}Pb$	28.2	21.29 [81]	20.91	20.89	20.34	20.98	20.14	22.74	19.79	19.04
$^{225}Ac \rightarrow ^{14}C + ^{211}Bi$	30.477	17.16 [82]	18.29	18.27	18.16	18.79	18.75	17.86	19.10	15.02
$^{228}Th \rightarrow ^{20}O + ^{208}Pb$	44.72	20.73 [83]	20.37	20.34	20.76	19.97	21.32	21.94	19.93	21.09
$^{230}U \rightarrow ^{22}Ne + ^{208}Pb$	61.4	19.56 [84]	18.84	18.83	18.23	21.33	19.85	19.21	19.60	19.62
$^{230}Th \rightarrow ^{24}Ne + ^{206}Hg$	57.571	24.61 [85]	24.01	23.99	25.04	27.62	24.96	23.87	22.39	20.75
$^{231}Pa \rightarrow ^{24}Ne + ^{207}Tl$	60.417	22.89 [85]	22.21	22.20	23.18	26.56	23.26	22.07	20.78	18.99
$^{232}U \rightarrow ^{24}Ne + ^{208}Pb$	62.31	20.39 [86]	21.32	21.30	22.27	25.62	20.11	21.25	21.32	21.32
$^{233}U \rightarrow ^{24}Ne + ^{209}Pb$	60.486	24.84 [85]	23.70	23.69	24.76	24.26	24.64	23.75	23.70	23.70
$^{234}U \rightarrow ^{26}Ne + ^{208}Pb$	59.466	25.93 [30,87]	24.55	27.39	25.88	23.75	26.21	24.46	24.55	27.41
$^{234}U \rightarrow ^{28}Mg + ^{206}Hg$	74.11	25.74 [88]	25.36	25.35	26.86	25.24	26.39	26.04	25.36	25.36
$^{236}Pu \rightarrow ^{28}Mg + ^{208}Pb$	79.67	21.65 [85]	21.94	21.93	20.46	21.68	20.39	22.67	21.94	21.94
$^{238}Pu \rightarrow ^{28}Mg + ^{210}Pb$	75.912	25.66 [89]	26.06	26.06	24.65	23.29	27.02	26.93	26.06	26.06
$^{238}Pu \rightarrow ^{30}Mg + ^{208}Pb$	77	25.66 [89]	24.70	24.68	23.12	23.28	26.21	25.26	24.70	24.70
$^{238}Pu \rightarrow ^{32}Si + ^{206}Hg$	91.19	25.3 [90]	26.49	26.48	25.03	23.44	24.28	27.85	26.49	26.49
$^{242}Cm \rightarrow ^{34}Si + ^{208}Pb$	96.509	23.11 [91]	22.20	22.18	23.82	22.26	24.05	23.24	22.20	22.20

Table 2

Standard deviation values between the experimental and different proximity functions such as σ_{MP77} , σ_{Prox77} , σ_{MP81} , σ_{Bass77} , σ_{Prox13} , σ_{Ng80} , σ_{DP00} and σ_{Prox00} .

σ_{MP77}	σ_{Prox77}	σ_{MP81}	σ_{Bass77}	σ_{Prox13}	σ_{Ng80}	σ_{DP00}	σ_{Prox00}
1.2586	0.544	0.546	1.298	0.624	0.406	1.587	1.54

In order to identify correct proximity function for cluster/HPR, we tried to reproduce available experimental cluster radioactivity half-lives using different proximity functions such as MP77, Prox77, MP81, Bass77, Prox13, Ng80, DP00 and Prox00. The Table 1 shows the tabulated values of logarithmic half-lives using different proximity potentials for the available experiments. In order to evaluate the $\log T_{1/2}$ values, we have considered experimental Q-values and it is tabulated in second column of the Table 1. From this table it is found that the proximity function Ng80 produces cluster-decay half-lives to closer to experiments than that of the other studied proximity potentials.

The standard deviation produced by each proximity potential is evaluated using following equations;

$$\sigma = \left(\frac{1}{(n-1)} \sum_{i=1}^n \left(\log_{1/2} T^{cal} - \log_{1/2} T^{exp} \right)^2 \right)^{1/2} \quad (28)$$

The evaluated standard deviation produced by different proximity potentials are tabulated in Table 2. From this table, it is clear that the deviation produced by proximity function Ng80 is about 0.406, which is smaller than that of other proximity potentials.

Later, we have used proximity Ng80 for the evaluation of logarithmic half-lives of heavy particle radioactivity in the superheavy nuclei $Z = 126$. In order to select the correct mass excess values for the study of HPR, Q-values corresponds to HPR were evaluated using the different mass excess values such as Kourra-Tachibaba-Uno-Yamada (KTUY) [72], finite-range liquid-drop model (FRLDM) [73], Weizsacker-Skyrme (WS4) model [74], Weizsacker-Skyrme (WS)+radial basis function (RBF) i.e. WS4+RBF [74], WS3+RBF [75], WS3 [76] and WS* [77]. The Q-values produced by the different mass excess were used to predict experimental HPR half-lives using Ng80 proximity potential. The Table 3 shows the logarithmic half-lives evaluated using different mass excess values along with the experimental cluster/HPR half-lives. The standard deviation is found using equation (28). The evaluated standard deviation of logarithmic half-lives obtained using different mass excess values [73–77] is shown in Table 4. From the table, it is clearly observed that the cluster/HPR half-lives obtained using mass excess values of FRLDM shows smaller deviation of about 0.33 when compared to other mass excess values available in the literature. However, the standard deviation produced WS4+RBF (0.84) and WS4(0.80) mass excess values are larger when compared to that of FRLDM.

In a systematic search for the suitable proximity potential and mass excess values, we are successfully identified proximity function Ng80 and mass excess values from FRLDM which produces cluster/HPR half-lives close to experiment. With this confidence, we have extended evaluation of HPR in the superheavy element $Z = 126$. The HPR is considered such that $Z_e^{min} = 28$ and maximum heavy particle emission is $Z_e^{max} = Z - 82$ [23]. Hence, we considered HPR of ^{60}Ni to ^{102}Ru from the superheavy nuclei $^{306}126$ to $^{326}126$. The Fig. 1 shows the variation of logarithmic half-lives as a function of neutron number of parent nuclei during HPR of ^{60}Ni to ^{102}Ru in the superheavy region $^{306}126$ to $^{326}126$. A small value of $\log T_{1/2}$ is observed in case of $N = 184$ which is near magic nuclei. Again gradual increase has been observed when the

Table 3

Comparison of logarithmic half-lives evaluated using different mass excess values [73–77] and Ng80 proximity potential with that of available experimental cluster/HPR half-lives.

Decay	Q_{Exp} (MeV)	$LogT_{1/2}(s)$							
		<i>Expt.</i>	<i>KTUY</i>	<i>FRLDM</i>	<i>WS4</i>	<i>WS4 + RBF</i>	<i>WS3</i>	<i>WS3 + RBF</i>	<i>WS*</i>
$^{221}Fr \rightarrow ^{14}C + ^{207}Tl$	31.317	14.51 [90]	15.50	15.16	14.47	14.36	14.20	15.91	14.29
$^{221}Ra \rightarrow ^{14}C + ^{207}Pb$	32.396	13.37 [90]	13.76	14.01	12.30	12.67	13.03	13.71	12.66
$^{222}Ra \rightarrow ^{14}C + ^{208}Pb$	33.05	11.05 [90]	11.18	12.38	11.09	11.13	11.65	11.72	10.50
$^{223}Ra \rightarrow ^{14}C + ^{209}Pb$	31.829	15.05 [90]	14.65	15.09	15.44	15.26	15.07	14.09	14.47
$^{224}Ra \rightarrow ^{14}C + ^{210}Pb$	30.54	15.9 [90]	15.91	15.73	16.70	16.33	16.30	16.73	16.72
$^{226}Ra \rightarrow ^{14}C + ^{212}Pb$	28.2	21.29 [90]	21.42	21.52	22.72	22.85	22.52	22.86	22.79
$^{225}Ac \rightarrow ^{14}C + ^{211}Bi$	30.477	19.28 [90]	19.30	19.37	19.46	18.07	19.05	18.50	18.12
$^{228}Th \rightarrow ^{20}O + ^{208}Pb$	44.72	20.73 [90]	19.87	21.64	20.83	19.19	20.79	21.17	20.99
$^{230}U \rightarrow ^{22}Ne + ^{208}Pb$	61.4	19.56 [90]	20.17	19.76	21.52	18.23	19.43	18.19	19.85
$^{231}Pa \rightarrow ^{24}Ne + ^{207}Tl$	60.417	26.02 [90]	26.89	27.54	28.21	26.80	25.14	27.64	26.46
$^{233}U \rightarrow ^{24}Ne + ^{209}Pb$	60.486	24.84 [90]	25.50	23.86	23.94	23.33	24.11	24.17	25.99
$^{234}U \rightarrow ^{24}Ne + ^{210}Pb$	58.826	25.93 [90]	25.28	26.73	26.61	23.49	26.78	24.07	25.88
$^{234}U \rightarrow ^{26}Ne + ^{208}Pb$	59.466	25.93 [90]	24.55	25.73	26.70	25.52	24.09	25.86	25.16
$^{234}U \rightarrow ^{28}Mg + ^{206}Hg$	74.11	25.74 [90]	24.40	26.21	27.52	26.89	24.80	24.03	25.08
$^{236}Pu \rightarrow ^{28}Mg + ^{208}Pb$	79.67	21.65 [90]	22.72	21.17	22.79	22.13	23.05	21.38	23.13
$^{238}Pu \rightarrow ^{28}Mg + ^{210}Pb$	75.912	25.66 [90]	24.67	26.80	27.10	24.14	23.90	26.02	23.95
$^{238}Pu \rightarrow ^{32}Si + ^{206}Hg$	91.19	25.3 [90]	27.46	26.23	27.59	27.58	24.18	23.57	24.04
$^{242}Cm \rightarrow ^{34}Si + ^{208}Pb$	96.509	23.11 [90]	21.79	21.99	22.11	21.81	22.24	21.67	22.89

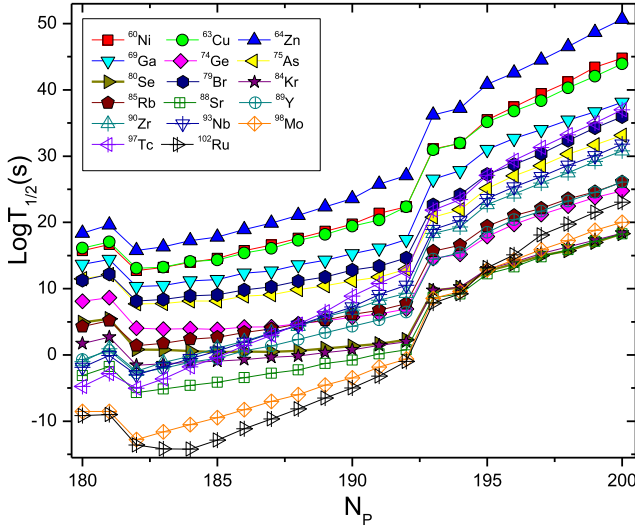


Fig. 1. The variation of heavy particle radioactivity half lives from ^{60}Ni to ^{102}Ru with the neutron number of parent in the superheavy nuclei $^{306}\text{126}$ to $^{326}\text{126}$. (For interpretation of the colours in the figure(s), the reader is referred to the web version of this article.)

Table 4

Standard deviation of logarithmic half-lives obtained using different mass excess values [73–77] with that of experiments.

KTUY	FRDM	WS4	WS4+RBF	WS3	WS3+RBF	WS1
0.48	0.33	0.80	0.84	0.46	0.71	0.44

neutron number moves away from the magic nuclei. On either side of the neutron number $N = 184$, smaller values of $\log T_{1/2}$ values were observed due to shell closures.

An effort was made to observe variation of logarithmic half-lives of HPR in the superheavy region $^{316}\text{126}$ to $^{326}\text{126}$ with the mass number of HPR. From the Fig. 2 it is observed that as the mass number of heavy particle emission increases $\log T_{1/2}$ values decreases. It is also observed that logarithmic half-lives of heavy particle emission of ^{102}Ru shows smaller value when compared to other heavy particle emissions.

The competing decay mode is identified by studying different decay modes such as α -decay [53], β -decay [92], spontaneous fission [93] and shortest half-lives among different HPR i.e. $T_{HPR} = ^{102}\text{Ru}$ were considered. The Fig. 3 shows the variation of logarithmic half-lives as function of mass number of parent nuclei. From this comparison it is clear that the superheavy nuclei $^{306,307,310}\text{126}$ having shorter half-lives when compared to other decay modes studied and alpha-decay half-lives are shorter in case of $^{309,311-318}\text{126}$. β^+ emitter is observed for the superheavy nuclei $^{319}\text{126}$ and spontaneous fission dominates in case of superheavy nuclei $Z \leq 319$.

The Table 5 shows tabulation of logarithmic half-lives of HPR of ^{102}Ru , α -decay, β -decay and spontaneous fission along with the dominant decay mode in the superheavy nuclei $^{306}\text{126}$ to $^{326}\text{126}$. The table gives better insight into dominant decay mode for the superheavy element $Z = 126$. Around 3 heavy particle emitters were observed from the superheavy nuclei $^{306}\text{126}$ to $^{314}\text{126}$. Ten α emitters, one β^+ emitter and seven spontaneous fission emitters were identified from the superheavy nuclei $^{315-318}\text{126}$, $^{319}\text{126}$ and $^{320-326}\text{126}$ respectively.

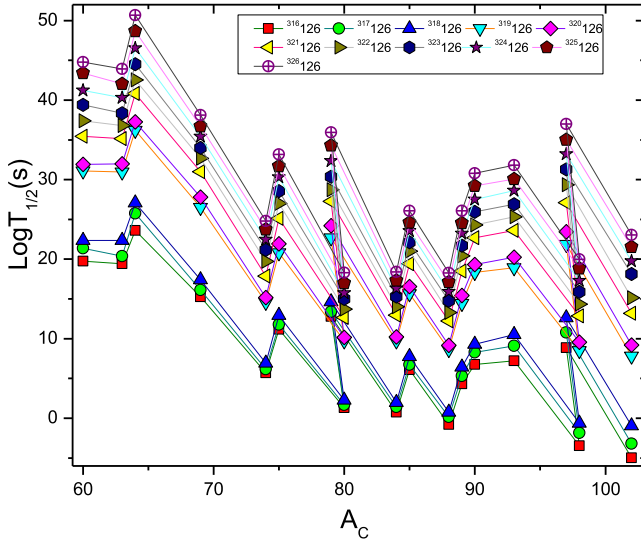


Fig. 2. The variation of logarithmic half-lives of heavy particle radioactivity from superheavy nuclei $^{316}126$ to $^{326}126$.

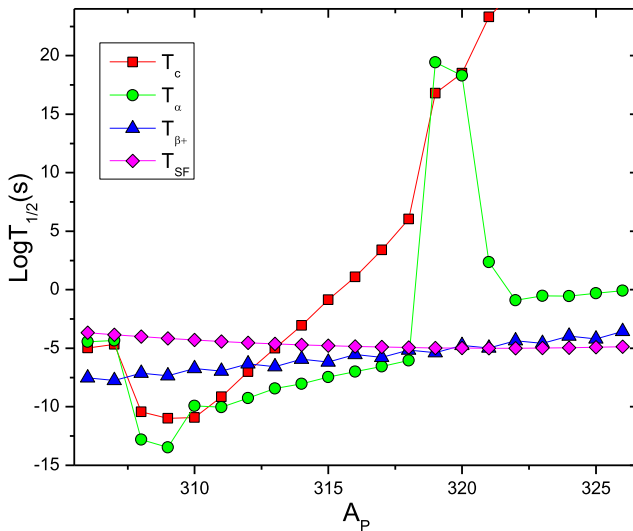


Fig. 3. Comparison of different logarithmic half-lives such as alpha decay, β -decay, heavy particle radioactivity (T_{HPR}) and spontaneous fission with that of mass number of parent nuclei in the superheavy nuclei $^{306}126$ to $^{326}126$.

4. Summary

In this work, we have evaluated HPR half-lives of superheavy nuclei $^{306}126$ to $^{326}126$ using two step process. Firstly, we have evaluated half-lives using eight proximity potentials. In the next step, using different mass excess values logarithmic half-lives were evaluated. The standard deviation obtained by both were evaluated by comparing with that of experiments. The heavy particle radioactivity of ^{60}Ni to ^{102}Ru were studied in the superheavy nuclei $^{306}126$ to $^{326}126$.

Table 5

Tabulation of $\log T_{1/2}$ values of HPR, α -decay, β -decay, spontaneous fission and dominant decay mode in the superheavy nuclei $^{306}_{126}$ to $^{326}_{126}$.

Parent nuclei	$\text{Log}T_{1/2}$				Decay mode
	HPR	α	$\beta+$	SF	
$^{306}_{126}$	-4.98	-4.44	-7.52	-3.68	HPR
$^{307}_{126}$	-4.68	-4.34	-7.75	-3.85	HPR
$^{308}_{126}$	-10.43	-12.80	-7.12	-4.01	α
$^{309}_{126}$	-10.99	-13.47	-7.36	-4.16	α
$^{310}_{126}$	-10.92	-9.92	-6.73	-4.29	HPR
$^{311}_{126}$	-9.14	-10.03	-6.96	-4.42	α
$^{312}_{126}$	-7.01	-9.26	-6.33	-4.53	α
$^{313}_{126}$	-4.99	-8.45	-6.57	-4.62	α
$^{314}_{126}$	-3.05	-8.03	-5.94	-4.71	α
$^{315}_{126}$	-0.85	-7.47	-6.17	-4.78	α
$^{316}_{126}$	1.09	-7.00	-5.54	-4.85	α
$^{317}_{126}$	3.41	-6.54	-5.78	-4.90	α
$^{318}_{126}$	6.04	-6.04	-5.15	-4.94	α
$^{319}_{126}$	16.81	19.42	-5.38	-4.97	$\beta+$
$^{320}_{126}$	18.51	18.31	-4.75	-4.99	SF
$^{321}_{126}$	23.31	2.36	-4.98	-4.99	SF
$^{322}_{126}$	25.66	-0.90	-4.36	-4.99	SF
$^{323}_{126}$	29.23	-0.53	-4.59	-4.98	SF
$^{324}_{126}$	31.18	-0.54	-3.96	-4.95	SF
$^{325}_{126}$	33.32	-0.29	-4.19	-4.92	SF
$^{326}_{126}$	35.11	-0.08	-3.56	-4.88	SF

The half-lives of superheavy nuclei $^{306}_{126}$ to $^{326}_{126}$ were evaluated using Ng80 proximity potential and FRDM mass excess values. The heavy particle radioactivity half-lives has been compared with the different decay modes such as α -decay, β -decay and spontaneous fission. Later, we have identified nine heavy particle emitters, four α emitters, one β^+ emitter and seven spontaneous fission from the superheavy nuclei $^{306-314}_{126}$, $^{315-318}_{126}$, $^{319}_{126}$ and $^{320-326}_{126}$ respectively.

CRediT authorship contribution statement

A.M. Nagaraja: Data curation. **H.C. Manjunatha:** Supervision. **N. Sowmya:** Writing – review & editing. **L. Seenappa:** Data curation. **P.S. Damodara Gupta:** Formal analysis. **N. Manjunatha:** Validation. **S. Alfred Cecil Raj:** Supervision.

Declaration of competing interest

The authors declare that they have no known competing financial interests or personal relationships that could have appeared to influence the work reported in this paper.

References

- [1] Y.T. Oganessian, V.K. Utyonkov, Y.V. Lobanov, F.S. Abdullin, A.N. Polyakov, I.V. Shirokovsky, Y.S. Tsyganov, G.G. Gulbekian, S.L. Bogomolov, B.N. Gikal, A.N. Mezentsev, S. Iliev, V.G. Subbotin, A.M. Sukhov, A.A. Voinov,

- G.V. Buklanov, K. Subotic, V.I. Zagrebaev, M.G. Itkis, J.B. Patin, K.J. Moody, J.F. Wild, M.A. Stoyer, N.J. Stoyer, D.A. Shaughnessy, J.M. Kenneally, P.A. Wilk, R.W. Lougheed, R.I. Il'kaev, S.P. Vesnovskii, Measurements of cross sections and decay properties of the isotopes of elements 112, 114, and 116 produced in the fusion reactions $^{233,238}\text{U}$, ^{242}Pu , and $^{248}\text{Cm} + ^{48}\text{Ca}$, Phys. Rev. C 70 (2004) 064609.
- [2] Y.T. Oganessian, V.K. Utyonkov, Y.V. Lobanov, F.S. Abdullin, A.N. Polyakov, R.N. Sagaidak, I.V. Shirokovsky, Y.S. Tsyganov, A.A. Voinov, G.G. Gulbekian, S.L. Bogomolov, B.N. Gikal, A.N. Mezentsev, S. Iliev, V.G. Subbotin, A.M. Sukhov, K. Subotic, V.I. Zagrebaev, G.K. Vostokin, M.G. Itkis, K.J. Moody, J.B. Patin, D.A. Shaughnessy, M.A. Stoyer, N.J. Stoyer, P.A. Wilk, J.M. Kenneally, J.H. Landrum, J.F. Wild, R.W. Lougheed, Synthesis of the isotopes of elements 118 and 116 in the ^{249}Cf and $^{245}\text{Cm} + ^{48}\text{Ca}$ fusion reactions, Phys. Rev. C 74 (2006) 044602.
- [3] Y.T. Oganessian, F.S. Abdullin, C. Alexander, J. Binder, R.A. Boll, S.N. Dmitriev, J. Ezold, K. Felker, J.M. Gostic, R.K. Grzywacz, J.H. Hamilton, R.A. Henderson, M.G. Itkis, K. Miernik, D. Miller, K.J. Moody, A.N. Polyakov, A.V. Ramayya, J.B. Roberto, M.A. Ryabinin, K.P. Rykaczewski, R.N. Sagaidak, D.A. Shaughnessy, I.V. Shirokovsky, M.V. Shumeiko, M.A. Stoyer, N.J. Stoyer, V.G. Subbotin, A.M. Sukhov, Y.S. Tsyganov, V.K. Utyonkov, A.A. Voinov, G.K. Vostokin, Experimental studies of the $^{249}\text{Bk} + ^{48}\text{Ca}$ reaction including decay properties and excitation function for isotopes of element 117, and discovery of the new isotope ^{277}Mt , Phys. Rev. C 87 (2013) 054621.
- [4] G. Munzenberg, S. Grevy, N. Alamanos, N. Amar, J. Angeli, R. Anne, G. Auger, F. Becker, R. Dayras, A. Drouart, et al., Experiment on the synthesis of element 113 in the reaction $^{209}\text{Bi}(^{70}\text{Zn},n)^{278}113$, Rev. Mod. Phys. 72 (2000) 733.
- [5] Y. Oganessian, Heaviest nuclei from 48Ca-induced reactions, J. Phys. G, Nucl. Part. Phys. 34 (2007) R165.
- [6] F. Heßberger, S. Hofmann, D. Ackermann, V. Ninov, M. Leino, G. Münzenberg, S. Saro, A. Lavrentev, A. Popeko, A. Yerebin, et al., Decay properties of neutron-deficient isotopes 256, 257 db, 255 rf, 252, 253 lr, Eur. Phys. J. A 12 (2001) 57.
- [7] J. Hamilton, S. Hofmann, Y.T. Oganessian, Search for superheavy nuclei, Annu. Rev. Nucl. Part. Sci. 63 (2013) 383.
- [8] S. Ćwiok, J. Dobaczewski, P.-H. Heenen, P. Magierski, W. Nazarewicz, Shell structure of the superheavy elements, Nucl. Phys. A 611 (1996) 211.
- [9] K. Rutz, M. Bender, T. Bürvenich, T. Schilling, P.-G. Reinhard, J.A. Maruhn, W. Greiner, Superheavy nuclei in self-consistent nuclear calculations, Phys. Rev. C 56 (1997) 238.
- [10] M. Bender, K. Rutz, P.-G. Reinhard, J.A. Maruhn, W. Greiner, Shell structure of superheavy nuclei in self-consistent mean-field models, Phys. Rev. C 60 (1999) 034304.
- [11] G. Adamian, N. Antonenko, W. Scheid, V. Volkov, Fusion cross sections for superheavy nuclei in the dinuclear system concept, Nucl. Phys. A 633 (1998) 409.
- [12] Y. Aritomo, T. Wada, M. Ohta, Y. Abe, Fluctuation-dissipation model for synthesis of superheavy elements, Phys. Rev. C 59 (1999) 796.
- [13] V.I. Zagrebaev, Synthesis of superheavy nuclei: nucleon collectivization as a mechanism for compound nucleus formation, Phys. Rev. C 64 (2001) 034606.
- [14] L. Zu-Hua, B. Jing-Dong, Effects of isospin equilibrium on cold fusion of superheavy nuclei, Chin. Phys. Lett. 22 (2005) 3044.
- [15] H. Manjunatha, K. Sridhar, Survival and compound nucleus probability of super heavy element $z = 117$, Eur. Phys. J. A 53 (2017) 1.
- [16] M. Itkis, E. Vardaci, I. Itkis, G. Knyazheva, E. Kozulin, Fusion and fission of heavy and superheavy nuclei (experiment), Nucl. Phys. A 944 (2015) 204.
- [17] H. Manjunatha, K. Sridhar, Projectile target combination to synthesis superheavy nuclei $z = 126$, Nucl. Phys. A 962 (2017) 7.
- [18] T. Nhan Hao, N. Duy, K. Chae, N. Quang Hung, N. Nhu Le, Investigation of the synthesis of the unknown superheavy nuclei 309, 312126, Int. J. Mod. Phys. E 28 (2019) 1950056.
- [19] Y.T. Oganessian, V.K. Utyonkov, Y.V. Lobanov, F.S. Abdullin, A.N. Polyakov, I.V. Shirokovsky, Y.S. Tsyganov, G.G. Gulbekian, S.L. Bogomolov, B.N. Gikal, A.N. Mezentsev, S. Iliev, V.G. Subbotin, A.M. Sukhov, O.V. Ivanov, G.V. Buklanov, K. Subotic, M.G. Itkis, K.J. Moody, J.F. Wild, N.J. Stoyer, M.A. Stoyer, R.W. Lougheed, Synthesis of superheavy nuclei in the $^{48}\text{Ca} + ^{244}\text{Pu}$ reaction: $^{288}114$, Phys. Rev. C 62 (2000) 041604.
- [20] Y.T. Oganessian, V. Utyonkov, Superheavy nuclei from 48Ca-induced reactions, Nucl. Phys. A 944 (2015) 62.
- [21] M. Thoennessen, Spontaneous fission, in: The Discovery of Isotopes, Springer, 2016, pp. 245–250.
- [22] D.N. Poenaru, R.A. Gherghescu, Spontaneous fission of the superheavy nucleus ^{286}Fl , Phys. Rev. C 94 (2016) 014309.
- [23] D.N. Poenaru, R.A. Gherghescu, W. Greiner, Heavy-particle radioactivity of superheavy nuclei, Phys. Rev. Lett. 107 (2011) 062503.

- [24] P.B. Price, Heavy-particle radioactivity ($a > 4$), *Annu. Rev. Nucl. Part. Sci.* 39 (1989) 19.
- [25] K.P. Santhosh, B. Priyanka, Heavy particle radioactivity from superheavy nuclei leading to 298114 daughter nuclei, *Nucl. Phys. A* 929 (2014) 20.
- [26] G. Sawhney, K. Sandhu, M.K. Sharma, R.K. Gupta, Role of nuclear deformations and proximity interactions in heavy particle radioactivity, *Eur. Phys. J. A* 50 (2014) 1.
- [27] H. Rose, G. Jones, A new kind of natural radioactivity, *Nature* 307 (1984) 245.
- [28] E. Hourani, M. Hussonnois, D. Poenaru, Radioactivities by light fragment (c, ne, mg) emission, *Ann. Phys.* 14 (1989) 311–396.
- [29] S.W. Barwick, P.B. Price, J.D. Stevenson, Radioactive decay of ^{232}U by ^{24}Ne emission, *Phys. Rev. C* 31 (1985) 1984.
- [30] R. Bonetti, C. Chiesa, A. Guglielmetti, C. Migliorino, A. Cesana, M. Terrani, P.B. Price, Neon radioactivity of uranium isotopes, *Phys. Rev. C* 44 (1991) 888.
- [31] P.B. Price, R. Bonetti, A. Guglielmetti, C. Chiesa, R. Matheoud, C. Migliorino, K.J. Moody, Emission of ^{23}F and ^{24}Ne in cluster radioactivity of ^{231}Pa , *Phys. Rev. C* 46 (1992) 1939.
- [32] R. Bonetti, C. Carbonini, A. Guglielmetti, M. Hussonnois, D. Trubert, C. Le Naour, Cluster decay of ^{230}U via ne emission, *Nucl. Phys. A* 686 (2001) 64.
- [33] K. Santhosh, B. Priyanka, M. Unnikrishnan, Cluster decay half-lives of trans-lead nuclei within the Coulomb and proximity potential model, *Nucl. Phys. A* 889 (2012) 29.
- [34] D.N. Poenaru, W. Greiner, M. Ivascu, A. Sandulescu, Heavy cluster decay of trans-zirconium “stable” nuclides, *Phys. Rev. C* 32 (1985) 2198.
- [35] S. Malik, S. Singh, R. Puri, S. Kumar, R.K. Gupta, Clustering phenomena in radioactive and stable nuclei and in heavy-ion collisions, *Pramana* 32 (1989) 419.
- [36] G. Shanmugam, B. Kamalaharan, Application of a cubic barrier in exotic decay studies, *Phys. Rev. C* 38 (1988) 1377.
- [37] S.S. Malik, R.K. Gupta, Theory of cluster radioactive decay and of cluster formation in nuclei, *Phys. Rev. C* 39 (1989) 1992.
- [38] M. Warda, L.M. Robledo, Microscopic description of cluster radioactivity in actinide nuclei, *Phys. Rev. C* 84 (2011) 044608.
- [39] Y.-J. Shi, W. Swiatecki, Estimates of radioactive decay by the emission of nuclei heavier than α -particles, *Nucl. Phys. A* 438 (1985) 450.
- [40] K. Santhosh, A. Joseph, Exotic decay in cerium isotopes, *Pramana* 58 (2002) 611.
- [41] A. Kobos, B. Brown, P. Hodgson, G. Satchler, A. Budzanowski, Folding model analysis of α -particle elastic scattering with a semirealistic density-dependent effective interaction, *Nucl. Phys. A* 384 (1982) 65.
- [42] C. Xu, Z. Ren, Global calculation of α -decay half-lives with a deformed density-dependent cluster model, *Phys. Rev. C* 74 (2006) 014304.
- [43] G. Royer, R. Moustabchir, Light nucleus emission within a generalized liquid-drop model and quasimolecular shapes, *Nucl. Phys. A* 683 (2001) 182.
- [44] M. Gonçalves, S.B. Duarte, Effective liquid drop description for the exotic decay of nuclei, *Phys. Rev. C* 48 (1993) 2409.
- [45] G. Royer, B. Remaud, Static and dynamic fusion barriers in heavy-ion reactions, *Nucl. Phys. A* 444 (1985) 477.
- [46] G. Royer, R. Gherghescu, On the formation and alpha decay of superheavy elements, *Nucl. Phys. A* 699 (2002) 479.
- [47] X. Bao, H. Zhang, B. Hu, G. Royer, J. Li, Half-lives of cluster radioactivity with a generalized liquid-drop model, *J. Phys. G, Nucl. Part. Phys.* 39 (2012) 095103.
- [48] J. Wang, H. Zhang, J. Li, α decay half-lives for $z = 108, 114, 120, 126$ isotopes and $n = 162, 184$ isotones, *J. Phys. G, Nucl. Part. Phys.* 40 (2013) 045103.
- [49] H. Zhang, W. Zuo, J. Li, G. Royer, α decay half-lives of new superheavy nuclei within a generalized liquid drop model, *Phys. Rev. C* 74 (2006) 017304.
- [50] H.C. Manjunatha, K.N. Sridhar, N. Sowmya, Investigations of the synthesis of the superheavy element $z = 122$, *Phys. Rev. C* 98 (2018) 024308.
- [51] H. Manjunatha, N. Sowmya, Decay modes of superheavy nuclei $z = 124$, *Int. J. Mod. Phys. E* 27 (2018) 1850041.
- [52] N. Sowmya, H. Manjunatha, Competition between different decay modes of superheavy element $z = 116$ and synthesis of possible isotopes, *Braz. J. Phys.* 49 (2019) 874.
- [53] H. Manjunatha, Alpha decay properties of superheavy nuclei $z = 126$, *Nucl. Phys. A* 945 (2016) 42.
- [54] H. Manjunatha, N. Sowmya, Competition between spontaneous fission ternary fission cluster decay and alpha decay in the super heavy nuclei of $z = 126$, *Nucl. Phys. A* 969 (2018) 68.
- [55] N. Sowmya, H. Manjunatha, N. Dhananjaya, A. Nagaraja, Competition between binary fission, ternary fission, cluster radioactivity and alpha decay of ^{281}ds , *J. Radioanal. Nucl. Chem.* 323 (2020) 1347.

- [56] A. Nagaraja, H. Manjunatha, N. Sowmya, N. Manjunath, S.A.C. Raj, Cluster radioactivity of superheavy nuclei 290–310 120 using different proximity functions, *Eur. Phys. J. Plus* 135 (2020) 1.
- [57] N. Sowmya, H. Manjunatha, P.D. Gupta, N. Dhananjaya, Competition between cluster and alpha decay in odd z superheavy nuclei $111 \leq z \leq 125$, *Braz. J. Phys.* 51 (2021) 99.
- [58] N. Sowmya, H. Manjunatha, Investigations on different decay modes of darmstadtium, *Phys. Part. Nucl. Lett.* 17 (2020) 370.
- [59] N. Sowmya, H. Manjunatha, et al., Decay properties of superheavy nuclei 269–290 fl, *Phys. Part. Nucl. Lett.* 18 (2021) 177.
- [60] J. Blocki, J. Randrup, W. Świątecki, C. Tsang, Proximity forces, *Ann. Phys.* 105 (1977) 427.
- [61] I. Dutt, The role of various parameters used in proximity potential in heavy-ion fusion reactions: new extension, *Pramana* 76 (2011) 921.
- [62] J. Blocki, W. Świątecki, A generalization of the proximity force theorem, *Ann. Phys.* 132 (1981) 53.
- [63] R. Bass, Nucleus-nucleus potential deduced from experimental fusion cross sections, *Phys. Rev. Lett.* 39 (1977) 265.
- [64] Y. Yao, G. Zhang, W. Qu, J. Qian, Comparative studies for different proximity potentials applied to α decay, *Eur. Phys. J. A* 51 (2015) 1.
- [65] G. Zhang, H. Zheng, W. Qu, Study of the universal function of nuclear proximity potential between α and nuclei from density-dependent nucleon-nucleon interaction, *Eur. Phys. J. A* 49 (2013) 1.
- [66] H. Ngô, C. Ngô, Calculation of the real part of the interaction potential between two heavy ions in the sudden approximation, *Nucl. Phys. A* 348 (1980) 140.
- [67] V. Denisov, Interaction potential between heavy ions, *Phys. Lett. B* 526 (2002) 315.
- [68] W. Myers, W. Świątecki, Nucleus-nucleus proximity potential and superheavy nuclei, *Phys. Rev. C* 62 (2000) 044610.
- [69] R. Blendowske, H. Walliser, Systematics of cluster-radioactivity-decay constants as suggested by microscopic calculations, *Phys. Rev. Lett.* 61 (1988) 1930.
- [70] K. Wei, H.F. Zhang, Cluster preformation law for heavy and superheavy nuclei, *Phys. Rev. C* 96 (2017) 021601.
- [71] K.P. Santhosh, C. Nithya, Systematic studies of α and heavy-cluster emissions from superheavy nuclei, *Phys. Rev. C* 97 (2018) 064616.
- [72] H. Koura, T. Tachibana, M. Uno, M. Yamada, Nuclidic mass formula on a spherical basis with an improved even-odd term, *Prog. Theor. Phys.* 113 (2005) 305.
- [73] P. Möller, J. Nix, W.D. Myers, W.J. Świątecki, *At. Data Nucl. Data Tables* 59 (1995) 185.
- [74] N. Wang, M. Liu, X. Wu, J. Meng, Surface diffuseness correction in global mass formula, *Phys. Lett. B* 734 (2014) 215.
- [75] N. Wang, M. Liu, Nuclear mass predictions with a radial basis function approach, *Phys. Rev. C* 84 (2011) 051303.
- [76] M. Liu, N. Wang, Y. Deng, X. Wu, Further improvements on a global nuclear mass model, *Phys. Rev. C* 84 (2011) 014333.
- [77] N. Wang, Z. Liang, M. Liu, X. Wu, Mirror nuclei constraint in nuclear mass formula, *Phys. Rev. C* 82 (2010) 044304.
- [78] R. Bonetti, C. Chiesa, A. Guglielmetti, C. Migliorino, P. Monti, A. Pasinetti, H. Ravn, Carbon radioactivity of 221fr and 221ra and the hindered decay of exotic odd- a emitters, *Nucl. Phys. A* 576 (1994) 21.
- [79] P.B. Price, J.D. Stevenson, S.W. Barwick, H.L. Ravn, Discovery of radioactive decay of ²²²Ra and ²²⁴Ra by ¹⁴C emission, *Phys. Rev. Lett.* 54 (1985) 297.
- [80] E. Hourani, L. Rosier, G. Berrier-Ronsin, A. Elayi, A. Mueller, G. Rappenecker, G. Rotbard, G. Renou, A. Liebe, L. Stab, et al., Fine structure in c 14 emission from ra 223 and ra 224, *Phys. Rev. C* 44 (1991) 1424.
- [81] E. Hourani, M. Hussonnois, L. Stab, L. Brillard, S. Gales, J. Schapira, Evidence for the radioactive decay of 226ra by 14c emission, *Phys. Lett. B* 160 (1985) 375.
- [82] R. Bonetti, C. Chiesa, A. Guglielmetti, R. Matheoud, C. Migliorino, A. Pasinetti, H. Ravn, Nuclear structure effects in the exotic decay of 225ac via 14c emission, *Nucl. Phys. A* 562 (1993) 32.
- [83] R. Bonetti, C. Chiesa, A. Guglielmetti, C. Migliorino, A. Cesana, M. Terrani, Discovery of oxygen radioactivity of atomic nuclei, *Nucl. Phys. A* 556 (1993) 115.
- [84] M. Hussonnois, J. Du Le, L. Brillard, J. Dalmaso, G. Ardisson, Search for a fine structure in the c 14 decay of ra 222, *Phys. Rev. C* 43 (1991) 2599.
- [85] K. Santhosh, R. Biju, A. Joseph, A semi-empirical model for alpha and cluster radioactivity, *J. Phys. G, Nucl. Part. Phys.* 35 (2008) 085102.
- [86] S. Barwick, P. Price, J. Stevenson, Radioactive decay of u 232 by ne 24 emission, *Phys. Rev. C* 31 (1985) 1984.
- [87] K. Moody, E. Hulet, S. Wang, P. Price, Heavy-fragment radioactivity of u 234, *Phys. Rev. C* 39 (1989) 2445.

- [88] S. Tretyakova, Y.S. Zamyatin, V. Kovantsev, Y.S. Korotkin, V. Mikheev, G. Timofeev, Observation of nucleon clusters in the spontaneous decay of ^{234}U , *Eur. Phys. J. A* 333 (1989) 349.
- [89] S. Wang, D. Snowden-Ifft, P. Price, K. Moody, E. Hulet, Heavy fragment radioactivity of ^{238}Pu : Si and Mg emission, *Phys. Rev. C* 39 (1989) 1647.
- [90] J. Dong, H. Zhang, J. Li, W. Scheid, Cluster preformation in heavy nuclei and radioactivity half-lives, *Eur. Phys. J. A* 41 (2009) 197.
- [91] A. Sandulescu, W. Greiner, Cluster decays, *Rep. Prog. Phys.* 55 (1992) 1423.
- [92] X. Zhang, Z. Ren, New exponential law of β^+ -decay half-lives of nuclei far from β -stable line, *Phys. Rev. C* 73 (2006) 014305.
- [93] C. Xu, Z. Ren, Systematical law of spontaneous fission half-lives of heavy nuclei, *Phys. Rev. C* 71 (2005) 014309.

Semi-empirical formula for alpha and cluster decay half-lives of superheavy nuclei

H. C. Manjunatha*[§], N. Sowmya*[†] and A. M. Nagaraja*[‡]

*Department of Physics, Government College for Women,
Kolar 563101, Karnataka, India

[†]Department of Physics, BMSIT, Affiliated to VTU,
Bangalore 560064, Karnataka, India

[‡]Department of Physics, St. Joseph's College, Tiruchirapalli 62002,
Affiliated to Bharathidasan University, India

[§]manjunathhc@rediffmail.com

Received 15 June 2019

Revised 6 August 2019

Accepted 11 September 2019

Published 5 November 2019

We have formulated a semi-empirical formula for alpha decay half-lives and cluster decay half-lives for superheavy nuclei of atomic number range $104 \leq Z \leq 130$. We have compared the logarithmic half-lives produced by the present formula with that of experiments and other formulae, such as universal decay law (UDL) [H. C. Manjunatha and K. N. Sridhar, *Eur. Phys. J. A* **53**, 156 (2017)] and Horoi *et al.* [Horoi *et al.*, *J. Phys. G: Nucl. Part. Phys.* **30**, 945 (2004)], Univ [D. Ni and Z. Ren, *Phys. Rev. C* **74**, 014304 (2006)], Royer [G. Royer, *J. Phys. G: Nucl. Part. Phys.* **26**, 1149 (2000)] and VSS [S. A. Gurvitz and G. Kalbermann, *Phys. Rev. Lett.* **59**, 262 (1987)]. The constructed formula produces logarithmic half-lives for alpha and cluster decay (^4He , ^9Be , $^{10,11}\text{B}$, ^{12}C , ^{14}N , ^{16}O , ^{19}F , $^{20-22}\text{Ne}$, ^{23}Na , $^{24-26}\text{Mg}$, ^{27}Al , $^{28-30}\text{Si}$, ^{31}P , $^{32-34}\text{S}$, ^{35}Cl , $^{36,38,40}\text{Ar}$, $^{39,41}\text{K}$ and $^{40,42-44,46}\text{Ca}$) in superheavy nuclei of atomic number range $104 \leq Z \leq 130$.

Keywords: Superheavy element; cluster radioactivity; alpha decay.

PACS Nos.: 21.10.Dr, 21.60.Gx, 23.60.+e, 25.85.Ca

1. Introduction

There are many models such as nuclear interaction potentials and semi-empirical models for the study of alpha decay and cluster radioactivity, and these are considered as effective method to study alpha decay half-lives and cluster decay half-lives. The cluster and alpha decay¹⁻⁴ were observed at the end of 20th century. Poenaru *et al.*^{5,6} studied competition between cluster and alpha decay. Geiger and Nuttal⁷

[§]Corresponding author.

proposed empirical relation and systematically observed variation of alpha decay half-lives. Gamow⁸ explained alpha decay half-lives by quantum tunneling effect. Viola and Seaborg⁹ constructed semi-empirical relation for alpha decay half-lives. Royer¹⁰ formulated an empirical formula for alpha decay half-lives based on liquid drop model which includes proximity effects. Brown¹¹ constructed an empirical formula based on experimental variation of logarithmic half-lives. Horoi *et al.*¹² suggested a scaling law for the decay time of alpha particle and it is generalized for cluster decay. Poenaru *et al.*¹³ proposed SemFIS formula for alpha decay half-lives of superheavy nuclei taking into account of magic numbers of nucleons, the analytical super asymmetric fission model, and the universal curves. Sobiczewski and Parkhomenko¹⁴ recommended formula for alpha decay half-lives of heavy and superheavy nuclei. Poenaru *et al.*¹⁵ presented single universal curve both for alpha decay and cluster radioactivity. Using recent data in NUBASE2012, Wang *et al.*¹⁶ evaluated alpha decay half-lives in which ground state spin and parity of parent and daughter were considered. Using WKB barrier penetration probability, Ni *et al.*¹⁷ derived semi-empirical formula for alpha decay half-lives and cluster decay half-lives. Previous works^{18,19} investigated the alpha decay energies and half-lives of superheavy elements. Mirea *et al.*²⁰ studied half-lives of different decay modes in ²²²Ra. Brown²¹ proposed empirical relation for alpha decay half-lives. Sobiczewski *et al.*²² studied alpha decay and spontaneous fission in superheavy nuclei. Using different relations, Akrawy *et al.*²³ systematically studied alpha decay half-lives in the superheavy region. Earlier works^{24–31} presented empirical formula for alpha decay half-lives in the heavy nuclei. Sobiczewski and Pomorski³² studied the properties of superheavy nuclei. Dong *et al.*³³ studied the alpha decay half-lives of heavy nuclei. Using multichannel cluster model, previous works^{34,35} evaluated alpha decay half-lives of deformed nuclei. Gurvitz and Kalbermann³⁶ studied decay width and energy shift in a metastable state. Sun *et al.*^{37,38} studied alpha decay half-lives in heavy and superheavy nuclei. Greiner *et al.*³⁹ studied cluster decay in ²²³Ra. Poenaru *et al.*⁴⁰ studied shell effects and alpha decay half-lives in superheavy nuclei.

Previous works^{41–44} studied the half-lives of spontaneous fission, ternary fission and cluster decay of this predicted nuclei for $Z = 122, 124$ and 126 , and compared with that of alpha decay. We have constructed the empirical formula for fusion barrier heights (V_B), positions (R_B), curvature of the inverted parabola ($\hbar\omega$) of superheavy nuclei with atomic number range $104 \leq Z \leq 136$, by studying the fusion barrier characteristics of 14,054 projectile target combinations. The values produced by the present formula with the simple inputs of mass number (A) and atomic number (Z) are compared with experiments.⁴⁵ Previous works⁴⁶ formulated semi-empirical formula for alpha decay half-lives of heavy and superheavy nuclei. Previous works⁴⁷ also parametrized the fusion–fission cross-section in case of heavy and superheavy nuclei. An alpha decay is the most dominant decay mode in superheavy nuclei and cluster radioactivity is usually observed in superheavy nuclei. There is a need to construct the simple empirical formula for alpha and cluster decay

half-lives. Hence in this work, we have formulated a general single semi-empirical formula for alpha decay half-lives and cluster decay half-lives.

2. Theoretical Framework for Alpha Decay and Cluster Decay

2.1. Theory

To study logarithmic the half-lives of superheavy nuclei, we have investigated the alpha decay and cluster decay process using the following theoretical framework. The potential $V(R)$ is considered as the sum of the Coulomb, the nuclear and the centrifugal potentials

$$V(R) = V_C(R) + V_N(R) + V_{cf}(R). \quad (1)$$

Coulomb potential $V_C(R)$ is written as

$$V_C(R) = Z_1 Z_2 e^2 \begin{cases} \frac{1}{R}, & (R > R_C), \\ \frac{1}{2R_C} \left[3 - \left(\frac{R}{R_C} \right)^2 \right], & (R < R_C), \end{cases} \quad (2)$$

where $R_C = 1.24 \times (R_1 + R_2)$, R_1 and R_2 are, respectively, the radii of the emitted alpha/cluster and daughter nuclei. Here, Z_1 and Z_2 are the atomic numbers of the daughter and emitted cluster the nuclear potential $V_N(R)$ is calculated from the proximity potential and it is given as

$$V_N(z) = 4\pi\gamma \left[\frac{C_1 C_2}{C_1 + C_2} \right] \Phi(\xi). \quad (3)$$

Using the droplet model,⁴⁸ matter radius C_i was calculated as

$$C_i = R_i + \frac{N_i}{A_i} t_i, \quad (4)$$

with

$$R_i(\alpha_i) = R_{0i} \left[1 + \sum_l b_l Y_\lambda^{(0)}(\alpha_i) \right]. \quad (5)$$

Here, α_i is the angle between the radius vector and symmetry axis of the i th nuclei. For this potential, R_{0i} denotes the half-density radii of the charge distribution and t_i is the neutron skin of the nucleus. The nuclear charge, is given by the relation

$$R_{00i} = 1.24 A_i^{1/3} \left(1 + \frac{1.646}{A_i} - 0.191 \frac{A_i - 2Z_i}{A_i} \right) \text{ fm}, \quad (i = 1, 2). \quad (6)$$

The half-density radius c_i was obtained from the relation

$$R_{0i} = R_{00i} \left(1 - \frac{7}{2} \frac{b^2}{R_{00i}^2} - \frac{49}{8} \frac{b^4}{R_{00i}^4} + \dots \right), \quad (i = 1, 2). \quad (7)$$

Using the droplet model, neutron skin t_i reads as

$$t_i = \frac{3}{2}r_0 \left(\frac{JI_i - \frac{1}{12}c_1Z_iA_i^{-1/3}}{Q + \frac{9}{4}JA_i^{-1/3}} \right), \quad (i = 1, 2), \quad (8)$$

where r_0 is 1.14 fm, the value of the nuclear symmetric energy coefficient $J = 32.65$ MeV, $I_i = (N_i - A_i)/Z_i$ and $c_1 = 3e^2/5r_0 = 0.757895$ MeV. The neutron skin stiffness coefficient Q was taken to be 35.4 MeV. The nuclear surface energy coefficient γ in terms of neutron skin was given as

$$\gamma = \frac{1}{4\pi r_0^2} \left[18.63 \text{ (MeV)} - Q \frac{t_1^2 + t_2^2}{2r_0^2} \right], \quad (9)$$

where t_1 and t_2 were calculated using the above equation. The universal function for this is given by

$$\Phi(\xi) = -0.1353 + \sum_{n=0}^5 \frac{c_n}{(n+1)} (2.5 - \xi)^{n+1} \quad \text{for } 0 \leq \xi \leq 2.5, \quad (10)$$

$$\Phi(\xi) = -\exp\left(\frac{2.75 - \xi}{0.7176}\right) \quad \text{for } \xi \geq 2.5, \quad (11)$$

where $\xi = R - C_1 - C_2$. The values of different constants c_n , where $c_0 = -0.1886$, $c_1 = -0.2628$, $c_2 = -0.15216$, $c_3 = -0.04562$, $c_4 = 0.069136$, and $c_5 = -0.011454$.

The Langer modified centrifugal barrier is adopted⁴⁹ in the present calculation

$$V_{cf} = \frac{h(l + \frac{1}{2})^2}{4\pi \times \mu R^2}. \quad (12)$$

According to the Wentzel-Kramers-Brillouin (WKB) approximation, the penetration probability P through the potential barrier is studied by the following equation:

$$P = \exp\left\{-\frac{2}{\hbar} \int_{R_a}^{R_b} \sqrt{2\mu(V_T(r) - Q)} dr\right\}, \quad (13)$$

where μ is the reduced mass alpha decay or cluster decay system, R_a/R_c and R_b are the inner and outer turning points and these turning points are calculated by

$$V_T(R_a/R_c) = Q = V_T(R_b). \quad (14)$$

The decay half-life of parent nuclei with the emission of alpha particle or cluster particle is studied by

$$T_{1/2} = \frac{\ln 2}{\lambda} = \frac{\ln 2}{\nu P}, \quad (15)$$

where λ is the decay constant and ν is the assault frequency and is expressed as

$$\nu = \frac{\omega}{2\pi} = \frac{2E_\nu}{\hbar}, \quad (16)$$

where E_ν is the empirical vibrational energy.⁵⁰

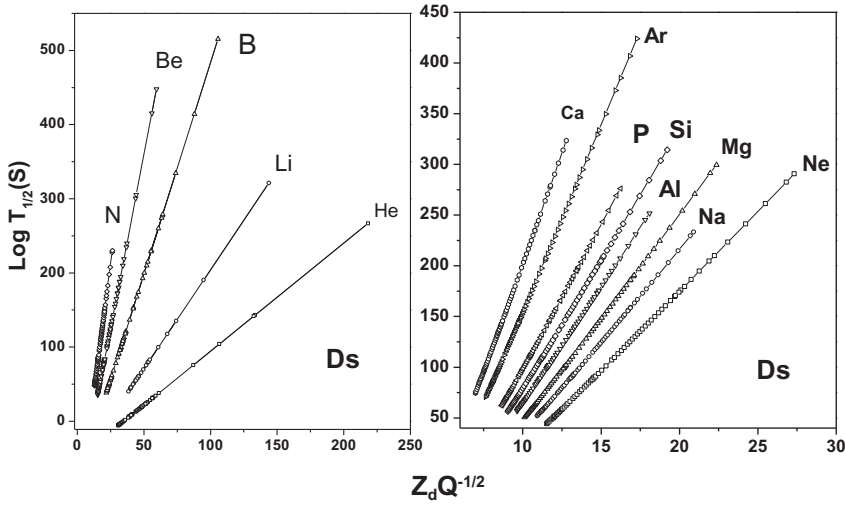


Fig. 1. The variation of logarithmic half-lives as a function of product of atomic number of daughter and inverse square root of energy released during the decay process for parent nuclei with $Z = 110$.

2.2. Derivation of universal semi-empirical formula for alpha decay and cluster decay

After evaluating the half-lives of alpha decay and cluster decay in the superheavy region $104 \leq Z \leq 130$, we have constructed universal semi-empirical formula for alpha decay and cluster decay. Derivation of semi-empirical formula is based on the following procedure. The variation of logarithmic half-lives with the product of atomic number of daughter and square root of reciprocal of energy released ($Z_d Q^{-1/2}$) is found to be linear. Figure 1 shows that variation of logarithmic half-lives with $Z_d Q^{-1/2}$ for instance parent nuclei $Z = 110$. From this figure, it is found that the linear equation is enough to fit for logarithmic half-lives in terms of $Z_d Q^{-1/2}$. The fitted equation for logarithmic half-lives in terms of $Z_d Q^{-1/2}$ is as follows:

$$\log_{10} T_{1/2} = A(Z_d Q^{-1/2}) + B. \quad (17)$$

In the above equation, A and B are the fitting parameters which depend on type of the cluster emitted and the parent nuclei. We can express the fitting parameters A and B as follows:

$$A = A(Z_c A_c) \quad \text{and} \quad B = B(Z_c A_c). \quad (18)$$

The fitting parameters A and B are evaluated by studying the variation of A and B with $Z_c A_c^{-1/3}$, where Z_c is the atomic number of cluster and A_c is the mass number of clusters. Figure 2 shows the variation of fitting constants (A and B) with product of atomic number and mass of cluster ($Z_c A_c^{-1/3}$) for instance $Z = 110$.

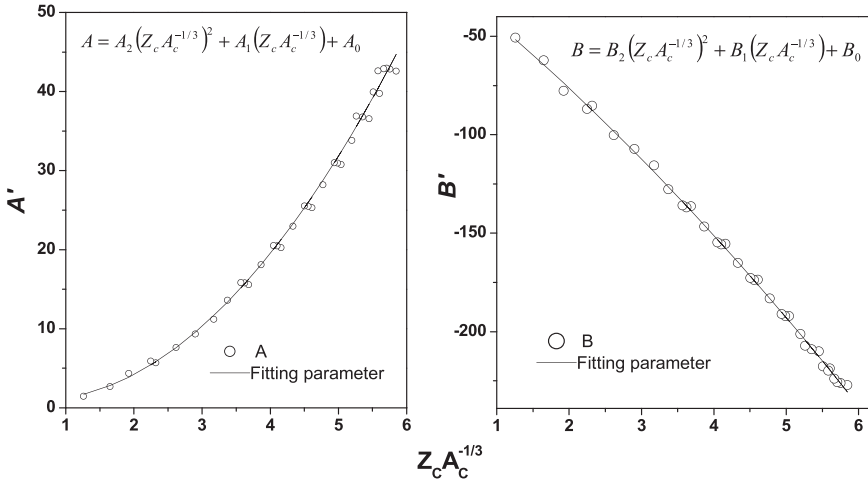


Fig. 2. Variation of fitting constants (A and B) with product of atomic number and mass of cluster ($Z_c A_c^{-1/3}$) for $Z = 110$.

Similar variation is observed for all the superheavy nuclei with atomic number range $104 \leq Z \leq 130$. Probability of emission of cluster depends on the size of the cluster and charge of the cluster. Hence, we attempt to parametrize them in terms of $Z_c A_c^{-1/3}$. Encouragingly, it can be seen that this function is also best suit function. By studying this variation we have fitted an equation for A 's and B 's in terms of $Z_c A_c^{-1/3}$.

$$A = A_2(Z_c A_c^{-1/3})^2 + A_1(Z_c A_c^{-1/3}) + A_0, \quad (19)$$

$$B = B_2(Z_c A_c^{-1/3})^2 + B_1(Z_c A_c^{-1/3}) + B_0. \quad (20)$$

Here, A_2 , A_1 , A_0 and B_2 , B_1 , B_0 are the fitting parameters which depend on the atomic number of the parent nuclei. So that we can express the above fitting parameters as $A_2 = A_2(Z)$, $A_1 = A_1(Z)$, $A_0 = A_0(Z)$, $B_2 = B_2(Z)$, $B_1 = B_1(Z)$, and $B_0 = B_0(Z)$. These fitting parameters are evaluated by studying the variation of A_2 , A_1 , A_0 , B_2 , B_1 and B_0 with the atomic number of parent nuclei. Figure 3 shows the variation of A_2 , A_1 , A_0 , B_2 , B_1 and B_0 with atomic number of parent nuclei. From this figure it is observed that there is systematic variation of fitting parameters with the atomic number of parent nuclei. We have fitted second-order polynomial for these fitting parameters in terms of atomic number of parent nuclei.

$$A_2 = \sum_{i=0}^2 A_{2i} Z^i, \quad A_1 = \sum_{i=0}^2 A_{1i} Z^i \quad \text{and} \quad A_0 = \sum_{i=0}^2 A_{0i} Z^i, \quad (21)$$

$$B_2 = \sum_{i=0}^2 0.53 \times B_{2i} Z^i, \quad B_1 = \sum_{i=0}^2 0.53 \times B_{1i} Z^i \quad \text{and} \quad B_0 = \sum_{i=0}^2 B_{0i} Z^i. \quad (22)$$

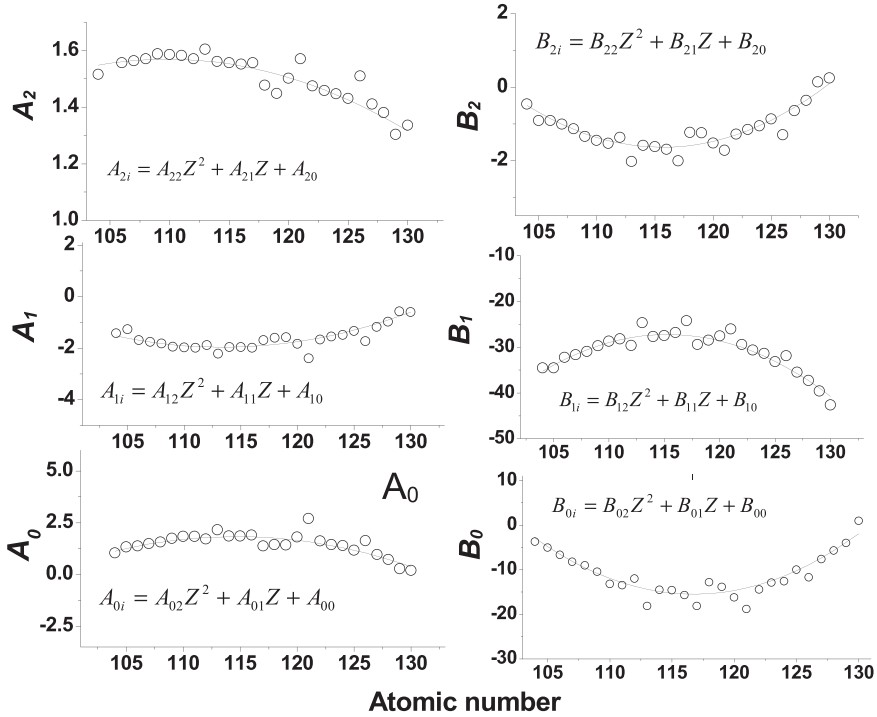


Fig. 3. Variation of A_2 , A_1 , A_0 , B_2 , B_1 and B_0 with atomic number of parent nuclei.

Table 1. Co-efficient sets of A^i and B^i .

i	A_{2i}	A_{1i}	A_{0i}	B_{2i}	B_{1i}	B_{0i}
2	-6.19E-04	4.93E-03	-6.17E-03	8.41E-03	-6.28E-02	7.73E-02
1	0.135994	-1.11765	1.414481	-1.94459	14.48453	-18.0448
0	-5.8946	61.40271	-79.2567	110.7946	-862.417	1037.946

In the above equations, A_{2i} , A_{1i} , A_{0i} , B_{2i} , B_{1i} and B_{0i} are the fitting parameters and it is given in Table 1. Final expression for logarithmic half-lives for alpha decay and cluster decay is constructed by substituting Eqs. (19)–(22) into Eq. (17), that is

$$\log T_{1/2} = \left\{ (Z_C A_C^{-1/3})^2 \sum_{i=0}^2 Z^i A_{2i} + (Z_C A_C^{-1/3}) \sum_{i=0}^2 Z^i A_{1i} + \sum_{i=0}^2 Z^i A_{0i} \right\} \\ \times \frac{Z_d Q^{-1/2}}{2} + \left\{ (Z_C A_C^{-1/3})^2 \sum_{i=0}^2 0.53 \times Z^i B_{2i} \right. \\ \left. + (Z_C A_C^{-1/3}) \sum_{i=0}^2 0.53 \times Z^i B_{1i} + \sum_{i=0}^2 Z^i B_{0i} \right\}. \quad (23)$$

This formula produces logarithmic half-lives for alpha and cluster decay from parent superheavy nuclei in the atomic number range $104 \leq Z \leq 130$.

3. Results and Discussions

In case of construction of formula for alpha decay half-lives, we have used the experimental half-lives available in the literature. It is observed from the literature, there is no experimental study on the cluster decay of superheavy nuclei but studies on the alpha decay of superheavy nuclei is available up to $Z = 118$. Goal of this work is to construct the semi-empirical formula for half-lives of cluster decay including alpha decay. For this, a reference data is required to evaluate the fitting parameters for cluster decay. Hence, we have first evaluated the half-lives for cluster decays using the formalism explained in Sec. 2.1, and these values are used to evaluate the fitting parameters. The values produced by the present formula is also compared with that of other models available in the literature. The amount of energy released Q (MeV) during cluster decay (${}^4\text{He}$, ${}^9\text{Be}$, ${}^{10,11}\text{B}$, ${}^{12}\text{C}$, ${}^{14}\text{N}$, ${}^{16}\text{O}$, ${}^{19}\text{F}$, ${}^{20-22}\text{Ne}$, ${}^{23}\text{Na}$, ${}^{24-26}\text{Mg}$, ${}^{27}\text{Al}$, ${}^{28-30}\text{Si}$, ${}^{31}\text{P}$, ${}^{32-34}\text{S}$, ${}^{35}\text{Cl}$, ${}^{36,38,40}\text{Ar}$, ${}^{39,41}\text{K}$ and ${}^{40,42-44,46}\text{Ca}$) including alpha decay from parent superheavy nuclei in the atomic number range $104 \leq Z \leq 130$ is calculated from the following equation:

$$Q = \delta M_P - (\delta M_i + \delta M_j) + k(Z_P^\epsilon - Z_d^\epsilon), \quad (24)$$

where δM_P , δM_i , and δM_j are the mass excess of parent and fission fragments. The last term in above equation represents the effect of atomic electrons. kZ^ϵ is the total binding energy of Z electrons in the atom, where $k = 8.7$ eV and $\epsilon = 2.517$ for $Z \geq 60$. In this work, we used the experimental mass excess values.⁵² We have considered the theoretical mass excess values⁵³⁻⁵⁶ wherever experimental mass excess values are not available. The half-lives of cluster decay (${}^4\text{He}$, ${}^9\text{Be}$, ${}^{10,11}\text{B}$, ${}^{12}\text{C}$, ${}^{14}\text{N}$, ${}^{16}\text{O}$, ${}^{19}\text{F}$, ${}^{20-22}\text{Ne}$, ${}^{23}\text{Na}$, ${}^{24-26}\text{Mg}$, ${}^{27}\text{Al}$, ${}^{28-30}\text{Si}$, ${}^{31}\text{P}$, ${}^{32-34}\text{S}$, ${}^{35}\text{Cl}$, ${}^{36,38,40}\text{Ar}$, ${}^{39,41}\text{K}$ and ${}^{40,42-44,46}\text{Ca}$) including alpha decay are evaluated for superheavy nuclei in the atomic number range $104 \leq Z \leq 130$ using the procedure explained in Sec. 2.1. We have constructed universal semi-empirical formula for alpha decay and cluster decay for superheavy nuclei of atomic number range $104 \leq Z \leq 130$ using the procedure explained in Sec. 2.2. The constructed universal formula for alpha decay and cluster decay is presented in Eq. (23). This formula produces logarithmic half-lives for alpha decay and cluster decay with simple inputs of mass number of cluster (A_c), mass number of daughter nuclei (A_d), amount of energy released during decay (Q) and atomic number of parent nuclei (Z). To validate this work, we have compared the logarithmic half-lives produced by the present formula with that of experiments and other formulae such as universal decay law (UDL)⁵¹ and Horoi *et al.*,¹² Univ,¹⁵ Royer¹⁰ and VSS.⁹

The comparison of calculated alpha half-lives with UDL,⁵¹ Horoi *et al.*,¹² Univ,¹⁵ Royer¹⁰ and VSS,⁹ and experimental values are tabulated in Table 2. From the detail literature survey, it is found that there are no experiments on the cluster

Semi-empirical formula for alpha and cluster decay half-lives of superheavy nuclei

Table 2. Comparison of half-lives (s) of this work with UDL, Horoi *et al.*, Univ, Royer and VSS and experimental values.

Isotopes	Experimental alpha decay half-lives (s)	Q_α (MeV)	Present work					
			alpha decay half-lives (s)	UDL(s)	Horoi <i>et al.</i> (s)	Univ (s)	Royer (s)	VSS (s)
$^{275}_{106}$	$144^{+4.3}_{-1.0}$ [Ref. 29]	8.65 ± 0.08	57.6	57.6	18.42	28.86	11.4	21.6
$^{271}_{106}$	$114^{+2.4}_{-0.6}$ [Ref. 26]	8.54 ± 0.08	90.6	90.6	45	62.4	30.6	59.4
$^{274}_{107}$	53^{+250}_{-24} [Ref. 27]	8.93 ± 0.08	9.51	6.88	8.51	3.56	6.86	12.58
$^{275}_{108}$	$0.19^{+0.22}_{-0.07}$ [Ref. 26]	9.30 ± 0.06	1.28	1.44	1.51	0.59	1.13	2.01
$^{275}_{108}$	$0.15^{+0.27}_{-0.06}$ [Ref. 29]	9.44 ± 0.07	0.76	0.60	0.62	0.23	0.43	0.77
$^{275}_{109}$	$0.097^{+46}_{-4.4}$ [Ref. 30]	10.48	12.49×10^{-3}	3.60×10^{-3}	2.92×10^{-3}	0.864×10^{-3}	1.39×10^{-3}	2.32×10^{-3}
$^{278}_{109}$	$7.7^{+37}_{-3.5}$ [Ref. 27]	9.69 ± 0.19	0.19	0.27	0.26	0.09	0.17	0.31
$^{279}_{110}$	$0.18^{+0.05}_{-0.03}$ [Ref. 29]	9.84 ± 0.06	0.078	0.25	0.21	0.07	0.14	0.25
$^{279}_{111}$	0.170^{+810}_{-80} [Ref. 30]	10.52	5.711×10^{-3}	0.12×10^{-3}	8.58×10^{-3}	2.60×10^{-3}	4.59×10^{-3}	7.65×10^{-3}
$^{282}_{111}$	$0.51^{+2.5}_{-0.23}$ [Ref. 27]	9.13 ± 0.10	0.998	43.07	36.43	17.62	39.15	73.54
$^{285}_{112}$	34^{+17}_{-9} [Ref. 29]	9.29 ± 0.06	0.492	31.79	25.17	11.45	25.86	50.80
$^{283}_{112}$	$4.0^{+1.3}_{-0.7}$ [Ref. 29]	9.67 ± 0.06	0.11	3.06	2.24	0.91	1.96	3.54
$^{283}_{112}$	$0.038^{+1.2}_{-0.37}$ [Ref. 26]	9.54 ± 0.06	0.18	6.86	5.03	2.18	4.79	8.66
$^{285}_{112}$	34^{+17}_{-9} [Ref. 28]	9.16 ± 0.06	0.84	74.89	59.50	29.08	66.80	131.18
$^{285}_{113}$	$5.5^{+5.0}_{-1.80}$ [Ref. 27]	9.88 ± 0.08	0.051	1.93	1.21	0.47	1.02	1.84
$^{286}_{113}$	0.02^{+94}_{-9} [Ref. 27]	9.76 ± 0.10	29.57×10^{-3}	191.3×10^{-3}	131.34×10^{-3}	46.51×10^{-3}	95.59×10^{-3}	158.4×10^{-3}
$^{283}_{113}$	0.1^{+490}_{-45} [Ref. 30]	10.26	169.822×10^{-3}	5.893	3.176	1.275	2.9141	5.473
$^{288}_{114}$	$0.018^{+2.1}_{-0.6}$ [Ref. 25]	9.83 ± 0.05	82.306×10^{-3}	1.596	1.014	0.386	0.859	1.545
$^{287}_{114}$	$0.00048^{+3.2}_{-0.09}$ [Ref. 26]	10.02 ± 0.06	0.035142	1.60	1.01	0.385	0.858	1.54
$^{289}_{114}$	$0.053^{+1.4}_{-19}$ [Ref. 28]	9.82 ± 0.06	176.523×10^{-3}	5.49	3.38	1.31	2.99	5.86
$^{288}_{114}$	$0.63^{+0.27}_{-0.14}$ [Ref. 28]	9.95 ± 0.08	0.11	2.35	1.541	0.583	1.31	2.451

Table 2. (Continued)

Isotopes	Experimental alpha decay half-lives (s)	Q_α (MeV)	Present work alpha decay half-lives (s)	UDL(s)	Horoi <i>et al.</i> (s)	Univ (s)	Royer (s)	VSS (s)
$^{286}_{114}$	$0.29^{+0.54}_{-0.11}$ [Ref. 28]	10.03 ± 0.31	0.079	1.51	0.954	0.376	0.84	1.45
$^{288}_{114}$	$0.63^{+0.27}_{-0.14}$ [Ref. 28]	9.95 ± 0.08	0.11	2.58	1.54	0.58	1.31	2.45
$^{286}_{114}$	$0.29^{+0.54}_{-0.11}$ [Ref. 28]	10.03 ± 0.31	0.079273	1.46	0.96	0.38	0.84	1.45
$^{289}_{114}$	$2.7^{+1.4}_{-0.7}$ [Ref. 29]	9.96 ± 0.06	0.12	2.283	1.454	0.526	1.171	2.29
$^{288}_{114}$	$0.8^{+0.32}_{-0.18}$ [Ref. 29]	10.09 ± 0.07	0.064	1.092	0.67	0.238	0.52	0.98
$^{287}_{114}$	$0.51^{+0.18}_{-0.10}$ [Ref. 29]	10.16 ± 0.06	0.049	0.75	0.45	0.16	0.35	0.63
$^{286}_{114}$	$0.16^{+0.07}_{-0.03}$ [Ref. 29]	10.35 ± 0.06	0.025	0.23	0.151	0.05	0.11	0.19
$^{289}_{114}$	$2.7^{+1.4}_{-0.7}$ [Ref. 29]	9.96 ± 0.06	0.10	2.28	1.45	0.53	1.17	2.29
$^{288}_{114}$	$0.8^{+0.32}_{-0.18}$ [Ref. 29]	10.09 ± 0.07	0.06	1.09	0.67	0.24	0.52	0.98
$^{289}_{115}$	0.220^{+260}_{-80} [Ref. 27]	10.45 ± 0.09	22.246×10^{-3}	0.315	0.164	0.053	0.12	0.21
$^{287}_{115}$	0.032^{+155}_{-14} [Ref. 30]	10.74	8.062×10^{-3}	57.91×10^{-3}	33.318×10^{-3}	10.39×10^{-3}	21.37×10^{-3}	35.1×10^{-3}
$^{290}_{115}$	0.016^{+75}_{-8} [Ref. 27]	10.09 ± 0.40	83.305×10^{-3}	2.36	1.29	0.48	1.1	2.1
$^{290}_{116}$	0.015^{+26}_{-26} [Ref. 23]	11.00 ± 0.08	4.826×10^{-3}	31.13×10^{-3}	15.78×10^{-3}	4.4×10^{-3}	8.943×10^{-3}	15.2×10^{-3}
$^{291}_{116}$	$0.063^{+2.5}_{+11.6}$ [Ref. 23]	10.89 ± 0.07	6.992×10^{-3}	59.46×10^{-3}	28.12×10^{-3}	7.881×10^{-3}	16.312×10^{-3}	28.88×10^{-3}
$^{292}_{116}$	0.018^{+6}_{+16} [Ref. 24]	10.80 ± 0.07	9.511×10^{-3}	87.29×10^{-3}	45.425×10^{-3}	12.71×10^{-3}	26.67×10^{-3}	49.3×10^{-3}
$^{293}_{116}$	0.053^{+19}_{+62} [Ref. 23]	10.67 ± 0.06	14.934×10^{-3}	177.1×10^{-3}	91.721×10^{-3}	26.09×10^{-3}	55.93×10^{-3}	107.9×10^{-3}
$^{286}_{116}$	$0.13^{+0.04}_{-0.02}$ [Ref. 26]	10.19 ± 0.06	0.086	2.63	1.35	0.64	1.55	2.22
$^{294}_{117}$	0.178^{+370}_{-36} [Ref. 27]	10.96 ± 0.10	9.013×10^{-3}	74.38×10^{-3}	36.193×10^{-3}	9.792×10^{-3}	20.86×10^{-3}	38.16×10^{-3}
$^{293}_{117}$	0.014^{+11}_{-4} [Ref. 27]	11.18 ± 0.08	4.315×10^{-3}	22.72×10^{-3}	11.568×10^{-3}	2.974×10^{-3}	6.071×10^{-3}	10.63×10^{-3}
$^{294}_{118}$	$0.00089^{+1.07}_{-0.31}$ [Ref. 26]	11.65 ± 0.06	1.738×10^{-3}	5.639×10^{-3}	2.054	0.471×10^{-3}	0.912×10^{-3}	1.506×10^{-3}
$^{294}_{118}$	$0.0018^{+75}_{-1.3}$ [Ref. 29]	11.81 ± 0.06	1.059×10^{-3}	1.994×10^{-3}	0.957×10^{-3}	0.208×10^{-3}	0.387×10^{-3}	0.637×10^{-3}

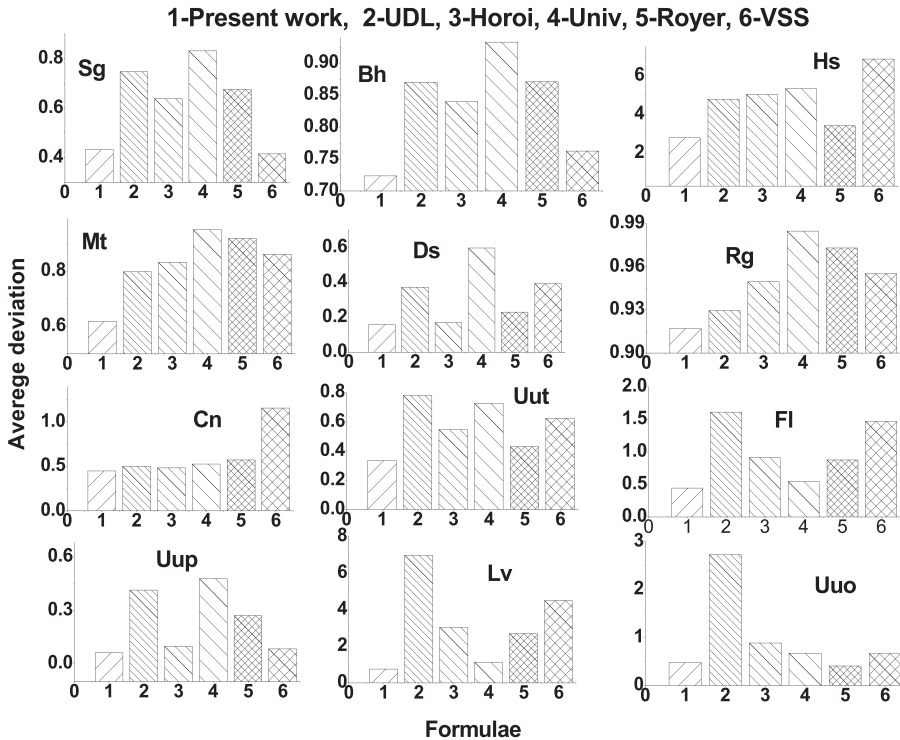


Fig. 4. The comparison of average deviation of alpha decay half-lives with atomic number for different semi-empirical relations.

decay of the superheavy nuclei, but experimental values for alpha decay in the superheavy nuclei region is available. Hence in this work, we have compared only the values produced by the present formula for alpha decay half-lives with that of the experiments. Comparison of experimental half-lives^{57–62} for alpha decay with the values produced by the present formula is as shown in Fig. 4.

We have also compared our work with calculated half-lives using different models^{17,63–67} and experimental half-lives of $Z = 114, 116$ and 118 with that of this work is tabulated in Table 3. From Table 3, it is observed that the half-lives of our work is in close agreement with the calculated and experimental half-lives in the superheavy region. Due to non-availability of experimental cluster decay half-lives in the superheavy region, we have compared cluster decay logarithmic half-lives of this work with the theoretical models such as Univ, NRDX, UDL and Horoi *et al.*, and it is tabulated in Table 4.

Since the predicted half-lives of superheavy nuclei is in close agreement with the experimental values, we have also predicted alpha decay half-lives in the superheavy region $Z = 118–126$ and it is presented in Fig. 5. To validate the logarithmic half-lives for cluster decay, we have compared this work with the other formulae available in the literature. In order to evaluate predictive power of present formula,

Table 3. Comparison of half-lives (s) of this work with Refs. 63–67.

Isotopes	Q (MeV)	$T_{1/2}^{\text{previous work}}$ (s)	$T_{1/2}^{\text{exp}}$ (s)	$T_{1/2}^{\text{present work}}$ (s)
^{286}Fl	10.35	8.48×10^{-3} [Refs. 63 and 64]	2×10^{-1}	1.05×10^{-2}
^{288}Fl	10.07	4.70×10^{-2} [Refs. 63 and 64]	6.6×10^{-1}	2.91×10^{-2}
^{286}Fl	9.94	6.14×10^{-2} [Ref. 66]	3.50×10^{-1}	4.76×10^{-2}
^{290}Lv	11	7.36×10^{-4} [Refs. 63 and 64]	8.3×10^{-3}	2.06×10^{-3}
^{292}Lv	10.78	2.51×10^{-3} [Refs. 63 and 64]	1.3×10^{-2}	4.36×10^{-3}
^{290}Lv	10.88	5.52×10^{-3} [Ref. 66]	8.00×10^{-3}	3.09×10^{-3}
^{292}Lv	10.92	1.93×10^{-2} [Ref. 66]	2.40×10^{-2}	2.70×10^{-3}
^{293}Og	12.241	0.354×10^{-3} [Ref. 65]	—	1.24×10^{-4}
^{293}Og	11.92	2.96×10^{-4} [Ref. 67]	1.00×10^{-3}	3.21×10^{-4}
^{294}Og	11.82	3.27×10^{-5} [Refs. 63 and 64]	6.9×10^{-4}	4.35×10^{-4}
^{294}Og	11.97	2.24×10^{-4} [Ref. 66]	1.15×10^{-3}	2.76×10^{-4}
^{295}Og	11.901	1.336×10^{-3} [Ref. 65]	—	3.40×10^{-4}
^{295}Og	11.7	5.49×10^{-4} [Ref. 67]	1.00×10^{-2}	6.29×10^{-4}
^{296}Og	11.655 ± 0.095	7.30×10^{-5} [Refs. 63 and 64]	8.25×10^{-4}	7.24×10^{-4}
^{296}Og	11.751	0.869×10^{-3} [Ref. 65]	—	5.37×10^{-4}
^{297}Og	12.103	0.361×10^{-3} [Ref. 65]	—	1.85×10^{-4}
^{297}Og	12	1.04×10^{-4} [Ref. 67]	—	2.52×10^{-4}

Table 4. A comparison of logarithmic half-lives (s) of this work with logarithmic half-lives (s) of UNIV, NRDX,¹⁷ UDL, and Horoi *et al.*

Isotopes		^{24}Mg	^{34}S	^{30}Si	^{40}Ca
^{263}Rf	This work	36.189	36.165	30.22	59.84
	$\text{Log } T_{1/2}^{\text{Univ}}$ (s)	44.406	41.94	37.06	64.762
	$\text{Log } T_{1/2}^{\text{NRDX}}$ (s)	45.8	45.5	41.5	68.672
	$\text{Log } T_{1/2}^{\text{UDL}}$ (s)	50.01	44.84	40.171	70.34
	$\text{Log } T_{1/2}^{\text{Horoi}}$ (s)	46.58	46.48	40.95	68.67
^{263}Rf	This work	48.49	47.546	41.016	63.85
	$\text{Log } T_{1/2}^{\text{Univ}}$ (s)	49.77	45.592	39.51	73.569
	$\text{Log } T_{1/2}^{\text{NRDX}}$ (s)	50.02	48.12	43.67	75.086
	$\text{Log } T_{1/2}^{\text{UDL}}$ (s)	56.034	49.356	43.21	80.639
	$\text{Log } T_{1/2}^{\text{Horoi}}$ (s)	52.02	50.69	43.977	77.09
^{259}Sg	This work	28.01	28.84	24.45	45.28
	$\text{Log } T_{1/2}^{\text{Univ}}$ (s)	32.57	32.05	29.41	43.8
	$\text{Log } T_{1/2}^{\text{NRDX}}$ (s)	33.4	33.58	31.153	44.73
	$\text{Log } T_{1/2}^{\text{UDL}}$ (s)	36.82	32.80	31.03	45.41
	$\text{Log } T_{1/2}^{\text{Horoi}}$ (s)	35.14	36.59	33.13	49.473

Table 4. (Continued)

Isotopes		^{24}Mg	^{34}S	^{30}Si	^{40}Ca
^{267}Bh	This work	40.182	41.35	30.45	55.89
	$\text{Log } T_{1/2}^{\text{Univ}}$ (s)	37.05	36.48	31.69	54.55
	$\text{Log } T_{1/2}^{\text{NRDX}}$ (s)	42.04	39.9	33.2	59.9
	$\text{Log } T_{1/2}^{\text{UDL}}$ (s)	42.086	38.49	33.97	58.76
	$\text{Log } T_{1/2}^{\text{Horo}}$ (s)	40.034	41.82	36.19	60.29
^{265}Hs	This work	38.18	38.31	35.75	51.89
	$\text{Log } T_{1/2}^{\text{Univ}}$ (s)	37.054	36.479	32.194	54.55
	$\text{Log } T_{1/2}^{\text{NRDX}}$ (s)	41.34	39.82	35.67	59.29
	$\text{Log } T_{1/2}^{\text{UDL}}$ (s)	42.085	38.49	34.59	58.76
	$\text{Log } T_{1/2}^{\text{Horo}}$ (s)	40.034	41.82	36.69	60.29
^{278}Mt	This work	42.7	42.21	46.17	55.63
	$\text{Log } T_{1/2}^{\text{Univ}}$ (s)	43.033	39.06	34.05	61.998
	$\text{Log } T_{1/2}^{\text{NRDX}}$ (s)	45.22	43.252	38.261	67.2
	$\text{Log } T_{1/2}^{\text{UDL}}$ (s)	49.056	41.94	37.09	67.97
	$\text{Log } T_{1/2}^{\text{Horo}}$ (s)	46.42	45.52	39.6	68.2
^{277}Ds	This work	37.85	38.65	33.04	49.93
	$\text{Log } T_{1/2}^{\text{Univ}}$ (s)	34.94	33.49	29.12	53.01
	$\text{Log } T_{1/2}^{\text{NRDX}}$ (s)	39.4	38.32	33.75	59.15
	$\text{Log } T_{1/2}^{\text{UDL}}$ (s)	39.98	35.084	31.089	57.35
	$\text{Log } T_{1/2}^{\text{Horo}}$ (s)	38.84	40.12	34.72	60.25
^{282}Rg	This work	49.42	47.13	41.64	60.85
	$\text{Log } T_{1/2}^{\text{Univ}}$ (s)	57.45	49.45	45.83	72.6
	$\text{Log } T_{1/2}^{\text{NRDX}}$ (s)	61.52	55.05	50.813	78.171
	$\text{Log } T_{1/2}^{\text{UDL}}$ (s)	64.983	54.59	51.19	80.53
	$\text{Log } T_{1/2}^{\text{Horo}}$ (s)	59.52	55.65	51.128	77.71
^{281}Cn	This work	26.12	26.87	21.51	47.05
	$\text{Log } T_{1/2}^{\text{Univ}}$ (s)	32.78	31.16	27.22	48.91
	$\text{Log } T_{1/2}^{\text{NRDX}}$ (s)	38.215	39.37	34.3	58.19
	$\text{Log } T_{1/2}^{\text{UDL}}$ (s)	37.67	32.29	28.86	52.60
	$\text{Log } T_{1/2}^{\text{Horo}}$ (s)	37.15	38.37	33.2	57.19

Table 4. (Continued)

Isotopes		²⁴ Mg	³⁴ S	³⁰ Si	⁴⁰ Ca
²⁸³ Nh	This work	25.43	26.16	20.99	46.001
	Log $T_{1/2}^{\text{Univ}}$ (s)	31.84	30.154	26.55	47.37
	Log $T_{1/2}^{\text{NRDX}}$ (s)	35.4	38.65	33.88	57.1
	Log $T_{1/2}^{\text{UDL}}$ (s)	36.62	31.072	28.097	50.81
	Log $T_{1/2}^{\text{Horoi}}$ (s)	36.44	37.552	32.88	56.098
²⁸⁹ Fl	This work	38.56	39.75	34.07	51.14
	Log $T_{1/2}^{\text{Univ}}$ (s)	37.56	36.37	32.09	55.92
	Log $T_{1/2}^{\text{NRDX}}$ (s)	43.72	45.35	38.42	63.92
	Log $T_{1/2}^{\text{UDL}}$ (s)	43.37	39.11	35.14	61.46
	Log $T_{1/2}^{\text{Horoi}}$ (s)	42.22	44.35	38.93	64.42
²⁸⁹ Mc	This work	35.87	36.98	31.79	46.69
	Log $T_{1/2}^{\text{Univ}}$ (s)	32.82	31.55	28.06	48.41
	Log $T_{1/2}^{\text{NRDX}}$ (s)	36.35	38.77	34.54	55.36
	Log $T_{1/2}^{\text{UDL}}$ (s)	37.99	33.06	30.17	52.36
	Log $T_{1/2}^{\text{Horoi}}$ (s)	37.85	39.77	35.036	57.86
²⁹² Lv	This work	38.73	38.93	33.66	48.90
	Log $T_{1/2}^{\text{Univ}}$ (s)	38.01	34.89	31.37	51.96
	Log $T_{1/2}^{\text{NRDX}}$ (s)	41.36	42.36	38.11	60.92
	Log $T_{1/2}^{\text{UDL}}$ (s)	44.05	37.41	34.41	56.88
	Log $T_{1/2}^{\text{Horoi}}$ (s)	42.86	43.36	38.61	61.42
²⁹⁴ Ts	This work	37.99	69.02	33.07	48.42
	Log $T_{1/2}^{\text{Univ}}$ (s)	36.43	74.17	30.08	50.87
	Log $T_{1/2}^{\text{NRDX}}$ (s)	40.086	77.25	37.07	60.24
	Log $T_{1/2}^{\text{UDL}}$ (s)	42.34	83.40	32.88	55.65
	Log $T_{1/2}^{\text{Horoi}}$ (s)	41.59	78.25	37.57	60.74
²⁹⁵ Og	This work	26.7	27.31	32.17	46.29
	Log $T_{1/2}^{\text{Univ}}$ (s)	33.8	31.52	28.18	46.91
	Log $T_{1/2}^{\text{NRDX}}$ (s)	37.75	39.55	35.37	56.92
	Log $T_{1/2}^{\text{UDL}}$ (s)	39.37	33.27	30.56	50.83
	Log $T_{1/2}^{\text{Horoi}}$ (s)	39.25	40.55	35.87	57.42

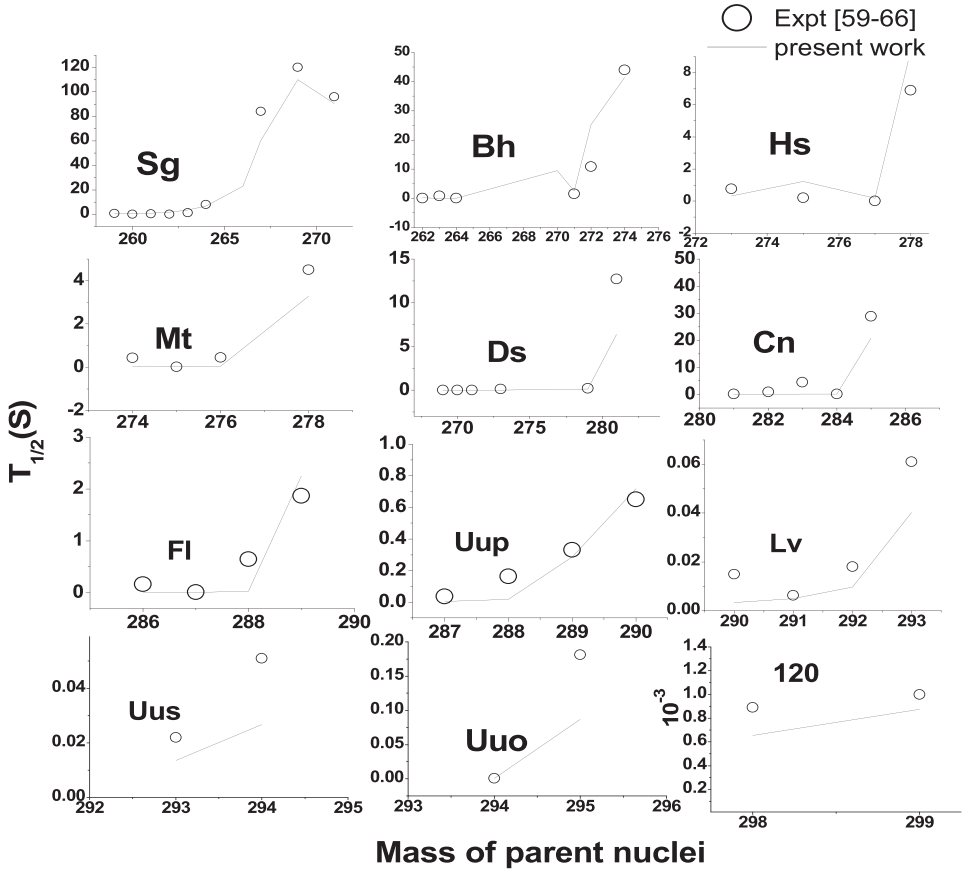


Fig. 5. A comparison of variation of available experimental values with this work.

we calculated percentage of deviation between calculated alpha decay half-lives and experimental alpha decay half-lives. The percentage of deviation are calculated from the following expression:

$$\text{Deviation} = \frac{\log_{10}(T_{1/2,i}^{\text{expt}}) - \log_{10}(T_{1/2,i}^{\text{cal}})}{\log_{10}(T_{1/2,i}^{\text{expt}})} \quad (25)$$

The average deviation factor of alpha decay half-lives for different atomic number in the superheavy region $104 \leq Z \leq 130$ is as shown in Fig. 6. The average deviation factor of present formula is small compared to UDL, Horoi *et al.*, Univ, Royer and VSS. Hence our universal semi-empirical formula produces alpha decay half-lives with less deviation than that of the other formulae such as UDL, Horoi *et al.*, Univ, Royer and VSS. The constructed formula for logarithmic half-lives of alpha decay and cluster decay is applicable only to superheavy nuclei of atomic number range $104 \leq Z \leq 130$.

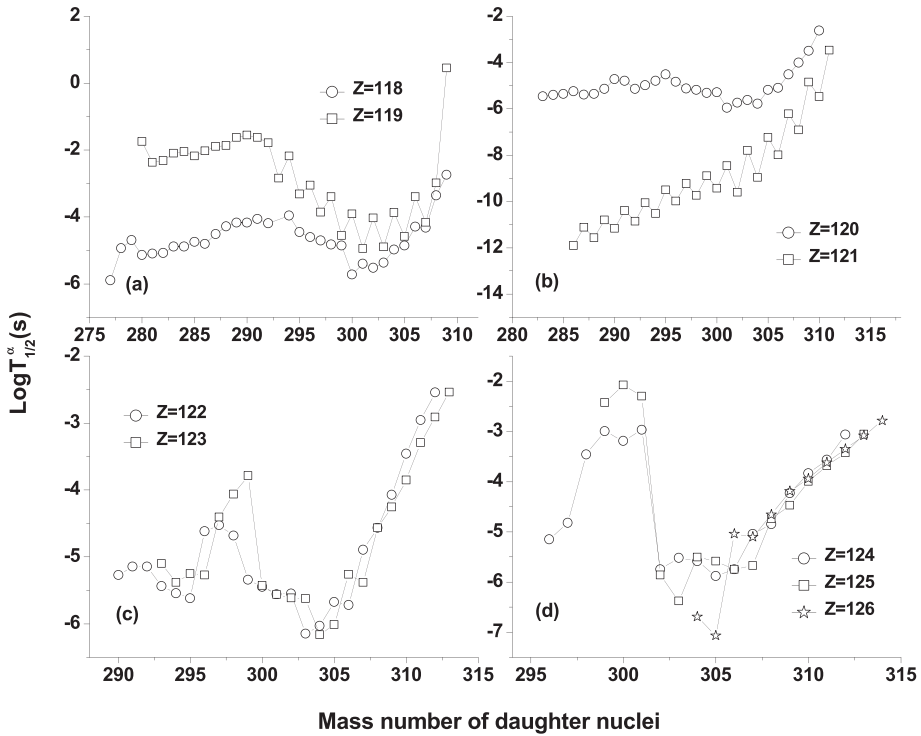


Fig. 6. A prediction of alpha decay half-lives in the superheavy region $Z = 118$ – 126 .

4. Conclusion

In this work, we have proposed a new empirical formula for alpha decay and cluster decay half-lives of superheavy region of atomic number range $104 \leq Z \leq 130$. Present formula agrees with the experiments and other formulae available in literature.

References

1. M. Greiner, W. Scheid and V. Oberacker, *Sov. J. Part. Nucl.* **11**, 528 (1980).
2. H. J. Rose and G. A. Jones, *Nature* **307**, 245 (1984).
3. J. K. Pansaers, *Comptes Rendus (Paris)* **122**, 420 (1896).
4. E. Rutherford, *Harper's Monthly Magazine* (1904), pp. 279–284.
5. D. N. Poenaru, R. A. Gherghescu and W. Greiner, *Phys. Rev. Lett.* **107**, 062504 (2011).
6. D. N. Poenaru, R. A. Gherghescu and W. Greiner, *Phys. Rev. C* **85**, 034615 (2012).
7. H. Geiger and J. M. Nuttall, *Philos. Mag.* **22**, 613 (1911).
8. G. Gamow, *Z. Phys.* **51**, 204 (1928).
9. V. E. Viola and G. T. Seaborg, *J. Inorg. Nucl. Chem.* **28**, 741 (1966).
10. G. Royer, *J. Phys. G: Nucl. Part. Phys.* **26**, 1149 (2000).
11. B. A. Brown, *Phys. Rev. C* **46**, 811 (1992).

12. M. Horoi, B. A. Brown and A. Sandulescu, *J. Phys. G: Nucl. Part. Phys.* **30**, 945 (2004).
13. D. N. Poenaru, I. H. Plonski and W. Greiner, *Phys. Rev. C* **74**, 014312 (2006).
14. A. Sobiczewski and A. Parkhomenko, *Prog. Part. Nucl. Phys.* **58**, 292 (2007).
15. D. N. Poenaru, R. A. Gherghescu and W. Greiner, *Phys. Rev. C* **83**, 014601 (2011).
16. Z. Y. Wang, Z. M. Niu, Q. Liu and J. Y. Guo, *J. Phys. G: Nucl. Part. Phys.* **42**, 5 (2015).
17. D. Ni, Z. Ren, T. Dong and C. Xu, *Phys. Rev. C* **78**, 044310 (2008).
18. Y. Z. Wang, S. J. Wang, Z. Y. Hou and J. Z. Gu, *Phys. Rev. C* **92**, 064301 (2015).
19. A. I. Budaca, R. Budaca and I. Silisteanu, *Nucl. Phys. A* **951**, 60 (2016).
20. M. Mirea, R. Budaca and A. Sandulescu, *Ann. Phys. (N. Y.)* **380**, 154 (2017).
21. B. A. Brown, *Phys. Rev. C* **46**, 811 (1992).
22. A. Sobiczewski, Z. Patyk and S. Ćwiok, *Phys. Lett. B* **224**, 1 (1989).
23. D. T. Akrawy, H. Hassanabadi, S. S. Hosseini and K. P. Santhosh, *Nucl. Phys. A* **971**, 130 (2018).
24. G. Royer, *Nucl. Phys. A* **848**, 279 (2010).
25. A. I. Budaca, R. Budaca and I. Silisteanu, *Nucl. Phys. A* **951**, 60 (2016).
26. D. N. Poenaru, I. H. Plonski and W. Greiner, *Phys. Rev. C* **74**, 014312 (2006).
27. B. Sahu, R. Paira and B. Rath, *Nucl. Phys. A* **908**, 40 (2013).
28. H. C. Manjunatha and K. N. Sridhar, *Eur. Phys. J. A* **53**, 156 (2017).
29. D. T. Akrawy and D. N. Poenaru, *J. Phys. G: Nucl. Part. Phys.* **44**, 105105 (2017).
30. R. Taagepera and M. Nurmia, *On the Relations between Half-Life and Energy Release in Alpha Decay*, Annales Academiae Scientiarum Fennicae. Series A, Vol. 78 (1961), 16 pp.
31. Z. Y. Wang, Z. M. Niu, Q. Liu and J. Y. Guo, *J. Phys. G: Nucl. Part. Phys.* **42**, 5 (2015).
32. A. Sobiczewski and K. Pomorski, *Prog. Part. Nucl. Phys.* **58**, 292 (2007).
33. J. Dong *et al.*, *Nucl. Phys. A* **832**, 198 (2010).
34. D. Ni and Z. Ren, *Phys. Rev. C* **74**, 014304 (2006).
35. C. Xu and Z. Ren, *Nucl. Phys. A* **760**, 303 (2005).
36. S. A. Gurvitz and G. Kalbermann, *Phys. Rev. Lett.* **59**, 262 (1987).
37. X. D. Sun, P. Guo and X. H. Li, *Phys. Rev. C* **93**, 034316 (2016).
38. X. D. Sun, P. Guo and X. H. Li, *Phys. Rev. C* **94**, 024338 (2016).
39. W. Greiner, M. Ivascu, D. N. Poenaru and A. Sandulescu, *Z. Phys. A* **320**, 347 (1985).
40. D. N. Poenaru, I. H. Plonski, R. A. Gherghescu and W. Greiner, *J. Phys. G: Nucl. Part. Phys.* **32**, 1223 (2006).
41. H. C. Manjunatha, K. N. Sridhar and N. Sowmya, *Phys. Rev. C* **98**, 024308 (2018).
42. H. C. Manjunatha and N. Sowmya, *Int. J. Mod. Phys. E* **27**, 1850041 (2018).
43. H. C. Manjunatha, *Nucl. Phys. A* **945**, 42 (2016).
44. H. C. Manjunatha and N. Sowmya, *Nucl. Phys. A* **969**, 68 (2018).
45. H. C. Manjunatha, K. N. Sridhar, N. Nagaraja and N. Sowmya, *Eur. Phys. J. Plus* **133**, 227 (2018).
46. H. C. Manjunatha and K. N. Sridhar, *Eur. Phys. J. A* **53**, 156 (2017).
47. H. C. Manjunatha and N. Sowmya, *Pramana-J. Phys.* **90**, 62 (2018).
48. W. D. Myers and W. J. Swiatecki, *Phys. Rev. C* **62**, 044610 (2000).
49. M. Ismail, A. Y. Ellithi, M. M. Botros and A. Adel, *Phys. Rev. C* **81**, 024602 (2010).
50. D. N. Poenaru, W. Greiner, M. Ivascu, D. Mazilu and I. H. Plonski, *Z. Phys. A* **325**, 435 (1986).
51. C. Qi, F. R. Xu, R. J. Liotta and R. Wyss, *Phys. Rev. Lett.* **103**, 072501 (2009).
52. <https://www-nds.iaea.org/RIPL-3/masses>.

53. H. Koura, T. Tachibana, M. Uno and M. Yamada, *Prog. Theor. Phys.* **113**, 305 (2005).
54. M. Kowal, P. Jachimowicz and J. Skalski, arXiv:1203.5013.
55. H. C. Manjunatha, B. M. Chandrika and L. Seenappa, *Mod. Phys. Lett. A* **31**, 1650162 (2016).
56. H. C. Manjunatha and N. Sowmya, *Mod. Phys. Lett. A* **34**, 1650162 (2019).
57. Yu. Ts. Oganessian *et al.*, *Phys. Rev. C* **69**, 054607 (2004).
58. Yu. Ts. Oganessian *et al.*, *Phys. Rev. C* **70**, 064609 (2004).
59. Yu. Ts. Oganessian *et al.*, *Phys. Rev. C* **63**, 011301 (2000).
60. Yu. Ts. Oganessian *et al.*, *Phys. Rev. C* **74**, 044602 (2006).
61. Yu. Ts. Oganessian *et al.*, *Phys. Rev. C* **83**, 054315 (2011).
62. H. Zhang, J. Li, W. Zuo, Z. Ma, B. Chen and S. Im, *Phys. Rev. C* **71**, 054312 (2005).
63. A. Sobczewsk, *Phys. Rev. C* **94**, 051302(R) (2016).
64. P. Mohr, *Phys. Rev. C* **95**, 011302(R) (2017).
65. X. J. Bao, S. Q. Guo, H. F. Zhang and J. Q. Li, *Phys. Rev. C* **95**, 034323 (2017).
66. J. G. Deng *et al.*, *Chinese Phys. C* **42**, 044102 (2018).
67. J. G. Deng, J. H. Cheng, B. Zheng and X. H. Li, *Chinese Phys. C* **41**, 124109 (2017).

An attempt to parameterize decay energies of superheavy nuclei $103 < Z < 126$ during alpha and cluster decay

H C Manjunatha^{1*}, A M Nagaraja^{1,2}, N Sowmya^{1,3} and K N Sridhar⁴

¹Department of Physics, Government College for Women, Kolar, Karnataka 563101, India

²Department of Physics, Affiliated to Bharathidasan University St. Joseph's College, Tiruchirappalli 62002, India

³Department of Physics, BMSIT&M, Affiliated to VTU, Bangalore, India

⁴Department of Physics, Government First Grade College, Kolar, Karnataka 563101, India

Received: 04 September 2020 / Accepted: 23 February 2021

Abstract: We have made an attempt to parameterize decay energies (Q) during the cluster emissions such as ${}^4\text{He}$, ${}^6\text{Li}$, ${}^9\text{Be}$, ${}^{20,22}\text{Ne}$, ${}^{23}\text{Na}$, ${}^{24-26}\text{Mg}$, ${}^{27}\text{Al}$, ${}^{28-30}\text{Si}$, ${}^{32-34}\text{S}$, ${}^{35}\text{Cl}$, ${}^{36,38,40}\text{Ar}$, ${}^{39,41}\text{K}$ and ${}^{40,42-44,46}\text{Ca}$ from the superheavy nuclei $103 < Z < 126$. We have formulated an empirical formula for decay energies of superheavy nuclei during the emission of different clusters of nuclei. To check the predictive power of constructed formula, we have compared the decay energies produced by the present formula with that of the experiments. The constructed empirical formula can reproduce the Q -values during the cluster emissions using simple inputs of mass number of daughter nuclei, atomic number of cluster emission and neutron number of parent nuclei.

Keywords: Decay energies; Alpha decay; Cluster decay

1. Introduction

The nuclear masses are the very important quantities in the nuclear physics. A large number of precise experimental data on the mass excess values have been collected by means of mass spectroscopy and the reaction Q -values. The knowledge about the Q -values has been further extended by the complete information on the binding energies. There were many remarkable successful formulae such as Weizsacker-Bethe [1, 2] mass formula. These mass formulae are not only useful for practical purpose but also gives relation between empirical and pure theories. Previous workers [3–5] studied the ground state properties within the Finite Liquid Droplet Model (FRDM). Audi et al., [5] and Goriely et al., [6] were studied the ground state properties of the nuclei within the Hartree-Fock_Bogoliubov (HFB) method. The experimental mass excess values were also included along with the FRDM and HFB-14 [7]. Audi et al., [8] presented the nuclear decay properties in the ground and isomeric states from the NUBASE

evaluation. Manjunatha et al., [9, 10] proposed semi-empirical formula for mass excess of nuclei in the atomic number range $57 < Z < 126$. The studied mass excess values using the semi-empirical formula were compared with the theoretical models such as Finite Liquid Droplet Model (FRDM) and Hartree-Fock_Bogoliubov (HFB). The proposed semi-empirical formula successfully reproduces the mass excess values, which are in agreement with the available values. Previous researchers [10] also proposed a semi-empirical formula for an alpha and cluster radioactivity, which exactly reproduces the experimental values. The experimental alpha decay half-lives of heavy nuclei were compared with the generalized liquid drop model and Viola-Seaborg-Sobiczewski formula by Royer and Zhang [11, 12] using the amount of energy released during an alpha decay. Negra et al., [13] studied the beta decay characteristics in case of neutron deficient isotopes such as Sr, Y and Zr and also deduced the mass excess values using Q_β measurements. Borrel et al., [14] studied the beta delayed two proton and mass excess values in the nuclei ${}^{31}\text{Ar}$ and ${}^{27}\text{S}$. Mayer et al., [15] investigated the mass excess values and the excited states of neutron-rich nuclei ${}^{33-35}\text{Si}$, ${}^{35-36}\text{P}$ and ${}^{37-38}\text{S}$ from the study of ${}^{14}\text{C}$ and ${}^{18}\text{O}$ induced reactions on ${}^{36}\text{S}$.

*Corresponding author, E-mail: manjunathhc@rediffmail.com

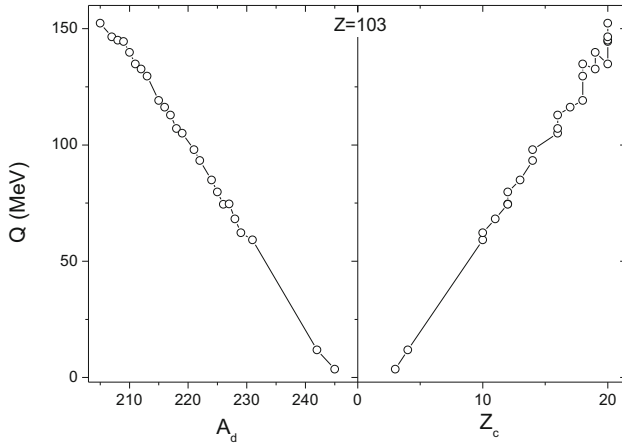


Fig. 1 The variation of Q-values with the mass number of daughter nuclei and atomic number of cluster nuclei

David [16] studied the mass excess values near the neutron-rich isotopes of iron. Scheerer et al., [17] measured Q-value of the reaction of $^{144}\text{Sm} (^3\text{He}, d)^{145}\text{Eu}$ and also evaluated the mass excess of ^{145}Eu , and it was found to be -77989KeV . Previous researchers [18, 19] experimentally measured the Q-values for the $^{40,42,51}\text{Ca}$ and hence determined the mass excess values. Earlier researchers [20–28] were extensively used the mass excess values and studied the Q-values of the reaction in heavy and superheavy nuclei region. Manjunatha et al., [29–31] were parameterized the fusion and fission cross sections, fusion barrier and barrier positions in case of heavy and superheavy heavy nuclei. From the detail study, it has been observed that there were many semi-empirical formulas for alpha and cluster decay half-lives, alpha decay energy, mass excess values, fusion and fission cross sections and fusion barriers. But there is no simple empirical formula to obtain the Q-values in case of cluster and an alpha decay. Hence, in

the present work, we made an attempt to parameterize decay energies during an alpha and cluster decay in the atomic number range $103 < Z < 126$. This paper is organized in the following order; Section 2 describes derivation of semi-empirical formula for Q-values, results and discussions were explained in Section 3 and conclusions in the Section 4.

2. Derivation of semi-empirical formula for Q-values

To derive the empirical formula for decay energy (Q) during the cluster emissions (^4He , ^6Li , ^9Be , $^{20,22}\text{Ne}$, ^{23}Na , $^{24-26}\text{Mg}$, ^{27}Al , $^{28-30}\text{Si}$, $^{32-34}\text{S}$, ^{35}Cl , $^{36,38,40}\text{Ar}$, $^{39,41}\text{K}$ and $^{40,42-44,46}\text{Ca}$), it is assumed that decay energy is directly proportional to the mass number of daughter nuclei (A_d) and inversely proportional to atomic number of cluster nuclei (Z_c). The Fig. 1 shows the variation of Q-values with the mass number of daughter nuclei (A_d) and atomic number of cluster nuclei (Z_c). The Geiger and Nuttall law (GNL) [32] and universal decay law (UDL) [33] relate the Q-values during cluster emission and depends on the daughter nucleus and emitted cluster nucleus.

The microscopic and macroscopic approaches [3, 34–37] were extensively used in the calculation of decay energy of alpha particle in the heavy and superheavy region. Furthermore, some of the formulae [38–42] were based on the ideology of liquid drop model, and shell-models assumed that decay energy is a function of atomic, mass and neutron number.

$$Q_\alpha = f(A, Z, N) \quad (1)$$

For an instance, Perlmann and Rasmussen [38] proposed the Q-value formula in the superheavy region for the alpha decay in terms of standard recoil energy and electron shielding corrections, and it is as follows;

Fig. 2 The variation of Q-values as a function of A_d/Z_c during different cluster emissions such as ^4He to ^{46}Ca for the neutron number = 148 and 150

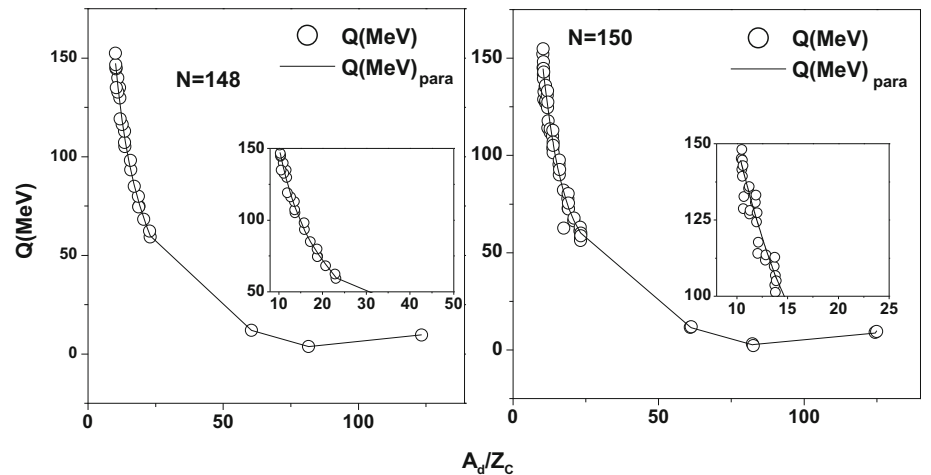


Table 1 Fitting parameters for present formula defined in Eq. (4) for even parent neutron number

Np	a_{62}	a_{61}	a_{60}	a_{52}	a_{51}	a_{50}
148-152	5.847718707E - 09	- 1.766676560E - 06	1.334346597E - 04	- 1.812370062E - 06	5.475851439E - 04	- 4.136238721E - 02
154-158	5.912525308E - 11	- 1.878646742E - 08	1.495389196E - 06	- 2.401845174E - 08	7.635230728E - 06	- 6.082073466E - 04
160-164	9.418879041E - 11	- 3.064941013E - 08	2.495873156E - 06	- 4.177148343E - 08	1.359261030E - 05	- 1.106944522E - 03
166-170	- 1.112380457E - 10	3.766826569E - 08	- 3.184435911E - 06	4.900664364E - 08	- 1.662274279E - 05	1.407444919E - 03
172-176	7.653701093E - 12	- 3.047609801E - 09	3.013214213E - 07	- 2.433934491E - 09	1.030792088E - 06	- 1.070339171E - 04
178-182	- 3.623620934E - 12	1.388448821E - 09	- 1.311978445E - 07	2.666310035E - 09	- 1.003426922E - 06	9.354381984E - 05
184-188	- 4.341816698E - 11	1.610594947E - 08	- 1.492032491E - 06	2.230833397E - 08	- 8.277984019E - 06	7.670884789E - 04
190-194	8.310606371E - 11	- 3.206394882E - 08	3.093538238E - 06	- 5.302429919E - 08	2.042396389E - 05	- 1.967180004E - 03
196-200	4.019136011E - 05	- 1.593646000E - 02	1.579554871E + 00	- 5.351532684E - 03	2.121960843E + 00	- 2.103198462E + 02
202-206	4.814175881E - 06	- 1.985825316E - 03	2.046392943E - 01	- 6.603989113E - 04	2.723525779E - 01	- 2.806010781E + 01
208-212	3.428784319E - 05	- 1.437743115E - 02	1.507158973E + 00	- 4.510174598E - 03	1.891006832E + 00	- 1.982122279E + 02
Np	a_{42}	a_{41}	a_{40}	a_{32}	a_{31}	a_{30}
148-152	2.038492841E - 04	- 6.159855413E - 02	4.653669178E + 00	- 1.034146920E - 02	3.125672492E + 00	- 2.362090773E + 02
154-158	3.756420434E - 06	- 1.194719035E - 03	9.524964220E - 02	- 2.830616883E - 04	9.007926952E - 02	- 7.189479330E + 00
160-164	7.141266164E - 06	- 2.323746809E - 03	1.892501379E - 01	- 5.893256505E - 04	1.917557365E - 01	- 1.561816483E + 01
166-170	- 8.258304740E - 06	2.806295788E - 03	- 2.380047961E - 01	6.659664818E - 04	- 2.267593094E - 01	1.926586349E + 01
172-176	2.423035785E - 07	- 1.179932007E - 04	1.345861991E - 02	- 2.085247871E - 06	3.657718757E - 03	- 5.984906945E - 01
178-182	- 6.696151123E - 07	2.496198150E - 04	- 2.309539200E - 02	7.657912641E - 05	- 2.836344125E - 02	2.609651811E + 00
184-188	- 4.421236379E - 06	1.641032553E - 03	- 1.521007462E - 01	4.230461589E - 04	- 1.570473753E - 01	1.455703254E + 01
190-194	1.252045729E - 05	- 4.817291665E - 03	4.634633781E - 01	- 1.380111984E - 03	5.305928820E - 01	- 5.100772486E + 01
196-200	2.924207238E - 01	- 1.159492676E + 02	1.149242204E + 04	- 8.384395965E + 00	3.324551256E + 03	- 3.295171040E + 05
202-206	3.733995244E - 02	- 1.539496117E + 01	1.585701627E + 03	- 1.112244703E + 00	4.584192739E + 02	- 4.720305333E + 04
208-212	2.421927344E - 01	- 1.015341678E + 02	1.064148258E + 04	- 6.787841379E + 00	2.845281259E + 03	- 2.981666740E + 05
Np	a_{22}	a_{21}	a_{20}	a_{12}	a_{11}	a_{10}
148-152	2.410849840E - 01	- 7.289909917E + 01	5.512240687E + 03	- 2.486481140E + 00	7.524616662E + 02	- 5.696272086E + 04
154-158	1.045598746E - 02	- 3.330628158E + 00	2.663182017E + 02	- 1.676149576E - 01	5.352502151E + 01	- 4.299818364E + 03
160-164	2.400977868E - 02	- 7.811971547E + 00	6.363932302E + 02	- 4.413342062E - 01	1.436098838E + 02	- 1.170698612E + 04
166-170	- 2.625096649E - 02	8.958157859E + 00	- 7.625148228E + 02	4.624089838E - 01	- 1.582117071E + 02	1.349279688E + 04
172-176	- 1.353345735E - 03	3.498704829E - 01	- 1.865174037E + 01	1.116563197E - 01	- 3.688772375E + 01	3.005812904E + 03
178-182	- 4.264610445E - 03	1.570896961E + 00	- 1.437670947E + 02	1.104809197E - 01	- 4.048972825E + 01	3.683388730E + 03
184-188	- 1.993375660E - 02	7.399772958E + 00	- 6.857375675E + 02	4.178312608E - 01	- 1.550569426E + 02	1.435654616E + 04
190-194	7.280682920E - 02	- 2.797578725E + 01	2.688004656E + 03	- 1.660868203E + 00	6.379396561E + 02	- 6.127831798E + 04
196-200	1.329121601E + 02	- 5.270212142E + 04	5.223663017E + 06	- 1.103624062E + 03	4.376100930E + 05	- 4.337478030E + 07
202-206	1.837625467E + 01	- 7.571137037E + 03	7.793234113E + 05	- 1.593728046E + 02	6.563730153E + 04	- 6.753811161E + 06
208-212	1.046304833E + 02	- 4.385138981E + 04	4.594633672E + 06	- 8.408028043E + 02	3.523208143E + 05	- 3.690859840E + 07
Np	a_{02}	a_{01}	a_{00}			

Table 1 continued

Np	a ₆₂	a ₆₁	a ₆₀	a ₅₂	a ₅₁	a ₅₀
148-152	9.299020413E + 00	- 2.817320729E + 03	2.137703873E + 05			
154-158	7.014099006E - 01	- 2.268605096E + 02	1.865986458E + 04			
160-164	3.150336986E + 00	- 1.025881256E + 03	8.382030958E + 04			
166-170	- 3.252437223E + 00	1.116598599E + 03	- 9.540410103E + 04			
172-176	- 3.032970202E + 00	1.049934540E + 03	- 9.045768767E + 04			
178-182	- 1.103723007E + 00	4.038214548E + 02	- 3.654291406E + 04			
184-188	- 3.170460158E + 00	1.176944722E + 03	- 1.088101887E + 05			
190-194	1.270224229E + 01	- 4.877486620E + 03	4.685758406E + 05			
196-200	3.748536102E + 03	- 1.486384417E + 06	1.473279656E + 08			
202-206	5.658595515E + 02	- 2.329574253E + 05	2.396181655E + 07			
208-212	2.752281816E + 03	- 1.153033566E + 06	1.207647837E + 08			

$$Q_\alpha = \frac{A}{A-4} E_\alpha + \left[6.53(Z-2)^{7/5} - 8.0(Z-2)^{2/5} \right] \times 10^{-5} \text{ MeV} \quad (2)$$

where A and Z are the mass number and atomic number of the parent nucleus. Babu and Kumar [39] removed the discrepancy between the Q_α and the experimental $Q_\alpha(\text{exp})$ by including the $\ln 2$ function in the Eq. (2), and it is as follows;

$$Q_\alpha = \frac{A}{A-4} E_\alpha + \left[6.53(Z-2)^{7/5} - 8.0(Z-2)^{2/5} \right] \times 10^{-5} - \ln 2 \text{ MeV} \quad (3)$$

The above defined relations are applicable in the superheavy region with atomic number range $110 \leq Z \leq 128$.

Later on, Dong et al., [40] proposed an alpha decay energy in the heavy and superheavy region ($Z \geq 92$ and $N \geq 140$) the Q_α value, and it is given as follows;

$$Q_\alpha = B(x) + [a_v(A-4) - a_v A] + [a_s A^{2/3} - a_s(A-4)^{2/3}] + [-a_c(Z-2)^2(A-4)^{-1/3} + a_c Z^2 A^{-1/3}] + \left[-a_a \left(\frac{N-Z}{2} \right)^2 (A-4)^{-1} + a_a \left(\frac{N-Z}{2} \right)^2 A^{-1} \right] + [a_p \delta(A-4)^{-1/2} - a_p \delta A^{-1/2}] + \left[a_6 \frac{|A-256|}{A-4} - a_6 \frac{|A-252|}{A} \right] + \left[a_7 \frac{|N-154|}{N-2} + a_7 \frac{|N-152|}{N} \right] + \left[a_8 \frac{|N-Z-50|}{A-4} - a_8 \frac{|N-Z-50|}{A} \right] \quad (4)$$

Here $a_v, a_s, a_c, a_a, a_p, a_6, a_7$ and a_8 are the fitting parameters [41]. Eventually, Dong et al., [40] simplified and proposed five-parameter Q-value formula by considering liquid drop model, and it is as follows;

$$Q_\alpha^{\text{Th}}(\text{MeV}) = \alpha Z A^{-4/3} (3A-Z) + \beta \left(\frac{N-Z}{A} \right)^2 + \gamma \left[\frac{|N-152|}{N} - \frac{|N-154|}{N-2} \right] + \delta \left[\frac{|Z-110|}{Z} - \frac{|Z-112|}{Z-2} \right] + \varepsilon \quad (5)$$

Further simplified formula was also given by Dong et al., [42] for the superheavy elements $Z > 110$ using liquid drop model by neglecting the effect of shell energy is as follows;

$$Q(\text{MeV}) = \alpha Z A^{-4/3} (3A-Z) + b \left(\frac{N-Z}{A} \right)^2 + e \quad (6)$$

Table 2 Fitting parameters for present formula defined in Eq. (4) for odd parent neutron number

Np	a_{62}	a_{61}	a_{60}	a_{52}	a_{51}	a_{50}
148-152	5.847718707E - 09	- 1.766676560E - 06	1.334346597E - 04	- 1.812370062E - 06	5.475851439E - 04	- 4.136238721E - 02
154-158	5.912525308E - 11	- 1.878646742E - 08	1.495389196E - 06	- 2.401845174E - 08	7.635230728E - 06	- 6.082073466E - 04
160-164	9.418879041E - 11	- 3.064941013E - 08	2.495873156E - 06	- 4.177148343E - 08	1.359261030E - 05	- 1.106944522E - 03
166-170	- 1.112380457E - 10	3.766826569E - 08	- 3.184435911E - 06	4.900664364E - 08	- 1.662274279E - 05	1.407444919E - 03
172-176	7.653701093E - 12	- 3.047609801E - 09	3.013214213E - 07	- 2.433934491E - 09	1.030792088E - 06	- 1.070339171E - 04
178-182	- 3.623620934E - 12	1.388448821E - 09	- 1.311978445E - 07	2.666310035E - 09	- 1.003426922E - 06	9.354381984E - 05
184-188	- 4.341816698E - 11	1.610594947E - 08	- 1.492032491E - 06	2.230833397E - 08	- 8.277984019E - 06	7.670884789E - 04
190-194	8.310606371E - 11	- 3.206394882E - 08	3.093538238E - 06	- 5.302429919E - 08	2.042396389E - 05	- 1.967180004E - 03
196-200	4.019136011E - 05	- 1.593646000E - 02	1.579554871E + 00	- 5.351532684E - 03	2.121960843E + 00	- 2.103198462E + 02
202-206	4.814175881E - 06	- 1.985825316E - 03	2.046392943E - 01	- 6.603989113E - 04	2.723252579E - 01	- 2.806010781E + 01
208-212	3.428784319E - 05	- 1.437743115E - 02	1.507158973E + 00	- 4.510174598E - 03	1.891006832E + 00	- 1.982122279E + 02
Np	a_{42}	a_{41}	a_{40}	a_{32}	a_{31}	a_{30}
148-152	2.038492841E - 04	- 6.159855413E - 02	4.653669178E + 00	- 1.034146920E - 02	3.125672492E + 00	- 2.362090773E + 02
154-158	3.756420434E - 06	- 1.194719035E - 03	9.524964220E - 02	- 2.830616883E - 04	9.007926952E - 02	- 7.189479330E + 00
160-164	7.141266164E - 06	- 2.323746809E - 03	1.892501379E - 01	- 5.893256505E - 04	1.917557365E - 01	- 1.561816483E + 01
166-170	- 8.258304740E - 06	2.806295788E - 03	- 2.380047961E - 01	6.659664818E - 04	- 2.267593094E - 01	1.926586349E + 01
172-176	2.423035785E - 07	- 1.179932007E - 04	1.345861991E - 02	- 2.085247871E - 06	3.657718757E - 03	- 5.984906945E - 01
178-182	- 6.696151123E - 07	2.496198150E - 04	- 2.309539200E - 02	7.657912641E - 05	- 2.836344125E - 02	2.609651811E + 00
184-188	- 4.421236379E - 06	1.641032553E - 03	- 1.521007462E - 01	4.230461589E - 04	- 1.570473753E - 01	1.455703254E + 01
190-194	1.252045729E - 05	- 4.817291665E - 03	4.634633781E - 01	- 1.380111984E - 03	5.305928820E - 01	- 5.100772486E + 01
196-200	2.924207238E - 01	- 1.159492676E + 02	1.149242204E + 04	- 8.384395965E + 00	3.324551256E + 03	- 3.295171040E + 05
202-206	3.733995244E - 02	- 1.539496117E + 01	1.585701627E + 03	- 1.112244703E + 00	4.584192739E + 02	- 4.720305333E + 04
208-212	2.421927344E - 01	- 1.015341678E + 02	1.064148258E + 04	- 6.787841379E + 00	2.845281259E + 03	- 2.981666740E + 05
Np	a_{22}	a_{21}	a_{20}	a_{12}	a_{11}	a_{10}
148-152	2.410849840E - 01	- 7.289909917E + 01	5.512240687E + 03	- 2.486481140E + 00	7.524616662E + 02	- 5.696272086E + 04
154-158	1.045598746E - 02	- 3.330628158E + 00	2.663182017E + 02	- 1.676149576E - 01	5.352502151E + 01	- 4.299818364E + 03
160-164	2.400977868E - 02	- 7.811971547E + 00	6.363932302E + 02	- 4.413342062E - 01	1.436098838E + 02	- 1.170698612E + 04
166-170	- 2.625096649E - 02	8.958157859E + 00	- 7.625148228E + 02	4.624089838E - 01	- 1.582117071E + 02	1.349279688E + 04
172-176	- 1.353345735E - 03	3.498704829E - 01	- 1.865174037E + 01	1.116563197E - 01	- 3.688772375E + 01	3.005812904E + 03
178-182	- 4.264610445E - 03	1.570896961E + 00	- 1.437670947E + 02	1.104809197E - 01	- 4.048972825E + 01	3.683388730E + 03
184-188	- 1.993375660E - 02	7.399772958E + 00	- 6.857375675E + 02	4.178312608E - 01	- 1.550569426E + 02	1.435654616E + 04
190-194	7.280682920E - 02	- 2.797578725E + 01	2.688004656E + 03	- 1.660868203E + 00	6.379396561E + 02	- 6.127831798E + 04
196-200	1.329121601E + 02	- 5.270212142E + 04	5.223663017E + 06	- 1.103624062E + 03	4.376100930E + 05	- 4.337478030E + 07
202-206	1.837625467E + 01	- 7.571137037E + 03	7.793234113E + 05	- 1.593728046E + 02	6.563730153E + 04	- 6.753811161E + 06
208-212	1.046304833E + 02	- 4.385138981E + 04	4.594633672E + 06	- 8.408028043E + 02	3.523208143E + 05	- 3.690859840E + 07
Np	a_{02}	a_{01}	a_{00}			

Table 2 continued

Np	a_{62}	a_{61}	a_{60}	a_{52}	a_{51}	a_{50}
148-152	9.299020413E + 00	- 2.817320729E + 03	2.137703873E + 05			
154-158	7.014099006E - 01	- 2.268605096E + 02	1.865986458E + 04			
160-164	3.150336986E + 00	- 1.025881256E + 03	8.382030958E + 04			
166-170	- 3.252437223E + 00	1.116598599E + 03	- 9.540410103E + 04			
172-176	- 3.032970202E + 00	1.049934540E + 03	- 9.045768767E + 04			
178-182	- 1.103723007E + 00	4.038214548E + 02	- 3.654291406E + 04			
184-188	- 3.170460158E + 00	1.176944722E + 03	- 1.088101887E + 05			
190-194	1.270224229E + 01	- 4.877486620E + 03	4.685758406E + 05			
196-200	3.748536102E + 03	- 1.486384417E + 06	1.473279656E + 08			
202-206	5.658595515E + 02	- 2.329574253E + 05	2.396181655E + 07			
208-212	2.752281816E + 03	- 1.153033566E + 06	1.207647837E + 08			

where a , b and e are fitting parameters [42]. The first two terms include the Coulomb energy and symmetry energy term, respectively. The above set of Eqs. (2-6) were defined by the previous researchers to predict the decay energies of an alpha by using atomic number (Z), mass number (A) and neutron number (N) of parent nucleus, atomic number of daughter nuclei ($Z_d = Z-2$), mass number of daughter nucleus ($A_d = A-4$) and neutron number of daughter nucleus ($N_d = N-2$). All the above formulae are used to predict the decay energies of the alpha only. A detail literature survey reveals that there is no empirical formula available for the prediction of the decay energies during the cluster emission.

Hence, in the present work, we have constructed empirical formula for decay energies of cluster emission by assuming the fact that decay energy is a function of mass number of the daughter nucleus, atomic number of the cluster nucleus and neutron number of the parent nucleus

$$Q = f(A_d, Z_c, N_p) \quad (7)$$

In the above function, the parent nuclei information is obtained from the neutron number (N_p), the cluster emission information is availed from the (Z_c), and daughter nuclei information is considered from (A_d), in the first step of the construction of this formula, we have evaluated the function;

$$Q = f(A_d/Z_c) \quad (8)$$

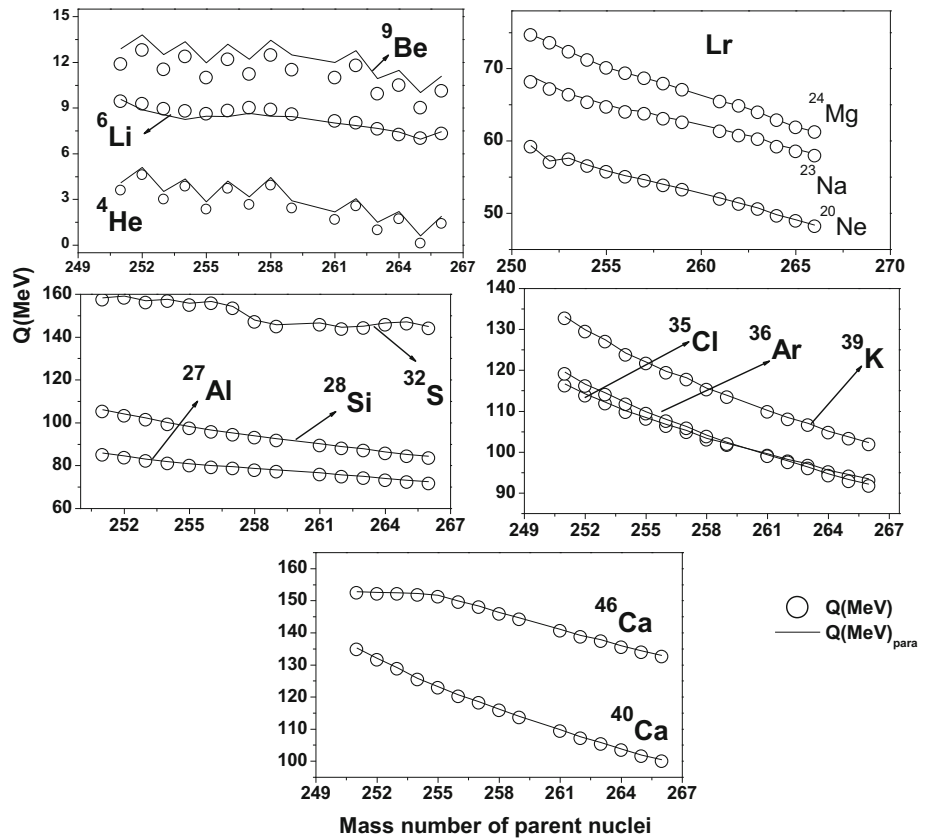
The function $f(A_d/Z_c)$ is evaluated by studying the variation of Q -values with A_d/Z_c . The variation of Q -values with that of A_d/Z_c is presented in Fig. 2. This figure shows the variation of Q -values as a function of A_d/Z_c during different cluster emissions such as ${}^4\text{He}$ to ${}^{46}\text{Ca}$ for the parent neutron number = 148 and 150. This type of variation is observed for all types of studied clusters. From the figure, it is observed that there is systematic variation of Q -values with the A_d/Z_c . Based on this variation, we have constructed the function for Q -values in terms of A_d/Z_c , and it is given as follows;

$$Q = \sum_{i=0}^6 a_i(N)(A_d/Z_c)^i \quad (9)$$

Here $a_6(N)$ to $a_0(Z)$ were the fitting constants, and these constants were evaluated by studying the variation of $a_i(N)$ with neutron number (N). In the present formulae, we have considered the sixth power of the polynomial function such that it has small co-efficient of determination and residual sum of powers nearly equal to unity, which produces the Q -values more accurately. In the above equation, we have considered a_i as function of neutron number by this the complete information for the decay process is considered while proposing the semi-empirical formulae for the Q -

Table 3 The range of isotopes and total number of isotopes considered for each atomic number (Z) in the present empirical formula

Z	Range of isotopes	Total isotopes	Z	Range of isotopes	Total isotopes
103	$251 \geq A \geq 266$	15	115	$287 \geq A \geq 290$	03
104	$253 \geq A \geq 270$	17	116	$288 \geq A \geq 294$	06
105	$258 \geq A \geq 272$	14	117	$290 \geq A \geq 310$	20
106	$258 \geq A \geq 271$	13	118	$290 \geq A \geq 300$	10
107	$260 \geq A \geq 278$	18	119	$290 \geq A \geq 300$	10
108	$263 \geq A \geq 277$	14	120	$295 \geq A \geq 310$	15
109	$266 \geq A \geq 282$	16	121	$295 \geq A \geq 310$	15
110	$267 \geq A \geq 281$	14	122	$299 \geq A \geq 310$	11
111	$272 \geq A \geq 286$	14	123	$297 \geq A \geq 339$	42
112	$277 \geq A \geq 286$	09	124	$309 \geq A \geq 320$	11
113	$278 \geq A \geq 290$	12	125	$303 \geq A \geq 339$	36
114	$284 \geq A \geq 290$	06	126	$306 \geq A \geq 339$	36

Fig. 3 A comparison of present formula with that of other theoretical method such as HFB [33]


values. The detail studies of fitting parameters $a_i(N)$ with neutron number enable us to construct the following function;

$$a_i = \sum_{j=0}^2 a_{ij} N^j \quad (10)$$

Final expression for decay energy (Q) is obtaining by substituting the Eq. (10) in Eq. (8);

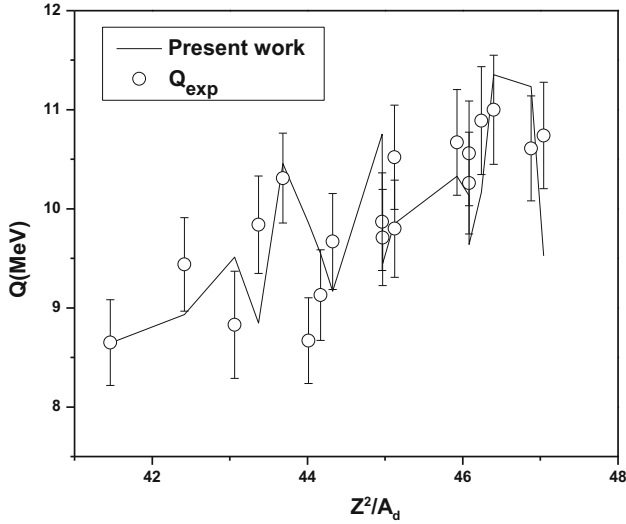


Fig. 4 A comparison of present formula with that of the experiments [33, 34]

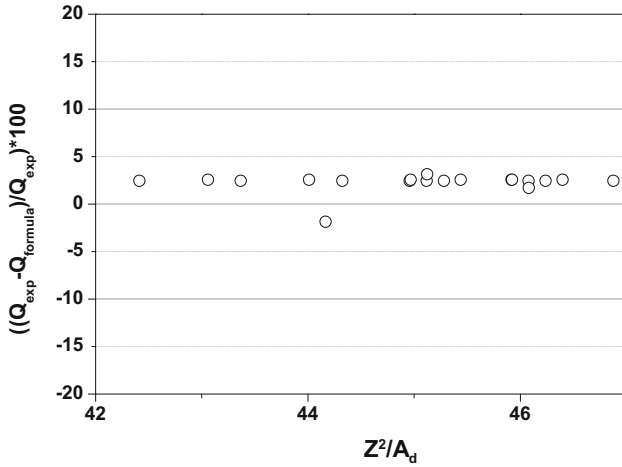


Fig. 5 Percentage of deviation of present formula with that of the experiments [33, 34]

Table 4 Root mean square error in the present formula, FRDM95 [35] and HFB14 [35]

Method	Present formula	FRDM95	HFB14
Root mean square error	0.919477465	1.137312	1.137324

$$Q = \left\{ \sum_{i=0}^6 \sum_{j=0}^2 a_{ij} N^j \left(\frac{A_d}{Z_c} \right)^i \right\} \quad (11)$$

The above equation produces the decay energies of superheavy nuclei during the emission of different clusters such as ${}^4\text{He}$, ${}^6\text{Li}$, ${}^9\text{Be}$, ${}^{20,22}\text{Ne}$, ${}^{23}\text{Na}$, ${}^{24-26}\text{Mg}$, ${}^{27}\text{Al}$, ${}^{28-30}\text{Si}$, ${}^{32-34}\text{S}$, ${}^{35}\text{Cl}$, ${}^{36,38,40}\text{Ar}$, ${}^{39,41}\text{K}$ and ${}^{40,42-44,46}\text{Ca}$

clusters. The values of fitting parameters for even parent neutron number and odd parent neutron number are given in the Tables 1, 2, respectively. Although the proposed semi-empirical formulae are in the sixth order, but the simple input of A_d , Z_c and neutron number of parent nuclei produces the Q-values more accurately and precisely without the knowledge of mass excess values.

3. Results and discussion

We have formulated an empirical formula for decay energies of superheavy nuclei during the emission of different clusters of nuclei. This formula produces the decay energies (Q-value) of superheavy nuclei of atomic number range $104 < Z_p < 126$ (corresponding mass numbers of isotopes are listed in Table 3) during the cluster emission of atomic number range $2 < Z_c < 20$ with mass number range $4 < A_c < 46$. In the present work, to evaluate the fitting parameters defined in Eqs. (11) to (13), we have used the mass excess values available in the literature [43]. This formula also predicts the different Q-values correspond to different cluster emissions of same A/Z ratio. The Fig. 2 shows the variation of Q-values with the function of ratio of mass number of daughter nuclei to the atomic number of emitted cluster.

We have compared the present work with that of the other theoretical methods. Figure 3 shows the comparison of present formula with that of other theoretical method such as HFB [6, 44] for superheavy element $Z = 104$. From the figure, it is clearly observed that there is close agreement of the present formula with that of HFB [6, 44]. Similarly, present formula produces Q-values close to the other theoretical methods. In order to check the predictive power of present constructed formula, we have compared the values produced by the present formula with that of the available experiments [45, 46].

The Fig. 4 shows the comparison of present formula with that of the experiments for different Z_p^2/A values. From the figure, it is clearly observed that the values produced by the present formula are close to the experiments. Hence, the constructed semi-empirical formula can produce the Q-values by simple inputs of mass number of daughter nuclei, atomic number of cluster emission and neutron number of parent nuclei.

To evaluate predictive power of the present formula, we have calculated the percentage of deviation and root mean square error (RMSE) of present formula using following equations;

Table 5 A comparison of experimental Q-values with the FRDM95, HFB14 and present formula having same A/Z during an alpha decay in the superheavy region $106 > Z > 118$

Parent	Daughter nuclei	A/Z	Q-values [32–36]			
			FRDM95	HFB14	EXP	Present formula
²⁶⁹ Sg	²⁶⁵ Rf	41.77	8.8	8.8	7.46 ± 0.06	8.64
²⁷¹ Sg	²⁶⁷ Rf	41.461	8.7	8.7	8.65 ± 0.4325	8.64
²⁷⁵ Hs	²⁷¹ Sg	42.415	9.199	9.199	9.44 ± 0.472	8.93
²⁷⁷ Ds	²⁷³ Hs	43.682	10.3	10.3	10.31 ± 0.453	10.46
²⁷⁹ Ds	²⁷⁵ Hs	43.369	9.6	9.6	9.84 ± 0.492	8.85
²⁸¹ Ds	²⁷⁷ Hs	43.06	8.958	8.958	8.83 ± 0.5415	9.51
²⁸³ Cn	²⁷⁹ Ds	44.325	9.62	9.62	9.67 ± 0.4835	9.17
²⁸⁴ Cn	²⁸⁰ Ds	44.169	9.301	9.301	9.13 ± 0.4565	9.55
²⁸⁵ Cn	²⁸¹ Ds	44.014	8.793	8.793	8.67 ± 0.4335	9.86
²⁸³ Nh	²⁷⁹ Rg	45.12	10.6	10.6	10.52 ± 0.526	9.86
²⁸⁴ Nh	²⁸⁰ Rg	44.961	10.25	10.25	9.87 ± 0.4935	10.75
²⁸⁶ Fl	²⁸² Cn	45.441	10.7	10.7	10.35 ± 0.5175	8.63
²⁸⁷ Fl	²⁸³ Cn	45.282	10.436	10.436	10.29 ± 0.5145	9.56
²⁸⁸ Fl	²⁸⁴ Cn	45.125	9.969	9.969	9.8 ± 0.49	9.85
²⁸⁹ Fl	²⁸⁵ Cn	44.969	9.847	9.847	9.71 ± 0.4855	9.45
²⁸⁷ Mc	²⁸³ Nh	46.08	11.3	11.3	10.26 ± 0.513	10.13
²⁸⁸ Mc	²⁸⁴ Nh	45.92	10.999	10.999	10.15 ± 0.5075	8.46
²⁹⁰ Lv	²⁸⁶ Fl	46.4	11.3	11.3	11 ± 0.55	11.35
²⁹¹ Lv	²⁸⁷ Fl	46.241	11	11	10.89 ± 0.5445	10.17
²⁹² Lv	²⁸⁸ Fl	46.082	10.707	10.707	10.56 ± 0.528	9.64
²⁹³ Lv	²⁸⁹ Fl	45.925	8.886	8.886	10.67 ± 0.5335	10.33
²⁹¹ Ts	²⁸⁷ Mc	47.041	11.9	11.9	10.74 ± 0.537	9.53
²⁹² Ts	²⁸⁸ Mc	46.88	11.6	11.6	10.61 ± 0.5305	11.23
²⁹⁴ Og	²⁹⁰ Lv	47.361	8.47	8.47	11.81 ± 0.06	9.98

$$\text{Deviation (\%)} = \left(\frac{Q_{\text{exp}} - Q_{\text{present formula}}}{Q_{\text{exp}}} \right) \times 100 \quad (12)$$

$$\text{RMSE} = \sqrt{\frac{\sum_{i=1}^N (Q_{\text{cal}} - Q_{\text{exp}})^2}{N}} \quad (13)$$

The evaluated percentage of deviation of present formula is shown in the Fig. 5. From this figure, it is observed that percentage of deviation is less than $\pm 5\%$. The evaluated root mean square error (RMSE) for present formula and also other theoretical methods given in the Table 4. Even though the ratio between A/Z corresponds to the same values, but due to different cluster emission, formation of daughter nuclei and isotope of the parent nuclei the Q-value released during the decay process changes. Hence, we have observed different Q-values for the same A/Z ratio. We have given the experimental results having same A/Z ratio during an alpha decay and corresponding Q-values in Table 5.

The available formulae [38–42] in the literature use up to eight terms to predict decay energies correspond to only

alpha emission. Eventually, we have used seven terms with sixth order to produce decay energies of (⁴He, ⁶Li, ⁹Be, ^{20,22}Ne, ²³Na, ^{24–26}Mg, ²⁷Al, ^{28–30}Si, ^{32–34}S, ³⁵Cl, ^{36,38,40}Ar, ^{39,41}K and ^{40,42–44,46}Ca) 27 clusters including alpha in the superheavy region. All the proposed semi-empirical formula produces the energy during an alpha decay only. The formula proposed to produce decay energies of cluster emission is first of its kind. Hence, the constructed new formula will be first of its kind to produce the decay energies of superheavy nuclei without the knowledge of the mass excess.

4. Conclusions

We have constructed the semi-empirical formula for Q-values of superheavy elements during the emission of ⁴He, ⁶Li, ⁹Be, ^{20,22}Ne, ²³Na, ^{24–26}Mg, ²⁷Al, ^{28–30}Si, ^{32–34}S, ³⁵Cl, ^{36,38,40}Ar, ^{39,41}K and ^{40,42–44,46}Ca clusters. Present formula successfully produces Q-values of superheavy elements during the cluster decay.


References

- [1] C F von Weizsacker *Z. Physik.* **96** 431 (1935)
- [2] H A Bethe and R F Bacher *Rev. Mod. Phys.* **8** 82 (1936)
- [3] P Moller, J R Nix, W D Myers and W J Swiatecki *At. Data and Nucl. Data Tables.* **59** 185 (1995)
- [4] P Moller and J R Nix *At. Data and Nucl. Data Tables.* **26** 165 (198)
- [5] G Audi and A H Wapstra *C Thibault Nucl. Phys. A.* **729** 337 (2003)
- [6] S Goriely, M Samyn and J M Pearson *Phys. Rev. C.* **75** 064312 (2007)
- [7] G Audi, O Bersillon, J Blachot and A H Wapstra *Nuclear Physics. A.* **624** 1 (2003)
- [8] H C Manjunatha, B M Chandrika and L Seenappa *Mod. Phys. Lett. A.* **31** 1650162(2016)
- [9] H C Manjunatha and N Sowmya *Mod. Phys. Lett. A* **34** 15 1950112 (2019)
- [10] H C Manjunatha, N Sowmya and A M Nagaraja *Mod. Phys. Lett. A* **35** 6 2050016 (2020)
- [11] G Royer and H F Zhang *Phys. Rev. C* **77** 037602 (2008)
- [12] H F Zhang and G Royer *Phys. Rev. C* **76** 047304 (2007)
- [13] S Della Negra, H Gauvin, D Jacquet and Y Le Beyec *Zeitschrift für Physik A, Atoms and Nuclei.* **307** 305 (1982)
- [14] V Borrel et al *Nucl. Phys. A.* **531** 353 (1991)
- [15] W A Mayer, W Henning, R Holzwarth and H J Körner *Zeitschrift für Physik A Atoms and Nuclei.* **319** 287 (1984)
- [16] C N Davids *Phys. Rev. C.* **13** 887 (1976)
- [17] H J Scheerer, D Pereira, A Chalupka, R Gyufko and C A Wiedner *Zeitschrift für Physik A Atoms and Nuclei.* **308** 183 (1982)
- [18] M Brauner, D Rychel, R Gyufko, C A Wiedler and S T Thornton *Phys Lett B.* **150** (1–3) 75–78 (1985)
- [19] Ph Ch Miehé, P BaumannDessagne, A Huck et al *Phys. Rev. C.* **39** 992 (1989)
- [20] H C Manjunatha, N Sowmya, K N Sridhar and L Seenappa *J. Radio anal Nucl. Chem.* **314** 991 (2017)
- [21] H C Manjunatha and N Sowmya *Nucl. Phys. A* **969** 68 (2018)
- [22] H C Manjunatha and N Sowmya *Inte. Jou of Mod Phy. E.* **27** 1850041 (2018)
- [23] H C Manjunatha, K N Sridhar and N Sowmya *Phy Rev. C.* **98** 024308 (2018)
- [24] H C Manjunatha, K N Sridhar and N Sowmya *Nuclear Physics. A.* **987** 382 (2019)
- [25] N Sowmya and H C Manjunatha *Bulg. J. Phys.* **46** 16 (2019)
- [26] N Sowmya and H C Manjunatha *Proceedings of the DAE Symp. on Nucl. Phys.* **63** 200 (2018)
- [27] N Sowmya and H C Manjunatha *Braz J Phys* **49** 874 (2019)
- [28] G R Sridhar, H C Manjunatha, N Sowmya, PSD Gupta and H B Ramalingam *Eur Phys Jour P.* **135** 1 (2020)
- [29] H C Manjunatha and N Sowmya *Pramana J. Phys.* **90** 62 (2018)
- [30] H C Manjunatha, K N Sridhar, N Nagaraja and N Sowmya *Eur. Phys. J. Plus* **133** 227 (2018)
- [31] H C Manjunatha et al *Phys. Rev. C.* **102** 064605 (2020)
- [32] H. Geiger and J.M. Nuttall, *Philos. Mag.* **22** 613 (1911); H. Geiger, *Z. Phys.* **8** 45 (1921)
- [33] C Qi, F R Xu, R J Liotta and R Wyss *Phys. Rev. Lett.* **103** 072501 (2009)
- [34] P Moller and J R Nix *J. Phys. G.* **20** 1681 (1994)
- [35] Y T Oganessian et al *Phys. Rev. C* **74** 044602 (2006)
- [36] M Brack et al *Rev. Mod. Phys.* **44** 320 (1972)
- [37] V M Strutinsky *Nucl. Phys. A* **95** 420 (1967)
- [38] I Perlman and J O Rasmussen *Handbuch der Physik.* **42** 145 (1957)
- [39] A V Babu and S S Kumar *Proceedings of the DAE Symp. on Nucl. Phys.* 58 (2013)
- [40] J Dong, W Zuo, J Gu, Y Wang and B Peng *Phys. Rev. C.* **81** 064309 (2010)
- [41] T. Dong and Z Ren *Phys. Rev. C.* **77** 064310 (2008)
- [42] J Dong, W Zuo and W Scheid *Phys. Rev. Lett.* **107** 012501 (2011)
- [43] P Moller, A J Sierk, T Ichikawa and H Sagawa *At. Data and Nucl. Data Tables.* **109** 1 (2016)
- [44] G Audi, A H Wapstra and C Thibault *Nucl. Phys. A* **729** 337 (2003)
- [45] H Zhang, W Zuo, J Li and G Royer *Phy Rev. C.* **74** 017304 (2006)
- [46] S B Duarte et al. *Journal of Physics G: Nuclear and Particle Physics.* **30** (2004)
- [47] G Audi and A H Wapstra *Nucl. Phys. A* **595** 409 (1995)

Publisher's Note Springer Nature remains neutral with regard to jurisdictional claims in published maps and institutional affiliations.



Surface, Asymmetric, Coulomb, Pairing and Shell Effects on Cluster Radioactivity of Superheavy Nuclei with $104 \leq Z \leq 126$

A. M. Nagaraja^{1,2} · K. N. Sridhar³ · L. Seenappa¹ · R. Munirathnam⁴ · N. Sowmya¹  · H. C. Manjunatha¹ · S. Alfred Cecil Raj²

Received: 2 March 2022 / Accepted: 23 March 2022
© The Author(s) under exclusive licence to Sociedade Brasileira de Física 2022

Abstract

The half-lives of cluster radioactivity are investigated using a modified generalized liquid-drop model (MGLDM). The radioactive decay with different cluster emissions in the isotopes of He, Li, Be, Ne, Na, Mg, Al, Si, P, Ar, K and Ca nuclei are studied. The cluster radioactivity half-lives have been evaluated within WKB integral method. The estimated cluster decay half-lives from the present work precisely reproduce the experimental data. Predictions are made in the even superheavy nuclei in the atomic number range $104 \leq Z \leq 126$. The role of Coulomb effect ($Z^2/A^{2/3}$), asymmetry effect ($(N - Z)^2/A$), pairing effect (\sqrt{A}) and shell effect on cluster radioactivity are studied.

Keywords Cluster radioactivity · Superheavy nuclei · Half-lives · Penetration probability

1 Introduction

Cluster radioactivity in the region of superheavy nuclei has become an interesting topic in the recent era. Cluster radioactivity is a type of highly asymmetric decay which exists between process of an alpha decay and spontaneous fission. During cluster radioactivity atom emits cluster of protons and neutrons whose number lies between an alpha particle and binary fission fragment. Cluster radioactivity is similar to that of an alpha decay which can occur only if the cluster passes through the potential barrier. Sandulescu et al. [1] discovered the first theoretically based prediction of cluster radioactivity. Experimental-based cluster radioactivity phenomenon was first found by Rose et al. [2] during decay

of ²²³Ra. Furthermore, systematics of cluster radioactivity and related decay constants calculation using microscopic approach is performed by Blendowske et al. [3].

Lovas et al. [4] investigated cluster radioactivity using different microscopic approaches. Poenaru and Griener [5] evaluated cluster radioactivity using macroscopic and microscopic approach. Furthermore, Santhosh et al. [6] proposed a semi-empirical formula for radioactive nuclei's exhibiting cluster radioactivity. In addition to the above empirical relations many microscopic models such as density dependent cluster model (DDCM) with usage of M3Y nucleon–nucleon interaction [7, 8], Density Functional Theory (DFT) [9], Optical potential calculations based on relativistic mean field (RMF) theory [10], exotic cluster decay in heavy nuclei using Folding Density Dependent M3Y (FDDM3Y) [11], super-fluid phenomena and resonance effects using Continuum Hopping Model (CHM) [12], generalized density-dependent cluster model (GDDCM) [13], Realistic α pre-formation factors of odd-A and odd-odd nuclei within the cluster-formation model (CFM) [14], preformed cluster model (PCM) [15], Analytical Super-Asymmetric Fission Model (ASAF) [16] and Skyrme-SLy4 effective nucleon–nucleon interaction (SLy4) [17] were extensively used to study cluster radioactivity.

Furthermore, cluster decay explained by macroscopic models viz., Half-lives of cluster radioactivity as an asymmetric spontaneous fission is studied by generalized

✉ N. Sowmya
sowmyaparakash8@gmail.com

✉ H. C. Manjunatha
manjunathhc@rediffmail.com

¹ Department of Physics, Government College for Women, Kolar 563101, Karnataka, India

² Department of Physics, St. Joseph's College, Affiliated to Bharathidasan University, Tiruchirappalli 62002, India

³ Department of Physics, Government First Grade College, Kolar 563101, Karnataka, India

⁴ Rajah Serfoji Government College (Autonomous), Thanjavur 613005, Tamil Nadu, India

liquid-drop model (GLDM) [18]. Cluster radioactivity of neutron-deficient nuclei in trans-tin region using Effective liquid-drop model (ELDM) [19], Cluster decay half-lives and preformation probabilities by Coulomb and proximity potential model (CPPM) were studied [20]. Earlier researchers [21–26] have studied cluster radioactivity in the superheavy region. Super-asymmetric fission theory is extended from cluster decay to nanophysics by Liquid-drop model (LDM) [16]. The half-lives of α and cluster radioactivity within a Gamow-like model (Gamow-like) for $Z \geq 84$ and $N \geq 104$ were studied [27].

Zhang et al. [28] deduced preformation factors using experimental cluster decay half-lives within preformed cluster model approach. Cluster radioactivity is investigated using Relativistic mean field (RMF) theory [29]. Experimental investigation of the cluster radioactivity of atomic nuclei is done by Tretyakova and Mikheev [30]. Ahmed et al. [31] studied the alpha and cluster preformation factors in the formation of even–even superheavy nuclei in the atomic numbers range $82 \leq Z \leq 114$. Ghodsi et al. studied alpha decay properties of even–even SHN by including the preformation factor within the Cluster formation model [32]. Various studies on cluster radioactivity using different proximity potentials within Coulomb and proximity potentials [33–38] are available in the literature. With the detailed analysis of the literature, we have carried out a comprehensive investigation using MGLDM and CPPM theoretical models to find effect of cluster radioactivity in the formation of even–even superheavy nuclei within the atomic range $104 \leq Z \leq 126$.

This paper is organized as follows. The theoretical framework is discussed in Sect. 2. Results and the corresponding discussion are given in Sect. 3, and the conclusions of this work are under Sect. 4.

2 Theory

2.1 Modified Generalized Liquid-drop Model (MGLDM)

In the Modified generalized liquid-drop model (MGLDM) [39, 40], total energy during cluster radioactivity is the sum of volume E_v , surface E_s , Coulomb E_c , proximity E_p and centrifugal energy E_ℓ and it is expressed as;

$$E = E_v + E_s + E_c + E_p + E_\ell \tag{1}$$

The total potential is evaluated as explained in the literature [41]. The term E_ℓ is expressed as;

$$E_\ell(r) = \frac{\hbar^2 \ell(\ell + 1)}{2\mu r^2} \tag{2}$$

where μ is the reduced mass, r is the distance between the mass centers and ℓ is the angular momentum. The nuclear proximity potential [42] is given by;

$$V_N(R) = 4\pi\gamma\bar{R}\Phi(s) \tag{3}$$

here \bar{R} is the mean curvature radius and it is given by $\bar{R} = \frac{C_1 C_2}{C_1 + C_2}$ and the Sussman central radii C_i is evaluated as follows;

$$C_i = R_i - \left(\frac{b^2}{R_i}\right) \tag{4}$$

Sharp radii R_i is expressed as;

$$R_i = 1.28A_i^{1/3} - 0.76 + 0.8A_i^{-1/3} \tag{5}$$

In Eq. (3), γ is defined as;

$$\gamma = \gamma_0 \left[1 - I_s \left(\frac{N - Z}{A} \right)^2 \right] \text{MeV}/\text{fm}^2 \tag{6}$$

where $\gamma_0 = 1.460734 \text{ MeV}/\text{fm}^2$ and $I_s = 4.0$ and the various universal proximity functions in Eq. 3 is evaluated using double-folding model (DFM) with the density-dependent nucleon–nucleon interaction. Zhang et al. [43] studied the universal function and it is expressed as;

$$\phi(S_0) = \frac{P_1}{1 + \exp\left(\frac{S_0 + P_2}{P_3}\right)} \tag{7}$$

with $S_0 = \frac{R - R_1 - R_2}{b}$ and P_1, P_2 and P_3 are the constants whose values are -7.65, 1.02 and 0.89, respectively [43]. The penetration probability using WKB integration;

$$P = \exp\left[-\frac{2}{\hbar} \int_{R_{in}}^{R_{out}} \sqrt{2B(r)E(r) - E(\text{sphere})}\right] \tag{8}$$

here R_{in} and R_{out} are the classical turning points with the conditions $V(r = R_{in}) = V(r = R_{out}) = Q$. μ is the reduced mass of the cluster and daughter nuclei. The half-lives of cluster emission from the odd superheavy nuclei in the atomic number range $105 \leq Z \leq 125$ were evaluated using the following equation;

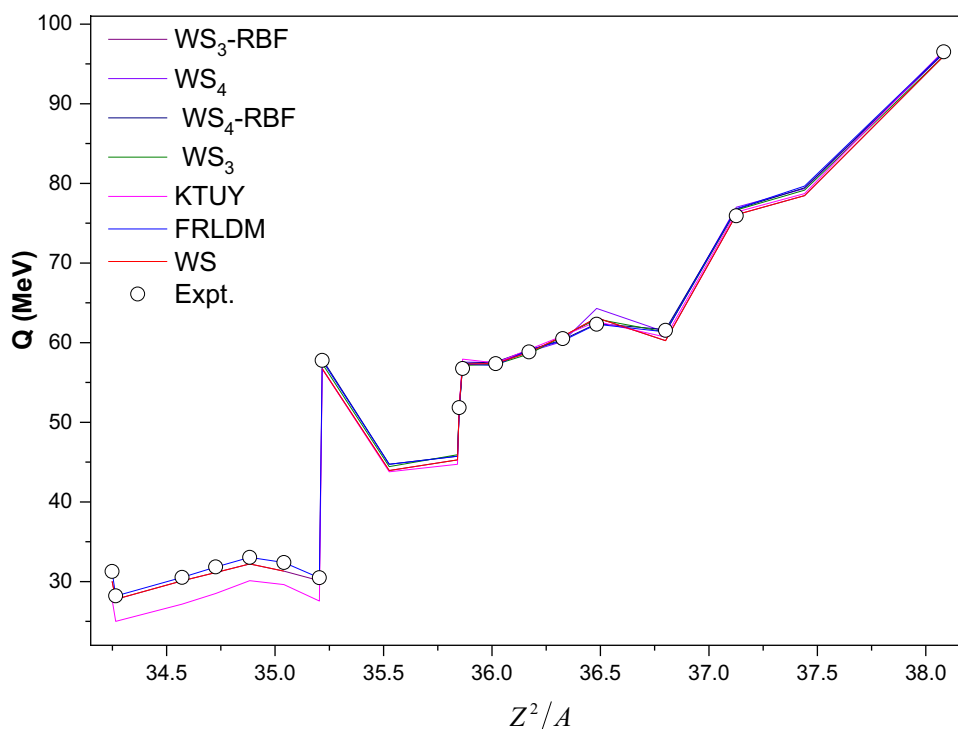
$$T_{1/2} = \left(\frac{\ln 2}{\lambda}\right) = \left(\frac{\ln 2}{vP}\right) \tag{9}$$

here decay constant λ is a function of assault frequency $v = \left(\frac{\omega}{2\pi}\right) = \left(\frac{2E_v}{\hbar}\right)$. Here, E_v is the empirical zero point vibrational energy and it is expressed as;

$$E_v = Q \left[0.056 + 0.039 \exp\left(\frac{4 - A_e}{2.5}\right) \right] \text{MeV} \tag{10}$$

Here, A_e is the mass number of the emitted cluster particle. The term P in Eq. (9) is the penetration probability of cluster decay.

Fig. 1 A plot of $Q(\text{MeV})$ of even nuclei within the atomic number range $104 \leq Z \leq 126$ as a function of Z^2/A



3 Results and Discussions

The sensitivity of Q-values in the evaluation of cluster decay half-lives using different mass excess values such as Finite-Range Liquid-Drop Model (FRLDM) [44], Kourra-Tachibaba-Uno-Yamada (KTUY) [45, 46], Weizsacker-Skyrme (WS4) model [47], WS3+RBF [48], WS3 [49], WS [50] and Weizsacker-Skyrme (WS)+radial basis function (RBF) i.e., WS4+RBF [47] were studied for the available experimental Q-values of cluster-radioactivity. Figure 1 shows plot of Q-values using different mass excess values as a function of Z^2/A . The Q-values increase with increase in the function Z^2/A . The overall behavior of Q-values is in good agreement with that of experimental Q-values. In order to identify the closure reproduction of experimental Q-values, the standard deviation is evaluated as follows;

$$\sigma = \left(\frac{1}{(n-1)} \sum_{i=1}^n (Q^{cal} - Q^{exp})^2 \right)^{1/2} \tag{11}$$

here n is the number of nuclei considered during cluster radioactivity. The deviation obtained using each mass excess values is tabulated in Table 1. From the table it is inferred that the deviation obtained using FRLDM is found to be

smaller when compared to other models studied. Hence, in further investigation of cluster decay half-lives we have used FRLDM mass excess values.

Furthermore, the suitable proximity potential is selected by plotting experimental $\log T_{1/2}(s)$ using different proximity functions as a function of Z/\sqrt{Q} and it is shown in Fig. 2. The standard deviation obtained for Prox-2013 is about $\sigma = 1.62$ with that of available experiments. Hence, in further analysis we have considered Prox-2013 proximity function for evaluation of cluster-decay half-lives. Evaluation of cluster emitters within the range He to Ca viz., ^4He , ^6Li , ^9Be , $^{20-22}\text{Ne}$, ^{23}Na , $^{24-26}\text{Mg}$, ^{27}Al , $^{28-30}\text{Si}$, ^{31}P , $^{32-34}\text{S}$, ^{35}Cl , $^{36,38,40}\text{Ar}$, ^{39}K and $^{40,42-4,46}\text{Ca}$ is evaluated for the even superheavy nuclei within the atomic number range $104 \leq Z \leq 126$.

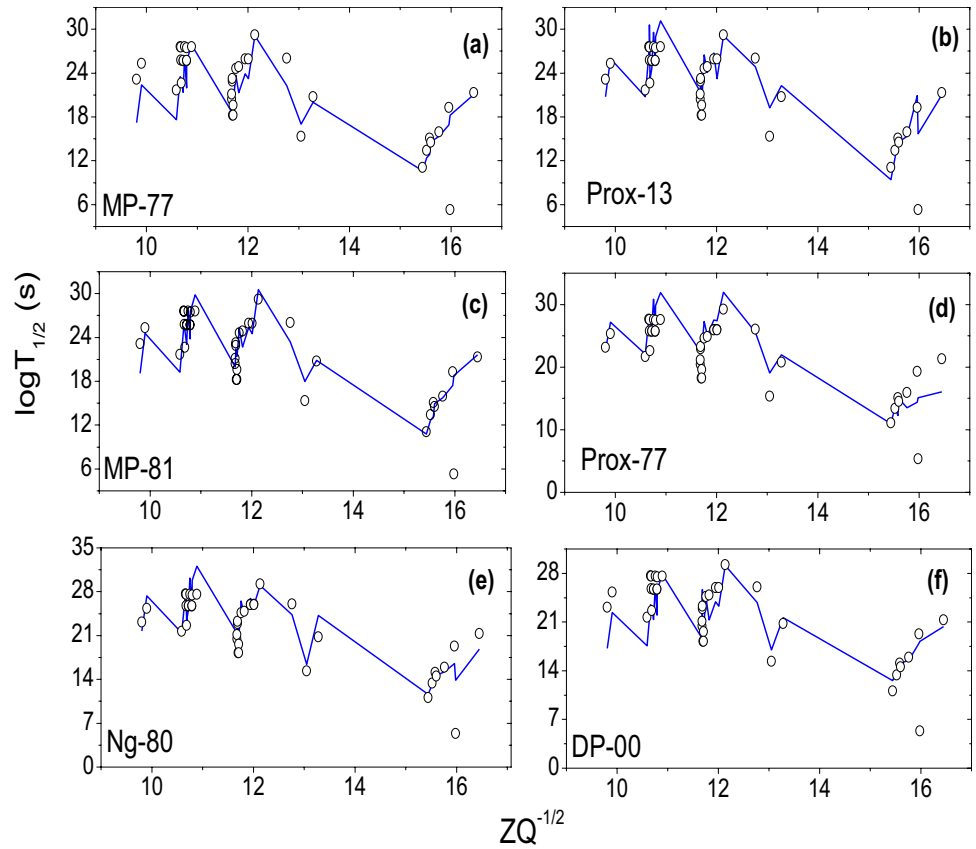
In Fig. 3, variation of Q-value with the Sussman central radii C_i is represented for even nuclei's within the atomic number range $104 \leq Z \leq 126$. From the graph it is clear that Q-value is varying inversely proportional to the Sussman central radii.

The penetration probability is evaluated within the atomic number range $104 \leq Z \leq 126$ and it is represented in Fig. 4. As the mass number of parent nuclei increases the penetration probability gradually decreases. There is a sudden

Table 1 The standard deviation obtained using different mass excess values with that of experimental Q-values

WS3-RBF	WS4	WS4-RBF	WS3	KTUY	FRLDM	WS
7.08	8.13	8.55	8.33	7.15	6.98	7.18

Fig. 2 A plot of experimental $\log T_{1/2}(s)$ as a function of Z/\sqrt{Q}



decrease in the penetration probability when $A=238$ and $A=253$ within the atomic number range $104 \leq Z \leq 126$. The penetration probability is inversely proportional to half-lives.

From this we can conclude that the smaller penetration probability leads to larger the half-lives when mass of the parent nuclei is equal to 238 and 253.

Fig. 3 A plot of Q value of even nuclei in the atomic number range $104 \leq Z \leq 126$ as a function of Sussman central radii C_i

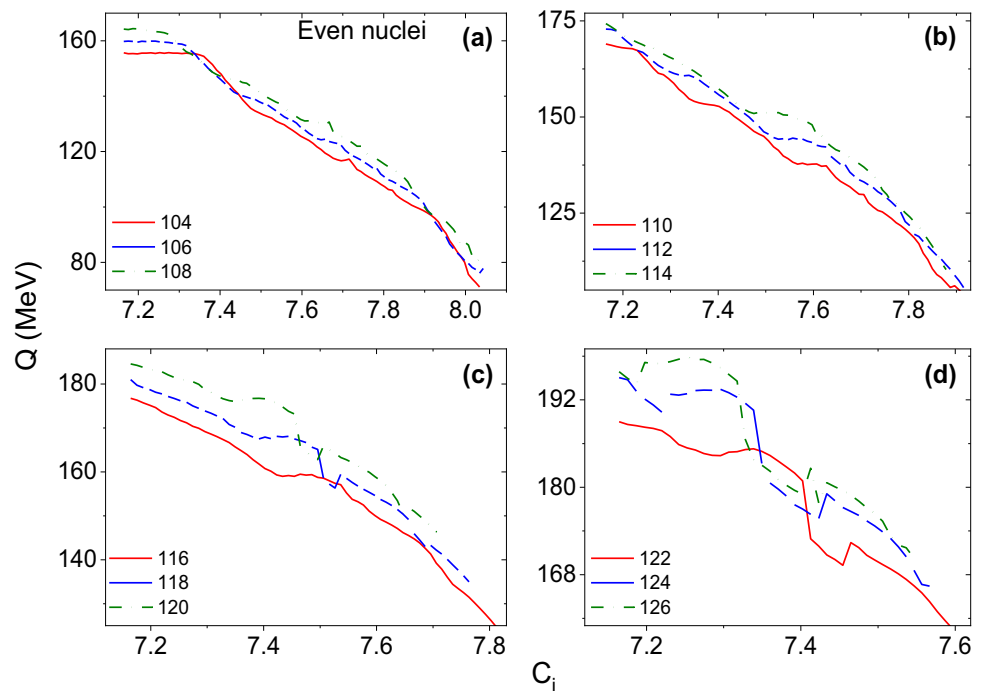
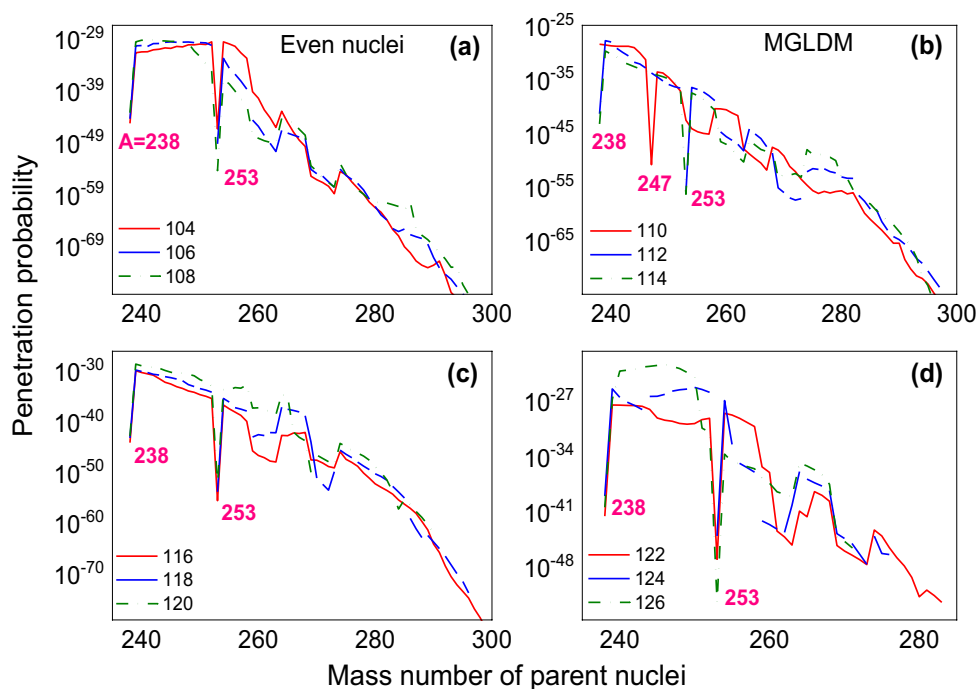


Fig. 4 A plot of penetration probability of even nuclei in the atomic number range $104 \leq Z \leq 126$ evaluated using MGLDM model with mass number of parent nuclei



Once the penetration probability is evaluated using the WKB integral with the boundary conditions, half-lives of even nuclei within the atomic number range $104 \leq Z \leq 126$ is studied. Figure 5 shows plot of $\log T_{1/2}(s)$ as a function of Z_d . In all the even superheavy nuclei, the larger $\log T_{1/2}$ is observed when Z_d is within atomic range 85 to 89. The larger value of $\log T_{1/2}$ is observed when atomic number is near the magic number.

In addition to plot of $\log T_{1/2}$ as a function of Z_d we have also plotted $\log T_{1/2}$ as function of N_C . Figure 6 shows an increase in logarithmic half-lives with increase in cluster neutron number. It reaches maximum when N_C is equal to 20 and again it gradually decreases. Figure 6(a) and (b) shows larger stability when N_C is equal to 20 and 23 when compared to their neighboring nuclei. Similarly, Fig. 6(c) shows peaks when N_C is equal to 16, 20 and 23. Furthermore, the

Fig. 5 A plot of $\log T_{1/2}(s)$ of even nuclei in the atomic number range $104 \leq Z \leq 126$ as a function of atomic number of daughter nuclei

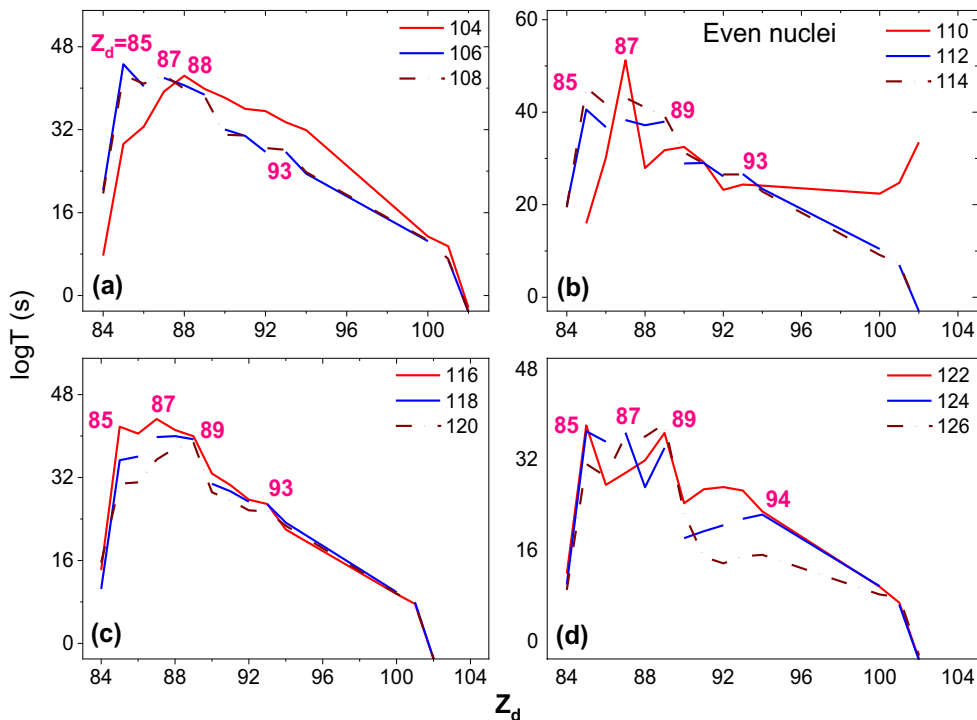
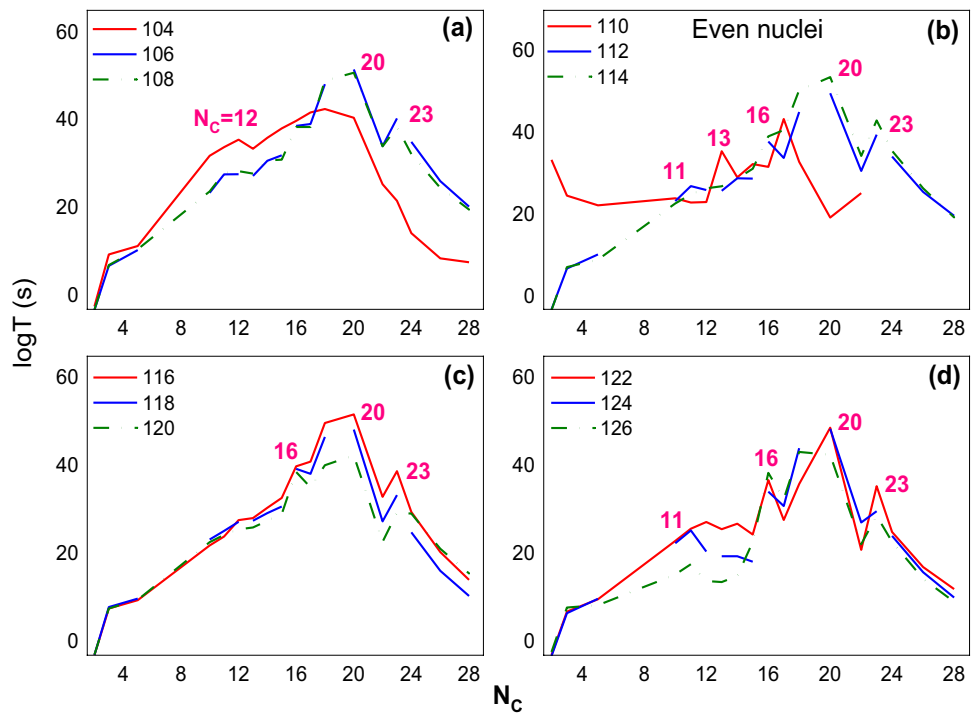


Fig. 6 Comparison of $\log T_{1/2}(s)$ of even nuclei as a function of neutron number of cluster nuclei (N_c)



logarithmic half-lives are larger in case of even superheavy nuclei with $Z=122$ and 124 at $N_c=11, 16, 20$ and 23 . Hence, the even superheavy nuclei with $104 \leq Z \leq 126$ shows stability against these cluster emissions with neutron number is between 11 and 23 .

The number of neutrons and protons significantly contributes to the logarithmic half-lives. A plot of logarithmic half-lives as a function of $(N - Z)^2/A$ is shown in Fig. 7. The

$\log T_{1/2}$ values increase with increase in $(N - Z)^2/A$ value. The disparity between emitted protons and neutrons causes a sudden increase in $\log T_{1/2}$ values when $(N - Z)^2/A$ is nearly equal to 12 and above in case of $Z=104$ during ^{12}C emission. Similarly, in case of $Z=114$, the $\log T_{1/2}$ value decreases when $(N - Z)^2/A$ is greater than 12 . In case of $Z=120$ and 126 the $(N - Z)^2/A$ is 18 and 14 , respectively, at which the $\log T_{1/2}$ value shows an unexpected increase.

Fig. 7 A plot of $\log T_{1/2}(s)$ of even nuclei within the atomic number range $104 \leq Z \leq 126$ as a function of $(N - Z)^2/A$ for different cluster emissions such as ^{12}C , ^{28}Si , ^{36}Ar and ^{40}Ca in case of (a) $Z=104$, (b) $Z=114$, (c) $Z=120$ and (d) $Z=126$

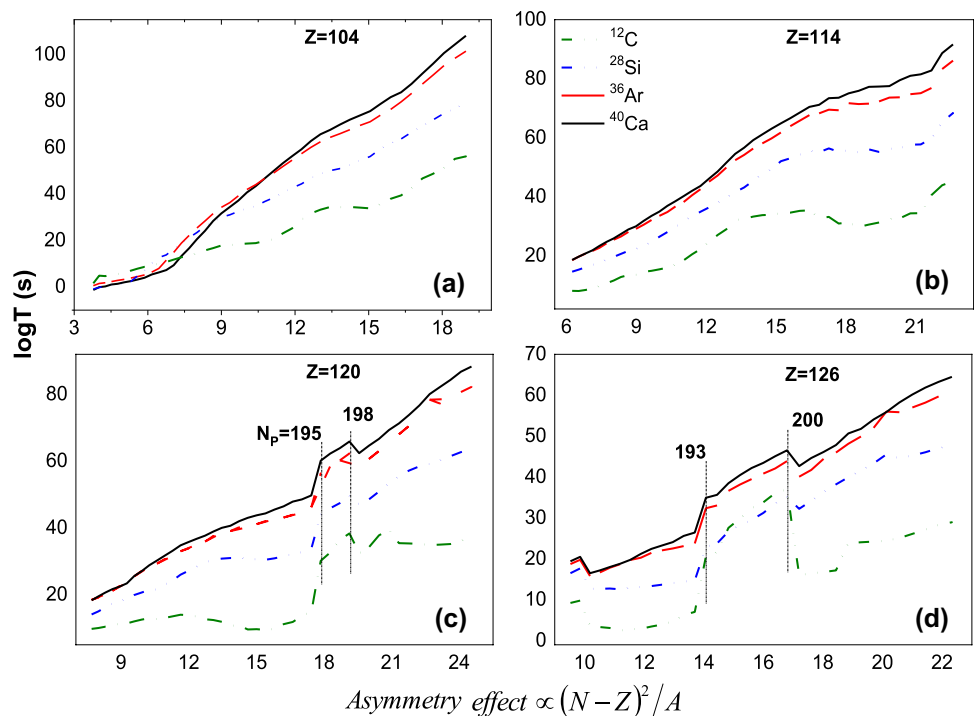
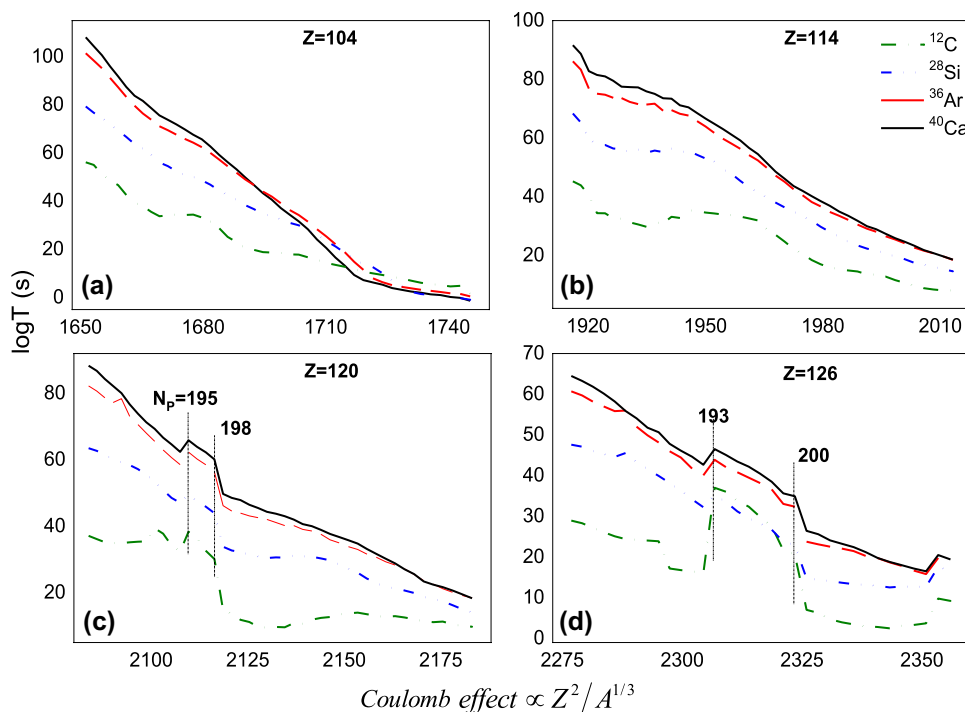


Fig. 8 A plot of $\log T_{1/2}(s)$ of even nuclei within the atomic number range $104 \leq Z \leq 126$ as a function of $Z^2/A^{1/3}$ for different cluster emissions such as ^{12}C , ^{28}Si , ^{36}Ar and ^{40}Ca in case of (a) $Z=104$, (b) $Z=114$, (c) $Z=120$ and (d) $Z=126$



The function $Z^2/A^{1/3}$ is involved in the Coulomb effect in the evaluation of binding energy. The repulsive force between two nuclei reduces the binding energy. It is also evident that as $Z^2/A^{1/3}$ increases the logarithmic half-lives gradually decrease, i.e., when there is an increase in Coulomb repulsive force then the life-time of the compound nuclei gradually decreases. A plot of $\log T_{1/2}$ as a function

of $Z^2/A^{1/3}$ is shown in Fig. 8(a-d) for atomic number $Z=104, 114, 120$ and 126 .

Another important term is pairing effect, it is an attractive interaction between two nucleons. Earlier studies [51, 52] were pointed out that the pairing energy of protons is greater than that of neutrons with $N=50$ and $N=82$. Figure 9(a-d) shows a plot of $\log T_{1/2}$ as function of pairing effect i.e.,

Fig. 9 A plot of $\log T_{1/2}(s)$ of even nuclei within the atomic number range $104 \leq Z \leq 126$ as a function of pairing effect (\sqrt{A})

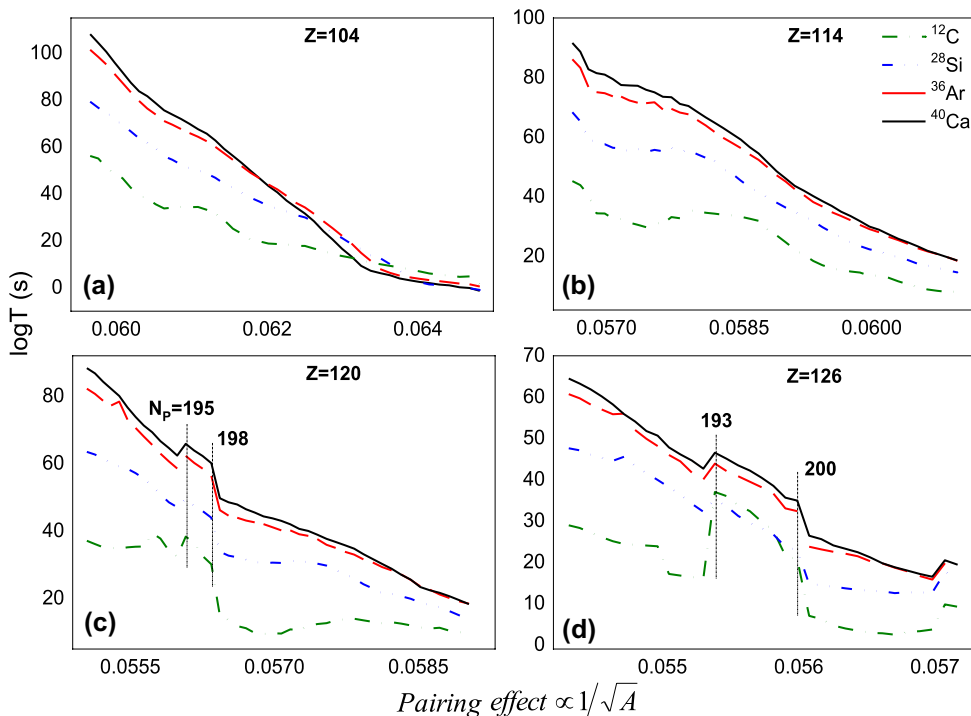
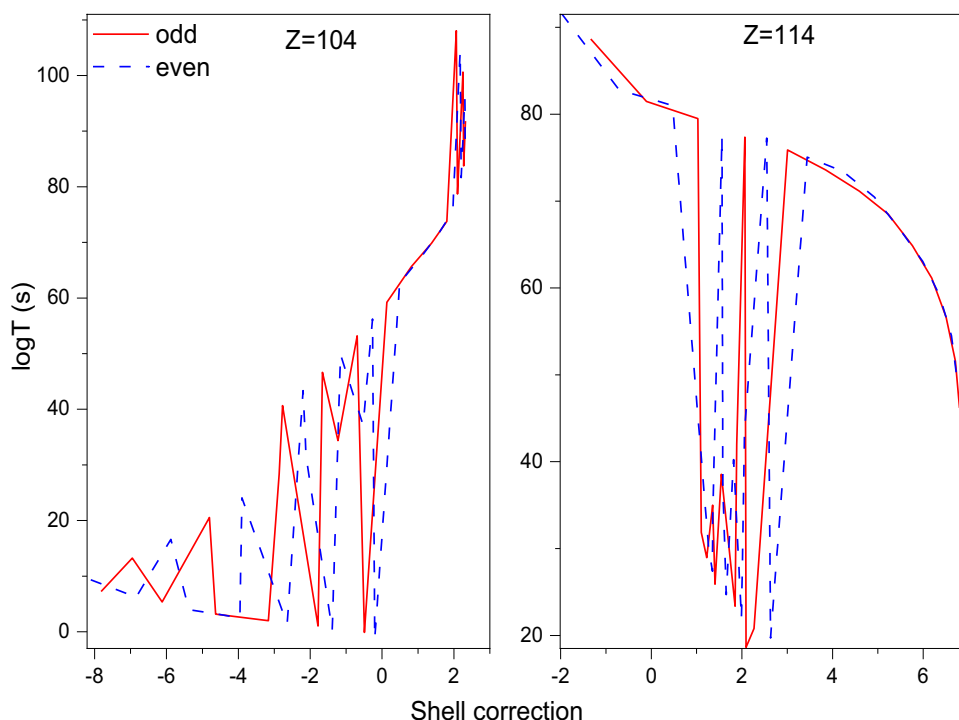


Fig. 10 A plot of logarithmic half-lives as function of shell corrections for (a) $Z=104$ and (b) 114



\sqrt{A} . As the effect of pairing effect increases between two nuclei the corresponding half-lives decrease. The attractive interaction between two nucleons decreases when the two nuclei are far apart. Hence, the half-lives of parent nuclei also decrease. From Fig. 9(c) we have observed stability of half-lives when pairing effect value is above 0.0560. That is when the neutron number is from 195 to 198 which is near the second generation magic number $N=196$. Hence, due to shell effects the unexpected increase in the $\log T_{1/2}$ values was observed from the parent nuclei $Z=120$. Similarly, in case of $Z=126$ unexpected increase in the $\log T_{1/2}$ values was observed when $N=193$ and $N=200$ and is as shown in Fig. 9d for the parent nuclei $Z=126$.

Seeger [53] effectively introduced the shell correction term which is function of neutron and proton number. The shell correction term allows for the explanation of magical nuclei by anticipating different factors such as proton separation energies, neutron separation energies, and so on. It also plays an important role in shell structure. Figure 10 illustrates the role of shell effects on the logarithmic half-lives in case of $Z=104$ and 114. Both odd and even mass of daughter nuclei is considered during an evaluation of half-lives. In both cases, the continuous line specifies the data corresponding to odd mass number of daughter nuclei and dotted lines for the even nuclei. However, no systematic variation of logarithmic half-lives is observed with respect to shell corrections. From the detailed analysis of logarithmic half-lives as function of Coulomb term, asymmetry term, pairing term

and shell corrections on cluster radioactivity half-lives in the even superheavy nuclei within the atomic number range $104 \leq Z \leq 126$ will guide for further investigations.

4 Conclusions

The phenomena of cluster radioactivity in even superheavy nuclei are studied using MGLDM approach. The radioactive decay with different cluster emissions in the isotopes of Helium to Calcium nuclei is studied. The nuclear proximity potential is studied using Prox-13 proximity function. The cluster radioactivity half-lives have been evaluated within WKB integral method. The estimated cluster decay half-lives from the present work precisely reproduce the experimental data. Predictions are made in the even superheavy nuclei in the atomic number range $104 \leq Z \leq 126$. The role of Coulomb effect ($Z^2/A^{2/3}$), asymmetry effect ($(N-Z)^2/A$), pairing effect (\sqrt{A}) and shell effect on half-lives gives an insight into future experiments on cluster radioactivity.

Declarations

Competing Interest The authors declare that they have no known competing financial interests or personal relationships that could have appeared to influence the work reported in this paper.

References

- A. Sandulescu, D.N. Poenaru, W. Greiner, New type of decay of heavy nuclei intermediate between fission and α decay. *Sov. J. Particles Nucl. (Engl. Transl.)*; (United States) **11**
- H. Rose, G. Jones, A new kind of natural radioactivity. *Nature* **307**(5948), 245–247 (1984)
- R. Blendowske, H. Walliser, Systematics of cluster-radioactivity-decay constants as suggested by microscopic calculations. *Phys. Rev. Lett.* **61**(17), 1930 (1988)
- R. Lovas, R. Liotta, A. Insolia, K. Varga, D. Delion, Microscopic theory of cluster radioactivity. *Phys. Rep.* **294**(5), 265–362 (1998)
- D.N. Poenaru, W. Greiner, in *Clusters in Nuclei* (Springer, 2010), pp. 1–56
- K. Santhosh, R. Biju, A. Joseph, A semi-empirical model for α and cluster radioactivity. *J. Phys. G: Nucl. Part. Phys.* **35**(8), 085102 (2008)
- Z. Ren, C. Xu, Z. Wang, New perspective on complex cluster radioactivity of heavy nuclei. *Phys. Rev. C* **70**, 034304 (2004)
- R. Zhong-Zhou, X. Chang, Density-dependent cluster model study of α -decay and cluster radioactivity of nuclei. *Nuclear Phys. Rev.* **22**(4), 344–350 (2005)
- Z. Matheson, S.A. Giuliani, W. Nazarewicz, J. Sadhukhan, N. Schunck, Cluster radioactivity of $\{294\}_{118}$ og $\{176\}$. arXiv preprint arXiv:1812.06490 (2018)
- B. Singh, M. Bhuyan, S. Patra, R.K. Gupta, Optical potential obtained from relativistic-mean-field theory-based microscopic nucleon–nucleon interaction: applied to cluster radioactive decays. *J. Phys. G: Nucl. Part. Phys.* **39**(2), 025101 (2012)
- T. Routray, J. Nayak, D. Basu, Cluster radioactivity in very heavy nuclei: a new perspective. *Nuclear Phys. A* **826**(3–4), 223–229 (2009)
- I. Silisteanu, W. Scheid, Half-lives of cluster radioactivity within a model including superfluid phenomena and resonance effects. *Phys. Rev. C* **51**(4), 2023 (1995)
- D. Ni, Z. Ren, Half-lives and cluster preformation factors for various cluster emissions in trans-lead nuclei. *Phys. Rev. C* **82**(2), 024311 (2010)
- D. Deng, Z. Ren, D. Ni, Y. Qian, Realistic α preformation factors of odd-a and odd-odd nuclei within the cluster-formation model. *J. Phys. G: Nucl. Part. Phys.* **42**(7), 075106 (2015)
- S.K. Arun, R.K. Gupta, S. Kanwar, B. Singh, M.K. Sharma, Cluster radioactivity with effects of deformations and orientations of nuclei included. *Phys. Rev. C* **80**(3), 034317 (2009)
- D.N. Poenaru, W. Greiner, Extension of superasymmetric fission theory from cluster decay to nanophysics. *Nuclear Phys. A* **834**(1–4), 163c–166c (2010)
- W. Seif, A. Abdulghany, Z. Hussein, Change in neutron skin thickness after cluster-decay. *J. Phys. G: Nucl. Part. Phys.* **48**(2), 025111 (2021)
- X. Bao, H. Zhang, B. Hu, G. Royer, J. Li, Half-lives of cluster radioactivity with a generalized liquid-drop model. *J. Phys. G: Nucl. Part. Phys.* **39**(9), 095103 (2012)
- Y. Gao, J. Cui, Y. Wang, J. Gu, Cluster radioactivity of neutron-deficient nuclei in trans-tin region. *Sci. Rep.* **10**(1), 1–15 (2020)
- M. Ismail, A. Ellithi, M. Selim, N. Abou-Samra, O. Mohamedien, Cluster decay half-lives and preformation probabilities. *Phys. Scr.* **95**(7), 075303 (2020)
- A.M. Nagaraja, H.C. Manjunatha, N. Sowmya, L. Seenappa, P.D. Gupta, N. Manjunatha, S.A.C. Raj, Heavy particle radioactivity of superheavy element $z=126$. *Nuclear Phys. A* **1015**, 122306 (2021)
- A.M. Nagaraja, H.C. Manjunatha, N. Sowmya, N. Manjunath, S.A.C. Raj, Cluster radioactivity of superheavy nuclei 290–310 120 using different proximity functions. *Eur. Phys. J. Plus* **135**(10), 1–16 (2020)
- A.M. Nagaraja, H.C. Manjunatha, N. Sowmya, P. Gupta, S. Raj, Decay of dinuclear systems formed from dubnium. *Pramana* **95**(4), 1–8 (2021)
- H.C. Manjunatha, S.A.C. Raj, A.M. Nagaraja, N. Sowmya, Cluster radioactivity in superheavy nuclei 299–306 122. *Journal of Nuclear Physics, Material Sciences, Radiation and Applications* **8**(1), 55–63 (2020)
- A.M. Nagaraja, H.C. Manjunatha, N. Sowmya, S. Raj, Cluster radioactivity in superheavy nuclei **299–302**, 120 (2020)
- H.C. Manjunatha, A.M. Nagaraja, in *Proceedings of the DAE Symp. on Nucl. Phys.*, vol. 64 (2019), p. 170
- A. Zdeb, M. Warda, K. Pomorski, Half-lives for α and cluster radioactivity within a gamow-like model. *Phys. Rev. C* **87**(2), 024308 (2013)
- H. Zhang, J. Dong, G. Royer, W. Zuo, J. Li, Preformation of clusters in heavy nuclei and cluster radioactivity. *Phys. Rev. C* **80**(3), 037307 (2009)
- O. Tavares, E. Medeiros, A simple description of cluster radioactivity. *Phys. Scr.* **86**(1), 015201 (2012)
- S. Tretyakova, V. Mikheev, Experimental investigation of the cluster radioactivity of atomic nuclei. *Il Nuovo Cimento A* (1971–1996) **110**(9–10), 1043–1048 (1997)
- S.M.S. Ahmed, R. Yahaya, S. Radiman, M.S. Yasir, Alpha-cluster preformation factors in α decay for even–even heavy nuclei using the cluster-formation model. *J. Phys. G: Nucl. Part. Phys.* **40**(6), 065105 (2013)
- O. Ghodsi, M. Hassanzad, α -decay properties of even-even superheavy nuclei. *Phys. Rev. C* **101**(3), 034606 (2020)
- N. Sowmya, H.C. Manjunatha, N. Dhananjaya, A.M. Nagaraja, Competition between binary fission, ternary fission, cluster radioactivity and α decay of 281 ds. *J. Radioanal. Nucl. Chem.* **323**(3), 1347–1351 (2020)
- N. Sowmya, H.C. Manjunatha, Investigations on different decay modes of darmstadtium. *Phys. Part. Nucl. Lett.* **17**(3), 370–378 (2020)
- H.C. Manjunatha, N. Sowmya, Competition between spontaneous fission ternary fission cluster decay and α decay in the super heavy nuclei of $z=126$. *Nuclear Phys. A* **969**, 68–82 (2018)
- H.C. Manjunatha, N. Sowmya, Decay modes of superheavy nuclei $z=124$. *International Journal of Modern Physics E* **27**(05), 1850041 (2018)
- H.C. Manjunatha, K.N. Sridhar, N. Sowmya, Investigations of the synthesis of the superheavy element $z=122$. *Phys. Rev. C* **98**, 024308 (2018)
- G.R. Sridhar, H.C. Manjunatha, N. Sowmya, P.S.D. Gupta, H.B. Ramalingam, Atlas of cluster radioactivity in actinide nuclei. *The European Physical Journal Plus* **135**(3), 1–28 (2020)
- G. Royer, R. Moustabchir, Light nucleus emission within a generalized liquid-drop model and quasimolecular shapes. *Nuclear Phys. A* **683**(1–4), 182–206 (2001)
- G. Royer, B. Remaud, Fission processes through compact and creviced shapes. *J. Phys. G: Nucl. Part. Phys.* **10**(8), 1057 (1984)
- K. Santhosh, T.A. Jose, Cluster pre-formation probabilities and decay half-lives for trans-lead nuclei using modified generalised liquid drop model (mgldm). *Pramana* **95**(4), 1–17 (2021)
- G. Zhang, Y. Yao, M. Guo, M. Pan, G. Zhang, X. Liu, Comparative studies for different proximity potentials applied to large cluster radioactivity of nuclei. *Nuclear Phys. A* **951**, 86–96 (2016)
- G. Zhang, H. Zheng, W. Qu, Study of the universal function of nuclear proximity potential between α and nuclei from density-dependent nucleon–nucleon interaction. *Eur. Phys. J. A* **49**(1), 1–6 (2013)
- P. Möller, J. Nix, Wd myers and wj swiatecki. *Atom. Data and Nucl. Data Tables* **59**, 185 (1995)
- H. Koura, T. Tachibana, M. Uno, M. Yamada, Nuclidic mass formula on a spherical basis with an improved even-odd term. *Prog. Theor. Phys.* **113**(2), 305–325 (2005)

46. H.K. et al. Calculated atomic masses and nuclear deformations (ktuy05). https://www.ndc.jaea.go.jp/nuclldata/mass/KTUY05_m246S12np.pdf
47. N. Wang, M. Liu, X. Wu, J. Meng, Surface diffuseness correction in global mass formula. *Phys. Lett. B* **734**, 215–219 (2014)
48. N. Wang, M. Liu, Nuclear mass predictions with a radial basis function approach. *Phys. Rev. C* **84**(5), 051303 (2011)
49. M. Liu, N. Wang, Y. Deng, X. Wu, Further improvements on a global nuclear mass model. *Phys. Rev. C* **84**(1), 014333 (2011)
50. N. Wang, Z. Liang, M. Liu, X. Wu, Mirror nuclei constraint in nuclear mass formula. *Phys. Rev. C* **82**(4), 044304 (2010)
51. H.E. Suess, Magic numbers and the missing elements technetium and promethium. *Phys. Rev.* **81**(6), 1071 (1951)
52. L. Kowarski, Magic numbers and elements with no stable isotopes. *Phys. Rev.* **78**(4), 477 (1950)
53. P.A. Seeger, Semiempirical atomic mass law. *Nuclear Phys.* **25**, 1–IN1 (1961)

Publisher's Note Springer Nature remains neutral with regard to jurisdictional claims in published maps and institutional affiliations.

Theoretical evidence for neutron magic number 184 from cluster radioactivity studies

A. M. Nagaraja^{*,†}, H. C. Manjunatha^{*,†}, N. Sowmya^{*,‡}, K. N. Sridhar[‡],
P. S. Damodara Gupta^{*} and S. Alfred Cecil Raj[†]

**Department of Physics, Government College for Women,
Kolar-563101, Karnataka, India*

*†Department of Physics,
St. Joseph's college (Autonomous), Affiliated to Bharathidasan,
University, Tiruchirappalli-620002, Tamil Nadu, India*

*‡Department of Physics, Government First Grade College,
Kolar-563101 Karnataka, India
†manjunathhc@rediffmail.com
‡sowmyaprakash8@gmail.com*

Received 23 November 2021

Revised 10 December 2021

Accepted 10 December 2021

Published 21 January 2022

The existence of neutron magic number 184 is demonstrated through the cluster decay studies. The alpha and cluster radioactivity have been studied in the superheavy region $104 \leq Z \leq 126$ using modified generalized liquid drop model (MGLDM). The values obtained from this work were compared with that of experiments. During the study of cluster radioactivity, surprisingly it is observed that the shortest half-lives of cluster decay in all superheavy elements are observed for daughter neutron number 184 and nearly equal to that. This is a clear evidence for the existence of the neutron magic number $N = 184$. This study is useful in the understanding of superheavy element nuclei structure.

Keywords: Superheavy nuclei; half-lives; probability of penetration; spontaneous fission.

1. Introduction

The cluster radioactivity is an asymmetric fission process which is an intermediate between spontaneous fission and α -decay. Before 1980s, the radioactive disintegration was experimentally observed either by α -decay or spontaneous fission. Later, the concept of cluster radioactivity phenomenon in the heavy and superheavy nuclei

^{†,‡}Corresponding authors.

was first suggested by Sandulescu *et al.*^[1] Rose and Jones^[2] experimentally observed cluster radioactivity in 1984 and later Aleksandrov *et al.*^[3] found ^{14}C cluster emission from ^{223}Ra . Later on, cluster emissions, such as ^{20}O , ^{23}F , $^{22,24,26}\text{Ne}$, $^{28,30}\text{Mg}$ and $^{32,34}\text{Si}$, were experimentally observed.^[4,5] The cluster ^{34}Si emission was experimentally observed^[6,7] in heavy nuclei ^{242}Cm and ^{238}U .

Several theoretical models, such as preformed cluster model (PCM) by Malik and Gupta^[8] and supersymmetric fission model by Poenaru *et al.*,^[9] explain the cluster radioactivity. There are also several theoretical models^[10,14] that successfully predict the cluster radioactivity in the heavy and superheavy nuclei. Microscopic measurements for the formation of cluster probability and barrier penetrability^[13,14] have been made by using R matrix description of the process. Within the microscopic model, Warda *et al.*^[15] investigated cluster radioactivity in the superheavy element $Z = 116$. In all of these different models, a collection of various proximity potentials is a benchmark to evaluate the half-lives.

Zhang *et al.*^[16] studied large cluster radioactivity in even-even nuclei by using 14 proximity potential functions. The results indicate that with experimental data, the effects of proximity potential such as Bass 77 and Denisov potentials are more appropriate. Raj Kumar^[17] investigated cluster radioactivity by using different proximity potential functions. Santhosh and Biju^[18] analyzed cluster radioactivity half-lives in the superheavy nuclei $^{280-314}116$ by studying Coulomb and proximity potentials. By using the folding density-dependent M3Y effective interaction method, Routray *et al.*^[19] investigated cluster radioactivity in heavy nuclei. Within the density-dependent cluster model, Ismail *et al.*^[20,21] studied the cluster radioactivity half-lives in the superheavy element $Z = 121$ and 122. The shorter half-lives were theoretically observed during cluster emissions of ^{14}C , ^{20}O , ^{20}Ne and ^{24}Ne cluster emissions from heavy and superheavy nuclei. The role of deformation parameter and the orientation of different nuclei during the cluster radioactivity leading to doubly magic nuclei ^{208}Pb were studied by Arun *et al.*^[22] Kuklin *et al.*^[23] examined cluster radioactivity by using dinuclear system concept in the actinide region. Iriondo *et al.*^[24] studied cluster radioactivity by using Gamow potential model for formation and then penetration probability of the particle through the Coulomb barrier. The earlier researchers^[25,36] extensively studied cluster radioactivity in heavy and superheavy region.

The stability of the nucleus is well defined by its magicity of protons or neutrons. Shell closure effects were studied using cluster decay in ^{218}U .^[37] Gupta *et al.*^[38] showed that stability of atom is either due to magicity of neutrons or protons. From the literature, it is observed that all these investigations give incomplete information of cluster radioactivity in the superheavy nuclei region $Z = 104-126$. Hence, in this work, we have analyzed cluster radioactivity in the superheavy region of wide range from $Z = 104-126$ using modified generalized liquid drop model (MGLDM). The half-lives of different cluster emissions such as ^4He , ^6Li , ^9Be , ^{20}Ne , ^{23}Na , ^{24}Mg , ^{27}Al , ^{28}Si , ^{31}P , ^{32}S , ^{35}Cl , ^{36}Ar , ^{39}K and ^{40}Ca were evaluated in the superheavy

region $Z = 104\text{--}126$ using Ng80³⁹ which produces less deviation when compared to other proximity functions as mentioned in the earlier work.²⁵ This study is structured according to the theory used to evaluate half-lives in the superheavy region $Z = 104\text{--}126$ during different cluster emissions and is given in Sec. 2. The analysis of different cluster emissions and corresponding results and discussions are presented in Sec. 3. Finally, conclusions of this work are given in Sec. 4.

2. Theoretical Framework

Among various models, the MGLDM is one of the successful models which describes the fusion, fission, α and light particle emissions^{40,46} and nuclear structure parameters such as nuclear radius and mass, investigation of charge asymmetry, deformation and proximity effects. For a deformed nucleus, total energy is the sum of the volume, surface, coulomb and proximity energies and the same were expressed as follows:

$$E = E_v + E_s + E_c + E_{\text{Prox}} + E_l. \quad (1)$$

For the deformed nuclei, the volume (E_V), surface (E_s) and coulomb energies (E_c) are given by

$$E_v = -15.494(1 - 1.8I^2)A \text{ MeV}, \quad (2)$$

$$E_s = 17.9439(1 - 2.6I^2)A^{2/3} \frac{S}{4\pi R_0^2} \text{ MeV}, \quad (3)$$

$$E_c = 0.6e^2(Z^2/R_0) \times 0.5 \int (V(\theta)/V_0)(R(\theta)/R_0)^3 \sin(\theta) d\theta \text{ MeV}, \quad (4)$$

where I and S are the relative neutron excess and surface area of the deformed nucleus, respectively. $V(\theta)$ and V_0 are the electrostatic potential at the surface and surface potential of the sphere, respectively. For the nuclei that are far apart, the equations are written as follows:

$$E_v = -15.494(1 - 1.8I_1^2)A_1 + (1 - 1.8I_2^2)A_2 \text{ MeV}, \quad (5)$$

$$E_s = 17.9439(1 - 2.6I_1^2)A_1^{2/3} + (1 - 2.6I_2^2)A_2^{2/3} \text{ MeV}, \quad (6)$$

$$E_c = 0.6e^2(Z_1^2/R_1) + 0.6e^2(Z_2^2/R_2) + e^2 Z_1 Z_2 / r \text{ MeV}. \quad (7)$$

Here, A_i , Z_i , R_i and I_i are with the usual notations such as mass number, atomic number, radii of the two nuclei and relative neutron excess of the two nuclei, respectively. $I_2 = 0$ such that E_V and E_S possess negative and positive values. The radii

R_i of the daughter nuclei are defined as follows:

$$R_i = (1.26A_i^{1/3} - 0.76 + 0.8A_i^{-1/3})fm \quad i = 1, 2, \dots \quad (8)$$

The centrifugal energy E_l of the emitted proton is expressed as follows:

$$E_l(r) = \frac{\hbar^2 \ell(\ell + 1)}{2\mu r^2}, \quad (9)$$

where μ , ℓ and r are the reduced mass, angular momentum and the distance between the mass centers, respectively. The proximity function is taken from Ref. [47] and it is expressed as follows:

$$V_p(z) = 4\pi\gamma\Phi\bar{R}\left(\frac{z}{b}\right). \quad (10)$$

Here, Φ is the universal proximity potential and z is the distance between the near surfaces of the fragments. $b \approx 0.99$ is the nuclear surface thickness. The mean curvature radius in Eq. (10) is calculated using the following relation:

$$\bar{R} = \frac{C_1 C_2}{C_1 + C_2}. \quad (11)$$

The Sussmann central radii C_i are given by

$$C_i = R_i - \left(\frac{b^2}{R_i}\right). \quad (12)$$

Sharp radii R_i are expressed as follows:

$$R_i = 1.28A_i^{1/3} - 0.76 + 0.8A_i^{-1/3}. \quad (13)$$

In Eq. (10), γ is given defined as follows:

$$\gamma = \gamma_0 \left[1 - K_s \left(\frac{N - Z}{A} \right)^2 \right] \text{MeV/fm}^2, \quad (14)$$

where $\gamma_0 = 1.460734$ MeV/fm² and $K_s = 4.0$ and universal proximity potential [39] is expressed as follows:

$$\Phi(\epsilon) = \begin{cases} -33 + 5.4(S - S_0)^2 & \text{for } S < S_0, \\ -33 \exp\left[-\frac{1}{5}\right] (S - S_0)^2 & \text{for } S \geq S_0. \end{cases} \quad (15)$$

The proximity and coulomb function are enough to achieve the α -decay and cluster radioactivity and the probability of penetration is studied using the WKB integration:

$$P = \exp \left[-\frac{2}{\hbar} \int_{R_{\text{in}}}^{R_{\text{out}}} \sqrt{2B(r)E(r) - E(\text{sphere})} \right]. \quad (16)$$

Here, R_{in} and R_{out} are the inside and outside classical turning points which can be evaluated from the condition $V(r = R_{\text{in}}) = V(r = R_{\text{out}}) = Q$ and μ is the reduced

mass of the cluster and daughter nuclei. The half-lives of cluster emission from the superheavy nuclei $Z = 104\text{--}126$ were evaluated using the following equation:

$$T_{1/2} = \frac{\ln 2}{\nu P_C P}. \quad (17)$$

Here, $\nu = 10^{20} \text{s}^{-1}$ is the assault frequency. P_C is the pre-formation factor^[48] as a function of amount of energy released during cluster decay is expressed as follows:

$$P_C = 10^{aQ+bQ^2+c}, \quad (18)$$

where Q is the amount of energy released during cluster radioactivity, the terms a , b and c are the parameters explained in detail in Ref. [48].

3. Results and Discussion

The cluster radioactivity half-lives of experimentally available cluster emitters were evaluated using MGLDM as explained in Sec. 2. Here, we have used experimental Q -values for the evaluation of cluster-decay half-lives for the experimentally available cluster emitters. Table 1 shows the evaluated cluster-decay half-lives using MGLDM with the available experiments. The average deviation and standard deviation are

Table 1. Comparison of cluster-decay half-lives evaluated using present work (PW) with the available experiments.

Decay	Q_{Exp} (MeV)	$\log T_{1/2}^{\text{exp}}$	$\log T_{1/2}^{\text{PW}}$
$^{221}\text{Fr} \rightarrow ^{14}\text{C} + ^{207}\text{Tl}$	31.317	14.51 ^[49]	15.59
$^{221}\text{Ra} \rightarrow ^{14}\text{C} + ^{207}\text{Pb}$	32.396	13.37 ^[49]	14.56
$^{222}\text{Ra} \rightarrow ^{14}\text{C} + ^{208}\text{Pb}$	33.05	11.05 ^[50]	13.70
$^{223}\text{Ra} \rightarrow ^{14}\text{C} + ^{209}\text{Pb}$	31.829	15.05 ^[50]	14.94
$^{224}\text{Ra} \rightarrow ^{14}\text{C} + ^{210}\text{Pb}$	30.54	15.9 ^[51]	16.52
$^{226}\text{Ra} \rightarrow ^{14}\text{C} + ^{212}\text{Pb}$	28.2	21.29 ^[52]	22.74
$^{225}\text{Ac} \rightarrow ^{14}\text{C} + ^{211}\text{Bi}$	30.477	17.16 ^[53]	17.86
$^{228}\text{Th} \rightarrow ^{20}\text{O} + ^{208}\text{Pb}$	44.72	20.73 ^[54]	21.94
$^{230}\text{U} \rightarrow ^{22}\text{Ne} + ^{208}\text{Pb}$	61.4	19.56 ^[55]	19.21
$^{230}\text{Th} \rightarrow ^{24}\text{Ne} + ^{206}\text{Hg}$	57.571	24.61 ^[56]	23.87
$^{231}\text{Pa} \rightarrow ^{24}\text{Ne} + ^{207}\text{Tl}$	60.417	22.89 ^[56]	22.07
$^{232}\text{U} \rightarrow ^{24}\text{Ne} + ^{208}\text{Pb}$	62.31	20.39 ^[57]	21.25
$^{233}\text{U} \rightarrow ^{24}\text{Ne} + ^{209}\text{Pb}$	60.486	24.84 ^[56]	23.75
$^{234}\text{U} \rightarrow ^{26}\text{Ne} + ^{208}\text{Pb}$	59.466	25.93 ^[58, 59]	24.46
$^{234}\text{U} \rightarrow ^{28}\text{Mg} + ^{206}\text{Hg}$	74.11	25.74 ^[60]	26.04
$^{236}\text{Pu} \rightarrow ^{28}\text{Mg} + ^{208}\text{Pb}$	79.67	21.65 ^[56]	22.67
$^{238}\text{Pu} \rightarrow ^{28}\text{Mg} + ^{210}\text{Pb}$	75.912	25.66 ^[61]	26.93
$^{238}\text{Pu} \rightarrow ^{30}\text{Mg} + ^{208}\text{Pb}$	77	25.66 ^[61]	25.26
$^{238}\text{Pu} \rightarrow ^{32}\text{Si} + ^{206}\text{Hg}$	91.19	25.3 ^[62]	27.85
$^{242}\text{Cm} \rightarrow ^{34}\text{Si} + ^{208}\text{Pb}$	96.509	23.11 ^[63]	23.24

evaluated using the following expressions:

$$\delta = \frac{1}{n} \sum_{i=1}^n |\log T_{1/2}^{\text{PW}} - \log_{1/2}^{\text{exp}}| \quad (19)$$

and

$$\sqrt{\delta^2} = \sqrt{\frac{1}{n} \sum_{i=1}^n [\log T_{1/2}^{\text{PW}} - \log_{1/2}^{\text{exp}}]^2}. \quad (20)$$

The average deviation (δ) and standard deviation ($\sqrt{\delta^2}$) are evaluated for 20 experimental values available in the literature. The values of δ and $\sqrt{\delta^2}$ are found to be 1.01 and 1.202, respectively.

The amount energy released during the cluster radioactivity is evaluated using the mass excess values available in the literature.^[64] In Figs. 1 and 2, we have studied the half-lives of possible cluster emissions from ${}^4\text{He}$ to ${}^{40}\text{Ca}$ and spontaneous fission in the superheavy region $104 \leq Z \leq 115$ and $116 \leq Z \leq 126$, respectively. Spontaneous fission half-lives of superheavy nuclei in the region $104 \leq Z \leq 126$ are

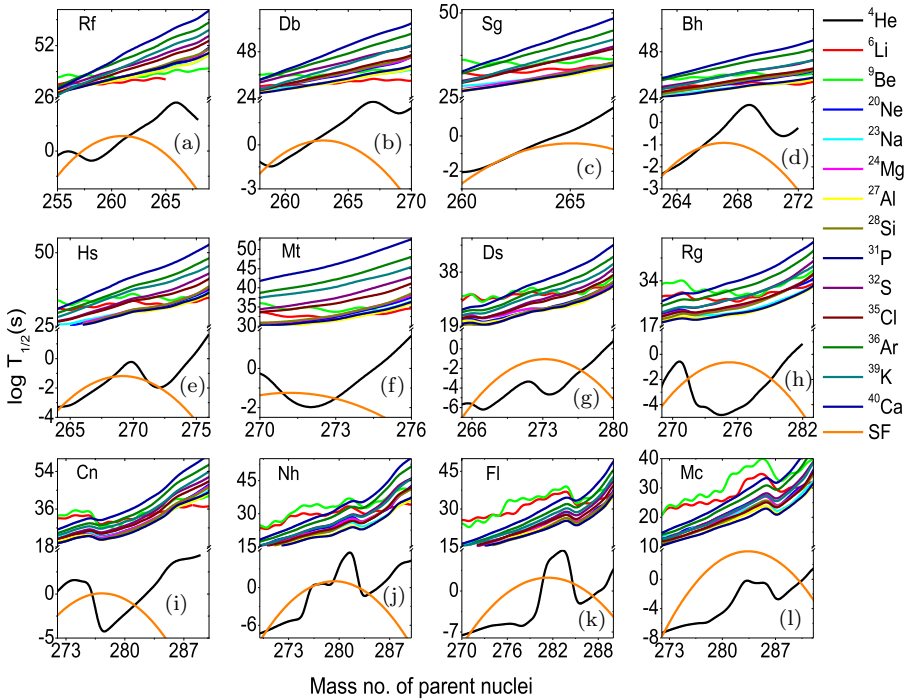


Fig. 1. Plot of evaluated $\log T_{1/2}$ values versus mass number of parent nuclei for the emission of cluster (${}^4\text{He}$ to ${}^{48}\text{Ca}$) and spontaneous fission from superheavy region $104 \leq Z \leq 115$.

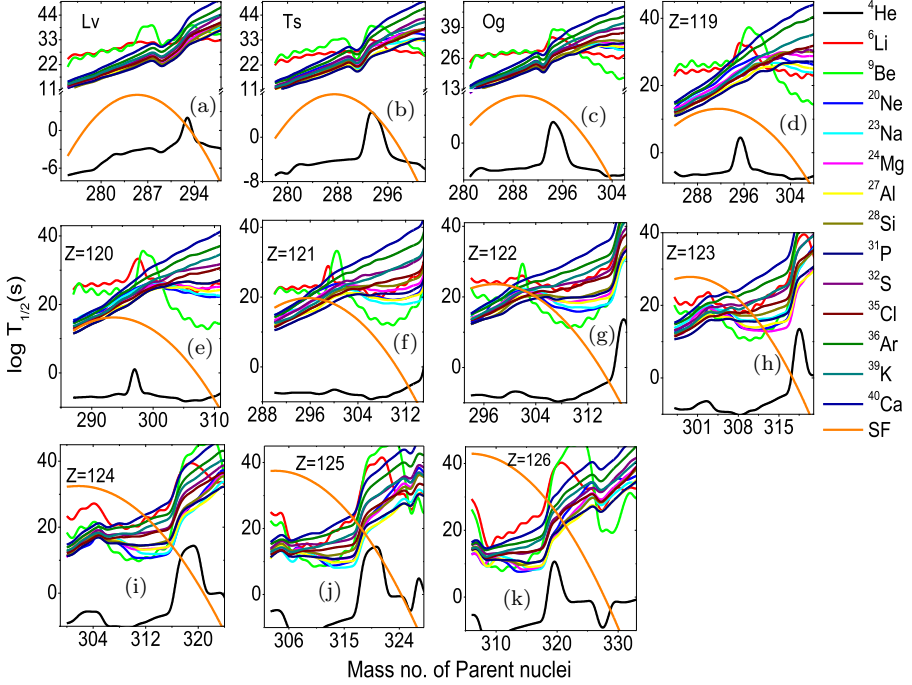


Fig. 2. Plot of evaluated $\log T_{1/2}$ values versus mass number of parent nuclei for the emission of cluster (${}^4\text{He}$ to ${}^{48}\text{Ca}$) and spontaneous fission from superheavy region $116 \leq Z \leq 126$.

evaluated using semi-empirical formula proposed by Xu *et al.*^[65] as follows:

$$T_{1/2} = \exp[2\pi(C_0 + C_1A + C_2A^2 + C_3Z^4 + C_4(N - Z)^2) - (0.13323Z^2/A^{1/3} - 11.64)], \quad (21)$$

where C_0, C_1, C_2, C_3 and C_4 are $-195.09227, 3.10156, -0.04386, 1.40301 \times 10^{-6}$ and -0.03199 , respectively.

From these plots, it is clear that the ${}^4\text{He}$ emission and spontaneous fission half-lives show smaller logarithmic half-life values when compared to other cluster emissions studied. Figure II(a) shows smaller half-lives in the isotopes of superheavy nuclei ${}^{257-262}\text{Rf}$ when compared to other cluster emissions studied. The neutron number corresponding to isotopes of superheavy nuclei ${}^{257-261}\text{Rf}$ varies between $N = 153-157$ which are near the magic numbers of 184. Similarly, Figs. II(b)-II(l) depict shorter α -decay half-lives when compared to other different decay modes in the isotopes of superheavy nuclei ${}^{259-262}\text{Db}$, ${}^{261-262}\text{Sg}$, ${}^{263-265}\text{Bh}$, ${}^{265-268}\text{Hs}$, ${}^{271-273}\text{Mt}$, ${}^{267-275}\text{Ds}$, ${}^{271-278}\text{Rg}$, ${}^{276-281}\text{Cn}$, ${}^{271-283}\text{Nh}$, ${}^{272-287}\text{Fl}$, ${}^{273-290}\text{Mc}$, ${}^{275-292}\text{Lv}$, ${}^{278-293, 295-298}\text{Ts}$, ${}^{281-301}\text{Og}$, ${}^{284-304}\text{119}$, ${}^{287-308}\text{120}$, ${}^{290-305, 308-311}\text{121}$, ${}^{294-314}\text{122}$, ${}^{297-317}\text{123}$, ${}^{300-305, 308-317}\text{124}$, ${}^{303-323}\text{125}$ and ${}^{306-325}\text{126}$.

In order to explore new isotopes of superheavy nuclei with magic nuclei, first we have analyzed shell closures of the atoms in heavy and superheavy nuclei in the

Table 2. Isotopes of heavy and superheavy nuclei having longer life time in the atomic number region $104 \leq Z \leq 118$.

Element	N	$\log T$	Element	N	$\log T$
$^{267}_{104}\text{Rf}$	163	3.67	$^{286}_{112}\text{Cn}$	174	2.82
$^{268}_{105}\text{Db}$	163	5.00	$^{286}_{113}\text{Nh}$	173	0.98
$^{269}_{106}\text{Sg}$	163	2.27	$^{290}_{114}\text{Fl}$	176	1.28
$^{278}_{107}\text{Bh}$	171	3.06	$^{290}_{115}\text{Mc}$	175	-0.19
$^{278}_{108}\text{Hs}$	170	3.06	$^{293}_{116}\text{Lv}$	177	-1.28
$^{282}_{109}\text{Mt}$	173	1.82	$^{294}_{117}\text{Ts}$	177	-1.29
$^{282}_{110}\text{Ds}$	172	1.82	$^{294}_{118}\text{Og}$	176	-3.24
$^{286}_{111}\text{Rg}$	175	2.82			

region $104 \leq Z \leq 118$. Table 2 presents the tabulation of nuclei having specific neutron number and larger half-lives. It has been observed that these tabulated nuclei with atomic number (Z) or neutron number (N) are much more stable than their neighboring nuclei. The tabulated atomic nucleus is having comparatively higher binding energy per nucleon. Thus, these nuclei possess longer half-lives and hence more stable against different nuclear decays. From the table, it is inferred that the neutron number $N = 163$ – 177 shows complete shell closures within the atomic nuclei. So, the neutron numbers with shell closures have larger half-lives which are

Table 3. Tabulation of parent (A_P), daughter (A_D) and cluster nuclei (A_C) along with the Q -values and $\log T_{1/2}$ values corresponding to magic number of neutrons of parent/daughter nuclei.

A_P	A_D	A_C	Q (MeV)	$\text{Log} T_{1/2}$
$^{309}_{120}_{189}$	$^{300}_{Lv}_{184}$	9Be_5	24.84	11.41
$^{310}_{121}_{189}$	$^{301}_{Ts}_{184}$	9Be_5	25.35	10.86
$^{311}_{122}_{189}$	$^{302}_{Og}_{184}$	9Be_5	25.93	10.22
$^{312}_{123}_{189}$	$^{303}_{119}_{184}$	9Be_5	26.31	10
$^{313}_{124}_{189}$	$^{304}_{120}_{184}$	9Be_5	26.81	9.56
$^{323}_{125}_{198}$	$^{296}_{Cn}_{184}$	$^{27}_{Al}_{14}$	105.15	24.59
$^{324}_{126}_{198}$	$^{297}_{Nh}_{184}$	$^{27}_{Al}_{14}$	106.15	24.66
$^{326}_{126}_{200}$	$^{295}_{Rg}_{184}$	$^{31}_{P}_{16}$	121.61	27.89
$^{302}_{118}_{184}$	$^{293}_{Fl}_{179}$	9Be_5	19.35	24.98
$^{303}_{119}_{184}$	$^{294}_{Mc}_{179}$	9Be_5	20.66	21.62
$^{304}_{120}_{184}$	$^{295}_{Lv}_{179}$	9Be_5	21.52	19.84
$^{305}_{121}_{184}$	$^{296}_{Ts}_{179}$	9Be_5	22.62	17.57
$^{306}_{122}_{184}$	$^{297}_{Og}_{179}$	9Be_5	23.33	16.37
$^{307}_{123}_{184}$	$^{298}_{119}_{179}$	9Be_5	24.46	14.27
$^{308}_{124}_{184}$	$^{299}_{120}_{179}$	9Be_5	25.27	13.05
$^{309}_{125}_{184}$	$^{300}_{121}_{179}$	9Be_5	26.59	10.77
$^{310}_{126}_{184}$	$^{301}_{122}_{179}$	9Be_5	27.25	10
$^{311}_{126}_{185}$	$^{302}_{122}_{180}$	9Be_5	28.95	6.69
$^{322}_{126}_{196}$	$^{295}_{Nh}_{182}$	$^{27}_{Al}_{14}$	108.47	22.14

near magic nuclei or magic nuclei. Hence, with this background, we have extended our work to predict magic or semi-magic neutron numbers in atomic number region $104 \leq Z \leq 126$.

Tables 4 and 5 show tabulated logarithmic half-lives of different decay modes such as α , β^+ , spontaneous fission half-lives and shortest logarithmic half-life correspond to cluster decay. The dominant decay mode among different decay mode studied is also shown in the 6th, 12th and 18th columns of Tables 4 and 5. From these tables, it is observed that the superheavy nuclei ^{262}Rf have neutron number $N = 158$ with logarithmic half-life of 1.13s which undergoes spontaneous fission. The nuclei ^{262}Rf are more stable when compared to their neighboring nuclei. Similarly, the superheavy nuclei ^{262}Db with $N = 157$ and α -decay logarithmic half-life of -0.44s , ^{262}Sg ($N = 156$) and $\log T_{1/2}$ of -1.88ms in case of α -decay, ^{266}Bh [$N = 159, -1.0\text{s(sf)}$], ^{272}Hs [$N = 164, -1.9\text{s(sf)}$], ^{273}Mt [$164, -1.73\text{s}(\alpha)$], ^{276}Ds [$166, -1.73\text{s(sf)}$], ^{279}Rg [$168, -1.86\text{s(sf)}$], ^{281}Cn [$169, -1.16\text{s}(\alpha)$], ^{283}Nh [$170, -1.55\text{s}(\alpha)$], ^{287}Fl [$173, -1.46\text{s}(\alpha)$], ^{289}Mc [$175, -2.03\text{s}(\alpha)$], ^{292}Lv [$176, -2.61\text{s}(\alpha)$], ^{299}Ts [$182, -4.03\text{s(sf)}$], ^{302}Og [$184, -3.62\text{s(sf)}$], $^{305}119$ [$186, -3.04\text{s(sf)}$], $^{309}120$ [$189, -4.94\text{s(sf)}$], $^{312}121$ [$191, -4.16\text{s(sf)}$], $^{315}122$ [$193, -3.18\text{s}(\alpha)$], $^{317}123$ [$194, -2.85\text{s}(\alpha)$], $^{317}124$ [$193, -3.92\text{s}(\alpha)$], $^{323}125$ [$198, -3.06\text{s}(\alpha)$] and $^{329}126$ [$203, -4.91\text{s(sf)}$] show comparably larger life times than their neighboring nuclei. This signifies that there may be semi-magic nuclei existing between the neutron numbers $N = 157-203$. More detailed experimental/theoretical study is necessary to draw the definite conclusion in this aspect.

Even though an alpha and spontaneous fission are dominant in the studied table, in our further analysis, we have considered cluster radioactivity of shorter half-lives. A map of nuclei reflects the shortest logarithmic half-lives of cluster emissions studied in the superheavy region $104 \leq Z \leq 126$ shown in Fig. 3. This figure enables us to predict shortest half-lives among the studied cluster emissions and it is shown on right side of the figure with the vertical bar. The shorter half-lives are shown with the color indigo which ranges from 6.6 to 10.97s in the superheavy region $121 \leq Z \leq 126$ which includes the cluster emissions such as ^9Be , ^{20}Ne , ^{23}Na , ^{24}Mg , ^{27}Al and ^{31}P . These shorter half-lives are due to magic number of neutrons in the superheavy region which ranges between 170 and 192. Among these half-lives the superheavy nuclei $^{309}125$ and $^{310}126$ have neutron number of 184 with $\log T_{1/2} = 10.77$ and 10s , respectively, for the cluster emission of ^9Be . Similarly, the $\log T_{1/2}$ corresponding to $^{311}126$ shows shortest value of 6.6 in which $Z = 126$ is a magic nuclei.

Further, dark blue color to light blue shows the $\log T_{1/2}$ values of 11.12 to 18.98 s within the superheavy region of $119 \leq Z \leq 126$ with the cluster emissions such as ^9Be , ^{20}Ne , ^{23}Na , ^{24}Mg , ^{27}Al and ^{31}P . Among these, the nucleus $^{322}126$ has magic neutron number $N = 196$, the nuclei $^{304}120$ $^{305}121$, $^{306}122$ and $^{308}124$ carry magic neutron number $N = 184$. Logarithmic half-lives from cyan to red color vary from 18 to 35.80 s in the superheavy region $104 \leq Z \leq 122$ and $124 \leq Z \leq 126$.

Table 4. Logarithmic half-lives of different decay modes such as α , β^+ , spontaneous fission, and shortest logarithmic half-life correspond to cluster decay.

Parent Nuclei	log $T_{1/2}$			Decay mode	Parent Nuclei	log $T_{1/2}$			Decay mode	Parent Nuclei	log $T_{1/2}$			Decay mode			
	α	β^+	Sf			Cluster	α	β^+			Sf	Cluster	α		β^+	Sf	Cluster
$^{257}\text{Rf}_{153}$	-2.11	0.23	-0.19	30.93(^{31}P)	α	$^{270}\text{Nh}_{157}$	-6.05	-3.77	-6.73	13.54(^{31}P)	Sf	$^{289}\text{Lv}_{173}$	-3.21	-2.19	4.53	20.32(^{31}P)	α
$^{258}\text{Rf}_{154}$	-1.86	0.46	0.43	32.43(^{27}Al)	α	$^{271}\text{Nh}_{158}$	-5.57	-3.55	-5.15	14.41(^{31}P)	α	$^{290}\text{Lv}_{174}$	-2.98	-1.97	3.80	22.75(^{31}P)	α
$^{259}\text{Rf}_{155}$	-1.22	5.17	0.88	31.77(^{6}Li)	α	$^{272}\text{Nh}_{159}$	-5.23	-3.33	-3.75	15.43(^{31}P)	α	$^{291}\text{Lv}_{175}$	-2.78	-1.76	2.90	24.25(^{31}P)	α
$^{260}\text{Rf}_{156}$	-0.29	1.14	1.14	34.1(^{27}Al)	α	$^{273}\text{Nh}_{160}$	-5.00	-3.11	-2.53	16.08(^{31}P)	α	$^{292}\text{Lv}_{176}$	-2.61	-1.54	1.82	26.76(^{27}Al)	α
$^{261}\text{Rf}_{157}$	0.39	1.82	1.23	32.77(^{6}Li)	α	$^{274}\text{Nh}_{161}$	-4.84	-2.89	-1.49	16.94(^{31}P)	α	$^{278}\text{Ts}_{161}$	-7.26	-5.41	-0.24	10.27(^{31}P)	α
$^{262}\text{Rf}_{158}$	1.17	2.06	1.13	35.71(^{6}Li)	Sf	$^{275}\text{Nh}_{162}$	-4.74	-2.67	-0.63	18.08(^{31}P)	α	$^{279}\text{Ts}_{162}$	-7.18	-5.19	1.37	11.49(^{31}P)	α
$^{259}\text{Db}_{154}$	-2.69	0.49	-1.12	27.14(^{31}P)	α	$^{276}\text{Nh}_{163}$	-4.69	-2.45	0.06	19.03(^{31}P)	α	$^{280}\text{Ts}_{163}$	-7.15	-4.98	2.80	11.96(^{31}P)	α
$^{260}\text{Db}_{155}$	-1.89	0.73	-0.49	28.3(^{27}Al)	α	$^{279}\text{Nh}_{166}$	-3.49	-1.79	1.04	19.98(^{31}P)	α	$^{281}\text{Ts}_{164}$	-7.14	-4.76	4.04	13.2(^{31}P)	α
$^{261}\text{Db}_{156}$	-1.26	0.96	-0.04	28.85(^{27}Al)	α	$^{283}\text{Nh}_{170}$	-1.55	-0.90	-0.15	22.2(^{31}P)	α	$^{282}\text{Ts}_{165}$	-6.76	-4.55	5.11	14.07(^{31}P)	α
$^{262}\text{Db}_{157}$	-0.44	1.20	0.23	29.82(^{6}Li)	α	$^{271}\text{Fl}_{157}$	-6.71	-4.40	-7.32	12.8(^{28}Si)	Sf	$^{289}\text{Ts}_{166}$	-6.41	-4.34	6.00	14.59(^{31}P)	α
$^{261}\text{Sg}_{155}$	-2.69	0.11	-1.86	27.73(^{28}Si)	α	$^{272}\text{Fl}_{158}$	-6.41	-4.18	-5.55	13.72(^{28}Si)	α	$^{284}\text{Ts}_{167}$	-6.04	-4.12	6.72	15.71(^{31}P)	α
$^{262}\text{Sg}_{156}$	-1.88	0.34	-1.22	28.74(^{28}Si)	α	$^{273}\text{Fl}_{159}$	-5.99	-3.96	-3.97	14.44(^{28}Si)	α	$^{285}\text{Ts}_{168}$	-5.47	-3.91	7.25	16.28(^{31}P)	α
$^{263}\text{Sg}_{156}$	-2.74	-0.28	-2.39	24.33(^{31}P)	α	$^{274}\text{Fl}_{160}$	-5.68	-3.74	-2.56	15.52(^{28}Si)	α	$^{286}\text{Ts}_{169}$	-5.09	-3.69	7.60	17.32(^{31}P)	α
$^{264}\text{Th}_{157}$	-1.92	-0.05	-1.75	25.17(^{31}P)	α	$^{275}\text{Fl}_{161}$	-5.49	-3.52	-1.34	16.35(^{28}Si)	α	$^{287}\text{Ts}_{170}$	-4.78	-3.48	7.78	18.43(^{31}P)	α
$^{265}\text{Th}_{158}$	-1.39	0.19	-1.28	25.83(^{31}P)	α	$^{276}\text{Fl}_{162}$	-5.38	-3.30	-0.29	17.41(^{28}Si)	α	$^{288}\text{Ts}_{171}$	-4.51	-3.27	7.78	19.75(^{31}P)	α
$^{266}\text{Th}_{159}$	-0.98	0.42	-1.00	26.89(^{27}Al)	Sf	$^{277}\text{Fl}_{163}$	-5.33	-3.08	0.58	18.17(^{28}Si)	α	$^{289}\text{Ts}_{172}$	-4.29	-3.05	7.59	20.62(^{31}P)	α
$^{264}\text{Hs}_{156}$	-3.32	-0.90	-3.53	23.74(^{28}Si)	Sf	$^{278}\text{Fl}_{164}$	-5.30	-2.86	1.27	18.92(^{28}Si)	α	$^{290}\text{Ts}_{173}$	-4.10	-2.84	7.24	22(^{31}P)	α
$^{265}\text{Hs}_{157}$	-2.83	-0.67	-2.70	24.31(^{31}P)	α	$^{279}\text{Fl}_{165}$	-4.84	-2.64	1.79	19.98(^{31}P)	α	$^{291}\text{Ts}_{174}$	-3.79	-2.63	6.70	18.22(^{31}P)	α
$^{266}\text{Hs}_{158}$	-2.17	-0.44	-2.05	25.41(^{31}P)	α	$^{280}\text{Fl}_{166}$	-4.43	-2.42	2.12	20.95(^{28}Si)	α	$^{292}\text{Ts}_{175}$	-3.52	-2.41	5.98	20.2(^{31}P)	α
$^{267}\text{Hs}_{159}$	-1.69	-0.21	-1.58	26.11(^{31}P)	α	$^{281}\text{Fl}_{167}$	-3.86	-2.20	2.28	21.86(^{31}P)	α	$^{293}\text{Ts}_{176}$	-3.30	-2.20	5.09	25.07(^{31}P)	α
$^{268}\text{Hs}_{160}$	-1.36	0.02	-1.29	27.61(^{27}Al)	α	$^{286}\text{Fl}_{172}$	-1.80	-1.11	0.37	24.79(^{31}P)	α	$^{295}\text{Ts}_{178}$	-2.92	-1.77	2.76	27.21(^{31}P)	α
$^{271}\text{Hs}_{163}$	-0.88	0.71	-1.48	29.73(^{27}Al)	Sf	$^{287}\text{Fl}_{173}$	-1.46	-0.89	-0.54	26.38(^{31}P)	α	$^{296}\text{Ts}_{179}$	-2.74	-1.56	1.33	27.57(^{6}Li)	α
$^{272}\text{Hs}_{164}$	-0.82	0.94	-1.90	30.77(^{27}Al)	Sf	$^{272}\text{Mc}_{157}$	-7.22	-5.02	-7.81	10.4(^{31}P)	Sf	$^{297}\text{Ts}_{180}$	-2.55	-1.34	-0.28	29.14(^{31}P)	α
$^{271}\text{Mt}_{162}$	-1.91	-0.15	-1.23	29.73(^{27}Al)	α	$^{273}\text{Mc}_{158}$	-6.90	-4.80	-5.86	11.1(^{31}P)	α	$^{299}\text{Ts}_{181}$	-2.35	-1.13	-0.26	27.1(^{6}Li)	α
$^{272}\text{Mt}_{163}$	-1.80	0.08	-1.29	30.77(^{27}Al)	α	$^{274}\text{Mc}_{159}$	-6.65	-4.58	-4.09	12(^{31}P)	α	$^{299}\text{Ts}_{182}$	-2.15	-0.91	-4.03	28.69(^{6}Li)	Sf
$^{273}\text{Mt}_{164}$	-1.73	0.31	-1.52	30.89(^{6}Li)	α	$^{275}\text{Mc}_{160}$	-6.47	-4.37	-2.49	12.74(^{31}P)	α	$^{281}\text{Og}_{163}$	-7.63	-5.61	3.78	10.74(^{24}Mg)	α
$^{266}\text{Ds}_{156}$	-5.16	-2.14	-5.69	19.85(^{28}Si)	Sf	$^{276}\text{Mc}_{161}$	-6.35	-4.15	-1.08	13.52(^{31}P)	α	$^{282}\text{Og}_{164}$	-7.63	-5.40	5.21	12.47(^{28}Si)	α

Table 4. (Continued)

Parent Nuclei	log T _{1/2}			Decay mode	Parent Nuclei	log T _{1/2}			Decay mode	Parent Nuclei	log T _{1/2}			Decay mode			
	α	β ⁺	Sf			α	β ⁺	Sf			α	β ⁺	Sf				
267Ds 157	-4.73	-1.91	-4.49	18.87(28Si)	α	277Mc 162	-6.28	-3.93	0.15	14.11(31P)	α	283Og 165	-7.20	-5.19	6.47	13.24(28Si)	α
268Ds 158	-4.21	-1.68	-3.47	19.83(28Si)	α	278Mc 163	-6.24	-3.71	1.21	15.14(31P)	α	284Og 166	-6.82	-4.97	7.54	14.01(28Si)	α
269Ds 159	-3.74	-1.46	-2.63	20.49(28Si)	α	279Mc 164	-6.23	-3.50	2.09	16.21(31P)	α	285Og 167	-6.49	-4.76	8.44	14.9(28Si)	α
270Ds 160	-3.43	-1.23	-1.96	22.09(31P)	α	280Mc 165	-5.52	-3.28	2.78	17.07(31P)	α	286Og 168	-6.19	-4.55	9.16	15.93(31P)	α
271Ds 161	-3.23	-1.00	-1.48	22.87(31P)	α	281Mc 166	-5.06	-3.06	3.30	17.77(31P)	α	287Og 169	-5.73	-4.34	9.70	16.85(31P)	α
272Ds 162	-3.09	-0.78	-1.17	24.3(31P)	α	282Mc 167	-4.65	-2.84	3.64	18.81(31P)	α	288Og 170	-5.34	-4.13	10.06	17.86(31P)	α
273Ds 163	-3.01	-0.55	-1.04	24.03(27Al)	α	283Mc 168	-4.30	-2.63	3.81	19.57(31P)	α	289Og 171	-5.05	-3.91	10.24	19.07(31P)	α
274Ds 164	-2.97	-0.33	-1.10	25.31(27Al)	α	284Mc 169	-3.77	-2.41	3.79	20.75(31P)	α	290Og 172	-4.81	-3.70	10.25	20(31P)	α
275Ds 165	-2.39	-0.10	-1.32	25.33(27Al)	α	285Mc 170	-3.34	-2.19	3.59	22.3(31P)	α	291Og 173	-4.60	-3.49	10.07	21.06(31P)	α
276Ds 166	-1.65	0.13	-1.73	26.42(27Al)	Sf	286Mc 171	-3.00	-1.97	3.22	23.69(31P)	α	292Og 174	-4.43	-3.28	9.72	22.41(31P)	α
277Ds 167	-1.10	0.35	-2.32	27.17(27Al)	Sf	287Mc 172	-2.73	-1.76	2.67	20.05(31P)	α	293Og 175	-4.28	-3.07	9.19	14.23(9Be)	α
278Ds 168	-0.62	0.58	-3.08	29.2(27Al)	Sf	288Mc 173	-2.49	-1.54	1.94	22.14(31P)	α	294Og 176	-4.14	-2.85	8.48	24.33(31P)	α
279Ds 169	0.12	0.81	-4.03	30.68(27Al)	Sf	289Mc 174	-2.29	-1.32	1.03	23.72(31P)	α	295Og 177	-4.00	-2.64	7.59	24.92(31P)	α
274Rg 160	-3.82	-1.86	-2.22	20.14(31P)	α	290Mc 175	-2.03	-1.10	-0.06	25.92(27Al)	α	296Og 178	-3.69	-2.43	6.52	26.34(31P)	α
272Rg 161	-3.59	-1.63	-1.55	19.02(31P)	α	275Lv 159	-7.12	-5.21	-4.09	10.92(28Si)	α	297Og 179	-3.45	-2.22	5.28	27.59(31P)	α
273Rg 162	-3.45	-1.41	-1.06	19.9(31P)	α	276Lv 160	-6.93	-4.99	-2.32	11.87(28Si)	α	298Og 180	-3.22	-2.00	3.86	27.49(31P)	α
274Rg 163	-3.37	-1.18	-0.75	20.33(27Al)	α	277Lv 161	-6.80	-4.78	-0.70	12.94(28Si)	α	299Og 181	-3.00	-1.79	2.26	24.57(9Be)	α
275Rg 164	-3.33	-0.96	-0.61	20.99(27Al)	α	278Lv 162	-6.73	-4.56	0.72	13.76(28Si)	α	300Og 182	-2.78	-1.58	0.48	27.78(9Be)	α
276Rg 165	-2.81	-0.73	-0.66	21.21(27Al)	α	279Lv 163	-6.70	-4.35	1.94	14.44(28Si)	α	301Og 183	-2.56	-1.37	-1.48	22.12(9Be)	α
277Rg 166	-2.20	-0.51	-0.88	21.84(27Al)	α	280Lv 164	-6.69	-4.13	3.00	15.85(28Si)	α	302Og 184	-2.33	-1.16	-3.62	24.98(9Be)	Sf
278Rg 167	-1.54	-0.29	-1.28	23.03(27Al)	α	281Lv 165	-6.33	-3.91	3.89	16.78(28Si)	α	303Og 185	-2.10	-0.94	-5.93	18.26(9Be)	Sf
279Rg 168	-1.03	-0.06	-1.86	24.16(27Al)	Sf	282Lv 166	-5.74	-3.70	4.59	17.59(28Si)	α	285 119 165	-7.69	-5.82	7.96	10.61(27Al)	α
276Cn 164	-3.90	-1.59	-0.06	23.5(31P)	α	283Lv 167	-5.26	-3.48	5.12	18.51(31P)	α	286 119 166	-7.26	-5.61	9.23	11.21(31P)	α
277Cn 165	-3.30	-1.37	0.08	20.71(31P)	α	284Lv 168	-4.87	-3.27	5.47	19.55(31P)	α	287 119 167	-6.90	-5.40	10.31	12.19(31P)	α
278Cn 166	-2.81	-1.15	0.04	21.69(27Al)	α	285Lv 169	-4.53	-3.05	5.64	20.45(31P)	α	288 119 168	-6.59	-5.19	11.21	12.87(31P)	α
279Cn 167	-2.37	-0.93	-0.18	22.45(31P)	α	286Lv 170	-4.25	-2.84	5.63	21.95(31P)	α	289 119 169	-6.31	-4.98	11.94	13.82(31P)	α
280Cn 168	-1.64	-0.70	-0.57	23.65(31P)	α	287Lv 171	-3.86	-2.62	5.44	23.3(31P)	α	290 119 170	-6.08	-4.77	12.49	14.33(31P)	α
281Cn 169	-1.16	-0.48	-1.14	24.98(31P)	α	288Lv 172	-3.48	-2.40	5.07	24.26(31P)	α	290 119 171	-5.68	-4.56	12.85	15.69(31P)	α

Table 5. Logarithmic half-lives of different decay modes such as α , β^+ , spontaneous fission, and shortest logarithmic half-life correspond to cluster decay.

Parent Nuclei	$\log T_{1/2}$			Decay mode	Parent Nuclei	$\log T_{1/2}$			Decay mode	Parent Nuclei	$\log T_{1/2}$			Decay mode			
	α	β^+	Sf			Cluster	α	β^+			Sf	Cluster	α		β^+	Sf	Cluster
291119 172	-5.37	-4.35	13.04	16.59(³¹ P)	α	304121 183	-4.55	-3.37	13.48	16.54(⁹ Be)	α	305124 181	-6.54	-5.78	31.54	17.06(²³ Na)	α
292119 173	-5.14	-4.14	13.05	17.49(³¹ P)	α	305121 184	-4.35	-3.17	11.90	17.57(⁹ Be)	α	308124 184	-6.10	-5.18	29.00	13.05(⁹ Be)	α
293119 174	-4.95	-3.93	12.89	18.6(³¹ P)	α	308121 187	-3.66	-2.55	6.09	11.15(⁹ Be)	α	309124 185	-5.94	-4.97	27.80	9(⁹ Be)	α
294119 175	-4.78	-3.72	12.54	19.78(³¹ P)	α	309121 188	-3.22	-2.34	3.79	13.36(⁹ Be)	α	310124 186	-5.78	-4.77	26.41	10.69(²⁰ Ne)	α
295119 176	-4.63	-3.51	12.02	20.49(³¹ P)	α	310121 189	-2.95	-2.13	1.32	10.86(⁹ Be)	α	311124 187	-5.40	-4.57	24.85	8.76(⁹ Be)	α
296119 177	-4.49	-3.30	11.31	21.04(³¹ P)	α	311121 190	-2.67	-1.93	-1.33	14.83(⁹ Be)	α	312124 188	-5.11	-4.37	23.11	10.61(²⁰ Ne)	α
297119 178	-4.35	-3.09	10.43	21.81(³¹ P)	α	312121 191	-2.39	-1.72	-4.16	12.65(⁹ Be)	Sf	313124 189	-4.85	-4.17	21.19	9.56(⁹ Be)	α
298119 179	-4.21	-2.88	9.37	23.62(³¹ P)	α	294122 172	-6.87	-6.29	22.39	12.23(²⁸ Si)	α	314124 190	-4.61	-3.97	19.10	11.12(²⁰ Ne)	α
299119 180	-4.06	-2.67	8.13	24.44(³¹ P)	α	295122 173	-6.70	-6.09	22.96	12.89(²⁸ Si)	α	315124 191	-4.37	-3.77	16.82	11.51(²⁰ Ne)	α
300119 181	-3.91	-2.46	6.72	24.14(³¹ P)	α	296122 174	-6.56	-5.88	23.34	13.69(³¹ P)	α	316124 192	-4.14	-3.56	14.37	12.44(²⁰ Ne)	α
301119 182	-3.51	-2.25	5.12	24.64(³¹ P)	α	297122 175	-6.44	-5.68	23.55	14.04(³¹ P)	α	317124 193	-3.92	-3.36	11.74	20.12(²³ Na)	α
302119 183	-3.23	-2.04	3.35	20.22(⁹ Be)	α	298122 176	-6.33	-5.48	23.59	14.71(³¹ P)	α	303125 178	-7.42	-7.04	37.47	10.84(²⁷ Al)	α
303119 184	-2.97	-1.83	1.40	21.62(⁹ Be)	α	299122 177	-6.22	-5.27	23.44	15.12(³¹ P)	α	304125 179	-7.27	-6.84	37.52	12.84(³¹ P)	α
304119 185	-2.71	-1.62	-0.73	16.24(⁹ Be)	α	300122 178	-6.11	-5.07	23.11	16.71(³¹ P)	α	305125 180	-7.13	-6.64	37.40	13.57(²³ Na)	α
305119 186	-2.46	-1.41	-3.04	18.72(⁹ Be)	Sf	301122 179	-6.00	-4.86	22.61	17.83(³¹ P)	α	306125 181	-6.98	-6.44	37.09	10.12(²³ Na)	α
306119 187	-2.21	-1.20	-5.53	14.1(⁹ Be)	Sf	302122 180	-5.88	-4.66	21.93	18.65(³¹ P)	α	307125 182	-6.83	-6.24	36.61	9.51(²³ Na)	α
307119 188	-1.96	-0.98	-8.19	16.53(⁹ Be)	Sf	303122 181	-5.58	-4.45	21.06	16.8(⁹ Be)	α	308125 183	-6.67	-6.04	35.94	10.16(⁹ Be)	α
287120 167	-7.34	-6.04	12.33	11.47(³¹ P)	α	305122 182	-5.33	-4.25	20.81	19.28(⁹ Be)	α	309125 184	-6.51	-5.85	35.10	10.77(⁹ Be)	α
288120 168	-7.00	-5.83	13.43	12.22(³¹ P)	α	305122 183	-5.11	-4.04	18.81	14.64(⁹ Be)	α	310125 185	-6.34	-5.65	34.08	7.74(⁹ Be)	α
289120 169	-6.71	-5.62	14.33	13.29(³¹ P)	α	306122 184	-4.89	-3.84	17.41	16.37(⁹ Be)	α	311125 186	-6.17	-5.45	32.89	9.31(⁹ Be)	α
290120 170	-6.46	-5.42	15.06	14.25(³¹ P)	α	307122 185	-4.67	-3.63	15.84	11.4(⁹ Be)	α	312125 187	-6.00	-5.25	31.51	8.07(⁹ Be)	α
291120 171	-6.26	-5.21	15.62	14.96(³¹ P)	α	309122 186	-4.46	-3.43	14.08	13.9(⁹ Be)	α	313125 188	-5.83	-5.05	29.96	7.97(²³ Na)	α
292120 172	-6.08	-5.00	15.99	15.71(³¹ P)	α	309122 187	-4.24	-3.22	12.15	10.13(⁹ Be)	α	314125 189	-5.56	-4.85	28.22	8.2(²³ Na)	α
293120 173	-5.93	-4.79	16.19	17.07(³¹ P)	α	310122 188	-4.03	-3.02	12.05	14.89(⁹ Be)	α	315125 190	-5.20	-4.65	26.31	8.11(²³ Na)	α
294120 174	-5.56	-4.58	16.20	18.17(³¹ P)	α	311122 189	-3.82	-2.81	7.75	10.22(⁹ Be)	α	316125 191	-4.92	-4.45	24.22	8.4(²³ Na)	α
295120 175	-5.36	-4.37	16.04	18.92(³¹ P)	α	312122 190	-3.41	-2.61	5.29	15.45(⁹ Be)	α	317125 192	-4.67	-4.25	21.95	8.76(²³ Na)	α
296120 176	-5.18	-4.16	15.70	19.77(³¹ P)	α	313122 191	-3.06	-2.40	2.65	12.2(⁹ Be)	α	318125 193	-4.43	-4.05	19.51	16.88(²³ Na)	α
297120 177	-5.02	-3.96	15.19	21.18(³¹ P)	α	314122 192	-2.76	-2.20	-0.18	17.22(²⁰ Ne)	α	319125 194	-4.20	-3.85	16.89	19.46(²³ Na)	α

Table 5. (Continued)

Parent Nuclei	$\log T_{1/2}$			Decay mode	Parent Nuclei	$\log T_{1/2}$			Decay mode	Parent Nuclei	$\log T_{1/2}$			Decay mode			
	α	β^+	Sf			Cluster	α	β^+			Sf	Cluster	α		β^+	Sf	Cluster
298 ₁₂₀ 178	-4.87	-3.75	14.49	22.38(³¹ P)	α	315 ₁₂₂ 193	-2.47	-1.99	-3.18	15.91(⁹ Be)	Sf	320 ₁₂₅ 195	-3.97	-3.65	14.08	20.73(²³ Na)	α
299 ₁₂₀ 179	-4.72	-3.54	13.62	23.69(²⁷ Al)	α	297 ₁₂₃ 174	-6.98	-6.54	27.19	10.6(³¹ P)	α	322 ₁₂₅ 197	-3.50	-3.25	7.94	23.26(²⁷ Al)	α
300 ₁₂₀ 180	-4.56	-3.33	12.56	24.4(²⁷ Al)	α	298 ₁₂₃ 175	-6.85	-6.33	27.58	10.96(³¹ P)	α	323 ₁₂₅ 198	-3.06	-3.05	4.61	24.59(²⁷ Al)	α
301 ₁₂₀ 181	-4.40	-3.12	11.33	24.76(²⁷ Al)	α	299 ₁₂₃ 176	-6.73	-6.13	27.80	11.4(³¹ P)	α	306 ₁₂₆ 180	-7.72	-7.31	42.98	12.78(²⁴ Mg)	α
302 ₁₂₀ 182	-4.22	-2.91	9.92	22.84(⁹ Be)	α	300 ₁₂₃ 177	-6.62	-5.93	27.84	12.14(³¹ P)	α	307 ₁₂₆ 181	-7.49	-7.11	42.86	13.39(²⁴ Mg)	α
303 ₁₂₀ 183	-4.05	-2.70	8.33	17.56(⁹ Be)	α	301 ₁₂₃ 178	-6.51	-5.72	27.70	13.29(³¹ P)	α	308 ₁₂₆ 182	-7.31	-6.91	42.56	8.14(²⁰ Ne)	α
304 ₁₂₀ 184	-3.86	-2.50	6.57	19.84(⁹ Be)	α	302 ₁₂₃ 179	-6.39	-5.52	27.38	14.76(³¹ P)	α	309 ₁₂₆ 183	-7.12	-6.71	42.08	8.13(⁹ Be)	α
305 ₁₂₀ 185	-3.43	-2.29	4.62	14.32(⁹ Be)	α	303 ₁₂₃ 180	-6.27	-5.32	26.88	16.16(³¹ P)	α	310 ₁₂₆ 184	-6.94	-6.52	41.43	10(⁹ Be)	α
306 ₁₂₀ 186	-3.13	-2.08	2.50	17.29(⁹ Be)	α	304 ₁₂₃ 181	-6.14	-5.11	26.20	15.12(⁹ Be)	α	311 ₁₂₆ 185	-6.76	-6.32	40.59	6.69(⁹ Be)	α
307 ₁₂₀ 187	-2.84	-1.87	0.20	12.21(⁹ Be)	α	305 ₁₂₃ 182	-6.01	-4.91	25.35	15.86(³¹ P)	α	312 ₁₂₆ 186	-6.58	-6.12	39.58	10.24(⁹ Be)	α
308 ₁₂₀ 188	-2.57	-1.66	-2.28	14.97(⁹ Be)	α	306 ₁₂₃ 183	-5.86	-4.71	24.32	13.31(⁹ Be)	α	313 ₁₂₆ 187	-6.40	-5.92	38.39	7.63(²⁰ Ne)	α
309 ₁₂₀ 189	-2.31	-1.45	-4.94	11.41(⁹ Be)	Sf	307 ₁₂₃ 184	-5.55	-4.51	23.11	14.27(⁹ Be)	α	314 ₁₂₆ 188	-6.22	-5.72	37.02	7.56(²⁰ Ne)	α
310 ₁₂₀ 190	-2.05	-1.25	-7.77	16.04(⁹ Be)	Sf	308 ₁₂₃ 185	-5.26	-4.30	21.72	9.96(⁹ Be)	α	315 ₁₂₆ 189	-6.04	-5.53	35.47	7.75(²⁰ Ne)	α
290 ₁₂₁ 169	-7.14	-6.27	16.89	10.45(³¹ P)	α	309 ₁₂₃ 186	-5.01	-4.10	20.15	11.95(⁹ Be)	α	316 ₁₂₆ 190	-5.86	-5.33	33.75	8.21(²⁰ Ne)	α
291 ₁₂₁ 170	-6.87	-6.06	17.80	10.97(³¹ P)	α	310 ₁₂₃ 187	-4.77	-3.90	18.40	9.48(⁹ Be)	α	317 ₁₂₆ 191	-5.69	-5.13	31.84	8.24(²³ Na)	α
292 ₁₂₁ 171	-6.65	-5.85	18.54	11.92(³¹ P)	α	311 ₁₂₃ 188	-4.54	-3.69	16.48	11.77(⁹ Be)	α	318 ₁₂₆ 192	-5.30	-4.93	29.76	8.83(²³ Na)	α
293 ₁₂₁ 172	-6.46	-5.65	19.10	12.59(³¹ P)	α	312 ₁₂₃ 189	-4.31	-3.49	14.38	10(⁹ Be)	α	319 ₁₂₆ 193	-5.00	-4.74	27.50	17.18(²⁷ Al)	α
294 ₁₂₁ 173	-6.31	-5.44	19.68	13.49(³¹ P)	α	313 ₁₂₃ 190	-4.09	-3.29	12.09	12.7(²⁴ Mg)	α	320 ₁₂₆ 194	-4.73	-4.54	25.06	17.93(²⁷ Al)	α
295 ₁₂₁ 174	-6.17	-5.23	19.69	14.06(³¹ P)	α	314 ₁₂₃ 191	-3.87	-3.08	9.64	12.2(⁹ Be)	α	321 ₁₂₆ 195	-4.49	-4.34	22.44	20.48(²⁷ Al)	α
296 ₁₂₁ 175	-6.05	-5.03	19.71	14.84(³¹ P)	α	315 ₁₂₃ 192	-3.61	-2.88	7.00	13.28(²⁴ Mg)	α	322 ₁₂₆ 196	-4.25	-4.14	19.65	22.14(²⁷ Al)	α
297 ₁₂₁ 176	-5.94	-4.82	19.56	15.61(³¹ P)	α	316 ₁₂₃ 193	-3.17	-2.68	4.18	13.61(²⁴ Mg)	α	323 ₁₂₆ 197	-4.02	-3.94	16.67	23.05(²⁷ Al)	α
298 ₁₂₁ 177	-5.70	-4.61	19.22	16.47(³¹ P)	α	317 ₁₂₃ 194	-2.85	-2.47	1.19	14.23(²⁴ Mg)	α	324 ₁₂₆ 198	-3.81	-3.75	13.52	24.66(²⁷ Al)	α
299 ₁₂₁ 178	-5.48	-4.41	18.71	17.22(³¹ P)	α	300 ₁₂₄ 176	-7.18	-6.79	32.21	10.85(²⁴ Mg)	α	325 ₁₂₆ 199	-3.59	-3.55	10.19	26.22(³¹ P)	β^+
300 ₁₂₁ 179	-5.29	-4.20	18.02	18.67(³¹ P)	α	301 ₁₂₄ 177	-7.05	-6.58	32.44	11.64(³¹ P)	α	326 ₁₂₆ 200	-3.18	-3.35	6.68	27.89(³¹ P)	β^+
301 ₁₂₁ 180	-5.11	-3.99	17.16	19.45(³¹ P)	α	302 ₁₂₄ 178	-6.93	-6.38	32.48	13.57(²⁰ Ne)	α	327 ₁₂₆ 201	-2.84	-3.15	3.00	17.42(⁹ Be)	β^+
302 ₁₂₁ 181	-4.93	-3.79	16.11	19.04(⁹ Be)	α	303 ₁₂₄ 179	-6.81	-6.18	32.35	14.3(²⁰ Ne)	α	328 ₁₂₆ 202	-2.54	-2.96	-0.86	21.39(⁹ Be)	β^+
303 ₁₂₁ 182	-4.74	-3.58	14.89	20.52(³¹ P)	α	304 ₁₂₄ 180	-6.68	-5.98	32.03	15.03(²⁰ Ne)	α	329 ₁₂₆ 203	-2.26	-2.76	-4.91	18.13(⁹ Be)	Sf

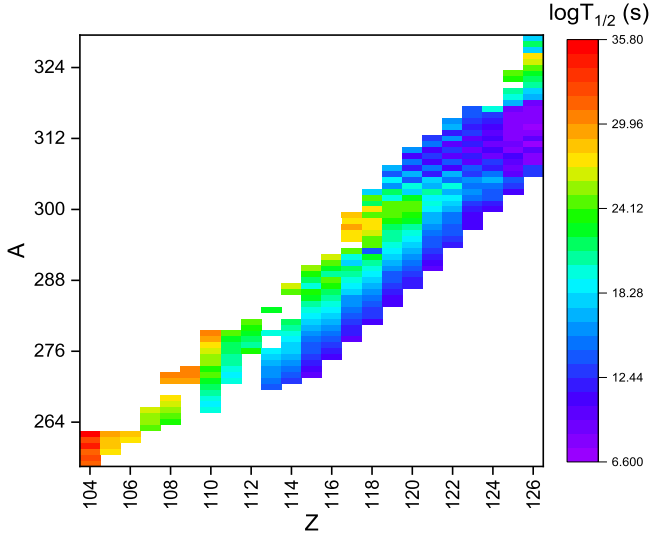


Fig. 3. Map of nuclei reflecting the logarithmic half-lives corresponding to shortest cluster-decay half-lives for the mass number and atomic number of parent nuclei in the superheavy element in the region $104 \leq Z \leq 126$.

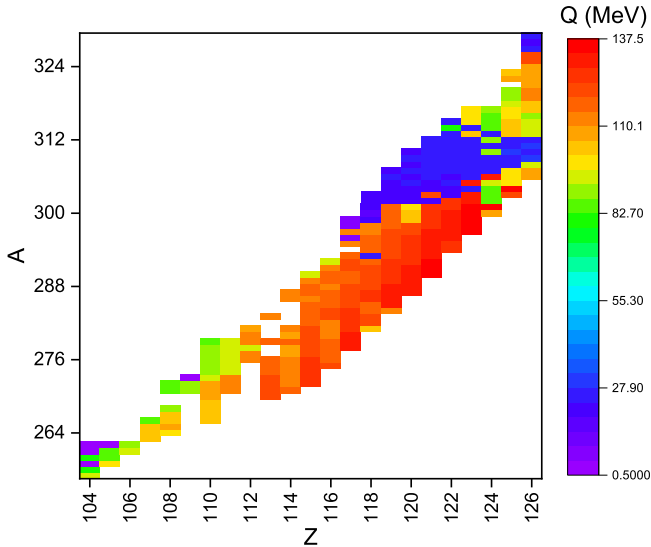


Fig. 4. Map of nuclei reflecting Q -values corresponding to shortest cluster-decay half-lives for the mass and atomic number of parent nuclei in superheavy element in the region $104 \leq Z \leq 126$.

The Q -values play a major role in the evaluation of cluster decay half-lives. Figure 4 shows Q -values corresponding to shortest cluster decay half-lives for the mass and atomic number of superheavy element in the region $104 \leq Z \leq 126$. The Q -value of cluster decay varies from 0.5 to 27.90 MeV from indigo to blue color for

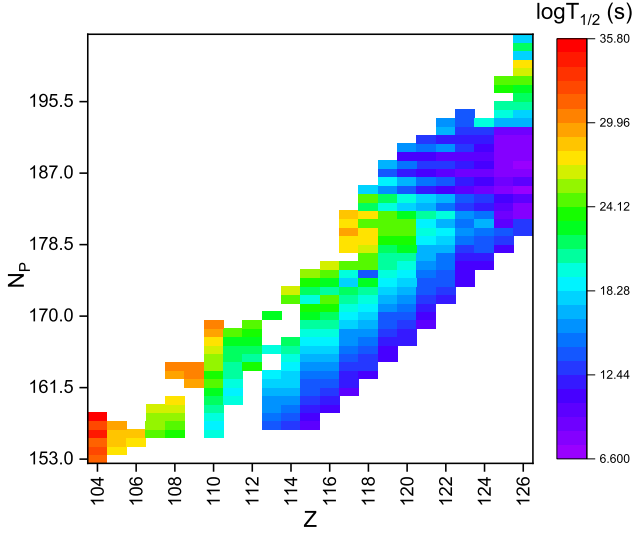


Fig. 5. Map of nuclei reflecting the logarithmic half-lives corresponding to shortest cluster-decay half-lives for the neutron number and atomic number of parent nuclei in the superheavy element in the region $104 \leq Z \leq 126$.

which logarithmic half-lives are smaller. Furthermore for the Q -values above 27.90 to 137.5 MeV corresponding to light blue to red color, the logarithmic half-lives were found to be larger.

Similarly, Fig. 5 shows the shortest cluster-decay half-lives for the neutron number and atomic number of parent nuclei in the superheavy element in the region $104 \leq Z \leq 126$. Indigo to blue color shows neutron number for which $\log T_{1/2}$ values present shorter half-lives and cyan to red color are related to larger half-lives.

Table 3 shows the tabulation of parent (A_P), daughter (A_D) and cluster nuclei (A_C) along with the Q -values and $\log T_{1/2}$ values corresponding to magic number of neutrons of parent/daughter nuclei. In case of parent nuclei, $^{309}_{120}_{189}$ $\log T_{1/2}$ value of 11.41 is observed with the Q -value of 24.84 MeV during the cluster emission of $^9\text{Be}_5$, resulting in the daughter nuclei $^{300}_{Lv}_{184}$ in which neutron number of daughter nuclei is $N = 184$. Similarly, we have also identified neutron number with magic number either in case of parent nuclei or daughter nuclei. From the detailed study of different decay modes and identification of shell closures in the superheavy region $104 \leq Z \leq 126$, there may exist daughter nuclei with magic number $N = 184$ or near magic number if the nuclei undergoes cluster radioactivity.

Detailed investigation on cluster radioactivity in superheavy elements reveals that the shortest half-lives are observed for decay of superheavy elements through ^9Be . The shortest half-lives corresponding to cluster decay are referred as T_c . Figure 6 exhibits the connection between the $\log T_c$ and neutron number of daughter nuclei (N_d). Surprisingly, it is observed that the shortest half-lives of cluster decay in all superheavy elements are observed for neutron number $N_d = 184$ and near to

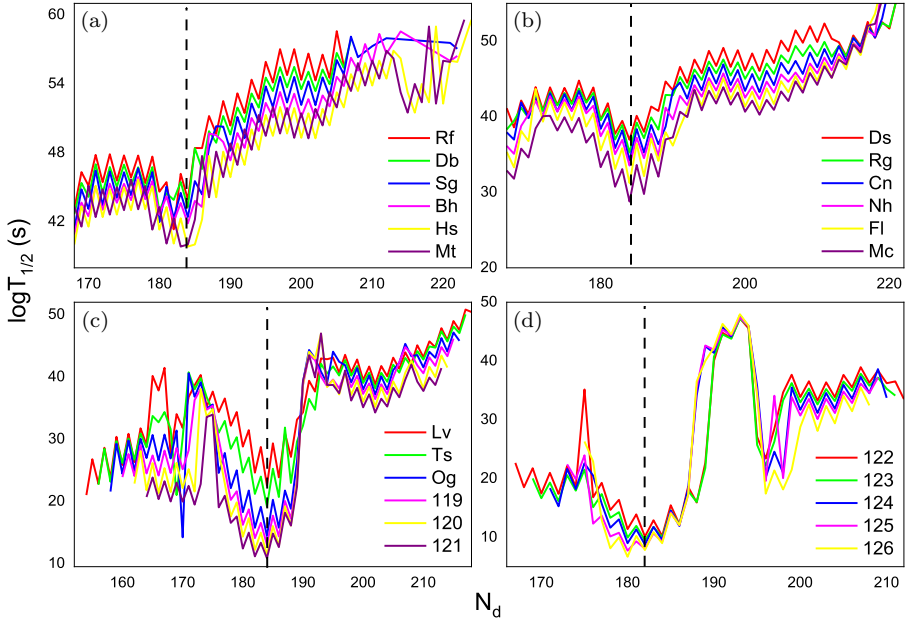


Fig. 6. (a) Variation of logarithmic half-lives ($\log T_{1/2}$) of ${}^9\text{Be}$ cluster-decay as a function of neutron number of the daughter nuclei in the region 104–109, similarly, (b) 110–115, (c) 116–121 and (d) 122–126.

that. However, many theoretical predictions also [66](#) [68](#) have shown stability of nuclei when neutron number is equal or nearly equal to 184. The shorter cluster decay half-lives are observed when $N_d = 184$ exhibits stronger shell effects due to their magicity when compared to their neighboring ones. This is the clear evidence for the existence of the magic number corresponding to the neutron number $N = 184$.

Furthermore, there is no experimental evidence on cluster radioactivity studies in the superheavy region. But, experimental cluster radioactivity in the actinide region is reported in [Table 1](#). The model used in this work is validated by producing cluster radioactivity half-lives of experiments. The cluster-decay half-lives tabulated in [Table 3](#) evaluated using present model show that the half-lives correspond to the daughter neutron number ≈ 184 are having smaller value. Eventually, there is a tendency to form daughter nucleus with neutron number $N = 184$. Hence, this may be the clue for the existence of neutron magic nuclei with $N = 184$.

4. Conclusion

The cluster radioactivity of superheavy nuclei in the region $104 \leq Z \leq 126$ was studied using MGLDM. The half-lives of different cluster emissions from ${}^4\text{He}$ to ${}^{40}\text{Ca}$ were studied. The values obtained in this work are in close agreement with the experiments. The neutron numbers corresponding to studied superheavy nuclei with $N = 179$ – 184 have shorter cluster decay half-lives. The shortest cluster decay

half-lives correspond to the superheavy nucleus $^{311}126_{185}$ with ^9Be cluster emission. The existence of neutron magic number 184 is also demonstrated through the cluster decay studies. In addition to this, shorter half-lives are also observed for the magic or near magic neutron number of daughter nuclei. Hence, we have predicted possibility of magic neutron number or near magic neutron number in the superheavy element $104 \leq Z \leq 126$.

References

1. A. Sandulescu, D. N. Poenaru and W. Greiner, *Sov. J. Particles Nucl. (Engl. Transl.); (United States)* **11**(6) (1980).
2. H. J. Rose and G. A. Jones, *Nature* **307** (1984) 245–247.
3. D. V. Aleksandrov, A. F. Belyatskij, Yu. A. Glukhov, E. Yu. Nkol'skij, B. G. Novatskij, A. A. Ogloblin and D. N. Stepanov, *Pis' ma v Zhurnal Eksperimental' noj i Teoreticheskoy Fiziki* **40** (1984) 152.
4. R. K. Gupta and W. Greiner, *Int. J. Mod. Phys. E* **3** (1994) 335.
5. Yu. S. Zamyatnin, V. L. Mikheev and S. P. Tret'yakova. V. I. furman, sg kadmenskii and yu. m. chulvil'skii, *Sov. J. Part. Nucl.* **21** (1990) 231.
6. R. Bonetti and A. Guglielmetti, *Rom. Rep. Phys.* **59** (2007) 301.
7. S. K. Arun, R. K. Gupta, S. Kanwar, B. Singh and M. K. Sharma, *Phys. Rev. C* **80** (2009) 034317.
8. S. S. Malik and R. K. Gupta, *Phys. Rev. C* **39** (1989) 1992.
9. D. N. Poenaru, M. Ivaşcu, A. Sandulescu and W. Greiner, *Phys. Rev. C* **32** (1985) 572.
10. M. Warda and L. M. Robledo, *Phys. Rev. C* **84** (2011) 044608.
11. R. Blendowske and H. Walliser, *Phys. Rev. Lett.* **61** (1988) 1930.
12. D. N. Poenaru, R. A. Gherghescu and W. Greiner, *Phys. Rev. C* **85** (2012) 034615.
13. R. G. Lovas, R. J. Liotta, A. Insolia, K. Varga and D. S. Delion, *Phys. Rep.* **294** (1998) 265–362.
14. C. Qi, F. R. Xu, R. J. Liotta and R. Wyss, *Phys. Rev. Lett.* **103** (2009) 072501.
15. M. Warda, A. Zdeb and L. M. Robledo, *Phys. Rev. C* **98** (2018) 041602.
16. G. L. Zhang, Y. J. Yao, M. F. Guo, M. Pan, G. X. Zhang and X. X. Liu, *Nucl. Phys. A* **951** (2016) 86.
17. R. Kumar, *Phys. Rev. C* **86** (2012) 044612.
18. K. P. Santhosh and R. K. Biju, *Pramana* **72** (2009) 689–707.
19. T. R. Routray, J. Nayak and D. N. Basu, *Nucl. Phys. A* **826** (2009) 223–229.
20. M. Ismail and A. Adel, *Phys. Rev. C* **101** (2020) 024607.
21. M. Ismail, W. M. Seif and A. Abdurrahman, *Phys. Rev. C* **94** (2016) 024316.
22. S. K. Arun, R. K. Gupta, B. Singh, S. Kanwar and M. K. Sharma, *Phys. Rev. C* **79** (2009) 064616.
23. S. N. Kuklin, G. G. Adamian and N. V. Antonenko, *Phys. At. Nucl.* **68** (2005) 1443.
24. M. Iriondo, D. Jerrestam and R. J. Liotta, *Nucl. Phys. A* **454** (1986) 252.
25. A. M. Nagaraja, H. C. Manjunatha, N. Sowmya and S. Raj, *J. Nucl. Phys. Mat. Sci. Rad. A* **8** (2020) 55.
26. H. C. Manjunatha and N. Sowmya, *Nucl. Phys. A* **969** (2018) 68.
27. N. Sowmya, H. C. Manjunatha, N. Dhananjaya and A. M. Nagaraja, *J. Radioanal. Nucl. Chem.* **323** (2020) 1347.
28. G. R. Sridhar, H. C. Manjunatha, N. Sowmya, P. S. Damodara Gupta and H. B. Ramalingam, *Eur. Phys. J. Plus* **135** (2020) 1.

29. H. C. Manjunatha, K. N. Sridhar and N. Sowmya, *Phys. Rev. C* **98** (2018) 024308.
30. H. C. Manjunatha and N. Sowmya, *Int. J. Mod. Phys. E* **27** (2018) 1850041.
31. N. Sowmya and H. C. Manjunatha, *Phys. Part. Nucl. Lett.* **17** (2020) 370.
32. N. Sowmya and H. C. Manjunatha, *Braz. J. Phys.* **49** (2019) 874.
33. N. Sowmya, H. C. Manjunatha and P. S. Damodara Gupta, *Int. J. Mod. Phys. E* (2020).
34. N. Sowmya and H. C. Manjunatha, *Braz. J. Phys.* **50** (2020) 317.
35. N. Sowmya, H. C. Manjunatha, P. S. Damodara Gupta and N. Dhananjaya, *Braz. J. Phys.* **51** (2021) 99.
36. K. N. Sridhar, H. C. Manjunatha and H. B. Ramalingam, *Phys. Rev. C* **98** (2018) 064605.
37. S. Kumar, R. Rani and R. Kumar, *J. Phys. G: Nucl. Part. Phys.* **36** (2018) 015110.
38. R. K. Gupta, S. Kumar, R. Kumar, M. Balasubramaniam and W. Scheid, *J. Phys. G: Nucl. Part. Phys.* **28** (2002) 2875.
39. H. Ngô and Ch. Ngô, *Nucl. Phys. A* **348** (1980) 140.
40. G. Royer and B. Remaud, *Nucl. Phys. A* **444** (1985) 477.
41. G. Royer and R. A. Gherghescu, *Nucl. Phys. A* **699** (2002) 479.
42. G. Royer and R. Moustabchir, *Nucl. Phys. A* **683** (2001) 182.
43. X. J. Bao, H. F. Zhang, B. S. Hu, G. Royer and J. Q. Li, *J. Phys. G: Nucl. Part. Phys.* **39** (2012) 095103.
44. G. Royer, *J. Phys. G: Nucl. Part. Phys.* **26** (2000) 1149.
45. G. Royer, K. Zbiri and C. Bonilla, *Nucl. Phys. A* **730** (2004) 355.
46. J. M. Wang, H. F. Zhang and J. Q. Li, *J. Phys. G: Nucl. Part. Phys.* **40** (2013) 045103.
47. J. Błocki, J. Randrup, W. J. Świątecki and C. F. Tsang, *Ann. Phys.* **105** (1977) 427.
48. K. P. Santhosh and T. A. Jose, *Indian J. Phys.* **95** (2021) 121.
49. R. Bonetti, C. Chiesa, A. Guglielmetti, C. Migliorino, P. Monti, A. L. Pasinetti and H. L. Ravn, *Nucl. Phys. A*, **576** (1994) 21–28.
50. P. B. Price, J. D. Stevenson, S. W. Barwick and H. L. Ravn, *Phys. Rev. Lett.* **54** (1985) 297, doi:10.1103/PhysRevLett.54.297.
51. E. Hourani et al., *Phys. Rev. C* **44** (1991) 1424.
52. E. Hourani, M. Hussonnois, L. Stab, L. Brillard, S. Gales and J. P. Schapira, *Phys. Lett. B* **160** (1985) 375.
53. R. Bonetti, C. Chiesa, A. Guglielmetti, R. Matheoud, C. Migliorino, A. L. Pasinetti and H. L. Ravn, *Nucl. Phys. A* **562** (1993) 32.
54. R. Bonetti, C. Chiesa, A. Guglielmetti, C. Migliorino, A. Cesana and M. Terrani, *Nucl. Phys. A* **556** (1993) 115.
55. M. Hussonnois, J.-F. Le Du, L. Brillard, J. Dalmasso and G. Ardisson, *Phys. Rev. C* **43** (1991) 2599.
56. K. P. Santhosh, R. K. Biju and A. Joseph, *J. Phys. G: Nucl. Part. Phys.*, **35** (2008) 085102.
57. S. W. Barwick, P. B. Price and J. D. Stevenson, *Phys. Rev. C* **31** (1985) 1984.
58. R. Bonetti, C. Chiesa, A. Guglielmetti, C. Migliorino, A. Cesana, M. Terrani and P. B. Price, *Phys. Rev. C* **44** (1991) 888.
59. K. J. Moody, E. K. Hulet, S. Wang and P. B. Price, *Phys. Rev. C* **39** (1989) 2445.
60. S. P. Tretyakova, Yu. S. Zamyatnin, V. N. Kovantsev, Yu. S. Korotkin, V. L. Mikheev and G. A. Timofeev, *Zeitschrift für Physik A At. Nucl.* **333** (1989) 349.
61. S. Wang, D. Snowden-Ifft, P. B. Price, K. J. Moody and E. K. Hulet, *Phys. Rev. C* **39** (1989) 1647.
62. J. M. Dong, H. F. Zhang, J. Q. Li and W. Scheid, *Eur. Phys. J. A* **41** (2009) 197.

63. A. Sandulescu and W. Greiner, *Rep. Prog. Phys.* **55** (1992) 1423.
64. M. Wang, W. J. Huang, F. G. Kondev, G. Audi and S. Naimi, *Chin. Phys. C* **45** (2021) 030003.
65. C. Xu, Z. Ren and Y. Guo, *Phys. Rev. C* **78** (2008) 044329, doi:10.1103/PhysRevC.78.044329.
66. A. T. Kruppa, M. Bender, W. Nazarewicz, P.-G. Reinhard, T. Vertse and S. Ćwiok, *Phys. Rev. C* **61** (2000) 034313, doi:10.1103/PhysRevC.61.034313.
67. S. Ćwiok, J. Dobaczewski, P.-H. Heenen, P. Magierski and W. Nazarewicz, *Nucl. Phys. A* **611** (1996) 211.
68. J. P. Cui, Y. L. Zhang, S. Zhang and Y. Z. Wang, *Phys. Rev. C* **97** (2018) 014316, doi:10.1103/PhysRevC.97.014316.



Investigation of decay modes of superheavy nuclei

H. C. Manjunatha¹ · N. Sowmya¹ · P. S. Damodara Gupta¹ · K. N. Sridhar² ·
A. M. Nagaraja^{1,3} · L. Seenappa¹ · S. Alfred Cecil Raj³

Received: 13 July 2021 / Revised: 28 August 2021 / Accepted: 31 August 2021 / Published online: 23 November 2021
© The Author(s), under exclusive licence to China Science Publishing & Media Ltd. (Science Press), Shanghai Institute of Applied Physics, the Chinese Academy of Sciences, Chinese Nuclear Society 2021

Abstract A detailed investigation of different decay modes, namely alpha decay, beta decay, cluster decay, including heavy particle emission ($Z_c > 28$), and spontaneous fission, was carried out, leading to the identification of new cluster and beta-plus emitters in superheavy nuclei with $104 \leq Z \leq 126$. For the first time, we identified around 20 beta-plus emitters in superheavy nuclei. Heavy-particle radioactivity was observed in superheavy elements of atomic number in the range $116 \leq Z \leq 126$. $^{292-293}\text{Og}$ were identified as ^{86}Kr emitters, and $^{298}122$ and $^{300}122$ were identified as ^{94}Zr emitters, whereas heavy-particle radioactivity from ^{91}Y was also observed in $^{299}123$. Furthermore, the nuclei $^{300}124$ and $^{306}126$ exhibit ^{96}Mo radioactivity. The reported regions of beta-plus and heavy-particle radioactivity for superheavy nuclei are stronger than those for alpha decay. The identified decay modes for superheavy nuclei are presented in a chart. This study is intended to serve as a reference for identifying possible decay modes in the superheavy region.

Keywords Alpha decay · Beta decay · Heavy-particle radioactivity · Branching ratios

1 Introduction

The most important unanswered questions in Nuclear Physics are to determine the heaviest superheavy nuclei that can exist, and to investigate whether very-long-lived superheavy nuclei exist in nature. The past ten years have been marked by remarkable progress in the science of superheavy elements and nuclei. The existence of superheavy nuclei above $Z = 103$ can be studied in terms of whether they can occur naturally or can be synthesized in the laboratory. There are no definitive conclusions regarding the existence of superheavy nuclei in nature. In contrast, such superheavy nuclei, with half-lives ranging between days to μs , can be synthesized using cold and hot fusion reactions. Cold fusion reactions involve either lead or bismuth as targets [1], whereas hot fusion reactions include ^{48}Ca beams on various actinide targets [2, 3]. Many theoretical predictions, such as microscopic–macroscopic [4] (single-particle potential) and self-consistent approaches, including nucleus–nucleus potential [5, 6], relativistic field models [7, 8], and multinucleon transfer reactions [9], provide information regarding the nucleus structure, shell closure location, and decay modes in heavy and superheavy nuclei.

The discovery of superheavy elements [10, 11] points to the island of stability. Boilley et al. [12] predicted the evaporation residue cross sections in superheavy elements and the influence of shell effects [13]. The entrance channel dynamics were studied using ^{48}Ca as a projectile and ^{208}Pb as target [14]. In 1966, two groups of researchers, namely Mayers and Swiatecki, and Viola and Seaborg [15], separately predicted the presence of heavy nuclei near the island of stability. Later, Sobiczewski et al. [16] predicted that the nucleus $Z = 114$ will be the center of the

✉ H. C. Manjunatha
manjunathhc@rediffmail.com

¹ Department of Physics, Government College for Women, Kolar, Karnataka 563101, India

² Department of Physics, Government First Grade College, Kolar, Karnataka 563101, India

³ Department of Physics, St. Joseph's College, Affiliated to Bharathidasan University, Tiruchirappalli, Tamil Nadu, India

island of stability, with neutron number $N = 184$. In 1955, Nilsson [17] proposed a shell model which includes deformation property of the nuclei. Bender et al. [18] used a Skyrme energy density functional model and studied the deformation properties of closed proton and neutron shells. The nuclear mass, radius, and spectroscopy far away from the valley of stability were experimentally analyzed earlier [19]. The investigation of isomers of the superheavy nucleus ^{254}No is a stepping stone toward the island of stability [20]. Previous researchers [21] analyzed the nuclear shell structure and discovered additional stability near magic nuclei. The present scenario is almost near the center of the presumed island of stability, but the final landing is yet to be completed, and the intriguing question is how these superheavy nuclei are still accessible.

The identification of superheavy nuclei is based on observations of decay chains. Superheavy element region $114 \leq Z \leq 118$ were observed owing to their consistent decay chains, which end in the isotopes of rutherfordium (Rf) and dubnium (Db). Spontaneous fission and α -decay are the dominant decay modes in superheavy nuclei and limit their stability. Furthermore, newly synthesized superheavy elements are primarily identified by their decay chains from unknown nuclei to known daughter nuclei by using the parent-and-daughter correlation.

The competition between different decay modes, such as ternary fission, spontaneous fission, cluster decay, proton decay, β -decay, and α -decay, in the heavy and superheavy region, has been extensively studied using various theoretical models, such as Coulomb and proximity potential models, modified generalized liquid drop models, effective liquid drop models, and temperature-dependent proximity potential models [22–33]. The possible decay modes in the superheavy nuclei $Z = 119$ and 120 are predicted in Ref. [34]. From Ref. [35], it is clearly observed that the isotopes of the superheavy nuclei $Z = 104$ – 112 have α -decay and spontaneous fission as dominant decay modes. However, only α -decay is dominant in the isotopes of superheavy nuclei $Z = 113, 115$ – 118 . The isotopes of the superheavy nucleus $Z = 114$ have spontaneous fission as the dominant decay mode in the nucleus ^{284}Fl , α -decay is dominant in the nuclei 286 – ^{289}Fl , and β^+ is dominant in the nucleus ^{290}Fl . Furthermore, the concept of heavy-particle radioactivity [36] in the superheavy region has important applications in the synthesis of superheavy nuclei. Despite the significant experimental and theoretical progress, there are many unanswered questions related to the decay modes of superheavy nuclei. Until now, only α -decay and spontaneous fission have been successfully observed in experiments.

Experimental results suggest a considerable increase in the lifetime of nuclei as they approach closed proton and

neutron shells [37]. The lifetimes of most known superheavy nuclei are governed by the competition between α -decay and spontaneous fission. The existence of the island of stability has been confirmed experimentally in the previous decade [38]. Some theoretical studies reveal that superheavy elements with 114 and 164 protons are stable against fission as well as alpha and beta decay [39]. Various phenomenological and microscopic models, such as the fission model [40], the cluster model [41], generalized liquid drop model [42], and the unified model for alpha decay and alpha capture [43], are available to study the different decay modes of superheavy nuclei. In addition, many studies have been concerned with the alpha decay and spontaneous fission of superheavy nuclei [44–46]. Simple empirical formulas are also available for determining the decay half-lives [47]. The possible isotopes of new superheavy elements are identified by studying the competition between different probable decay modes, such as α -decay, β -decay, cluster decay, and spontaneous fission. This study focuses on the different decay modes of superheavy nuclei in the atomic number range $104 \leq Z \leq 126$. After a detailed investigation of the competition between different decay modes, the possible isotopes and their decay modes with branching ratios are identified in the superheavy nuclei region. Hence, the contribution of this study is in the prediction of the most possible decay mode in superheavy nuclei, and in the identification of possible emitters in this superheavy region. The formalism is explained in Sect. 2. The analysis of different decay modes and possible emitters in the superheavy region is explained in Sect. 2.4. The paper is concluded in Sect. 3.

2 Theory

2.1 Alpha decay and cluster decay

In the effective liquid-drop model (ELDM), the α -decay half-life is computed using the relation

$$T_{1/2}(s) = \frac{\ln 2}{v_0 P P_\alpha}, \quad (1)$$

where v_0 is the assault frequency on the barrier, and $v_0 = 1.8 \times 10^{22} \text{s}^{-1}$ [48]. P_α is the preformation factor, which is closely related to the shell structure [49]. The empirical formula for P_α is expressed as

$$\log P_\alpha = p_1 + p_2(Z - Z_1)(Z_2 - Z) + p_3(N - N_1)(N_2 - N) + p_4A, \quad (2)$$

where N , Z , and A are the neutron, charge, and mass number of the parent nucleus, respectively, Z_1 and Z_2 are

the proton magic numbers around Z ($Z_1 \leq Z \leq Z_2$), and N_1 and N_2 are the neutron magic numbers around N ($N_1 \leq N \leq N_2$). $p_1, p_2,$ and p_3 correspond to parameters in the region even(Z)-even(N), even(Z)-odd(N), odd(Z)-even(N), and odd(Z)-odd(N). They are presented in Table I of Ref. [50]. P is the Gamow penetrability factor, given by the expression

$$P = \exp \left[-\frac{2}{\hbar} \int_{\zeta_0}^{\zeta_c} \sqrt{2\mu[V(\zeta) - Q]} d\zeta \right], \tag{3}$$

where μ is the inertial coefficient resulting from the Werner–Wheeler approximation [51]. The limits of integration ζ_0 and ζ_c are the inner and outer turning points, expressed as $\zeta_0 = R_p - \bar{R}_1$ and $\zeta_c = \frac{Z_1 Z_2 e^2}{Q}$. R_p is the radius of the parent nucleus, and \bar{R}_1 is the final radius of the emitted cluster. In the ELDM, the total potential has been demonstrated to be the sum of Coulomb, proximity, and centrifugal potential [52, 53]. Hence, we can use the effective one-dimensional total potential energy as follows:

$$V = V_C + V_S + V_\ell. \tag{4}$$

To evaluate the Coulomb contribution in terms of the deformation parameter, we used V_C as defined in Ref. [54]:

$$V_C(R) = \frac{e^2 Z_1 Z_2}{R} + 3Z_1 Z_2 e^2 \sum_{\lambda, i=1,2} \times \frac{R_i^\lambda(\alpha_i, T)}{(2\lambda + 1)} Y_\lambda^{(0)}(\theta_i) \left[\beta_{\lambda i} + \frac{4}{7} \beta_{\lambda i}^2 Y_\lambda^{(0)}(\theta_i) \right], \tag{5}$$

with

$$R_i(\alpha_i) = R_{oi} \left[1 + \sum_{\lambda} \beta_{\lambda i} Y_\lambda^{(0)}(\alpha_i) \right], \tag{6}$$

where $\beta_{\lambda i}$ is the deformation parameter, $Y_{\lambda(0)}$ are the spherical harmonics, and $R_{oi} = 1.28A_i^{1/3} - 0.76 + 0.8A_i^{-1/3}$. The effective surface potential can be calculated by

$$V_S = \sigma_{\text{eff}}(S_1 + S_2), \tag{7}$$

where S_1 and S_2 are the surface areas of the spherical fragments. σ_{eff} is the effective surface tension, which is defined as

$$\sigma_{\text{eff}} = \frac{1}{4(R^2 - R_1^2 - R_2^2)} \left(Q - \frac{3}{20\pi\epsilon_0} e^2 \left[\frac{Z^2}{R} - \frac{Z_1^2}{R_1} - \frac{Z_2^2}{R_2} \right] \right), \tag{8}$$

where R_2 is the final radius of the daughter fragment. The centrifugal potential energy is determined by

$$V_\ell = \frac{\hbar^2 \ell(\ell + 1)}{2\mu\zeta^2}, \tag{9}$$

where ℓ is the angular momentum of the emitted alpha/cluster and is calculated using the selection rules. In the case of alpha/cluster decay [55, 56], the selection rules follow the condition

$$|J_p - J_d| \leq \ell_\alpha \leq |J_p + J_d| \quad \text{and} \quad \frac{\pi_p}{\pi_d} = (-1)^{\ell_\alpha}, \tag{10}$$

where J_p, π_p and J_d, π_d are the spin and parity of the parent and daughter nuclei, respectively. $\mu = \frac{M_1 M_2}{M_1 + M_2}$ is the reduced mass of the fragments, where M_1 and M_2 denote their atomic masses.

In ELDM, a system with two intersecting spherical nuclei with different radii is considered [52]. A schematic diagram for the representation of four independent coordinates, namely $R_1, R_2, \zeta,$ and $\xi,$ is shown in Fig. 1. Three constraints are used to reduce the four-dimensional spherical problem to an equivalent one-dimensional problem. The geometric constraint given below is introduced so that the spherical segments remain in contact:

$$R_1^2 - (\zeta - \xi)^2 = R^2 - \xi^2. \tag{11}$$

The variables ζ and ξ represent the distance between the geometrical centers and the distance between the center of the heavier fragment and the circular sharp neck of the radius, respectively [53, 57]. Assuming that nuclear matter is incompressible, the constraint for the conservation of the total volume of the system is

$$2(R_1^3 + R_2^3) + 3[R_1^2(\zeta - \xi) + R_2^2 \xi] - [(\zeta - \xi)^2 + \xi^3] = 4R^3, \tag{12}$$

where $R = r_0 A^{1/3}$ is the radius of the parent nucleus ($r_0 = 1.34$ fm is an adjustable parameter), with A being the mass number of the parent.

The radius of the α particle, $R_1,$ is assumed to be constant in the varying mass asymmetry shape description:

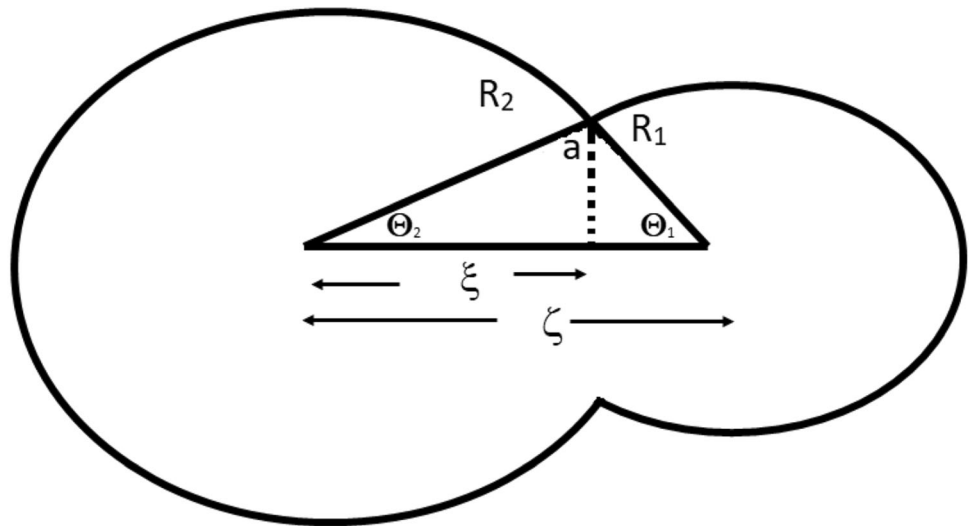
$$R_1 - \bar{R}_1 = 0, \tag{13}$$

where $\bar{R}_1 = (\frac{Z}{Z})^{1/3} R, i = 1, 2; \bar{R}_1$ provides the final radius of the α particle. Here, $Z_1, Z_2,$ and Z are the atomic numbers of the α particle, daughter nucleus, and parent nucleus, respectively.

2.2 Beta decay

For all types of β processes, the expression for the half-life T_β is given by [58]

Fig. 1 Schematic presentation of molecular phase of the di-nuclear system (the daughter nucleus and the emitted (smaller) fragments). The distance between their geometrical centers and the distance between the center of the heavier fragment and the circular sharp neck of radius a are denoted by ζ and ξ , respectively



$$\frac{1}{T_\beta} = \frac{1}{T_{\beta^+}} + \frac{1}{T_{\beta^-}} + \frac{1}{EC}. \tag{14}$$

Here, EC is the electron capture. For a particular type of β -decay, the half-life is expressed as follows:

$$f_0^b T_b = \ln 2 \left[\frac{g^2 m_e^5 c^4}{2\pi^3 \hbar^7} |M_{if}|^2 \right]^{-1}. \tag{15}$$

Here, f_0^b is the Fermi function, $b = \beta^\pm$ or EC , m_e is the mass of the electron, and M_{if} is the transition matrix element between the initial and final states. The right-hand side of the above may be approximated by a constant for each type of β -decay [59]. This constant is different for allowed and forbidden cases of beta decay. For allowed β -decay, this constant has been determined as 5.7 ± 1.1 [60]. Equation (15) is reduced to

$$\log_{10} [f_0^b T_b (\text{sec})] = 5.7 \pm 1.1, \tag{16}$$

$$\log_{10} [f_0^b T_b] = 4.7. \tag{17}$$

2.2.1 β^\pm decay

The Fermi function for β -decay is expressed as

$$f_0^\beta \pm = \int_1^{E_0} F(E, Z) P(E) (E_0 - E)^2 dE. \tag{18}$$

Here, $P(E)$ is the momentum of the particle, and $F(E, Z)$ can be computed at the nuclear surface using the magnitude of the radial electron/positron wave function. The first approximation of $F(E, Z)$ is

$$F_0(E, Z) = \frac{2(\gamma + 1)(2pR)^{2(\gamma-1)} \exp\left[\frac{\pi\xi}{p}\right] |\Gamma(\gamma + i\frac{\xi}{p})|^2}{\Gamma^2(2\gamma + 1)}. \tag{19}$$

Here, $\gamma = \sqrt{1 - \alpha^2 Z^2}$, $\xi = \pm \alpha Z E$ (+ for β^- decay and - for β^+ decay), $\alpha = 1/137$ is the fine structure constant, R is the radius of the nucleus, and Γ is the gamma function.

At the surface of the nucleus (for β^+ decay), the orbital electron screening effect has a significant impact on the β electron/positron wave function. Thus, $F(E, Z)$ becomes

$$F(E, Z) = F_0(E \mp V_0, Z)^\mp (E \mp V_0, Z) \frac{p(E \mp V_0)(E \mp V_0)}{p(E)E}. \tag{20}$$

Here, $V_0 = 1.81\alpha^2 Z^4/3$, is the finite wavelength of the β particle, $p(E) = \sqrt{E^2 - 1}$ is the momentum of the β particle, $E_0 = 1 + Q_{\beta^\pm}/m_e c^2$ is the total limit energy of the β decay, $E = 1 + \varepsilon/m_e c^2$, and ε is the kinetic energy of the β particle

The expression for the energy released in β^+ decay is

$$Q_{\beta^+} = M(A, Z) - M(A, Z - 1) - 2m_e c^2. \tag{21}$$

Similarly, for β^- decay,

$$Q_{\beta^-} = M(A, Z) - M(A, Z - 1). \tag{22}$$

2.2.2 Electron capture

The value of Q for electron capture is given by

$$\begin{aligned} Q_{EC} &= M(A, Z) - M(A, Z - 1) - B_e \\ &= Q_{\beta^+} + 2m_e c^2 - B_e. \end{aligned} \tag{23}$$

Here, B_e is the electron binding energy. Hence, even for the forbidden β^+ decay, electron capture is allowed. The capture of electrons of the K -shell for lower Z , and of the L -shell for higher Z is the major contributor to electron

capture. The contributions of the electrons of higher shells are negligible. Thus, the Fermi function becomes

$$f_0^{\text{EC}} = f_0^K + f_0^{L\text{I}} + f_0^{L\text{II}}. \tag{24}$$

In general, for any shell,

$$f_0^X = \frac{\pi}{2} [E(Q_{\text{EC}}) + E_X]^2 [g_X^2(Z_X) + f_X^2(Z_X)] \tag{25}$$

$$X = K, L\text{I}, L\text{II}.$$

Here, E_X is the total energy of the electron:

$$E_K = \gamma, E_L = \left(\frac{1 + \gamma}{2}\right)^{1/2}, \tag{26}$$

where Z_X is the effective charge, which considers the screening of the Coulomb field of the nucleus by other electrons [61]:

$$Z_K = Z - 0.35 \quad \text{and} \quad Z_L = Z - 4.15. \tag{27}$$

The nonzero components of the radial parts (g_X & f_X) of the wave function of the relativistic electron of orbit X are

Table 1 Cluster-decay half-lives obtained from present study (PS) and available experiments (exp)

Decay	Q_{Exp} (MeV)	$\log T_{1/2}^{\text{exp}}$ [71]	$\log T_{1/2}^{\text{PS}}$
$^{221}\text{Fr} \rightarrow ^{14}\text{C} + ^{207}\text{Tl}$	31.317	14.51	14.91
$^{221}\text{Ra} \rightarrow ^{14}\text{C} + ^{207}\text{Pb}$	32.396	13.37	13.56
$^{222}\text{Ra} \rightarrow ^{14}\text{C} + ^{208}\text{Pb}$	33.05	11.05	12.70
$^{223}\text{Ra} \rightarrow ^{14}\text{C} + ^{209}\text{Pb}$	31.829	15.05	13.94
$^{224}\text{Ra} \rightarrow ^{14}\text{C} + ^{210}\text{Pb}$	30.54	15.9	15.52
$^{226}\text{Ra} \rightarrow ^{14}\text{C} + ^{212}\text{Pb}$	28.2	21.29	22.74
$^{225}\text{Ac} \rightarrow ^{14}\text{C} + ^{211}\text{Bi}$	30.477	17.16	17.06
$^{228}\text{Th} \rightarrow ^{20}\text{O} + ^{208}\text{Pb}$	44.72	20.73	22.04
$^{230}\text{U} \rightarrow ^{22}\text{Ne} + ^{208}\text{Pb}$	61.4	19.56	20.21
$^{230}\text{Th} \rightarrow ^{24}\text{Ne} + ^{206}\text{Hg}$	57.571	24.61	25.07
$^{231}\text{Pa} \rightarrow ^{24}\text{Ne} + ^{207}\text{Tl}$	60.417	22.89	23.07
$^{232}\text{U} \rightarrow ^{24}\text{Ne} + ^{208}\text{Pb}$	62.31	20.39	22.25
$^{233}\text{U} \rightarrow ^{24}\text{Ne} + ^{209}\text{Pb}$	60.486	24.84	25.05
$^{234}\text{U} \rightarrow ^{26}\text{Ne} + ^{208}\text{Pb}$	59.466	25.93	25.62
$^{234}\text{U} \rightarrow ^{28}\text{Mg} + ^{206}\text{Hg}$	74.11	25.74	26.04
$^{236}\text{Pu} \rightarrow ^{28}\text{Mg} + ^{208}\text{Pb}$	79.67	21.65	22.07
$^{238}\text{Pu} \rightarrow ^{28}\text{Mg} + ^{210}\text{Pb}$	75.912	25.66	25.98
$^{238}\text{Pu} \rightarrow ^{30}\text{Mg} + ^{208}\text{Pb}$	77	25.66	26.25
$^{238}\text{Pu} \rightarrow ^{32}\text{Si} + ^{206}\text{Hg}$	91.19	25.3	26.05
$^{242}\text{Cm} \rightarrow ^{34}\text{Si} + ^{208}\text{Pb}$	96.509	23.11	24.24

Table 2 Comparison of logarithm half-lives (years) of spontaneous fission in the superheavy region $104 \leq Z \leq 114$ from present study with those from available experiments

Parent nuclei	$\log_{\text{SF}}^{\text{Expt}} \text{yr}$ [72]	$\log_{\text{SF}}^{\text{Th}} \text{yr}$
^{254}Rf	- 12.1	- 10.91
^{256}Rf	- 9.71	- 8.48
^{258}Rf	- 9.35	- 7.06
^{260}Rf	- 9.2	- 6.35
^{262}Rf	- 7.18	- 6.36
^{258}Sg	- 10	- 11.33
^{260}Sg	- 9.65	- 10.17
^{262}Sg	- 9.32	- 8.722
^{264}Sg	- 8.93	- 7.98
^{266}Sg	- 7.86	- 7.96
^{264}Hs	- 10.2	- 11.02
^{270}Ds	- 8.6	- 9.46
^{282}Cn	- 10.6	- 9.39
^{284}Cn	- 8.5	- 7.98
^{286}Fl	- 8.08	- 7.58

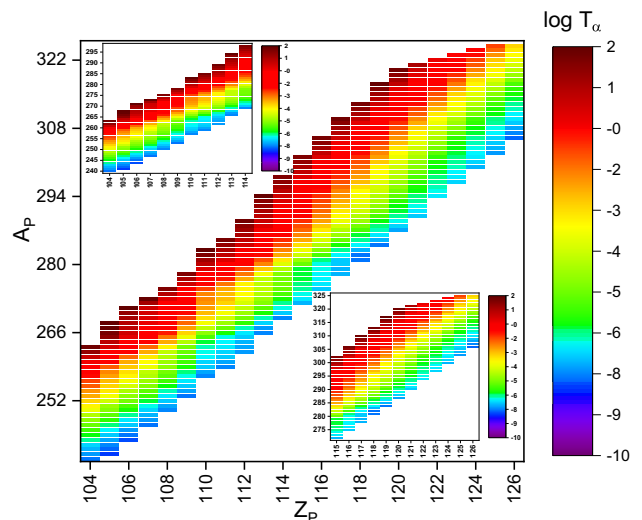


Fig. 2 (Color online) Map of nuclei reflecting the logarithmic α -decay half-lives for the isotopes of elements from $Z = 104$ to 126 . The Q -values were estimated using AME16 and FRDM95. The vertical line on the right side of the figure shows an increase in the $\log T_{1/2}$ values from the navy-blue region to the brown region

$$g_K^2(Z) = \frac{4(1 + \gamma)(2\alpha ZR)^{2(\gamma-1)}(\alpha Z)^3}{\Gamma(2\gamma + 1)}, \tag{28}$$

Table 3 Comparison of alpha-decay half-lives from the present study (PS) and those from available experimental (Exp) values

Parent nuclei	Q_α (MeV)	$\log T_{1/2}$ (Exp)	$\log T_{1/2}$ (PS)
^{261}Bh	8.649	1.515	1.86
^{260}Db	9.379	- 0.295	0.11
^{269}Sg	8.8	2.27	2.12
^{265}Sg	9.078	0.869	1.15
^{263}Sg	9.391	- 0.932	0.12
^{261}Sg	9.803	- 1.469	- 1.21
^{272}Bh	9.3	1.025	0.78
^{271}Bh	9.5	0.176	0.18
^{270}Bh	9.3	1.785	1.02
^{277}Hs	8.4	- 2.523	- 1.02
^{273}Hs	9.9	- 0.119	- 0.32
^{269}Hs	9.629	0.851	0.65
^{274}Hs	9.5	0.079	0.21
^{278}Mt	9.1	0.653	1.65
^{276}Mt	9.8	- 0.284	0.05
^{274}Mt	10.5	- 0.357	- 0.98
^{281}Ds	8.958	1.104	1.45
^{282}Rg	9.38	2	1.85
^{280}Rg	9.98	0.623	0.55
^{279}Rg	10.45	- 1.046	- 1.04
^{285}Cn	8.793	1.447	2.85
^{283}Cn	9.62	0.623	0.89
^{281}Cn	10.28	- 0.886	- 0.68
^{284}Cn	9.301	1.013	1.78
^{277}Cn	11.622	- 2.551	- 2.65
^{286}Nh	9.68	0.978	1.22
^{285}Nh	10.02	0.623	0.76
^{284}Nh	10.25	- 0.013	0.08
^{283}Nh	10.6	- 1.125	- 0.98
^{289}Fl	9.847	0.279	0.96
^{288}Fl	9.969	- 0.18	- 0.16
^{287}Fl	10.436	- 0.319	- 0.28
^{286}Fl	10.7	- 0.921	- 0.87
^{285}Fl	11	- 0.824	- 1.89
^{290}Mc	10.3	- 0.187	0.18
^{289}Mc	10.6	- 0.481	- 0.35
^{293}Lv	8.886	- 1.244	0.12
^{292}Lv	10.707	- 1.886	- 0.96
^{291}Lv	11	- 1.721	- 1.45
^{289}Lv	11.7	- 2.848	- 2.97
^{294}Ts	8.963	- 1.292	0.06
^{294}Og	8.47	- 3.161	- 2.45
^{295}Og	9.056	- 1.745	0.58
$^{298}\text{120}$	13.355	- 3.051	- 4.68
$^{299}\text{120}$	13.105	- 3.15	- 1.58

Fig. 3 (Color online) Predicted cluster-decay logarithmic half-lives in the atomic number range $Z = 104-126$ using AME16 and FRDM95 mass excess values. The hallow bin with different color in each panel shows the cluster emission corresponding to minimum half-lives

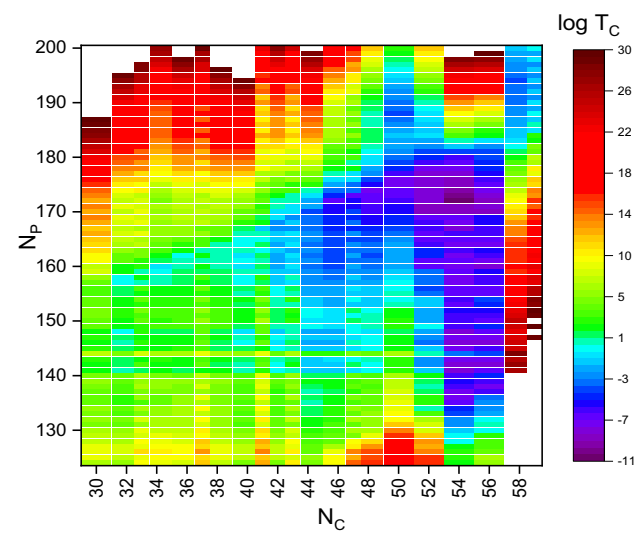
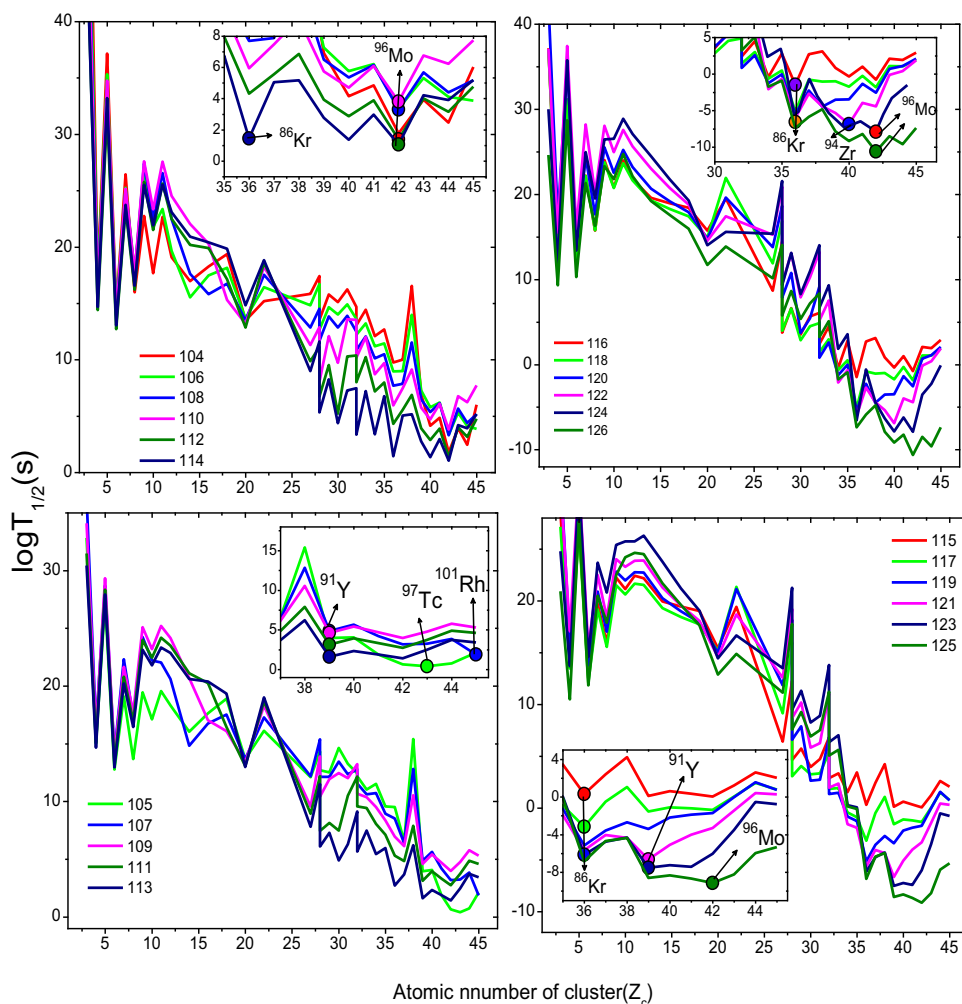


Fig. 4 (Color online) Map of nuclei reflecting the logarithmic cluster-decay half-lives for neutron number of parent and cluster isotopes of elements with $Z = 104-126$

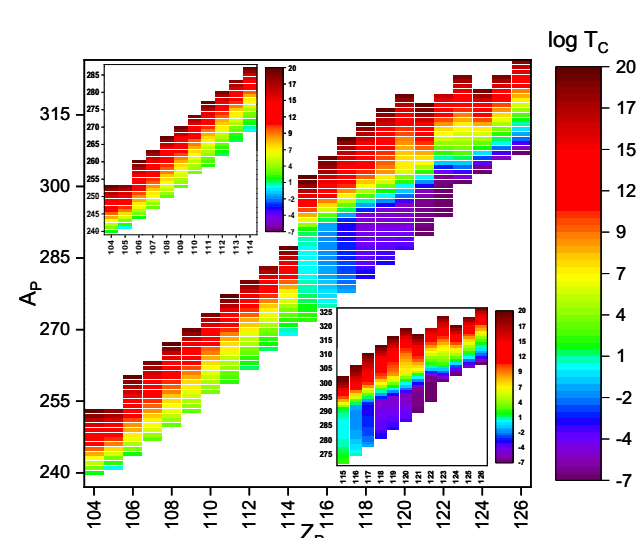


Fig. 5 (Color online) Heat map showing the variations of lowest logarithmic half lives of clusters with $104 < Z < 126$

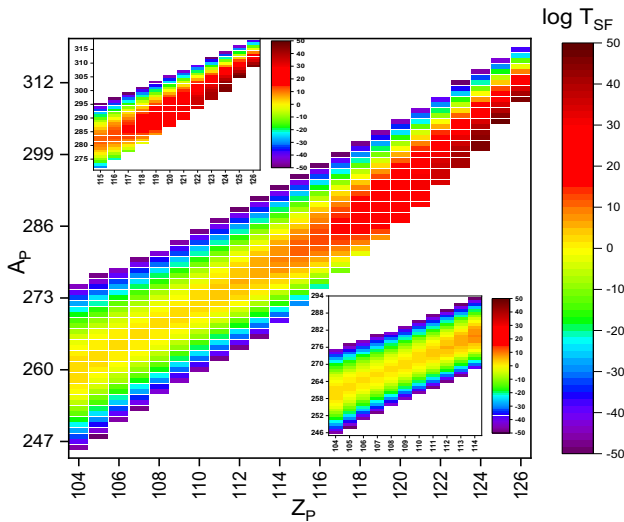


Fig. 6 (Color online) Heat map of the variations of logarithmic half-lives for spontaneous fission for $104 < Z < 126$

$$g_{LI}^2(Z) = \frac{[(2\gamma + 2)^{1/2} + 2](2\gamma + 1)(2\alpha ZR)^{2(\gamma-1)}(\alpha Z)^3}{\Gamma(2\gamma + 1)[(2\gamma + 2)^{1/2} + 1](2\gamma + 2)^\gamma}, \tag{29}$$

$$g_{LII}^2(Z) = \frac{3}{16}(\alpha Z)^2 g_{LI}^2(Z). \tag{30}$$

2.3 Spontaneous fission

Spontaneous fission decay is studied by employing the quantum tunneling effect through the potential barrier. The decay constant of spontaneous fission is expressed as

$$\lambda = \frac{\ln 2}{T_{sf}} = \nu SP_S, \tag{31}$$

where ν , S , and P_S are model-dependent quantities, namely assault frequency, preformation probability, and barrier penetrability, respectively. In the above equation, $P = SP_S$ and the spontaneous-fission half-lives are calculated as

$$T = \frac{\ln 2}{\nu P} = \frac{h \ln 2}{2 E_\nu P}, \tag{32}$$

where h is the Planck constant, and $E_\nu = h\nu/2$ is the zero-point vibration energy. The penetration probability is evaluated using the action integral K :

$$P = \exp(-K), \tag{33}$$

and hence, the decimal logarithm of $T(s)$ is given by

$$\log_{10} T = 0.43429K - 20.8436 - \log_{10} E_\nu. \tag{34}$$

If $E_\nu = 0.5$ MeV, then the above equation becomes

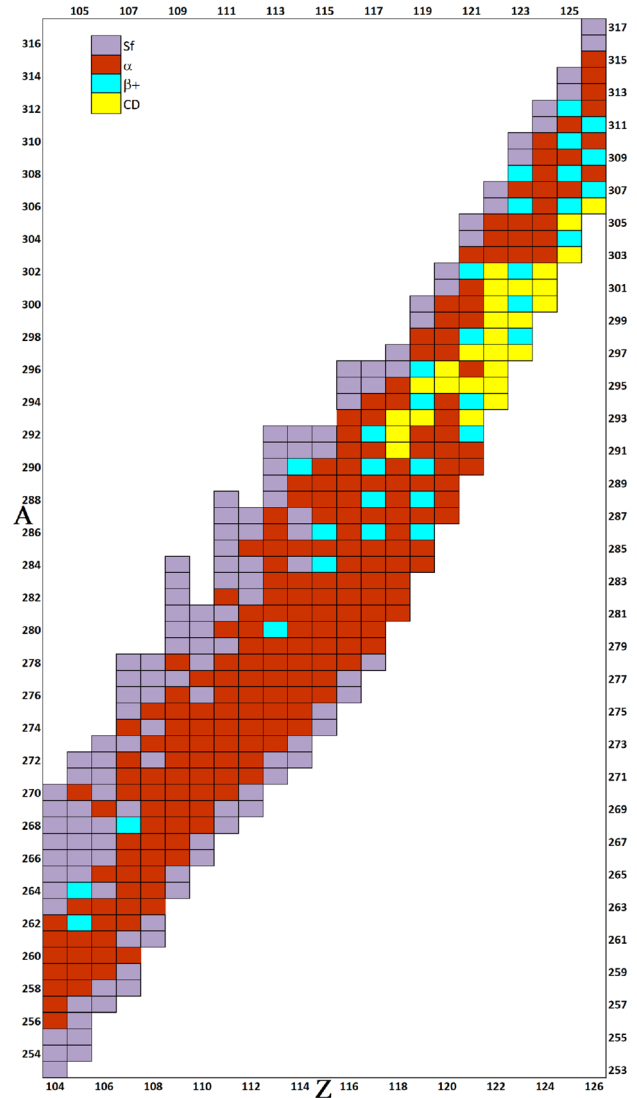


Fig. 7 (Color online) Chart of spontaneous fission (purple), alpha decay (brown), β^+ -decay (cyan), and cluster emitters (yellow) with atomic numbers $Z = 104-126$. The Q -values were calculated using the FRDM95 mass tables

Table 4 Identified cluster emitters in the superheavy nuclei region

Parent nuclei	Q (MeV)	$\log T_{1/2}$	Cluster
^{292}Og	304.08	- 5.08	^{86}Kr
^{293}Og	303.63	- 4.63	^{86}Kr
$^{298}\text{122}$	338.25	- 6.02	^{94}Zr
$^{300}\text{122}$	337.45	- 6.21	^{94}Zr
$^{299}\text{123}$	338.66	- 7.18	^{91}Y
$^{300}\text{124}$	356.06	- 7.35	^{96}Mo
$^{306}\text{126}$	364.27	- 8.78	^{96}Mo

Table 5 Identified alpha emitters in the superheavy nuclei region

Parent nuclei	Q (MeV)	$\log T_{1/2}$	Parent nuclei	Q (MeV)	$\log T_{1/2}$	Parent nuclei	Q (MeV)	$\log T_{1/2}$
²⁵⁶ Rf	10.15	0.92	²⁷⁷ Ds	10.34	- 2.51	²⁸⁰ Lv	13.59	- 6.78
²⁵⁷ Rf	10.05	0.78	²⁷¹ Rg	11.61	- 3.72	²⁸¹ Lv	13.35	- 6.98
²⁵⁸ Rf	9.94	- 0.16	²⁷³ Rg	11.44	- 3.56	²⁸² Lv	13.13	- 5.14
²⁵⁹ Rf	9.67	0.35	²⁷⁵ Rg	11.37	- 3.42	²⁸³ Lv	12.91	- 5.78
²⁶⁰ Rf	9.4	- 1.12	²⁷⁷ Rg	10.88	- 2.21	²⁸⁴ Lv	12.7	- 3.89
²⁶¹ Rf	9.14	1.56	²⁷⁹ Rg	10.44	- 1.23	²⁸⁵ Lv	12.51	- 3.99
²⁶² Rf	8.92	0.52	²⁸⁰ Rg	10.24	0.62	²⁸⁶ Lv	12.34	- 4.25
²⁵⁸ Db	10.45	0.55	²⁸² Rg	9.89	2.15	²⁸⁷ Lv	12.19	- 3.98
²⁵⁹ Db	10.36	- 0.35	²⁷¹ Cn	12.1	- 4.89	²⁸⁸ Lv	12.06	- 3.56
²⁶⁰ Db	10.08	0.26	²⁷² Cn	11.96	- 4.65	²⁹⁰ Lv	11.83	- 1.75
²⁶¹ Db	9.81	0.65	²⁷³ Cn	11.87	- 4.33	²⁹¹ Lv	11.73	- 2.36
²⁶³ Db	9.34	1.52	²⁷⁴ Cn	11.8	- 4.16	²⁹² Lv	11.64	- 1.88
²⁷⁰ Db	8.45	3.25	²⁷⁵ Cn	11.76	- 3.98	²⁹³ Lv	11.55	- 1.23
²⁵⁹ Sg	10.84	- 0.15	²⁷⁶ Cn	11.74	- 2.98	²⁷⁹ Ts	14.06	- 7.36
²⁶⁰ Sg	10.74	- 2.16	²⁷⁷ Cn	11.49	- 3.15	²⁸¹ Ts	14.02	- 8.25
²⁶¹ Sg	10.47	- 0.48	²⁷⁸ Cn	11.25	- 2.47	²⁸³ Ts	13.56	- 5.36
²⁶² Sg	10.2	- 1.86	²⁷⁹ Cn	11.03	- 2.36	²⁸⁵ Ts	13.14	- 5.12
²⁶³ Sg	9.95	0.25	²⁸⁰ Cn	10.81	- 1.78	²⁸⁷ Ts	12.78	- 4.88
²⁶⁹ Sg	9.16	2.56	²⁸¹ Cn	10.62	- 0.99	²⁸⁹ Ts	12.5	- 4.65
²⁶⁰ Bh	11.21	- 1.42	²⁸⁵ Cn	10	1.56	²⁹¹ Ts	12.28	- 2.98
²⁶³ Bh	10.59	- 1.76	²⁷³ Nh	12.4	- 5.65	²⁹⁴ Ts	12	- 1.45
²⁶⁵ Bh	10.12	0.12	²⁷⁵ Nh	12.24	- 4.79	²⁸¹ Og	14.44	- 7.65
²⁶⁶ Bh	9.94	0.22	²⁷⁶ Nh	12.2	- 4.78	²⁸² Og	14.43	- 7.63
²⁷⁰ Bh	9.56	1.89	²⁷⁷ Nh	12.18	- 4.52	²⁸³ Og	14.19	- 7.45
²⁷¹ Bh	9.53	0.18	²⁷⁹ Nh	11.7	- 2.89	²⁸⁴ Og	13.97	- 6.25
²⁷² Bh	9.27	1.12	²⁸¹ Nh	11.26	- 2.12	²⁸⁵ Og	13.76	- 6.41
²⁷⁴ Bh	8.78	1.23	²⁸² Nh	11.07	- 1.69	²⁸⁶ Og	13.56	- 6.24
²⁶³ Hs	11.27	- 2.56	²⁸⁴ Nh	10.73	- 0.16	²⁸⁷ Og	13.37	- 5.25
²⁶⁵ Hs	10.77	- 4.56	²⁸⁵ Nh	10.59	0.78	²⁸⁸ Og	13.21	- 5.98
²⁶⁶ Hs	10.55	- 1.85	²⁸⁶ Nh	10.47	0.88	²⁹⁴ Og	12.53	- 3.88
²⁶⁷ Hs	10.37	- 1.42	²⁸⁷ Nh	10.35	0.76	²⁹⁵ Og	12.44	- 1.25
²⁶⁸ Hs	10.23	0.69	²⁷⁵ Fl	12.78	- 4.69	²⁸⁵ 119	14.37	- 5.69
²⁶⁹ Hs	10.13	1.42	²⁷⁶ Fl	12.72	- 5.12	²⁸⁷ 119	13.96	- 4.25
²⁷⁰ Hs	10.05	1.78	²⁷⁷ Fl	12.68	- 5.36	²⁸⁹ 119	13.62	- 5.97
²⁷¹ Hs	10	0.45	²⁷⁸ Fl	12.66	- 5.46	²⁹² 119	13.23	- 5.28
²⁷³ Hs	9.71	- 0.56	²⁷⁹ Fl	12.42	- 4.12	²⁹⁷ 119	12.78	- 3.97
²⁷⁵ Hs	9.23	- 0.15	²⁸⁰ Fl	12.19	- 4.36	²⁸⁷ 120	14.56	- 6.58
²⁶⁶ Mt	11.27	- 1.93	²⁸¹ Fl	11.96	- 3.78	²⁸⁸ 120	14.37	- 6.25
²⁶⁷ Mt	11.06	- 2.52	²⁸² Fl	11.76	- 3.15	²⁹⁰ 120	14.03	- 6.46
²⁶⁹ Mt	10.74	- 2.32	²⁸³ Fl	11.56	- 2.99	²⁹² 120	13.76	- 5.85
²⁷¹ Mt	10.57	- 1.85	²⁸⁸ Fl	10.86	- 0.25	²⁹⁸ 120	13.2	- 3.87
²⁷³ Mt	10.49	- 1.23	²⁸⁹ Fl	10.75	0.62	²⁹⁹ 120	13.11	- 4.12
²⁷⁴ Mt	10.23	- 0.12	²⁷⁷ Mc	13.19	- 6.85	³⁰⁰ 120	13.02	- 4.36
²⁷⁵ Mt	9.99	- 1.25	²⁷⁸ Mc	13.16	- 6.48	²⁹⁰ 121	14.59	- 6.28
²⁷⁶ Mt	9.75	- 0.36	²⁷⁹ Mc	13.14	- 5.96	²⁹⁶ 121	13.87	- 5.48
²⁷⁸ Mt	9.33	1.36	²⁸⁰ Mc	12.9	- 5.12	³⁰⁰ 121	13.53	- 5.22

Table 5 continued

Parent nuclei	Q (MeV)	$\log T_{1/2}$	Parent nuclei	Q (MeV)	$\log T_{1/2}$	Parent nuclei	Q (MeV)	$\log T_{1/2}$
^{268}Ds	11.62	− 3.56	^{281}Mc	12.67	− 5.36	$^{303}_{122}$	13.77	− 4.98
^{269}Ds	11.45	− 3.24	^{283}Mc	12.24	− 4.25	$^{304}_{122}$	13.67	− 4.99
^{270}Ds	11.31	− 3.68	^{285}Mc	11.88	− 3.12	$^{304}_{123}$	14.18	− 5.12
^{271}Ds	11.21	− 0.58	^{288}Mc	11.47	− 0.89	$^{306}_{124}$	14.49	− 5.66
^{272}Ds	11.14	− 3.09	^{289}Mc	11.36	− 0.52	$^{308}_{124}$	14.28	− 5.98
^{273}Ds	11.1	− 2.96	^{290}Mc	11.26	− 0.25	$^{310}_{124}$	14.05	− 5.87
^{274}Ds	11.07	− 2.45	^{278}Lv	13.64	− 6.75			
^{275}Ds	10.81	− 2.12	^{279}Lv	13.61	− 6.12			

$\log_{10} T = -\log_{10} P - 20.5426$. The action integral K is evaluated as follows:

$$K = \frac{2\sqrt{2m}}{\hbar} \int_{R_a}^{R_b} (B(r)[E(R) - Q])^{1/2} dR. \quad (35)$$

The term $E(R)$ is the macroscopic energy in terms of the surface, volume, Coulomb, proximity energy, shell correction, and pairing energy term [62], and m is the rest mass of the neutron. A few superheavies are spherical, the rest are deformed, primarily prolate or oblate. To include this effect, deformations are also involved in the calculation of $E(r)$, which is adopted from Ref. [62]. In the above equation, R is the separation distance between the center of the fission fragments, and R_a and R_b are the turning points, which are evaluated using the boundary conditions $E(R_a)$ and $E(R_b) = Q$. However, the term $B(r)$ is the inertia with respect to r and is evaluated using the semi-empirical model for inertia [63]:

$$B(r) = \mu \left(1 + k \exp \left[-\frac{128}{51} (r - R_{\text{sph}}/R_0) \right] \right), \quad (36)$$

where μ and k are the reduced mass of the fission fragments and a semi-empirical constant ($k = 14.8$), respectively. R_{sph} is the distance between the center of mass of the fission fragments, set as $R_{\text{sph}}/R_0 = 0.75$ in the symmetric case. The decay constant (λ) and the total fission decay constant are evaluated as described in Ref. [62].

2.4 Results and discussion

The mass excess values play a major role in the prediction of the decay mode and the corresponding half-lives. The predicted half-lives are sensitive to the Q -values, and small changes in the Q -values result in a notable change in the half-lives, with a magnitude of order 10^1 to 10^2 [36]. Mass excess tables such as WS4 [64], EBW [65], HFB28 and HFB29 [66], DZ10 [67], KTUY [68], finite-range droplet model (FRDM) [69], and AME16 [70] are available

Table 6 Identified β^+ emitters in the superheavy nuclei region

Parent nuclei	Q (MeV)	$\log T_{1/2}$
^{264}Db	2.24	− 0.04
^{268}Bh	2.93	− 0.83
^{290}Fl	0.79	1.28
^{286}Mc	4.53	− 3.68
^{292}Ts	4.96	− 4.12
$^{290}_{119}$	7.20	− 6.27
$^{296}_{119}$	5.75	− 5.01
$^{292}_{121}$	8.29	− 7.56
$^{294}_{121}$	8.06	− 7.15
$^{298}_{121}$	6.83	− 6.32
$^{302}_{121}$	5.12	− 5.49
$^{298}_{123}$	8.42	− 8.04
$^{300}_{123}$	8.27	− 7.64
$^{302}_{123}$	6.72	− 7.23
$^{306}_{123}$	5.73	− 6.42
$^{304}_{125}$	7.81	− 8.55
$^{306}_{125}$	7.61	− 8.15
$^{308}_{125}$	6.99	− 7.75
$^{310}_{125}$	6.47	− 7.35
$^{312}_{125}$	5.79	− 6.96

in the literature. In the present study, we used the updated AME16 [70] mass excess values up to $Z = 118$, and above $Z > 118$, the mass excess values are taken from the FRDM [69]. The dominant decay mode is identified by studying the competition between different decay modes: α -decay, β -decay, cluster decay, and spontaneous fission in the superheavy nuclei region $104 \leq Z \leq 126$.

A detailed literature review indicates that there is no experimental evidence for cluster radioactivity in the superheavy region. Furthermore, experimental studies of cluster decay in the actinide region are available. To validate the present study, the cluster-decay half-lives obtained

Table 7 Superheavy nuclei with dual decay mode and branching ratio

Parent nuclei	$\log T_{1/2}$		Decay mode		Parent nuclei		$\log T_{1/2}$		Decay mode				
	Sf	α	β^+	CD	Sf	α	β^+	CD	Sf	α	β^+	CD	
²⁶³ Rf	1.25	1.98	1.65	36.6	Sf = 57%	²⁹⁶ 120	β^+ = 43%	19.58	- 4.87	- 4.38	- 5.45	CD = 53%	α = 47%
²⁶² Db	2.31	- 0.48	- 0.51	34.76	β^+ = 52%	²⁹¹ 120	α = 48%	25.45	- 6.21	- 5.85	- 4.69	α = 51%	β^+ = 49%
²⁶⁴ Bh	0.71	- 1.65	- 1.75	20.58	β^+ = 51%	²⁹⁷ 120	α = 49%	15.36	- 4.25	- 4.6	- 3.62	β^+ = 52%	α = 48%
²⁶² Bh	- 3.25	- 3.25	- 2.22	17.73	Sf = 50%	²⁸⁹ 120	Sf = 50%	21.36	- 6.31	- 6.27	- 4.3	α = 50%	β^+ = 50%
²⁶⁶ Bh	1.62	- 1.89	- 1.29	23.6	α = 59%	²⁹³ 120	β^+ = 41%	25.32	- 5.18	- 5.43	- 5.06	β^+ = 51%	α = 49%
²⁶⁴ Hs	- 2.98	- 3.15	- 1.11	15.37	α = 51%	²⁹³ 121	Sf = 49%	29.32	- 6.98	- 6.29	- 6.47	α = 52%	CD = 48%
²⁷⁰ Mt	2.11	- 2.45	- 2.08	19.43	α = 54%	²⁹⁹ 121	β^+ = 46%	18.56	- 4.75	- 5.05	- 5.43	CD = 52%	β^+ = 48%
²⁷² Mt	1.35	- 1.65	- 1.63	22.66	α = 50%	³⁰³ 121	β^+ = 50%	- 4.36	- 3.52	- 4.22	2.35	Sf = 51%	β^+ = 49%
²⁶⁸ Mt	0.99	- 2.78	- 2.54	16.53	α = 52%	²⁹¹ 121	β^+ = 48%	25.87	- 5.94	- 6.7	- 6.65	β^+ = 50%	CD = 50%
²⁷⁶ Ds	- 1.72	- 1.65	- 0.09	23.61	Sf = 51%	²⁹⁵ 121	α = 49%	30.36	- 5.78	- 5.88	- 6.34	CD = 52%	β^+ = 48%
²⁷² Rg	2.22	- 3.15	- 3.34	12.55	β^+ = 51%	²⁹⁷ 121	α = 49%	26.9	- 4.77	- 5.46	- 6.33	CD = 54%	β^+ = 46%
²⁷⁶ Rg	2.42	- 2.16	- 2.44	18.44	β^+ = 53%	³⁰¹ 121	α = 47%	8.25	- 5.36	- 4.64	- 1.47	α = 54%	β^+ = 46%
²⁶⁹ Rg	- 3.98	- 3.86	- 2.95	9.04	Sf = 51%	²⁹⁴ 122	α = 49%	30.65	- 5.98	- 6.51	- 6.89	CD = 51%	β^+ = 49%
²⁷⁰ Rg	- 1.56	- 3.87	- 3.79	10.12	α = 51%	²⁹⁵ 122	β^+ = 49%	34.25	- 5.99	- 6.73	- 6.78	CD = 50%	β^+ = 50%
²⁷⁸ Rg	- 1.32	- 1.54	- 1.99	21.54	β^+ = 56%	²⁹⁶ 122	α = 44%	36.89	- 6.24	- 6.1	- 6.83	CD = 52%	α = 48%
²⁷⁴ Rg	3.56	- 3.22	- 2.89	15.4	α = 53%	²⁹⁷ 122	β^+ = 47%	34.22	- 6.96	- 6.32	- 6.77	α = 51%	CD = 49%
²⁸³ Nh	- 1.55	- 1.89	- 1.55	18.55	α = 55%	³⁰⁵ 122	Sf = 45%	- 0.58	- 4.98	- 4.68	- 0.68	α = 52%	β^+ = 48%
²⁷⁴ Nh	0.65	- 4.01	- 4.6	6.88	β^+ = 53%	³⁰² 122	α = 47%	18.21	- 5.27	- 4.87	- 6.31	CD = 54%	α = 46%
²⁸⁰ Nh	4.98	- 2.78	- 3.27	14.3	β^+ = 54%	³⁰¹ 122	α = 46%	23.56	- 5.96	- 5.5	- 6.46	CD = 52%	α = 48%
²⁷⁸ Nh	5.88	- 3.87	- 3.72	11.51	α = 51%	²⁹⁹ 122	β^+ = 49%	30.89	- 6.14	- 5.91	- 6.7	CD = 52%	α = 48%
²⁷⁴ Fl	- 5.12	- 4.89	- 3.95	3.62	Sf = 51%	³⁰³ 122	α = 49%	13.77	- 5.11	- 5.09	- 4.33	α = 50%	β^+ = 50%
²⁸⁵ Fl	- 0.45	- 2.11	- 1.97	16.71	α = 52%	³⁰³ 123	β^+ = 48%	27.89	- 6.36	- 5.96	- 3.66	α = 52%	β^+ = 48%
²⁸³ Mc	11.02	- 3.78	- 4.55	0.52	β^+ = 55%	²⁹⁷ 123	α = 45%	38.48	- 6.17	- 7.18	- 7.51	CD = 51%	β^+ = 49%
²⁸⁷ Mc	1.32	- 2.98	- 2.4	0.5	α = 55%	³⁰¹ 123	β^+ = 45%	35.02	- 6.18	- 6.37	- 6.86	CD = 52%	β^+ = 48%
²⁸⁴ Mc	8.98	- 3.58	- 4.12	0.37	β^+ = 54%	³⁰⁷ 123	α = 46%	2.18	- 4.98	- 5.15	2.81	β^+ = 51%	α = 49%
²⁷⁶ Mc	- 3.12	- 5.89	- 5.86	1.45	α = 50%	³⁰⁵ 123	β^+ = 50%	15.58	- 5.48	- 5.56	- 0.65	β^+ = 50%	α = 50%
²⁷⁷ Lv	- 6.85	- 5.78	- 5.42	0.18	Sf = 54%	³⁰⁸ 123	α = 46%	- 4.89	- 5.26	- 6.01	3.61	β^+ = 53%	α = 47%
²⁸⁹ Lv	3.15	- 3.05	- 2.83	- 1.32	α = 52%	³⁰³ 124	β^+ = 48%	40.25	- 6.25	- 6.83	- 6.77	β^+ = 50%	CD = 50%
²⁹³ Ts	- 2.98	- 3.58	- 2.84	- 2.88	α = 55%	³⁰⁵ 124	Sf = 45%	33.21	- 5.12	- 6.42	- 4.29	β^+ = 56%	α = 44%
²⁸⁴ Ts	13.25	- 5.25	- 5.83	- 2.5	β^+ = 53%	³⁰² 124	α = 47%	40.25	- 5.96	- 6.6	- 7.13	CD = 52%	β^+ = 48%
²⁸⁶ Ts	14.55	- 5.16	- 5.4	- 2.6	β^+ = 51%	³⁰⁴ 124	α = 49%	35.85	- 6.01	- 6.19	- 6.45	CD = 51%	β^+ = 49%
²⁹⁰ Ts	9.18	- 4.36	- 4.55	- 3.09	β^+ = 51%	³⁰⁷ 124	α = 49%	22.14	- 5.97	- 6.02	- 0.09	β^+ = 50%	α = 50%

Table 7 continued

Parent nuclei	$\log T_{1/2}$		Decay mode			Parent nuclei	$\log T_{1/2}$		Decay mode			
	<i>Sf</i>	α	β^+	<i>CD</i>			<i>Sf</i>	α	β^+	<i>CD</i>		
²⁸⁸ Ts	13.78	- 4.87	- 4.98	- 2.91	$\beta^+ = 51\%$	³⁰¹ 124	44.14	- 6.04	- 7.23	- 7.53	$CD = 51\%$	$\beta^+ = 49\%$
²⁸⁰ Ts	0.68	- 6.25	- 6.69	- 2.01	$\beta^+ = 52\%$	³⁰⁹ 124	6.87	- 5.11	- 5.62	3.17	$\beta^+ = 52\%$	$\alpha = 48\%$
²⁸² Ts	8.58	- 5.85	- 6.26	- 2.19	$\beta^+ = 52\%$	³⁰⁹ 125	26.25	- 6.51	- 6.49	0.26	$\alpha = 50\%$	$\beta^+ = 50\%$
²⁹⁰ Og	16.98	- 3.78	- 3.91	- 4.72	$CD = 55\%$	³⁰⁷ 125	38.21	- 6.21	- 6.89	- 3.75	$\beta^+ = 53\%$	$\alpha = 47\%$
²⁹¹ Og	14.89	- 3.78	- 4.13	- 4.9	$CD = 54\%$	³¹¹ 125	11.58	- 5.75	- 6.09	2.43	$\beta^+ = 51\%$	$\alpha = 49\%$
²⁸⁹ Og	18.74	- 5.25	- 4.56	- 4.46	$\alpha = 54\%$	³⁰⁵ 125	45.35	- 6.87	- 7.29	- 7.5	$CD = 51\%$	$\beta^+ = 49\%$
²⁸⁴ 119	5.95	- 6.68	- 7.53	- 3.17	$\beta^+ = 53\%$	³⁰³ 125	45.25	- 6.96	- 7.69	- 8.07	$CD = 51\%$	$\beta^+ = 49\%$
²⁹³ 119	18.29	- 3.98	- 4.57	- 5.15	$CD = 53\%$	³¹⁵ 126	- 1.58	- 5.75	- 6.17	2.82	$\beta^+ = 52\%$	$\alpha = 48\%$
²⁸⁶ 119	14.98	- 7.25	- 7.11	- 3.79	$\alpha = 50\%$	³¹³ 126	15.25	- 6.24	- 6.57	0.85	$\beta^+ = 51\%$	$\alpha = 49\%$
²⁹⁴ 119	15.98	- 3.89	- 5.43	- 5.15	$\beta^+ = 51\%$	³⁰⁸ 126	48.21	- 6.87	- 7.12	- 5.37	$\beta^+ = 51\%$	$\alpha = 49\%$
²⁸⁸ 119	19.35	- 5.85	- 6.69	- 4.15	$\beta^+ = 53\%$	³¹¹ 126	32.21	- 5.12	- 6.96	- 0.97	$\beta^+ = 58\%$	$\alpha = 42\%$
²⁹⁸ 119	- 4.85	- 3.22	- 4.59	0.23	$Sf = 51\%$	³¹⁰ 126	39.21	- 6.32	- 6.73	- 1.99	$\beta^+ = 52\%$	$\alpha = 48\%$
²⁹¹ 119	21.25	- 4.58	- 4.99	- 4.74	$\beta^+ = 51\%$	³⁰⁹ 126	44.58	- 6.58	- 7.36	- 3.69	$\beta^+ = 53\%$	$\alpha = 47\%$
²⁹⁵ 119	11.35	- 4.23	- 4.15	- 5.03	$CD = 54\%$	³¹² 126	26.12	- 5.74	- 6.33	0.01	$\beta^+ = 52\%$	$\alpha = 48\%$
²⁹⁵ 120	22.15	- 4.78	- 5.02	- 5.46	$CD = 52\%$	³⁰⁷ 126	51.32	- 7.11	- 7.75	- 6.99	$\beta^+ = 52\%$	$\alpha = 48\%$
²⁹⁴ 120	23.58	- 4.22	- 4.79	- 5.36	$CD = 53\%$	³¹⁴ 126	7.56	- 6.21	- 5.94	1.7	$\alpha = 51\%$	$\beta^+ = 49\%$

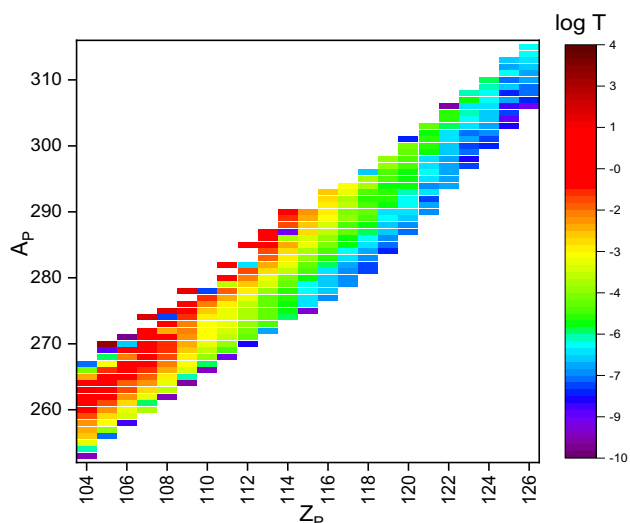


Fig. 8 (Color online) Heat map showing the variations of atomic number, mass number of parent and logarithmic half-lives of different decay modes (life times) for $104 < Z < 126$

in the present study in the actinide region were compared with the experiments, and good agreement was observed. With this confidence, we studied cluster decay in the superheavy region, and the results are presented in Table 1. Similarly, Table 2 shows a comparison of the studied logarithmic half-lives (in years) of spontaneous fission from the present study with those from available experiments. It can be seen that the cluster-decay and spontaneous-fission half-lives obtained in the present study are close to those of the experiments.

As a part of this investigation, we studied the α -decay properties of superheavy nuclei using the formalism explained in the theory section. The predicted alpha-decay half-lives were validated by comparison with those from available experiments in the superheavy region. The results are given in Table 3.

From the comparison, it is observed that the predicted half-lives are in good agreement with those of the experiments. With this confidence, we obtained the alpha-decay half-lives of superheavy nuclei in the region $104 \leq Z \leq 126$ Fig. 2.

shows a wide range of α -decay half-lives. For a given superheavy nucleus, the alpha decay half-lives increase as the neutron number of its isotopes increases. For instance, the α -decay half-lives are of the order of nanoseconds at $N/Z = 1.307692$ for Rutherfordium, whereas for the same superheavy element, the α -decay half-lives are of the order of 10^2 s at $N/Z = 1.504762$. Similarly, all neutron-rich superheavy nuclei have comparably longer α -decay half-lives, which is in agreement with the report available in Ref. [73]. The obtained α -decay half-lives of all possible superheavy nuclei are presented in the heat map in Fig. 2.

The right vertical bar shows the magnitude of the $\log T_{1/2}$ values. The color variation from navy blue to wine indicates values in the range 10^{-10} – 10^2 s. The contrast in the blue region lies between 10^{-10} s and 10^{-7} s, in the green region, it lies in the range 10^{-6} – 10^{-4} s, and the range 10^{-4} – 10^{-3} s is presented in the yellow region. Finally, the red-to-wine region shows higher half-lives in the range 10^{-2} – 10^2 s. The inset of Fig. 2 on the top left side provides information on the magnified portion of α -decay half-lives in the superheavy region $Z = 104 - 114$, whereas the bottom-right inset provides information on the magnified portion of the superheavy region $Z = 115 - 126$. After the detailed investigation of the α -decay, a search was made to identify the cluster emitters in the superheavy region. Cluster radioactivity is energetically favorable if the Q-values are positive. We studied the possibility of cluster decay with $3 \leq Z_C \leq 45$ in the superheavy region $104 \leq Z \leq 126$. For a given parent nucleus, the half-lives corresponding to various cluster emission were evaluated, and the cluster corresponding to shorter half-lives was identified. Furthermore, the cluster emitters corresponding to shorter half-lives for different isotopes of a given superheavy element were also identified. Eventually, cluster emissions corresponding to the shortest half-lives T_C were identified; these are referred to as cluster-decay half-lives (T_C). The predicted cluster decay half-lives in the atomic number region $104 \leq Z \leq 126$ correspond to all the studied cluster emissions, as shown in Fig. 3.

This figure enables us to identify the cluster emission corresponding to the shorter half-lives of a given superheavy element. The half-lives of superheavy nuclei with $Z = 115$ – 120 against cluster radioactivity are shorter for ^{86}Kr than those of the other studied clusters. The superheavy nuclei with $Z = 104, 106, 108, 110, 112, 114, 124,$ and 126 have shorter half-lives against ^{96}Mo cluster emissions than those of the other studied clusters. The decay half-lives are shorter for the ^{91}Y emission from superheavy nuclei with $Z = 109, 111, 113, 121,$ and 123 . Similarly, the half-lives of superheavy nuclei with $Z = 105$ and 107 against cluster radioactivity are shorter for ^{97}Tc and ^{101}Rh than those of the other studied clusters.

Cluster radioactivity in the superheavy nuclei region has shorter half-lives for cluster neutron numbers 44–48 from parent nuclei with neutron numbers 130–200, as shown in Fig. 4.

The range of cluster decay half-lives for superheavy elements with $104 \leq Z \leq 126$ is shown in Fig. 5.

Shorter half-lives are observed for $N/Z > 1.37068$, and larger half-lives are observed for $N/Z < 1.37068$. From the figure, it is clear that up to superheavy nuclei $104 \leq Z \leq 115$, larger cluster-decay half-lives are observed, whereas shorter cluster-decay half-lives are observed in the

superheavy region $116 \leq Z \leq 126$. The inset of Fig. 5 on the top-left side shows a magnified portion of the logarithmic half-lives (T_C) in the superheavy region $104 \leq Z \leq 115$, whereas the inset at the right bottom shows a magnified portion of the shorter logarithmic half-lives (T_C) in the superheavy region $116 \leq Z \leq 126$. This figure also shows that some of the superheavy nuclei have lifetimes of the order of ns to μ s and exhibit cluster decay.

The other prominent decay mode that was studied is spontaneous fission, which is also energetically feasible in heavy and superheavy nuclei. It may occur in such nuclei owing to an increase in the Coulomb interactions. References [10, 11, 38, 74–77] report consistent α -decay chains from superheavy nuclei followed by spontaneous fission. The spontaneous fission half-lives are studied using the theory explained in Sect. 2.3. The variations of spontaneous fission half-lives in the superheavy region $Z = 104$ –126 are shown in Fig. 6.

The $\log T_{SF}$ values vary between -50 (dark blue region) and 50 (dark-red region). For instance, at atomic number $Z = 104$, for isotopes 245–275, the $\log T_{1/2}(SF)$ values ranging from -50 to 5 are shown, whereas the half-lives with smaller values are indicated by the color range from navy blue to blue. The half-lives ranging from nanoseconds to 10^5 s are indicated by the color range from yellow to light orange. Similarly, in the atomic number range $Z = 119$ and above, larger values of spontaneous-fission logarithmic half-lives are indicated by the red color range. Thus, on either side of Fig. 6, for isotopes corresponding to the atomic number range $Z = 104$ –126, smaller half-lives are observed, whereas in the middle region of the figure, larger values of $\log T_{1/2}$ are observed up to $Z = 116$. In contrast, smaller half-lives are observed for higher isotopes ($Z > 116$), and larger $\log T_{1/2}$ for lower isotopes ($Z < 116$). A similar trend was also observed in a previous study [78], in which the half-lives of nuclei $Z = 92$ –104 were compared with experimentally available values.

A detailed investigation of the Q -values corresponding to β -decay in the superheavy region demonstrates that β^+ -decay is energetically possible with $Z = 105, 107, 113, 114, 115, 117, 119, 121, 123, 125,$ and 126 , whereas β^- -decay is not energetically possible. Furthermore, we also studied β -decay half-lives using the formalism explained in Sect. 2.2.1.

The competition between different possible decay modes, namely α -decay, cluster-decay, β -decay and spontaneous fission, enables us to identify the dominant decay mode for superheavy elements in the atomic number region $104 \leq Z \leq 126$ of all possible isotopes Fig. 7.

shows the decay modes of the superheavy nuclei. In the studied superheavy region, we identified around 20 β^+ emitters, which are presented in Table 6. We also

identified 35 cluster emitters, which are presented in Table 4.

It was demonstrated that the majority of superheavy nuclei undergo α -decay and spontaneous fission. The α -emitting superheavy nuclei are listed in Table 5.

The identified alpha emitters have half-lives of approximately μ s to 100 s in the superheavy region $104 \leq Z \leq 126$. Table 4 lists the identified cluster emissions with the corresponding half-lives. The amount of energy released during cluster emission, cluster emitted, and $\log T_{1/2}$ values are presented in the table. The minimum cluster decay half-lives correspond to ^{86}Kr , ^{94}Zr , ^{91}Y , and ^{96}Mo for the nuclei $^{292-293}\text{Og}$, $^{298,300}\text{122}$, $^{299}\text{123}$, $^{300}\text{124}$, and $^{306}\text{126}$, respectively. From the available literature, it is also evident that the heavy particle radioactivity of ^{86}Kr is observed in the superheavy nucleus $Z = 118$ [36, 79]. In addition, Rb, Sr, Y, Zr, Nb, and Mo cluster emissions [80] were observed for $Z = 119$ –124, respectively. As in previous studies, in the present study, shorter half-lives in the superheavy region $Z = 118, 122$ –124, and 126 were observed, with ^{86}Kr , ^{94}Zr , ^{91}Y , and ^{96}Mo cluster emissions, respectively. Similarly, approximately 20 possible β^+ emitters were identified in the superheavy region $105 \leq Z \leq 125$, and they are presented in Table 6.

The information provided Table 7 regarding the half-lives and branching ratios presents ambiguities in terms of determining a single decay mode. The branching ratios relative to the minimum half-lives among the studied decay modes are obtained, and the second column of the table shows the $\log T_{1/2}$ values corresponding to spontaneous-fission, α -decay, β^+ -decay, and cluster-decay half-lives. For instance, the superheavy nucleus ^{263}Rf exhibits shorter $\log T_{1/2}$ values for spontaneous fission and β^+ -decay than for other decay modes. The branching ratio of spontaneous fission and β^+ -decay was obtained, and it was found that the branching ratio corresponding to spontaneous fission and β^+ was 55% and 45%, respectively. Similarly, we identified the branching ratios for the superheavy region $104 \leq Z \leq 126$, which are presented in Table 7.

Finally, Fig. 8 shows the lifetimes of the superheavy elements after the competition between different decay modes was studied.

It can be seen that the lifetime varies from ns to min and decreases as the atomic number increases. For instance, the average lifetime of a superheavy element with $Z = 104$ is approximately 10 min, whereas that of a hypothetical superheavy element with $Z = 126$ is of the order of ms.

3 Conclusion

We systematically investigated all possible decay modes, namely α -decay, β -decay, cluster decay, and spontaneous fission, in the superheavy region $104 \leq Z \leq 126$. The findings of this study were validated by comparison with experiments. Approximately 20 β^+ and 7 heavy particle emitters were found in the superheavy region. Furthermore, the nuclei with almost the same half-lives for the two decay modes were also reported, with the corresponding branching ratios. However, an experimental study is necessary to draw definite conclusions.

Author contributions All authors contributed to the study conception and design. Conceived of the original idea, developed the theory formulation of work and writing by HCM and NS. Performed the computations and performed, analytic calculations and graphical representation by PSDG, KNS and AMN, data analysis by LS and SACR. All authors read and approved the final manuscript.

References

1. F.P. Heberger, S. Hofmann, D. Ackermann et al., Decay properties of neutron-deficient isotopes 256,257 Db, 255 Rf, 252,253 Lr. *Eur. Phys. J. A* **12**, 57–67 (2001). <https://doi.org/10.1007/s100500170039>
2. Y.T. Oganessian, V.K. Utyonkov, Y.V. Lobanov et al., Publisher's note: Measurements of cross sections and decay properties of the isotopes of elements 112, 114, and 116 produced in the fusion reactions 233,238 U, 242 Pu, and 248 Cm + 48 Ca. *Phys. Rev. C* **70**, 064609 (2004). <https://doi.org/10.1103/PhysRevC.71.029902>
3. Y.T. Oganessian, V.K. Utyonkov, Y.V. Lobanov et al., Publisher's note: measurements of cross sections and decay properties of the isotopes of elements 112, 114, and 116 produced in the fusion reactions ^{233,238}U, ²⁴²Pu, and ²⁴⁸Cm + ⁴⁸Ca. *Phys. Rev. C* **71**, 029902 (2005). <https://doi.org/10.1103/PhysRevC.71.029902>
4. G.G. Adamian, N.V. Antonenko, W. Scheid, High-spin isomers in some of the heaviest nuclei: spectra, decays, and population. *Phys. Rev. C* **81**, 024320 (2010). <https://doi.org/10.1103/PhysRevC.81.024320>
5. A.T. Kruppa, M. Bender, W. Nazarewicz et al., Shell corrections of superheavy nuclei in self-consistent calculations. *Phys. Rev. C* **61**, 034313 (2000). <https://doi.org/10.1103/PhysRevC.61.034313>
6. Y. Shi, D.E. Ward, B.G. Carlsson et al., Structure of superheavy nuclei along decay chains of element 115. *Phys. Rev. C* **90**, 014308 (2014). <https://doi.org/10.1103/PhysRevC.90.014308>
7. X. Meng, B. Lu, S. Zhou, Ground state properties and potential energy surfaces of ²⁷⁰Hs from multidimensionally-constrained relativistic mean field model. *Sci. China I Phys. Mech. Astron.* **63**, 1–11 (2020). <https://doi.org/10.1007/s11433-019-9422-1>
8. R. Swain, B. Sahu, Structure and reaction dynamics of she Z = 130. *Chin. Phys. C* **43**, 104103 (2019). <https://doi.org/10.1088/1674-1137/43/10/104103>
9. F. Niu, P.-H. Chen, H.-G. Cheng et al., Multinucleon transfer dynamics in nearly symmetric nuclear reactions. *Nucl. Sci. Tech.* **31**, 59 (2020). <https://doi.org/10.1007/s41365-020-00770-1>
10. S. Hofmann, V. Ninov, F.P. Heberger et al., Production and decay of ²⁶⁹110. *Zeitschrift fur Physik A Hadrons and Nuclei* **350**, 277–280 (1995). <https://doi.org/10.1007/BF01291181>
11. S. Hofmann, G. Munzenberg, The discovery of the heaviest elements. *Rev. Mod. Phys.* **72**, 733–767 (2000). <https://doi.org/10.1103/RevModPhys.72.733>
12. D. Boilley, B. Cauchois, H. Lv et al., How accurately can we predict synthesis cross sections of superheavy elements? *Nucl. Sci. Tech.* **29**, 172 (2018). <https://doi.org/10.1007/s41365-018-0509-7>
13. D. Naderi, S.A. Alavi, Influence of the shell effects on evaporation residue cross section of superheavy nuclei. *Nucl. Sci. Tech.* **29**, 161 (2018). <https://doi.org/10.1007/s41365-018-0498-6>
14. X. Li, Z. Wu, L. Guo, Entrancechannel dynamics in the reaction ⁴⁰Ca + ²⁰⁸Pb. *Sci. China-Phys. Mech. Astron.* **62**, 12 (2019). <https://doi.org/10.1007/s11433-019-9435-x>
15. Y.T. Oganessian, K.P. Rykaczewski, A beachhead on the island of stability. *Phys. Today* (2015). <https://doi.org/10.1063/PT.3.2880>
16. A. Sobiczewski, F.A. Gareev, B.N. Kalinkin, Closed shells for Z > 82 and N > 126 in a diffuse potential well. *Phys. Lett.* **22**, 500–502 (1966). [https://doi.org/10.1016/0031-9163\(66\)91243-1](https://doi.org/10.1016/0031-9163(66)91243-1)
17. S. Nilsson, Binding states of individual nucleons in strongly deformed nuclei. *Dan. Mat. Fys. Med.* **29**, 1–69 (1955)
18. M. Bender, K. Bennaceur, T. Duguet et al., Tensor part of the skyrme energy density functional: ii: deformation properties of magic and semimagic nuclei. *Phys. Rev. C* **80**, 064302 (2009). <https://doi.org/10.1103/PhysRevC.80.064302>
19. B.A. Brown, The nuclear shell model towards the drip lines. *Prog. Part. Nucl. Phys.* **47**, 517–599 (2001). [https://doi.org/10.1016/S0146-6410\(01\)00159-4](https://doi.org/10.1016/S0146-6410(01)00159-4)
20. R.D. Herzberg, P.T. Greenlees, P.A. Butler et al., Nuclear isomers in superheavy elements as stepping stones towards the island of stability. *Nature* **442**, 896–899 (2006). <https://doi.org/10.1038/nature05069>
21. D. Tománek, M.A. Schlüter, Calculation of magic numbers and the stability of small si clusters. *Phys. Rev. Lett.* **56**, 1055–1058 (1986). <https://doi.org/10.1103/PhysRevLett.56.1055>
22. A.M. Nagaraja, H.C. Manjunatha, N. Sowmya et al., Cluster radioactivity in superheavy nuclei ^{299–302}120. *Indian J. Pure Appl. Phys.* **58**, 207–212 (2020)
23. H.C. Manjunatha, N. Sowmya, Competition between spontaneous fission ternary fission cluster decay and alpha decay in the super heavy nuclei of Z = 126. *Nucl. Phys. A* **969**, 68–82 (2018). <https://doi.org/10.1016/j.nuclphysa.2017.09.008>
24. N. Sowmya, H.C. Manjunatha, N. Dhananjaya et al., Competition between binary fission, ternary fission, cluster radioactivity and alpha decay of ²⁸¹Ds. *J. Radioanal. Nucl. Chem.* **323**, 1347–1351 (2020). <https://doi.org/10.1007/s10967-019-06706-3>
25. G.R. Sridhar, H.C. Manjunatha, N. Sowmya et al., Atlas of cluster radioactivity in actinide nuclei. *Eur. Phys. J. Plus* **135**, 1–28 (2020). <https://doi.org/10.1140/epjp/s13360-020-00302-1>
26. H.C. Manjunatha, K.N. Sridhar, N. Sowmya, Investigations of the synthesis of the superheavy element Z = 122. *Phys. Rev. C* **98**, 024308 (2018). <https://doi.org/10.1103/PhysRevC.98.024308>
27. H.C. Manjunatha, N. Sowmya, Decay modes of superheavy nuclei Z = 124. *Int. J. Mod. Phys. E* **27**, 1850041 (2018). <https://doi.org/10.1142/S0218301318500416>
28. N. Sowmya, H.C. Manjunatha, Investigations on different decay modes of darmstadtium. *Phys. Particles Nuclei Lett.* **17**, 370–378 (2020). <https://doi.org/10.1134/S1547477120030140>
29. N. Sowmya, H.C. Manjunatha, Competition between different decay modes of superheavy element Z = 116 and synthesis of possible isotopes. *Braz. J. Phys.* **49**, 874–886 (2019). <https://doi.org/10.1007/s13538-019-00710-4>

30. N. Sowmya, H.C. Manjunatha, P.S.D. Gupta, Competition between decay modes of superheavy nuclei $^{281-310}\text{Og}$. *Int. J. Mod. Phys. E* (2020). <https://doi.org/10.1142/S0218301320500871>
31. N. Sowmya, H.C. Manjunatha, Investigations on the synthesis and decay properties of roentgenium. *Braz. J. Phys.* **50**, 317–330 (2020). <https://doi.org/10.1007/s13538-020-00747-w>
32. N. Sowmya, H.C. Manjunatha, P.S.D. Gupta et al., Competition between cluster and alpha decay in odd Z superheavy nuclei $111 \leq Z \leq 125$. *Braz. J. Phys.* **51**, 99–135 (2021). <https://doi.org/10.1007/s13538-020-00801-7>
33. K.N. Sridhar, H.C. Manjunatha, H.B. Ramalingam, Search for possible fusion reactions to synthesize the superheavy element $Z = 121$. *Phys. Rev. C* **98**, 064605 (2018). <https://doi.org/10.1103/PhysRevC.98.064605>
34. A. Soylyu, Search for decay modes of heavy and superheavy nuclei. *Chin. Phys. C* **43**, 074102 (2019). <https://doi.org/10.1088/1674-1137/43/7/074102>
35. Nuclear live chart. <https://www-nds.iaea.org/relnsd/vcharthtml/VChartHTML.html>
36. D.N. Poenaru, R.A. Gherghescu, W. Greiner, Heavy-particle radioactivity of superheavy nuclei. *Phys. Rev. Lett.* **107**, 062503 (2011). <https://doi.org/10.1103/PhysRevLett.107.062503>
37. Y.T. Oganessian, Route to islands of stability of superheavy elements. *Phys. Atom. Nuclei* **63**, 1315–1336 (2000). <https://doi.org/10.1134/1.1307456>
38. Y. Oganessian, Heaviest nuclei from ^{48}Ca induced reactions. *J. Phys. G* **34**, R165 (2007). <https://doi.org/10.1016/j.nuclphysa.2015.07.003>
39. J. Grumann, U. Mosel, B. Fink et al., Investigation of the stability of superheavy nuclei around $Z = 114$ and $Z = 164$. *Zeitschrift für Physik* **228**, 371–386 (1969). <https://doi.org/10.1007/BF01406719>
40. D.N. Poenaru, M. Ivaşcu, A. Sndulescu et al., Atomic nuclei decay modes by spontaneous emission of heavy ions. *Phys. Rev. C* **32**, 572–581 (1985). <https://doi.org/10.1103/PhysRevC.32.572>
41. B. Buck, A.C. Merchant, S.M. Perez, α decay calculations with a realistic potential. *Phys. Rev. C* **45**, 2247–2253 (1992). <https://doi.org/10.1103/PhysRevC.45.2247>
42. H.F. Zhang, G. Royer, Theoretical and experimental α decay half-lives of the heaviest odd- Z elements and general predictions. *Phys. Rev. C* **76**, 017304 (2007). <https://doi.org/10.1103/PhysRevC.76.047304>
43. V.Y. Denisov, H. Ikezoe, α -nucleus potential for α -decay and sub-barrier fusion. *Phys. Rev. C* **72**, 064613 (2005). <https://doi.org/10.1103/PhysRevC.72.064613>
44. P. Möller, G.A. Leander, J.R. Nix, On the stability of the trans-steinium elements. *Zeitschrift für Physik A Atomic Nuclei* **323**, 41–45 (1986). <https://doi.org/10.1007/BF01294553>
45. F.R. Xu, E.G. Zhao, R. Wyss et al., Enhanced stability of superheavy nuclei due to high-spin isomerism. *Phys. Rev. Lett.* **92**, 252501 (2004). <https://doi.org/10.1103/PhysRevLett.92.252501>
46. C. Wong, Additional evidence of stability of the superheavy element 310126 according to the shell model. *Phys. Lett.* **21**, 688–690 (1966). [https://doi.org/10.1016/0031-9163\(66\)90127-2](https://doi.org/10.1016/0031-9163(66)90127-2)
47. D.N. Poenaru, R.A. Gherghescu, W. Greiner, Single universal curve for cluster radioactivities and α decay. *Phys. Rev. C* **83**, 014601 (2011). <https://doi.org/10.1103/PhysRevC.83.014601>
48. S.B. Duarte, F.G. Oap, T.A. Dimarco, Half-lives for proton emission, alpha decay, cluster radioactivity, and cold fission processes calculated in a unified theoretical framework. *Atom. Data Nucl. Data Tables* **80**, 235 (2002). <https://doi.org/10.1006/andn.2002.0881>
49. H.F. Zhang, G. Royer, Y.J. Wang et al., Analytic expressions for α particle preformation in heavy nuclei. *Phys. Rev. C* **80**, 057301 (2009). <https://doi.org/10.1103/PhysRevC.80.057301>
50. Z. Shan, Z. Yanli, C. Jianpo et al., Improved semi-empirical relationship for α -decay half-lives. *Phys. Rev. C* **95**, 014311 (2017). <https://doi.org/10.1103/PhysRevC.95.014311>
51. D.N. Poenaru, J.A. Maruhn, W. Greiner et al., Inertia and fission paths in a wide range of mass asymmetry. *Zeitschrift für Physik A Atomic Nuclei* **333**, 291 (1989). <https://doi.org/10.1007/BF01294517>
52. M. Gongalves, S.B. Duarte, Effective liquid drop description for the exotic decay of nuclei. *Phys. Rev. C* **48**, 2409–2414 (1993). <https://doi.org/10.1103/PhysRevC.48.2409>
53. M. Gonçalves, N. Teruya, O. Tavares et al., Twoproton emission half-lives in the effective liquid drop model. *Phys. Lett. B* **774**, 14–19 (2017). <https://doi.org/10.1016/j.physletb.2017.09.032>
54. K. Santhosh, R. Biju, Stability of $^{248,254}\text{Cf}$ isotopes against alpha and cluster radioactivity. *Ann. Phys.* **334**, 280–287 (2013). <https://doi.org/10.1016/j.aop.2013.04.008>
55. H.C. Manjunatha, G.R. Sridhar, N. Sowmya et al., A systematic study of alpha decay in actinide nuclei using modified generalized liquid drop model. *Int. J. Mod. Phys. E* **30**, 2150013 (2021). <https://doi.org/10.1142/S0218301321500130>
56. N. Maroufi, V. Dehghani, S.A. Alavi, Alpha and cluster decay of some deformed heavy and superheavy nuclei. *Nucl. Phys. A* **983**, 77–89 (2019). <https://doi.org/10.1016/j.nuclphysa.2018.12.023>
57. M. Gonçalves, S.B. Duarte, Effective liquid drop description for the exotic decay of nuclei. *Phys. Rev. C* **48**, 2409–2414 (1993). <https://doi.org/10.1103/PhysRevC.48.2409>
58. B.S. Dzhelepov, L.N. Zyryanova, Y.P. Suslov, Beta processes functions for the analysis of beta spectra and electron capture. **373**(1972)
59. A.V. Karpov, V.I. Zagrebaev, Y. MartinezPalenzuela et al., Decay properties and stability of heaviest elements. *Int. J. Mod. Phys. E* **21**, 1250013 (2012). <https://doi.org/10.1142/S0218301312500139>
60. C.S. Wu, S.A. Moszkowski, Beta decay. **183**(1966)
61. M. A. Preston. Addison-Wesley Publishing Company, Inc., (1962)
62. X. Bao, H. Zhang, G. Royer et al., Spontaneous fission half-lives of heavy and superheavy nuclei within a generalized liquid drop model. *Nucl. Phys. A* **906**, 1–13 (2013). <https://doi.org/10.1016/j.nuclphysa.2013.03.002>
63. J. Randrup, S.E. Larsson, P. Moller et al., Spontaneous-fission half-lives for even nuclei with $Z \geq 92$. *Phys. Rev. C* **13**, 229–239 (1976). <https://doi.org/10.1103/PhysRevC.13.229>
64. N. Wang, M. Liu, X. Wu et al., Surface diffuseness correction in global mass formula. *Phys. Lett. B* **734**, 215–219 (2014). <https://doi.org/10.1016/j.physletb.2014.05.049>
65. M.W. Kirson, Mutual influence of terms in a semi-empirical mass formula. *Nucl. Phys. A* **798**, 29–60 (2008). <https://doi.org/10.1016/j.nuclphysa.2007.10.011>
66. S. Goriely, Further explorations of skyrme-hartree-fock-bogoliubov mass formulas. XV. The spin-orbit coupling. *Nucl. Phys. A* **933**, 68–81 (2015). <https://doi.org/10.1016/j.nuclphysa.2014.09.045>
67. J. Duflo, A. Zuker, Microscopic mass formulas. *Phys. Rev. C* **52**, R23–R27 (1995). <https://doi.org/10.1103/PhysRevC.52.R23>
68. H. Koura, T. Tachibana, M. Uno et al., Nuclidic mass formula on a spherical basis with an improved even-odd term. *Prog. Theor. Phys.* **113**, 305–325 (2005). <https://doi.org/10.1143/PTP.113.305>
69. Reference input parameter library (ripl-3). <https://www-nds.iaea.org/RIPL-3>
70. M. Wang, G. Audi, F.G. Kondev et al., The ame2016 atomic mass evaluation (ii): tables, graphs and references. *Chin. Phys. C*

- 41, 030003 (2017). <https://doi.org/10.1088/1674-1137/41/3/030003>
71. K.P. Santhosh, R.K. Biju, A. Joseph, A semi-empirical model for alpha and cluster radioactivity. *J. Phys. G* **35**, 082102 (2008). <https://doi.org/10.1088/0954-3899/35/8/085102>
72. C. Xu, Z. Ren, Y. Guo, Competition between α decay and spontaneous fission for heavy and superheavy nuclei. *Phys. Rev. C* **78**, 044329 (2008). <https://doi.org/10.1103/PhysRevC.78.044329>
73. J.P. Wieleczko, E. Bonnet, J. Gomez del Campo et al., Influence of the n/z ratio on disintegration modes of compound nuclei. *AIP Conf. Proc.* **1098**, 64–69 (2009). <https://doi.org/10.1063/1.3108862>
74. Y.T. Oganessian, V.K. Utyonkov, Y.V. Lobanov et al., Synthesis of superheavy nuclei in the $^{48}\text{Ca}+^{244}\text{Pu}$ reaction: $^{288}114$. *Phys. Rev. C* **62**, 041604 (2000). <https://doi.org/10.1103/PhysRevC.62.041604>
75. Y.T. Oganessian, V.K. Utyonkov, Y.V. Lobanov et al., Observation of the decay of $^{292}116$. *Phys. Rev. C* **63**, 011301 (2000). <https://doi.org/10.1103/PhysRevC.63.011301>
76. Y.T. Oganessian, V.K. Utyonkov, Y.V. Lobanov et al., Measurements of cross sections for the fusion-evaporation reactions $^{244}\text{Pu}(^{48}\text{Ca}, xn)^{292-x}114$ and $^{245}\text{Cm}(^{48}\text{Ca}, xn)^{293-x}116$. *Phys. Rev. C* **69**, 054607 (2004). <https://doi.org/10.1103/PhysRevC.69.054607>
77. K. Morita, K. Morimoto, D. Kaji et al., Experiment on the synthesis of element 113 in the reaction $^{209}\text{Bi}(^{70}\text{Zn}, n)^{278}113$. *J. Phys. Soc. Jpn.* **73**, 2593–2596 (2004). <https://doi.org/10.1143/JPSJ.73.2593>
78. A. Baran, K. Pomorski, A. Lukasiak et al., A dynamic analysis of spontaneous-fission halfives. *Nucl. Phys. A* **361**, 83–101 (1981). [https://doi.org/10.1016/0375-9474\(81\)90471-1](https://doi.org/10.1016/0375-9474(81)90471-1)
79. Z. Matheson, S.A. Giuliani, W. Nazarewicz et al., Cluster radioactivity of $^{294}_{118}\text{Og}_{176}$. *Phys. Rev. C* **99**, 041304 (2019). <https://doi.org/10.1103/PhysRevC.99.041304>
80. D.N. Poenaru, R.A. Gherghescu, W. Greiner, Heavy-particle radioactivity. *J. Phys. Conf. Ser.* (2013). <https://doi.org/10.1088/1742-6596/436/1/012056>



Cluster Radioactivity in Super-Heavy Nuclei ²⁹⁹⁻³⁰⁶122

H.C. Manjunatha¹ , S. Alfred Cecil Raj² , A.M. Nagaraja^{1,2} and N. Sowmya^{1,3}

¹Department of Physics, Government College for Women, Kolar-563101, Karnataka, India

²Department of Physics, St. Joseph's College, Tiruchirapalli-620002, Tamilnadu, India

³Department of Physics, BMS Institute of Technology and Management, Bengaluru-560064, Karnataka, India

²sac63raj@gmail.com

^{1,2}amnagaraja@yahoo.com

^{1,3}sowmyaprakash8@gmail.com

¹manjunathhc@rediffmail.com (Corresponding Author)

ARTICLE INFORMATION

Received: August 28, 2020

Revised: October 07, 2020

Accepted: October 09, 2020

Published Online: November 09, 2020

Keywords:

Super-heavy Nuclei, Cluster Radioactivity

ABSTRACT

Cluster radioactivity is an intermediate process between alpha decay and spontaneous fission. It is also an exotic decay mode in super-heavy nuclei. When super-heavy nuclei undergo cluster decay, the daughter nuclei is having near or equal to doubly magic nuclei. We have investigated cluster decay of isotopes of He, Li, Be, Ne, N, Mg, Si, P, S, Cl, Ar and Ca in the super-heavy nuclei region ²⁹⁹⁻³⁰⁶122. We have also compared the logarithmic half-lives of cluster decay with that of other models such as Univ [1], NRDX [2], UDL [3] and Horoi [4]. From this study it is concluded that an alpha decay is the dominant decay mode in the superheavy nuclei ²⁹⁹⁻³⁰⁶122.



DOI: 10.15415/jnp.2020.81007

1. Introduction

Super-heavy elements are not natural elements. These super-heavy elements have to be synthesized and their synthesis plays a very dynamic role in the extension of the periodic table. Poenaru et al., [1] plotted single line universal curve both for alpha and cluster radioactivity by plotting the sum of decimal logarithm of the half-life and cluster preformation probability against the decimal logarithmic penetration probability. They considered fission theory for large mass asymmetry based on the quantum mechanical tunnelling process. Ni et al., [2] proposed NRDX formula by considering quantum tunnelling through the potential barrier. The half-lives were evaluated by using the preformation probability, which varies from one decay mode to another but does not significantly change for a given radioactivity. Qi et al., [3] presented universal decay formula by considering microscopic mechanism of the charged-particle emission. The half-lives were evaluated by using Q-values of the outgoing particles as well as the masses and charges of the nuclei involved in the decay. Horoi et al., [4] proposed independent model and analysed the accumulated data by pointing important variables in case of alpha and cluster decay of the even-even heavy nuclei.

Cluster emission, and decay from super-heavy elements leads to cluster radioactivity. Poenaru et al., [5-6] studied branching ratios and half-lives in the super-heavy region. Ismail and Seif [7] studied half-lives of cluster ¹⁴C, ²⁰O, ²⁰Ne and ²⁴Ne in heavy and super-heavy nuclei region. Zang et al., [8] evaluated half-lives of heavy and super-heavy nuclei using WKB approximation. Zhang and Wang [9] studied cluster and alpha decay in the isotopes of super-heavy nuclei ²⁹⁴118, ²⁹⁶120 and ²⁹⁸122. Wang et al., [10] studied preformation probability using generalised liquid drop model. Zagrebaev et al., [11] studied ternary fission in doubly magic nuclei of tin. Ismail et al., [12] studied alpha decay half-lives in the super-heavy nuclei. Shanmugam et al., [13] studied alpha decay chains in the super-heavy region Z=114-116 and 118. Previous workers [14-15] studied alpha decay half-lives of super-heavy region using generalized liquid-drop model (GLDM) and density-dependent cluster model.

Agbemava et al., [16] theoretically studied the properties such as charge radii and neutron skins of the hyperheavy nuclei using density functional theory. Cui et al., [17] studied alpha decay half-lives with in the frame of the effective liquid drop model (ELDM). Previous workers

[18-20] estimated the alpha decay half-lives in the super-heavy region using generalised density dependent model. The alpha decay half-lives of spherical and deformed nuclei for the study of nuclear structure of super-heavy elements was reported by earlier workers [21-22]. Matheson et al., [23] reported dependence of Q value on cluster emissions. Warda et al., [24] predicted a sharp fission fragment mass distribution with the heavy fragment close to ^{208}Pb . Karim and Ahmed [25] investigated alpha decay half-lives in the super-heavy nuclei $Z=120$. Routray et al., [26] evaluated half-lives using WKB integral method in the very heavy nuclei region.

Earlier workers [27-44] studied different decay modes such as spontaneous fission, ternary fission, cluster decay and alpha decay in the heavy and super-heavy region and also predicted suitable projectile-target combinations to synthesize these super-heavy nuclei. Karpeshin [45] has shown that the choice of a specific shape of the proximity potential affects not only the shape of the barrier, but can also change the total kinetic energy of fragments by tens of MeV. From the available literature it is witnessed that the cluster decay plays a very important role in identifying the existence of the super-heavy nuclei.

Extensive theoretical and experimental search for cluster emission from various heavy and super-heavy nuclei ranging from ^{14}C to ^{80}Ge [46-49] have been studied. The present study focus on the cluster decay such as ^4He , ^{22}Ne , ^{26}Mg , $^{28,30}\text{Si}$, ^{34}S , ^{40}Ca and ^{46}Ca which are magic nuclei or near the magic nuclei whose half-lives are maximum. The hypothetical super-heavy nuclei such as $Z=120$, 122, 124 and 126 are most predictable super-heavy nuclei in the island of stability. From the literature [50] it is observed that the super-heavy nuclei $^{299-306}122$ survives fission. In order to check whether, the isotopes of $Z=122$ also survives the cluster decay such as Li, Be, Ne, N, Mg, Si, P, S, Cl, Ar and Ca, we made an attempt to study different cluster decay in the super-heavy nuclei region of $^{299-306}122$ by using proximity potential 2013. The overlap between the two nuclei increases, the proximity potential model becomes more complex due to the nuclear potential interacting within the shorter distance of the nuclear surfaces. Hence in the present work we have used the DFM with the density-dependent nucleon-nucleon interaction and studied nuclear potential with the universal function (Prox13) [51].

The present paper is organised as follows. The Sec II consists of theory for the present model and semi-empirical formulae

2. a. Theory

The total interacting potential is the sum of the coulomb potential and proximity potential and it is studied using the following equation;

$$V(R) = V_N(R) + V_C(R) \quad (1)$$

The interaction with atom is given by

$$V_C(r) = Z_1 Z_2 e^2 \begin{cases} \frac{1}{R} & (R > R_C) \\ \frac{1}{2R_C} \left[3 - \left(\frac{R}{R_C} \right)^2 \right] & (R < R_C) \end{cases} \quad (2)$$

where Z_1 and Z_2 are the atomic number of emitted cluster/alpha particle and daughter nuclei. $R_C = 1.24 \times (R_1 + R_2)$ where R_1 and R_2 are the radii of the emitted alpha/cluster and daughter nuclei respectively. The proximity potential is based on proximity force theorem [52]. The nuclear proximity potential is given by

$$V_p(Z) = 4\pi\gamma\bar{R}\Phi\left(\frac{z}{b}\right) \quad (3)$$

where z is the distance between the near surfaces of the fragments, and b is the nuclear surface thickness ($b=0.99$). where Φ is the universal proximity potential which depends on the minimum separation distance and is independent of geometry and shape of the nuclei. The surface tension co-efficient is given by $\gamma = 1.25284 \left[1 - 2.345 \left(\frac{N-Z}{A} \right)^2 \right]$ MeV/fm². The mean curvature is given by $\bar{R} = C_1 C_2 / C_1 + C_2$ where C_1 and C_2 are the Sussmann's central radius of cluster/alpha nuclei and daughter nuclei respectively. The Sussmann central radii C_1 and C_2 are related to sharp radii R_i and it is expressed as $C_i = R_i - (b^2/R_i)$. The sharp radii R_i is written as $R_i = 1.28A_i^{1/3} - 0.76 + 0.8A_i^{-1/3}$. The proximity function specially defined for cluster/alpha decay is as follows;

$$\Phi(s_0) = \frac{p_1}{1 + \exp\left(\frac{s_0 + p_2}{p_3}\right)} \quad (4)$$

The constants $p_1 = -7.65$, $p_2 = 1.02$ and $p_3 = 0.89$. The S_0 is evaluated from the equation $s_0 = R - R_1 - R_2/b$ where R , R_1 and R_2 are the radii of parent, daughter and emitted cluster. The half-lives of the cluster decay can also be evaluated by using Hill-Wheeler formalism, since the coulomb interaction is not included in the formalism [53] we have evaluated the cluster decay half-lives using WKB integral;

$$P = \exp\left\{-\frac{2}{\hbar} \int_{R_2}^{R_3} \sqrt{2\mu(V_T(r) - Q)} dr\right\} \quad (5)$$

where μ is the reduced mass of the fission fragments. R_a and R_b are the initial and finishing turning points, and it can be evaluated as $V_T(R_a) = Q = V_T(R_b)$. The half-life of the cluster decay is given by

$$T_{1/2} = \frac{\ln 2}{\lambda} = \frac{\ln 2}{vP} \quad (6)$$

where $v = \frac{\omega}{2\pi} = \frac{2E_v}{h}$ represent assaults frequency and λ is the decay constant. E_v is the empirical vibration energy and expressed as;

$$E_v = Q \left\{ 0.056 + 0.039 \exp \left[\frac{4 - A_2}{2.5} \right] \right\} \text{ for } A_2 \geq 4. \quad (7)$$

2. b. Comparison of Prox 13 with the other Models:

i. UNIV Formula: Poenaru et al., [1] derived single line of universal (UNIV) curve for alpha and cluster decay by plotting the sum of the decimal logarithm of the half-life and cluster preformation probability versus the decimal logarithm of the penetrability of external barrier. This formula is referred as UNIV formula it is expressed as,

$$\log T_{1/2}^{UNIV} = -\log P_s - 22.169 + 0.598(A_e - 1) \quad (8)$$

Where $-\log P_s = c_{AZ} \left[\arccos \sqrt{r} - \sqrt{r(1-r)} \right]$ with $c_{AZ} = 0.22873(\mu_A Z_d Z_e R_b)^{1/2}$, $r = R_t/R_b$, $R_b = 1.43998 Z_d Z_e/Q$ and $\mu_A = A_d A_e/A$

ii. NRDX formula: Ni et al., [2] derived semi-empirical formula for alpha and cluster decay half-lives from the WKB barrier penetration probability with certain approximations. The proposed formula is

$$\log T_{1/2}^{NRDX} = a\sqrt{\mu} Z_a Z_d Q^{-1/2} + b\sqrt{\mu} (Z_a Z_d)^{1/2} + c \quad (9)$$

where a, b, and c are fitting coefficients and corresponding values are 6.8, 6.9 and -22.4 respectively. This is referred as NRDX in the present work.

iii. Universal Decay Law (UDL): Qi et al., [3] presented a linear universal decay formula from the microscopic mechanism of the charged-particle emission. It relates the half-lives of monopole radioactive decays with the Q values of the outgoing particles as well as the masses and charges. This formula is used in the calculation of half-lives of alpha decay and cluster decay.

$$\log T_{1/2}^{UDL} = aZ_c Z_d A^{1/2} Q^{-1/2} + b \left(AZ_c Z_d \left[A_d^{1/3} + A_c^{1/3} \right] \right)^{1/2} + c \quad (10)$$

where $A = \sqrt{A_c A_d / (A_c + A_d)}$

where a, b, and c are fitting coefficients and corresponding values are 0.3949, -0.3693 and -23.7615 respectively.

iv. Horoi et al. formula: Horoi et al., [4] proposed scaling law for the decay time of alpha particles and it is generalized for cluster decay. They proposed that $\log T_{1/2}$ depends linearly on the scaling variable $(Z_c Z_d)^{0.6}/Q_c$ and on the square root of the reduced mass of cluster and daughter.

$$\log T_{1/2}^H = \left(a_1 \sqrt{\mu} + b_1 \right) \left[(Z_a Z_d)^y Q^{-1/2} - 7 \right] + \left(a_2 \sqrt{\mu} + b_2 \right) \quad (11)$$

here the fitting constants $a_1=6.8$, $b_1=-7.5$, $a_2=6.9$ and $b_2=-22.4$

3. Results and Discussions

The amount of energy released from the cluster decay such as ${}^4\text{He}$, ${}^6\text{Li}$, ${}^9\text{Be}$, ${}^{12}\text{C}$, ${}^{14}\text{N}$, ${}^{20,22}\text{Ne}$, ${}^{23}\text{N}$, ${}^{24-26}\text{Mg}$, ${}^{28-30}\text{Si}$, ${}^{31}\text{P}$, ${}^{32-34}\text{S}$, ${}^{35}\text{Cl}$, ${}^{36,38,40}\text{Ar}$, and ${}^{40,46}\text{Ca}$ are studied using mass excess values available in the reference [54]. The Figure 1 shows the variation of scattering potential with the mass number of clusters. From the figure it is observed that as the mass number of cluster increases scattering potential also increases. The studied scattering potential of ${}^6\text{Li}$, ${}^9\text{Be}$, ${}^{22}\text{Ne}$, ${}^{26}\text{Mg}$, ${}^{28,30}\text{Si}$, ${}^{34}\text{S}$, and ${}^{40,46}\text{Ca}$ in the isotope of super-heavy element ${}^{299}122$ with the variant of separation distance between the two nuclei is presented in Figure 2. From the figure it has been examined that the driving potential for ${}^{299}122$ varies between 80MeV to 184MeV during the cluster emission of ${}^{22}\text{Ne}$ and ${}^{46}\text{Ca}$ respectively.

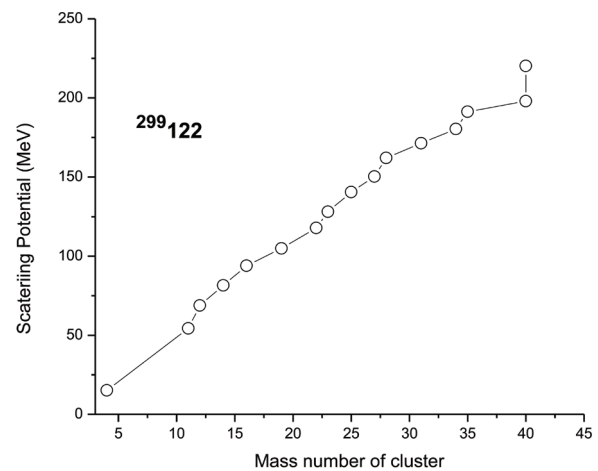


Figure 1: A variation of scattering potential with the mass number of clusters.

In order to show the variation of scattering potential, we have considered negative separation between the two nuclei. For an instance, let us consider the total scattering potential as function of separation distance between the two nuclei is as shown in Figure 3 during an alpha emission from the nuclei $^{299}_{122}$. It is observed that the total scattering potential consists of three classical turning points such as R_1 , R_2 and R_3 . The WKB integral by using equation (5) is evaluated using the first boundary condition i.e $V(R_1)=Q$ is close to origin and second boundary condition $V(R_3)=Q$ which is away from the origin. Hence the total scattering potential helps us to analyse the half-lives. These half-lives are inversely proportional to the penetration probability and it is evaluated using the WKB integral. If the penetration probability is more, then the corresponding half-lives were small.

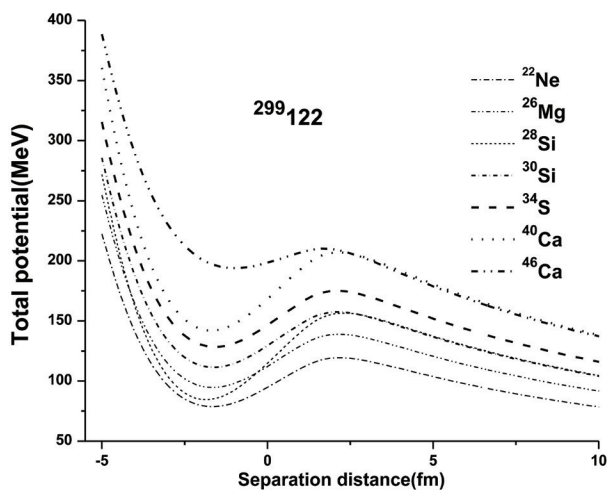


Figure 2: The variation of total potential with the separation distance between the fission fragments in the cluster decay of super-heavy element $^{299}_{122}$.

We have also studied half-lives of different cluster emission using driving potential and penetration probability in the super-heavy nuclei $^{299-306}_{122}$ using the equations (1) to (6). The half-life values of Prox 13 compared with the different models such as Univ [1], NRDX [2], UDL [3] and Horoi [4] Figures 4 shows the variation of logarithmic half-lives of Prox 13 and different models such as Univ, NRDX, UDL Horoi with the mass number of clusters. The half-lives of the cluster emission of ^4He , ^6Li , ^9Be , ^{22}Ne , ^{26}Mg , $^{28,30}\text{Si}$, ^{34}S , and $^{40,46}\text{Ca}$ are calculated for the super-heavy nuclei $^{299-306}_{122}$. Among all the studied clusters, alpha decay has minimum half-lives. Earlier workers [6] have observed unexpected results. They predict that the half-lives of cluster radioactivity (T_c) are

smaller compared to alpha decay half-lives. But the present study contradicts the earlier work. We obtained that $T_\alpha < T_c$ by using available mass excess values [54]. Thus, we took into account that the half-lives are sensitive to the amount of energy released. Half-lives of cluster emission using the Prox 13 is compared with that of the other model such as Univ, NRDX, UDL and Horoi and it is also presented in Table 1. The values obtained using the present model is close to the UNIV model.

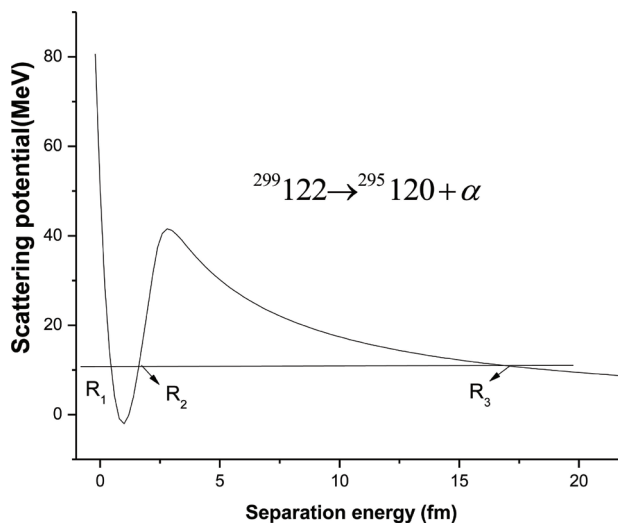


Figure 3: The variation of scattering potential with the separation distance between fission fragments in the alpha-decay of super-heavy element $^{299}_{122}$.

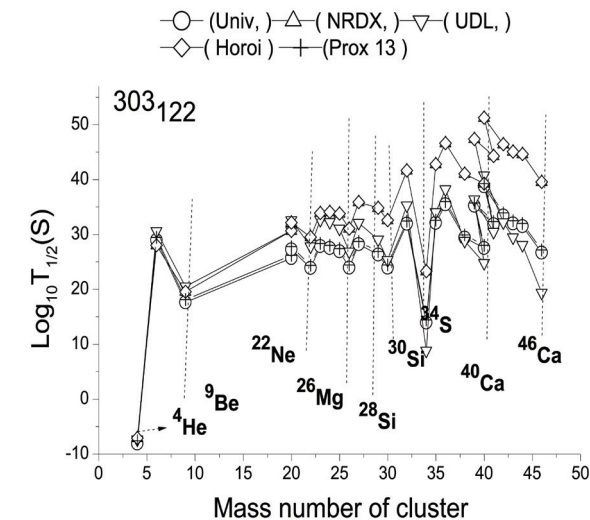


Figure 4: Comparison of logarithmic half-lives of present work with the Univ, NRDX, UDL, Horoi in the super-heavy element $^{303-306}_{122}$.

Table 1: A comparison of different cluster emissions (${}^4\text{He}$, ${}^6\text{Li}$, ${}^9\text{Be}$, ${}^{22}\text{Ne}$, ${}^{26}\text{Mg}$, ${}^{28,30}\text{Si}$, ${}^{34}\text{S}$, and ${}^{40,46}\text{Ca}$) half-lives of Prox 13 with the different models such as, NRDX, UDL, Horoi and Univ.

Parent nuclei	Cluster emission	Half-lives(s)				
		Prox 13	NRDX	UDL	Horoi	UNIV
${}^{299}\text{122}$	${}^4\text{He}$	-5.506	-7.775	-7.542	-5.446	-7.506
	${}^6\text{Li}$	26.793	28.484	25.949	25.529	26.793
	${}^9\text{Be}$	18.149	21.045	19.973	19.973	18.149
	${}^{22}\text{Ne}$	22.501	26.111	27.857	22.801	22.502
	${}^{26}\text{Mg}$	21.535	23.787	28.364	16.167	21.535
	${}^{28}\text{Si}$	12.752	6.983	21.582	9.158	12.752
	${}^{30}\text{Si}$	20.971	21.384	29.267	19.330	20.971
	${}^{34}\text{S}$	23.698	23.083	33.502	24.033	23.698
	${}^{40}\text{Ca}$	25.693	22.161	36.973	24.061	34.660
${}^{300}\text{122}$	${}^4\text{He}$	-5.893	-6.063	-6.009	5.571	-6.893
	${}^6\text{Li}$	36.621	37.901	34.745	35.330	34.621
	${}^9\text{Be}$	22.695	25.668	24.439	24.286	22.695
	${}^{22}\text{Ne}$	23.471	27.281	28.881	13.312	23.471
	${}^{26}\text{Mg}$	22.561	25.097	29.470	16.751	22.561
	${}^{28}\text{Si}$	14.188	9.236	23.334	10.049	14.188
	${}^{30}\text{Si}$	21.820	22.530	30.220	19.856	21.820
	${}^{34}\text{S}$	24.755	24.544	34.670	24.705	24.755
	${}^{40}\text{Ca}$	26.568	23.430	37.989	24.626	36.265
${}^{301}\text{122}$	${}^4\text{He}$	-6.754	-5.914	-5.863	-4.333	-5.625
	${}^6\text{Li}$	31.618	33.130	30.320	30.912	30.504
	${}^9\text{Be}$	19.301	22.230	21.167	20.848	21.410
	${}^{22}\text{Ne}$	24.217	28.176	29.680	30.709	29.939
	${}^{26}\text{Mg}$	23.580	26.387	30.560	28.326	30.770
	${}^{28}\text{Si}$	13.744	22.551	22.913	21.829	22.201
	${}^{30}\text{Si}$	22.938	24.025	31.439	20.531	31.767
	${}^{34}\text{S}$	25.328	25.334	35.340	25.086	35.487
	${}^{40}\text{Ca}$	27.068	24.152	38.607	24.967	38.021
${}^{302}\text{122}$	${}^4\text{He}$	-5.027	-6.199	-6.103	5.507	-6.642
	${}^6\text{Li}$	40.100	41.217	37.879	17.037	37.314
	${}^9\text{Be}$	22.438	25.417	24.258	4.204	24.545
	${}^{22}\text{Ne}$	24.204	28.167	29.733	13.732	29.344
	${}^{26}\text{Mg}$	23.888	26.781	30.940	17.524	30.624
	${}^{28}\text{Si}$	14.723	10.072	24.124	10.442	18.328
	${}^{30}\text{Si}$	23.620	24.934	32.210	20.956	30.384
	${}^{34}\text{S}$	25.799	25.980	35.904	25.408	34.780
	${}^{40}\text{Ca}$	27.476	24.742	39.134	25.255	37.334
${}^{46}\text{Ca}$	26.690	19.394	39.461	23.766	37.689	

$^{303}122$	^4He	-5.618	-7.117	-7.355	-7.117	-8.251
	^6Li	29.446	27.979	30.572	27.979	27.765
	^9Be	18.090	19.556	20.489	19.556	17.897
	^{22}Ne	24.382	29.483	27.789	29.330	23.882
	^{26}Mg	28.013	34.076	32.236	32.544	27.515
	^{28}Si	24.435	31.061	26.845	30.498	23.934
	^{30}Si	26.834	34.834	29.053	31.765	26.334
	^{34}S	24.407	32.581	25.318	30.682	23.907
	^{40}Ca	40.408	23.279	28.816	23.415	28.908
	^{46}Ca	27.986	39.246	24.764	39.753	27.486
$^{304}122$	^4He	-5.804	-7.279	-7.551	-7.203	-8.305
	^6Li	33.350	31.493	34.318	31.708	32.850
	^9Be	20.497	21.950	22.952	20.840	19.997
	^{22}Ne	23.768	28.944	27.061	25.582	23.267
	^{26}Mg	27.885	34.021	32.083	33.705	27.384
	^{28}Si	24.207	30.908	26.567	29.342	23.707
	^{30}Si	28.346	36.382	30.989	35.634	27.847
	^{34}S	24.455	32.710	25.387	31.636	23.954
	^{40}Ca	15.253	24.334	20.127	24.957	14.754
	^{46}Ca	28.212	29.579	25.093	29.433	27.712
$^{305}122$	^4He	-5.004	-7.453	-7.762	-7.124	-8.504
	^6Li	26.685	25.550	27.920	25.911	26.185
	^9Be	16.049	17.606	18.396	17.497	15.548
	^{22}Ne	23.176	28.423	26.356	28.665	22.676
	^{26}Mg	27.553	33.780	31.691	32.389	27.053
	^{28}Si	24.013	30.788	26.328	30.584	23.512
	^{30}Si	27.158	35.312	29.483	35.061	26.660
	^{34}S	24.617	32.954	25.609	31.408	24.117
	^{40}Ca	14.567	23.637	19.072	23.435	14.068
	^{46}Ca	28.260	39.730	25.170	35.483	27.761
$^{306}122$	^4He	-5.003	-7.439	-7.759	-7.397	-8.503
	^6Li	31.941	30.286	32.979	31.305	31.441
	^9Be	17.732	19.305	20.134	19.489	17.233
	^{22}Ne	22.360	27.679	25.380	27.817	21.860
	^{26}Mg	26.572	32.918	30.507	32.648	26.072
	^{28}Si	23.595	30.447	25.810	30.502	23.093
	^{30}Si	28.236	36.435	30.860	36.634	27.735
	^{34}S	24.494	32.914	25.453	32.788	23.994
	^{40}Ca	15.290	24.551	10.193	24.450	14.790
	^{46}Ca	28.130	39.698	24.993	39.100	27.631

Conclusions

We have studied driving potential, amount of energy released, penetration probability and half-lives for the super-heavy nuclei $^{299-306}122$. We have also compared Prox 13 results with the Univ, NRDX, UDL and Horoi. The cluster emission of ^4He , ^6Li , ^9Be , ^{22}Ne , ^{26}Mg , $^{28,30}\text{Si}$, ^{34}S , and $^{40,46}\text{Ca}$ in super-heavy nuclei $^{299-306}122$, it is evident that the cluster radioactivity is possible only when a daughter or cluster nuclei are nearly magic or doubly magic nuclei. In the present work, it is observed that the alpha decay is the dominant decay mode in the super-heavy nuclei $^{299-306}122$.

References

- [1] D.N. Poenaru, R.A. Gherghescu and W. Greiner, Phys. Rev. C **83**, 014601 (2011). <https://doi.org/10.1103/PhysRevC.83.014601>
- [2] D. Ni, Z. Ren, T. Dong and C. Xu, Phys. Rev. C **78**, 044310 (2008). <https://doi.org/10.1103/PhysRevC.78.044310>
- [3] C. Qi, F.R. Xu, R.J. Liotta and R. Wyss, Phys. Rev. Lett. **103**, 072501 (2009). <https://doi.org/10.1103/PhysRevLett.103.072501>
- [4] M. Horoi, J. Phys. G: Nucl. Part. Phys. **30**, 945 (2004). <https://doi.org/10.1088/0954-3899/30/7/010>
- [5] D.N. Poenaru, R.A. Gherghescu and W. Greiner, Phys. Rev. Lett. **107**, 062503 (2011). <https://doi.org/10.1103/PhysRevLett.107.062503>
- [6] D.N. Poenaru, R.A. Gherghescu and W. Greiner, Phys. Rev. C **85**, 034615 (2012). <https://doi.org/10.1103/PhysRevC.85.034615>
- [7] M. Ismail, W.M. Seif and A. Abdurrahman, Phys. Rev. C **94**, 024316 (2016). <https://doi.org/10.1103/PhysRevC.94.024316>
- [8] G.L. Zhang, X.Y. Le and H.Q. Zhang, Phys. Rev. C **80**, 064325 (2009). <https://doi.org/10.1103/PhysRevC.80.064325>
- [9] Y.L. Zhang and Y.Z. Wang, Phys. Rev. C **97**, 014318 (2018). <https://doi.org/10.1103/PhysRevC.97.014318>
- [10] Y.Z. Wang, J.Z. Gu and Z.Y. Hou, Phys. Rev. C **89**, 047301 (2014). <https://doi.org/10.1103/PhysRevC.89.047301>
- [11] V.I. Zagrebaev, A.V. Karpov and W. Greiner, Phys. Rev. C **81**, 044608 (2010). <https://doi.org/10.1103/PhysRevC.81.044608>
- [12] M. Ismail, A.Y. Ellithi, M.M. Botros and A. Adel, Phys. Rev. C **81**, 024602 (2010). <https://doi.org/10.1103/PhysRevC.81.024602>
- [13] G. Shanmugam, S. Sudhakar and S. Niranjani, Phys. Rev. C **72**, 034310 (2005). <https://doi.org/10.1103/PhysRevC.72.034310>
- [14] H.F. Zhang, G. Royer and J.Q. Li, Phys. Rev. C **84**, 027303 (2011). <https://doi.org/10.1103/PhysRevC.84.027303>
- [15] Y. Qian and Z. Ren, Phys. Rev. C **85**, 027306 (2012). <https://doi.org/10.1103/PhysRevC.85.027306>
- [16] S.E. Agbemava, A.V. Afanasjev, A. Taninah and A. Gyawali, Phys. Rev. C **99**, 034316 (2019). <https://doi.org/10.1103/PhysRevC.99.034316>
- [17] J.P. Cui, Y.L. Zhang, S. Zhang and Y.Z. Wang, Phys. Rev. C **97**, 014316 (2018). <https://doi.org/10.1103/PhysRevC.97.014316>
- [18] D. Ni and Z. Ren, Nuclear Physics A **893**, 13 (2012). <https://doi.org/10.1016/j.nuclphysa.2012.08.006>
- [19] J. Dong, W. Zuo and W. Scheid, Nuclear Physics A **861**, 1 (2011). <https://doi.org/10.1016/j.nuclphysa.2011.06.016>
- [20] C. Samanta P.R. Chowdhury and D.N. Basu, Nuclear Physics A **789**, 142 (2007). <https://doi.org/10.1016/j.nuclphysa.2007.04.001>
- [21] D. Ni and Z. Ren, Annals of Physics **358**, 108 (2015).
- [22] A.I. Budaca, R. Budaca and I. Silisteanu, Nuclear Physics A **951**, 60 (2016). <https://doi.org/10.1016/j.nuclphysa.2016.03.048>
- [23] Z. Matheson, S.A. Giuliani, W. Nazarewicz, J. Sadhukhan and N. Schunck, Phys. Rev. C **99**, 041304(R) (2019). <https://doi.org/10.1103/PhysRevC.99.041304>
- [24] M. Warda, A. Zdeb and L.M. Robledo, Phys. Rev. C **98**, 041602(R) (2018). <https://doi.org/10.1103/PhysRevC.98.041602>
- [25] A. Karim and S. Ahmad, Chinese Journal of Physics **59**, 606 (2019). <https://doi.org/10.1016/j.cjph.2019.04.014>
- [26] T.R. Routray J. Nayak and D.N. Basu, Nuclear Physics A **826**, 223 (2009). <https://doi.org/10.1016/j.nuclphysa.2009.06.018>
- [27] H.C. Manjunatha, Nuclear Physics A, **945**, 42 (2016). <https://doi.org/10.1016/j.nuclphysa.2015.09.014>
- [28] H.C. Manjunatha and N. Sowmya, Nuclear Physics A **969**, 68 (2018). <https://doi.org/10.1016/j.nuclphysa.2017.09.008>
- [29] H.C. Manjunatha, K.N. Sridhar and N. Sowmya, Nuclear Physics A **987**, 382 (2019). <https://doi.org/10.1016/j.nuclphysa.2019.05.006>
- [30] M.G. Srinivas, H.C. Manjunatha, K.N. Sridhar and N. Sowmya and A.C. Raj, Nuclear Physics A

- 995**, 121689 (2020). <https://doi.org/10.1016/j.nuclphysa.2019.121689>
- [31] H.C. Manjunatha and N. Sowmya, International Journal of Modern Physics E **27**, 1850041 (2018). <https://doi.org/10.1142/S0218301318500416>
- [32] H.C. Manjunatha, K.N. Sridhar and N. Sowmya, Phys. Rev. C **98**, 024308 (2018). <https://doi.org/10.1103/PhysRevC.98.024308>
- [33] K.N. Sridhar, H.C. Manjunatha and H.B. Ramalingam, Phys. Rev. C **98**, 064605 (2018). <https://doi.org/10.1103/PhysRevC.98.064605>
- [34] H.C. Manjunatha, K.N. Sridhar and N. Sowmya, Nuclear Physics A **987**, 382 (2019). <https://doi.org/10.1016/j.nuclphysa.2019.05.006>
- [35] N. Sowmya and H.C. Manjunatha, Bulg. J. Phys. **46**, 16 (2019).
- [36] H.C. Manjunatha, International Journal of Modern Physics E **25**, 1650074 (2016). <https://doi.org/10.1142/S0218301316500749>
- [37] H.C. Manjunatha, N. Sowmya, K.N. Sridhar and L. Seenappa, Journal of Radioanalytical and Nuclear Chemistry **314**, 991 (2017). <https://doi.org/10.1007/s10967-017-5450-4>
- [38] H.C. Manjunatha and N. Sowmya, International Journal of Modern Physics E **27**, 1850041 (2018). <https://doi.org/10.1142/S0218301318500416>
- [39] N. Sowmya and H.C. Manjunatha, Brazillian Journal of Physics **49**, 874 (2019). <https://doi.org/10.1007/s13538-019-00710-4>
- [40] N. Sowmya and H.C. Manjunatha, Physics of Particles and Nuclei Letters **17**, 370 (2020). <https://doi.org/10.1134/S1547477120030140>
- [41] H.C. Manjunatha and K.N. Sridhar, Eur. Phys. J. A **53**, 156 (2017). <https://doi.org/10.1140/epja/i2017-12337-y>
- [42] N. Sowmya, H.C. Manjunatha, N. Dhananjaya and A.M. Nagaraja, Journal of Radioanalytical and Nuclear Chemistry **323**, 1347 (2020). <https://doi.org/10.1007/s10967-019-06706-3>
- [43] G.R. Sridhar, H.C. Manjunatha, N. Sowmya, P.S.D. Gupta and H.B. Ramalingam, The European Physical Journal Plus **135**, 291 (2020). <https://doi.org/10.1140/epjp/s13360-020-00302-1>
- [44] N. Sowmya and H.C. Manjunatha, Proceedings of the DAE Symp. on Nucl. Phys. **63**, 200 (2018).
- [45] F.F. Karpeshin, <https://arxiv.org/pdf/1904.10598.pdf>
- [46] R.K. Gupta, Clusters in Nuclei. Lecture Notes in Physics (Springer, Berlin, Heidelberg, 2010) Vol. 818, p. 223 (2010), *Collective Clusterization in Nuclei and Excited Compound Systems: The Dynamical Cluster-Decay Model*; Beck C. (eds). https://doi.org/10.1007/978-3-642-13899-7_6
- [47] R. Bonetti, A. Guglielmetti, Rom. Rep. Phys. **59**, 301 (2007).
- [48] K.P. Santhosh and B. Priyanka, Nucl Phys A **929**, 20 (2014). <https://doi.org/10.1016/j.nuclphysa.2014.05.015>
- [49] G. Sawhney, A. Kaur, M.K. Sharma and R.K. Gupta, Phy Rev C **92**, 064303 (2015). <https://doi.org/10.1103/PhysRevC.92.064303>
- [50] H.C. Manjunatha, International Journal of Modern Physics E **25**, 1650100 (2016). <https://doi.org/10.1142/S0218301316501007>
- [51] G.L. Zhang, H.B. Zheng and W.W. Qu, Eur. Phys. Jour. A **49**, 10 (2013). <https://doi.org/10.1140/epja/i2013-13010-3>
- [52] J. Blocki and W.J. Swiatecki, Ann. Phys. **132**, 53 (1981). [https://doi.org/10.1016/0003-4916\(81\)90268-2](https://doi.org/10.1016/0003-4916(81)90268-2)
- [53] N.B. de Takacsy Phys. Rev. C **5**, 1883 (1972). <https://doi.org/10.1103/PhysRevC.5.1883>
- [54] P. Möller, A.J. Sierk, T. Ichikawa and H. Sagawa, At. Dat. Nucl. Dat. Tables **109**, 1 (2016). <https://doi.org/10.1016/j.adt.2015.10.002>



Journal of Nuclear Physics, Material Sciences, Radiation and Applications

Chitkara University, Saraswati Kendra, SCO 160-161, Sector 9-C,
Chandigarh, 160009, India

Volume 8, Issue 1

August 2020

ISSN 2321-8649

Copyright: [© 2020 H.C. Manjunatha et al.] This is an Open Access article published in Journal of Nuclear Physics, Material Sciences, Radiation and Applications (J. Nucl. Phy. Mat. Sci. Rad. A.) by Chitkara University Publications. It is published with a Creative Commons Attribution- CC-BY 4.0 International License. This license permits unrestricted use, distribution, and reproduction in any medium, provided the original author and source are credited.



Cluster radioactivity in superheavy nuclei $^{299-302}120$

Nagaraja A M^{a,b}, H C Manjunatha^{a*}, N Sowmya^{a,c} & S Alfred Cecil Raj^b

^aDepartment of Physics, Government College for Women, Kolar 563 101, India

^bDepartment of Physics, St. Joseph's College, Tiruchirappalli 620 002, India

^cDepartment of Physics, BMSIT, Bangalore 560 064, India

Received 17 February 2020

The cluster radioactivity is an unusual decay process observed in superheavy nuclei. When a cluster nuclei are emitted, the residual or daughter nuclei is having doubly magic nuclei or it may be neighbourhood of the same. We have studied cluster radioactivity [^4He , ^6Li , ^9Be , $^{20,22}\text{Ne}$, ^{23}N , $^{24-26}\text{Mg}$, $^{28-30}\text{Si}$, ^{31}P , $^{32-34}\text{S}$, ^{35}Cl , $^{36,38,40}\text{Ar}$, $^{40-46}\text{Ca}$] in the superheavy nuclei $^{299-302}120$ using the nuclear and proximity model. The calculated cluster decay half-lives are compared with that of the other theoretical models such as Univ¹, NRDX², UDL³ and Horoi⁴. From the comparison of different models we have observed that the cluster nuclei with ^4He , ^9Be , ^{22}Ne , ^{26}Mg , ^{30}Si , ^{34}S , ^{40}Ca and ^{46}Ca are having smaller logarithmic half-lives than the exotic cluster decay modes.

Keywords: Superheavy nuclei, Cluster radioactivity, Exotic cluster decay, Proximity model

1 Introduction

The cluster radioactivity is the process in which heavy nuclei disintegrates into asymmetric combination of fission fragments. It is the process in which it emits light nuclei from the parent nuclei. The cluster radioactivity has been the curiosity of the present consequences. The cluster radioactivity was observed during the year 1984⁵⁻⁷. Only few papers are available on both theoretical and experimental aspects of cluster radioactivity. Experiment⁸⁻¹⁴ becomes crucial in discriminating different theoretical models of cluster radioactivity. The cluster decay is the intermediate of alpha and spontaneous fission. Recent discovery of superheavy elements play a very important role in the material world. The different decay modes of superheavy elements are found in experimental and theoretical works on cluster radioactivity. Ni and Ren² studied alpha decay rates and Xu and Ren³ studied alpha decay using Density-dependent cluster model. Using quantum scattering process Sahu *et al.*¹⁵ developed general decay formula for cluster radioactivity. Cui *et al.*¹⁶ employed alpha decay half-lives from the study of different models in the heavy and superheavy region $Z=80-118$. Santhosh and Priyanka¹⁷ studied competition between spontaneous fission and alpha decay in the superheavy region $Z=99-129$. Using generalized

density-dependent cluster model, Qian and Ren¹⁸ studied half-lives in the superheavy region. Zhang and Wang¹⁹ used unified description formula to study cluster radioactivity in superheavy region $Z \geq 118$. Previous workers²⁰⁻²⁴ studied exotic cluster decay in heavy and superheavy nuclei.

Using cluster preformation law, Wei and Zhang²⁵ investigated cluster radioactivity in the heavy and superheavy region. Poenaru *et al.*²⁶ studied branching ratios with respect to alpha decay half-lives in the superheavy region. Dong *et al.*²⁷ were studied alpha decay half-lives of superheavy nuclei using two potential approach. Previous workers²⁸⁻³⁰ studied the decay properties and half-lives of the different decay modes in the superheavy region $Z=121$ and 125 . Using liquid drop model Wang *et al.*³¹ studied alpha decay and proton decay half-lives in neutron deficient nuclei. Earlier workers³²⁻⁴⁰ studied different decay modes and the projectile-target combinations to synthesis the superheavy element. Hence, the purpose of our work is to identify cluster radioactivity [^4He , ^6Li , ^9Be , $^{20,22}\text{Ne}$, ^{23}N , $^{24-26}\text{Mg}$, $^{28-30}\text{Si}$, ^{31}P , $^{32-34}\text{S}$, ^{35}Cl , $^{36,38,40}\text{Ar}$, $^{40-46}\text{Ca}$] in the superheavy nuclei $^{299-302}120$. At the end we have compared our work with the Univ, NRDX, UDL and Horoi.

2 Theoretical Framework

The cluster radioactivity is the fission like process in which parent nuclei split into a daughter nuclei and

*Corresponding author: (E-mail: manjunathhc@rediffmail.com)

a fragment nucleus. For a spherical daughter nuclei and fragment nuclei, the total potential is written as:

$$V(r) = V_n(r) + \frac{Z_1 Z_2 e^2}{r} + \frac{\ell(\ell+1)\hbar^2}{2\mu r^2} \quad \dots (1)$$

The nuclear interaction between the two spherical nuclei is given by:

$$V_n(r) = 4\pi\gamma b \frac{C_1 C_2}{C_1 + C_2} \phi(\varepsilon) \quad \dots (2)$$

here b is the nuclear surface width ≈ 1 fm, C_i is the central radii of a nuclei, $\phi(\varepsilon)$ is the universal function⁴⁰ Which depends on $\varepsilon = (r - C_1 - C_2)/b$ and γ is the nuclear surface tension and given by

$$\gamma = \gamma_0 \left[1 - k(N - Z)^2 / A^2 \right] \text{MeV/fm}^2 \quad \dots (3)$$

where N is the neutron number, Z is the charge number and A is the mass number of parent nuclei. The $\gamma_0 = 0.9517$ and $k = 1.7826$ ⁴¹. The central radii in terms of sharp radius is given as:

$$C_i = R_i - \frac{b^2}{R_i} \text{fm} \quad \dots (4)$$

and the sharp radii is expressed as

$$R_i = 1.28A_i^{1/3} - 0.76 + 0.8A_i^{-1/3} \quad \dots (5)$$

For cluster radioactivity, the barrier penetrability P is evaluated numerically and analytically and it is expressed as:

$$P = \exp \left\{ -\frac{2}{\hbar} \int_a^b \sqrt{2\mu(V-Q)} dz \right\} \quad \dots (6)$$

where reduced mass $\mu = \frac{A_1 A_2}{A_1 + A_2}$, where A_1 , and A_2

are masses of daughter and emitted cluster, respectively. The turning points a and b are studied using the following condition $V(a) = Q$ and $V(b) = 0$. The half-life of cluster radioactivity is given by:

$$T_{1/2} = \frac{\ln 2}{\lambda} = \frac{\ln 2}{\nu P} \quad \dots (7)$$

where $\nu = \frac{\omega}{2\pi} = \frac{2E_v}{h}$, ν is the assault frequency

and λ is the decay constant. The empirical vibration energy is expressed as:

$$E_v = Q \left\{ 0.056 + 0.039 \exp \left[\frac{4 - A_2}{2.5} \right] \right\} \text{ for } A_2 \geq 4 \quad \dots (8)$$

3 Results and Discussion

The amount of energy released during the cluster radioactivity is studied using the following equation;

$$Q = \Delta M(A, Z) - \Delta M(A_d, Z_d) - \Delta M(A_c, Z_c) \quad \dots (9)$$

where $\Delta M(A, Z)$ is the mass excess of the parent, $\Delta M(A_d, Z_d)$ is the mass excess of daughter nuclei and $\Delta M(A_c, Z_c)$ is the mass excess of cluster nuclei.

In the work, we have used both experimental and theoretical mass excess values available in the literature⁴²⁻⁴⁶. The amount of energy released during the emission of clusters such as ⁴He, ⁶Li, ⁹Be, ^{20,22}Ne, ²³N, ²⁴⁻²⁶Mg, ²⁸⁻³⁰Si, ³¹P, ³²⁻³⁴S, ³⁵Cl, ^{36,38,40}Ar, and ⁴⁰⁻⁴⁶Ca are plotted as function of mass number of clusters and depicted in Fig. 1. The variation of amount of energy released during cluster radioactivity with the neutron number of cluster is as shown in Fig. 2. From the Figs 1 and 2 it is observed that as the mass number of cluster/neutron number of cluster increases the amount of energy released also increases. It is observed from the two figures that the amount of energy released is higher for ⁴⁰Ca [$Z=20$, $N=20$], which may be due to the presence of magic nuclei. We have studied half-lives for different cluster emission such as ⁴He, ⁶Li, ⁹Be, ^{20,22}Ne, ²³N, ²⁴⁻²⁶Mg, ²⁸⁻³⁰Si, ³¹P, ³²⁻³⁴S, ³⁵Cl, ^{36,38,40}Ar, and ⁴⁰⁻⁴⁶Ca in the isotopes of ²⁹⁹⁻³⁰²120 as explained in detail in the theoretical frame work. The studied half-lives of different cluster emission with the neutron mass number is presented in Fig. 3. In the present graph, we observed smaller half-lives for the neutron number 2, 5, 12, 14, 16, 18, 20 and 26, which are near or equal to magic number of the nuclei.

We have also studied the logarithmic half-lives of different models such as Univ, NRDX, UDL, Horoi. Figure 4 describes the variation of logarithmic half-lives of different models such as Univ, NRDX, UDL, Horoi and present work with the mass number of cluster in the superheavy region ²⁹⁹⁻³⁰²120 and it is

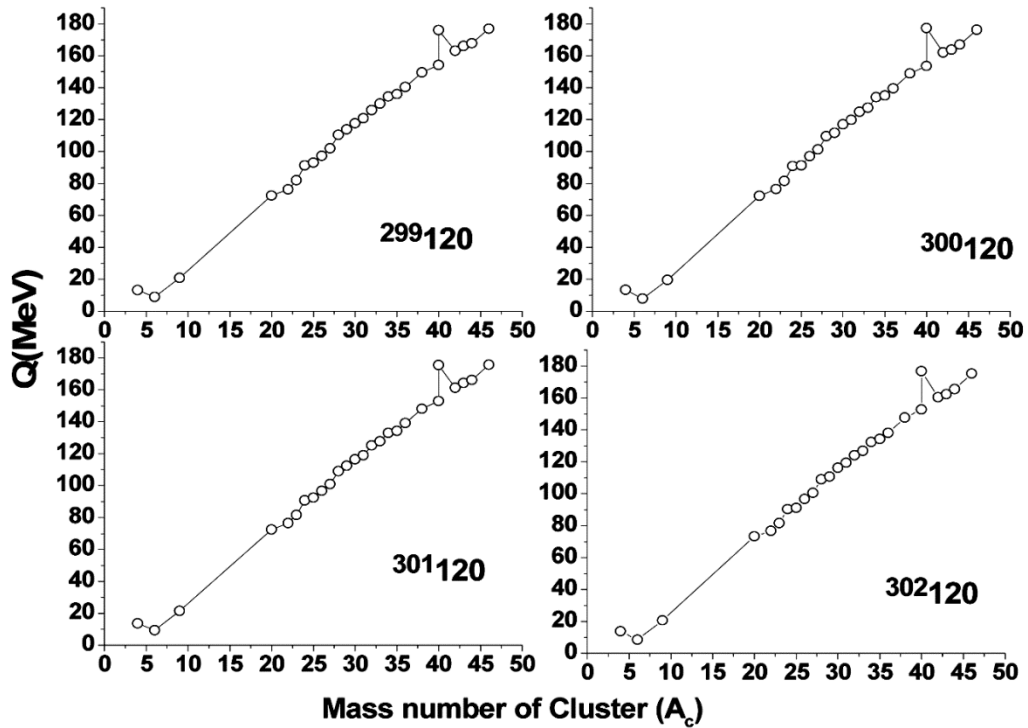


Fig. 1 – Variation of amount of energy released during cluster radioactivity with mass number of cluster (A_c) for the isotopes of superheavy nuclei $^{299-302}_{120}$

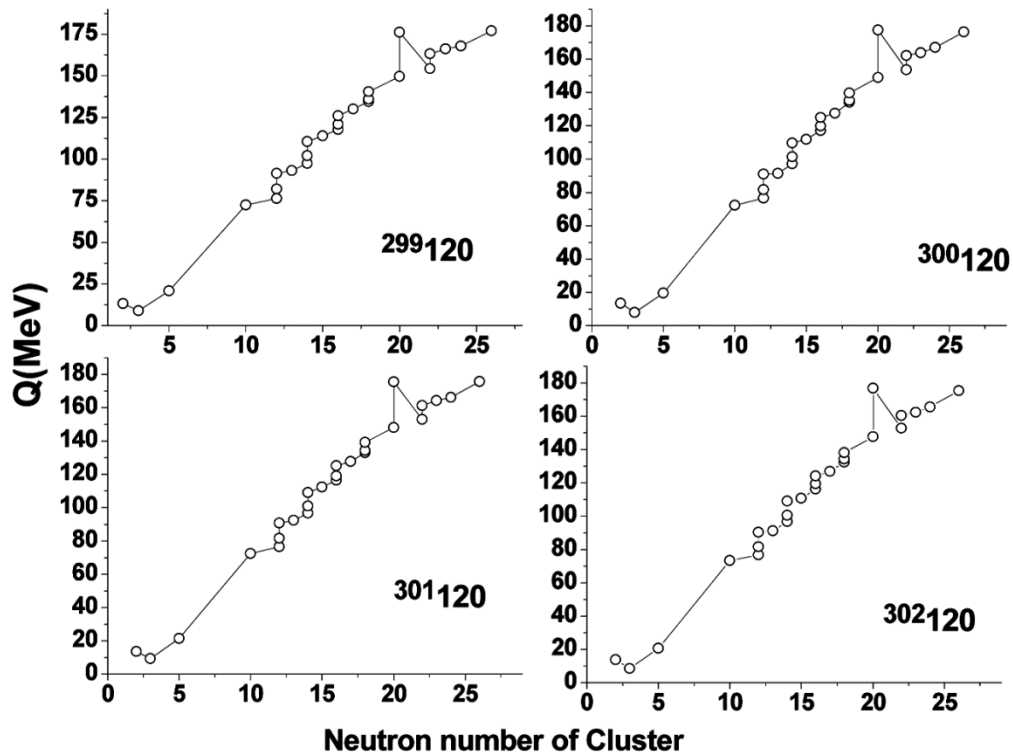


Fig. 2 – A Variation of amount of energy released during cluster radioactivity with the neutron number of cluster for the isotopes of superheavy nuclei $^{299-302}_{120}$.

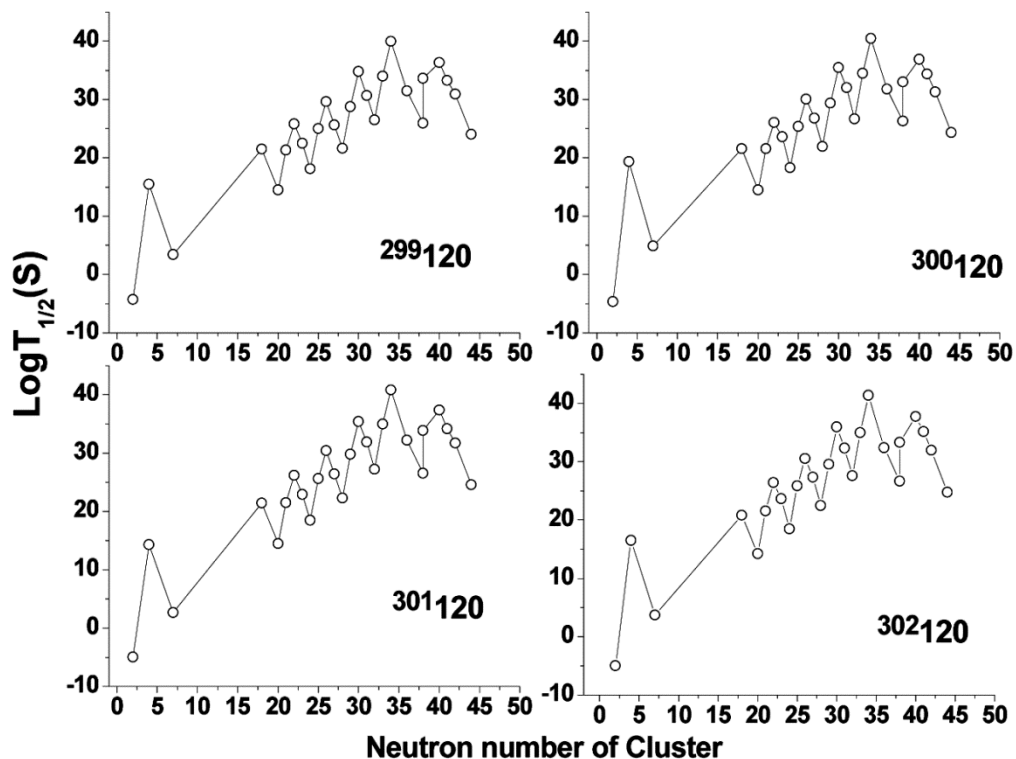


Fig 3 – A variation of logarithmic half-lives of cluster radioactivity with the neutron number of cluster for the isotopes of superheavy nuclei $^{299-302}_{120}$.

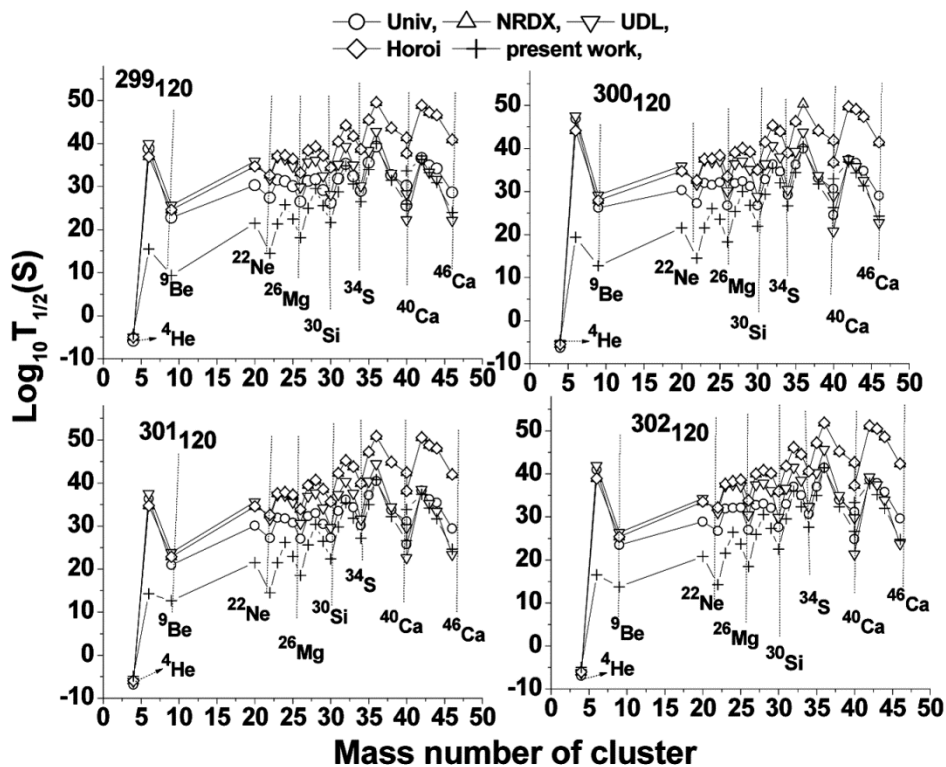


Fig. 4 – A comparison of logarithmic half-lives of different decay modes such as Univ, NRDX, UDL, Horoi and present work with the mass number of cluster for the isotopes of superheavy nuclei $^{299-302}_{120}$.

presented in Fig. 4. From the figure we observed that the logarithmic half-lives of cluster emission such as ⁴He, ⁹Be, ²²Ne, ²⁶Mg, ³⁰Si, ³⁴S, ⁴⁰Ca and ⁴⁶Ca are

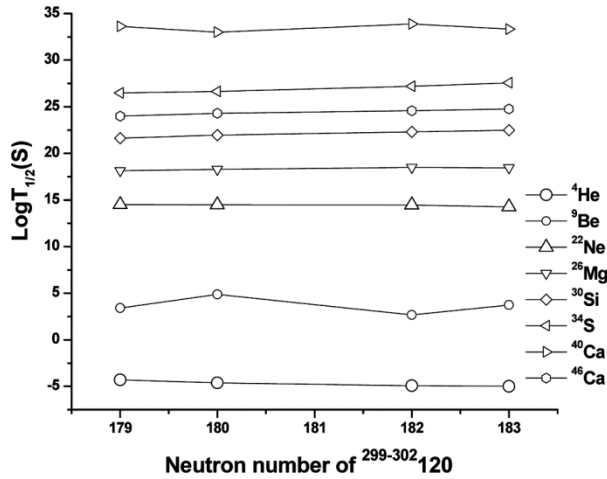


Fig. 5 – The variation of logarithmic half-lives of different clusters as a function of neutron number for the isotopes of superheavy nuclei ²⁹⁹⁻³⁰²120.

Table 1 – Tabulation of logarithmic half-lives of different cluster emission in the isotopes of superheavy nuclei ²⁹⁹⁻³⁰²120.

Cluster emission	Log T _{1/2} (S)			
	²⁹⁹ 120	³⁰⁰ 120	³⁰¹ 120	³⁰² 120
⁴ He	-4.303	-4.633	-4.931	-4.985
⁶ Li	15.496	19.367	14.292	16.545
⁹ Be	3.398	4.871	2.662	3.736
²⁰ Ne	21.509	21.544	21.453	20.840
²² Ne	14.507	14.474	14.467	14.243
²³ N	21.301	21.532	21.525	21.555
²⁴ Mg	25.834	26.058	26.195	26.404
²⁵ Mg	22.472	23.574	22.918	23.663
²⁶ Mg	18.144	18.279	18.493	18.454
²⁸ Si	25.004	25.391	25.622	25.888
²⁹ Si	29.590	30.033	30.400	30.519
³⁰ Si	25.630	26.806	26.429	27.341
³¹ P	21.630	21.960	22.315	22.485
³² S	28.785	29.370	29.812	29.550
³³ S	34.816	35.482	35.392	35.948
³⁴ S	30.652	32.019	31.870	32.339
³⁵ Cl	26.475	26.649	27.198	27.570
³⁶ Ar	33.982	34.449	34.994	34.966
³⁸ Ar	39.980	40.465	40.788	41.397
⁴⁰ Ar	31.475	31.788	32.185	32.402
⁴⁰ Ca	25.957	26.271	26.573	26.669
⁴² Ca	33.634	32.999	33.887	33.332
⁴³ Ca	36.351	36.862	37.389	37.747
⁴⁴ Ca	33.247	34.351	34.154	35.156
⁴⁵ Ca	30.887	31.291	31.696	31.978
⁴⁶ Ca	24.002	24.308	24.582	24.770

having smaller half-lives compared to other cluster emission in the isotopes of superheavy nuclei ²⁹⁹⁻³⁰²120. From this study, it is found that the cluster decay half-lives are smaller for the cluster nuclei whose mass number or neutron numbers are nearer/equal to magic number. We have also studied the variation of logarithmic half-lives of cluster emission with the neutron number and we presented the same in Fig. 5. From the figure we have observed that as the mass number of cluster increases, the logarithmic half-life increases with the increase in neutron number. We have tabulated corresponding values of logarithmic half-lives and amount of energy released in the isotopes of superheavy nuclei ²⁹⁹⁻³⁰²120 are tabulated in Tables 1 and 2. From the tables and graphs, it is found that alpha decay (⁴He) is having smaller half-lives compared to other cluster decay mode.

Table 2 – The tabulation of amount of energy released during different cluster emission in the isotopes of superheavy nuclei ²⁹⁹⁻³⁰²120.

Cluster emission	Q(MeV)			
	²⁹⁹ 120	³⁰⁰ 120	³⁰¹ 120	³⁰² 120
⁴ He	13.105	13.395	13.665	13.715
⁶ Li	8.923	7.823	9.313	8.603
⁹ Be	20.792	19.612	21.422	20.512
²⁰ Ne	72.384	72.334	72.463	73.342
²² Ne	76.361	76.415	76.427	76.797
²³ N	82.049	81.692	81.703	81.657
²⁴ Mg	91.301	90.951	90.738	90.414
²⁵ Mg	93.188	91.38	92.45	91.237
²⁶ Mg	97.276	97.03	96.642	96.712
²⁸ Si	101.941	101.284	100.895	100.449
²⁹ Si	110.484	109.735	109.122	108.923
³⁰ Si	113.815	111.706	112.377	110.764
³¹ P	117.819	117.173	116.484	116.155
³² S	120.91	119.853	119.064	119.531
³³ S	126.132	124.982	125.136	124.186
³⁴ S	130.03	127.522	127.792	126.946
³⁵ Cl	134.543	134.196	133.108	132.378
³⁶ Ar	136.108	135.251	134.262	134.314
³⁸ Ar	140.573	139.723	139.162	138.112
⁴⁰ Ar	149.531	148.904	148.116	147.686
⁴⁰ Ca	154.251	153.569	152.916	152.709
⁴² Ca	176.112	177.492	175.566	176.766
⁴³ Ca	163.278	162.261	161.223	160.523
⁴⁴ Ca	166.243	163.96	164.363	162.325
⁴⁵ Ca	167.93	167.063	166.2	165.603
⁴⁶ Ca	177.105	176.371	175.716	175.269

4 Conclusions

In summary, we have carried out the study of cluster radioactivity in the isotopes of superheavy nuclei $^{299-302}120$. We have studied logarithmic half-lives for the ground-to ground transitions in the emission of clusters such as ^4He , ^6Li , ^9Be , $^{20,22}\text{Ne}$, ^{23}N , $^{24-26}\text{Mg}$, $^{28-30}\text{Si}$, ^{31}P , $^{32-34}\text{S}$, ^{35}Cl , $^{36,38,40}\text{Ar}$, $^{40-46}\text{Ca}$. We have studied the amount of energy released and logarithmic half-lives in the super-heavy nuclei $^{299-302}120$. From this study, it is found that the cluster radioactivity half-lives are smaller for the cluster nuclei whose atomic or neutron number are nearer/equal to magic number. The present results are in good agreement with the other models such as Univ, NRDx, UDL and Horoi. From the outcomes of the present work, it emphasizes on the dependence of logarithmic half-lives and Q-values near or equal to the magic number. Hence, the superheavy nuclei $^{299-302}120$ are stable against the cluster decay and the dominant decay mode is ^4He (alpha decay). The present study on the superheavy nuclei $^{299-302}120$ finds an important role in the future experiments.

References

- 1 Poenaru D N, Gherghescu R A & Greiner W, *Phys Rev C*, 83 (2011) 014601.
- 2 Ni D, Ren Z, Dong T & Xu C, *Phys Rev C*, 78 (2008) 044310.
- 3 Qi C, Xu F R, Liotta R J & Wyss R, *Phys Rev Lett*, 103 (2009) 072501.
- 4 Horoi M, Brown B A & Sandulescu A, *J Phys G: Nucl Part Phys*, 30 (2004) 945.
- 5 Rose H J & Jones G A, *Nature*, 307 (1984) 245.
- 6 Price P B, *Ann Rev Nucl Part Sci*, 39 (1989) 19.
- 7 Hasegan D & Tretyakova S P, in Particle Emission from Nuclei, Vol II, Ed Poenaru D N & Ivascu S M, CRC, Boca Raton, FL, USA, 1989.
- 8 Ogloblin A A, Bonetti R, Denisov V A & Guglielmetti A, *Phys Rev*, C61 (2000) 034301.
- 9 Blendowske R & Walliser H, *Phys Rev Lett*, 61 (1988) 1930.
- 10 Zamyatnin Y S, Kadmenski S G, 57, *Sov J Nucl Phys*, (1994) 1981.
- 11 Poenaru D N, Schnabel D, Greiner W, Mazilu D & Gherghescu R, *At Data Nucl Data Tables*, 48 (1991) 231.
- 12 Pik-Pichak G A, Fiz Y, *Sov J Nucl Phys*, 44 (1986) 1421.
- 13 Poenaru D, Nuclear Decay Modes, Ed Poenaru D N, Institute of Physics, Bristol, UK, 1996.
- 14 Bonetti R, Carbonini C, Guglielmetti A, Hussonnois M, Trubert D & Naour C L, *Nucl Phys A*, 686 (2001) 64.
- 15 Sahu B, Paira R & Rath B, *Nucl Phys A*, 908 (2013) 40.
- 16 Cui J P, Xiao Y, Gao Y H & Wang Y Z, *Nucl Phys A*, 987(2019) 99.
- 17 Santhosh K P & Priyanka B, *Nucl Phys A*, 940 (2015) 21.
- 18 Qian Y & Ren Z, *Phys Lett B*, 738 (2014) 87.
- 19 Zhang Y L & Wang Y Z, *Phys Rev C*, 97 (2018) 014318.
- 20 Warda M, Zdeb A & Robledo L M, *Phys Rev C*, 98 (2018) 041602.
- 21 Routray T R, Nayak J & Basu D N, *Nucl Phys A*, 826 (2009) 223.
- 22 Gupta R K & Greiner W, *Int J Mod Phys E*, 3 (1994) 335.
- 23 Blendowske R & Walliser H, *Phys Rev Lett*, 61 (1988) 1930.
- 24 Kaur A, Sawhney G, Sharma M K & Gupta R K, *Int J Mod Phys E*, 27 (2018) 1850043.
- 25 Wei K & Zhang H F, *Phys Rev C*, 96 (2017) 021601(R).
- 26 Poenaru D N, Gherghescu R A & Greiner W, *Phys Rev C*, 85 (2012) 034615.
- 27 Sun X D, Guo P & Li X H, *Phys Rev C*, 93 (2016) 034316.
- 28 Qian Y & Ren Z, *Phys Rev C*, 90 (2014) 064308.
- 29 Zdeb A, Warda M & Pomorski K, *Phys Rev C*, 87 (2013) 024308.
- 30 Santhosh K P & Nithya C, *Phys Rev C*, 97 (2018) 044615.
- 31 Wang Y Z, Cui J P, Zhang Y L, Zhang S & Gu J Z, *Phys Rev C*, 95 (2017) 014302.
- 32 Manjunatha H C, Sowmya N, Sridhar K N & Seenappa L, *J Radio Anal Nucl Chem*, 314 (2017) 991.
- 33 Manjunatha H C & Sowmya N, *Nucl Phys A*, 969 (2018) 68.
- 34 Manjunatha H C & Sowmya N, *Int J Mod Phys E*, 27 (2018) 1.
- 35 Manjunatha H C, Sridhar K N & Sowmya N, *Phys Rev C*, 98 (2018) 024308.
- 36 Sridhar K N, Manjunatha H C & Ramalingam H B, *Phys Rev C*, 98 (2018) 064605.
- 37 Manjunatha H C, Sridhar K N & Sowmya N, *Nucl Phys A*, 987 (2019) 382.
- 38 Sowmya N & Manjunatha H C, *Bulg J Phys*, 46 (2019) 16.
- 39 Sowmya N & Manjunatha H C, *Proc DAE Symp Nucl Phys*, 63 (2018) 200.
- 40 Sowmya N & Manjunatha H C, *Braz J Phys*, 49 (2019) 874.
- 41 Bocki J, Randrup J, Swiatecki W & Tsang C, *Ann Phys*, 105 (1977) 427.
- 42 <https://www-nds.iaea.org/RIPL-3>.
- 43 Möller P, Sierk A J, Ichikawa T & Sagawa H, *At Data Nucl Data Tables*, 109 (2016) 1.
- 44 Manjunatha H C, Chandrika B M & Seenappa L, *Mod Phys Lett A*, 31 (2016) 1650162.
- 45 Wang M, Audi G, Wapstra A H, Kondev FG, MacCormick M, Xu X & Pfeiffer B, *Chin Phys C*, 36 (2012) 1603.
- 46 Manjunatha H C & Sowmya N, *Mod Phys Lett A*, 34 (2019) 1950112.



Decay of dinuclear systems formed from dubnium

A M NAGARAJA^{1,2}, H C MANJUNATHA^{1,*}, N SOWMYA¹ , P S DAMODARA GUPTA¹ and S ALFRED CECIL RAJ²

¹Department of Physics, Government College for Women, Kolar 563 101, India

²Department of Physics, St. Joseph's College (Autonomous), Affiliated to Bharathidasan University, Tiruchirappalli 620 002, India

*Corresponding authors. E-mail: manjunathhc@rediffmail.com; sowmyaparakash8@gmail.com

MS received 25 April 2021; revised 7 July 2021; accepted 9 July 2021

Abstract. The radioactivity of the superheavy nuclei $^{250-275}\text{Db}$ is studied and presented using the Coulomb and proximity potentials. The half-lives corresponding to different decay modes such as α , cluster decay (^{12}C , ^{14}N , $^{18,20}\text{O}$, ^{23}F , ^{20}Ne , ^{34}S , ^{28}Mg and ^{40}Ca) and spontaneous fission in the superheavy nuclei $^{250-275}\text{Db}$ are studied. The studied half-lives are compared with the available experiments. The decay modes and the branching ratios of isotopes of dubnium are presented. The isotopes of dubnium, $^{254-263}\text{Db}$, are identified as α emitters, whereas isotopes such as $^{250-253}\text{Db}$ and $^{264-275}\text{Db}$ are identified as having spontaneous fission. The identified alpha emitting isotopes of dubnium have decay energies from 6 MeV to 10 MeV and half-lives 1 ms to 100 s. The possible projectile–target combinations to synthesise the superheavy nuclei $^{253-263}\text{Db}$ were predicted. The fusion of spherical projectile and target yields larger evaporation residue cross-sections.

Keywords. Superheavy; half-lives; alpha-decay; penetration probability; decay mode.

PACS Nos 25.85.Ca; 24.10.–I; 23.60.+e; 21.60.–n

1. Introduction

The analysis of radioactivity in the transactinide elements with $Z \geq 104$ provides an opportunity to understand the structure and properties of matter. The cold fusion reactions with lead and bismuth as the targets and hot fusion reactions with the ^{48}Ca projectile on an actinide target are used to synthesise superheavy elements [1–11]. By the cold and hot fusion reactions, the formed compound nuclei achieve a stable state by many decay methods such as α -decay, cluster decay, β -decay and spontaneous fission. However, in the superheavy region, the formed nuclei decay mainly through an α -decay followed by the spontaneous fission and in a few cases mainly by the spontaneous fission. The possibility of the heavy particle radioactivity (HPR) was also predicted in the superheavy nuclei [12,13].

Many theoretical models such as cluster model [14], multichannel cluster model [15], density-dependent M3Y (DDM3Y) effective interaction [16,17], generalised liquid drop model (GLDM) [18], Coulomb and proximity potential model (CPPM) [19], generalised

density-dependent cluster model [20] and unified model for α -decay and α -capture (UMADAC) [21] were involved to evaluate the α -decay half-lives. The method of quasiparticle random phase approximation (QRPA) was used to evaluate the β -decay half-lives [22]. The β -decay half-lives are evaluated using the widely accepted models [23–25].

The spontaneous fission half-lives were first predicted by Wheeler and Bohr [26] and later on experimentally confirmed by Flerov and Petrzak [27]. During the year 1955, Swiatecki [28] evaluated spontaneous fission half-lives using the fissility parameter Z^2/A in a liquid drop model. Previous researchers [29–31] studied spontaneous fission half-lives using shell correction in a modified liquid drop model. Furthermore, cluster decay is an intermediate between an α decay and spontaneous fission [32] which was experimentally confirmed during the year 1984 [33]. Cluster decays such as ^{14}C , $^{16,18}\text{O}$, $^{22,24,26}\text{Ne}$, ^{23}F , $^{28,30}\text{Mg}$, ^{34}Si and so on were experimentally observed from the parent nuclei ^{221}Fr to ^{242}Cm [34]. The cluster decay half-lives are evaluated using various models such as super-asymmetric fission model (SAFM) [35,36], unified fission model

[37,38] and preformation cluster model (PCM) [39,40]. The cluster decay half-lives are also evaluated using semi-microscopic methods [41–43]. Earlier researchers studied different decay modes using different models and semi-empirical relations to evaluate the half-lives [44–57].

In the present work, we have investigated decay properties such as α , cluster decay and spontaneous fission half-lives and identified decay mode of the superheavy nuclei dubnium with $Z = 105$. The α and cluster decay half-lives are evaluated using the Coulomb and proximity potential model and spontaneous fission is studied using the semi-empirical relation. The theory used to evaluate the decay half-lives and decay modes are given in §2. The corresponding results are discussed in §3 and conclusions of the present work are presented in §4.

2. Theory

2.1 Alpha and cluster decay

By quantum tunnelling process, the cluster and α decay are feasible. In the theoretical context, overall potential at this stage is a significant consideration. The ultimate potential is well established with regard to Coulomb, nuclear and centrifugal potentials.

$$V(R) = V_N(R) + V_c(R) + \frac{\hbar^2 \ell(\ell + 1)}{2\mu r^2}. \quad (1)$$

Here ℓ is the angular momentum and μ is the reduced mass of the emitted α /cluster nuclei and daughter nuclei. r is the distance between fragment centres. In the present work, we have considered Coulomb and proximity potential to evaluate total scattering potential by neglecting the centrifugal potential. The value corresponding to the centrifugal potential is almost zero for ground state to ground state transitions. The short-range Coulomb potential is evaluated as follows:

$$V_c(R) = Z_1 Z_2 e^2 \begin{cases} \frac{1}{R} & \text{for } R > R_c, \\ \frac{1}{2R_c} \left[3 - \left(\frac{R}{R_c} \right) \right] & \text{for } R < R_c, \end{cases} \quad (2)$$

where Z_1 and Z_2 are the atomic numbers of the daughter and emitted α /cluster respectively. The radial distance is obtained using the equation $R_c = 1.24(R_e + R_d)$.

The long-range proximity potential function ($V_N(R)$) is the product of two functions and it depends on the shape and geometry of the colliding system. The second

is the universal function and it is expressed as follows:

$$V_p(Z) = 4\pi\gamma\Phi\bar{R} \left(\frac{r - C_1 - C_2}{b} \right) \text{MeV}. \quad (3)$$

The proximity potential is evaluated using the set of equations described in [45]. Using the total interacting potential and proximity potential, the penetration probability P is evaluated using the WKB approximation as follows:

$$P = \exp \left[-\frac{2}{\hbar} \int_{R_{\text{in}}}^{R_{\text{out}}} \sqrt{2\mu[V(r) - Q]} dr \right], \quad (4)$$

where R_{in} and R_{out} are the classical turning points and are evaluated using the following boundary conditions: $V(r - R_{\text{in}}) = V(r = R_{\text{out}}) = Q$. Here Q is the decay energy of the emitted cluster/ α and it is defined as

$$Q = M_p - M_d - M_c, \quad (5)$$

where M_p , M_d and M_c are mass excess of the parent, the daughter and the cluster/ α nuclei, respectively and these are adopted from ref. [58]. Both α and cluster decay half-lives are evaluated as follows:

$$T_{1/2} = \frac{h \ln 2}{2E_v P}, \quad (6)$$

where the empirical vibrational energy E_v is calculated using the following equation:

$$E_v = Q \left[0.056 + 0.039 \exp \left(\frac{4 - A_e}{2.5} \right) \right] \text{MeV}. \quad (7)$$

Here, A_e is the mass number of the emitted α /cluster particle.

2.2 Spontaneous fission

Spontaneous fission is the most complicated process. Bao *et al* [59] proposed semi-empirical relation for spontaneous fission by including the shell correction and isospin effect for the Swiatecki's formula [28]. Ren and Xu [60] proposed semi-empirical relation for the spontaneous fission based on the blocking effect of unpaired nucleon in the case of even–even nuclei and odd-A nuclei. Furthermore, Santhosh *et al* [61] proposed a relation for spontaneous fission half-lives based on fissility parameter and isospin effect. Karpov *et al* [62] proposed the semi-empirical relation for the spontaneous fission based on barrier height (B_f) on the potential energy surface. By including the systematics of fission isomer half-lives, Metag *et al* [63,64] proposed semi-empirical relation for the fission half-lives. Among the different semi-empirical relations available in the literature, we have considered Karpov's semi-empirical relation [62] which is based on the fission barrier height, and it is expressed as follows:

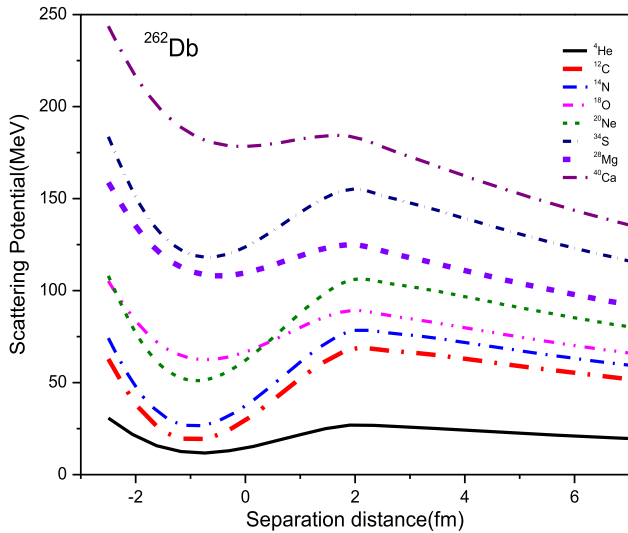


Figure 1. Variation of scattering potential as a function of separation distance during the cluster emission (${}^4\text{He}$ – ${}^{40}\text{Ca}$) from the superheavy nucleus ${}^{262}\text{Db}$.

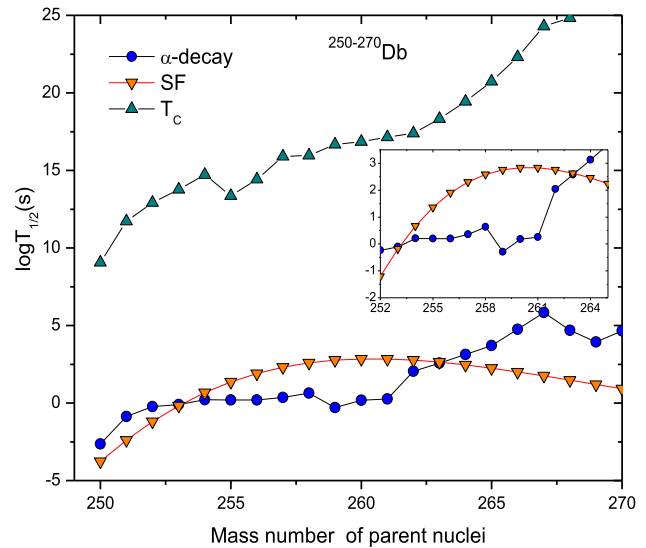


Figure 2. Variation of $\log T_{1/2}$ for different decay modes (SF, α -decay and ${}^{12}\text{C}$ emission) with mass number of the parent nuclei A_p for the superheavy element $Z = 105$.

$$\begin{aligned} \log T_{\text{SF}}(s) = & 1146.44 - 75.3153 \left(\frac{Z^2}{A}\right) \\ & + 1.63792 \left(\frac{Z^2}{A}\right)^2 - 0.0119827 \left(\frac{Z^2}{A}\right)^3 \\ & + B_f(7.23613 - 0.0947022Z^2/A) \\ & + \begin{cases} 0, & Z \text{ and } N \text{ are even,} \\ 1.53897, & A \text{ is odd,} \\ 0.80822, & Z \text{ and } N \text{ are odd.} \end{cases} \end{aligned} \tag{8}$$

Here B_f is the fission barrier and it is evaluated as the sum of the liquid drop barrier B_f (LDM) and shell correction term (δU). In the present study, we have evaluated the fission barriers using the semi-relation available in [65] for the heavy and superheavy regions.

3. Results and discussions

The half-lives of the cluster and α decay of $Z = 105$ are studied using the Coulomb and proximity potential model as explained in §2.1. During the cluster emissions, we have studied all the cluster emissions from ${}^{12}\text{C}$ to ${}^{40}\text{Ca}$. All possible isotopes of cluster emissions were considered during the cluster decay.

Figure 1 presents the variation of scattering potential with the separation distance between the daughter and the emitted cluster nuclei (${}^4\text{He}$ – ${}^{40}\text{Ca}$) for the superheavy nucleus ${}^{262}\text{Db}$. From the figure it is inferred that the short-range attractive nuclear force is dominant up

to the separation distance of 0 fm. However, the value of the nuclear force varies depending on the type of cluster emitted during the decay mode. Again, the Coulomb repulsive force will be dominant and maximum value of force is observed at 2 fm. The scattering potential almost becomes constant as the separation distance increases.

Similarly, we have studied cluster and α decay half-lives in isotopes of superheavy nuclei ${}^{250}\text{Db}$ to ${}^{270}\text{Db}$. Then the studied half-lives are compared with the spontaneous fission as explained in §2.2. Different decay modes for the isotopes of dubnium from ${}^{250}\text{Db}$ to ${}^{270}\text{Db}$ are presented in figure 2. The half-lives corresponding to ${}^{254}\text{Db}$ to ${}^{263}\text{Db}$ are shorter than the other decay modes which have been studied. The magnified portion of the region from 252 – ${}^{264}\text{Db}$ is clearly shown in the inset of the same figure. But, the nuclei below ${}^{254}\text{Db}$ and above ${}^{263}\text{Db}$ have shorter half-lives for the spontaneous fission. Hence, the superheavy nuclei ${}^{254}\text{Db}$ to ${}^{263}\text{Db}$ shows maximum probability of an α -decay only. After identifying the dominant decay mode in dubnium, the corresponding half-lives are compared with the available experimental values.

Table 2 shows the comparison between the present work and the experimental values. A good agreement between the studied half-lives and available experimental values can be observed. However, there is a deviation of calculated half-lives around 10 times with the experiment in the case of ${}^{262}\text{Db}$ and ${}^{263}\text{Db}$. Once the values obtained are comparable with the experimental values, the study is extended to other isotopes of dubnium.

Table 1. Tabulation of Q -values, $\log T_{1/2}$ and the corresponding decay mode in the isotopes of Db.

Parent nuclei	Daughter nuclei	Q (MeV)	$\log T_{1/2}$ (s)	Decay mode
^{250}Db	^{246}Lr	10.41	-3.775	SF
^{251}Db	^{247}Lr	10.07	-2.39	SF
^{252}Db	^{248}Lr	9.83	-1.19	SF
^{253}Db	^{249}Lr	9.78	-0.17	SF
^{254}Db	^{250}Lr	9.66	-1.29	α
^{255}Db	^{251}Lr	9.44	0.204	α
^{256}Db	^{252}Lr	9.34	0.21	α
^{257}Db	^{253}Lr	9.207	0.36	α
^{258}Db	^{254}Lr	9.5	0.63	α
^{259}Db	^{255}Lr	9.62	-0.29	α
^{260}Db	^{256}Lr	9.5	0.18	α
^{261}Db	^{257}Lr	9.22	0.255	α
^{262}Db	^{258}Lr	8.19	2.04	α
^{263}Db	^{259}Lr	7.9	2.57	α
^{264}Db	^{260}Lr	8.2	2.45	SF
^{265}Db	^{261}Lr	8.4	2.25	SF
^{266}Db	^{262}Lr	8.2	2.01	SF
^{267}Db	^{263}Lr	7.78	1.75	SF
^{268}Db	^{264}Lr	7.635	1.475	SF
^{269}Db	^{265}Lr	7.75	1.19	SF
^{270}Db	^{266}Lr	7.12	0.92	SF

Table 2. Comparison of α decay half-lives of the present work (PW) with that of the available experiments.

Parent nuclei	$T_{1/2}^{\text{Exp}}$	$\log T_{1/2}^{\text{Exp}}$	$\log T_{1/2}^{\text{PW}}$	Ref.
^{255}Db	20 ms	-1.6	0.204	[66]
^{256}Db	$1.6^{+0.5}_{-0.3}$ s	0.20s	0.21	[1]
^{257}Db	$1.50^{+0.19}_{-0.15}$	0.17	0.36	[1]
^{258}Db	3.6 s	0.55	0.63	[67]
^{258}Db	$4.4^{+0.9}_{-0.6}$ s	0.64	0.63	[68]
^{259}Db	0.51 ± 0.16 s	-0.29	-0.29	[69]
^{260}Db	1.52 ± 0.13 s	0.181	0.18	[70]
^{261}Db	1.8 s	0.26	0.255	[71]
^{262}Db	40.9 s	1.61	2.04	[72]
^{263}Db	27 s	1.43	2.57	[73]

The emitted cluster particle energy (Q -value) is studied by the difference of initial and final (daughter+emitted nuclei) mass excess values and these mass excess values are taken from [58]. Based on the above studies, we have predicted the half-lives and Q -values of isotopes of dubnium from ^{250}Db to ^{275}Db . The values corresponding to the decay, Q -values and $\log T_{1/2}$ are tabulated in table 1.

After the identification of possible decay mode in the isotopes of dubnium, we have studied the corresponding decay products and the decay modes. Table 3

presents the daughter nuclei, amount of energy released during the process and $\log T_{1/2}$ of α and spontaneous fission half-lives and decay mode. The superheavy nucleus ^{254}Db has shorter half-life with α decay than with spontaneous fission and hence it is terminated to ^{253}Lr with α_1 decay and again the nucleus ^{253}Lr is not stable against α decay and hence it is ended with the spontaneous fission. Similarly, we have shown decay chains corresponding to nuclei from ^{255}Db to ^{263}Db . ^{255}Db is terminated with the single α decay followed by the spontaneous fission, whereas the nuclei ^{256}Db to

Table 3. A comparison of logarithmic α decay and spontaneous fission and its decay mode for the superheavy nuclei ^{254}Db to ^{263}Db .

Parent nuclei	Daughter nuclei	Q -values	$\log T_{1/2} (\alpha)$	$\log T_{1/2} (\text{SF})$	Decay mode
^{254}Db	^{250}Lr	9.66	0.21	0.68	α_1
^{250}Lr	^{246}Md	9.43	-2.81	-3.78	SF
^{255}Db	^{251}Lr	9.44	0.20	1.37	α_1
^{251}Lr	^{247}Md	9.43	-2.81	-2.40	SF
^{256}Db	^{252}Lr	9.34	0.20	1.91	α_1
^{252}Lr	^{248}Md	9.26	-2.34	-1.20	α_2
^{248}Md	^{244}Es	8.70	-1.28	-7	SF
^{257}Db	^{253}Lr	9.21	0.36	2.31	α_1
^{253}Lr	^{249}Md	8.94	-1.36	-0.17	α_2
^{249}Md	^{245}Es	8.46	-0.53	-5.32	SF
^{258}Db	^{254}Lr	9.50	0.63	2.59	α_1
^{254}Lr	^{250}Md	8.79	-0.9	0.68	α_2
^{250}Md	^{245}Es	9.62	-1.28	2.88	SF
^{259}Db	^{255}Lr	9.62	-0.29	2.76	α_1
^{255}Lr	^{251}Md	8.61	-0.31	1.37	α_2
^{251}Md	^{247}Es	7.99	1.08	-2.40	SF
^{260}Db	^{256}Lr	9.50	0.18	2.84	α_1
^{256}Lr	^{252}Md	8.82	-1.02	1.91	α_2
^{252}Md	^{248}Es	7.90	1.40	-1.2	α_3
^{261}Db	^{257}Lr	9.22	0.26	2.84	α_1
^{257}Lr	^{253}Md	9.01	-1.65	2.31	α_2
^{253}Md	^{249}Es	7.70	2.05	2.76	α_3
^{262}Db	^{258}Lr	8.19	2.05	2.76	α_1
^{258}Lr	^{254}Md	8.90	-1.34	2.59	α_2
^{254}Md	^{250}Es	7.86	1.53	0.68	SF
^{263}Db	^{259}Lr	7.90	2.58	2.63	α_1
^{259}Lr	^{255}Md	8.58	-0.31	2.76	α_2
^{255}Md	^{251}Es	7.91	1.34	1.37	α_3
^{251}Es	^{247}Bk	6.60	6.07	-2.4	SF

^{262}Db are determined by the 2 α decay chain and hence terminated with the spontaneous fission and ^{263}Db follows the 3 α decay chain with the ^{259}Lr , ^{255}Md , ^{251}Es daughter nuclei and finally ended with the spontaneous fission. However, if the Q -values are reliable, then the obtained $\log T_{1/2}$ values show consistent decay chains followed by the spontaneous fission in the case of ^{254}Db to ^{263}Db and it is shown in table 3. The branching ratios [45] of an α with respect to cluster decay are evaluated and are presented in table 4. From the table it is inferred that the ratio of α with respect to the clus-

ter decay shows higher value of magnitude of an order of 10^{24} to 10^{83} . From the table it is clearly observed that the branching ratios corresponding to ^{12}C , ^{14}N , ^{20}Ne , ^{34}S and ^{40}Ca show an increasing trend with mass number of the parent nuclei. However, branching ratio remains almost constant in the case of ^{18}O . These values may be due to the amount of energy released during the ^{18}O cluster emission from the isotopes of dubnium.

As smaller half-lives and higher magnitude of branching ratios are observed in the isotopes of dubnium, we

Table 4. Logarithmic values of branching ratio of α -decay with respect to cluster decay (^{12}C , ^{14}N , ^{18}O , ^{20}Ne , ^{34}S and ^{40}Ca) for the isotopes of superheavy nuclei ^{251}Db to ^{275}Db .

Isotopes	$\frac{\lambda_{\alpha}}{\lambda_{^{12}\text{C}}}$	$\frac{\lambda_{\alpha}}{\lambda_{^{14}\text{N}}}$	$\frac{\lambda_{\alpha}}{\lambda_{^{18}\text{O}}}$	$\frac{\lambda_{\alpha}}{\lambda_{^{20}\text{Ne}}}$	$\frac{\lambda_{\alpha}}{\lambda_{^{34}\text{S}}}$	$\frac{\lambda_{\alpha}}{\lambda_{^{40}\text{Ca}}}$
^{251}Db	25.95	32.89	34.32	33.68	25.63	29.79
^{252}Db	25.59	30.46	34.43	34.11	27.11	32.18
^{253}Db	25.81	33.99	35.29	34.97	28.80	35.31
^{254}Db	25.66	32.02	34.99	35.70	30.18	37.84
^{255}Db	26.91	34.05	33.74	35.38	30.77	40.06
^{256}Db	27.09	31.61	33.73	35.78	31.50	42.55
^{257}Db	27.80	35.23	33.82	36.41	32.82	45.08
^{258}Db	30.08	33.95	34.39	37.79	34.70	48.69
^{259}Db	32.51	37.83	34.97	39.26	36.44	51.68
^{260}Db	32.35	35.12	34.32	39.45	37.10	54.19
^{261}Db	32.75	37.73	34.36	40.27	37.73	56.18
^{262}Db	32.64	35.12	33.83	40.64	38.46	58.40
^{263}Db	36.87	38.39	33.75	41.64	39.24	60.48
^{264}Db	35.95	35.94	33.01	41.94	39.78	63.55
^{265}Db	34.62	39.75	33.12	42.96	40.45	65.47
^{266}Db	35.22	37.79	32.73	43.54	40.75	67.26
^{267}Db	35.97	41.85	32.57	44.13	41.09	68.93
^{268}Db	38.99	40.84	34.26	46.43	43.34	72.46
^{269}Db	41.80	45.84	35.74	48.44	45.05	75.11
^{270}Db	45.10	42.92	35.63	50.68	45.46	76.75
^{271}Db	45.23	51.42	37.57	53.85	47.16	79.72
^{272}Db	46.89	46.64	36.77	54.16	47.12	80.77
^{273}Db	50.23	50.71	38.68	55.27	48.29	83.05
^{274}Db	47.89	45.25	36.78	54.26	46.79	82.98
^{275}Db	47.36	48.57	34.80	53.25	45.84	83.26

have also made an effort to predict possible projectile–target combinations to synthesise the isotopes of dubnium. We have selected around 218 possible projectile–target combinations to synthesise superheavy nuclei ^{254}Db to ^{263}Db as predicted in table 3. We have selected the projectile–target combination in such a way that the evaporation residue cross-section is maximum. The evaporation residue cross-section is evaluated as explained in refs [74–76]. Later, we have selected 24 possible projectile–target combinations with maximum evaporation residue cross-sections to synthesise the superheavy nuclei ^{254}Db to ^{263}Db and tabulated in table 5. Among all these predicted projectile–target combinations, the fusion reaction $^{51}\text{V}+^{208}\text{Pb}$, both projectile and target being spherical ($\beta_2 = 0$), shows a larger evaporation residue cross-section of 896.2nb. The second larger production cross-section is observed for

the projectile with magic nuclei (^{48}Ca) and target almost spherical fusion reaction shows a larger evaporation residue cross-section of 812.7 nb.

4. Conclusions

The half-lives and branching ratios of isotopes in the superheavy nuclei $^{254-275}\text{Db}$ have been studied using recent proximity potential. The study of smaller half-lives of ^4He and larger branching ratio reveals that α decay is dominant compared to other clusters such as ^{12}C , ^{14}N , $^{18,20}\text{O}$, ^{23}F , ^{20}Ne , ^{34}S , ^{28}Mg and ^{40}Ca . The evaluated half-lives are compared with the available experimental values and a close agreement of values of the present work with the available experimental value is observed. α and spontaneous fis-

Table 5. Tabulation of the predicted projectile–target combination to synthesise the isotopes of superheavy nuclei ^{253}Db to ^{263}Db along with the centre of mass energy (E_{cm}), fusion barrier (B_{fu}), deformation parameter (β_2) of the projectile and the target and evaporation residue cross-sections.

Reaction	E_{cm} (MeV)	B_{fu} (MeV)	β_2		σ_{ER} (nb)
			Proj.	Targ.	
$^{49}\text{V} + ^{206}\text{Pb} \rightarrow ^{254}\text{Db} + 1\text{n}$	184	202.3	0	− 0.008	13.1
$^{45}\text{Ca} + ^{211}\text{At} \rightarrow ^{254}\text{Db} + 2\text{n}$	178	181.3	0	0.008	4.4
$^{46}\text{Sc} + ^{210}\text{Po} \rightarrow ^{254}\text{Db} + 2\text{n}$	183	188.9	− 0.008	0	3.1
$^{47}\text{Ca} + ^{210}\text{At} \rightarrow ^{255}\text{Db} + 2\text{n}$	178	180.4	0	− 0.018	43.9
$^{47}\text{Sc} + ^{210}\text{Po} \rightarrow ^{255}\text{Db} + 2\text{n}$	184	188.3	− 0.008	0	30.4
$^{48}\text{Sc} + ^{210}\text{Po} \rightarrow ^{256}\text{Db} + 2\text{n}$	185	187.7	− 0.044	0	184.5
$^{30}\text{Si} + ^{230}\text{Pa} \rightarrow ^{256}\text{Db} + 4\text{n}$	138	144.4	0	0.190	2.8
$^{48}\text{Ti} + ^{210}\text{Bi} \rightarrow ^{257}\text{Db} + 1\text{n}$	176	195.2	0	− 0.018	242.8
$^{48}\text{Ca} + ^{211}\text{At} \rightarrow ^{257}\text{Db} + 2\text{n}$	179	179.6	0	0.008	812.7
$^{51}\text{V} + ^{208}\text{Pb} \rightarrow ^{257}\text{Db} + 2\text{n}$	197	200.8	0	0	896.2
$^{40}\text{Ar} + ^{221}\text{Fr} \rightarrow ^{257}\text{Db} + 4\text{n}$	166	166.8	0	0.120	5.7
$^{39}\text{K} + ^{222}\text{Rn} \rightarrow ^{257}\text{Db} + 4\text{n}$	170	174.7	0	0.137	0.14
$^{40}\text{K} + ^{222}\text{Rn} \rightarrow ^{257}\text{Db} + 5\text{n}$	174	174.1	− 0.035	0.137	1.4
$^{50}\text{Ti} + ^{210}\text{Bi} \rightarrow ^{258}\text{Db} + 2\text{n}$	191	194.1	0	− 0.018	533.9
$^{41}\text{Ar} + ^{221}\text{Fr} \rightarrow ^{259}\text{Db} + 3\text{n}$	159	166.3	0	0.120	5.1
$^{42}\text{Ar} + ^{221}\text{Fr} \rightarrow ^{259}\text{Db} + 4\text{n}$	166	165.8	0	0.120	9.4
$^{41}\text{K} + ^{222}\text{Rn} \rightarrow ^{259}\text{Db} + 4\text{n}$	169	173.5	0	0.137	0.9
$^{42}\text{Ar} + ^{222}\text{Fr} \rightarrow ^{260}\text{Db} + 4\text{n}$	166	165.7	0	0.138	7.4
$^{41}\text{Ar} + ^{223}\text{Fr} \rightarrow ^{260}\text{Db} + 4\text{n}$	164	165.9	0	0.146	2.5
$^{42}\text{Ar} + ^{223}\text{Fr} \rightarrow ^{261}\text{Db} + 4\text{n}$	165	165.5	0	0.146	7.7
$^{32}\text{P} + ^{234}\text{Th} \rightarrow ^{261}\text{Db} + 5\text{n}$	144	150.5	0	0.215	2.4
$^{32}\text{Si} + ^{234}\text{Pa} \rightarrow ^{262}\text{Db} + 4\text{n}$	135	142.5	0	0.215	9.1
$^{14}\text{N} + ^{253}\text{Cf} \rightarrow ^{262}\text{Db} + 5\text{n}$	79	75.1	0	0.226	4.5
$^{33}\text{P} + ^{234}\text{Th} \rightarrow ^{263}\text{Db} + 4\text{n}$	141	150.1	0	0.215	2.6

sion emitters are identified in the superheavy region $^{250}\text{--}^{270}\text{Db}$. The possible projectile–target combinations to synthesise the superheavy nuclei ^{254}Db to ^{263}Db are predicted.

References

[1] F P Heßberger *et al*, *Eur. Phys. J. A* **12**, 57 (2001)
 [2] Y T Oganessian, A G Demin, A S Iljinov, S P Tretyakova, A A Pleve, Y E Penionzhkevich, M P Ivanov and Y P Tretyakov, *Nucl. Phys. A* **239**, 157 (1975)
 [3] G Müntzenberg *et al*, *Z. Phys. A* **322**, 227 (1985)
 [4] C M Folden III, S L Nelson, C E Düllmann, J M Schwantes, R Sudowe, P M Zielinski, K E Gregorich, H Nitsche and D C Hoffman, *Phys. Rev. C* **73**, 014611 (2006)
 [5] S Hofmann, F P Heßberger, V Ninov, P Armbruster, G Müntzenberg, C Stodel, A G Popeko, A V Yeremin, S Saro and M Leino, *Z. Phys. A* **358**, 377 (1997)
 [6] S Hofmann *et al*, *Z. Phys. A* **350**, 277 (1995)
 [7] S Hofmann *et al*, *Eur. Phys. J. A* **14**, 147 (2002)
 [8] K Morita *et al*, *Eur. Phys. J. A* **73**, 2593 (2004)
 [9] Y T Oganessian *et al*, *Phys. Rev. C* **70**, 064609 (2004)
 [10] Y T Oganessian *et al*, *Phys. Rev. C* **62**, 041604 (2000)
 [11] Y T Oganessian *et al*, *Phys. Rev. C* **69**, 041601 (2004)
 [12] D N Poenaru, R A Gherghescu, W Greiner, *Phys. Rev. C* **6**, 062503 (2011)
 [13] D N Poenaru, R A Gherghescu and W Greiner, *J. Phys.: Conf. Ser.* **436**, 012056 (2013)
 [14] B Buck, A C Merchant and S M Perez, *Mod. Phys. Lett. A* **6**, 2453 (1991)
 [15] D Ni and Z Ren, *Phys. Rev. C* **81**, 064318 (2010)
 [16] P R Chowdhury, C Samanta and D N Basu, *Phys. Rev. C* **77**, 044603 (2008)
 [17] C Samanta, P R Chowdhury and D N Basu, *Nucl. Phys. A* **789**, 142 (2007)
 [18] Y Z Wang, J M Dong, B B Peng and H F Zhang, *Phys. Rev. C* **81**, 067301 (2010)
 [19] V Y Denisov and H Ikezoe, *Phys. Rev. C* **72**, 064613 (2005)
 [20] D Ni and Z Ren, *Nucl. Phys. A* **893**, 13 (2012)

- [21] V Y Denisov and A Khudenko, *At. Data Nucl. Data Tables* **95**, 815 (2009)
- [22] J Engel, M Bender, J Dobaczewski, W Nazarewicz and R Surman, *Phys. Rev. C* **60**, 014302 (1999)
- [23] P Möller, J R Nix, W D Wyers and W J Swiatecki, *At. Data Nucl. Data Tables* **66**, 131 (1997)
- [24] P Möller, B Pfeiffer and K Kratz, *At. Data Nucl. Data Tables* **67**, 055802 (2003)
- [25] I N Borzov, S Goriely and J M Pearson, *Nucl. Phys. A* **621**, 307 (1997)
- [26] N Bohr and J A Wheeler, *Phys. Rev.* **56**, 426 (1936)
- [27] G N Flerov and K A Petrzhak, *Phys. Rev.* **58**, 275 (1940)
- [28] W J Swiatecki, *Phys. Rev.* **100**, 937 (1955)
- [29] V M Strutinsky, *Nucl. Phys. A* **95**, 420 (1967)
- [30] P Möller, D G Madland, A J Sierk and A Iwamoto, *Nature* **409**, 6822 (2001)
- [31] A Sobiczewski and K Pomorski, *Prog. Part. Nucl. Phys.* **58**, 292 (2007)
- [32] A Sandulescu, D N Poenaru and W Greiner, *Sov. J. Part. Nucl. (Engl. Transl.)* **11**, 6 (1980)
- [33] H J Rose and G A Jones, *Nature* **307**, 245 (1984)
- [34] K P Santhosh and T A Jose, *Nucl. Phys. A* **992**, 121626 (2009)
- [35] D N Poenaru, M Ivaşcu, A Sandulescu and W Greiner, *Phys. Rev. C* **32**, 572 (1985)
- [36] W Greiner, M Ivaşcu, D N Poenaru and A Sandulescu, *Z. Phys. A* **320**, 347 (1985)
- [37] Y J Shi and W J Swiatecki, *Phys. Rev. Lett.* **54**, 300 (1989)
- [38] B Buck and A C Merchant, *J. Phys. G* **15**, 615 (1989)
- [39] S S Malik and R K Gupta, *Phys. Rev. C* **39**, 1992 (1989)
- [40] S Kumar and R K Gupta, *Phys. Rev. C* **55**, 218 (1997)
- [41] D N Poenaru, Y Nagame, R A Gherghescu and W Greiner, *Phys. Rev. C* **66**, 049902 (2002)
- [42] D N Poenaru, Y Nagame, R A Gherghescu and W Greiner, *Phys. Rev. C* **65**, 054308 (2002)
- [43] M A Hooshyar, I Reichstein and F B Malik, *Nuclear fission and cluster radioactivity* (Springer Science and Business Media, 2005)
- [44] A M Nagaraja, H C Manjunatha, N Sowmya, N Manjunath and S A C Raj, *The Eur. Phys. J. Plus* **135**, 1 (2020)
- [45] H C Manjunatha and N Sowmya, *Nucl. Phys. A* **969**, 68 (2018)
- [46] N Sowmya, H C Manjunatha, N Dhananjaya and A M Nagaraja, *J. Rad. Nucl. Chem.* **323**, 1347 (2020)
- [47] A M Nagaraja, H C Manjunatha, N Sowmya and S C Raj, NISCAIR-CSIR, India (2020)
- [48] G R Sridhar, H C Manjunatha, N Sowmya, P S Damodara Gupta and H B Ramalingam, *The Eur. Phys. J Plus* **135**, 1 (2020)
- [49] G R Sridhar, H C Manjunatha, N Sowmya, P S D Gupta and H B Ramalingam, *Phys. Rev. C* **98**, 024308 (2018)
- [50] H C Manjunatha and N Sowmya, *Int. J. Mod. Phys. E* **27**, 1850041 (2018)
- [51] N Sowmya and H C Manjunatha, *Phys. Part. Nucl. Lett.* **17**, 370 (2020)
- [52] N Sowmya and H C Manjunatha, *Braz. J. Phys.* **49**, 874 (2019)
- [53] N Sowmya, H C Manjunatha and P S Damodara Gupta, *Int. J. Mod. Phys. E* **29**, 2050087 (2020)
- [54] N Sowmya and H C Manjunatha, *Braz. J. Phys.* **50**, 317 (2020)
- [55] N Sowmya, H C Manjunatha, P S Damodara Gupta and N Dhananjaya, *Braz. J. Phys.* **17**, 1 (2020)
- [56] N Sowmya, H C Manjunatha and N Dhananjaya, *Proceedings of the Fourteenth Biennial DAE-BRNS symposium on Nuclear and Radiochemistry: Book of Abstracts* (2019)
- [57] K N Sridhar, H C Manjunatha and H B Ramalingam, *Phys. Rev. C* **98**, 064605 (2018)
- [58] Reference Input Parameter Library (RIPL-3), <https://www-nds.iaea.org/RIPL-3.html>
- [59] X J Bao, S Q Guo, H F Zhang, Y Z Xing, J M Dong and J Q Li, *J. Phys. G: Nucl. Part. Phys.* **42**, 085101 (2015)
- [60] Z Ren and C Xu, *Nucl. Phys. A* **759**, 64 (2005)
- [61] K P Santhosh, R K Biju and S Sahadevan, *Nucl. Phys. A* **832**, 220 (2010)
- [62] A V Karpov, V I Zagrebaev, Y Martinez Palenzuela, L Felipe Ruiz and W Greiner, *Int. J. Mod. Phys. E* **21**, 1250013 (2012)
- [63] V Metag, R Repnow and P Von Brentano, *Nucl. Phys. A* **165**, 289 (1971)
- [64] V Metag, *Nukleonika* **20**, 7 (1975)
- [65] H C Manjunatha, *Indian J. Phys.* **92**, 507 (2018)
- [66] A Leppnen, *Alpha decay and decay-tagging studies of heavy elements using the RITU separator* (University of Jyväskylä, 2005)
- [67] G Müntenberg, S Hofmann, F P Heßberger, W Reisdorf, K H Schmidt, J H R Schneider, P Armbruster, C C Sahn and B Thuma, *Z. Phys. A* **300**, 107 (1981)
- [68] M Vostinar *et al*, *Eur. Phys. J. A* **55**, 1 (2019)
- [69] Z Gan *et al*, *Eur. Phys. J. A* **10**, 21 (2001)
- [70] K Morita *et al*, *J. Phys. Soc. Jpn.* **73**, 1738 (2004)
- [71] Z G Gan *et al*, *Eur. Phys. J. A* **20**, 385 (2004)
- [72] K Morita *et al*, *J. Phys. Soc. Jpn.* **81**, 103201 (2012)
- [73] H Ikezoe, T Ikuta, S Mitsuoka, Y Nagame, I Nishinaka, Y Tsukada, T Ohtsuki, T Kizimaki and J Lu, Jaeri Tandem & VDG Annual Report 1997 (April 1, 1997–March 31, 1998) **98**, 47 (1998)
- [74] H C Manjunatha, K N Sridhar and N Sowmya, *Nucl. Phys. A* **987**, 388 (2019)
- [75] H C Manjunatha, L Seenappa and N Sowmya, *Can. J. Phys.* **99**, 16 (2021)
- [76] H C Manjunatha, N Sowmya, N Manjunatha, P S Damodara Gupta, L Seenappa, K N Sridhar, T Ganesh and T Nandi, *Phys. Rev. C* **102**, 064605 (2020)

Systematics of ^{12}C Emission from Superheavy Nuclei

A.M. Nagaraja^{1,3}, H.C. Manjunatha¹, K.N. Sridhar²,
S. Alfred Cecil Raj³

¹Department of Physics, Government College for Women,
Kolar-563101 Karnataka, India

²Department of Physics, Government First Grade College,
Kolar-563101 Karnataka, India

³Department of Physics, St. Joseph's College (autonomous),
Thiruchirapalli-620 002, Tamilnadu, India

Received: 4 May 2019

Abstract. We have theoretically studied the systematics of ^{12}C emission in superheavy nuclei with $Z = 104\text{--}130$. We have also compared the ^{12}C decay half-lives with that of alpha decay and spontaneous fission. It is found that ^{12}C decay half-lives are greater than that of alpha decay and spontaneous fission. The variation of logarithmic ^{12}C decay half-lives with $Z_d^{0.6}Q^{-1/2}$ is found to be exact straight line. The superheavy nuclei which are having shorter ^{12}C half-lives are highlighted.

PACS codes: 36.10.-k

1 Introduction

Study of exotic/cluster decay is important in the field of superheavy nuclei. There is an expectation that the decay of superheavy nuclei through the cluster emission of nuclei. The study of alpha decay and cluster radioactivity plays an important role in the identification and synthesis of superheavy elements. From the detail literature survey it has been observed theoretical as well as experimental works on the synthesis and decay modes of superheavy elements. The alpha and heavy particle decay in $Z=116\text{--}124$ was reported by Santhosh and Priyanka [1]. Manjunatha [2] studied alpha decay properties of $Z = 126$ in the range of $288 \leq A \leq 339$. Previous workers [3] extended systematics of alpha decay half-lives for exotic superheavy nuclei. Santhosh and Nithya [4] studied different decay modes of even Z superheavy isotopes. Santhosh et al. [5] reported cluster emission in $^{210\text{--}226}\text{Ra}$ isotopes. Alpha decay half-lives of superheavy nuclei with $Z = 116\text{--}118$ are reported by previous workers [6]. The competition between spontaneous fission and α -decay process for superheavy

Systematics of ^{12}C Emission from Superheavy Nuclei

element with $Z = 112$ was reported by previous researchers [7]. Alpha decay properties and structure of superheavy nuclei $Z = 102\text{--}120$ was studied by Silișteanu and Budaca [8]. A study on α -decay rates of spherical and deformed nuclei was reported by Ni and Ren [9]. Nuclear lifetimes of cluster radioactivities with $Z = 52\text{--}122$, were empirically calculated by Poenaru et al. [10]. There has been several detail reports on alpha decay half-lives of superheavy nuclei [11–24]. From the literature survey [25–29], it is also observed that there was some studies on preformation probabilities of alpha decay. There were some studies reported on cluster decay and heavy particle radioactivity [30–40]. Some of the researchers [41–46], studied both alpha and cluster emission in superheavy nuclei.

The study of cluster radioactivity is important for heavy and superheavy nuclei. Most of the researchers studied the cluster radioactivity except ^{12}C emission. A detail literature survey reveals that there is no systematic study of ^{12}C emission in superheavy nuclei. Hence in the present work, we have theoretically studied the systematics of ^{12}C emission in superheavy nuclei. This paper is organized in to three sections. First part is introduction and in the second part, we have explained the theoretical frame work used in the calculations of half-lives of ^{12}C emission. The results obtained in the present work are analyzed in the third section.

2 Theoretical Frame Work

The decay half-life of parent nuclei with the emission of ^{12}C cluster is studied by

$$T_{1/2} = \frac{\ln 2}{\lambda} = \frac{\ln 2}{\nu P}, \quad (1)$$

where λ is the decay constant and ν is the assault frequency and is expressed as

$$\nu = \frac{\omega}{2\pi} = \frac{2E_\nu}{h}, \quad (2)$$

where E_ν is the empirical vibrational energy [47]. According to WKB approximation (Wentzel-Kramers-Brillouin) the penetration probability P through the potential barrier studied by the following equation:

$$P = \exp \left\{ -\frac{4\pi}{h} \int_{R_a}^{R_b} \sqrt{2\mu(V_T(r) - Q)} dr \right\}, \quad (3)$$

where μ is the reduced mass of fission fragments of cluster decay and alpha decay system, R_a and R_b are the inner and outer turning points and these turning points are calculated by

$$V_T(R_a) = Q = V_T(R_b). \quad (4)$$

The total interacting potential is

$$V_T(r) = V_N(r) + V_C(r) + V_l(r), \quad (5)$$

where $V_N(r)$ is the attractive nuclear potential, $V_C(r)$ is the repulsive Coulomb potential and $V_l(r)$ is the centrifugal potential. The Coulomb potential $V_C(r)$ for cluster decay and alpha decay is given by

$$V_C(r) = Z_\alpha Z_b e^2 \begin{cases} \frac{1}{R} & (R > R_C) \\ \frac{1}{2R_c} \left[3 - \left(\frac{R}{R_c} \right)^2 \right] & (R < R_C) \end{cases}, \quad (6)$$

where R_c is touching radial separation between fission fragments in cluster decay and alpha decay. The nuclear potential $V_N(r)$ between cluster/alpha decay nuclei and daughter nuclei is

$$V_N(r) = 4\pi\gamma\bar{R}\Phi(\varepsilon). \quad (7)$$

The nuclear potential intern depends upon geometry and shape of the nuclei and universal function $\Phi(\varepsilon)$ and surface coefficient γ is calculated as [48]

$$\gamma = \gamma_0 \left[1 - K_s \left(\frac{N-Z}{A} \right)^2 \right] \text{ MeV/fm}^2, \quad (8)$$

where γ_0 is the surface energy constant and K_s is the surface asymmetry constant. $\gamma_0 = 1.25284 \text{ MeV/fm}^2$ and $K_s = 2.345$ [49]. \bar{R} is the mean curvature as

$$\bar{R} = \frac{C_1 C_2}{C_1 + C_2}, \quad (9)$$

where C_1 and C_2 are the süssmann's central radii of cluster/alpha nuclei and daughter nuclei, respectively. Based on droplet model [50] C_i is written as

$$C_i = c_i + \left(\frac{N_i}{a_i} \right) t_i, \quad (i = 1, 2), \quad (10)$$

where t_i is the neutron skin and is given as

$$t_i = \frac{3}{2} r_0 \left(\frac{J I_i - \frac{1}{12} c_i Z_i A_i^{-1/3}}{Q + \frac{9}{4} J A_i^{-1/3}} \right), \quad (i = 1, 2), \quad (11)$$

r_0 is the radius constant and $r_0 = 1.14 \text{ fm}$, the symmetry energy coefficient $J = 32.65 \text{ MeV}$, $I = (N-Z)/A$, $c_i = 3e^2/5r_0 = 0.757895 \text{ MeV}$ and neutron skin stiffness coefficient $Q = 35.4 \text{ MeV}$, c_i is the half-density radius of the charge distribution and it is defined as [50]

$$c_i = R_{00i} \left(1 - \frac{7}{2} \frac{b^2}{R_{00i}^2} - \frac{49}{8} \frac{b^4}{R_{00i}^4} + \dots \right), \quad (i = 1, 2), \quad (12)$$

Systematics of ^{12}C Emission from Superheavy Nuclei

R_{00i} is charge radius formula and is expressed as

$$R_{00i} = 1.171A_i^{1/3} + 1.472A_i^{-1/3}, \quad (i = 1, 2). \quad (13)$$

Universal proximity potential is given by [51]

$$\Phi(\varepsilon) = \begin{cases} -1.7817 + 0.9270\varepsilon + 0.143\varepsilon^2 - 0.09\varepsilon^3 & \text{for } \varepsilon \leq 0.0, \\ -1.7817 + 0.9270\varepsilon + 0.0169\varepsilon^2 - 0.05148\varepsilon^3 & \text{for } 0 \leq \varepsilon \leq 1.9475, \\ -4.41 \exp\left(\frac{-\varepsilon}{0.7176}\right) & \text{for } \varepsilon \geq 1.9475 \end{cases}, \quad (14)$$

where $\varepsilon = s/b$ is the minimum separation between fission fragments and $b \approx 0.99$ is the nuclear surface thickness and s is the distance between the near surfaces of the fragments.

Table 1. Highlighted ^{12}C emitters in the superheavy nuclei

Parent nucleus	Daughter nucleus	Q , (MeV)	$T_{1/2}$, (s)	Parent nucleus	Daughter nucleus	Q , (MeV)	$T_{1/2}$, (s)
$^{257}_{107}$	$^{245}_{101}$	29.63	24678.2	$^{312}_{126}$	$^{300}_{120}$	45.61	426.5356
$^{308}_{123}$	$^{296}_{117}$	37.90	397111.2	$^{313}_{126}$	$^{301}_{120}$	32.10	480.2658
$^{309}_{123}$	$^{297}_{118}$	37.87	8667.157	$^{314}_{126}$	$^{302}_{120}$	32.30	1232.562
$^{310}_{123}$	$^{298}_{117}$	37.68	41863.62	$^{315}_{126}$	$^{303}_{120}$	33.40	3671.034
$^{311}_{123}$	$^{299}_{117}$	36.89	33121.23	$^{316}_{126}$	$^{304}_{120}$	31.30	13081.06
$^{312}_{123}$	$^{300}_{117}$	37.55	43938.14	$^{310}_{127}$	$^{298}_{121}$	33.59	73.15606
$^{314}_{123}$	$^{302}_{117}$	37.92	532.7464	$^{311}_{127}$	$^{299}_{121}$	33.08	46.28831
$^{308}_{124}$	$^{296}_{118}$	39.96	55384.92	$^{312}_{127}$	$^{300}_{121}$	32.73	17.52527
$^{312}_{124}$	$^{300}_{118}$	41.44	20280.27	$^{313}_{127}$	$^{301}_{121}$	32.71	42.9559
$^{313}_{124}$	$^{301}_{118}$	41.85	44699.79	$^{314}_{127}$	$^{302}_{121}$	32.58	63.11274
$^{306}_{125}$	$^{294}_{119}$	41.32	16016.39	$^{315}_{127}$	$^{303}_{121}$	32.42	275.5344
$^{307}_{125}$	$^{295}_{119}$	41.76	11912.69	$^{316}_{127}$	$^{304}_{121}$	32.19	705.3964
$^{309}_{125}$	$^{297}_{119}$	41.72	2749.136	$^{317}_{127}$	$^{305}_{121}$	32.67	2993.247
$^{310}_{125}$	$^{298}_{119}$	42.32	683.8953	$^{313}_{128}$	$^{301}_{122}$	34.97	3.719666
$^{311}_{125}$	$^{299}_{119}$	42.98	473.7727	$^{314}_{128}$	$^{302}_{122}$	34.98	6.717327
$^{312}_{125}$	$^{300}_{119}$	43.83	1185.967	$^{315}_{128}$	$^{303}_{122}$	34.89	39.61285
$^{313}_{125}$	$^{301}_{119}$	43.66	3526.878	$^{316}_{128}$	$^{304}_{122}$	34.76	130.3004
$^{314}_{125}$	$^{302}_{119}$	43.96	8568.358	$^{317}_{128}$	$^{305}_{122}$	34.67	524.9683
$^{315}_{125}$	$^{303}_{119}$	43.66	30641.77	$^{318}_{128}$	$^{306}_{122}$	35.98	2318.064
$^{308}_{126}$	$^{296}_{120}$	44.47	2103.65	$^{316}_{129}$	$^{304}_{123}$	36.89	10.09031
$^{309}_{126}$	$^{297}_{120}$	44.60	977.4565	$^{317}_{129}$	$^{305}_{123}$	36.85	52.34164
$^{310}_{126}$	$^{298}_{120}$	44.92	646.8053	$^{319}_{130}$	$^{307}_{124}$	39.51	228.5082
$^{311}_{126}$	$^{299}_{120}$	45.74	199.4518	$^{320}_{130}$	$^{308}_{124}$	39.96	1499.252

3 Results and Discussion

We have studied the half-lives of ^{12}C decay from superheavy nuclei of $104 < Z < 130$. The energy released (Q) during the ^{12}C decay is plotted as a function of neutron number of the parent nuclei and it is shown in Figure 1. Figure 2 shows the variation of logarithmic half-lives with neutron number of parent nuclei for studied superheavy nuclei. From this figure it is found that half-lives of ^{12}C decay is shorter for superheavy nuclei with $Z > 120$. The highlighted ^{12}C emitters in the superheavy emitters are given in Table 1. To study the competition between the ^{12}C decay and other dominant decay modes such as alpha decay and spontaneous fission, we have also calculated the half-lives corresponds to the alpha decay and spontaneous fission. The comparison of ^{12}C decay half-lives with that of alpha decay and spontaneous fission are shown in Figure 3. From this figure it is found that ^{12}C decay half-lives are greater than that of alpha decay and spontaneous fission.

The variation of logarithmic half-lives for ^{12}C decay with mass number reveals that there is peaks correspond to the nuclei ^{286}Fl , $^{297}\text{120}$, $^{301}\text{121}$, $^{301}\text{122}$ and $^{303}\text{123}$. These nuclei are having longer ^{12}C decay half-lives than that of neighbour. This means these nuclei are having extra stability against ^{12}C decay. The variation of logarithmic half-lives for ^{12}C decay with mass number reveals that there is peaks correspond to the nuclei ^{286}Fl , $^{297}\text{120}$, $^{301}\text{121}$, $^{301}\text{122}$ and $^{303}\text{123}$. These nuclei are having longer ^{12}C decay half-lives than that of neighbour. This means these nuclei are having extra stability against ^{12}C decay.

To test the validity of Geiger–Nuttall law [52] for ^{12}C decay, we have plotted the logarithmic ^{12}C decay half-lives with inverse of square root of energy released (Q). Figure 3 shows the variation of logarithmic ^{12}C decay half-lives with inverse of square root of energy released (Q). From this figure it is found that variation of logarithmic ^{12}C decay half-lives with $Q^{-1/2}$ is found to be straight line. We have also evaluated the fitting coefficients 'a' and 'b' and these are included in the Figure 4. Experimental data of branching ratios between alpha and ^{12}C decay in superheavy nuclei are not available in the literature.

To validate the present calculations, we have evaluated branching ratios for some actinide nuclei where the experimental data is available. We have compared the calculated branching ratios between alpha and carbon cluster radioactivity with that of the experiments (Ref. [53]) and this comparison is as shown in Table 2. From the detail study of variation of logarithmic half-lives with energy released (Q) and atomic number of daughter nuclei reveals that the logarithmic half-lives can be expressed linearly using $Z_d^{0.6}Q^{-1/2}$. Figure 5 shows the variation of logarithmic ^{12}C decay half-lives with $Z_d^{0.6}Q^{-1/2}$. The variation of logarithmic ^{12}C decay half-lives with $Z_d^{0.6}Q^{-1/2}$ is found to be exact straight line. For each superheavy element, we have expressed logarithmic half-lives in terms linear equation of $Z_d^{0.6}Q^{-1/2}$. In Figure 5, to show the exactness of the fit, we have

Systematics of ^{12}C Emission from Superheavy Nuclei

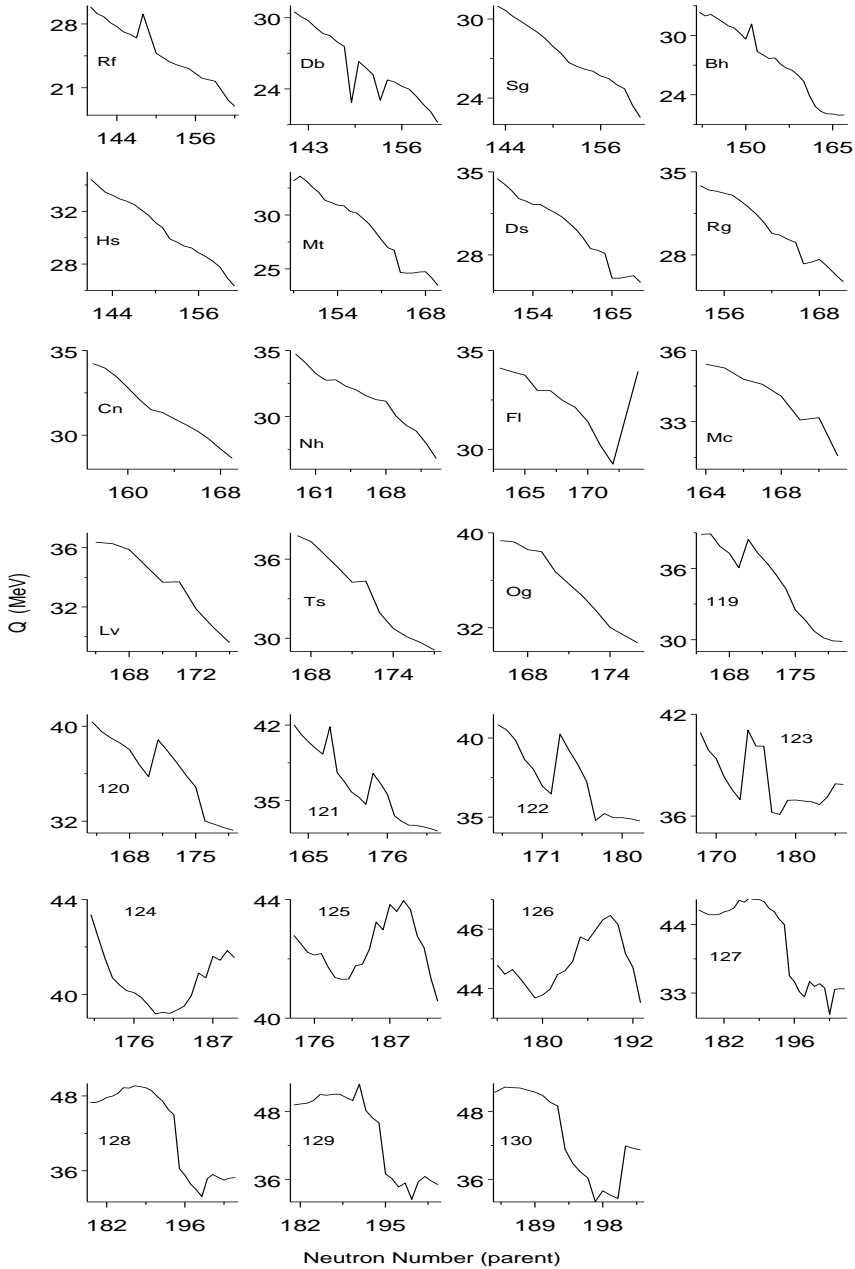


Figure 1. Variation of Q (MeV) with neutron number of parent nuclei.

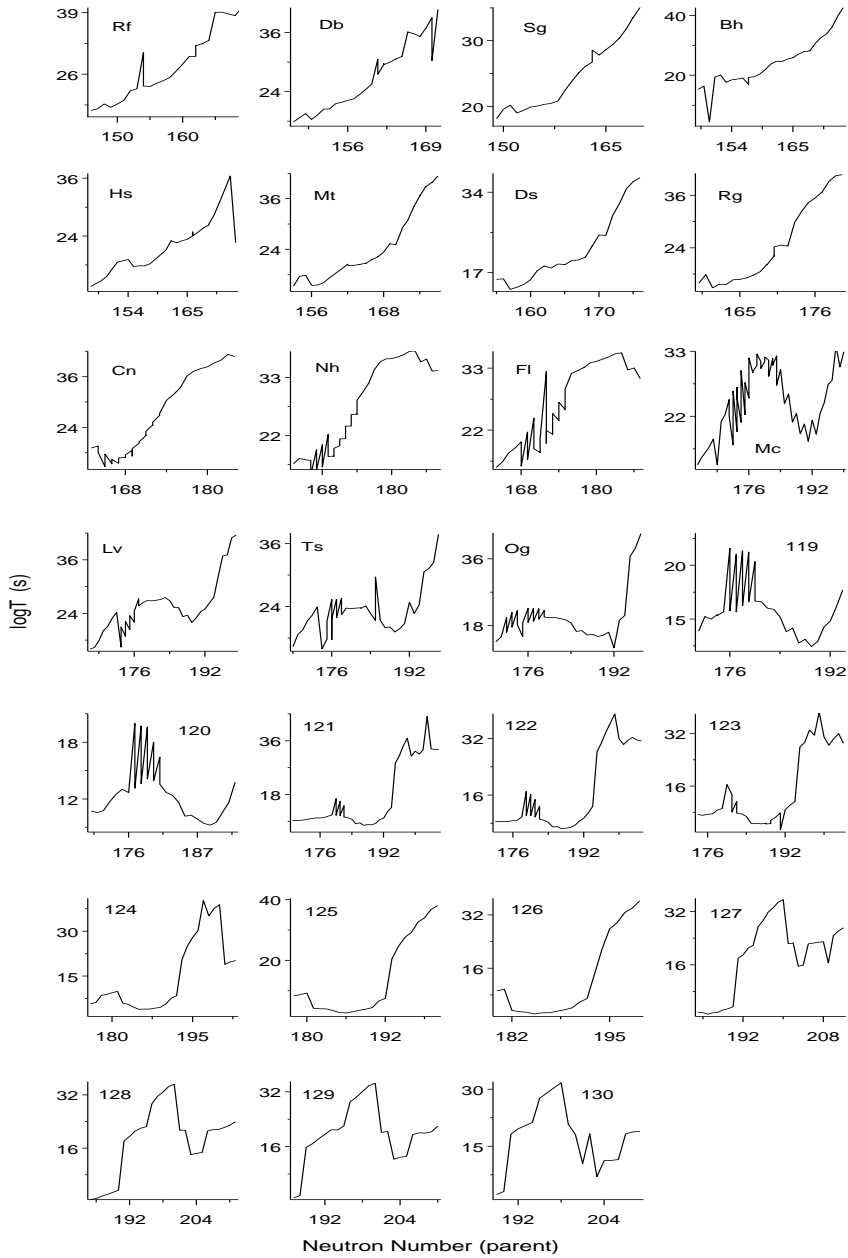


Figure 2. Variation of logarithmic half-lives with neutron number of parent nuclei.

Systematics of ^{12}C Emission from Superheavy Nuclei

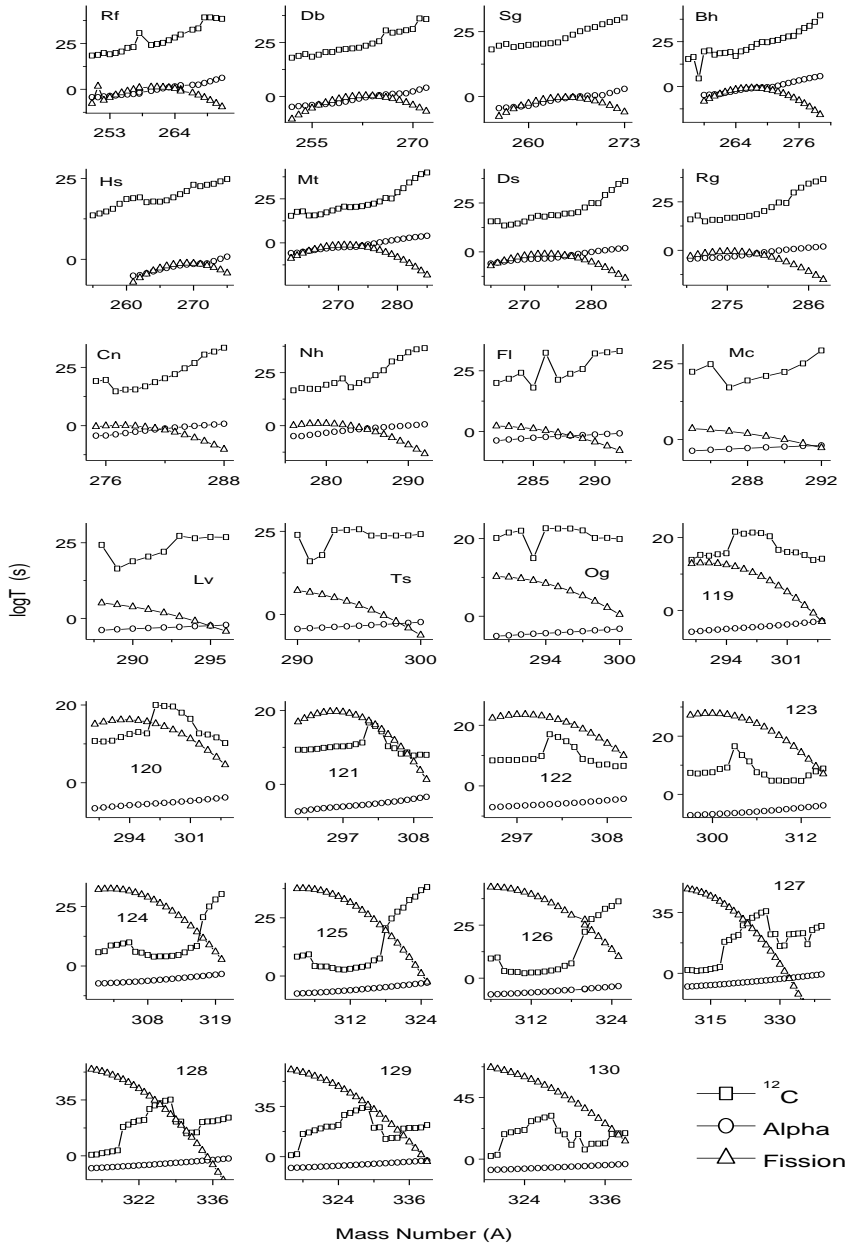


Figure 3. Comparison of logarithmic half-lives of ^{12}C decay with that of alpha decay and spontaneous fission. ^{258}Rf , ^{286}Fl , $^{297}\text{120}$, $^{301}\text{121}$, $^{301}\text{122}$, $^{303}\text{123}$.

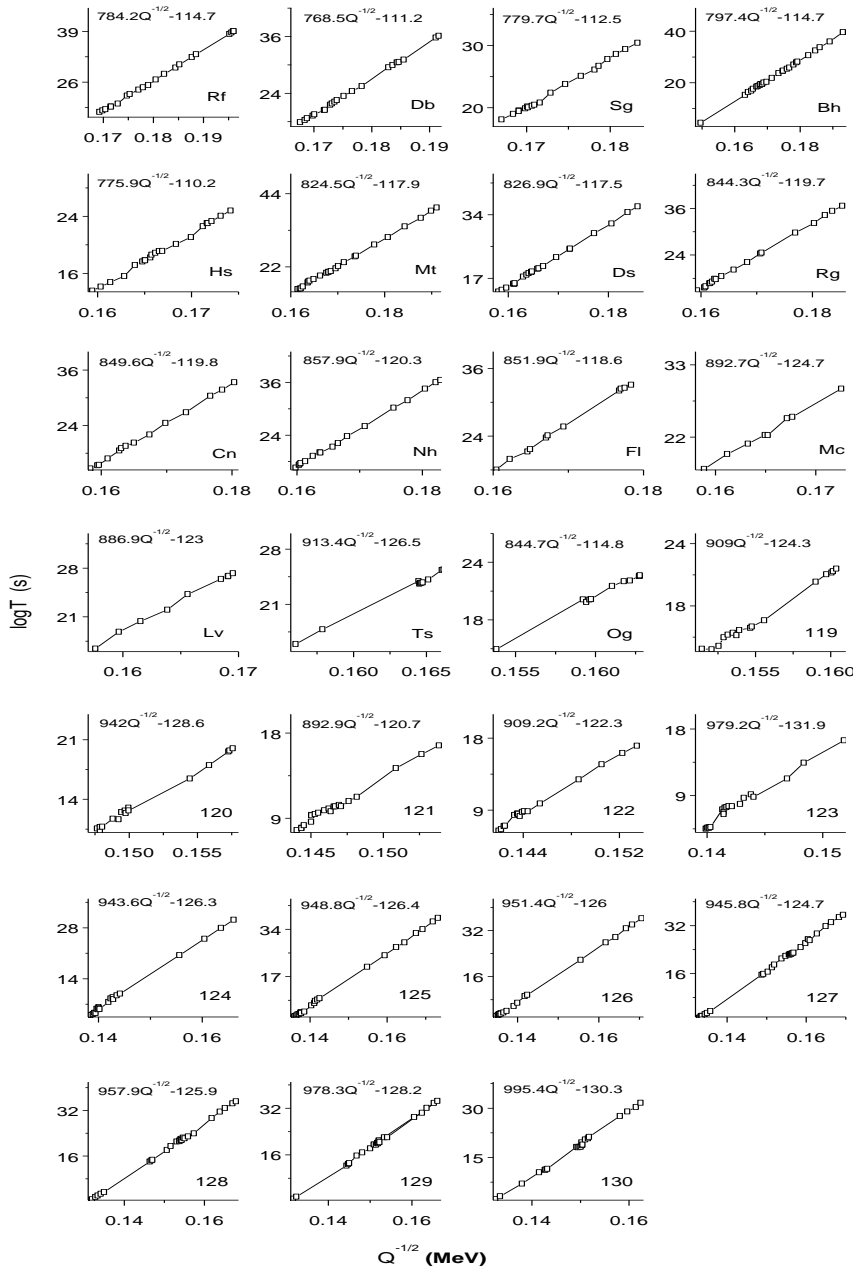


Figure 4. Variation of logarithmic ^{12}C decay half-lives with $Q^{-1/2}$ (MeV).

Systematics of ^{12}C Emission from Superheavy Nuclei

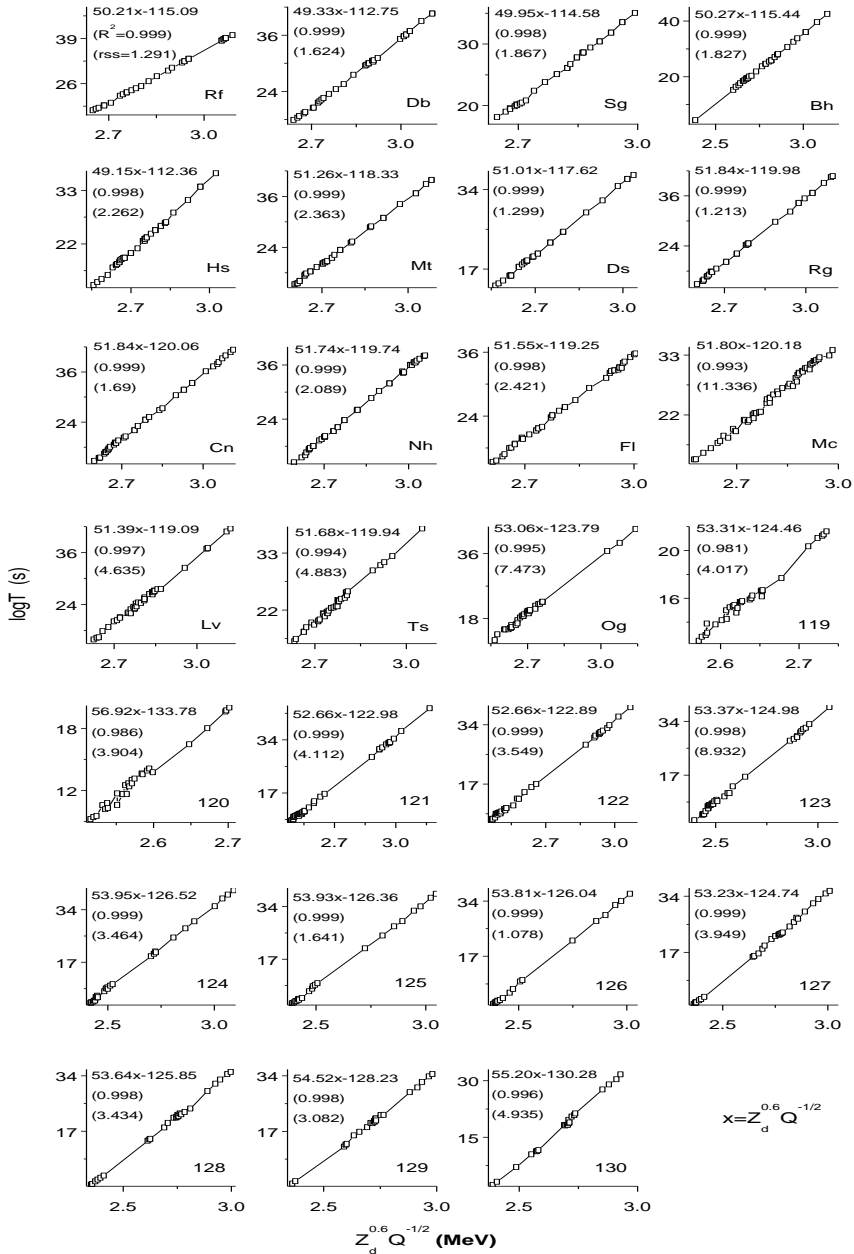


Figure 5. Variation of logarithmic of ^{12}C decay half-lives with $Z_d^{0.6} Q^{-1/2}$.

Table 2. Comparison of calculated branching ratios between alpha and cluster radioactivity with that of the experiments (Ref. [53]).

Emitter	Cluster	Detection	Branching ratios	
		System (Ref. [53])	Experiment (Ref. [53])	Present work
^{221}Fr	^{14}C	BP1 (Ref. [53])	$(8.14 \pm 1.14)10^{-13}$	9.6×10^{-13}
^{221}Ra	^{14}C	BP1 (Ref. [53])	$(1.15 \pm 0.91)10^{-12}$	1.93×10^{-12}
^{222}Ra	^{14}C	BP1 (Ref. [53])	$(3.7 \pm 0.6)10^{-10}$	3.94×10^{-10}
^{222}Ra	^{14}C	POLY (Ref. [53])	$(3.1 \pm 1.0)10^{-10}$	3.293×10^{-10}
^{222}Ra	^{14}C	SOLENO (Ref. [53])	$(2.3 \pm 0.3)10^{-10}$	2.63×10^{-10}
^{223}Ra	^{14}C	SOLENO (Ref. [53])	$(8.5 \pm 2.5)10^{-10}$	10.94×10^{-10}
^{223}Ra	^{14}C	E X Δ E (Ref. [53])	$(5.5 \pm 2.0)10^{-10}$	6.97×10^{-10}
^{223}Ra	^{14}C	SOLENO (Ref. [53])	$(7.6 \pm 3.0)10^{-10}$	9.74×10^{-10}
^{223}Ra	^{14}C	E X Δ E (Ref. [53])	$(6.1 \pm 1.0)10^{-10}$	7.13×10^{-10}
^{223}Ra	^{14}C	POLY (Ref. [53])	$(4.7 \pm 1.3)10^{-10}$	5.61×10^{-10}
^{223}Ra	^{14}C	SPLIT-POLE (Ref. [53])	$(6.4 \pm 0.4)10^{-10}$	7.13×10^{-10}
^{223}Ra	^{14}C	SOLENO (Ref. [53])	$(7.0 \pm 0.4)10^{-10}$	7.41×10^{-10}
^{223}Ra	^{14}C	SOLENO (Ref. [53])	$(8.9 \pm 0.4)10^{-10}$	8.91×10^{-10}
^{224}Ra	^{14}C	SOLENO (Ref. [53])	$(4.3 \pm 1.2)10^{-11}$	5.53×10^{-11}
^{224}Ra	^{14}C	POLY (Ref. [53])	$(6.5 \pm 1.0)10^{-11}$	6.63×10^{-11}
^{225}Ac	^{14}C	SOLENO (Ref. [53])	$(6.0 \pm 1.3)10^{-12}$	7.15×10^{-12}
^{225}Ac	^{14}C	BP1 (Ref. [53])	$(4.5 \pm 1.4)10^{-12}$	5.16×10^{-12}
^{226}Ra	^{14}C	BP1 (Ref. [53])	$(3.2 \pm 1.6)10^{-11}$	4.23×10^{-11}

also included the residual sum of squares (RSS) and coefficient of determination (R^2). The studied systematics of ^{12}C emission in superheavy nuclei with $Z = 104\text{--}130$ is important in the field of superheavy element.

References

- [1] K.P. Santhosh, B. Priyanka (2014) *Nucl. Phys. A* **929** 20.
- [2] H.C. Manjunatha (2016) *Nucl. Phys. A* **945** 4.
- [3] A.I. Budaca R. Budaca I. Silisteanu (2016) *Nucl. Phys. A* **951** 60.
- [4] K.P. Santhosh C. Nithya (2018) *At. Data Nucl. Data Tables* **119** 33.
- [5] K.P. Santhosh, Sabina Sahadevan, B. Priyanka, M.S. Unnikrishnan (2012) *Nucl. Phys. A* **882** 49.
- [6] X. Bao, H. Zhang, H. Zhang, G. Royer, J. Li (2014) *Nucl. Phys. A* **921** 85.
- [7] Y.L. Zhang, Y.Z. Wang (2017) *Nucl. Phys. A* **966** 102.
- [8] I. Silişteanu, I. Budaca (2012) *At. Data Nucl. Data Tables* **98** 1096.
- [9] D. Ni, Z. Ren (2015) *Ann. Phys.* **358** 108.
- [10] D.N. Poenaru, D. Schnabel, W. Greiner (1991) *At. Data Nucl. Data Tables* **48** 231.
- [11] J. Dong, W. Zuo, J. Gu, Y. Wang, B. Peng (2010) *Phys. Rev. C* **81** 064309.
- [12] D. Ni, Z. Ren (2011) *Phys. Rev. C* **83** 014310.
- [13] D. Ni, Z. Ren, T. Dong, Y. Qian (2013) *Phys. Rev. C* **87** 024310.

Systematics of ^{12}C Emission from Superheavy Nuclei

- [14] K.P. Santhosh, C. Nithya (2016) *Phys. Rev. C* **94** 054621.
- [15] C. Xu, Z. Ren, Y. Guo (2008) *Phys. Rev. C* **78** 044329.
- [16] Y. Ren, Z. Ren (2012) *Phys. Rev. C* **85** 044608.
- [17] Y. Qian, Z. Ren, D. Ni (2011) *Phys. Rev. C* **83** 044317.
- [18] D.N. Poenaru, I.-H. Plonski, W. Greiner (2006) *Phys. Rev. C* **74** 014312.
- [19] Madhubrata Bhattacharya, G. Gangopadhyay (2008) *Phys. Rev. C* **77** 047302.
- [20] Y. Qian, Z. Ren (2011) *Phys. Rev. C* **84** 064307.
- [21] M. Ismail, A.Y. Ellithi, M.M. Botros, A. Adel (2010) *Phys. Rev. C* **81** 024602.
- [22] Y.K. Gambhir, A. Bhagwat, M. Gupta, Arun K. Jain (2003) *Phys. Rev. C* **68** 044316.
- [23] Y. Qian, Z. Ren (2013) *Phys. Rev. C* **88** 044329.
- [24] X. Dong Sun, P. Guo, X. Li (2016) *Phys. Rev. C* **94** 024338.
- [25] M. Ismail, A. Adel (2014) *Phys. Rev. C* **89** 034617.
- [26] H.F. Zhang, G. Royer (2008) *Phys. Rev. C* **77** 054318.
- [27] G.L. Zhang, X.Y. Le, H.Q. Zhang (2009) *Phys. Rev. C* **80** 064325.
- [28] W.M. Seif (2015) *Phys. Rev. C* **91** 014322.
- [29] H.F. Zhang, G. Royer, J.Q. Li (2011) *Phys. Rev. C* **84** 027303.
- [30] M. Warda, A. Zdeb, L.M. Robledo (2018) *Phys. Rev. C* **98** 041602(R).
- [31] K. Wei, H.F. Zhang (2017) *Phys. Rev. C* **96** 021601(R).
- [32] Y.L. Zhang, Y.Z. Wang (2018) *Phys. Rev. C* **97** 014318.
- [33] R.K. Gupta, S. Dhaulta, R. Kumar, M. Balasubramaniam (2003) *Phys. Rev. C* **68** 034321.
- [34] D.N. Poenaru, R.A. Gherghescu, W. Greiner (2011) *Phys. Rev. Lett.* **107** 062503.
- [35] M. Warda, L.M. Robledo (2011) *Phys. Rev. C* **84** 044608.
- [36] B.D.C. Kimene Kaya, S.M. Wyngaardt, T.T. Ibrahim, W.A. Yahya (2018) *Phys. Rev. C* **98** 044308.
- [37] G. Sawhney, A. Kaur, M.K. Sharma, R.K. Gupta (2015) *Phys. Rev. C* **92** 064303.
- [38] D.N. Poenaru, R.A. Gherghescu, W. Greiner (2006) *Phys. Rev. C* **73** 014608.
- [39] BirBikram Singh, S.K. Patra, R.K. Gupta (2010) *Phys. Rev. C* **82** 014607.
- [40] Y.Z. Wang, J.P. Cui, Y.L. Zhang, S. Zhang, J.Z. Gu (2017) *Phys. Rev. C* **95** 014302.
- [41] D. Ni, Z. Ren, T. Dong, C. Xu (2008) *Phys. Rev. C* **78** 044310.
- [42] K.P. Santhosh, C. Nithya (2018) *Phys. Rev. C* **97** 064616.
- [43] Y. Qian, Z. Ren, D. Ni (2013) *Phys. Rev. C* **87** 054323.
- [44] D.N. Poenaru, R.A. Gherghescu (2018) *Phys. Rev. C* **97** 044621.
- [45] G. Sawhney, A. Kaur, M.K. Sharma, R.K. Gupta (2015) *Phys. Rev. C* **92**, 064303.
- [46] E. Shin, Y. Lim, C. Ho Hyun, Y. Oh (2016) *Phys. Rev. C* **94** 024320.
- [47] D.N. Poenaru, W. Greiner, M. Ivaşcu, D. Mazilu, and I.-H. Plonski (1986) *Z. Phys. A: At. Nucl.* **325** 435.
- [48] W.D. Myers, W.J. Świątecki (1966) *Nucl. Phys.* **81** 1.
- [49] P. Möller, J.R. Nix, W.D. Myers, W.J. Świątecki (1995) *At. Data Nucl. Data Tables* **59** 185.
- [50] W.D. Myers, W.J. Świątecki (2000) *Phys. Rev. C* **62** 044610b.
- [51] J. Blocki, W.J. Świątecki (1981) *Ann. Phys. (NY)* **132** 53.
- [52] H. Geiger, J.M. Nuttall (1911) *Phil. Mag.* **22** 613.
- [53] R. Bonetti, A. Guglielmetti (2007) *Rom. Rep. Phys.* **59** 301.



Competition between binary fission, ternary fission, cluster radioactivity and alpha decay of ^{281}Ds

N. Sowmya^{1,2} · H. C. Manjunatha¹ · N. Dhananjaya² · A. M. Nagaraja^{1,3}

Received: 10 April 2019

© Akadémiai Kiadó, Budapest, Hungary 2019

Abstract

The competition between different decay modes such as binary fission, ternary fission, cluster and alpha decay modes finds an important role in the synthesis of superheavy nuclei. The nuclei ^{281}Ds is the most stable among the isotopes of Ds. We have studied the different decay modes in superheavy nuclei ^{281}Ds . It is observed that alpha decay half-lives are smaller compared to other modes. The alpha decay mode of ^{281}Ds is observed with greater probability compared to binary fission.

Keywords Superheavy nuclei · Alpha decay · Cluster decay · Fission

Introduction

The quest for superheavy element started in the decades of 1930's. These superheavy elements which are rich in protons splits into fission fragments by different decay modes. In most of the cases superheavy element undergoes decay through alpha decay and spontaneous fission [1–3]. In addition to alpha and binary fission, superheavy nuclei undergo cluster radioactivity and ternary fission [4–7]. Even though the probability of ternary fission small compared to other decay modes, but it is successfully observed in experiments. Oganessian and Utyonkov [8] synthesised $Z = 113–118$ using calcium induced reactions. Mirea et al. [9] studied different disintegration modes such as spontaneous fission, cluster emission and alpha decay from the parent nuclei radium. Xu et al. [10, 11] theoretically studied the competition between alpha decay and spontaneous fission in superheavy elements. Earlier workers [12, 13] synthesised superheavy element $Z = 112, 114$ using fusion of high intense calcium beam with lead. Hofmann et al. [14] investigated an alpha decay chains of ^{269}Ds . Ninov et al. [15] experimentally

synthesised $Z = 118$ by the fusion of lead with krypton ions. Earlier workers also studied the different decay modes of superheavy nuclei [16–23]. Superheavy nuclei are synthesised after recognising its dominant decay mode. Hence, it is important to identify the dominant decay channel for the superheavy nuclei. The dominant decay mode can be identified by studying the competition between different possible decay modes such as binary fission, ternary fission, cluster and alpha decay. Hence in the present work, we have identified the dominant decay mode of ^{281}Ds . To identify the most dominant decay mode, we studied half-lives of different decay modes such as binary fission, ternary fission, cluster and alpha decay in ^{281}Ds . We also studied branching ratios of the different decay modes.

Theoretical framework

(a) Cluster and alpha decay

The decay half-life of parent nuclei during the emission of cluster and alpha particle is studied by [24]

$$T_{1/2} = \frac{\ln 2}{\lambda} = \frac{\ln 2}{\nu P} \quad (1)$$

where λ is the decay constant and ν is the assault frequency. The penetration probability P through the potential barrier studied by the following equation [24]

✉ H. C. Manjunatha
manjunathhc@rediffmail.com

¹ Department of Physics, Government College for Women, Kolar, Karnataka 563101, India

² Department of Physics, BMSIT&M, Affiliated to VTU, Bangalore, India

³ Department of Physics, St. Joseph's College, Affiliated to Bharathidasan University, Tiruchirapalli 620002, India

$$P = \exp \left\{ -\frac{2}{\hbar} \int_{R_a}^{R_b} \sqrt{2\mu(V_T(r) - Q)} dr \right\} \quad (2)$$

The total interacting potential is the sum of nuclear, coulomb and centripetal potential, where

$$V_T(r) = V_N(r) + V_C(r) + V_l(r) \quad (3)$$

where $V_N(r)$ is the nuclear potential, $V_C(r)$ is the Coulomb potential and $V_l(r)$ is the centrifugal potential. These potentials are calculated as suggested from the previous workers [25, 26]. The universal proximity potential is given by [27]

$$\Phi(\varepsilon) = \begin{cases} -1.7817 + 0.9270\varepsilon + 0.143\varepsilon^2 - 0.09\varepsilon^3 & \text{for } \varepsilon \leq 0.0, \\ -1.7817 + 0.9270\varepsilon + 0.0169\varepsilon^2 - 0.05148\varepsilon^3 & \text{for } 0 \leq \varepsilon \leq 1.9475, \\ -4.41 \exp\left(\frac{-\varepsilon}{0.7176}\right) & \text{for } \varepsilon \geq 1.9475 \end{cases} \quad (4)$$

where $\varepsilon = s/b$, is the minimum separation between fission fragments and $b \approx 0.99$ and s is the distance between the near surfaces of the fragments, where s is determined by [24].

$$s = r - C_1 - C_2 \text{ fm.} \quad (5)$$

(b) *Binary and ternary fission* To study the binary and ternary fission the coulomb potential is taken as

$$V_C(R) = \frac{Z_i Z_j e^2}{r_{ij}} \quad (6)$$

$$\Phi(\varepsilon) = \begin{cases} -4.41 \exp\left(\frac{-\varepsilon}{0.7176}\right) & \text{for } 0 \leq \varepsilon \leq 1.9475 \\ -1.7817 + 0.9270\varepsilon + 0.0169\varepsilon^2 - 0.05148\varepsilon^3 & \text{for } 0 \leq \varepsilon \leq 1.9475 \end{cases} \quad (12)$$

here Z_i and Z_j are the atomic numbers of the products and r_{ij} is the distance between spherical fragments. The nuclear potential $V_N(r)$ between fission fragments is given by [28].

$$V_N(r) = 4\pi\gamma\bar{R}\Phi(\varepsilon) \quad (7)$$

The nuclear potential intern depends upon geometry and shape of the nuclei and universal function $\Phi(\varepsilon)$. \bar{R} is the mean curvature as

$$\bar{R} = \frac{C_1 C_2}{C_1 + C_2} \quad (8)$$

The Sussmann central radii C_i of the products related to sharp radii R_i is expressed as

$$C_i = R_i - \left(\frac{b^2}{R_i}\right) \quad (9)$$

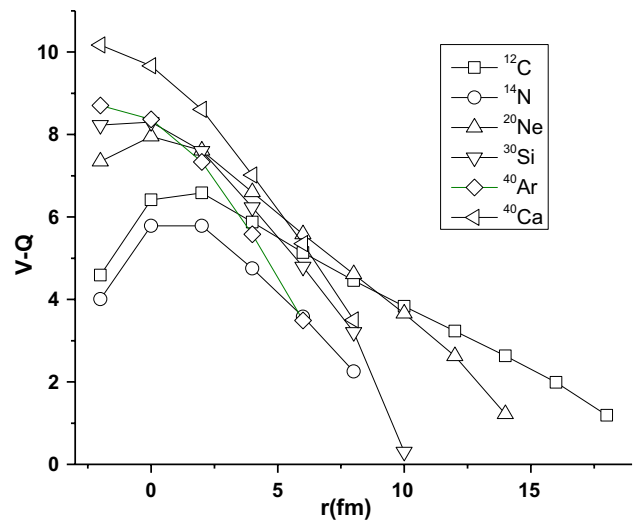


Fig. 1 Variation of driving potential with respect to distance between cluster fission fragments

where R_i is given by

$$R_i = 1.28A_i^{1/3} - 0.76 + 0.8A_i^{-1/3} \quad (10)$$

and surface energy coefficient γ is as follows

$$\gamma = \gamma_0 \left[1 - K_s \left(\frac{N-Z}{A} \right)^2 \right] \text{ MeV/fm}^2 \quad (11)$$

where $\gamma_0 = 1.460734 \text{ MeV/fm}^2$ and $K_s = 4.0$ [29].

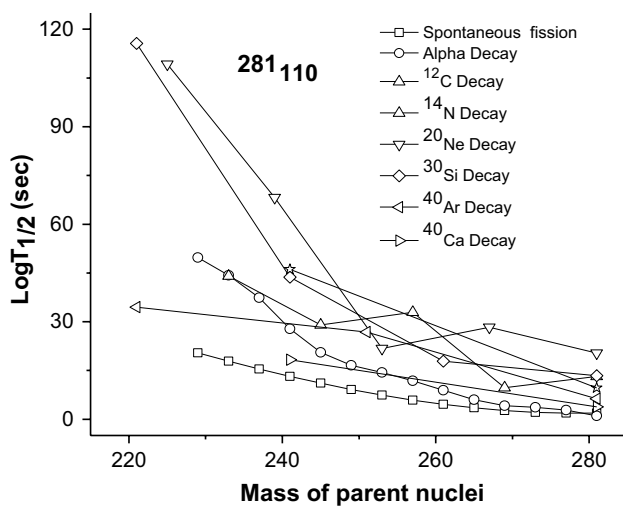
The nuclear proximity potential is given by [27]

Results and discussions

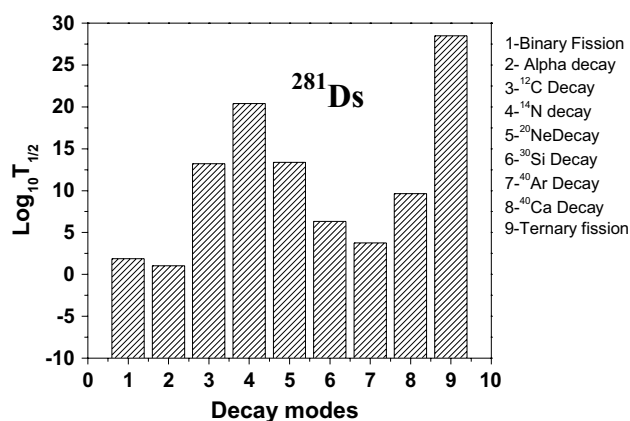
We systematically studied different decay modes in ^{281}Ds . The total interaction potential between the fragments using different decay modes is calculated by the sum of coulomb, nuclear proximity and centrifugal potential. The value of angular momentum from ground state to ground state is taken to be minimum ($l = l_{\min}$) which leads to minimum centrifugal potential. The amount of energy released during different decay modes is studied using mass excess values [30–33]. The driving potential is the difference between total potential and amount of energy released. Figure 1 gives the variation of driving potential with the distance between the two fragments. The calculated half-lives of

Table 1 Comparison of half lives and branching ratio's with different decay modes such as binary, ternary, cluster radioactivity with that of alpha decay

Different decay modes in ^{281}Ds	Log ($T_{1/2}$)	Branching ratio	
Alpha decay	1.022	—	—
C-12	13.203	$\lambda_\alpha/\lambda_{CR}$	6.96E+00
N-14	20.381		2.83E+27
Ne-20	13.371		1.52E+12
Si-30	6.321		2.29E+19
Ar-40	3.796		2.23E+12
Ca-40	9.623		1.99E+05
Ternary fission	28.474	$\lambda_\alpha/\lambda_{TF}$	5.94E+02
Binary fission	1.865	$\lambda_\alpha/\lambda_{SF}$	3.99E+08

**Fig. 2** Variation of logarithmic half-lives with respect to mass number of parent nuclei

different decay modes in ^{281}Ds and branching ratios of different decay modes [21] is tabulated as shown in Table 1. The comparison of alpha decay half lives with other three decay half lives shows that alpha decay half lives are having smaller value compared to others. It is observed from calculation that alpha decay half-life is 1.022 s and spontaneous fission logarithmic half-life is 1.865 s. That is half-lives of alpha decay and spontaneous fission are close (difference ≈ 0.843 s). The decay chains of different decay modes such as binary, ternary, alpha decay and cluster radioactivity (^{12}C , ^{14}N , ^{20}Ne , ^{30}Si , ^{40}Ar and ^{40}Ca) for ^{281}Ds is as shown

**Fig. 3** A comparison of logarithmic half-lives among the studied decay modes (binary, ternary, alpha decay and cluster radioactivity such as ^{12}C , ^{14}N , ^{20}Ne , ^{30}Si , ^{40}Ar and ^{40}Ca) for ^{281}Ds

in Fig. 2. This figure enables to identify the decay mode for each nuclei. The nuclei ^{281}Ds undergoes alpha decay with termination into Hs, Sg, Rf, No, Fm, Cf, Cm, Pu, U, Th, Ra and so on. We have calculated percentage of yield to identify the maximum probability of different decay modes. Figure 3 gives the comparison of logarithmic half-lives with respect to different decay modes and observed minimum logarithmic half-lives for alpha decay. The detail investigations of logarithmic half-lives, barrier penetrability and decay constant during the emission of different clusters from ^{281}Ds is given in Table 2. The superheavy nuclei is detected through the energy released during the decay and corresponding decay chains of the compound nuclei. The energy released during the decay is measured by identifying the specific decay mode. The dominant decay mode is identified by studying the competition between the different decay modes such as binary fission, ternary fission, cluster and alpha decay. Thus the study of competition between the different decay modes plays important role in the synthesis of superheavy nuclei.

Conclusions

We have systematically studied different decay modes such as spontaneous, ternary, cluster radioactivity and alpha decay in ^{281}Ds . The comparison of different decay half-lives imparts alpha decay half-lives are smaller than other decay modes. The detail study of half-lives and branching ratio results in most dominant decay mode in ^{281}Ds . The

Table 2 The characteristics cluster decay during the emission of $^{12,14}\text{C}$, ^{14}N , $^{20,22,24}\text{Ne}$, $^{28,30,32,34}\text{Si}$, $^{36,38,40,42,44}\text{Ar}$, $^{40,42,44,46,48}\text{Ca}$ from the ^{281}Ds

Parent nuclei	Emitted cluster	Daughter nuclei	Q value (MeV)	Penetrability P	Decay constant λ	$T_{1/2}(S)$
^{281}Ds	^4He	^{277}Hs	9.5718	$2.54\text{E}-22$	$6.58\text{E}-02$	$1.05\text{E}+01$
	^{12}C	^{269}Rf	33.6990	$1.98\text{E}-31$	$1.81\text{E}-10$	$3.83\text{E}+09$
	^{14}C	^{267}Rf	34.735	$4.55\text{E}-30$	$4.28\text{E}-09$	$1.62\text{E}+08$
	^{14}N	^{267}Lr	35.776	$5.76\text{E}-38$	$5.58\text{E}-17$	$1.24\text{E}+16$
	^{20}Ne	^{261}Fm	59.021	$9.28\text{E}-35$	$1.48\text{E}-13$	$4.67\text{E}+12$
	^{22}Ne	^{259}Fm	64.297	$1.91\text{E}-30$	$3.32\text{E}-09$	$2.08\text{E}+08$
	^{24}Ne	^{257}Fm	69.412	$8.08\text{E}-27$	$1.52\text{E}-05$	$4.56\text{E}+04$
	^{28}Si	^{253}Cm	88.702	$1.35\text{E}-32$	$3.25\text{E}-11$	$2.13\text{E}+10$
	^{30}Si	^{251}Cm	98.744	$1.29\text{E}-26$	$3.44\text{E}-05$	$2.01\text{E}+04$
	^{32}Si	^{249}Cm	104.29	$7.45\text{E}-23$	0.210307	$3.29\text{E}+00$
	^{34}Si	^{247}Cm	105.382	$3.68\text{E}-22$	$2.85\text{E}+21$	$6.59\text{E}-01$
	^{36}Ar	^{245}U	111.711	$7.25\text{E}-34$	$2.19\text{E}-12$	$3.16\text{E}+11$
	^{38}Ar	^{243}U	122.924	$4.33\text{E}-28$	$1.44\text{E}-06$	$4.80\text{E}+05$
	^{40}Ar	^{241}U	129.802	$2.21\text{E}-24$	0.007756	$8.92\text{E}+01$
	^{42}Ar	^{239}U	134.808	$1.78\text{E}-22$	0.648832	$1.07\text{E}+00$
	^{44}Ar	^{237}U	139.99	$1.77\text{E}-20$	67.08587	$1.03\text{E}-02$
	^{40}Ca	^{241}Th	122.215	$2.93\text{E}-34$	$9.71\text{E}-13$	$7.13\text{E}+11$
	^{42}Ca	^{239}Th	128.995	$6.83\text{E}-31$	$2.38\text{E}-09$	$2.90\text{E}+08$
	^{44}Ca	^{237}Th	135.603	$2.8\text{E}-28$	$1.03\text{E}-06$	$6.72\text{E}+05$
	^{46}Ca	^{235}Th	141.55	$1.49\text{E}-25$	0.000572	$1.21\text{E}+03$
^{48}Ca	^{233}Th	156.44	$6.21\text{E}-19$	2628.812	$2.63\text{E}-04$	

detail study of different decay modes reveals that the alpha decay leads spontaneous fission process by 0.843 s and it is also observed with greater probability compared to binary fission.

References

- Petrjak KA, Flerov GN (1940) Spontaneous fission of uranium. *Phys Rev* 58:89
- Pansaers JK (1896) *Table des comptes-rendus*. Paris 122:420
- Rutherford E (1904) Disintegration of the radioactive elements. *Harper's Mon Mag* 108:279–284
- San Tsiang T, Zah-Wel H, Vigneron L, Chastel R (1947) Ternary and quaternary fission of uranium nuclei. *Nature* 159:773–774
- San-Tsiang T (1947) Sur la bipartition et la tripartition des éléments lourds. *J Phys Radium* 8:165–178
- Greiner M, Scheid W, Oberacker V (1988) Coulomb-induced α decay and cluster emission within the superasymmetric fission model for the collision of ^{238}U on ^{238}U . *J Phy G* 14:589
- Rose HJ, Jones GA (1984) A new kind of natural radioactivity. *Nature* 307:245
- Oganessian YT, Utyonkov VK (2015) Superheavy nuclei from ^{48}Ca -induced reactions. *Nucl Phys A* 944:62–98
- Mirea M, Budaca R, Sandulescu A (2017) Spontaneous fission, cluster emission and alpha decay of ^{222}Ra in a unified description. *Ann Phys* 380:154–167
- Xu C, Zhang X, Ren Z (2013) Stability of superheavy nuclei against α -decay and spontaneous fission. *Nucl Phys A* 898:24–31
- Zhang YL, Wang YZ (2017) Systematic study on the competition between α -decay and spontaneous fission of superheavy nuclei. *Nucl Phys A* 966:102–112
- Oganessian YT, Yeremin AV, Popeko AG, Bogomolov SL et al (1991) Synthesis of nuclei of the superheavy element 114 in reactions induced by ^{48}Ca . *Nature* 400(6741):242
- Oganessian YT, Yeremin AV, Gulbekian GG, Bogomolov SL et al (1999) Search for new isotopes of element 112 by irradiation of ^{238}U with ^{48}Ca . *Eur Phys J A-Hadron Nucl* 5(1):63–68
- Hofmann S, Ninov V, Heffberger FP, Armbruster P (1995) Production and decay of ^{269}Ds . *Z Phys A* 350:277–280
- Ninov V, Gregorich KE, Loveland W, Ghiorso A et al (1999) Observation of superheavy nuclei produced in the reaction of ^{86}Kr with ^{208}Pb . *Phys Rev Lett* 83(6):1104
- Fiset EO, Nix JR (1972) Calculation of half-lives for superheavy nuclei. *Nucl Phys A* 193:641–671
- Manjunatha HC (2016) Theoretical prediction of probable isotopes of superheavy nuclei of $Z=122$. *Int J Mod Phys E* 25(11):1–20, 1650100
- Manjunatha HC (2016) Comparison of alpha decay with fission for isotopes of superheavy nuclei $Z=124$. *Int J Mod Phys E* 25(9):1–11, 1650074
- Manjunatha HC (2016) Alpha decay properties of superheavy nuclei $Z=126$. *Nucl Phys A* 945:42–57
- Manjunatha HC, Sowmya N, Sridhar KN, Seenappa L (2017) A study of probable alpha-ternary fission fragments of ^{257}Fm . *J Radioanal Nucl Chem* 314(2):991–999
- Manjunatha HC, Sowmya N (2018) Competition between spontaneous fission ternary fission cluster decay and alpha decay in the super heavy nuclei of $Z=126$. *Nucl Phys A* 969:68–82
- Manjunatha HC, Sowmya N (2018) Decay modes of superheavy nuclei $Z=124$. *Int J Mod Phys E* 27(5):1–17, 1850041

23. Manjunatha HC, Sridhar KN, Sowmya N (2018) Investigations of the synthesis of the superheavy element $Z=122$. *Phys Rev C* 98:024308
24. Daei-Ataollah A, Ghodsi ON, Mahdavi M (2018) Proximity potential and temperature effects on α -decay half-lives. *Phys Rev C* 97:054621
25. Dutt I (2011) The role of various parameters used in proximity potential in heavy-ion fusion reactions: new extension. *Pramana* 76:921–931
26. Ghodsi ON, Daei-Ataollah A (2016) Systematic study of α decay using different versions of proximity formalism. *Phys Rev C* 93:024612
27. Blocki J, Świątecki WJ (1981) A generalization of the proximity force theorem. *Ann Phys (NY)* 132:53
28. Myers WD, Świątecki WJ (1966) Nuclear masses and deformations. *Nucl Phys* 81:1
29. Dutt I, Puri RK (2010) Role of surface energy coefficients and nuclear surface diffuseness in the fusion of heavy-ions. *Phys Rev C* 81:047601
30. Koura H, Tachibana T, Uno M, Yamada M (2005) Nuclidic mass formula on a spherical basis with an improved even-odd term. *Prog Theor Phys* 113:305
31. Kowal M, Jachimowicz P, Skalski J (2012) Ground state and saddle point: masses and deformations for even-even superheavy nuclei with $98 \leq Z \leq 126$ and $134 \leq N \leq 192$. [arXiv:1203.5013](https://arxiv.org/abs/1203.5013)
32. Manjunatha HC, Chandrika BM, Seenappa L (2016) Empirical formula for mass excess of heavy and superheavy nuclei. *Mod Phys Lett A* 31(28):1650162
33. Manjunatha HC, Sowmya N (2019) Pocket formula for mass excess of nuclei range $57 < Z < 103$. *Mod Phys Lett A* 34(15):1950112

Publisher's Note Springer Nature remains neutral with regard to jurisdictional claims in published maps and institutional affiliations.

Cluster radioactivity in superheavy nuclei Z=124

H.C.Manjunatha¹, Nagaraja A.M^{1&2}, N. Sowmya^{1&3},

¹Department of Physics, Government College for Women, Kolar-563101, Karnataka,

²Department of Physics, St. Joseph's College, Tiruchirapalli-62002

³Department of Physics, BMSIT, Affiliated to VTU, Bangalore.

Email: manjunathhc@rediffmail.com

Introduction

Cluster radioactivity of superheavy elements plays an important role in the identification and synthesis of superheavy elements. In 1984 Rose and Jones [1] for the first time observed emission of ¹⁴C nucleus from ²²³Ra. Warda, et al., [2] studied cluster radioactivity in heavy and superheavy nuclei. Zachary Matheson, et al., [3] studied alpha decay properties and cluster emission in Z=118. Zhang and Wang [4] studied cluster radioactivity in the superheavy region Z=118, 120 and 122. Previous workers [5-7] studied different decay modes in superheavy nuclei Z= 122, 124 and 126. Using unified fission model and preformed cluster model [8-10] studied cluster radioactivity in actinides. From the literature studies it is clearly observed that, the study on cluster radioactivity in the superheavy region is required for the synthesis of the superheavy element and also the possible decay mode for the same. Hence in the present work we have studied cluster radioactivity of ²⁷Al, ³⁶Ar, ⁹Be, ⁴⁰Ca, ⁴²Ca, ⁴³Ca, ⁴⁴Ca, ⁴⁶Ca, ³⁵Cl, ⁴He, ³⁹K, ⁴¹K, ⁶Li, ²⁴Mg, ²⁵Mg, ²³Na, ²⁰Ne, ²²Ne, ³²S, ³³S, ³⁴S, ²⁸Si, ²⁹Si and ³⁰Si in the superheavy nuclei Z=124 and also identified possible decay mode.

Theory:

The total interacting potential is the sum of coulomb potential, proximity potential and centrifugal force and it is given as follows;

$$V(R) = V_N(R) + V_C(R) + \frac{l(l+1)\hbar^2}{2\mu \times R^2} \quad (1)$$

We have studied the total potential of the superheavy nuclei Z=124 as explained in previous work [9]. Using WKB approximation,

we have studied penetration probability and half-lives of the superheavy element Z=124. The barrier penetration probability given by

$$P = \exp \left\{ -\frac{2}{\hbar} \int_{R_a}^{R_b} \sqrt{2\mu(V_l(r) - Q)} dr \right\} \quad (2)$$

where μ is the reduced mass fission fragments of cluster decay system, R_a and R_b are the initial and final turning points. The half-lives of cluster decay is studied using the relation,

$$T_{1/2} = \frac{\ln 2}{\lambda} = \frac{\ln 2}{\nu P} \quad (3)$$

where $\nu = \frac{\omega}{2\pi} = \frac{2E_v}{h}$ represent assaults frequency

and λ is the decay constant. E_v is the empirical vibration energy.

Results and discussions:

The amount of energy released during cluster decay is given by;

$$Q = \Delta M(A, Z) - \sum_i^n \Delta M(A_i, Z_i) \quad (4)$$

where $\Delta M(A, Z)$ and $\Delta M(A_i, Z_i)$ are mass excess of the parent and for (i=1,2) for daughter nuclei and cluster nuclei respectively. The amount of energy released (Q in MeV) of a parent nuclei against different decay modes are studied using mass excess values [12]. Where ever experimental values are not available we have used the theoretical values available in the literature [13-15]. We have studied cluster radioactivity by calculating driving potential, penetration probability and half-lives in the superheavy nuclei Z=124. The driving potential is the difference between total potential and the amount of energy released. The variation of energy released and logarithmic half-lives with the mass number of cluster nuclei are as shown

in figure 1. From the figure it is observed that as mass number of cluster increases the amount of energy released and logarithmic half-lives also increases. The variation logarithmic half-lives of cluster decay such as (^{27}Al , ^{36}Ar , ^9Be , ^{40}Ca , ^{42}Ca , ^{43}Ca , ^{44}Ca , ^{46}Ca , ^{35}Cl , ^4He , ^{39}K , ^{41}K , ^6Li , ^{24}Mg , ^{25}Mg , ^{23}Na , ^{20}Ne , ^{22}Ne , ^{32}S , ^{33}S , ^{34}S , ^{28}Si , ^{29}Si and ^{30}Si) are shown in figure 2. The figure 2 depicts that the logarithmic half-lives of ^4He is less compared to all other cluster decay modes.

Fig. 1: The variation of energy released and logarithmic half-lives with the mass number of cluster nuclei.

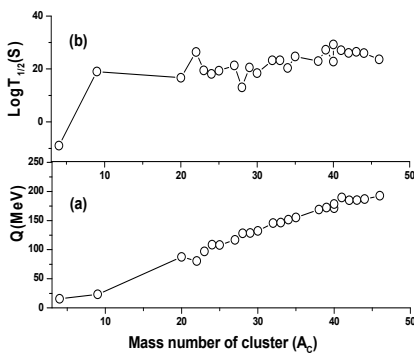
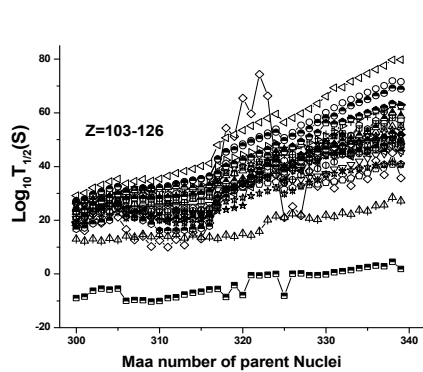


Fig. 2: The variation of logarithmic half-lives with mass number of parent nuclei.



Conclusions:

To summarize our work, we have studied the driving potential, penetration probability and cluster decay (^{27}Al , ^{36}Ar , ^9Be , ^{40}Ca , ^{42}Ca , ^{43}Ca , ^{44}Ca , ^{46}Ca , ^{35}Cl , ^4He , ^{39}K , ^{41}K , ^6Li , ^{24}Mg , ^{25}Mg , ^{23}Na , ^{20}Ne , ^{22}Ne , ^{32}S , ^{33}S , ^{34}S ,

^{28}Si , ^{29}Si and ^{30}Si) half-lives of superheavy nuclei $Z=124$. From the study of cluster decay half-lives, we observed that alpha decay half-lives are smaller compared to other exotic decay modes. Hence the SHE $Z=124$ undergoes alpha decay only.

References

[1] H. J. Rose and G. A. Jones, Nature 307, 245 (1984).
 [2] M. Ward A. Zdeb, and L. M. Robledo Phys. Rev. C 98, 041602(R) (2018).
 [3] Zachary Matheson, Samuel A. Giuliani, et al., Phys. Rev. C 99, 041304(2019).
 [4] Y. L. Zhang and Y. Z. Wang. Phys. Rev. C 97, 014318 (2018).
 [5] H. C. Manjunatha, K. N. Sridhar, N. Sowmya, Phys. Rev. C 98, 024308 (2018).
 [6] H. C. Manjunatha and N. Sowmya International Journal of Modern Physics E 27, 05, 1850041 (2018)
 [7] H.C.Manjunatha and N.Sowmya Nuclear Physics A Volume 969,(2018).
 [8] Raj K. Gupta and Walter Greiner International Journal of Modern Physics E 03, 1, 335-433 (1994).
 [9] R. Blendowske and H. Walliser Phys. Rev. Lett. 61, 1930 (1988).
 [10] H. F. Zhang, J. M. Dong, et al., Phys. Rev. C 80, 037307 (2009).
 [11] <https://www-nds.iaea.org/RIPL-3>.
 [12] P. Möller, A.J. Sierk, T. Ichikawa, H. Sagawa At. Dat. Nucl. Dat. Tables 109 1(2016).
 [58] H.C. Manjunatha, B.M. Chandrika, L. Seenappa, Mod. Phys. Lett. A 31, 28, 1650162 (2016).
 [59] M. Wang, G. Audi, A. H. Wapstra, F. G. Kondev, et al., Chin. Phys. C 36 1603(2012).
 [60] H. C. Manjunatha, N. Sowmya Modern Physics Letters A 34 (15) 1950112 (2019).

Study of heavy particle radioactivity of $^{294}118$

A.M.Nagaraja^{1&2}, N. Sowmya^{1*}, H.C. Manjunatha^{1*}, P.S.Damodara Gupta¹,
S.Alfred Cecil Raj²

¹Department of Physics, Government College for Women, Kolar, Karnataka, India.

²Department of Physics, St.Joseph's college (Autonomous), Affiliated to Bharathidasan University,
Tiruchirappalli-620002

Corresponding Author: manjunathhc@rediffmail.com, sowmyaprakash8@gmail.com

Introduction

In heavy-particle radioactivity, emitted particles may have atomic number $Z_e > 28$ and $Z_e^{\max} = Z - 82$. Poenaru and Gherghescu [1] observed shorter half-lives and a larger branching ratios for heavy particle emission from superheavy elements. Nagaraja et al., [2] also identified heavy particle radioactivity from superheavy element $Z=126$ under modified generalised liquid drop model formalism. The logarithmic half-lives of HPR are calculated using eight different proximity functions, these are compared to experimental results. The Coulomb and proximity potential models have been used [3] to investigate the feasibility of alpha decay and heavy particle decay from even-even superheavy nuclei with $Z = 116-124$. A comparison of their predicted half lives with that of empirical formulas shows good agreement.

The Coulomb and proximity potential models were also used [4] to study cluster radioactivity of even-even superheavy nuclei with $Z = 122-132$. Sowmya et al., [5] investigated the various decay modes of superheavy nuclei ^{281}Ds . The cluster and alpha decay half-lives of the superheavy nuclei $Z = 120$ were studied by Nagaraja et al., [6]. In the super-heavy nuclei region $^{299-306}122$, Cluster decay of He, Li, Be, Ne, N, Mg, Si, P, S, Cl, Ar, and Ca isotopes was studied by Manjunatha et al., [7]. The logarithmic half-lives of cluster decay were also compared to those of other models like Univ NRDX and Horoi. The systematics of ^{12}C emission in superheavy nuclei with $Z = 104-130$ are also studied by previous researcher [8]. There is a scope to study the heavy particle radioactivity in the nuclei with atomic number $Z=118$. Hence, the aim of the present work is to study heavy particle radioactivity in superheavy nuclei $^{294}118$.

Theoretical Frame work

The half-lives of heavy particle radioactivity in the superheavy nuclei $^{294}118$ is studied using the following equation;

$$T_{1/2} = \hbar \ln(2) / \Gamma \quad (1)$$

here Γ is the decay width and it is evaluated as follows;

$$\Gamma = \frac{1}{4\pi} \int \gamma(\theta, \phi) d\Omega \quad (2)$$

where $\gamma(\theta, \phi)$ is the partial width of heavy particle emission. The total width in terms of θ as follows;

$$\Gamma = \int_0^{\pi/2} \gamma(\theta) \sin(\theta) d\theta \quad (3)$$

here $\gamma(\theta) = \hbar \xi t(Q, \theta, \ell)$ [is the width of the heavy particle emitted in the direction of θ . The penetration probability is as follows;

$$t(Q, \theta, \ell) = \left\{ 1 + \exp \left[\frac{2}{\hbar} \int_{r_2(\theta)}^{r_3(\theta)} dr \sqrt{2\mu(V(r, \theta, \ell, Q) - Q)} \right] \right\}^{-1} \quad (4)$$

here $r_2(\theta)$ and $r_3(\theta)$ are the turning points and the total potential $V(r, \theta, \ell, Q)$ is evaluated as explained in detail in literature [9] using Ng0 proximity potential.

Results and Discussions:

The heavy particle radioactivity of a superheavy heavy nuclei $^{294}118$ is determined by taking sum of repulsive coulomb potential, attractive nuclear potential and centrifugal potential. The amount of energy released during heavy particle radioactivity is evaluated using recent mass excess values. The possibility of heavy particle emissions were considered using the condition that $Z_e^{\min} = 28$ and $Z_e^{\max} = Z - 82$ i.e the heavy particle emission from the superheavy element $Z=118$ is up to $Z=36$. The figure 1 shows the variation of amount of energy released during heavy particle radioactivity with

mass number of heavy particle emitted. From this figure it is observed that as the mass number of heavy particle increases the Q-values also increases. Which shows that the Q-values directly depend on the heavy particle emitted.

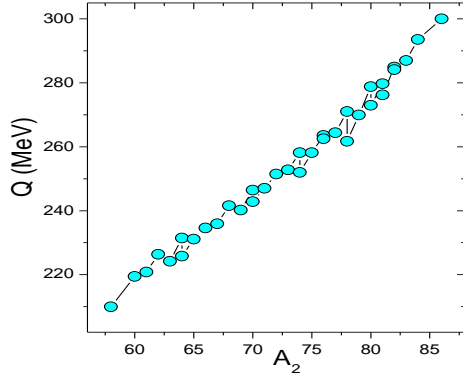


Fig 1: Variation of Q-values during heavy particle radioactivity with mass number of heavy particle emitted from the parent nuclei $^{294}118$.

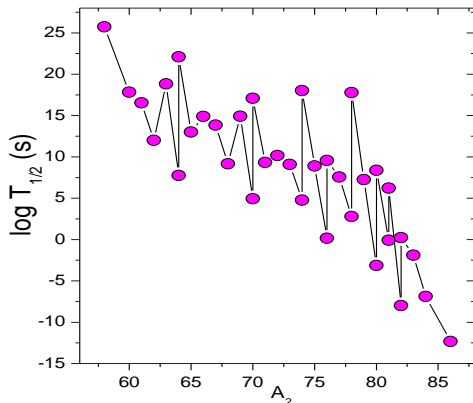


Fig 2: A plot of $\log T_{1/2}$ of heavy particle radioactivity from the parent nuclei $^{294}118$ with that of mass number of heavy particle emission.

The half-lives evaluated during cluster and heavy particle radioactivity are plotted as a function of mass number of cluster and heavy particle radioactivity and it is presented in figure 2. From this figure it is observed that the heavy particle emission of ^{86}Kr shows shorter half-lives when compared to their neighboring ones. This may be due to the shell closure effects of both daughter and heavy particle emission i.e $^{208}\text{Pb} + ^{86}\text{Kr}$ nuclei. Among which the daughter nuclei is doubly magic nuclei.

Conclusions:

The heavy particle radioactivity of superheavy element $^{294}118$ is studied using Coulomb and proximity potential model. The logarithmic half-lives of heavy particle radioactivity from $^{294}118$ is shorter for ^{86}Kr emission. The corresponding daughter nuclei is ^{208}Pb . Shorter half-lives due to doubly magic nuclei ^{208}Pb ($Z=82, N=126$). This study finds an important role in the identification of decay mode of superheavy element $Z=118$.

References

- [1] D. N. Poenaru, R. A. Gherghescu. Phys. Rev. Lett.. 107.062503 (2021).
- [2] A.M.Nagaraja, H.C.Manjunatha, N.Sowmya, L.Seenappa, P.S.Damodara Gupta, N.Manjunatha S. Alfred CecilRaj. Nucl. Phys. A. 1015, 122306 (2021).
- [3]K.P.Santhosh B.Priyanka. Nucl. Phys. A. 929 , 20-37 (2014).
- [4] K.P. Santhosh, InduSukumaran. Can.J. Phys. 95, 1 (2017).
- [5] N.Sowmya, H.C.Manjunatha, N.Dhananjaya and A. M. Nagaraja. J.Radioanal. Nucl. Chem. 323, 1347 (2020).
- [6] A. M. Nagaraja, H. C. Manjunatha, N. Sowmya, N. Manjunath and S. Alfred Cecil Raj. E. Phys. J. Plus. 135,814 (2020)
- [7] H.C. Manjunatha , S. Alfred Cecil Raj, A.M. Nagaraja, and N. Sowmya. J. Nucl. Phys. Mat. Sci. Rad. A. 8, 1 (2020).
- [8] H. C. Manjunatha, N. Sowmya and A. M. Nagaraja. M. Phys. Lett.. 35, 06,2050016(2020).
- [9] G.R.Sridhar, H.C.Manjunatha, N.Sowmya, P.S. Damodara Gupta, H.B. Ramalingam, Eur. Phys. J. Plus 135:291 (2020).

CLUSTER RADIOACTIVITY IN ^{287}Mc USING MODIFIED GENERALIZED LIQUID DROP MODEL

N. Manjunatha*¹, A.M. Nagaraja^{1,3}, N. Sowmya¹, H.C. Manjunatha*¹, P.S. Damodara Gupta¹,
L. Seenappa¹, K.N.Sridhar², S. Alfred Cecil Raj³

¹Department of Physics, Government College for Women, Kolar, Karnataka, India

²Department of Physics, Government First Grade College, Kolar, Karnataka, India

³Department of Physics, St. Joseph's college (Autonomous), Affiliated to Bharathidasan University, Tiruchirappalli, Tamil Nadu, India

*Corresponding author: manjunathhc@rediffmail.com

ABSTRACT

Using modified generalized liquid drop model, we have studied all possible cluster decay modes of superheavy nuclei ^{287}Mc using different nuclear potentials. The daughter or residual nuclei is having magic nuclei or semi-magic nuclei. The total potential is evaluated by considering quantum tunneling process. The lower limit of cluster emission is from $Z_e^{\text{min}} = 2$ and upper limit of cluster emission considered is $Z_e^{\text{max}} = Z - 82$. The studied different nuclear potentials such as Danisov, AW-91, BW-91 and Bass-73 shows shorter half-lives and larger relative yield for the cluster emission ^{74}Ge . Hence, the possible cluster decay is with the combination $^{74}\text{Ge} + ^{213}\text{Bi}$.

Keywords: Cluster decay, Quantum tunneling, Superheavy element, Half-lives.

1. INTRODUCTION

As a first attempt to synthesize a transuranic element heavier than Uranium, a group of Italian scientists led by Enrico Fermi bombarded uranium nuclei with free neutrons in 1934. Neptunium was the first such element to be synthesized, with an atomic number of 93. Since then, several new elements have been synthesised in the lab, and their properties have been studied. Hot fusion reactions with ^{48}Ca projectiles produced three new elements with the atomic numbers 114, 116, and 118. Denisov and Hofmann [1] investigated shell structure and nuclear stability of the projectile and target combination using cold fusion reactions. Brodzinski and Skalski [2] theoretically predicted fission half-lives of superheavy element $Z=128-148$ using microscopic-macroscopic models. Using preformation cluster model, Wei and Zhang [3] studied an alpha and cluster radioactivity in the heavy and superheavy nuclei. To provide insight into the physics of cold-fusion reactions leading to the formation of elements at the end of the periodic system, Takatoshi Ichikawa [4] assumed that the target and projectile remain spherical during the collision and that the barrier can be described as a sum of Coulomb interaction and a short-range nuclear interaction. The experiments described by Oganessian [5] were targeted at producing nuclides with $Z = 113-$

116, 118, and $N = 170-177$ in the fusion reactions of heavy isotopes of Pu, Am, Cm and Cf with ^{48}Ca projectiles. Using the Cubic plus Yukawa Plus Exponential Model in two sphere approximations and including parent deformation and parent cluster deformations [6], computed the heavy cluster radioactivity half-lives of some of the set of isotopes of Superheavy nuclei. The values of the preformation factors were calculated using the experimental cluster decay half-lives, assuming that the heavy-ion emission decay constant equals the product of the assault frequency, the preformation factor, and the penetrability. D.N. Poenaru and R.A. Gherghescu [7] described the analytical superasymmetric fission (ASAF) model, which is widely used to forecast the half-lives of heavy and superheavy ($Z > 104$) elements. For the 26 cluster decays that have already been measured (from ^{14}C to $^{32,34}\text{Si}$ of parent nuclides with $Z = 87-96$). The Skyrem-Hartree-Fock method with a density-independent contact pairing interaction and the macroscopic-microscopic approach with an average Woods-Saxon potential and a monopole pairing interaction are used by S. Cwiok et al, [8] to investigate the ground-state properties of the superheavy elements (SHE) with $108 \leq Z \leq 128$ and $150 \leq N \leq 192$. Rafelski et al., [9] observed that the energy eigenvalues and wave

functions of atomic electrons bound to superheavy nuclei diverge dramatically when the electric field strength is limited. Samanta et al., [10] theoretically estimated alpha-decay half-lives of 314 heavy and superheavy elements in the region $Z = 102-120$ in the WKB frame work with DDM3Y interaction. Aritomo et al., [11] applied the Smoluchowski equation to study the fusion-fission process in heavy systems, with the finite-range droplet model potential.

Oganessian et al., [12] has explained the nuclear stability with $Z=114$ and 184 . The Coulomb and proximity potential models for deformed nuclei (CPPMDN) [13] are used to compute alpha-decay half-lives. Poenaru et al., [14] investigated heavy particle radioactivity with $Z_c > 28$. The UD, UNIV, Horoi, and UDL formulae were used by Zhang and Wang [15] investigated cluster radioactivity of $^{294}118$, $^{296}120$, and $^{298}122$. Warda et al., [16] used a microscopic theory to study the disintegration in heavier nuclei up to Lv ($Z=116$). Using CPPM and CPPMDN [17], alpha-decay half-lives of SHN $Z=122$ are theoretically studied. The macroscopic-microscopic model [18] for the ^{24}Ne emission from ^{232}U is used to calculate the dynamical path for cluster decay. For superheavy nuclei with atomic numbers between 104 and 130, Manjunatha et al., [20] developed a semi-empirical formula for alpha decay half-lives and cluster decay half-lives and compared the logarithmic half-lives generated by the current formula to those obtained from other equations such as the universal decay law (UDL). Earlier researchers [20-34] were used different models such as modified generalized liquid drop model, Coulomb and proximity potential model, effective liquid drop model and different decay modes such as alpha, cluster, proton, beta-decay and spontaneous fission. Literature survey shows inadequate theoretical studies on cluster radioactivity of Maseovium ($Z=115$). Hence in the present work, we have studied cluster radioactivity of ^{287}Mc using modified generalized liquid drop model and various versions of nuclear potential.

2. THEORETICAL FRAMEWORK

The total energy of the system including volume (E_V), surface (E_S), Coulomb (E_C), proximity ($E_{P_{prox}}$) and centrifugal energies (E_l) are given by;

$$E = E_V + E_S + E_C + E_{P_{prox}} + E_l \tag{1}$$

For compound nuclei, the volume, surface and coulomb energies are given by

$$E_V = -15.494(1 - 1.8I^2)A \text{ MeV} \tag{2}$$

$$E_S = 17.9439(1 - 2.6I^2)A^{2/3}(S/4\pi R_0^2) \text{ MeV} \tag{3}$$

$$E_C = 0.6e^2(Z^2/R_0) \times 0.5 \int (V(\theta)/V_0)(R(\theta)/R_0)^3 \sin \theta d\theta \tag{4}$$

where I , S , $V(\theta)$ and V_0 are with usual notations as explained in the literature [35]. When the nuclei are far apart, the equations (2-4) can be expressed as;

$$E_V = -15.494[(1 - 1.8I_1^2)A_1 + (1 - 1.8I_2^2)A_2] \text{ MeV} \tag{5}$$

$$E_S = 17.9439[(1 - 2.6I_1^2)A_1^{2/3} + (1 - 2.6I_2^2)A_2^{2/3}] \text{ MeV} \tag{6}$$

$$E_C = 0.6e^2 Z_1^2/R_1 + 0.6e^2 Z_2^2/R_2 + e^2 Z_1 Z_2/r \tag{7}$$

Here A_i is the mass number, Z_i is the atomic number, R_i is the radii of the two nuclei and I_i is the relative neutron excess of the two nuclei. The radii R_i is determined by;

$$R_i = (1.28A_i^{1/3} - 0.76 + 0.8A_i^{-1/3}) \text{ fm}, i = 1, 2 \tag{8}$$

In the equation (1) the centrifugal energy E_l of the emitted nuclei is expressed as;

$$E_l(r) = \frac{\hbar^2 l(l+1)}{2\mu r^2} \tag{9}$$

Where $\hbar = \frac{h}{2\pi}$. The μ , r and l are the reduced mass, distance between the mass centers of the two nuclei and angular momentum respectively.

The nuclear proximity function Danisov [36] is defined as;

$$V_P(r) = -1.989843 \frac{R_1 R_2}{R_1 + R_2} \varphi(r - R_1 - R_2 - 2.65) \times \left[1 + 0.003525139 \left(\frac{A_1}{A_2} + \frac{A_2}{A_1} \right)^{3/2} - 0.4113263(I_1 + I_2) \right] \tag{10}$$

where the effective nuclear radius is expressed as;

$$R_i = R_{ip} \left(1 - \frac{11.65415}{R_{ip}} \right) + 1.284589 \left(I_i - \frac{0.4A_i}{A_i + 200} \right) (i = 1, 2) \tag{11}$$

where R_{ip} is studied using the relation;

$$R_{ip} = 1.24A_i^{3/2} \left[1 + \frac{1.646}{A_i} - 0.19I \left(\frac{A_i - 2Z_i}{A_i} \right) \right] \text{ with } I_i = \frac{N_i - Z_i}{A_i} \tag{12}$$

The universal function is expressed as;

$$\varphi(s) = \begin{cases} 1 - S(0.7881663 + 1.229218S^2 - 0.2234277S^3 - 0.1038769S^4) - \frac{R_1 R_2}{R_1 + R_2} (0.1844935S^2 + 0.07570101S^3) + (I_1 + I_2) (0.04470645S^2 + 0.03346870S^3) & \text{for } -5.65 \leq S \leq 0 \\ 1 - S^2 \left[0.05410106 \frac{R_1 R_2}{R_1 + R_2} \exp\left(-\frac{S}{1.760580}\right) \right] & \\ -0.5395420 (I_1 + I_2) \exp\left(-\frac{S}{2.424408}\right) \times \exp\left(-\frac{S}{0.7881663}\right) & \text{for } S \geq 0 \end{cases} \tag{13}$$

where $s = r - R_1 - R_2 - 2.65$ is the separation between the two nuclei. Similarly, the nuclear potentials are evaluated using different potentials such as Bass73, AW-91 and BW-91 were studied as explained in detail in reference [37].

The barrier penetration probability is expressed as;

$$P = \exp\left[-\frac{2}{\hbar} \int_{R_{in}}^{R_{out}} \sqrt{2B(r)(E(r) - E(sphere))} dr\right] \tag{14}$$

Where $R_{in} = R_d + R_\alpha$ and $B(r) = \mu$ is the reduced mass and $R_{out} = e^2 Z_d Z_\alpha / Q_\alpha$. The decay half-life is defined as;

$$T_{1/2} = \frac{\ln 2}{\lambda} = \frac{\ln 2}{\nu_0 P} \quad (15)$$

here ν_0 is the assault frequency and whose value is 10^{20}S^{-1} and P is the barrier penetration probability evaluated using the equation (14).

3. RESULTS AND DISCUSSION

The total potential is evaluated for different possible cluster emissions from the superheavy nuclei ^{287}Mc using the theory explained in the section II.

The Fig. 1 gives the plots of scattering potential versus mass number of cluster emission A_1 in from the superheavy nuclei ^{287}Mc using different proximity functions such as Denisov, BW91, AW91 and Bass73. The variation of scattering potential is minimum for the cluster radioactivity of $^8\text{Be} + ^{279}\text{Rg}$, $^{16}\text{O} + ^{271}\text{Bh}$,

$^{31}\text{P} + ^{254}\text{Fm}$, $^{44}\text{Ca} + ^{243}\text{Am}$, $^{50}\text{Ti} + ^{237}\text{Np}$, $^{64}\text{Ni} + ^{223}\text{Fr}$, $^{74}\text{Ge} + ^{213}\text{Bi}$ using different proximity potentials with the mass number of one of the fragments for ^{287}Mc is observed. Scattering potential is highest for the cluster $^{31}\text{P} + ^{254}\text{Fm}$ and it is lowest for the clusters with magic numbers that is $^8\text{Be} + ^{279}\text{Rg}$ and $^{74}\text{Ge} + ^{213}\text{Bi}$. The graphical representation of scattering potential is useful to analyze the half-life values for the emitted clusters.

The variation of penetration probability with the mass number of one of the fragments for ^{287}Mc for different proximity functions is shown in Fig. 2. From this Fig. it is found that penetration probability is inversely proportional to logarithmic half lives for the emitted clusters. Penetration probability is small for the emitted cluster $^{31}\text{P} + ^{254}\text{Fm}$ and high for the cluster $^{74}\text{Ge} + ^{213}\text{Bi}$ for all the proximity functions. Similar variation will be found for decay constant for all the emitted clusters and it is presented in Fig. 3.

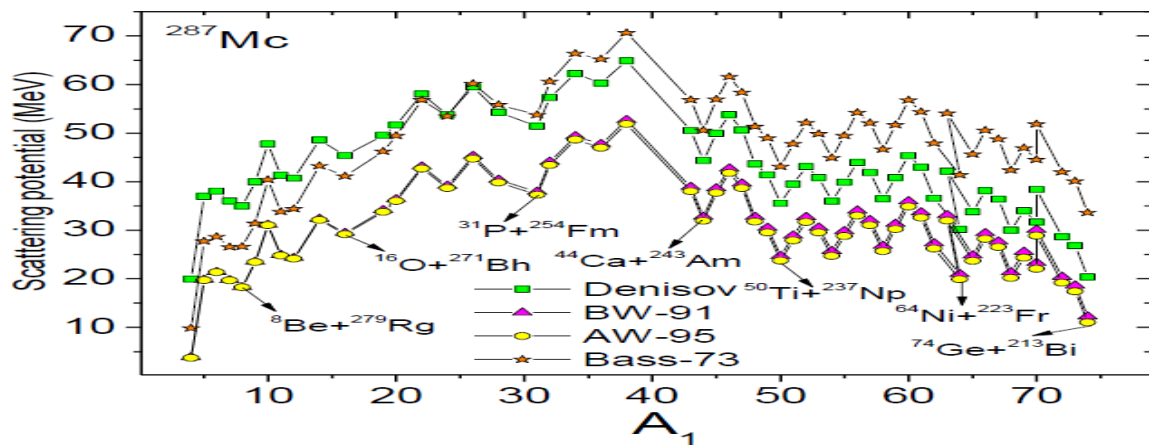


Fig. 1: The scattering potentials as a function of the mass number of one of the fragments for ^{287}Mc for different proximity functions

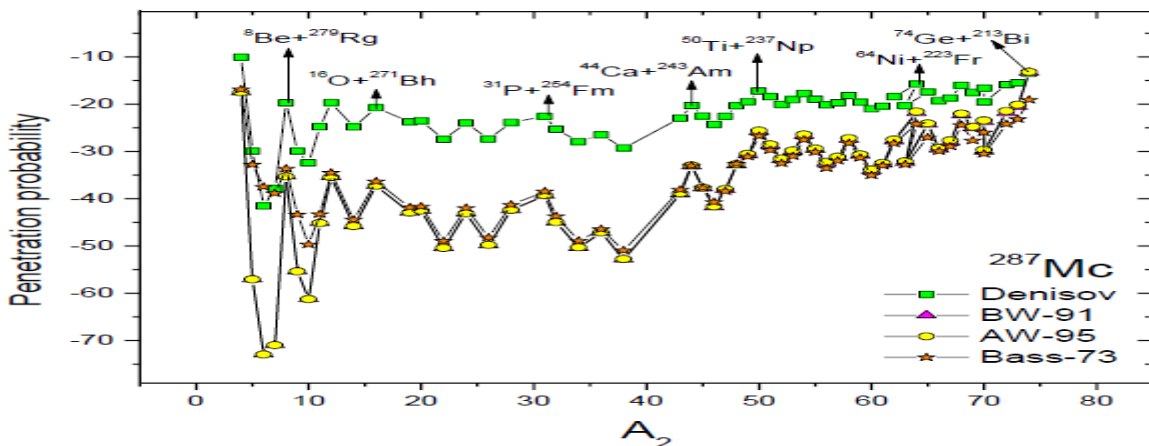


Fig. 2: The penetration probability as a function of the mass number of one of the fragments for ^{287}Mc for different proximity functions.

The variation of logarithmic half-lives with the mass number of one of the fragments for ^{287}Mc for different proximity functions is shown in Fig. 4. From this variation it is found that logarithmic half-life is more for

the cluster $^{31}\text{P}+^{254}\text{Fm}$ and small for the cluster $^{74}\text{Ge}+^{213}\text{Bi}$ for all the proximity functions. These results are due to the presence of magic nuclei in the daughter nuclei.

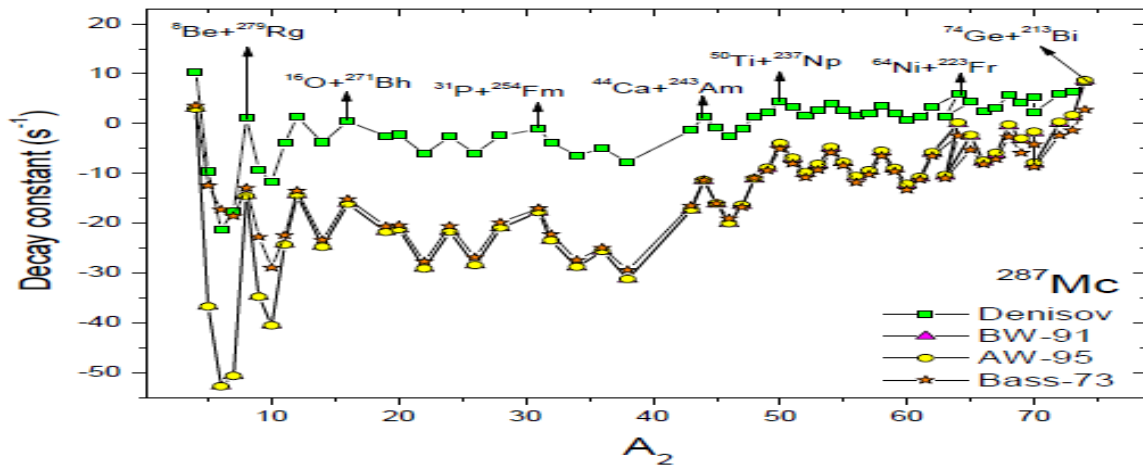


Fig. 3: The decay constant as a function of the mass number of one of the fragments for ^{287}Mc for different proximity functions

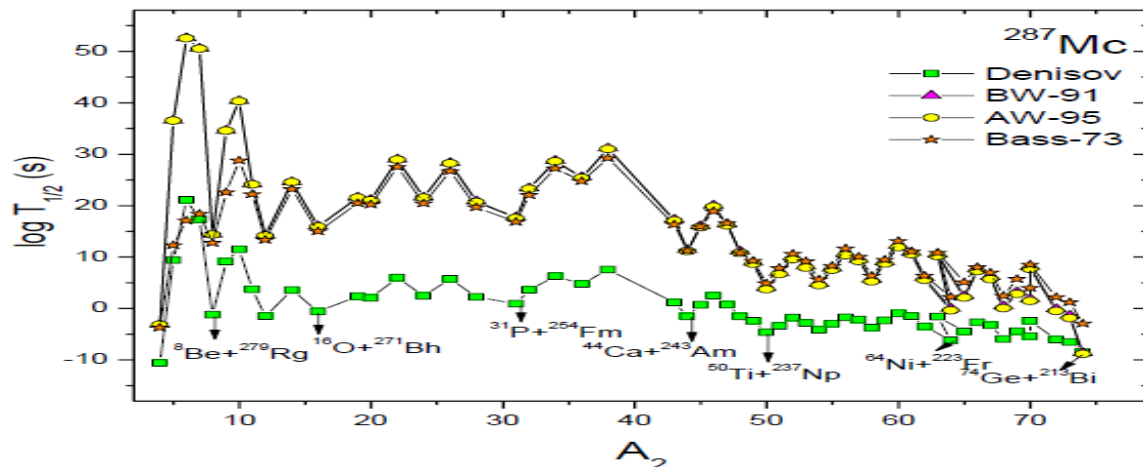


Fig. 4: The logarithmic half-lives as a function of the mass number of one of the fragments for ^{287}Mc for different proximity functions.

4. CONCLUSION

The cluster radioactivity of all cluster emissions were investigated using MGLDM and different nuclear potentials in superheavy nuclei ^{287}Mc . The studied different nuclear potentials such as Danisov, AW-91, BW-91 and Bass-73 shows shorter half-lives and larger relative yield for the cluster emission ^{74}Ge . The logarithmic half-lives corresponding to daughter nuclei $Z=83$ shows shorter half-lives and larger relative yield when compared to other different combinations studied. Hence, the possible cluster decay is with the $^{74}\text{Ge}+^{213}\text{Bi}$.

5. REFERENCES

1. Denisov VY, Hofmann S. *Phys Rev C*, 2000; **61**:034606.
2. Brodziński W, Skalski J. *Phys Rev C*, 2013; **88**:044307.
3. Wei K, Zhang HF. *Phys Rev C*, 2020; **102**: 034318.
4. Takatoshi I. *Phys Rev C*, 2005; **71**:044608.
5. Yury T, Oganessian. *Pure Appl Chem*, 2004; **76**:1715.
6. Carmel Vigila Bai GM, Revathi R. *First ICAPSM IOP*, 2020; **1706**:012021.

7. Poenaru DN, Gherghescu RA. *J Nucl.Phys Mat Sci.Rad A*, 2020; **8**:65.
8. Cwiok S, Dobaczewska J, Heenen PH, Magierski P, Nazarewicz W. *Nuclear Physics A*, 1996; **611**:211.
9. Rafelski J, Lewis P, Fulcher, Greiner W. *Phys Rev Lett*, 1971; **27**:958.
10. Samantaa C, Roy Chowdhury P, Basu DN. *Nucl Phys A*, 2007; **789**:142-154.
11. Aritomo Y, Wada T, Ohta M. *Phys Rev C*, 1977; **55**:3.
12. Oganessian Y. *Pure Appl. Chem*, 2006; **78**: 889–904.
13. Santhosh KP, Nithya. C. *Phys Rev C*, 2016; **94**:054621.
14. Poenaru DN, Gherghescu RA, Greiner W. *Phys Rev C*, 2012; **85**: 034615.
15. Zhang YL, Wang YZ. *Phys Rev C*, 2018; **97**: 014318.
16. Warda M. Zdeb A., Robledo LM. *Phys Rev C*, 2018; **98**:041602.
17. Manjunatha HC. *Int J Mod Phys E*, 2016; **25**:1650100.
18. Mirea M, Săndulescu A, Delion DS. *Proc Rom Acad A*, 2011; **12**:203-208.
19. Manjunatha HC, Sowmya N, Nagaraja AM. *Mod Phys Lett A*, 2020; **35**: 2050016.
20. Zagrebaev VI, Karpov AV, Greiner W. *Phys Rev C*, 2010; **81**: 044608.
21. Vijayaraghavan KR, Balasubramaniam M, Oertzen WV. *Phys Rev C*, 2015; **91**: 044616.
22. Diehl H, Greiner W. *Nucl Phys A*, 1974; **229**: 29-46.
23. Manjunatha HC, Sowmya N, *Nucl Phys A*, 2018; **969**:68-82.
24. Manjunatha HC, Sowmya N, *Int J Mod Phys E*, 2018; **27**:1850041.
25. Manjunatha HC, Sridhar KN, Sowmya N. *Phys Rev C*, 2018; **98**:024308.
26. Sowmya N, Manjunatha HC. *Bulg J Phys*, 2019; **46**:16-27.
27. Manjunatha HC, Sowmya N, Sridhar KN, Seenappa L. *J Radioanal Nucl Chem*, 2017; **314**:991-999.
28. Sowmya N, Manjunatha HC, Dhananjaya N. *J Radioanal Nucl Chem*, 2020; **323**:1347-1351.
29. Sowmya N, Manjunatha HC. *Braz J Phys*, 2019; **49**:874.
30. Sowmya N, Manjunatha HC. *Braz J Phys*, 2020; **50**:317.
31. Srinivas MG, Manjunatha HC, Sridhar KN, Sowmya N, Raj AC. *Nucl Phys A*, 2020; **995**:1216.
32. Sridhar GR, Manjunatha, HC, Sowmya N, Gupta PSD, Ramalingam HB. *Eur Phys. J Plus*, 2020; **135**:291.
33. Sowmya N, Manjunatha HC. *Phys of Part and Nucl Lett*, 2020; **17**:370.
34. Sridhar GR, Manjunatha, HC, Gupta PSD, Ramalingam HB. *Indian J Pure Appl.Phys.* 2020; **58**:234-240.
35. Manjunatha HC, Sowmya, N. Manjunath N, Seenappa L. *Int J Mod Phys E*, 2020; **29**:2050028.
36. Denisov VY. *Phys.Lett B*, 2002; **526**:315.
37. Zhang GL, Yao YJ. Guo MF, Pan M. *Nucl Phys A*, 2016; **951**:86-96.